Flinders University

Solvent Induced S-S Metathesis of Trisulfides

By

Alfrets Daniel Tikoalu
S.Pd. (Chemistry Education), M.Sc. (Chemistry)

Thesis
Submitted to Flinders University
for the degree of

Doctor of Philosophy

College of Science and Engineering
14 May 2025

TABLE OF CONTENTS

ABSTRACT

Polymers containing high sulfur content such as those made by inverse vulcanization have opened many opportunities for researchers to develop functional materials that can be used in many different applications such as polymers for energy storage, sorbents for toxic and precious metals, sorbents for oil spill remediation, infrared optics, adhesives, and composite materials. Inverse vulcanization is versatile to make polymer systems with sulfur rank 3 or more by altering the ratio of sulfur and alkenes starting materials. Due to its high S-S crosslink, however, polymers made by inverse vulcanization are difficult to process in common organic solvents, and pyridine is often the only solvent that can dissolve the polymers. It is thought that pyridine actually breaks the S-S bond in the polymer and converts it into soluble polymeric species. Phosphines such as tributyl phosphine can also do the similar thing but more rapidly and vigorously, which can facilitate desulfurization via an ionic mechanism.

A remarkable finding from our lab is that amide solvents such as dimethyl formamide can dissolve polysulfides made by inverse vulcanization with sulfur rank 3 or more. This result suggests that amide solvents could play a role in breaking and reforming the S-S bond in the polysulfide. A model S-S metathesis reaction employing dimethyl trisulfide and di-*n*-propyl trisulfide was used to test the theory. Dimethyl formamide, dimethyl acetamide, and *N*-methyl pyrrolidone were found to induce S-S metathesis in the trisulfide system to give a new trisulfide (methyl *n*-propyl trisulfide) in a reversible manner, while no reaction was observed in the disulfide analogues. This S-S metathesis reaction of organic trisulfides by amide solvents is unusual.

This thesis reported the investigation of the scope and mechanisms of the solvent induced S-S metathesis of organic trisulfides. Firstly, various organic trisulfides and tetrasulfides were synthesized and tested for the S-S metathesis. Different methods to access trisulfides were reported: 1) a trisulfide from thiosulfoxide salt (Bunte salt) and sodium sulfide, 2) a trisulfide from a thiol and sulfur dichloride (SCl_2), and 3) a trisulfide from a thiol and *N,N'*-thiobisphthalimide (a monosulfur transfer reagent). In this thesis, three new trisulfides (diisobutyl trisulfide, di-*n*-hexyl trisulfide, and bis(4-methoxybenzyl) trisulfide) were reported for the first time. Secondly, the effect of various solvents on the trisulfide metathesis was explored. Dry and excess solvent were the key to rapid trisulfide metathesis. An additional experiment for S-S metathesis involving a cyclic trisulfide, norbornane trisulfide, is demonstrated.

Furthermore, in this thesis the rapid S-S metathesis chemistry was demonstrated. The preparation of an unsymmetrical trisulfide from two symmetrical trisulfides, the production of trisulfide-based dynamic combinatorial library, and the late-stage modification of a complex natural product containing trisulfide moiety, calicheamicin-γ_1, can be achieved rapidly in the presence of amide solvents such as dimethyl formamide.

The mechanistic investigation of this solvent induced S-S metathesis of trisulfides was studied. Several mechanistic proposals involving radical, ionic, and thiosulfoxide intermediates were proposed. Experiments were conducted to find evidence for or against these mechanistic hypotheses. Primary evidence by electron paramagnetic resonance (EPR) suggests that no radical present in the reaction. While TEMPO can inhibit the trisulfide metathesis reaction, other small molecules such as acids, dienophiles (i.e., maleic anhydride and benzoquinone), and water also inhibit the reaction. These results suggest that the trisulfide metathesis reaction may not follow a radical pathway. Thiosulfoxide intermediate is proposed for the metathesis reaction. However, until now this intermediate has not been directly observed and reported. Future investigations, theoretically and experimentally, are suggested in order to successfully characterise the intermediate and to understand this solvent induced S-S metathesis chemistry.

DECLARATION

I certify that this thesis does not incorporate without acknowledgment any material previously submitted for a degree or diploma in any university; and the research within will not be submitted for any other future degree or diploma without the permission of Flinders University; and that to the best of my knowledge and belief it does not contain any material previously published or written by another person except where due reference is made in the text.

Signed: Alfrets Daniel Tikoalu

Date: 29 January 2025

ACKNOWLEDGEMENTS

First of all, I would like to thank my primary supervisor, Prof. Justin M. Chalker, for his unwavering guidance, immense support, and encouragement throughout my PhD journey. His insightful advice, patience, and belief in my abilities have been instrumental in shaping this thesis. Words cannot adequately convey how much I appreciate his mentorship and the countless hours he dedicated to guiding me. I would also like to extend my heartfelt thanks to my co-supervisor, Assoc. Prof. Michael V. Perkins, for his valuable insights and support. His expertise and constructive feedback have significantly contributed to the quality of this work.

I could not have completed my PhD without the generous financial support from Flinders University through the Flinders University International Tuition Fee Sponsorship (2021–2025) and Australian Research Council Discovery Project DP 200100090 (2021–2025). Their funding has provided me with the resources and opportunities to carry out this work. Their support also afforded me the opportunity to share my research at several universities in Indonesia and international conferences in Australia and New Zealand.

I am deeply grateful to Assoc. Prof. Zhongfan Jia and Dr. Harshal D. Patel for their guidance and motivation, which have been a source of inspiration throughout this journey. Their encouragement and advice have been pivotal in overcoming challenges and achieving milestones. I also thank Dr. Jasmine Pople, Dr. Maximillian Mann for their help during my PhD studies.

My sincere thanks go to all the other PhD, masters, and honours students in the lab. Your companionship, discussions, and shared experiences have made my time in the lab truly memorable. Working alongside such a talented and supportive group has been a privilege. Finally, I would like to thank my family and friends. To Meykke and Julio, words cannot describe how thankful I am to have you both by my side. I thank for their unconditional love and support.

Alfrets Daniel Tikoalu
29 January 2025
Flinders University
Chalker Research Lab

PUBLISHED WORK

The following is a list of peer-reviewed articles that were published, and conference presentations that were presented during the candidate's candidature.

Draft article related to the work presented in this thesis:

1. Harshal D. Patel, **Alfrets D. Tikoalu**, James N. Smith, Zhipeng Pei, Ryan Shapter, Samuel J. Tonkin, Peiyao Yan, Witold M. Bloch, Martin R. Johnston, Jeffrey R. Harmer, Christopher T. Gibson, Michael V. Perkins, Tom Hasell, Michelle L. Coote, Zhongfan Jia, and Justin M. Chalker. **2025**. Spontaneous Trisulfide Metathesis in Polar Aprotic Solvents. *Manuscript in preparation*.

Peer-reviewed articles not related to the work presented in this thesis:

2. Carbonisation of a polymer made from sulfur and canola oil. Mann, M.; Luo, X.; **Tikoalu, A.D.**; Gibson, C.T.; Yin, Y.; Al-Attabi, R.; Andersson, G.G.; Raston, C.L.; Henderson, L.C.; Pring, A.; Hasell, T. *Chem. Commun.* **2021**, *57*, 6296-6299.
3. Modelling mercury sorption of a polysulfide coating made from sulfur and limonene. Worthington, M.J.; Mann, M.; Muhti, I.Y.; **Tikoalu, A.D.**; Gibson, C.T.; Jia, Z.; Miller, A.D.; and Chalker, J.M. *Phys. Chem. Chem. Phys.*, **2022**, *24*, 12363-12373.

Conference presentations:

Chemical depolymerisation of a poly(trisulfide). **Alfrets D. Tikoalu**, Jasmine M. M. Pople, Dr. Harshal D. Patel, Assoc. Prof. Michael V. Perkins, Prof. Justin M. Chalker. Poster presentation for 12th Annual Conference of The Flinders Institute for Nanoscale Science & Technology, Flinders University at Tonsley, Adelaide, South Australia, 14 June 2023.

Amide solvent induced S-S metathesis of organotrisulfides and its application for polymer recycling. **Alfrets D. Tikoalu**, Harshal D. Patel, Zhipeng Pei, Ryan Shapter, Witold M. Bloch, Peiyao Yan, Samuel J. Tonkin, Michael V. Perkins, Martin R. Johnston, Jeffrey R. Harmer, Tom Hasell, Michelle L. Coote, Zhongfan Jia, Justin M. Chalker. Speaker for 38th Australasian Polymer Symposium, Auckland, New Zealand, 18 – 21 February 2024.

Trisulfide metathesis induced by polar aprotic solvents. **Alfrets D. Tikoalu**, Harshal D. Patel, Zhipeng Pei, Michael V. Perkins, Jeffrey R. Harmer, Tom Hasell, Michelle L. Coote, Zhongfan Jia, Justin M. Chalker. Poster presentation for RACI Organic Chemistry Symposium (Organic24), Adelaide, Australia, 18 – 20 November 2024.

CHAPTER 1: INTRODUCTION TO THE CHEMISTRY OF ORGANIC TRISULFIDES

1.1 Acknowledgement

Dr. Harshal D. Patel for the advice and discussion on the chemistry of organic trisulfides

1.2 Background and Motivations

Despite its high volume production (~80 million tons/year), sulfur recovered from refining processes is still underutilised and mainly used to make sulfuric acid.[1] However, sulfur and its derivatives have recently become a significant area of interest for researchers. Construction of sulfur compounds directly from elemental sulfur can be achieved through sulfuration, reduction, oxidation, and redox condensation processes.[2] Sulfur compounds have been an important part of our lives. Hundreds of FDA approved drugs contain sulfur.[3] Other sulfur compounds such as organic polysulfides from allium family of garlic and onions have been studied as endogenous H_2S releasing compounds for antitumour drugs.[4]

With many diverse applications of sulfur, many efforts have been made to convert sulfur into value added materials, such as polymers. One of the most notable ways to directly convert sulfur into value-added high sulfur content polymers (typically 20–90% sulfur) is via inverse vulcanization. This technique was introduced in a landmark paper published in Nature Chemistry in 2013 by Pyun and co-workers.[5] By using this technique, sulfur polymers can be made via radical copolymerization with polyenes. Since then, sulfur has been used via inverse vulcanization to make various value-added materials such as polymers for energy storage[6, 7], sorbents for toxic and or precious metals[8-10], sorbents for oil spill remediation[11], antimicrobial agents[12], infrared optics[13, 14], sustainable adhesives[15, 16], and composite materials.[17-19]

Inverse vulcanization offers researchers to explore various functional sulfur polymers (often called organic polysulfides or simply polysulfides). The physical and chemical properties of inverse vulcanized polymers depend primarily on the alkene starting material and the ratio of sulfur to the alkene. The ratio of sulfur to the alkene determines the average number of sulfur atoms that crosslink to the alkene (sulfur rank). At 1:1 ratio of sulfur to alkene, for example, inverse vulcanized sulfur polymer made from aromatic hydrocarbons such as 1,3-diisopropenyl benzene (DIB) is glassy and brittle[5, 20], while if it is made from unsaturated triglycerides, the resulting polymer is soft and rubbery.[11, 21] The properties of the sulfur polymers can also be altered by combining two alkenes in a single synthesis step or more to make a terpolymer, or by doing post-modification of an inverse vulcanized polymer.[22-24]

In 2022, Hasell group at the University of Liverpool and Chalker group at Flinders University carried out a study on post-modification of an inverse vulcanized polymer made from Span-80 and sulfur, followed by crosslinking it with bisphenol epoxides (BADGE). The aim of this study was to

design sulfur polymers that are solvent processable and recyclable. It is important to note that most of the inverse vulcanized sulfur polymers are insoluble in many organic solvents. Pyridine is often a solvent used to dissolve these polymers. However, this nucleophilic amine is thought to actually breaking the S-S bond in the sulfur polymer made by inverse vulcanisation via an ionic mechanism.[25] In their study, Hasell and Chalker developed a stretchable and durable inverse vulcanized polymer made from Span-80, sulfur, and BADGE. The remarkable finding is that this polymer can be dissolved in amide solvents (DMF, DMAc, and NMP). GPC analysis of the DMF soluble fraction of the polymer provided evidence that the molecular weight of the soluble fraction of the polymer decreased.[22] This result suggests that the amide solvents could play a role in breaking and reforming S-S bonds in the polymer. This theory was tested by using a model S-S metathesis reaction employing dimethyl and di-*n*-propyl trisulfide for the trisulfide system and the disulfide analogues for the disulfide system. DMF, DMAc, and NMP were found to induce the S-S metathesis in the trisulfide system at room temperature (Figure 1.1), while no reaction was observed in the disulfide system. The results of this investigation support the theory that polysulfide system with the sulfur rank 3 can be reprocessed via S-S metathesis in these solvents, though the mechanism was not fully understood at the time.

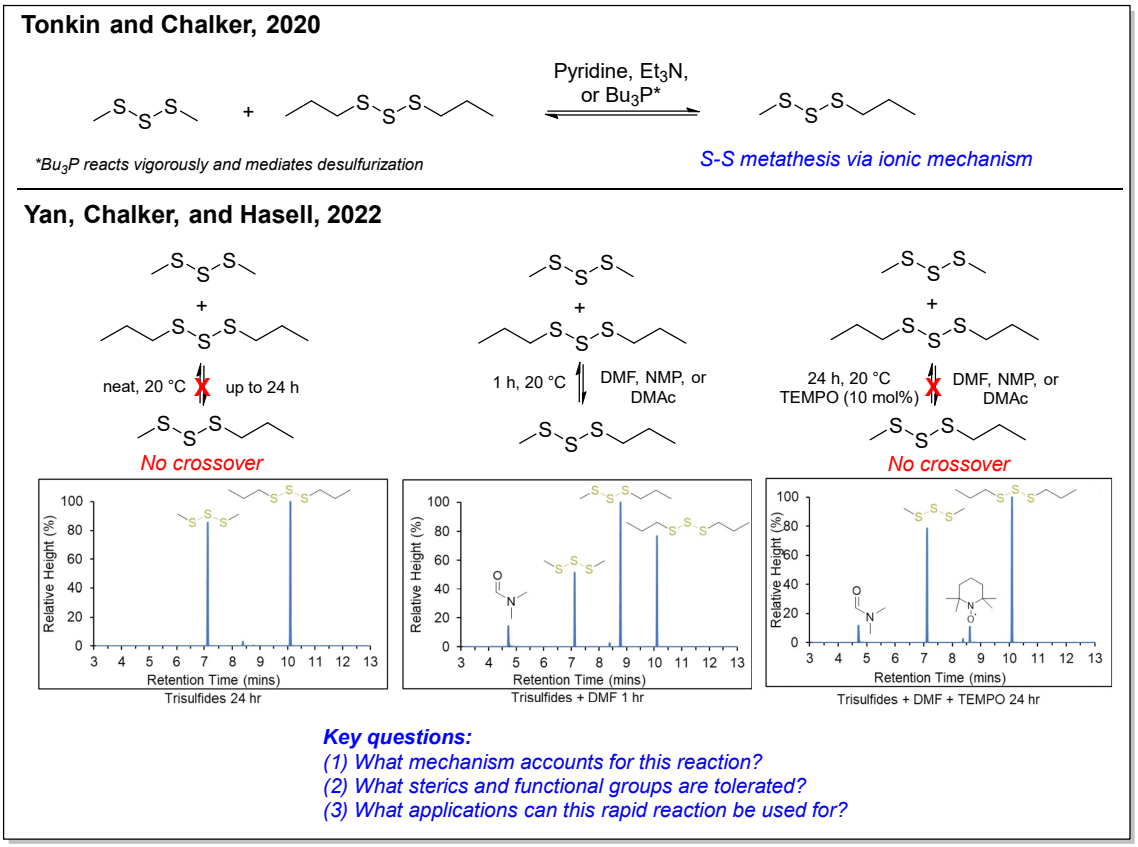

Figure 1.1: Previous works on the solvent induced S-S metathesis of trisulfides[22, 25] and the research questions in this study. The GC images were reproduced from ref. 22, under a Creative Commons Licence: CC-BY 4.0.

This room temperature trisulfide metathesis reaction induced by polar amide solvents is quite unusual. In the report, a complete S-S exchange between the trisulfides in DMF occurs within one hour. As shown in Figure 1.1, the exchange reaction selectively gave only a new trisulfide, and no disulfides or tetrasulfides were formed.[22] The room temperature trisulfide metathesis has also been reported previously by Harpp[26] and our group[25] but it is required nucleophilic phosphines or amines. In some case, desulfurization caused by the phosphine nucleophiles is unavoidable, especially for longer reaction time. In an Honours project, Shapter also found that other polar aprotic solvents like DMSO can also induce the trisulfide metathesis. Acetonitrile, acetone, and alcohols could also induce the metathesis but the rate was much slower compared to those amides. Hence, in general polar solvents can induce trisulfide metathesis, but the mechanism by which this occurs are not established.

Furthermore, Hasell and co-worker found that TEMPO can inhibit the trisulfide metathesis reaction which suggests that the reaction may follow a radical pathway. In another study by Shapter[27], the rate of reaction between the trisulfides in DMF was found to reduce in the presence of acetic acid. Because the trisulfide metathesis in DMF is inhibited by TEMPO, it was thought that the thiyl radical could be trapped using a methacrylate monomer. If this idea was successful, it would be a novel and mild way to initiate radical polymerization. The polymerization of methyl methacrylate in the mixture of dimethyl trisulfide, di-*n*-propyl trisulfide, and DMF was investigated by Shapter. Despite these efforts, no polymer product was observed and the radical mechanism was called into doubt.

The discovery of the unusual S-S metathesis reaction of organic trisulfides in polar solvents opens up many questions. From a mechanistic perspective, if the radical mechanism is involved, a disulfide and a tetrasulfide should be formed in the reaction, but only trisulfides were formed. What mechanism accounts for this observation? What steric effects and functional groups are tolerated? What applications can the rapid reaction be used for? Indeed, a better understanding of this chemistry can be crucial as it would allow us to explore the reactivity of organic trisulfides in polymer synthesis and recycling, modification of biomolecules, or synthetic chemistry. Therefore, the aim of this thesis is to study this trisulfide metathesis chemistry in detail to better understand its mechanism and scope. To provide the context for this trisulfide metathesis research, a literature review on the S-S metathesis chemistries, theories and knowledge gaps is provided in the next sections of this chapter.

1.3 Introduction to Organic Polysulfides

Organic polysulfides (RS_nR), consist of a chain of sulfur atoms (n > 2) that link to alkyl or aryl via carbon atoms. The number of sulfur atoms (n) in the organic polysulfide is often called “sulfur rank”.[28] For example, dimethyl trisulfide (CH_3SSSCH_3) has a sulfur rank of 3. Today, polymers containing high sulfur contents are also colloquially called “polysulfides” such as polymers made by inverse vulcanization.[5] Organic trisulfides are important in our everyday life. They exist in natural products[29],

polymers[30], biological molecules[4], and energy materials[6, 7] (Figure 1.2). In addition, organic polysulfides can be found in antitumor medicines such as Calicheamicin γ_1 and Shishijimicin A – contains trisulfides in their structures.[31-33] Because of the significance of polysulfides, researchers have become more interested in the synthesis of polysulfides, in both small molecules and polymeric materials.

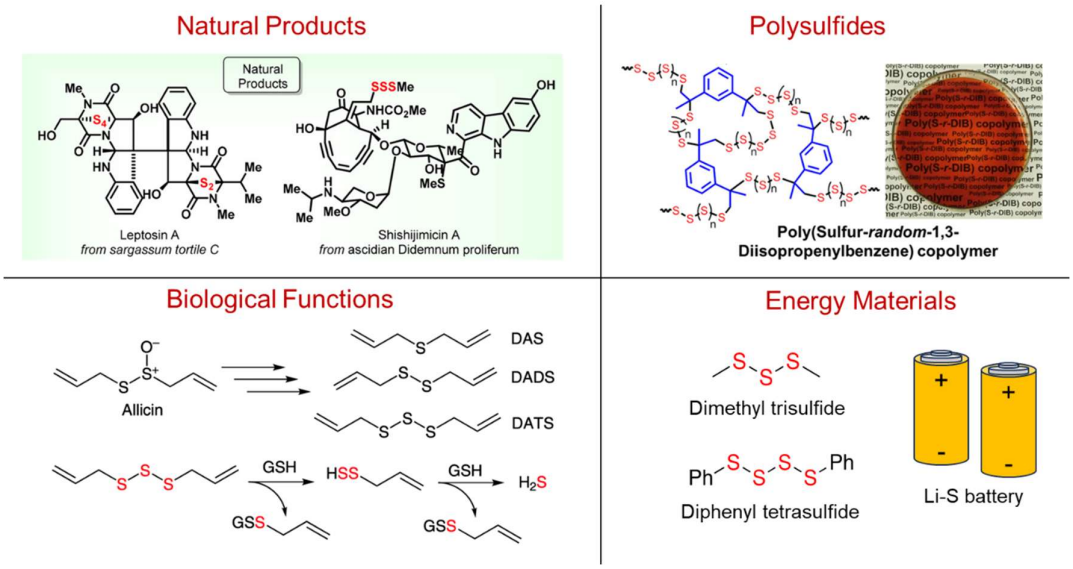

Figure 1.2: Significance of organic polysulfides.[4, 6, 7, 29, 30] Natural products image was reproduced with permission from ref. 29. © 2020 American Chemical Society. Polysulfides image was reproduced with permission from ref. 30. © 2014 American Chemical Society. Biological functions image was reproduced with permission from ref. 4. © 2015 Georg Thieme Verlag KG.

The reactivity of organic polysulfides is related to the S-S bond energy. In general, the S-S bond dissociation energy in organic polysulfides decreases as the number of sulfur atom increases.[34, 35] Theoretical calculation of S-S bond dissociation energies (BDEs) in polysulfides (Table 1.1) has been reported by Lundquist et al.[17] The values of the S-S BDEs obtained by the ab initio G4 thermochemical protocol (chemical accuracy ± 4 kJ mol^{-1}) are consistent with the experimental observation of dimethyl polysulfides by Tobolsky.[36] From Table 1, the S-S bond strength weakens considerably from disulfide to tetrasulfide (215 to 98.9 kJ mol^{-1}, respectively). With this reactivity, it is anticipated that a polysulfide with higher sulfur rank tends to be more reactive than the lower one.

Table 1.1: S-S bond dissociation energy (BDE) of dimethyl polysulfides (MeS_nMe, n = 2 – 4) (ref.[17])

Polysulfide	MeS_2Me	MeS_3Me	MeS_4Me
S-S BDE (ΔG_{298K}) in kJ mol^{-1}	215.0	160.2	98.9

Polysulfides can undergo several types of reactions, such as interconversion (sulfur atom exchange between molecules containing S-S bond or known as S-S metathesis), sulfur transfer reactions, replacement reactions, nucleophilic displacement reactions at S-S bonds, and oxidation reactions.[28, 37] The focus on this review is the discussion of interconversion reaction and nucleophilic displacement reaction since it is related to the PhD project.

1.4 Interconversion Reaction of Organic Trisulfide (Trisulfide Metathesis)

Trisulfide Metathesis Induced by Thermal, UV and Nucleophiles

The exchange of sulfur atom in polysulfides can occur by several mechanisms and the rate of reaction at certain temperature heavily depends on the polysulfide compounds and solvents. A study by Tobolsky and co-worker showed that neat dimethyl trisulfide (Me_2S_3), with exclusion of light, decomposes at 80 ºC to give dimethyl disulfide (Me_2S_2) and dimethyl tetrasulfide (Me_2S_4) (Figure 1.3). This reaction takes almost 3 days to give approximately 1:1 mixture of disulfide and tetrasulfide. Also, prolonged heating of the trisulfide (> 9 days) can lead to the formation of dimethyl penta- and hexasulfide (Me_2S_5 and Me_2S_6).[36] This thermal reaction is notably slow and lead to the formation of a mixture of di-, tri-, tetra-, and higher polysulfides.

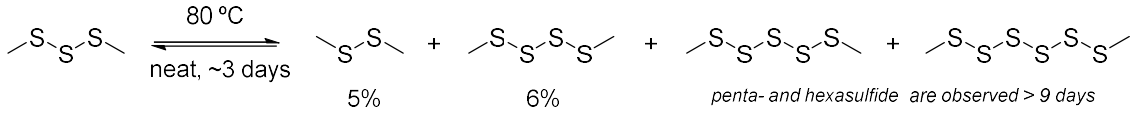

Figure 1.3: Decomposition of dimethyl trisulfide at 80 °C. Prolonged heating of the trisulfide leads to the formation of dimethyl penta- and hexasulfide.[36]

However, if the trisulfide is heated in benzene, it takes around 20 days for the reaction to reach equilibrium.[36] In another study by Trivette and Coran[38], the crossover reaction between an equimolar mixture of two dialkyl trisulfides (Figure 1.4A), diethyl trisulfide (Et_2S_3) and di-*n*-propyl trisulfide ($^{n}Pr_2S_3$), at 132 – 148 °C yield to a new trisulfide, ethyl *n*-propyl trisulfide ($EtS_3{}^{n}Pr$). In a control experiment, the S-S exchange reaction does not occur at room temperature after storage in the dark for around 30 days. For the thermal S-S metathesis involving more hindered trisulfides, the reaction does not occur. Chauvin et al.[35] reported that the crossover reaction between di-*tert*-butyl trisulfide ($^{t}Bu_2S_3$) and diisopropyl trisulfide ($^{i}Pr_2S_3$) at 100 °C in chlorobenzene (Figure 1.4B) does not occur. This is due to the higher S-S bond strength of a trisulfide, which is ~70 kJ mol^{-1} higher, compared to a tetrasulfide. In addition to this, perthiyl radical ($RSS^{\bullet}$) is more stable than thiyl radical ($RS^{\bullet}$).[35] In the reaction employing the tetrasulfides analogues, Chauvin et al.[35] observed that the S-S exchange reaction had reached equilibrium after ~2 hours. Trivette and Coran[38] also observed that the S-S exchange of the trisulfide shown in Figure 1.4A is accelerated when a small portion of tetrasulfide is presence in the mixture.

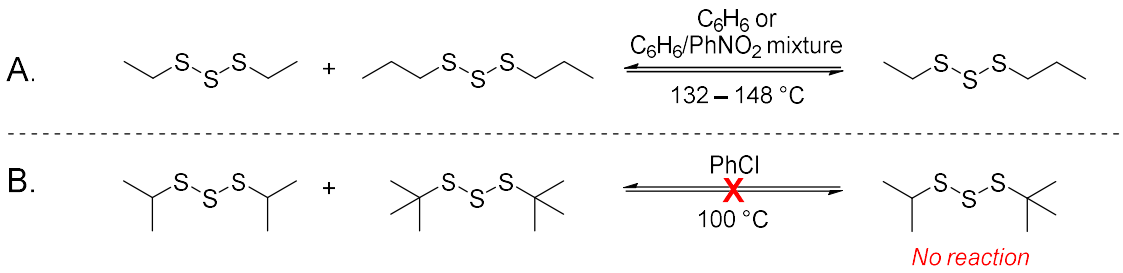

Figure 1.4: Several examples of thermal S-S exchange between trisulfides reported by (A) Trivette and Coran[38] and (B) Chauvin and co-workers[35].

Uncatalyzed S-S metathesis at elevated temperature is thought to follow a radical pathway. This mechanism is illustrated in Figure 1.5. In the initiation process, two thiyl radicals are formed by an unsymmetrical dissociation of the trisulfide. The generated thiyl radicals would then attack the central sulfur atom (more electron rich) of a trisulfide to yield the new trisulfide and another thiyl radical during the propagation step. Similarly, the perthiyl radical can attack the trisulfide and yield the same thiyl radical. In the termination process, two radicals can undergo a recombination which then leads to the formation of disulfide, trisulfide and tetrasulfide.[35, 37, 38]

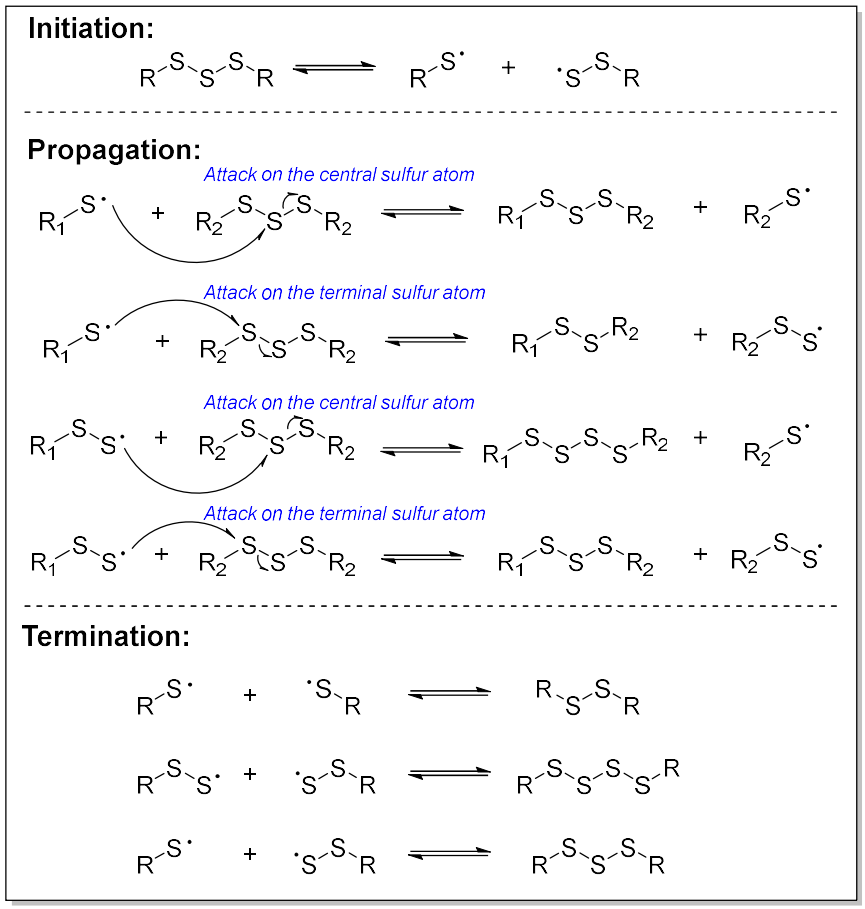

Figure 1.5: A radical mechanism in trisulfide metathesis reaction.

The light promoted S-S metathesis of polysulfides also proceeds via a radical pathway. The light promoted trisulfide metathesis was discussed by Guryanova.[39] Birch and co-workers[40] studied the decomposition of dimethyl trisulfide under the UV light of a medium pressure mercury lamp. During the UV exposure, dimethyl trisulfide is converted to its corresponding di- and tetrasulfide (Figure 1.6A). Milligan and co-workers[41] studied the photolysis of several trisulfides (i.e., Me_2S_3, Et_2S_3, and $^{i}Pr_2S_3$) using 254 nm (UV mercury lamp) or sunlight (midsummer) in some cases as the irradiation sources (Figure 1.6B). They found the similar result as reported by Birch et al. where a mixture of di-, tri-, and tetrasulfide is observed and can be isolated by distillation. Interestingly, upon UV irradiation of dimethyl and diethyl trisulfide, hydrocarbons are formed but the yield was low. The results suggest that C-S bond scission also occurs but the S-S bond scission occurs preferentially.

Evidence on the radical mechanism for the trisulfide metathesis induced by UV light is supported by several reported experiments. A study by Burkey et al. showed that *tert*-BuSS$^{\bullet}$ is generated upon photolysis of frozen *tert*-butyl tetrasulfide (-160 °C, 20% v/v in toluene) and this radical can be characterised by means of electron paramagnetic resonance (EPR).[42] Everett et al. also reported the formation of perthiyl radicals from photolysis penicillamine and cysteine trisulfide.[43]

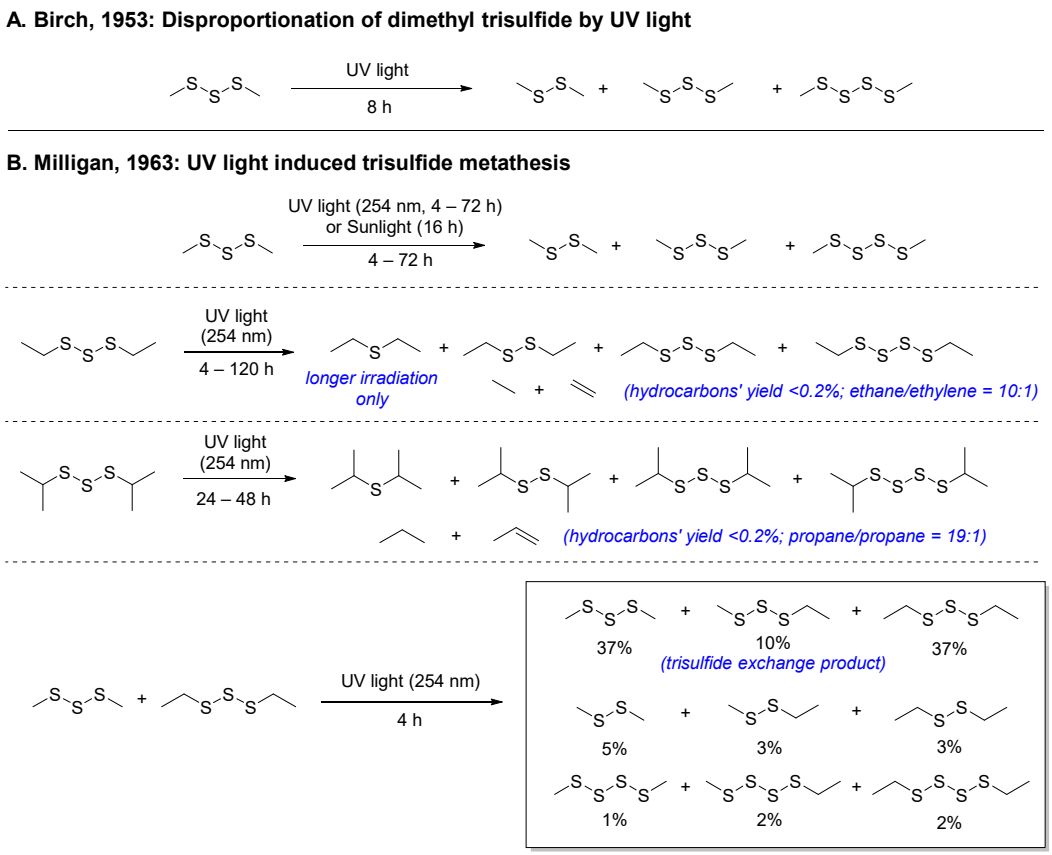

Figure 1.6: UV light promoted trisulfide metathesis. A. Disproportionation of dimethyl trisulfide under UV studied by Birch et al.[40] B. Disproportionation of various trisulfides (i.e., dimethyl, diethyl, and diisopropyl trisulfide) and the trisulfide exchange between dimethyl trisulfide and diethyl trisulfide under UV light studied by Milligan et al.[41]

Several amines such as pyridine and triethylamine can also catalyse the S-S metathesis between the two organic polysulfides. However, the results depend on the concentration of the amine. In a study by Tonkin et al.[25], in an excess molar of pyridine (~105 eq. to the trisulfide), dimethyl trisulfide (Me_2S_3) and di-*n*-propyl trisulfide ($^nPr_2S_3$), the crossover reaction between the trisulfides occurs rapidly with the equilibrium reached within 5 minutes (Figure 1.7A). This reaction, in contrast, does not occur if an equimolar mixture of pyridine and the trisulfides is reacted as a chloroform solution (115 mM) for 24 h (Figure 1.7B). However, when pyridine is replaced by triethylamine (also the same concentration of 115 mM), the trisulfide crossover did occur (Figure 1.7C). This phenomenon could be explained by nucleophilic parameter (*N*) of the amines. Triethylamine (*N* = 17.3 in CH_2Cl_2) is more nucleophilic than pyridine (*N* = 12.9 in CH_2Cl_2).[44, 45] Hence, the trisulfides crossover reaction can occur in triethylamine.

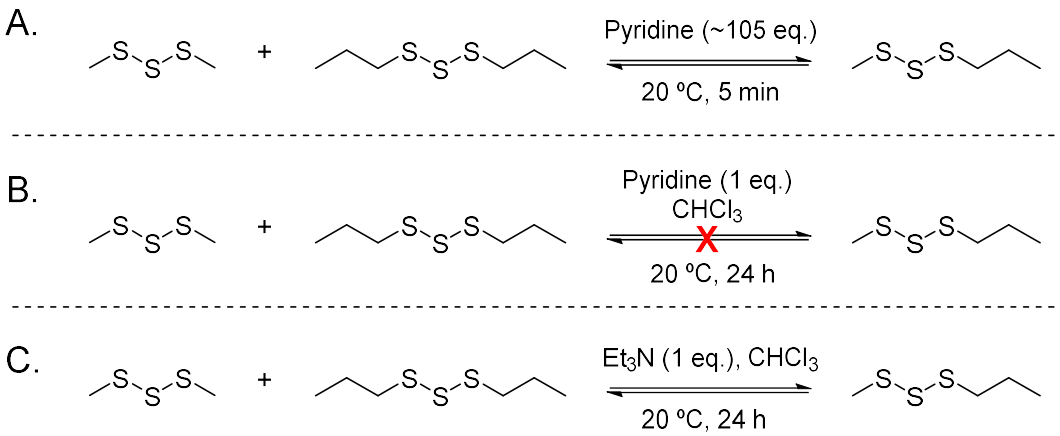

Figure 1.7: Trisulfide metathesis reaction in (A) neat pyridine after 5 min, (B) 115 mM pyridine (1 eq. to the trisulfide) after 24 h, and (C) 115 mM triethylamine.

Unlike the reactions with pyridine or triethylamine, some strong nucleophiles e.g., phosphines (R_3P, R= alkyl, aryl, dialkylamino), sulfite ions (SO_3^{2-}) and cyanide ions (CN^-) can even desulfurize the polysulfide (Figure 1.8).[26, 37] For example, Harpp et al. reported that organic trisulfides can be desulfurized to disulfides by triphenyl phosphine (Ph_3P). They also reported that tris(dialkylamino) phosphines are particularly efficient to desulfurize trisulfides to disulfides.[26] Recently, Tonkin et al.[25] demonstrated the rapid and vigorous trisulfide metathesis reaction in the presence of tributylphosphine. The phosphine catalysed trisulfide metathesis and desulfurization is discussed in more detail in Chapter 3. Sulfite can react with a tetrasulfide to give disulfide and cyanide can react with a trisulfide to give a thioether.[37, 46] The reactivity of these nucleophiles toward organic polysulfides depends on the steric and strain requirements of the S-S bonds to be broken.[37] These reactions are not categorised as interconversion reactions but a nucleophilic displacement reaction or desulfurization.

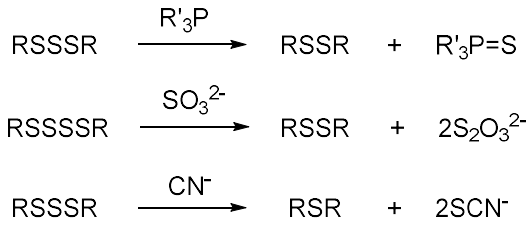

Figure 1.8: Several reaction between organic tri- or tetrasulfide and phosphines, sulfite, and cyanide ion.[37]

The mechanism of nucleophilic induced trisulfides crossover reaction can be explained via an ionic mechanism. For desulfurization of organic trisulfides, the S_N2 displacement could occur either via central or terminal sulfur atom. This mechanism is shown in Figure 1.9 below. In addition to this, polar solvents such as acetonitrile and acetone were found far more effective to assist desulfurization via removal a central sulfur atom of the trisulfide (Table 1.2) compared to those less polar solvents.

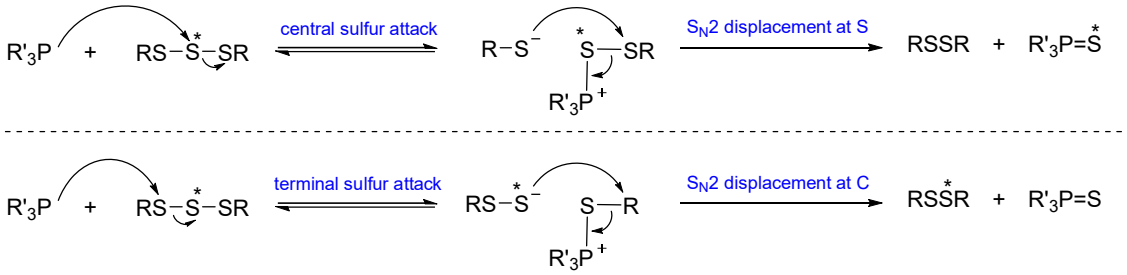

Figure 1.9: Harpp's discussion on the mechanistic desulfurization of organic trisulfides catalysed by phosphines.[26]

Table 1.2: Desulfurization of (R,R)-bis(1-phenylethyl) trisulfide by tris(dimethylamino) phosphine.[26] Data was reprinted with permission from ref. 26. © 1982 American Chemical Society.

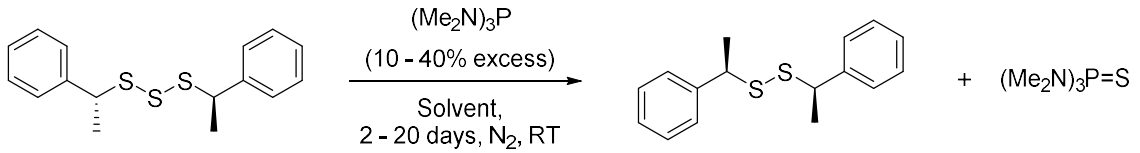

Reaction solvent	Solvent Polarity (E_T value)	Average $[\alpha]^{20}$ D of Product in benzene (degree)*	% central sulfur removal**
MeCN	46.0	252	82
Acetone ($Me_2C=O$)	42.2	200	65
EtOAc	38.1	106	34
THF	37.4	80	26
Et_2O	34.6	102	33
C_6H_6	34.5	62.9	20
Cyclohexane (cy-C_6H_{12})	31.2	150	49

* Average data obtained from 3 – 6 experiments.

** Each optical rotation value $[a]^{20}$ D was divided by 309° to obtain the percentage central sulfur removal since a 1:1 mixture of (R,R)-bis(1-phenylethyl) disulfide and $(Me_2N)_3P=S$ had $[a]^{20}$ +309° (c 2.01, C_6H_6) (addition of up to 0.5 mol eq. of the phosphine to this sample had a negligible effect on this optical rotation)

Trisulfide Metathesis Induced by Polar Solvents

In general, the crossover reaction between two dialkyl trisulfides requires heating at elevated temperature (> 80 °C), UV light, or a strong nucleophile to cleavage the S-S bond. These processes allow the formation of thiyl radicals or thiolate ions which can then proceed the crossover reaction. A recent discovery from the work of Hasell and Chalker laboratory demonstrated that the crossover reaction of dialkyl trisulfides can now be done in the presence of polar aprotic solvents at room temperature (20 °C).[22] A model study using small molecules trisulfides, dimethyl and di-*n*-propyl trisulfide, was investigated by Tonkin and Chalker. The trisulfide models were selected to mimic the nature of polysulfide bonds in the polymer system with sulfur rank of 3. As mentioned in the introduction of this chapter, upon addition of amide solvents (i.e., DMF, DMAc, or NMP) to the trisulfide mixture, a new trisulfide, methyl *n*-propyl trisulfide, is formed and the equilibrium has reached within 1 hour (Figure 1.10). After longer reaction time (~24 h), the mixture only consists of the starting materials and the new trisulfide. THF was also found to induce the exchange, however, the rate was much slower than those amides.

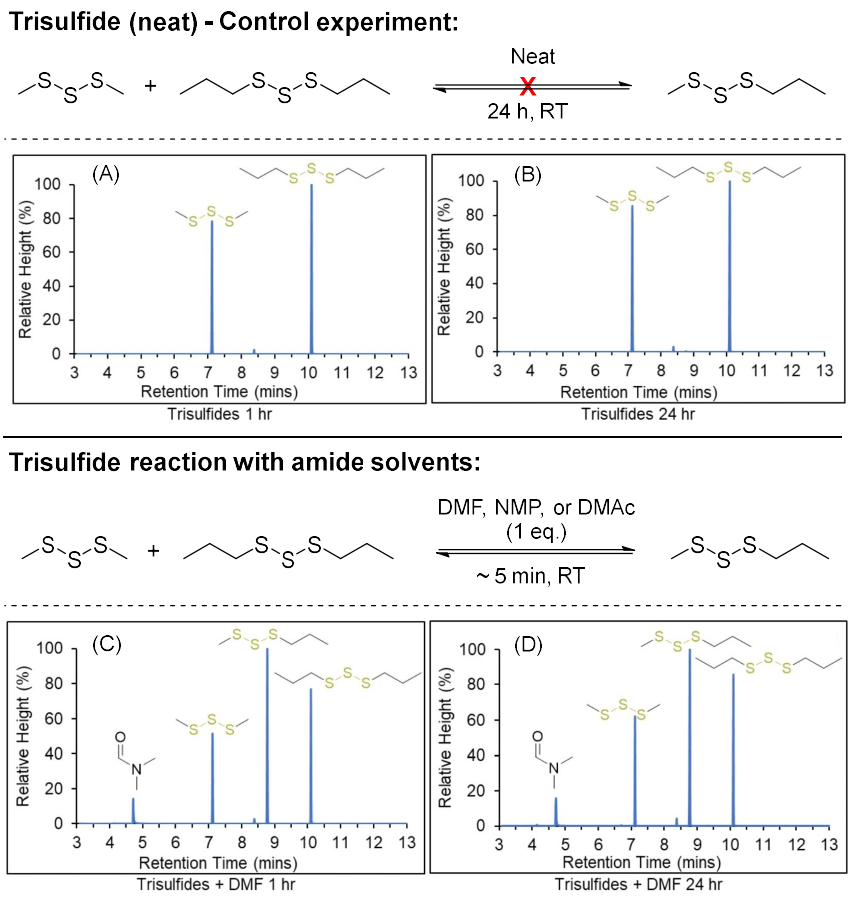

Figure 1.10: Crossover reaction between dimethyl trisulfide and di-*n*-propyl trisulfide. A, B. No crossover product formed after 1 h and 24 h reaction in the trisulfides (neat). C, D. An equimolar amide solvents (DMF, NMP or DMAc) yielded a crossover product (methyl propyl trisulfide) at 20 °C within 1 hour and no other product formed after 24 h.[22] The GC images were reproduced from ref. 22, under a Creative Commons Licence: CC-BY 4.0.

The metathesis investigation using other polar solvents was also studied by Shapter[27] in his Honour project in the Chalker Lab. The same trisulfide models were used in the experiments. DMSO was also found to effectively induce the trisulfide metathesis in which the rate of metathesis is comparable with other amides such as DMF, NMP, and DMAc. It has been known that DMSO possesses unique properties. This high boiling point polar aprotic solvent has been known for its ability to improve organic reactions by enhancing solubility, participating as a reagent, and stabilising the reaction intermediates.[47, 48] It also has a high dielectric constant (46.6 at 25°C)[49], and DMSO is a nucleophile at either oxygen or sulfur,[50] which might also be important in this reaction. Furthermore, other polar aprotic solvents such as acetonitrile and acetone were investigated by Shapter for the trisulfide metathesis reaction. These common solvents were also found to induce the trisulfide metathesis reaction, but the rate is generally slower than those amides. Protic solvents such as alcohols also induce the metathesis but it took days to generate the new trisulfide. The exact mechanism on how these polar aprotic solvents interacts with a trisulfide in the trisulfide metathesis

reaction is unknown. Nevertheless, Steudel had previously proposed that the metathesis reaction could possibly occur due to the presence of trace nucleophiles as impurities on the glass surface.[37]

It was initially proposed by Hasell and Chalker that the solvent-induced metathesis was a radical pathway. This hypothesis was put forth because TEMPO was found to inhibit the reaction. In the pervious study reported by Hasell and Chalker[22], the trisulfide metathesis was inhibited by 10 mol% TEMPO even after 24 h in solvents such as DMF. Shapter re-investigated the inhibition reaction by varying the amount of TEMPO. He found that TEMPO inhibition depends on the concentration of TEMPO where higher concentration of TEMPO leads to the greater inhibition. The inhibition mechanism by TEMPO could be explained via a radical-coupling process (Figure 1.11A).[51] A thiyl or perthiyl radical (RS• or RSS•), which could be generated from the reaction between the trisulfides and DMF, is trapped by TEMPO; thus, the inhibition occurs. With that said, GC-MS analysis of the reaction mixture showed only all starting materials: the trisulfides, DMF, and TEMPO (Figure 1.11B).

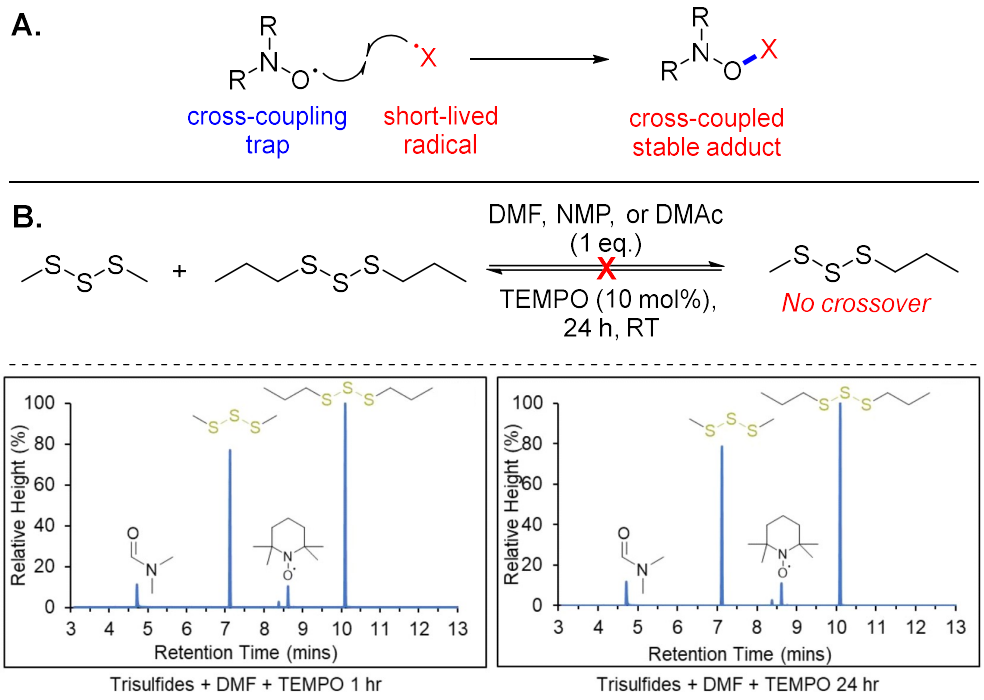

Figure 1.11: A. Radical-radical recombination to form a stable adduct. B. TEMPO radical inhibits the crossover reaction between the trisulfides in DMF, suggesting the reaction involves radical mechanism. The GC images were reproduced from ref. 22, under a Creative Commons Licence: CC-BY 4.0.

If the thiyl radical exists in the reaction mixture, a radical-radical recombination will occur between TEMPO ($R_2NO^•$) and thiyl/perthiyl radical ($RS^•$) could form an adduct (R_2NO-SR). Goldstein et al.[52] reported that the deprotonated form of this adduct was unstable and prone to decomposition via heterolysis of N-O bond to yield an amine (>NH) and sulfinic acid (RS(O)OH) while the protonated form of the adduct decomposes via homolysis of N-O bond to aminium radical ($>NH^{•+}$) and sulfenyl

radical ($RSO^{\bullet}$) which could produce an amine and sulfonic acid ($RS(O)_2OH$) in the presence of a thiol and nitroxide (Figure 1.12). They also reported that in physiological conditions the unstable adduct (>NO-SR) decomposes mainly to amine via heterolysis process. In the amide-trisulfides system, considering the mixture is neutral and if the adduct is formed it would not be decomposed or slightly decomposed if a small amount of water present. The adduct can, therefore, be analysed by either mass spectroscopy techniques or NMR spectroscopy.

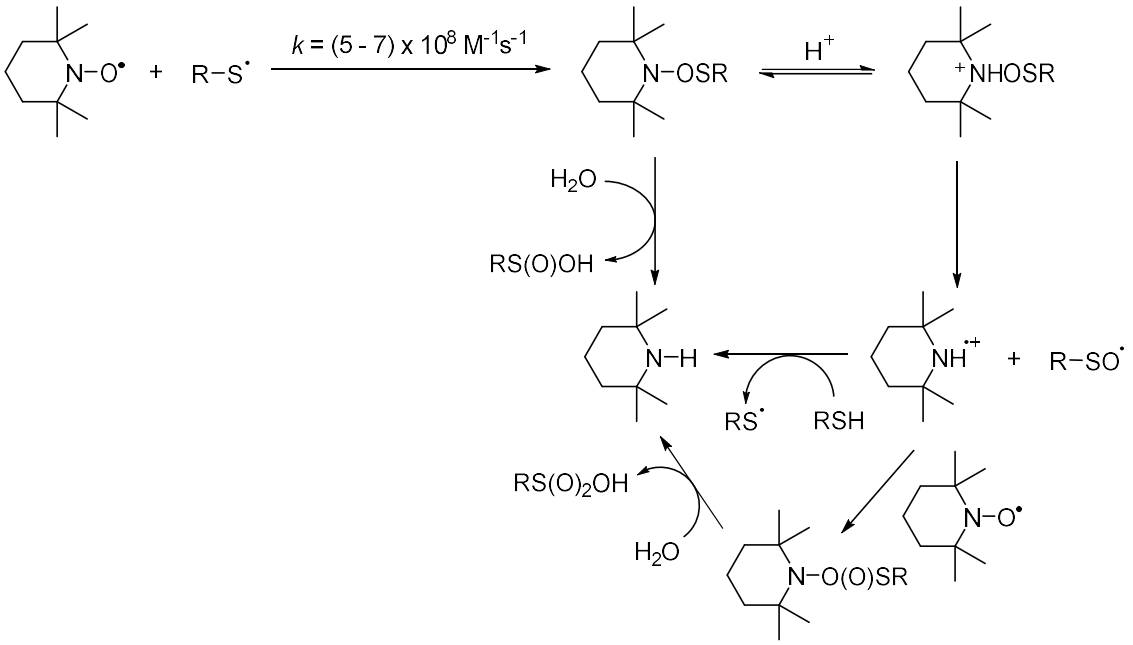

Figure 1.12: TEMPO recombination with a thiyl radical to form N-O-SR bond. This product can undergo decomposition in the presence of water and acid.[52]

The inhibition of trisulfide metathesis was also observed when in the presence of acetic acid. Shapter observed that the addition of 10 mol% of acetic acid does decrease the rate of the metathesis reaction, particularly in DMF (Figure 1.13).[27] The same reaction was also carried out in NMP and DMSO. The results showed that there is no significant change in the reaction rate compared to the normal reaction (without the addition of acid). Because reaction was analysed after 1 hour of the reaction, it is difficult to see how the reaction can significantly be influenced by the acid. Moreover, acetic acid can react with the trace of basic impurity such as amines which may present in the solvents. The metathesis reaction was found to still occur in the presence of acid which suggests that the reaction is not affected by the impurity.

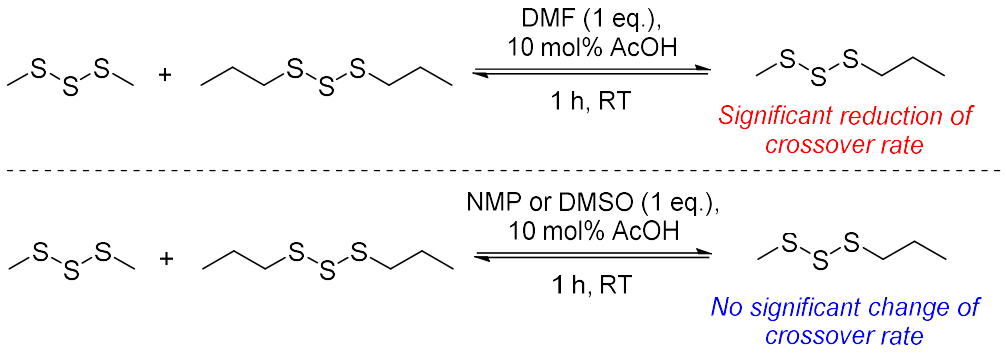

Figure 1.13: Trisulfide metathesis reaction in the presence of acetic acid.[27]

In these solvent-promoted trisulfide metathesis studies[22, 27], the focus was mainly to identify which solvents induce the metathesis reaction. The mechanisms by which this may occur are still unknown. The most puzzling feature of these studies is that TEMPO inhibits the S-S metathesis reaction, suggesting a radical mechanism. However, only trisulfides are formed (no disulfides and no tetrasulfides), which is difficult to explain if a radical process is involved. Furthermore, the limited scope of the trisulfides being studied in the previous works is also a barrier to fully understand this chemistry and the specific role of the solvent is not clear. Therefore, by studying the substrate scope, the effect of solvent polarity, and the inhibition by other small molecules, this thesis aims to provide insight into the scope and mechanism of this unusual reaction.

1.5 Solvents Effect in Chemical Reactions: Solvent Polarity and Trisulfide Metathesis

Solvents can affect chemical reactions in many different ways and influence the reaction rate, selectivity, and yield.[53] There are basically two approaches that can be used to understand the solvent effects: the phenomenological and physical approaches. The phenomenological approach is split into two aspects which are the dielectric and chemical considerations. Early understanding of the solvent effects invoked the term "*solvent polarity*", but this term is not always precisely defined.[54] Solvent polarity is often discussed in conjunction with dielectric constant. However, it is not always sufficient to correlate the solvent effects with solvent polarity based on the pure electrostatic approach (dielectric constant). It is because other aspects such as solute-solvent interactions such as intermolecular forces (i.e., Electron-Pair Acceptor (EPA) and Electron-Pair Donor (EPD), dipole-dipole, hydrogen bonding interactions) must be considered.[53, 55]

To quantify the solvent polarity based on the interaction between solute and solvent experimentally by spectroscopic measurements, empirical solvent polarity parameters are often used. There are several common solvent polarity parameters: Z-scale (Kosower), E_T (Dimroth-Reichardt), π^* (Dipolarity), α (Kamlet and Taft – Hydrogen Bond Donor Acidity), β (Kamlet and Taft – Hydrogen Bond Donor Basicity), AN (Acceptor Number, Gutman), and DN (Donor Number,

Gutman).[53, 54, 56] Among these solvent polarity parameters, Dimroth and Reichardt E_T (30) scale are the most widely studied and utilized solvent polarity. Z value, or E_T (molar transition energy) defined by Kosower, is a measurement of solvent polarity based on the shift of the longest-wavelength absorption band of 1-ethyl-4-(methoxycarbonyl)pyridinium iodide in the appropriate solvent. The E_T value is obtained from the formula in Equation 1. A high Z value corresponds to a high solvent polarity. For example, the Z value of MeOH (83.6 kcal/mol) is higher than dichloromethane (64.2 kcal/mol). Thus, methanol is more polar than dichloromethane.[57] Analogous to Z value, Dimroth and Reichardt[58, 59] established the E_T(30) which a molar electronic transition energy of Reichardt's dye (Betaine **1** or B30, Figure 1.14) and E_T^N value which is the dimensionless value derived from E_T(30) or absolute measured of solvent polarity. The value is also determined based on Equation 1. While Kosower Z value is more general to interpret the solvent polarity, E_T(30) value is specific to betaine dyes and has focus on dipolarity and hydrogen bonding interaction within solute-solvent. The E_T(30) and E_T^N value of selected organic solvents are shown in Table 1.3. From this table, we know that, for instance, acetonitrile is more polar than acetone.

$$E_T \text{ (kcal mol}^{-1}) = h.\ c.\ \nu.\ N_A = 2.859 \times 10^{-3} \text{ v/cm}^{-1} \equiv Z \qquad \text{Eq. 1}$$

where, h = Planck's constant (6.626×10^{-34} J s), c = the velocity of light (3×10^8 m s^{-1}), ν = the wavenumber of the photon, N_A = Avogadro's number (6.022×10^{22}).

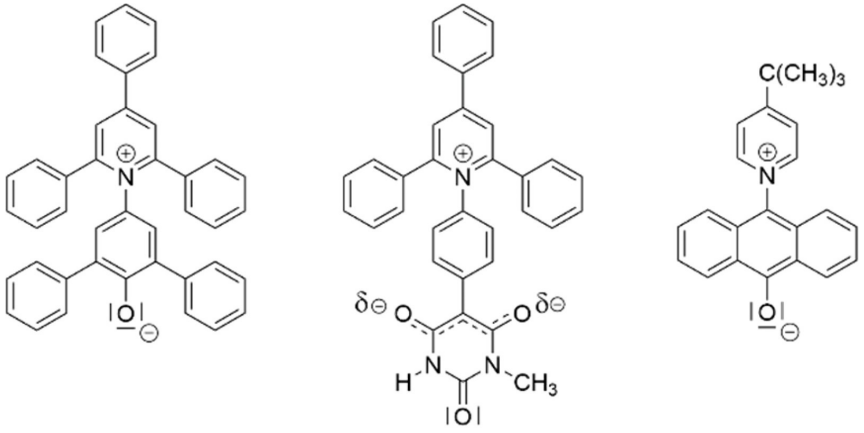

1 (= B30) **2** **3**

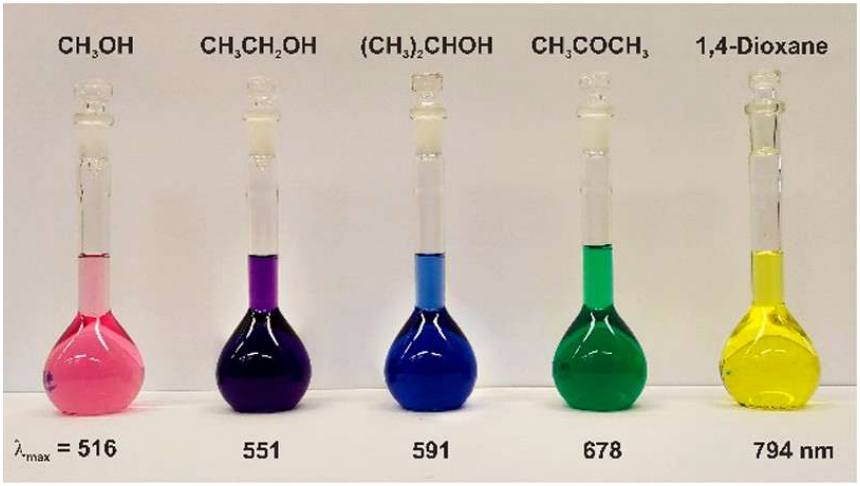

Figure 1.14: (Top) Three solvent sensitive betaine dyes used to study solvent polarity. E_T (30) value is obtained from the betaine **1** (B30). (Bottom) Colour changes and visible absorption maxima of the negatively solvatochromic betaine dye **1** (B30) dissolved in five solvents of increasing polarity: methanol (red), ethanol (violet), 2-propanol (blue), acetone (green), and 1,4-dioxane (yellow).[54, 60] This image was reproduced with permission from ref. 54. © 2021 American Chemical Society.

Table 1.3: E_T (30) and E_T^N value of selected organic solvents. Data was reproduced with permission from ref.55. Copyright © 2011 Wiley-VCH Verlag GmbH & Co. KGaA

Solvents	Protic/Aprotic	E_T (30)/(kcal mol^{-1})	E_T^N
Tetramethylsilane (TMS)	Aprotic	30.7	0.000
Cyclohexane	Aprotic	30.9	0.006
n-hexane	Aprotic	31.0	0.009
Triethylamine	Aprotic	32.1	0.043
Toluene	Aprotic	33.9	0.099
Diethyl ether	Aprotic	34.5	0.117
Chlorobenzene	Aprotic	36.8	0.188
Ethyl acetate	Aprotic	38.1	0.228
Chloroform	Aprotic	39.1	0.259
Pyridine	Aprotic	40.5	0.302
Dichloromethane	Aprotic	40.7	0.309
Nitrobenzene	Aprotic	41.2	0.324
Acetone	Aprotic	42.4	0.355
N,N-dimethylacetamide	Aprotic	42.9	0.377
N,N-dimethylformamide	Aprotic	43.2	0.386
tert-butanol	Protic	43.3	0.389
Dimethyl sulfoxide	Aprotic	45.1	0.444
Acetonitrile	Aprotic	45.6	0.460

2-propanol (isopropanol)	Protic	48.4	0.546
Acetic acid	Protic	51.7	0.648
Ethanol	Protic	51.9	0.654
Phenol	Protic	53.4	0.701
Methanol	Protic	55.4	0.762
Water	Protic	63.1	1.000

Polar solvents have been shown to influence the rate of reaction. For instance, Harpp and co-workers[26] demonstrated that desulfurization of an organic trisulfide by a phosphine catalyst improve in polar solvents (Table 1.2). This indeed was rationalized by the act of polar solvent in stabilising the charged intermediate (formation of the phosphonium ion). Furthermore, for nucleophilic reactions with anions such as a thiolate/disulfide metathesis (Figure 1.15), the reaction rate was greater in DMSO than in water.[61] The increase in the rate of reaction is due to better solvation of the charged delocalised polar activated complex by DMSO, which can lead to the decrease in the activation barrier.

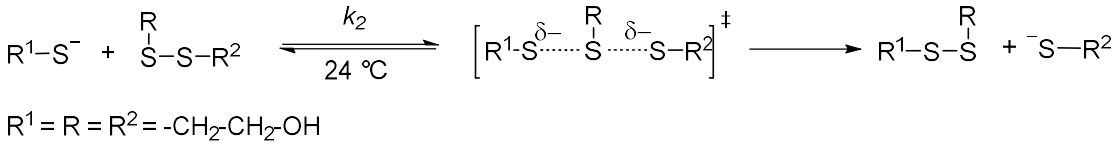

Figure 1.15: A thiolate/disulfide exchange reaction.[61]

Unlike many examples of disulfide metathesis reactions[62-65], the trisulfide metathesis reaction described here is unique in that it proceeds without the need of nucleophilic catalysts such as phosphines or amines.[25] From preliminary studies in the Chalker Lab, the trisulfide metathesis reaction generally takes place rapidly in polar aprotic solvents, while the reaction was found to be much slower in polar protic solvents. Figure 1.16 shows the solvents which have been tested for the trisulfide metathesis studies.[22, 27] Since this trisulfide metathesis is new, the role of solvents on this chemistry is poorly understood.

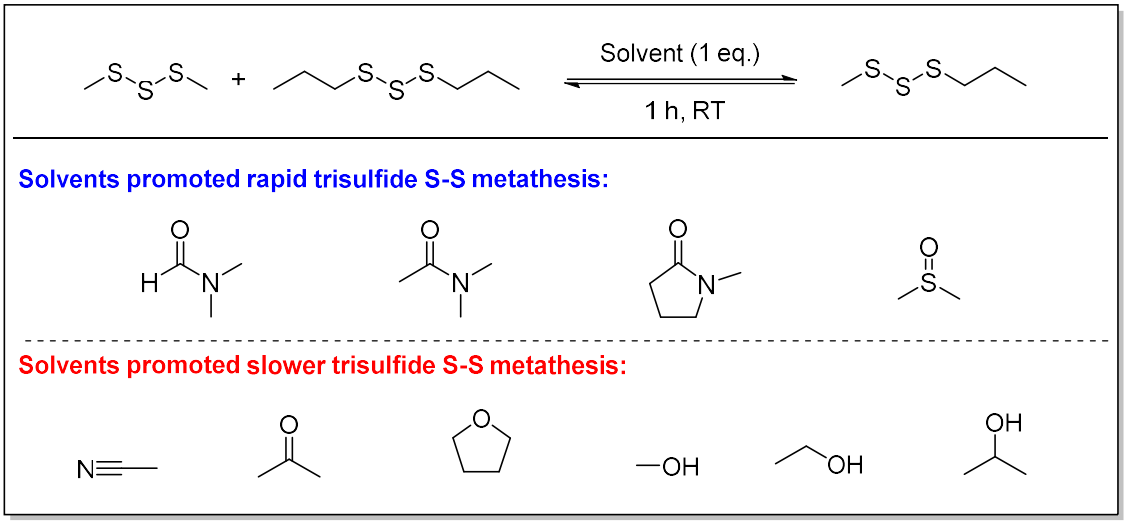

Figure 1.16: Various solvents tested for trisulfide metathesis from previous studies.[22, 27]

The influence of solvents on the trisulfide metathesis reaction is a critical aspect of understanding the fundamental mechanism of the reaction. Besides stabilizing polar transition states or intermediates generated in the reaction, polar aprotic solvents could also induce polarization in non-polar bonds such as S-S bond in a trisulfide molecule. This could result in weakening the S-S bond and induce a chemical reaction. Moreover, polar protic solvents such as alcohols could protonate the sulfur atom in a trisulfide and activate the charged sulfur species. However, the previously reported S-S metathesis showed that reaction in polar protic solvents such as alcohols is very slow compared to that of polar aprotic solvents such as DMF, NMP, and DMSO.[27] Lastly, the solute-solvent interaction could also occur between the lone pair electrons in sulfur atom of a trisulfide and the solvent. It has been discussed previously that compounds containing S-S bond such as di-, tri- and tetrasulfides may exist as thiosulfoxide, (a branch structure).[37, 66-69] Theoretical studies by Steudel have indicated that thiosulfoxide is highly polar (Figure 1.17).[70] Thus, this species should be stabilized in polar solvents. The sulfur atoms in the trisulfide could interact with the solvent and undergo rearrangement to form this polar species. This species could then participate in the trisulfide metathesis reaction. However, the mechanism on how solvents participate in the S-S exchange is unknown. The area of this research is still developing.

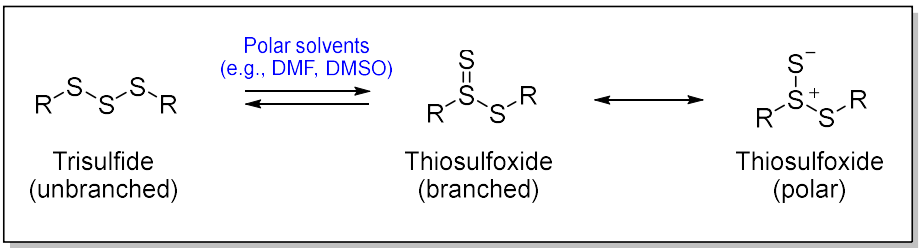

Figure 1.17: Polar solvents may interact with a trisulfide to form a highly polar thiosulfoxide, which are intermediates considered in this thesis.

1.6 Synthesis of Organic Trisulfides and Tetrasulfides

This section provides a review on the synthesis of organic trisulfides via several methods. The discussions on the synthesis of organic trisulfides and tetrasulfides have been recently reviewed by Ali and co-workers.[71] In this discussion, several trisulfide synthesis methodologies are presented. The main purpose of this review is to provide readers with simplest and most general ways to access organic trisulfides. The following methods for synthesizing organic trisulfides are discussed: (1) Direct synthesis from a thiol and sulfur dichloride, (2), Direct synthesis from a thiol and a sulfur transfer reagent, and (3) A two-step process from an alkyl halide via thiosulfate salt (Bunte salt). The reaction between a thiol and sulfur monochloride (S_2Cl_2) will be discussed for a tetrasulfide synthesis.

Direct Trisulfide Synthesis from A thiol and Sulfur Dichloride

Organic trisulfides can be quickly prepared using a direct synthetic method employing a thiol (R-SH) and sulfur dichloride (SCl_2). A general reaction scheme is shown in Figure 1.18. Two equivalents of thiol are required for this synthesis. This synthesis is first demonstrated by Clayton and Etzler in 1947 where they prepared hexadecyl trisulfide in a fair yield (~60%). This first demonstration of trisulfide synthesis was experimentally done in petroleum ether solution employing sulfur dichloride and the corresponding hexadecyl thiol. This reaction is exothermic, with the temperature of the mixture rising from 17 to 27 °C after the addition of sulfur dichloride. Hydrogen chloride gas is a by-product of this reaction.

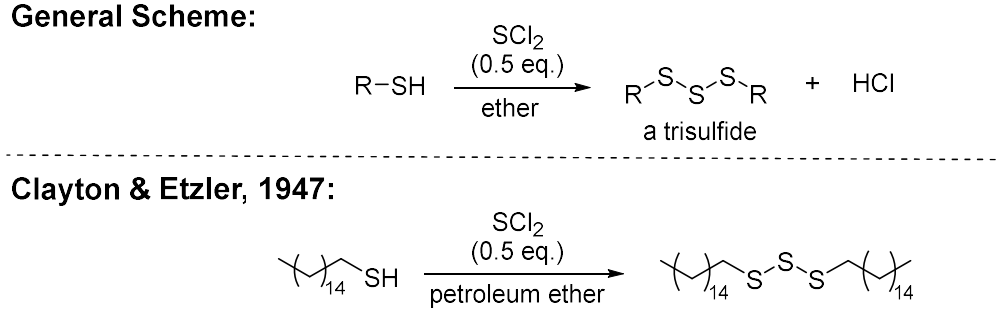

Figure 1.18: A general scheme for the trisulfide synthesis from a thiol and sulfur dichloride.

In 1994, Derbessy and Harpp[72] further developed this trisulfide synthesis method by altering the reaction conditions. The reaction was set to a low temperature (-78°C, dry ice/acetone bath) and a tertiary amine (i.e., Et_3N, pyridine) was used to neutralize the resulting hydrochloric acid. The reaction is relatively quick (typically complete within 3 h). At low temperatures, the first reaction between a thiol and sulfur dichloride would provide an intermediate alkyl thiosulfenyl chloride (or alkyl chlorodisulfide). This reactive intermediate can react in the second step with another thiol molecule *in situ* to produce a trisulfide. This method improves the yield and purity of the resulting trisulfide. For instance, Derbessy and Harpp[72] reported that the synthesis of various symmetrical trisulfides can be achieved with the yield typically > 94%, except for diallyl trisulfide which is only

46% (Figure 1.19). Unsymmetrical trisulfides can also be prepared using this procedure, although several of them are obtained in moderate yield. The low yield of diallyl trisulfide is because sulfur dichloride (SCl_2) and sulfur monochloride (S_2Cl_2) can react with alkenes to form episulfonium intermediate.[73, 74] Indeed, copolymerization of sulfur monochloride with polyenes has recently been reported as an alternative to inverse vulcanization.[75]

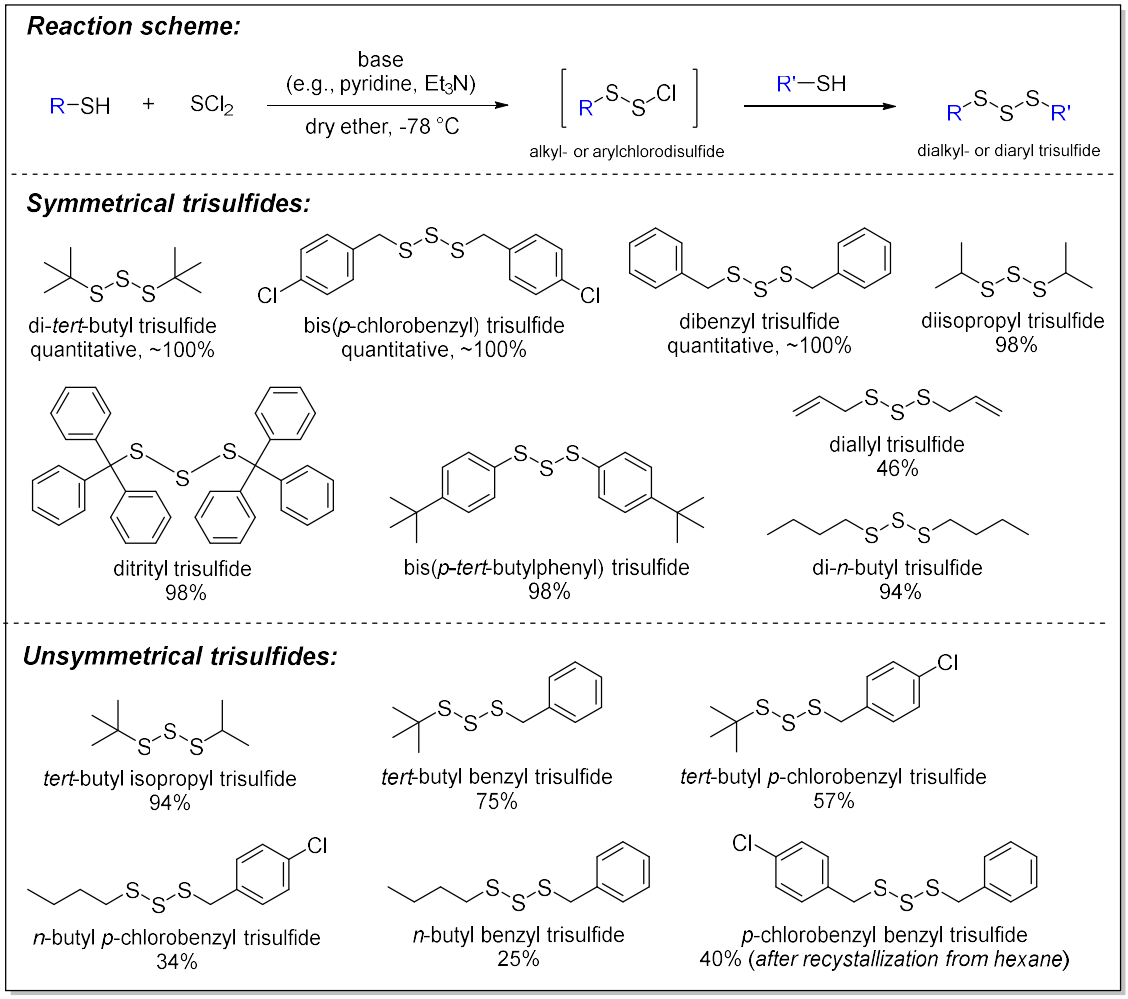

Figure 1.19: Examples of various symmetrical trisulfide prepared from a thiol and sulfur dichloride using Harpp's method.[72] Yields for the synthesis of symmetrical trisulfides are generally excellent.

In general, this method is operationally simple. However, there are several disadvantages of using sulfur dichloride. First, sulfur dichloride is relatively unstable at room temperature and undergoes decomposition to other sulfur chlorides, chlorine gas, and elemental sulfur.[76-78] For this reason, it is best to use freshly distilled sulfur dichloride. The addition of phosphorus trichloride (PCl_3)[79] or phosphorus pentachloride (PCl_5)[80] to this sulfur dichloride aims to prevent decomposition during distillation. However, this process does not inhibit the decomposition for a long period of time.[79] Therefore, freshly distilled sulfur dichloride should be used soon after purification. The synthesis of sulfur chlorides (SCl_2 and S_2Cl_2) is provided in more detail in Chapter 2 of this Thesis.

If sulfur dichloride is heavily contaminated with other decomposition products such as sulfur monochloride, for instance, this sulfur dichloride reaction with a thiol can result in the formation of polysulfides (Figure 1.20).[66, 78] Indeed, this issue can cause significant inconvenience because organic polysulfides can be difficult to separate by column chromatography due to the similar polarity. Second, due to its high reactivity, sulfur dichloride may not be suitable for making linear alkyl trisulfides containing alkene group (i.e., diallyl trisulfide[72]) or cyclic trisulfides such as trithiane.[81, 82] The reactions could give low yield or a mixture of di-, tetra-, or pentasulfide.

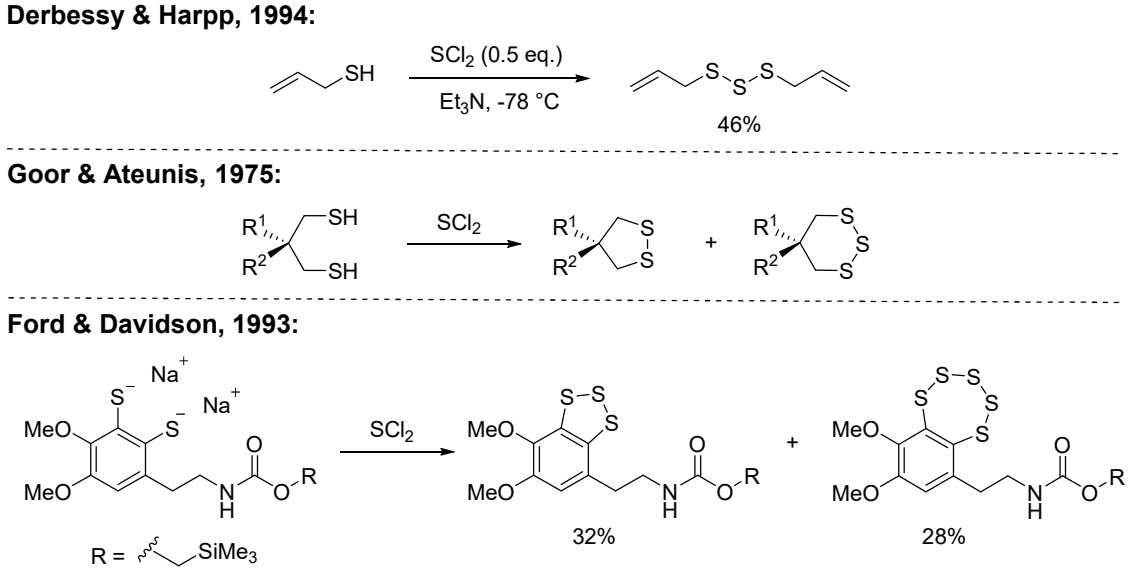

Figure 1.20: Sulfur dichloride (SCl_2) could give a mixture of polysulfides.

Direct Trisulfide Synthesis from a Thiol and a Monosulfur Transfer Reagent

Because sulfur dichloride is unstable at room temperature and not easy to handle, the synthesis of organic trisulfides can alternatively be achieved via reaction between a thiol and a sulfur transfer reagent with nitrogen heterocycles as a leaving group.[78, 83] One example of stable sulfur transfer reagent is *N,N'*-thiobisphthalimide. However, this monosulfur transfer reagent possesses lower reactivity compared to sulfur dichloride, which can be a disadvantage. In a study by Harpp and co-workers[78] reported that an attempt to prepare cyclic trisulfides using *N,N'*-thiobisphthalimide was not successful.

The sulfur transfer reagents shown in Figure 1.22 can be synthesized from hexamethyldisilazane (HMDS) with the nitrogen heterocycles. The silylated of heterocycles are then treated with a half equivalent of sulfur dichloride to obtain the sulfur transfer reagents (Figure 1.21).[78] *N,N'*-thiobisphthalimide can also be prepared from sulfur monochloride (S_2Cl_2) and phthalimide (Figure 1.21). Kalnins[84] demonstrated that phthalimide or its potassium salt in dry DMF reacts very readily with sulfur monochloride to give *N,N'*-thiobisphthalimide as a white solid with the melting point of 315 – 317 °C. *N,N'*-thiobisphthalimide can alternatively be obtained from the reaction between

potassium phthalimide and sulfur dichloride in dry petroleum ether as a solvent. However, owing to its stability sulfur monochloride is much more preferable reagent to use than sulfur dichloride for the synthesis of *N,N'*-thiobisphthalimide. To date, the most commonly method to prepare *N,N'*-thiobisphthalimide is a reaction between phthalimide and sulfur monochloride in dry DMF.

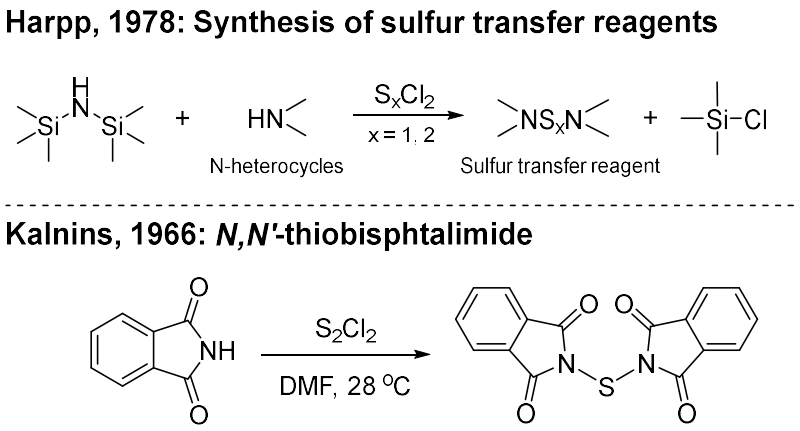

Figure 1.21: Synthesis of sulfur transfer reagents from N-heterocycle compounds and sulfur chlorides. Harpp's method can also be used to prepare *N,N'*-dithiobis compounds.

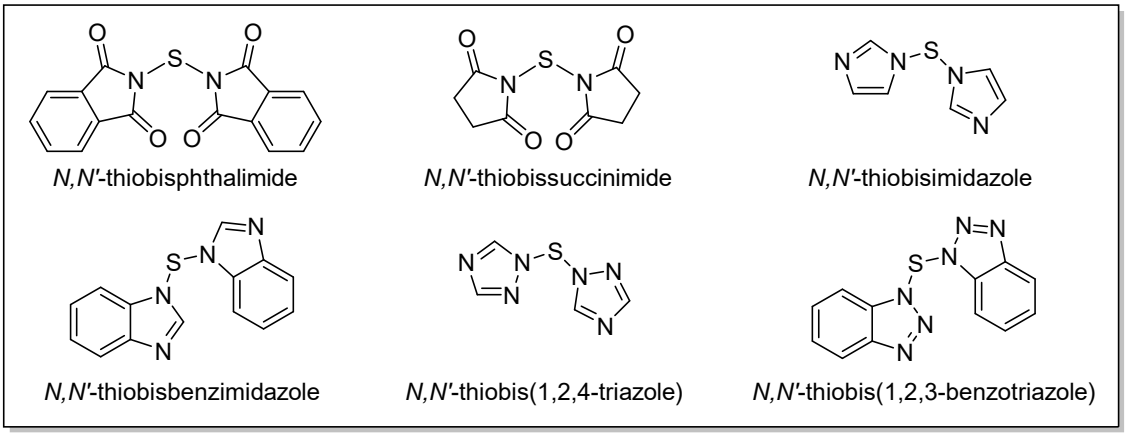

Figure 1.22: Several sulfur transfer reagents with N-heterocycles.[78]

The reactivity toward nucleophiles of sulfur transfer reagents shown in Figure 1.22 above has been qualitatively assessed by Harpp and co-workers.[78] The order of reactivity for these reagents are as follow: imidazole > 1,2,4-triazole > benzimidazole > 1,2,3-benzotriazole > succinimide > phthalimide. All of these reagents can transform benzyl thiol to dibenzyl trisulfide in good to excellent yields (> 84%), which is far superior to *N,N'*-thiobisphthalimide (27%). Due to its low reactivity, the reaction involving *N,N'*-thiobisphthalimide is often carried out under reflux. In terms of the mechanism, the authors suggested that the first step involves a protonation of these sulfur transfer reagents, followed by a nucleophilic attack from the thiolate (Figure 1.23A).[78] The synthesis of dibenzyl and diallyl trisulfide are shown in Figure 1.23B.

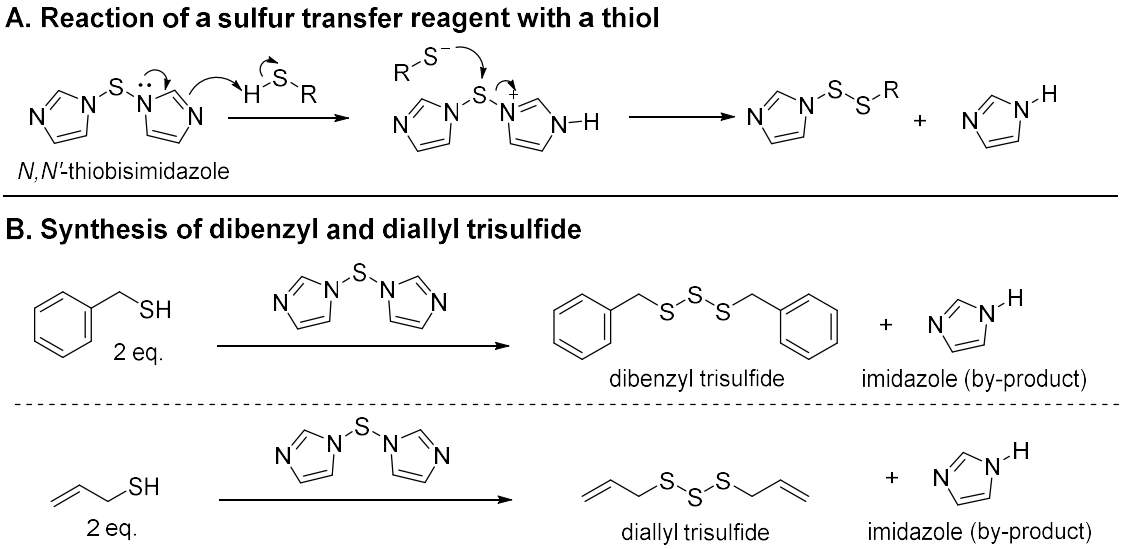

Figure 1.23: A. A proposed mechanism of protonation of a sulfur transfer reagent and nucleophilic attack to the sulfur atom by thiolate. B. Synthesis of dibenzyl trisulfide using *N,N'*-thiobisimidazole.

The use of sulfur transfer reagents in the synthesis of organic trisulfides offers several advantages. First, it allows the synthesis of trisulfides containing functional groups such as alkene. In contrast to the use of sulfur dichloride, *N,N'*-thiobisimidazole reacts with allyl thiol to give diallyl trisulfide in a very good yield (80%).[85] The use of sulfur transfer reagents can effectively improve the synthesis of trisulfide containing functional groups which cannot be tolerated by sulfur dichloride. Second, the synthesis of trisulfides employing the monosulfur azole reagents (Figure 1.22) is relatively quick, where the reaction is complete within few minutes. Only *N,N'*-thiobisphthalimide is less reactive in which the reaction can be controlled until a monosubstitution stage. This, however, can be an advantage especially for the synthesis of unsymmetrical trisulfide.[86, 87] Lastly, the N-heterocycle compound as the by- product of the reaction between the sulfur transfer reagent and a thiol can be reused. For instance, in Figure 1.23B the by-product imidazole from the reaction can be isolated and reused to make the sulfur transfer reagent by reacting them with HDMS and sulfur chlorides.

Trisulfide Synthesis from an Alkyl Halide via Sodium *S*-Alkyl Thiosulfate Salt

Another strategy to access an organic trisulfide is via Bunte salt or sodium *S*-alkyl thiosulfate ($RSSO_3^-Na^+$). A Bunte salt is prepared from the reaction between an alkyl halide (R-X) and sodium thiosulfate ($Na_2S_2O_3$) via an S_N2 reaction. In a report by Lecher and Hardy[88], thallium(I) thiosulfate can also be used in place of sodium thiosulfate. In the original method reported by Bunte[89], the salt is obtained by heating an aqueous solution of sodium thiosulfate and alkyl halides (Figure 1.24, the first reaction). This method becomes a general method for the preparation of sodium *S*-alkyl thiosulfate. In the synthesis of this salt, aqueous methanol, ethanol, dioxane, and DMSO are

commonly used.[90, 91] Various methods for making the salt such as from disulfides and alkali metal bisulfites, from thiols and alkali metal sulfites, chlorosulfonic acid, sulfur trioxide, sulfur trioxide-pyridine complexes, and so on, had been reviewed by Distler.[90] Moreover, the reaction of sodium *S*-alkyl thiosulfate salt with sodium sulfide leads to the formation of organic trisulfides (Figure 1.24, the second reaction).

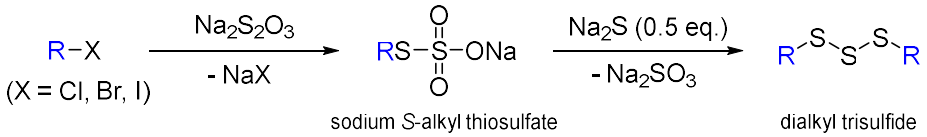

Figure 1.24: A synthetic route to make a trisulfide via sodium *S*-alkyl thiosulfate (Bunte Salt).

Upon addition of sodium sulfide to a solution of sodium *S*-alkyl thiosulfate, the target trisulfide is formed. However, sodium sulfite is also produced in this reaction. Sulfite is found to react with organic trisulfide to give a disulfide. Milligan and co-workers[92] demonstrated that the reaction between dimethyl trisulfide and sodium sulfite at pH ~8 results in the formation of dimethyl disulfide (Figure 1.25A). In a case of dimethyl trisulfide synthesis from sodium *S*-methyl thiosulfate and sodium sulfide, Milligan and co-workers[92] found that the molar ratio between dimethyl disulfide and trisulfide was 3 : 2. Dimethyl trisulfide was found to be relatively soluble in water compared to the higher dialkyl trisulfides. In comparison, solubility of dimethyl trisulfide in water (0.025%) was ten times higher than that of diethyl trisulfide.[92] This was thought to be the cause of low trisulfide ratio because the sulfite can react with dimethyl trisulfide and yield the corresponding disulfide. Later, Milligan and co-workers then found that the addition of light petroleum, which extracts the trisulfide, and saturating the mixture with sodium chloride, which decreases the solubility of the trisulfide in water, could increase the yield of trisulfide over disulfide. They also found that combination of these techniques does not significantly improve the trisulfide yield.

These approaches only minimize the formation of disulfide by removing the trisulfide from aqueous phase, and so it does not remove the main problem, the sulfite anions. The removal of sulfite anions can be achieved through the addition of formaldehyde.[93, 94] Thus, Milligan and co-workers[92] then explored the synthesis of trisulfides by using of formaldehyde in phosphate buffer solution at pH around 8. Sodium sulfite reacts with formaldehyde to form a stable adduct, sodium formaldehyde bisulfite ($HOCH_2$-$NaSO_3$).[95] By doing so, the sulfite is chemically removed from the solution. The addition of formaldehyde solution to the mixture of sodium *S*-alkyl thiosulfate and sodium sulfide improve the trisulfide synthesis significantly. Milligan and co-workers reported that disulfide formation could be supressed by the addition of formaldehyde (Figure 1.25B). Acetaldehyde in place of formaldehyde also gave similar result.[92] The use of paraformaldehyde or other aldehydes in the synthesis has not been reported yet in the literature. Thus, this can be an alternative additive to formaldehyde.

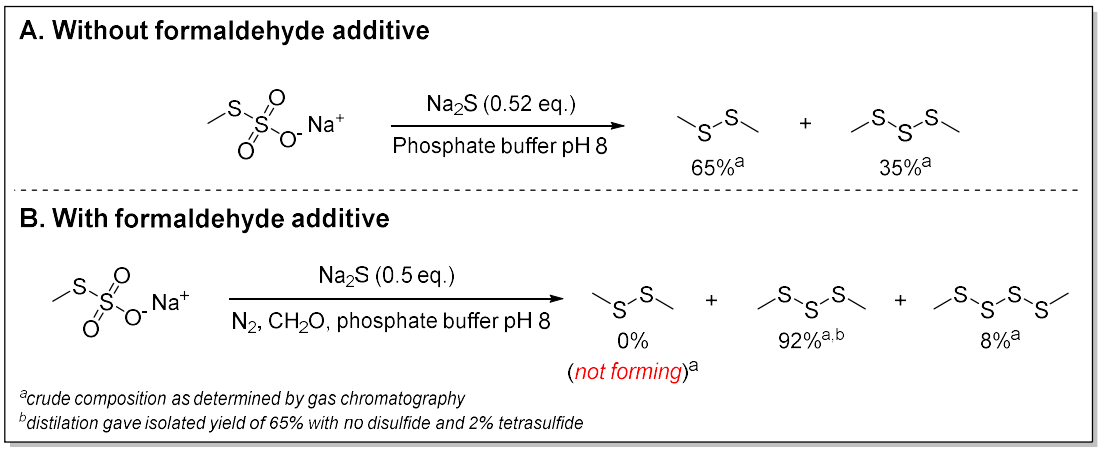

Figure 1.25: Examples of the synthesis of dimethyl trisulfide from its sodium *S*-methyl thiosulfate (A) without and (B) with formaldehyde additive reported by Milligan and co-workers.[92]

Besides formaldehyde, altering the reaction temperature and selecting the right solvent are other way to improve the synthesis of trisulfide. Bhattacherjee and coworkers[96] recently reported the optimization process for synthesis organic trisulfide via Bunte salt and sodium sulfide by altering the temperature and solvent. Water was found to be the best solvent for the synthesis of trisulfide. In addition, maintaining the reaction temperature to 0 °C is also the key to a successful synthesis of trisulfides. Excess sodium sulfide (Entry 3, Figure 1.26) and higher temperature reaction at 80 °C (Entry 8, Figure 1.26) can lead to the significant formation of disulfide. The best reaction conditions for the synthesis of trisulfide were achieved when 0.5 equivalent of sodium sulfide was employed and the reaction temperature was maintained at 0 °C for 8 hours.

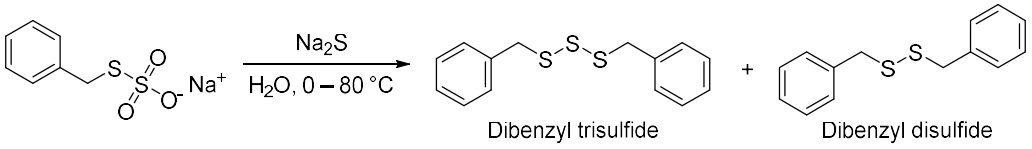

Entry	Na_2S (eq.)	Temp. (°C)	Time (h)	Yield Trisulfide (%)*	Yield Disulfide (%)*
1	0.5	RT	24	59	7
2	1.0	RT	24	27	6
3	3.0	RT	24	37	21
4	0.5	RT	4	61	5
5	0.5	RT	8	70	6
6	***0.5***	***0***	***8***	***77***	***1***
7	0.5	0	12	68	2
8	0.5	80	4	41	27

**yield was calculated from the peak intensity of benzylic proton (-S-CH_2-) of a product mixture in ^{1}H NMR*

Figure 1.26: Optimization process for the synthesis of dibenzyl trisulfide from sodium *S*-benzyl thiosulfate and sodium sulfide reported by Bhattacherjee and coworkers.[96] Data was reproduced with permission from ref. 96. © 2019 Royal Society of Chemistry; permission conveyed through Copyright Clearance Center, Inc.

One of the advantages of this synthetic strategy for the synthesis of organic trisulfides is the use of inexpensive reagents such as alkyl halides and sodium thiosulfate via Bunte salt. More importantly, unlike sulfur dichloride this method tolerates alkene functional group. Therefore, the synthesis of organic trisulfide containing allyl group, which is reactive to sulfur dichloride, become possible via Bunte salt chemistry with sodium sulfide.[92, 96] Milligan and co-workers reported the synthesis of diallyl trisulfide containing only 2% of diallyl disulfide (Figure 1.27). The synthesis of Bunte salt containing propargyl group has been reported previously in the literature.[91] Yet, no report on the synthesis of dipropargyl trisulfide has been made using this chemistry.

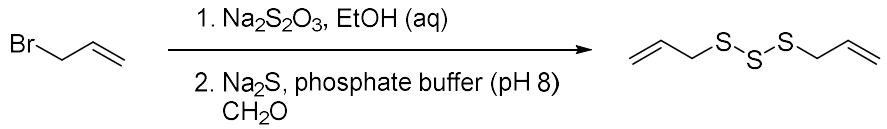

Figure 1.27: Diallyl trisulfide synthesis of via sodium *S*-allyl thiosulfate and sodium sulfide.[92]

Drawbacks of making trisulfide using this method include longer reaction times, multiple steps, and limited scope for hindered substrates. Additionally, the preparation of the *S*-alkyl thiosulfate from the alkyl halide can take several hours. The salt is often purified by alcohol extraction prior to the next step.[96]

All in all, each synthetic strategy for making trisulfide can be chosen after considering the reactivity and availability of the starting materials. For example, it requires additional precautions when using a thiol in the trisulfide synthesis because molecular oxygen can oxidise thiol to a disulfide. Consequently, reaction should be carried out under inert atmosphere (i.e., N_2 or Argon). Hindered trisulfides such as di-*tert*-butyl trisulfide can be obtained via sulfur dichloride but it cannot be obtained from Bunte salt chemistry. The use of sulfur transfer reagents-based N-heterocycle compounds such as *N,N'*-thiobisimidazole and *N,N'*-thiobisphthalimide can also be an alternative to sulfur dichloride.

Direct Tetrasulfide Synthesis from a thiol and Sulfur Monochloride

Organic tetrasulfides are typically prepared from the reaction between a thiol (R-SH) and sulfur monochloride (S_2Cl_2). This reaction is practically simple and unlike sulfur dichloride (SCl_2), sulfur monochloride is relatively stable. In 1932, Chakravarti[97] first reported the synthesis of several organic tetrasulfides such as diethyl, diphenyl, and dibenzyl tetrasulfide. The process involves treatment of an alcoholic caustic potash solution of thiol with sulfur monochloride. Extraction with ether, followed by solvent removal was carried out to afford the tetrasulfide (Figure 1.28A). The synthesis method was developed by Harpp and co-workers for the general synthesis of symmetrical organic tetrasulfides.[72, 98] The method involves the use of amine and reaction at low temperature (-78 °C) (Figure 1.28B). Ramaraju and coworkers[99] also reported the synthesis of organic tetrasulfides (Figure 1.28C). Dichloromethane was used as a solvent and the temperature was relatively higher

(~20 °C to room temperature). Figure 1.29 shows several examples of tetrasulfides prepared from a thiol and sulfur monochloride.

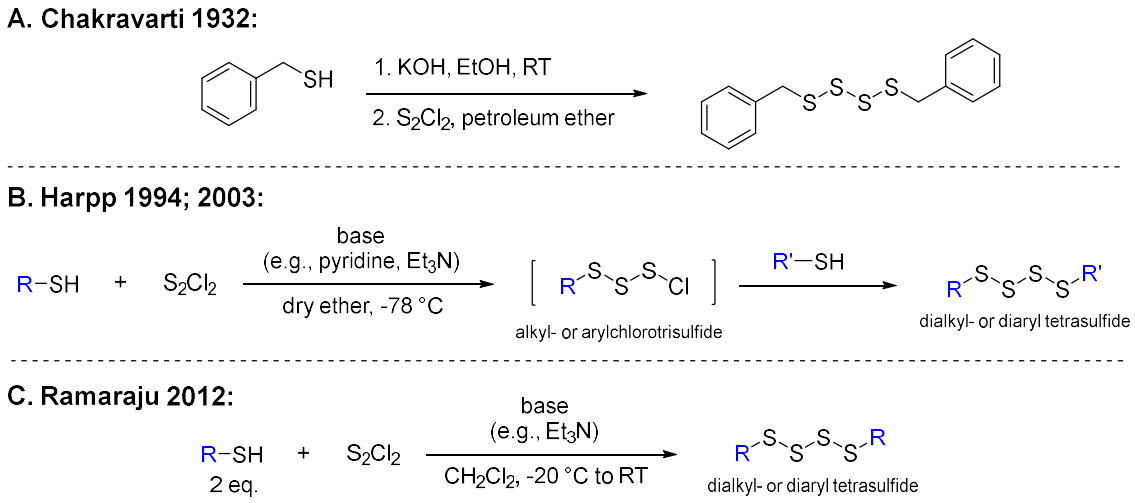

Figure 1.28: A. An example of dibenzyl tetrasulfide synthesis reported by Chakravarti.[97] A general scheme for the tetrasulfide synthesis developed by: B. Harpp and co-workers.[72, 80] and C. Ramaraju and co-workers.[99]

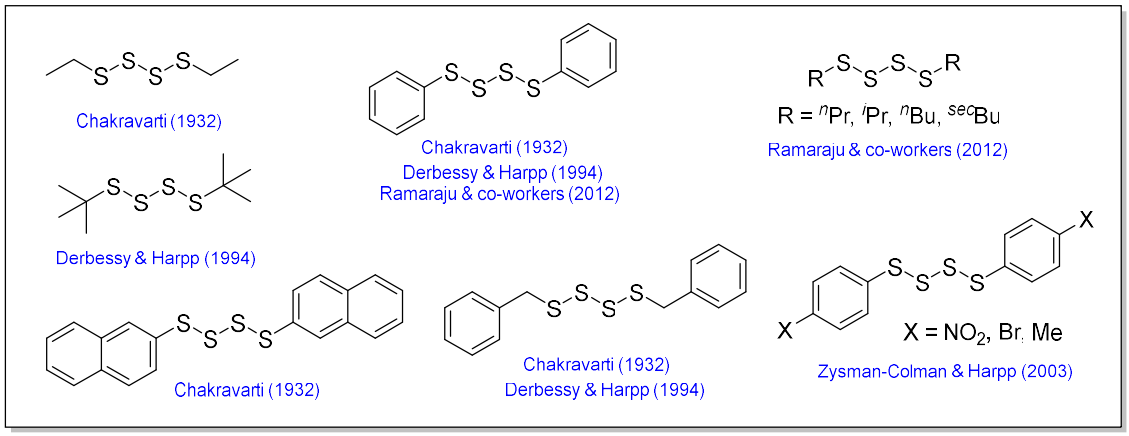

Figure 1.29: Several examples of organic tetrasulfides prepared from the reaction between a thiol and sulfur monochloride.

1.7 Thesis Objectives

The general goal of this thesis is to understand the reaction mechanism of the trisulfide metathesis induced by the polar aprotic solvents, particularly DMF. With this understanding, this chemistry can provide new tools for synthetic chemistry methodologies, polymer synthesis, recycling, and depolymerisation under mild conditions.

In Chapter 2, the syntheses of various organic trisulfides and tetrasulfides are reported. With the limited understanding on the effect of different substituents (R group) of trisulfides on the metathesis reaction induced by DMF, various trisulfides containing primary, secondary, and tertiary alkyl groups were made and used in the metathesis reaction in DMF. In addition to this, several organic tetrasulfides are reported and used to investigate the tetrasulfide metathesis to see how it compares to the corresponding trisulfide. Disulfides were obtained commercially. All metathesis studies involving di-, tri-, and tetrasulfides are reported in Chapter 3. To access those trisulfides, we reported various trisulfide synthetic methods: 1) a trisulfide from thiosulfoxide salt (Bunte salt) and sodium sulfide, 2) a trisulfide from a thiol and sulfur dichloride (SCl_2), and 3) a trisulfide from a thiol and *N,N'*-thiobisphthalimide (a monosulfur transfer reagent). All tetrasulfides were prepared using a thiol and sulfur monochloride (S_2Cl_2). In the synthesis of trisulfides via Bunte salt chemistry, we explored the use of paraformaldehyde to improve the synthesis process. Several new trisulfides (i.e., diisobutyl trisulfide, di-*n*-hexyl trisulfide, and bis(4-methoxybenzyl) trisulfide) are reported for the first time in this Chapter.

In Chapter 3, the effect of various solvents on the trisulfide metathesis between dimethyl trisulfide and di-*n*-propyl trisulfide are reported. This study aims to evaluate how solvents with different polarity influence the rate of trisulfide metathesis. Examples of trisulfide metathesis are also demonstrated in a binary solvent system (e.g., DMF and chlorobenzene). The S-S metathesis study between dimethyl trisulfide and various trisulfides made in Chapter 2 is presented. In a special case study, S-S metathesis reaction involving a cyclic trisulfide, norbornane trisulfide, is demonstrated. This Chapter also discusses several applications of this metathesis chemistry for the preparation of unsymmetrical trisulfide directly from two symmetrical trisulfides, the production of trisulfide-based dynamic combinatorial library, and the late-stage modification of a complex natural product containing trisulfide moiety (i.e., calicheamicin-γ_1). In the last section of this Chapter, the investigation of disulfide and tetrasulfide metathesis are presented. The goal of this study was to understand the reactivity of disulfides and tetrasulfides and how they compare or differ to the key trisulfide substrates of interest.

Chapter 4 describes the mechanistic investigations of trisulfide metathesis. Several mechanistic proposals involving radical, ionic, and thiosulfoxide intermediate were proposed. Several key experiments were conducted to find evidence for or against these mechanistic hypotheses. For instance, Electron Paramagnetic Resonance (EPR) spectroscopy experiments were carried out to obtain determine whether or not thiyl radical signals are present in the trisulfide metathesis. NMR spectroscopy experiments to identify the presence of possible intermediates. This

chapter also presents trapping experiments to sequester putative thiyl or thiolate intermediates. The reaction between a thiolate and trisulfide, or a trisulfide in the presence of UV light, are also studied to assess the product distributions of these ionic or radical processes, respectively. The overall aims of these key experiments were to rule out some proposed mechanisms and determine the underlying process. Moreover, TEMPO is not the only molecule that can inhibit the trisulfide metathesis reaction, other small molecules such as acids, dienophiles (i.e., maleic anhydride and benzoquinone), and water can also inhibit the metathesis reaction. The metathesis inhibition is also discussed in this Chapter. Finally, a proposed mechanism via a thiosulfoxide intermediate is discussed in this Chapter. Until now, the thiosulfoxide intermediate is not directly observed and reported. Future investigations, theoretically and experimentally, are suggested in order to successfully characterise the intermediate and to understand the reaction behaviour of trisulfide metathesis.

The ultimate goal of this Thesis is for us to be able to use the trisulfide metathesis chemistry for broader applications. The dynamic nature of the S-S metathesis, for instance, was applied to a novel dynamic library synthesis of trisulfides. The reaction is also rapid and selective, providing a method to modify therapeutic trisulfides. The reversibility of the reaction was also proposed for use in polymerization and depolymerization of novel poly(trisulfide)s. Discussion on the future research regarding this chemistry is presented in Chapter 5.

1.8 References

(1) U. S. Geological Survey. *Mineral commodity summaries 2024*; Reston, Virginia, 2024. DOI: 10.3133/mcs2024.

(2) Nguyen, T. B. Recent advances in organic reactions involving elemental sulfur. *Adv. Synth. Catal.* **2017**, *359* (7), 1066-1130. DOI: 10.1002/adsc.201601329.

(3) Scott, K. A.; Njardarson, J. T. Analysis of US FDA-Approved Drugs Containing Sulfur Atoms. In *Sulfur Chemistry*, Jiang, X. Ed.; Springer International Publishing, 2019; pp 1-34.

(4) Pluth, M. D.; Bailey, T. S.; Hammers, M. D.; Hartle, M. D.; Henthorn, H. A.; Steiger, A. K. Natural products containing hydrogen sulfide releasing moieties. *Synlett* **2015**, *26* (19), 2633-2643. DOI: 10.1055/s-0035-1560638

(5) Chung, W. J.; Griebel, J. J.; Kim, E. T.; Yoon, H.; Simmonds, A. G.; Ji, H. J.; Dirlam, P. T.; Glass, R. S.; Wie, J. J.; Nguyen, N. A.; et al. The use of elemental sulfur as an alternative feedstock for polymeric materials. *Nat. Chem.* **2013**, *5* (6), 518-524. DOI: 10.1038/nchem.1624.

(6) Wang, D.-Y.; Guo, W.; Fu, Y. Organosulfides: An Emerging Class of Cathode Materials for Rechargeable Lithium Batteries. *Acc. Chem. Res.* **2019**, *52* (8), 2290-2300. DOI: 10.1021/acs.accounts.9b00231.

(7) Gu, S.; Jin, J.; Zhuo, S.; Qian, R.; Wen, Z. Organic Polysulfides Based on −S−S−S− Structure as Additives or Cosolvents for High Performance Lithium-Sulfur Batteries. *ChemElectroChem* **2018**, *5* (13), 1717-1723. DOI: 10.1002/celc.201800196.

(8) Chalker, J. M.; Mann, M.; Worthington, M. J. H.; Esdaile, L. J. Polymers Made by Inverse Vulcanization for Use as Mercury Sorbents. *Org. Mater.* **2021**, *03* (02), 362-373. DOI: 10.1055/a-1502-2611.

(9) Lundquist, N. A.; Chalker, J. M. Confining a spent lead sorbent in a polymer made by inverse vulcanization prevents leaching. *Sustain. Mater. Technol.* **2020**, *26*, e00222. DOI: 10.1016/j.susmat.2020.e00222.

(10) Eder, M. L.; Call, C. B.; Jenkins, C. L. Utilizing Reclaimed Petroleum Waste to Synthesize Water-Soluble Polysulfides for Selective Heavy Metal Binding and Detection. *ACS Appl. Polym. Mater.* **2022**, *4* (2), 1110-1116. DOI: 10.1021/acsapm.1c01536.

(11) Worthington, M. J. H.; Shearer, C. J.; Esdaile, L. J.; Campbell, J. A.; Gibson, C. T.; Legg, S. K.; Yin, Y.; Lundquist, N. A.; Gascooke, J. R.; Albuquerque, I. S.; et al. Sustainable polysulfides for oil spill remediation: repurposing industrial waste for environmental benefit. *Adv. Sustain. Syst.* **2018**, *2* (6), 1800024. DOI: 10.1002/adsu.201800024.

(12) Deng, Z.; Hoefling, A.; Théato, P.; Lienkamp, K. Surface Properties and Antimicrobial Activity of Poly(sulfur-co-1,3-diisopropenylbenzene) Copolymers. *Macromol. Chem. Phys.* **2018**, *219* (5), 1700497. DOI: 10.1002/macp.201700497.

(13) Tonkin, S. J.; Pham, L. N.; Gascooke, J. R.; Johnston, M. R.; Coote, M. L.; Gibson, C. T.; Chalker, J. M. Thermal Imaging and Clandestine Surveillance using Low-Cost Polymers with Long-Wave Infrared Transparency. *Adv. Opt. Mater.* **2023**, *11* (16), 2300058. DOI: 10.1002/adom.202300058.

(14) Pyun, J.; Norwood, R. A. Infrared plastic optics and photonic devices using chalcogenide hybrid inorganic/organic polymers via inverse vulcanization of elemental sulfur. *Prog. Polym. Sci.* **2024**, *156*, 101865. DOI: 10.1016/j.progpolymsci.2024.101865.

(15) Herrera, C.; Ysinga, K. J.; Jenkins, C. L. Polysulfides Synthesized from Renewable Garlic Components and Repurposed Sulfur Form Environmentally Friendly Adhesives. *ACS Appl. Mater. Interfaces* **2019**, *11* (38), 35312-35318. DOI: 10.1021/acsami.9b11204.

(16) Wickramasingha, Y. A.; Simon, Ž.; Hayne, D. J.; Eyckens, D. J.; Dharmasiri, B.; Chalker, J. M.; Henderson, L. C. Adhesives Made from Sulfur Copolymer Composites Reinforced with Recycled Carbon Fiber. *Ind. Eng. Chem. Res.* **2024**, *63* (28), 12490-12501. DOI: 10.1021/acs.iecr.4c01280.

(17) Lundquist, N. A.; Tikoalu, A. D.; Worthington, M. J. H.; Shapter, R.; Tonkin, S. J.; Stojcevski, F.; Mann, M.; Gibson, C. T.; Gascooke, J. R.; Karton, A.; et al. Reactive Compression Molding Post-Inverse Vulcanization: A Method to Assemble, Recycle, and Repurpose Sulfur Polymers and Composites. *Chem. Eur. J.* **2020**, *26* (44), 10035-10044. DOI: 10.1002/chem.202001841.

(18) Wickramasingha, Y. A.; Stojcevski, F.; Eyckens, D. J.; Hayne, D. J.; Chalker, J. M.; Henderson, L. C. Exploring Inverse Vulcanized Dicyclopentadiene As a Polymer Matrix for Carbon Fiber Composites. *Macromol. Mater. Eng.* **2024**, *309* (3), 2300298. DOI: 10.1002/mame.202300298.

(19) Stojcevski, F.; Stanfield, M. K.; Hayne, D. J.; Mann, M.; Lundquist, N. A.; Chalker, J. M.; Henderson, L. C. Inverse Vulcanisation of canola oil as a route to recyclable chopped carbon fibre composites. *Sustain. Mater. Technol.* **2022**, *32*, e00400. DOI: 10.1016/j.susmat.2022.e00400.

(20) Bao, J.; Martin, K. P.; Cho, E.; Kang, K.-S.; Glass, R. S.; Coropceanu, V.; Bredas, J.-L.; Parker, W. O. N., Jr.; Njardarson, J. T.; Pyun, J. On the Mechanism of the Inverse Vulcanization of Elemental Sulfur: Structural Characterization of Poly(sulfur-random-(1,3-diisopropenylbenzene)). *J. Am. Chem. Soc.* **2023**, *145* (22), 12386-12397. DOI: 10.1021/jacs.3c03604.

(21) Hoefling, A.; Lee, Y. J.; Theato, P. Sulfur-Based Polymer Composites from Vegetable Oils and Elemental Sulfur: A Sustainable Active Material for Li–S Batteries. *Macromol. Chem. Phys.* **2017**, *218* (1), 1600303. DOI: 10.1002/macp.201600303 (acccessed 2024/12/11).

(22) Yan, P.; Zhao, W.; Tonkin, S. J.; Chalker, J. M.; Schiller, T. L.; Hasell, T. Stretchable and Durable Inverse Vulcanized Polymers with Chemical and Thermal Recycling. *Chem. Matter.* **2022**, *34* (3), 1167-1178. DOI: 10.1021/acs.chemmater.1c03662.

(23) Smith, J. A.; Green, S. J.; Petcher, S.; Parker, D. J.; Zhang, B.; Worthington, M. J. H.; Wu, X.; Kelly, C. A.; Baker, T.; Gibson, C. T.; et al. Crosslinker Copolymerization for Property Control in Inverse Vulcanization. *Chem. Eur. J.* **2019**, *25* (44), 10433-10440. DOI: 10.1002/chem.201901619.

(24) Yan, P.; Wang, H.; Dodd, L. J.; Hasell, T. Processable crosslinked terpolymers made from elemental sulfur with wide range of thermal and mechanical properties. *Commun. Mater.* **2023**, *4* (1), 89. DOI: 10.1038/s43246-023-00417-9.

(25) Tonkin, S. J.; Gibson, C. T.; Campbell, J. A.; Lewis, D. A.; Karton, A.; Hasell, T.; Chalker, J. M. Chemically induced repair, adhesion, and recycling of polymers made by inverse vulcanization. *Chem. Sci.* **2020**, *11* (21), 5537-5546. DOI: 10.1039/D0SC00855A.

(26) Harpp, D. N.; Smith, R. A. Organic sulfur chemistry. 42. Sulfur-sulfur bond cleavage processes. Selective desulfurization of trisulfides. *J. Am. Chem. Soc.* **1982**, *104* (22), 6045-6053. DOI: 10.1021/ja00386a034.

(27) Shapter, R. Investigating reactions of trisulfide system. Undergraduate thesis, Flinders University, Bedford Park, South Australia, 2021.

(28) Steudel, R. Sulfur: Organic Polysulfanes. In *Encyclopedia of Inorganic Chemistry*, R.B. King, R. H. C., C.M. Lukehart, D.A. Atwood, R.A. Scott, Ed.; 2007.

(29) Xue, J.; Jiang, X. Polysulfuration via a Bilateral Thiamine Disulfurating Reagent. *Organic Lett.* **2020**, *22* (20), 8044-8048. DOI: 10.1021/acs.orglett.0c02992.

(30) Simmonds, A. G.; Griebel, J. J.; Park, J.; Kim, K. R.; Chung, W. J.; Oleshko, V. P.; Kim, J.; Kim, E. T.; Glass, R. S.; Soles, C. L.; et al. Inverse Vulcanization of Elemental Sulfur to Prepare Polymeric Electrode Materials for Li–S Batteries. *ACS Macro Lett.* **2014**, *3* (3), 229-232. DOI: 10.1021/mz400649w.

(31) Zein, N.; Sinha, A. M.; McGahren, W. J.; Ellestad, G. A. Calicheamicin γ1I: an Antitumor Antibiotic That Cleaves Double-Stranded DNA Site Specifically. *Science* **1988**, *240* (4856), 1198-1201. DOI: doi:10.1126/science.3240341.

(32) Wiedemeyer, W. R.; Gavrilyuk, J.; Schammel, A.; Zhao, X.; Sarvaiya, H.; Pysz, M.; Gu, C.; You, M.; Isse, K.; Sullivan, T. ABBV-011, a novel, calicheamicin-based antibody–drug conjugate, targets SEZ6 to eradicate small cell lung cancer tumors. *Mol. Cancer Ther.* **2022**, *21* (6), 986-998. DOI: 10.1158/1535-7163.MCT-21-0851.

(33) Oku, N.; Matsunaga, S.; Fusetani, N. Shishijimicins A−C, Novel Enediyne Antitumor Antibiotics from the Ascidian Didemnum proliferum. *J. Am. Chem. Soc.* **2003**, *125* (8), 2044-2045. DOI: 10.1021/ja0296780.

(34) Steudel, R. Properties of Sulfur-Sulfur Bonds. *Angew. Chem., Int. Ed. Engl.* **1975**, *14* (10), 655-664. DOI: 10.1002/anie.197506551.

(35) Chauvin, J.-P. R.; Griesser, M.; Pratt, D. A. The antioxidant activity of polysulfides: it's radical! *Chem. Sci.* **2019**, *10* (19), 4999-5010. DOI: 10.1039/C9SC00276F.

(36) Pickering, T. L.; Saunders, K. J.; Tobolsky, A. V. Disproportionation of organic polysulfides. *J. Am. Chem. Soc.* **1967**, *89* (10), 2364-2367. DOI: 10.1021/ja00986a021.

(37) Steudel, R. The Chemistry of Organic Polysulfanes R− S n− R (n> 2). *Chem. Rev.* **2002**, *102* (11), 3905-3946. DOI: 10.1021/cr010127m

(38) Trivette Jr, C.; Coran, A. Polysulfide Exchange Reactions. I. Kinetics and Mechanism of the Thermal Exchange between Diethyl Trisulfide and Di-n-propyl Trisulfide. *J. Org. Chem.* **1966**, *31* (1), 100-104. DOI: 10.1021/jo01339a020.

(39) Guryanova, E.; Vasilyeva, V.; Kuzina, L. Sulfur Exchange in Polysulfides and in Various Vulcanization Accelerators. In *Conference of the Academy of Sciences of the USSR on the Peaceful Uses of Atomic Energy, July 1-5, 1955*, United States Atomic Energy Commission: Vol. 1.

(40) Birch S. F.; Cullum T. V.; Dean R. A. The Preparation and Properties of Dialkyl Di- and Poly-sulphides. Some Disproportionation Reactions *J. Inst. Petrol.* **1953**, *39*, 206.

(41) Milligan, B.; Rivett, D.; Savige, W. The photolysis of dialkyl sulphides, disulphides, and trisulphides. *Aust. J. Chem.* **1963**, *16* (6), 1020-1029. DOI: 10.1071/CH9631020.

(42) Burkey, T.; Hawari, J.; Lossing, F.; Lusztyk, J.; Sutcliffe, R.; Griller, D. The tert-butylperthiyl radical. *J. Org. Chem.* **1985**, *50* (24), 4966-4967. DOI: 10.1021/jo00224a064.

(43) Everett, S. A.; Schoeneich, C.; Stewart, J. H.; Asmus, K. D. Perthiyl radicals, trisulfide radical ions, and sulfate formation: a combined photolysis and radiolysis study on redox processes with organic di- and trisulfides. *J. Phys. Chem.* **1992**, *96* (1), 306-314. DOI: 10.1021/j100180a058.

(44) Ammer, J.; Baidya, M.; Kobayashi, S.; Mayr, H. Nucleophilic reactivities of tertiary alkylamines. *J. Phys. Org. Chem.* **2010**, *23* (11), 1029-1035. DOI: 10.1002/poc.1707.

(45) Brotzel, F.; Kempf, B.; Singer, T.; Zipse, H.; Mayr, H. Nucleophilicities and Carbon Basicities of Pyridines. *Chem. Eur. J.* **2007**, *13* (1), 336-345. DOI: 10.1002/chem.200600941.

(46) Foss, O. CHAPTER 9 - IONIC SCISSION OF THE SULFUR-SULFUR BOND. In *Organic Sulfur Compounds*, Kharasch, N. Ed.; Pergamon, 1961; pp 83-96.

(47) Martin, D.; Weise, A.; Niclas, H. J. The Solvent Dimethyl Sulfoxide. *Angew. Chem., Int. Ed. Engl.* **1967**, *6* (4), 318-334. DOI: 10.1002/anie.196703181.

(48) Xiang, J.-C.; Gao, Q.-H.; Wu, A.-X. The Applications of DMSO. In *Solvents as Reagents in Organic Synthesis*, 2017; pp 315-353.

(49) Ritzoulis, G. Excess properties of the binary liquid systems dimethylsulfoxide + isopropanol and propylene carbonate + isopropanol. *Can. J. Chem.* **1989**, *67* (6), 1105-1108. DOI: 10.1139/v89-166.

(50) Fuchs, R.; McCrary, G. E.; Bloomfield, J. J. Mechanisms of Nucleophilic Displacement in Aqueous Dimethyl Sulfoxide Solutions. *J. Am. Chem. Soc.* **1961**, *83* (20), 4281-4284. DOI: 10.1021/ja01481a043.

(51) Williams, P. J. H.; Boustead, G. A.; Heard, D. E.; Seakins, P. W.; Rickard, A. R.; Chechik, V. New Approach to the Detection of Short-Lived Radical Intermediates. *J. Am. Chem. Soc.* **2022**, *144* (35), 15969-15976. DOI: 10.1021/jacs.2c03618.

(52) Goldstein, S.; Samuni, A.; Merenyi, G. Kinetics of the Reaction between Nitroxide and Thiyl Radicals: Nitroxides as Antioxidants in the Presence of Thiols. *J. Phys. Chem. A* **2008**, *112* (37), 8600-8605. DOI: 10.1021/jp804743g.

(53) Schmid, R. Effect of Solvent on Chemical Reactions and Reactivity. In *Handbook of Solvents*, Wypych, G. Ed.; ChemTec Publishing, 2001; pp 737-846.

(54) Reichardt, C. Solvation Effects in Organic Chemistry: A Short Historical Overview. *J. Org. Chem.* **2022**, *87* (3), 1616-1629. DOI: 10.1021/acs.joc.1c01979.

(55) Reichardt, C.; Welton, T. Empirical Parameters of Solvent Polarity. In *Solvents and Solvent Effects in Organic Chemistry*, Reichardt, C., Welton, T. Eds.; 2010; pp 425-508.

(56) Gutmann, V. *The donor-acceptor approach to molecular interactions*; Springer New York, 1978.

(57) Kosower, E. M. The Effect of Solvent on Spectra. I. A New Empirical Measure of Solvent Polarity: Z-Values. *J. Am. Chem. Soc.* **1958**, *80* (13), 3253-3260. DOI: 10.1021/ja01546a020.

(58) Dimroth, K.; Reichardt, C.; Siepmann, T.; Bohlmann, F. Über Pyridinium-N-phenol-betaine und ihre Verwendung zur Charakterisierung der Polarität von Lösungsmitteln. *Justus Liebigs Ann. Chem.* **1963**, *661* (1), 1-37. DOI: 10.1002/jlac.19636610102.

(59) Reichardt, C.; Harbusch-Görnert, E. Über Pyridinium-N-phenolat-Betaine und ihre Verwendung zur Charakterisierung der Polarität von Lösungsmitteln, X. Erweiterung, Korrektur und Neudefinition der ET-Lösungsmittelpolaritätsskala mit Hilfe eines lipophilen penta-tert-butyl-substituierten Pyridinium-N-phenolat-Betainfarbstoffes. *Liebigs Ann. Chem.* **1983**, *1983* (5), 721-743. DOI: 10.1002/jlac.198319830502.

(60) Rao, P. Molecule of the month: Molecular-Chameleon: Solvatochromism at its iridescent best! *Resonance* **1997**, *2* (5), 69-72. DOI: 10.1007/BF02838017.

(61) Singh, R.; Whitesides, G. M. Comparisons of rate constants for thiolate-disulfide interchange in water and in polar aprotic solvents using dynamic proton NMR line shape analysis. *J. Am. Chem. Soc.* **1990**, *112* (3), 1190-1197. DOI: 10.1021/ja00159a046.

(62) Arisawa, M.; Yamaguchi, M. Rhodium-Catalyzed Disulfide Exchange Reaction. *J. Am. Chem. Soc.* **2003**, *125* (22), 6624-6625. DOI: 10.1021/ja035221u.

(63) Song, M.; Hu, Q.; Li, Z.-Y.; Sun, X.; Yang, K. NFSI-catalyzed SS bond exchange reaction for the synthesis of unsymmetrical disulfides. *Chin. Chem. Lett.* **2022**, *33* (9), 4269-4272. DOI: 10.1016/j.cclet.2021.12.073.

(64) Caraballo, R.; Rahm, M.; Vongvilai, P.; Brinck, T.; Ramström, O. Phosphine-catalyzed disulfide metathesis. *Chem.Commun.* **2008**, (48), 6603-6605. DOI: 10.1039/B815710C.

(65) Tanaka, K.; Ajiki, K. Phosphine-free cationic rhodium(I) complex-catalyzed disulfide exchange reaction: convenient synthesis of unsymmetrical disulfides. *Tetrahedron Lett.* **2004**, *45* (29), 5677-5679. DOI: 10.1016/j.tetlet.2004.05.092.

(66) Clennan, E. L.; Stensaas, K. L. Recent progress in the synthesis, properties and reactions of trisulfanes and their oxides. *Org. Prep. Proced. Int.* **1998**, *30* (5), 551-600. DOI: 10.1080/00304949809355321.

(67) Steudel, R. Homocyclic sulfur molecules. *Top. Curr. Chem.* **1982**, 149-176. DOI: 10.1007/3-540-11345-2_10.

(68) Hoefle, G.; Baldwin, J. E. Thiosulfoxides. Intermediates in rearrangement and reduction of allylic disulfides. *J. Am. Chem. Soc.* **1971**, *93* (23), 6307-6308. DOI: 10.1021/ja00752a073.

(69) Kutney, G. W.; Turnbull, K. Compounds containing the S=S bond. *Chem. Rev.* **1982**, *82* (4), 333-357. DOI: 10.1021/cr00050a001.

(70) Steudel, R.; Drozdova, Y.; Miaskiewicz, K.; Hertwig, R. H.; Koch, W. How unstable are thiosulfoxides? An ab initio MO study of various disulfanes RSSR (R= H, Me, Pr, all), their branched isomers R2SS, and the related transition states1, 2. *J. Am. Chem. Soc.* **1997**, *119* (8), 1990-1996. DOI: 10.1021/ja9624026.

(71) Ali, D.; Amer, Y.; Petersen, W. F.; Kaschula, C. H.; Hunter, R. A Review of Heterolytic Synthesis Methodologies for Organotri-and Organotetrasulfane Synthesis. *SynOpen* **2021**, *5* (01), 49-64. DOI: 10.1055/s-0040-1706018.

(72) Derbesy, G.; Harpp, D. N. A simple method to prepare unsymmetrical di- tri- and tetrasulfides. *Tetrahedron Lett.* **1994**, *35* (30), 5381-5384. DOI: 10.1016/S0040-4039(00)73505-2.

(73) Gundermann, K. D. Neighboring Group and Substituent Effects in Organosulfur Compounds. *Angew. Chem., Int. Ed. Engl.* **1963**, *2* (11), 674-683. DOI: 10.1002/anie.196306741.

(74) Abu-Yousef, I. A.; Harpp, D. N. New sulfenyl chloride chemistry: Synthesis, reactions and mechanisms toward carbon-carbon double bonds. *Sulfur Rep.* **2003**, *24* (3), 255-282. DOI: 10.1080/01961770308047977.

(75) Kang, K.-S.; Olikagu, C.; Lee, T.; Bao, J.; Molineux, J.; Holmen, L. N.; Martin, K. P.; Kim, K.-J.; Kim, K. H.; Bang, J.; et al. Sulfenyl Chlorides: An Alternative Monomer Feedstock from Elemental Sulfur for Polymer Synthesis. *J. Am. Chem. Soc.* **2022**, *144* (50), 23044-23052. DOI: 10.1021/jacs.2c10317.

(76) Lowry, T. M.; Jessop, G. CLXXXII.—The properties of the chlorides of sulphur. Part II. Molecular extinction coefficients. *J. Chem. Soc.* **1929**, (0), 1421-1435. DOI: 10.1039/JR9290001421.

(77) Thompson, Q. E. Organic Esters of Bivalent Sulfur. III. Sulfoxylates. *J. Org. Chem.* **1965**, *30* (8), 2703-2707. DOI: 10.1021/jo01019a046.

(78) Harpp, D. N.; Steliou, K.; Chan, T. H. Organic sulfur chemistry. 26. Synthesis and reactions of some new sulfur transfer reagents. *J. Am. Chem. Soc.* **1978**, *100* (4), 1222-1228. DOI: 10.1021/ja00472a032.

(79) Stone, B. D.; Nielsen, M. L. The Reaction of Sulfur Dichloride with Methylamine1. *J. Am. Chem. Soc.* **1959**, *81* (14), 3580-3584. DOI: 10.1021/ja01523a025.

(80) Zysman-Colman, E.; Harpp, D. N. Optimization of the Synthesis of Symmetric Aromatic Tri- and Tetrasulfides. *J. Org. Chem.* **2003**, *68* (6), 2487-2489. DOI: 10.1021/jo0265481.

(81) Ford, P. W.; Davidson, B. S. Synthesis of varacin, a cytotoxic naturally occurring benzopentathiepin isolated from a marine ascidian. *J. Org. Chem.* **1993**, *58* (17), 4522-4523. DOI: 10.1021/jo00069a006.

(82) Goor, G.; Anteunis, M. Synthesis of 5,5-Disubstituted-1,2,3-trithianes. *Synthesis* **1975**, *1975* (05), 329-330. DOI: 10.1055/s-1975-23749.

(83) Harpp, D. N.; Back, T. G. N,N′-thiobisphthalimide - a useful sulfur-transfer reagent. *Tetrahedron Lett.* **1972**, *13* (15), 1481-1484. DOI: 10.1016/S0040-4039(01)84662-1.

(84) Kalnins, M. V. Reactions of phthalimide and potassium phthalimide with sulfur monochloride. *Can. J. Chem.,* **1966**, *44* (17), 2111-2113. DOI: 10.1139/v66-318.

(85) Banerji, A.; Kalena, G. P. A new synthesis of organic trisulfides. *Tetrahedron Lett.* **1980**, *21* (31), 3003-3004. DOI: 10.1016/0040-4039(80)88021-X.

(86) Dao, N. V.; Ercole, F.; Kaminskas, L. M.; Davis, T. P.; Sloan, E. K.; Whittaker, M. R.; Quinn, J. F. Trisulfide-Bearing PEG Brush Polymers Donate Hydrogen Sulfide and Ameliorate Cellular Oxidative Stress. *Biomacromolecules* **2020**, *21* (12), 5292-5305. DOI: 10.1021/acs.biomac.0c01347.

(87) Ercole, F.; Li, Y.; Whittaker, M. R.; Davis, T. P.; Quinn, J. F. H2S-Donating trisulfide linkers confer unexpected biological behaviour to poly(ethylene glycol)–cholesteryl conjugates. *J. Mater. Chem. B* **2020**, *8* (17), 3896-3907. DOI: 10.1039/C9TB02614B.

(88) Lecher, H. Z.; Hardy, E. M. Some new methods for preparing Bunte Salts. *J. Org. Chem.* **1955**, *20* (4), 475-487. DOI: 10.1021/jo01122a010.

(89) Bunte, H. Zur Constitution der unterschwefligen Säure. *Ber. Dtsch. Chem. Ges.* **1874**, *7* (1), 646-648. DOI: 10.1002/cber.187400701201.

(90) Distler, H. The Chemistry of Bunte Salts. *Angew. Chem., Int. Ed. Engl.* **1967**, *6* (6), 544-553. DOI: 10.1002/anie.196705441.

(91) Reeves, J. T.; Camara, K.; Han, Z. S.; Xu, Y.; Lee, H.; Busacca, C. A.; Senanayake, C. H. The Reaction of Grignard Reagents with Bunte Salts: A Thiol-Free Synthesis of Sulfides. *Org. Lett.* **2014**, *16* (4), 1196-1199. DOI: 10.1021/ol500067f.

(92) Milligan, B.; Saville, B.; Swan, J. M. 680. Trisulphides and tetrasulphides from Bunte salts. *J. Chem. Soc.* **1963**, 3608-3614. DOI: 10.1039/JR9630003608.

(93) Foss, O. Thiosulphate Catalysis on Mixtures of Tetrathionate and Monoselenotrithionate. *Acta Chem. Scand.* **1950**, *4*, 866-869. DOI: 10.3891/acta.chem.scand.04-0866.

(94) Foss, O.; Kringlebotn, I. Displacement of Sulphite Groups of Polythionates by Thiosulphate. *Acta Chem. Scand.* **1961**, *15*, 1608-1609. DOI: 10.3891/acta.chem.scand.15-1608.

(95) Carrico, R. J. Apparatus and method for determining whether formaldehyde in aqueous solution has been neutralized. US6426182B1, 2002.

(96) Bhattacherjee, D.; Sufian, A.; Mahato, S. K.; Begum, S.; Banerjee, K.; De, S.; Srivastava, H. K.; Bhabak, K. P. Trisulfides over disulfides: highly selective synthetic strategies, anti-proliferative activities and sustained H_2S release profiles. *Chem. Commun.* **2019**, *55* (90), 13534-13537. DOI: 10.1039/C9CC05562B.

(97) Chakravarti, G. C. CX.—Action of sulphur monochloride on mercaptans. *J. Chem. Soc., Trans.* **1923**, *123* (0), 964-968. DOI: 10.1039/CT9232300964.

(98) Derbesy, G. Synthesis and Oxidative Reactivity of Organopolysulphides. McGill University, Canada, 1994. https://escholarship.mcgill.ca/concern/theses/t148fk37t?locale=en.

(99) Ramaraju, P.; Gergeres, D.; Turos, E.; Dickey, S.; Lim, D. V.; Thomas, J.; Anderson, B. Synthesis and antimicrobial activities of structurally novel S,S′-bis(heterosubstituted) disulfides. *Bioorg. Med. Chem. Lett.* **2012**, *22* (11), 3623-3631. DOI: 10.1016/j.bmcl.2012.04.056.

CHAPTER 2: THE SYNTHESIS OF ORGANIC TRISULFIDES AND TETRASULFIDES

2.1 Acknowledgement

Dr. Harshal D. Patel for the assistance in the synthesis and characterization of organic tetrasulfides, and HRMS measurement of both trisulfides and tetrasulfides. Dr. Witold Bloch for the measurement of X-ray diffraction data of crystalline organic trisulfides and tetrasulfides. Steven Tsoukatos for the assistance in trisulfide crystal data processing. Abigail Mann for the assistance in trisulfide IR data processing.

2.2 Introduction

For the purposes of studying the scope and mechanism of S-S metathesis, several trisulfides and some tetrasulfides needed to be synthesised. This chapter explored the synthesis of a variety of symmetrical organic trisulfides, R-SSS-R, (Figure 2.1) via several previously reported reagents such as Bunte salt (sodium *S*-alkyl thiosulfate)[1-3], sulfur dichloride (SCl_2)[4], and a monosulfur transfer reagent, *N*,*N*'-thiobisphthalimide.[5] The selection of these synthetic methodologies was based on the availability and the ease of handling the starting materials. The aim was to provide a library of trisulfides (and tetrasulfides) for metathesis mechanistic studies, and to assess the generality of each synthesis method for application to novel trisulfide targets. Several new, previously unreported, trisulfides, diisobutyl trisulfide **2.4** and di-*n*-hexyl trisulfide **2.11**, were successfully synthesized using the Bunte salt method.

Sodium *S*-alkyl thiosulfate ($RSSO_3^-Na^+$), also referred to as a Bunte salt, is a valuable intermediate that can be used to prepare organic trisulfides.[6] The thiosulfate salt can be easily prepared from an alkyl halide and sodium thiosulfate via an S_N2 reaction (Figure 2.1A). The addition of sodium sulfide (Na_2S) to the thiosulfate salt yields an organic trisulfide (Figure 2.1B).[1, 2] A major advantage of this synthetic method is that it does not require thiols, which can be malodorous. For the synthesis of unsaturated trisulfides from alkyl halides (i.e., conversion of allyl bromide to diallyl trisulfide), the Bunte salt method could be the method of choice because it can tolerate a reaction involving olefinic group. However, there are some drawbacks when employing this method for making trisulfide. Typically, it takes almost a day or more to produce the desired trisulfide. Additionally, tertiary alkyl halides do not react with sodium thiosulfate due to steric hindrence.[7] The Bunte salt method cannot be used, therefore, in the synthesis of di-*tert*-butyl trisulfide ($^tBu_2S_3$) or any sterically hindered trisulfide. For these substrates, an alternative method to make organic trisulfides was required.

A. An alkyl halide to sodium S-alkyl thiosulfate or "Bunte salt"

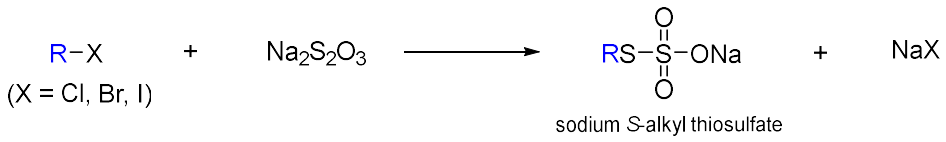

B. Sodium S-alkyl thiosulfate to a trisulfide

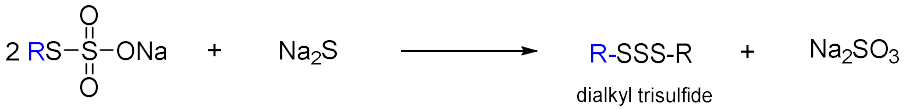

Figure 2.1: A. Synthesis of sodium *S*-alkyl thiosulfate (Bunte Salt). B. Synthesis of an organic trisulfide from sodium *S*-alkyl thiosulfate (Bunte Salt).

Trisulfides can also be synthesized using a classic and efficient method of reacting a thiol with sulfur dichloride (SCl_2) in a dry solvent such as diethyl ether. The use of sulfur dichloride in trisulfide synthesis can be traced back to 1947 where Clayton and Etzler first attempted to prepare hexadecyl trisulfide.[8] Since then, the method has been used and developed further. In 1994, Harpp reported a comprehensive study on the use of sulfur dichloride for synthesis of symmetrical and unsymmetrical trisulfides.[4] This method is generally simple and quick (~3 hours of reaction time) compared to that of sodium *S*-alkyl/aryl thiosulfate method. However, it requires the use of a thiol, a base such as a tertiary amine (e.g., pyridine, triethylamine), and low temperature (-78 °C) (Figure 2.2A). The amine is used to neutralise the HCl generated in the reaction. Harpp et al.[4] also believe that the amine could form an activated intermediate e.g., sulfenyl pyridinium or thiosulfenyl pyridinium complex to assist the reaction by nucleophilic catalysis. Although sulfur dichloride is an efficient sulfenylating agent, this reagent needs to be freshly distilled prior to use. This is because sulfur dichloride is slowly decomposed at room temperature to give sulfur monochloride and chlorine gas.[9]

The use of sulfur monochloride (S_2Cl_2) and a thiol for the synthesis of symmetrical tetrasulfide was first explored by Chakravarti[10] in 1923. Harpp further developed the method for the general synthesis of symmetrical organic tetrasulfides.[4, 11] For symmetrical aromatic tetrasulfides, optimisation of the synthesis was reported by Zysman-Colman and Harpp.[12] In general, tetrasulfides are prepared in a similar way to that of trisulfides (Figure 2.2B).

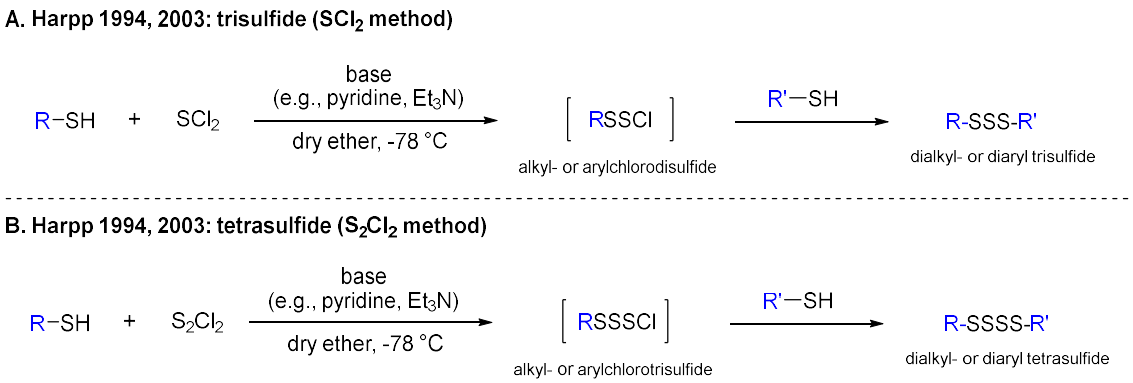

Figure 2.2: A. Synthesis of organic trisulfide from a thiol (R-SH) and sulfur dichloride (SCl_2) B. Synthesis of organic tetrasulfide from a thiol (R-SH) and sulfur monochloride (S_2Cl_2).

Due to the need of freshly distilled sulfur dichloride for the synthesis of organic trisulfides, we decided to synthesize sulfur dichloride from elemental sulfur and chlorine gas. Sulfur dichloride was synthesized and purified according to the procedures adapted from Brauer[13] and Harpp.[5, 12] There are two main steps in the synthesis. Briefly, as shown in Figure 2.3, chlorine gas is first generated from the reaction between trichloroisocyanuric acid (TCCA) and hydrochloric acid (step 1). The chlorine gas, after being carefully dried using concentrated sulfuric acid (or calcium chloride), is then bubbled through the molten sulfur (step 2). As reaction progress, the viscosity of the molten sulfur decreases and the colour of the mixture changes from yellow to dark red, indicating the formation of sulfur chlorides (mainly sulfur dichloride and sulfur monochloride). The mixture containing sulfur chlorides can be easily separated by fractional distillation (SCl_2 b.p. 59 – 60 °C and S_2Cl_2 b.p. 137 – 138 °C). The collected fraction of sulfur dichloride was redistilled in the presence of phosphorus pentachloride (typically 0.05 – 0.10% PCl_5) prior to use in the trisulfide synthesis.[12] When sulfur monochloride was required for the synthesis of organic tetrasulfides, it was purified by distillation in the presence of elemental sulfur. Otherwise, sulfur monochloride is also available commercially with a typical purity of approximately 98%.

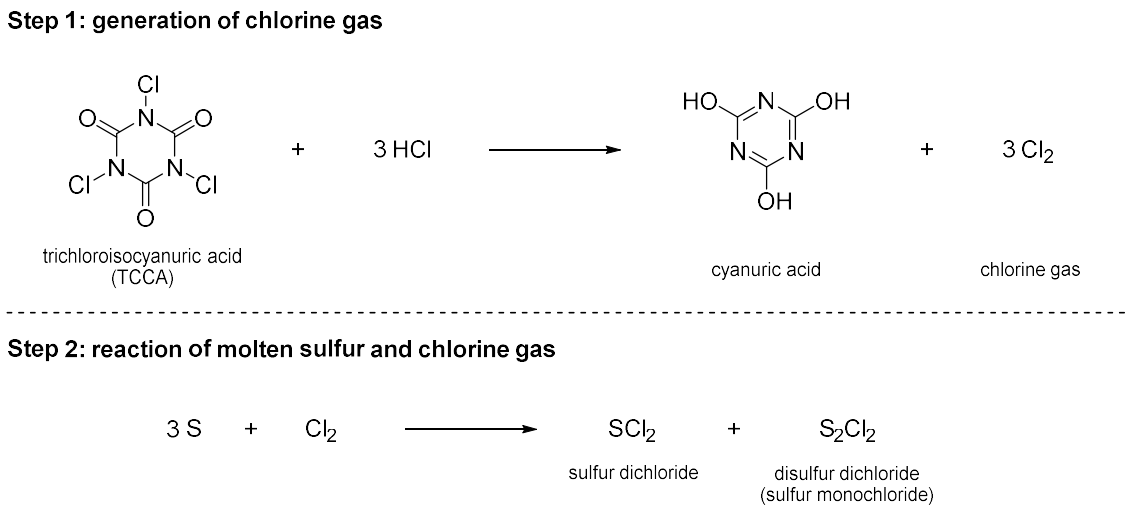

Figure 2.3: Synthesis of sulfur dichloride (SCl_2) from elemental sulfur and chlorine gas.

The use of a stable monosulfur transfer reagent, *N*,*N*'-thiobisphthalimide, for trisulfide synthesis has also been reported. This sulfur transfer reagent was exclusively used in this thesis for the synthesis of bis(2-hydroxyethtyl) trisulfide. This reagent was also reported to be useful for the synthesis of unsymmetrical trisulfides. Both symmetrical and unsymmetrical trisulfide are generally prepared using a two-step reaction. First, the synthesis of an alkyl or arylphtalimido disulfide is achieved from the reaction between a thiol and *N*,*N*'-thiobisphthalimide. Second, the isolated alkyl or arylphtalimido disulfide is then reacted with another thiol to obtain the trisulfide. The by-product of this reaction is phthalimide. Phthalimide can be recovered from this reaction and reused for the synthesis of *N*,*N*'-thiobisphthalimide. The general synthetic scheme is shown in Figure 2.4.

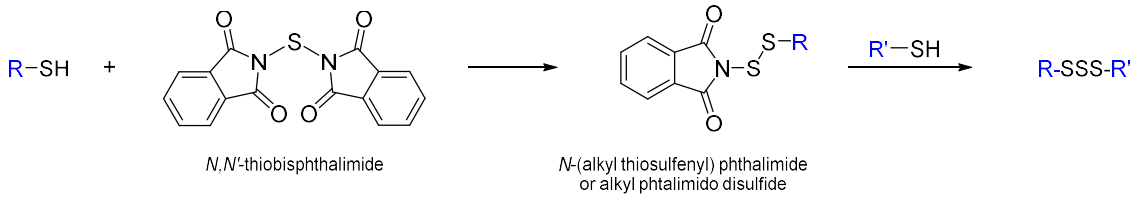

Figure 2.4: Synthesis of trisulfide using *N*,*N*'-thiobisphthalimide as a sulfur transfer reagent.

Despite their potent smell, sulfur dichloride and thiols are still the reagents of choice for reliably making trisulfides. The use of sodium *S*-alkyl thiosulfate was also an alternative option used to make trisulfides from primary and secondary alkyl halides. In addition, a reaction of a stable monosulfur transfer reagent, *N,N'*-thiobisphthalimide, with a thiol can be another alternative method to access trisulfide. The use of these methods for making trisulfides, and their associated challenges, are discussed in this chapter.

2.3 Results and Discussion

Organic trisulfides from Bunte salt (sodium S-alkyl thiosulfate) and sodium sulfide

Among ten organic trisulfides reported in this chapter, four trisulfides i.e., diallyl trisulfide, diethyl trisulfide, di-*n*-hexyl trisulfide, and di-*iso*-butyl trisulfide were synthesized using this method. For the synthesis of these trisulfides, alkyl bromides were first converted to their sodium *S*-alkyl thiosulfates, typically in aqueous EtOH at temperature of refluxing. In some cases, this transformation can also be done using only water, aqueous MeOH, dioxane.[6, 7] In a study of the synthesis of *S*-aryl or *S*-vinyl Bunte salt (sodium *S*-aryl thiosulfate), a polar aprotic solvent such as DMSO is typically used. For this, we suggest the reader to see the study by Reeves for a more comprehensive study on the synthesis of *S*-aryl or *S*-vinyl Bunte salt.[6] Since we only prepared sodium *S*-alkyl thiosulfates, aqueous EtOH is a preferrable solvent for this synthesis. After isolating the Bunte salt, the salts were reacted with sodium sulfide to yield the targeted trisulfides.

Synthesis of diallyl trisulfide, di-iso-butyl trisulfide, and dibenzyl trisulfide via Bunte salt and sodium sulfide

The synthesis of three trisulfides i.e. diallyl trisulfide (**2.2**), di-*iso*-butyl trisulfide (**2.4**), and dibenzyl trisulfide (**2.6**) were first attempted using the protocol described by Srivastava and Bhabak.[3] Allyl bromide, isobutyl bromide, and benzyl bromide were converted to sodium *S*-allyl thiosulfate (**2.1**), sodium *S*-isobutyl thiosulfate (**2.3**), and sodium *S*-benzyl thiosulfate (**2.5**), respectively. The thiosulfate salts were obtained by reacting the bromides (each 10 mmol) with excess of sodium thiosulfate (1.2 eq.) in 30% aqueous ethanol at 65 ºC. The addition of the bromide to a solution of sodium thiosulfate creates a two-phase mixture. With vigorous stirring and heating, the mixture became homogeneous after few minutes. This indicates that the alkyl halide is being converted to *S*-alkyl thiosulfate sodium salt. For allyl bromide and benzyl bromide, it took only 5 – 10 minutes for the mixture to become one phase, while for isobutyl bromide it took around 5 – 6 hours upon heating at 65 ºC. To push reaction into completion, heating for a total of 4 hours was applied for allyl bromide mixture (Figure 2.5A) and benzyl bromide mixture (Figure 2.5C), whereas isobutyl bromide mixture (Figure 2.5B) was heated for at least 16 hours. Although those bromides are classified as a primary alkyl halide, longer reaction time was required for the conversion of isobutyl bromide to the thiosulfate salt **2.3**. This occurs because of the steric hindrance of the isobutyl group, impeding nucleophilic attack which slows down the S_N2 reaction.[14] After solvent removal, the crude thiosulfate salt was ready to be used for the next step. NMR analysis of the crude salts in D_2O indicates the clean conversion of the bromides to their corresponding the thiosulfate salt **2.1**, **2.3**, and **2.5**, respectively.

With the crude Bunte salts in hand, the next step was to convert these salts to the desired trisulfides by reacting the salts with sodium sulfide (Figure 2.5). The reaction was continued without any further purification. The addition of sodium sulfide solution to each thiosulfate salt solution in water was done at 0 °C for 8 hours (based on the optimum condition for the trisulfide synthesis reported in the literature method[3]). It should be noted that the reaction temperature has to be

maintained at 0 ºC and this is crucial; otherwise, the reaction would favour the formation of disulfide.[3] This method yields trisulfide **2.2** in 86% yield, **2.4** in 90% yield, and **2.6** in 73% yield. Trisulfides obtained from this method also contain their disulfides which can be observed by GC-MS. Trisulfide **2.6** was recrystallised from hexane to yield a high purity product (>99% by ^{1}H NMR spectroscopy). The yield of those trisulfides were good but NMR analysis showed that the purity of trisulfide **2.2** was 90% (10% diallyl disulfide) and trisulfide **2.4** was 97% (3% di-*iso*-butyl disulfide). The result was not satisfactory, especially for the synthesis of diallyl trisulfide, because in general post-synthetic separation of organic polysulfides is difficult to achieve due to similar polarity. Trisulfides with high purity are desirable for the S-S metathesis study, otherwise the presence of any disulfide impurity could confound experiments designed to understand the mechanism.

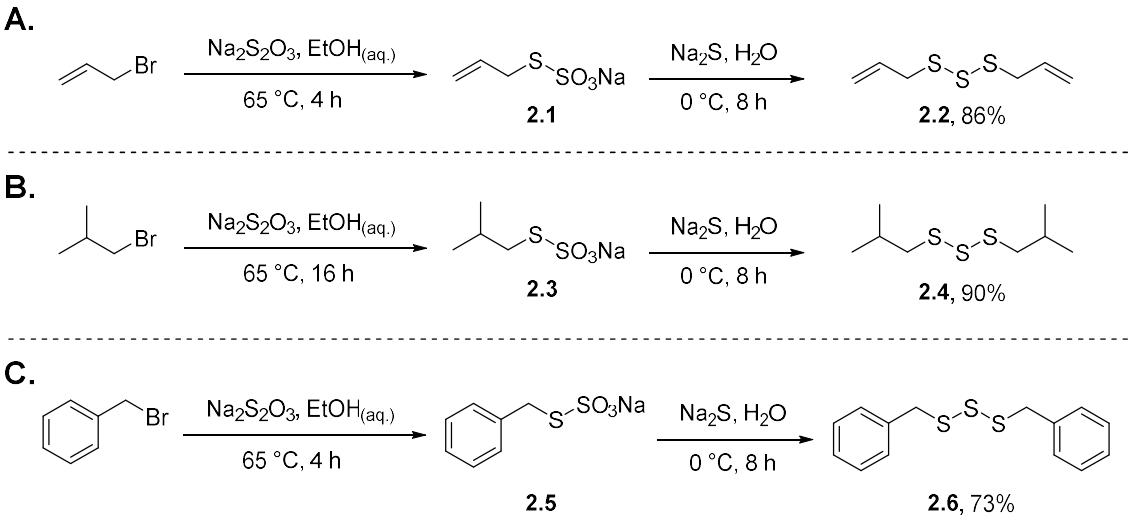

Figure 2.5: Synthesis of diallyl trisulfide (**2.2**), di-*iso*-butyl trisulfide (**2.4**), and dibenzyl trisulfide (**2.6**) via sodium *S*-alkyl thiosulfate and sodium sulfide.

Synthesis of diallyl trisulfide, di-iso-butyl trisulfide, diethyl trisulfide, di-n-hexyl trisulfide, and dibenzyl trisulfide via Bunte salt and sodium sulfide with paraformaldehyde additive

The synthetic methodologies for trisulfide synthesis via Bunte salt method were then re-evaluated with the goal to improve the overall purity. Milligan reported several experimental techniques to obtain high purity dialkyl trisulfides from their Bunte salts, and one of them is by the addition of formaldehyde.[2] Instead of using formaldehyde, the conversion of sodium *S*-alkyl thiosulfate to dialkyl trisulfide was carried out in the presence of paraformaldehyde (polymeric formaldehyde) as the additive. The solution pH was not buffered and remained high after the sodium sulfide addition (pH = ~12). This was intentionally set to meet condition so that paraformaldehyde can be slowly depolymerised to formaldehyde which can react and form stable adducts with sulfite anions. Unlike the previous attempt, the obtained Bunte salt was extracted using methanol and filtered to remove excess sodium thiosulfate and sodium bromide. This was done in order to avoid any potential side reaction between the product and thiosulfate ion.

The conversion of allyl bromide to trisulfide **2.2** was tested (Figure 2.6A). The synthesis was carried out by reacting the bromide (100 mmol) and excess sodium thiosulfate (1.1 eq.) in 50% aqueous ethanol at 70 ºC. Under this condition, it took around 20 minutes for the mixture to become one phase. The total reaction time was shortened to 2.5 hours instead of 4 hours. Prolonged heating was seen to be unnecessary because the reaction is generally complete when the mixture becomes homogenous.[7] After extraction with hot methanol and solvent removal, salt **2.1** was then subjected to reaction with sodium sulfide in the presence of paraformaldehyde. After the dropwise addition of the sulfide (pH= ~12), the paraformaldehyde solid was slowly dissolved, indicating that the depolymerization of paraformaldehyde occurs. However, it is not clear at this time whether paraformaldehyde is partially or fully converted to formaldehyde under this condition (0 ºC, pH= ~12). Normally, this conversion occurs in a basic medium (pH = ~10) with the temperature of 60 – 75 ºC.[15, 16] After a total of 4 hours, the reaction was stopped. Following the workup, trisulfide **2.2** was isolated in 88% yield as a clear pale-yellow oil. Gratifyingly, this improved method gave diallyl trisulfide with the high purity of 99% when analysed by ^{1}H NMR spectroscopy and GC-MS. This method is advantageous due to shorter reaction time for the conversion of sodium *S*-alkyl thiosulfate to dialkyl trisulfide. Most importantly, no further separation techniques such as column chromatography, distillation, or any other separation technique are required.

With the successful synthesis of diallyl trisulfide (**2.2**), three other trisulfides: di-*iso*-butyl trisulfide (**2.4**), diethyl trisulfide (**2.9**), and di-*n*-hexyl trisulfide (**2.11**), were also prepared using the same paraformaldehyde method. The schematic synthesis of these trisulfides is shown in Figure 2.6. First, the conversion of isobutyl bromide to salt **2.3** was achieved after a 24-hour reflux at 100 ºC. It should be noted that isobutyl bromide was not fully reacted (two phases observed) after several hours of refluxing. This is, as previously discussed, due to the steric effect of isobutyl group. Hence, a longer reaction time was necessary to complete this conversion. After the reaction with sodium sulfide and paraformaldehyde for 5.5 hours at 0 ºC, trisulfide **2.4** was isolated in 82% as a beige oil with the purity of 99.7% (GC-MS). Second, trisulfide **2.9** was synthesized from ethyl bromide. Using the same condition for the synthesis of diallyl trisulfide (**2.2**), trisulfide **2.9** was successfully isolated in 72% yield as a beige oil with the purity of above 99% (GC-MS). Lastly, trisulfide **2.11** was successfully synthesized from *n*-hexyl bromide. Salt **2.10** was prepared from the reaction between *n*-hexyl bromide and sodium thiosulfate at 100 °C for 6 hours. The resulting sodium *S*-hexyl thiosulfate (**2.10**) was isolated and then further reacted with sodium sulfide in the presence of paraformaldehyde at 0 °C for 4 hours to give trisulfide **2.11** in 70% yield with the purity of 99.9% (GC-MS). To the best of our knowledge, both trisulfide **2.4** and **2.11** have not been reported previously in any literature using this synthetic method. The results suggest that the addition of paraformaldehyde in the synthesis of dialkyl trisulfides is essential. It allows the selective conversion of sodium S-alkyl thiosulfate to a highly pure trisulfide. This improved method not only gives trisulfides with good to excellent yield but also require no tedious purification steps such as column chromatography and distillation.

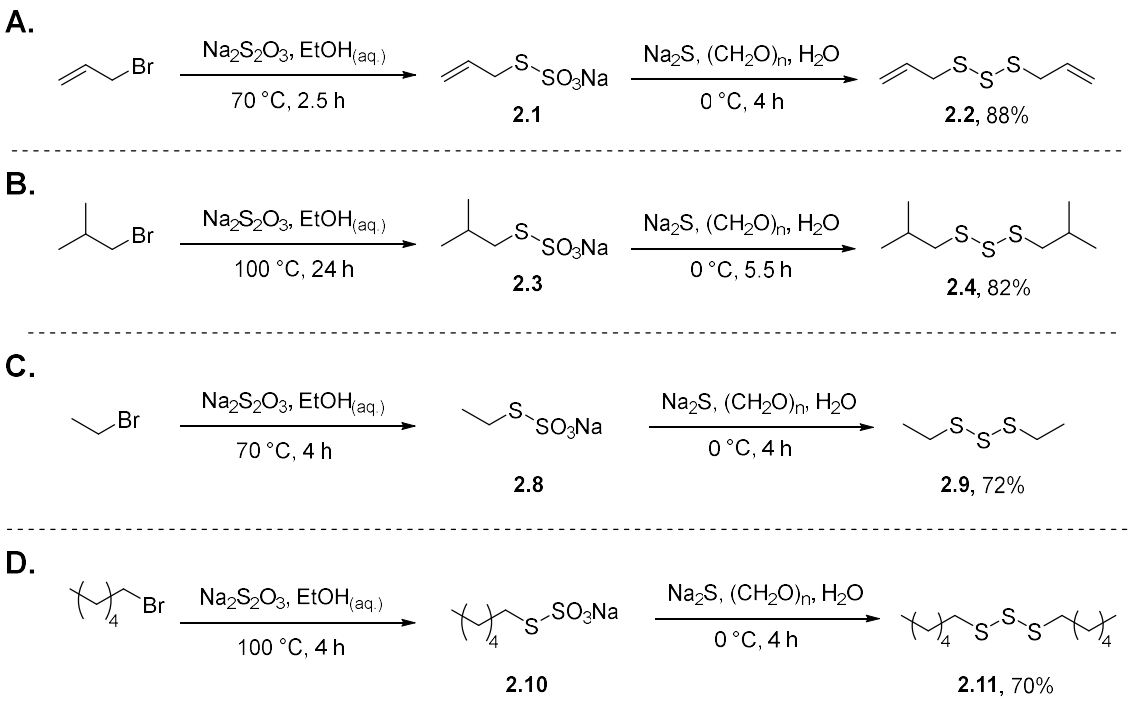

Figure 2.6: Synthesis of diallyl trisulfide (**2.2**), di-*iso*-butyl trisulfide (**2.4**), diethyl trisulfide (**2.8**), and di-*n*-hexyl trisulfide (**2.10**) via sodium *S*-alkyl thiosulfates and Na_2S with paraformaldehyde as the additive.

The synthesis of dibenzyl trisulfide was also attempted using the paraformaldehyde method (Figure 2.7). In this case, benzyl chloride was used as the starting alkyl halide. At the first stage, the conversion of benzyl chloride to its *S*-benzyl thiosulfate salt was successfully achieved. After the addition of sodium sulfide, the reaction was continued for a total of 4 hours similar to that of normal method (without paraformaldehyde additive). ^{1}H NMR analysis of the aliquot revealed that the crude mixture consists of around 95% of dibenzyl trisulfide (**2.6**) and around 5% of dibenzyl disulfide (**2.7**). However, when paraformaldehyde was used in the synthesis, the crude mixture contains 80% of dibenzyl trisulfide (d Ph-C**H$_2$**-S = 4.03 ppm) and 20% of dibenzyl disulfide (d Ph-C**H$_2$**-S = 3.60 ppm). The result was even worse when the mixture was continued to stir for nearly 8 hours where the composition of dibenzyl trisulfide as the target product monitored by ^{1}H NMR spectroscopy was reduced to 67%. This experiment suggests that the synthesis of dibenzyl trisulfide using paraformaldehyde additive did not improve product purity. This method appears to have most benefit in the synthesis of dialkyl trisulfides. Therefore, the sulfur dichloride method was employed to synthesize trisulfide **2.6**.

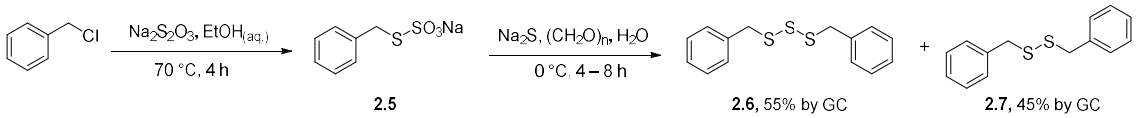

Figure 2.7: Synthesis of dibenzyl trisulfide via sodium *S*-benzyl thiosulfate and sodium sulfide with paraformaldehyde as the additive.

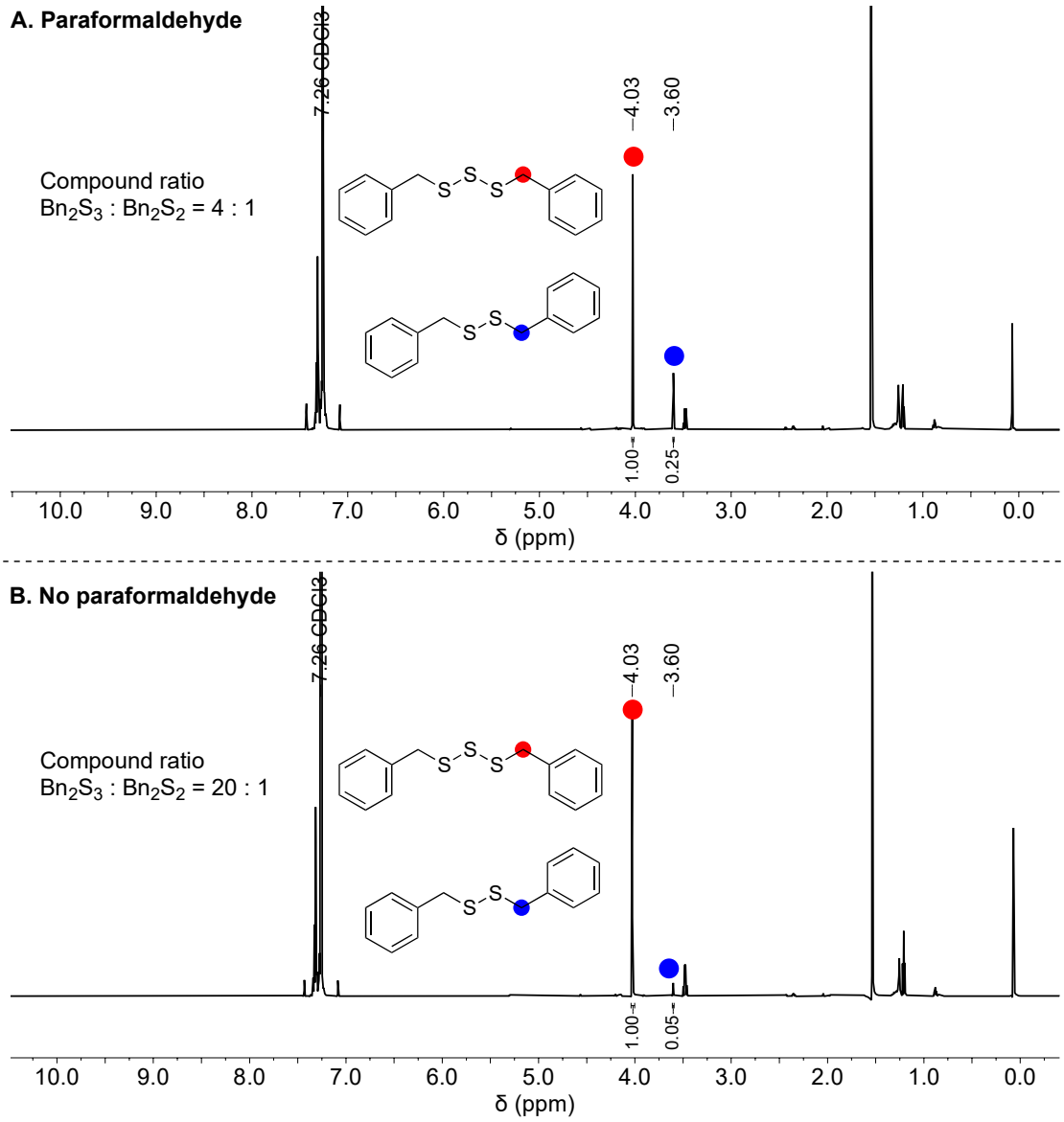

Figure 2.8: ^{1}H NMR spectra of the crude mixture for the synthesis of dibenzyl trisulfide after 4 hours of reaction time: A. Reaction with paraformaldehyde (B) Reaction without paraformaldehyde.

Organic trisulfides from thiols and sulfur dichloride (SCl_2)

Three trisulfides: di-*tert*-butyl trisulfide (**2.12**), dibenzyl trisulfide (**2.6**), and bis(1-adamantyl) trisulfide (**2.13**) were synthesized from their thiols and sulfur dichloride. The synthesis of trisulfide **2.12** was adapted from the protocol described by Harpp.[4] Trisulfide **2.6** and **2.13** were synthesized using a modified method from Zysman-Colman and Harpp.[4, 12]

Synthesis of sulfur dichloride

Sulfur dichloride is not a commercially available compound and for the use in the trisulfide synthesis we, therefore, had to prepared it form sulfur and chlorine gas as described in Figure 2.3. An alternative way to prepare sulfur dichloride is by reacting sulfur monochloride with excess chlorine

gas.[13] Trichloroisocyanuric and concentrated hydrochloric acid were used because these reagents does not react violently to generate chlorine gas. In addition to this, both reagents are inexpensive. Hydrochloric acid had to be slowly dropped to granular TCCA in order to control the production of chlorine gas. Wet chlorine gas is produced by this method, and it was carefully dried by passing through concentrated sulfuric acid. Drying chlorine gas before reacting with molten sulfur is important. Any traces of water can hydrolyse the resulting sulfur chlorides into sulfur dioxide, hydrochloric acid, and elemental sulfur.[17] Therefore, all glassware used for the synthesis of sulfur chlorides must be rigorously dried. Since excess of chlorine gas was used in the synthesis, it is also important to trap chlorine gas using sodium hydroxide solution. The obtained red liquid containing sulfur chlorides (SCl_2 and S_2Cl_2) was then distilled in the presence of phosphorus pentachloride to obtain sulfur dichloride (b.p. 59 – 60 ºC). Another distillation is also required to obtain high purity of sulfur dichloride since it is easily to decompose at room temperature or the presence of light.

Synthesis of di-tert-butyl trisulfide

Trisulfide **2.12** was prepared according to a method of Derbesy and Harpp (Figure 2.9).[4] The reaction was performed under an atmosphere of nitrogen. This is typically to prevent oxidation of the thiol to the disulfide by molecular oxygen.[18, 19] The orange solution of sulfur dichloride in dry ether (-78 °C, dry ice/acetone bath) disappeared upon a slow addition of a solution of *tert*-butyl thiol and triethylamine in ether. In this reaction, the first equivalent of *tert*-butyl thiol (^{t}BuSH) was reacted with sulfur dichloride to give *tert*-butyl thiosulfenyl chloride (^{t}BuSSCl). Besides obtaining a stable thiosulfenyl chloride in the reaction[4, 11], the low temperature aimed to ensure a controlled reaction. This is because the reaction of sulfur dichloride and most nucleophiles is exothermic.[20] A good example of this is the synthesis of hexadecyl trisulfide demonstrated by Clayton and Etzler where the reaction temperature increased from 17 °C to 27 °C after the slow addition of sulfur dichloride to hexadecyl thiol dissolved in petroleum ether.[8] Harpp et al.[21] also described that in some cases sulfur dichloride addition to ethereal solution of a thiol required cooling (an ice-water bath) otherwise the ether would start to reflux. Next, *tert*-butyl thiosulfenyl chloride (^{t}BuSSCl) has been reported in the literature as a stable compound so it can be isolated and characterized at room temperature. In the subsequent reaction, *tert*-butyl thiosulfenyl chloride was then reacted with another equivalent of *tert*-butyl thiol to yield *tert*-butyl trisulfide. Following workup, this desired trisulfide was isolated as a beige oil in 79% yield (Figure 2.9).

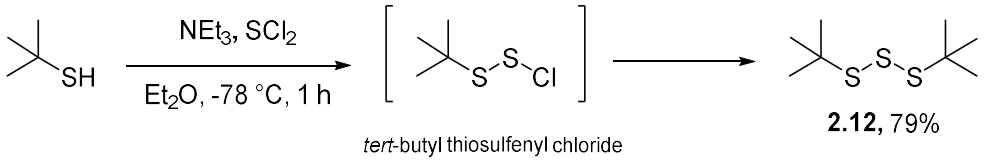

Figure 2.9: Synthesis of di-*tert*-butyl trisulfide.

During the reaction, a cloudy white suspension was formed, which is due to the reaction between hydrochloric acid and triethylamine to produce triethylamine hydrochloride salt (white solid) which is insoluble in dry ether. The role of a tertiary amine in this reaction is to neutralise the hydrochloric acid and to enhance the nucleophilicity of the thiol.[11, 12] However, it was not clear until now whether the nucleophilic enhancement occurs via the deprotonation of the thiol to form a thiolate (Figure 2.10A) by the amine (e.g., triethylamine, pyridine), the formation of an activated sulfenyl-amine complex (Figure 2.10B), or the combination of both pathways (Figure 2.10C). To date, no studies related to the mechanism have been reported so far. However, in some relevant studies such as in a thiol-Michael addition reaction, amines are mostly used as a base to deprotonate thiols into their reactive thiolates.[22, 23] If we look back to the original method, even without the presence of a tertiary amine, a nucleophilic substitution reaction between a thiol and sulfur dichloride still produces a trisulfide in a moderate to excellent yield.[20] The benefit of using a tertiary amine, however, is clear. Hydrochloric acid gas can be trapped *in situ* while reaction is progressing. This can make the synthesis process become more efficient because it does not require reflux to drive off the acid gas by-product from the trisulfide solution. Refluxing can even be problematic as it could lead to the formation of other polysulfides because of increased temperature. Organic trisulfides have been reported to undergo decomposition at high temperature to their corresponding di- and tetrasulfide or even higher polysulfides.[24]

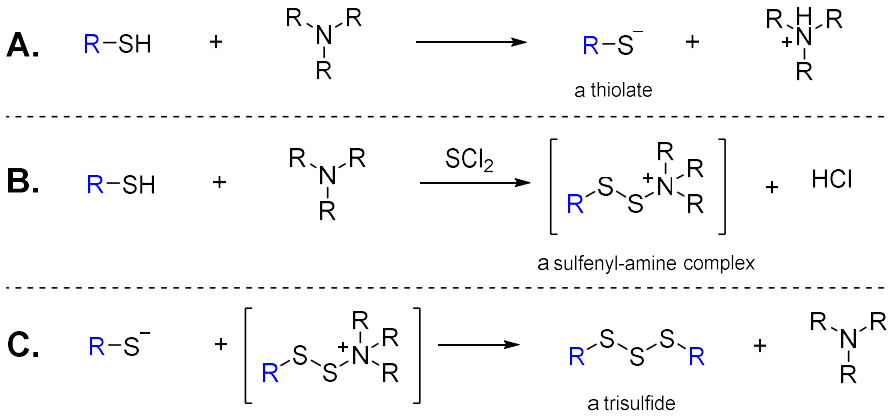

Figure 2.10: Possible roles of amine in the synthesis of organic trisulfides from a thiol and sulfur dichloride.

Synthesis of dibenzyl trisulfide

The synthesis of dibenzyl trisulfide from benzyl thiol and sulfur dichloride, without a tertiary amine, has been previously reported by Harpp.[25] In earlier discussion, we demonstrated that this trisulfide can also be prepared from a reaction of sodium *S*-benzyl thiosulfate with sodium sulfide (see Figure 2.5C). Although the synthesis of dibenzyl trisulfide from its sodium *S*-benzyl thiosulfate was a success, the method is laborious. Therefore, we attempted to prepare the trisulfide using the alternative pyridine-sulfur dichloride method developed by Zysman-Colman and Harpp.[12] Pyridine

was used as a base for this reaction. No attempt on using different bases, e.g., triethylamine, were made. A slow addition of benzyl thiol and pyridine to a cooled solution of sulfur dichloride in dry diethyl ether gave crude dibenzyl trisulfide as an oil. This reaction only took a total of two hours which is efficient compared to that of the thiosulfate salt method. This oil was dissolved in hexane and stored in a freezer at –25 °C for overnight to obtain white needle-like crystals of dibenzyl trisulfide (**2.6**) in 80% yield. X-ray crystallography revealed the structure of dibenzyl trisulfide as monoclinic with space group C2 (Figure 2.11). The crystallography data also revealed the length of S-S bond for this trisulfide which is around 2.05 Å. This value is in the range of S-S bond for trisulfides (2.012 to 2.086 Å) reported in the Cambridge Structural Database.[20] The length of S-S bond in organic polysulfides can provide information about their bond dissociation energy (BDE) which is a crucial factor to understand the reactivity. Generally, BDEs for disulfide is higher than those of tri- and tetrasulfides in polysulfide (Table 1.1, Chapter 1).

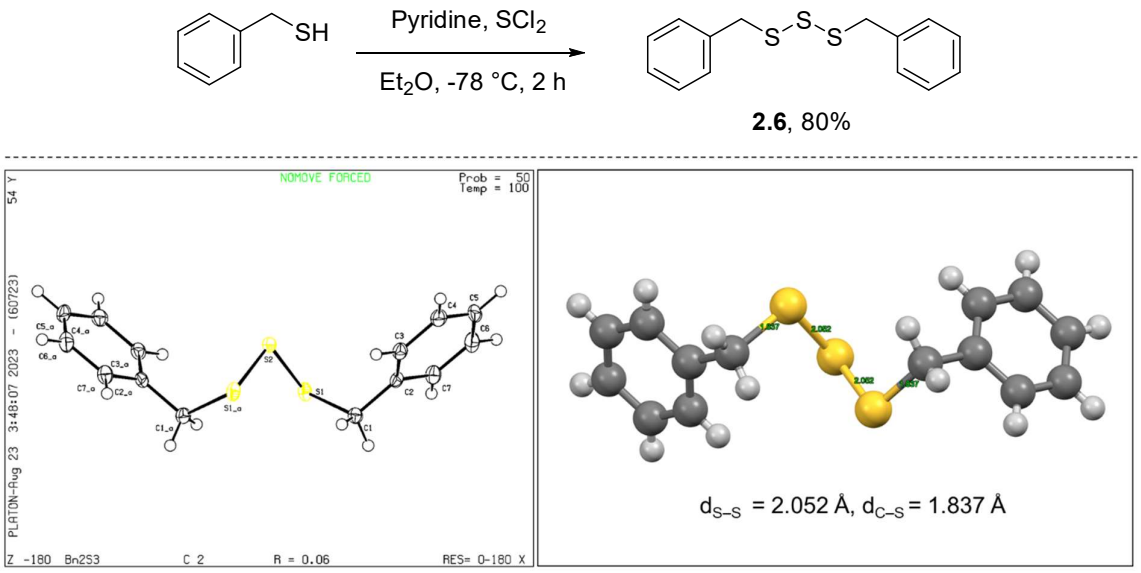

Figure 2.11: Synthesis of dibenzyl trisulfide via sulfur dichloride method and a crystal structure of dibenzyl trisulfide.

Synthesis of bis(1-adamantyl) trisulfide

Bis(1-adamantyl) trisulfide (**2.13**) is a sterically bulky trisulfide with non-polar adamantyl groups (Figure 2.12). To date, there is very limited study about the synthesis and applications of this compound. Two synthetic methods from Sirakawa[26] and Gorjian[27] have been reported for the synthesis of **2.13**, and only one study by Pavelko[28] on thermochemical and tribological behaviour of trisulfide **2.13** was reported. Another literature method of Pavelko[29] in 1989 describes the synthesis of bis(1-adamantyl trisulfide) from 1-adamantyl thiol and sulfur dichloride. In this publication, only melting point data was determined and compared to the one reported by Sirakawa.[26] In 1994, Derbesy and Harpp[4] then reported the NMR data of bis(1-adamantyl) trisulfide; however, Derbesy[11],

in his PhD thesis, only reported the synthesis of bis(1-adamantyl) disulfide and the NMR data for bis(1-adamantyl) disulfide and the trisulfide are nearly identical. Therefore, it was important in this study to unambiguously characterise this trisulfide. For the synthesis of trisulfide **2.13**, we adapted the general procedure reported by Zysman-Colman and Harpp.[12] Similar to the preparation of trisulfide **2.6**, the reaction of 1-adamantyl thiol and sulfur dichloride with pyridine was carried out in dry diethyl ether at -78 ºC to give trisulfide **2.13** as a white solid. Recrystallisation of this solid from chloroform/methanol gave pure trisulfide **2.13** in 61% yield. An attempt to recrystallize this solid for obtaining a single crystal XRD was not successful. Thus, no crystal data is obtained for this compound. Elemental analysis for the obtained white solid confirmed that it was a trisulfide ($C_{20}H_{30}S_3$ requires C, 65.52%; H, 8.25%; N, 0%; S, 26.23%. Found C, 65.74%; H, 8.72%; N, 0%; S, 27.92%.)

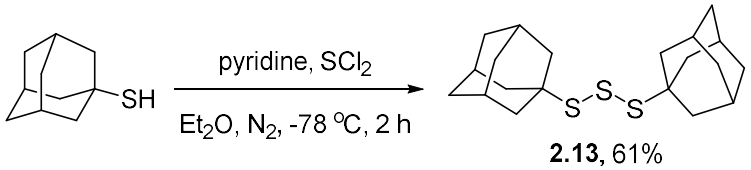

2.13, 61%

Figure 2.12: Synthesis of bis(1-adamantyl) trisulfide.

Synthesis of diphenyl trisulfide

We also attempted to synthesize diphenyl trisulfide (**2.14**). The synthesis protocol was adapted from Zysman-Colman and Harpp.[12] A solution of sulfur dichloride in dry ether was added dropwise to a solution of thiophenol and pyridine for 0.5 hour at -78 °C (Figure 2.13). The reaction was continued to stir at that temperature for an additional 1.5 hours. Following the workup, trisulfide **2.14** was obtained as a yellow oil. This oil was directly dissolved in *n*-pentane. Upon recrystallization from *n*-pentane at -25 ºC (freezer) overnight, a white crystal was formed. Initially, we thought that trisulfide **2.14** was successfully obtained. However, it was ultimately found that the crystal was diphenyl disulfide (**2.15**). First, X-ray structure analysis showed that this crystal was diphenyl disulfide (S-S bond length 2.026 Å). Second, GC-MS analysis of this crystal (Figure 2.14) showed that a single GC peak with the mass fragments (base peak m/z 218) similar to that of diphenyl disulfide (**2.15**). While Zysman-Colman and Harpp[12] reported HRMS data for the obtained crystal was 249.9936 (HMRS calculated for diphenyl trisulfide, $C_{12}H_{10}S_3$ = 249.9945), the mass spectrum data of their obtained crystal by electron ionization (EI) gave a base peak of m/z 218 (100%) and the molecular ion peak [$M^{+\bullet}$] of 250 with only 4% relative intensity. This MS data was consistent with MS-EI data of diphenyl disulfide by NIST (National Institute of Standards and Technology, US Department of Commerce). Further analysis revealed another evidence that the melting point of this white crystal was 61 – 62 °C in which this value was consistent with the melting point of diphenyl disulfide.[30] Therefore, in the first attempt, recrystallization of the oil product has led to the formation of diphenyl disulfide.

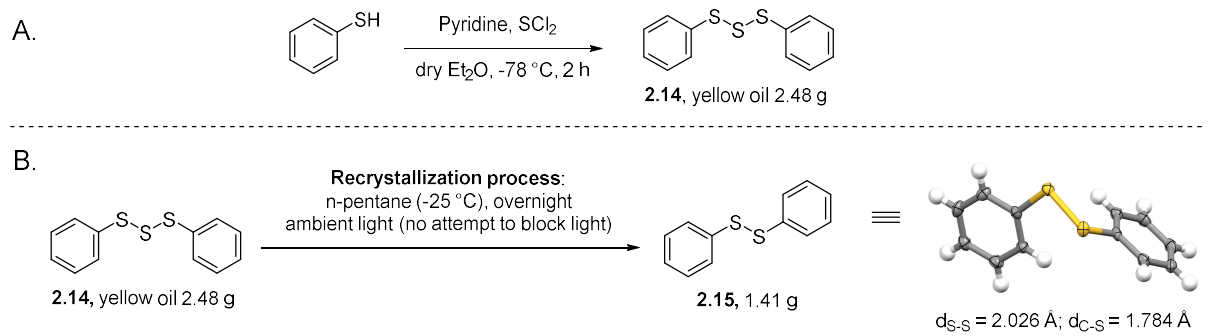

Figure 2.13: A. Synthesis of diphenyl trisulfide. B. Attempt on recrystallization of the oil product leading to the formation of diphenyl disulfide.

In the second attempt, trisulfide **2.14** was again synthesized from thiophenol and sulfur dichloride following the procedure described previously. The result gave a consistent yield. The yellow oil was stored in the round bottom flask covered with aluminium foil to exclude any light. This precaution was made as Zysman-Colman and Harpp[12] found that trisulfide **2.14** would be decomposed upon exposure to light in a matter of hours. Instead of doing recrystallization from *n*-pentane, the oil was directly characterized by NMR and GC-MS. First, both the ^{1}H and ^{13}C NMR spectra looked like pure trisulfide. Three proton peaks gave integrations of 10 protons in total. Four carbon peaks indicated four different carbon environments (see experimental details and characterizations). NMR data comparison of the oil and diphenyl disulfide (purchased from TCI) showed very close chemical shifts (Figure 2.14). For ^{1}H NMR analysis, the chemical shift of the protons of the phenyl group of disulfide **2.15** was slightly higher than that of diphenyl trisulfide. Interestingly, the chemical shifts of the carbons of disulfide **2.15** showed the opposite values which is slightly lower compared to that of diphenyl trisulfide **2.14**. Next, GC-MS analysis of this oil show two peaks at retention time of 18.3 min and 25.9 min with the percent composition of 1% and 99%, respectively. The former GC peak was assigned to be diphenyl disulfide (m/z calcd.: 218.0; m/z found: 218.0) and the latter peak was assigned to be diphenyl trisulfide (m/z calcd.: 250.0; m/z found: 250.0). It is important to note that a correct GC method should be applied for analysis trisulfide **2.14**. We adapted a GC method by Wu et al.[31] that was suitable for the analysis (Figure 2.15). A lower ramp rate of 8 ºC/min with MS transfer line set at 180 ºC gave a good separation while a higher ramp rate of 50 ºC/min with MS transfer line set at 250 ºC gave poor separation and caused decomposition. However, for analysis most other trisulfides the latter GC method did not give any problem.

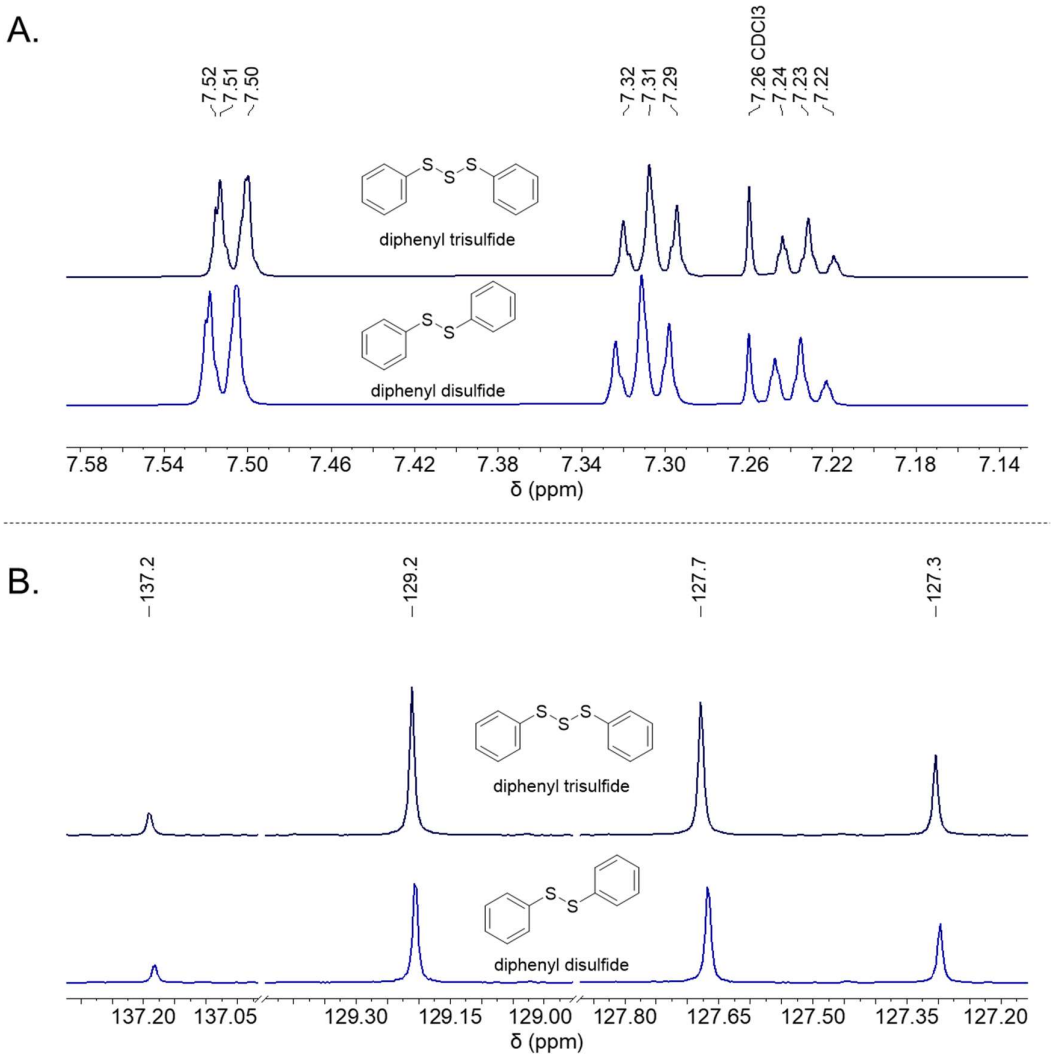

Figure 2.14: A. ^{1}H NMR (600 MHz, $CDCl_3$) and B. ^{13}C NMR (150 MHz, $CDCl_3$) spectra of as synthesized diphenyl trisulfide (yellow oil) in comparison to diphenyl disulfide (white solid) purchased from TCI (Tokyo Chemical Industry). Peaks highlighted for as synthesized diphenyl trisulfide (yellow oil). Chemical shift was calibrated to the residual solvent ($CDCl_3$: δ 7.26 ppm for ^{1}H NMR and δ 77.16 ppm for ^{13}C NMR).

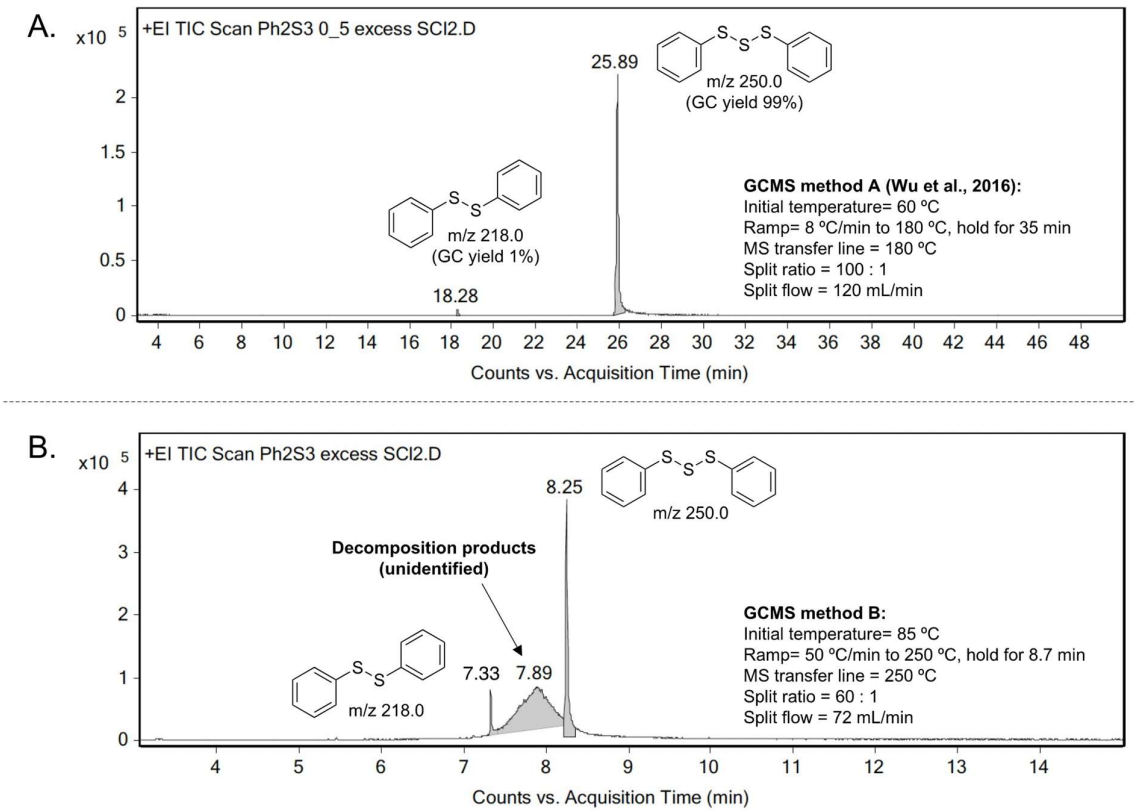

Figure 2.15: A. GC-MS analysis of the yellow oil containing diphenyl trisulfide using an analysis method by Wu et al.[31] B. GC-MS analysis of the same oil using a method developed by author to analyse other common trisulfides.

After several hours of storing trisulfide **2.14** in dark by wrapping with aluminium foil to exclude light, we checked again by running NMR and GC-MS analysis. As shown in Figure 2.16, a significant change was observed in both proton and carbon NMR profile of trisulfide **2.14** just after synthesis and a mere 6-hour storage in the dark at room temperature (11 – 13 ºC). From the ^{13}C NMR spectrum (Figure 2.16D), it seems that trisulfide **2.14** had been transformed into several polysulfides. GC-MS analysis (Figure 2.17) confirmed that only two compounds were observed i.e. diphenyl trisulfide (m/z 250.0) at 18.3 min and diphenyl disulfide (m/z 218.0) at 26 min with the percent area of 73% and 27%, respectively. It is still not clear how and why trisulfide **2.14** was converted to its corresponding disulfide, but desulfurization reactions of trisulfides have been reported. And because of the instability of trisulfide **2.14**, it was not employed in the S-S metathesis study.

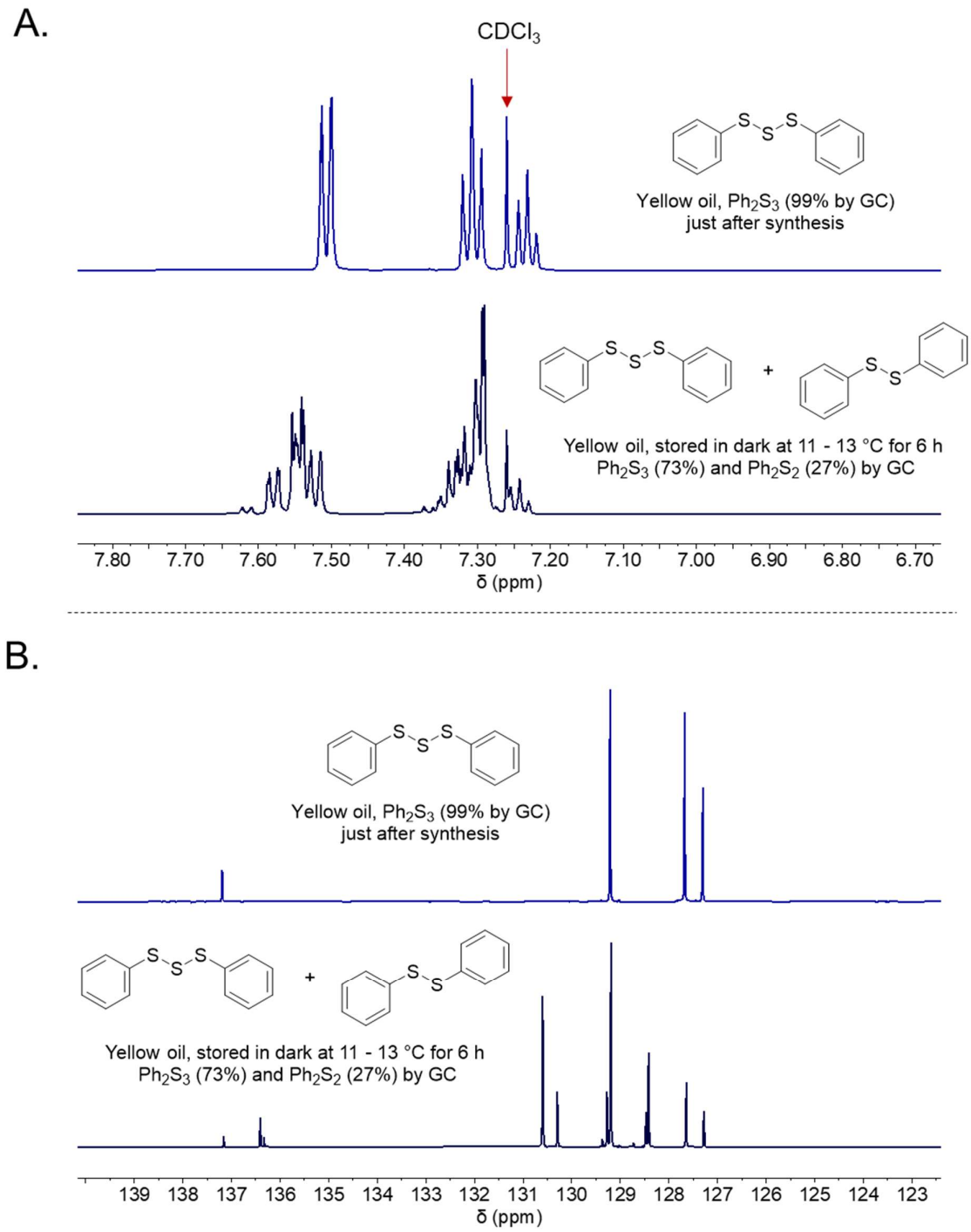

Figure 2.16: ^{1}H NMR spectra of: A. Trisulfide **2.14** after synthesis. B. Trisulfide **2.14** after stored for 6 hours in dark at 11 – 13 ºC. ^{13}C NMR of: C. Trisulfide **2.14** after synthesis. D. Trisulfide **2.14** after stored for 6 hours in dark at 11 – 13 ºC.

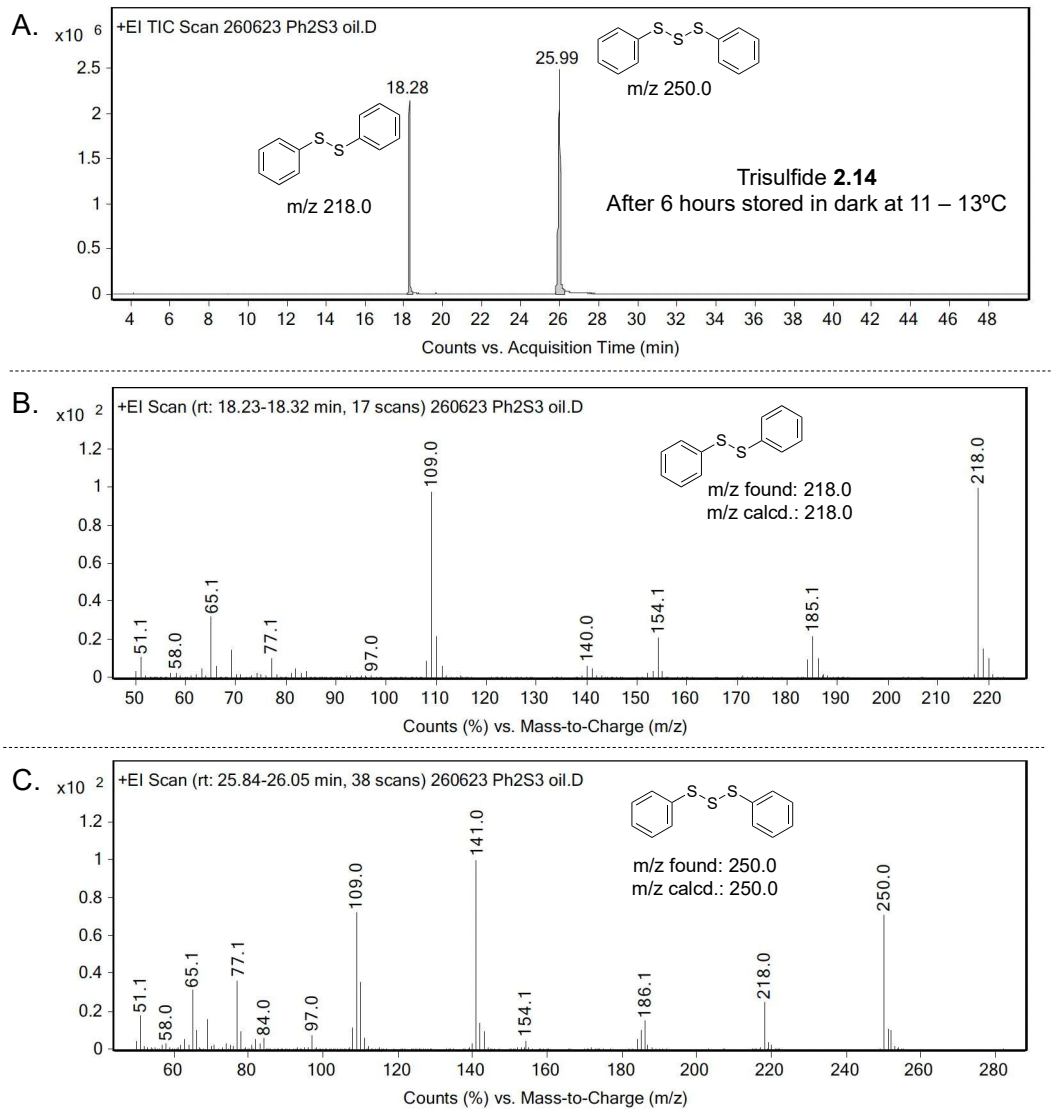

Figure 2.17: A. Gas chromatogram profile of trisulfide 2.14 after a 6-hour store in dark at 11 – 13 ºC. B. MS spectrum of the peak at 18.3 min, indicating the mass fragments of diphenyl disulfide. C. MS spectrum of the peak at 26 min, indicating the mass fragments of diphenyl trisulfide.

Organic trisulfides from thiols and *N,N'*-thiobisphthalimide

Bis(2-hydroxyethyl) trisulfide and bis(4-methoxybenzyl) trisulfide were prepared from the reaction between their thiol starting materials (i.e., 2-mercaptoethanol and 4-methoxybenzyl thiol), and the monosulfur transfer reagent *N,N'*-thiobisphthalimide (**2.16**, Figure 2.18). This compound is used as an alternative reagent for the synthesis of organic trisulfides, replacing the unstable and malodorous sulfur dichloride. Another benefit of using *N,N'*-thiobisphthalimide is that it can be advantageous for the preparation of unsymmetrical trisulfide due to its low reactivity towards nucleophiles.[5]

Synthesis of N,N'-thiobisphthalimide

In our study, *N,N'*-thiobisphthalimide (**2.16**) was prepared using the reported method by Kalnins[32] with minor modification. Phthalimide was first dissolved in dry DMF (dried and stored over molecular sieves type 4A). To this solution was added sulfur monochloride in portions and the mixture was heated at 28 ºC. A precipitate starts to form typically after 20 – 30 minutes of the reaction, indicating the formation of *N,N'*-thiobisphthalimide. This was shown by Kalnins[32] that the product has a low solubility in DMF which is around 1.87 g/100 mL. After 20 hours, the solid product was isolated by filtration and dried under high vacuum to remove the remaining DMF. A complete DMF removal can be done at 100 ºC under vacuum (~30 mbar) without any sign of decomposition. Recrystallisation of the product from chloroform/hexane gave a product as a white solid in 59% yield. In another experiment, we also attempted the purification by washing crude **2.16** with methanol to remove DMF and other impurities. After filtration and vacuum drying, pure **2.16** can be obtained in 62% yield. The obtained spectral data is in agreement with the literature.[33]

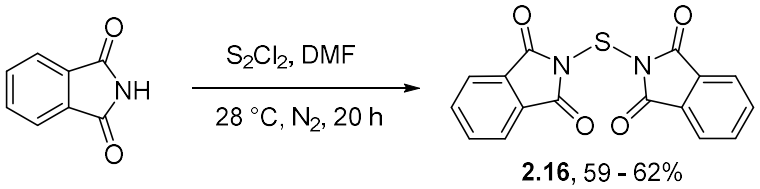

2.16, 59 - 62%

Figure 2.18: Synthesis of *N,N'*-thiobisphthalimide.

Synthesis of bis(2-hydroxyethyl) trisulfide

The synthesis of bis(2-hydroxyethyl) trisulfide (**2.17**) was carried out by reacting β-mercaptoethanol with **2.16** in toluene at 80 ºC under nitrogen atmosphere. In this first attempt, 2-mercaptoethanol (3.0 mmol, 2 eq.) was added in a single portion to a suspension of monosulfur transfer reagent **2.16** (1.67 mmol, 1.1 eq.) in toluene (Figure 2.19). ^{1}H NMR analysis of the crude mixture (Figure 2.20) showed that reagent **2.16** was fully consumed after heating for 1 hour. Proton signals for the target trisulfide **2.17** can be observed at δ 3.98, 3.09, and 2.25 ppm (Figure 2.20, green dot). In the mixture, we also observed the formation of **2.18** which appears at δ 7.97 – 7.91, 7.83 – 7.78, 4.06, 3.23, and 1.93 ppm (Figure 2.15, red square). Ercole et al.[34] reported the synthesis of **2.17** in two steps: (1) the conversion of **2.16** and 2-mercaptoethanol to **2.18** and (2) the conversion of **2.18** and another equivalent of the thiol to trisulfide **2.17**. Therefore, both **2.16** and **2.17** were expected to form during the reaction. This one-pot synthesis method gave trisulfide **2.17** in 67% yield (187.3 mg, 1.01 mmol) along with **2.18** in (102.7 mg, 0.46 mmol) and phthalimide (127.3 mg, 0.87 mmol). Our focus of this study was only to obtain **2.17** and we were not interested in the by-products. Nevertheless, if a large-scale reaction is established, it is worth to consider the recovery of **2.18** and phthalimide. In that way, **2.18** can be used as a precursor to synthesize trisulfide **2.17** or other unsymmetrical trisulfides. Phthalimide later can be used to regenerate monosulfur transfer reagent **2.16** (see the reaction shown in Figure 2.18).

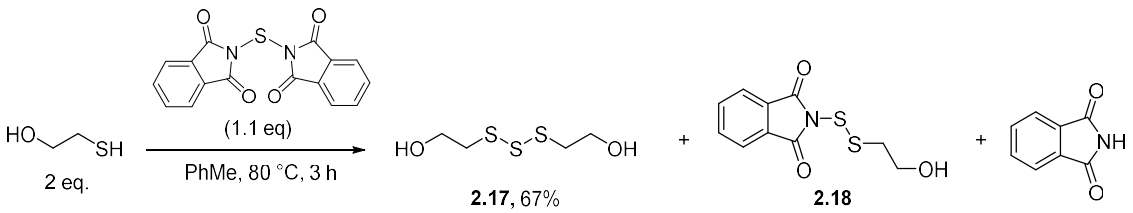

Figure 2.19: Synthesis of bis(2-hydroxyethyl) trisulfide.

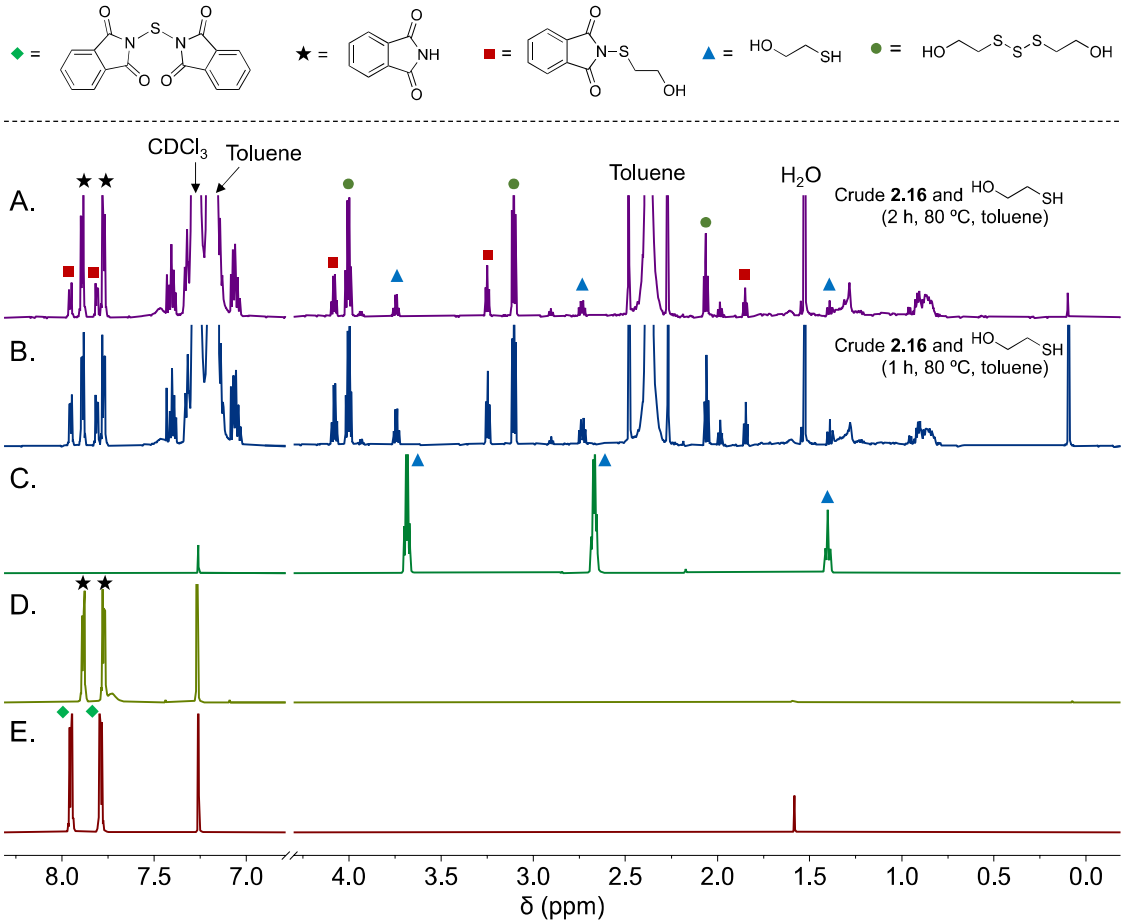

Figure 2.20: ^{1}H NMR studies of the reaction between *N,N'*-thiobisphthalimide (**2.16)** and 2-mercaptoethanol at 80 ºC in toluene. ^{1}H NMR spectra of (A) the crude mixture after heating for 2 h heating, (B) the crude mixture after heating for 1 h, (C) 2-mercaptoethanol, (D) phthalimide, and (E) *N,N'*-thiobisphthalimide (**2.16**).

Moreover, the synthesis of **2.17** was also attempted using sulfur dichloride method (Figure 2.21A). However, the product contains a mixture of trisulfide **2.17** and disulfide **2.19** (Figure 2.21B-D). This is due to the unstable sulfur dichloride which could undergo decomposition during the synthesis.

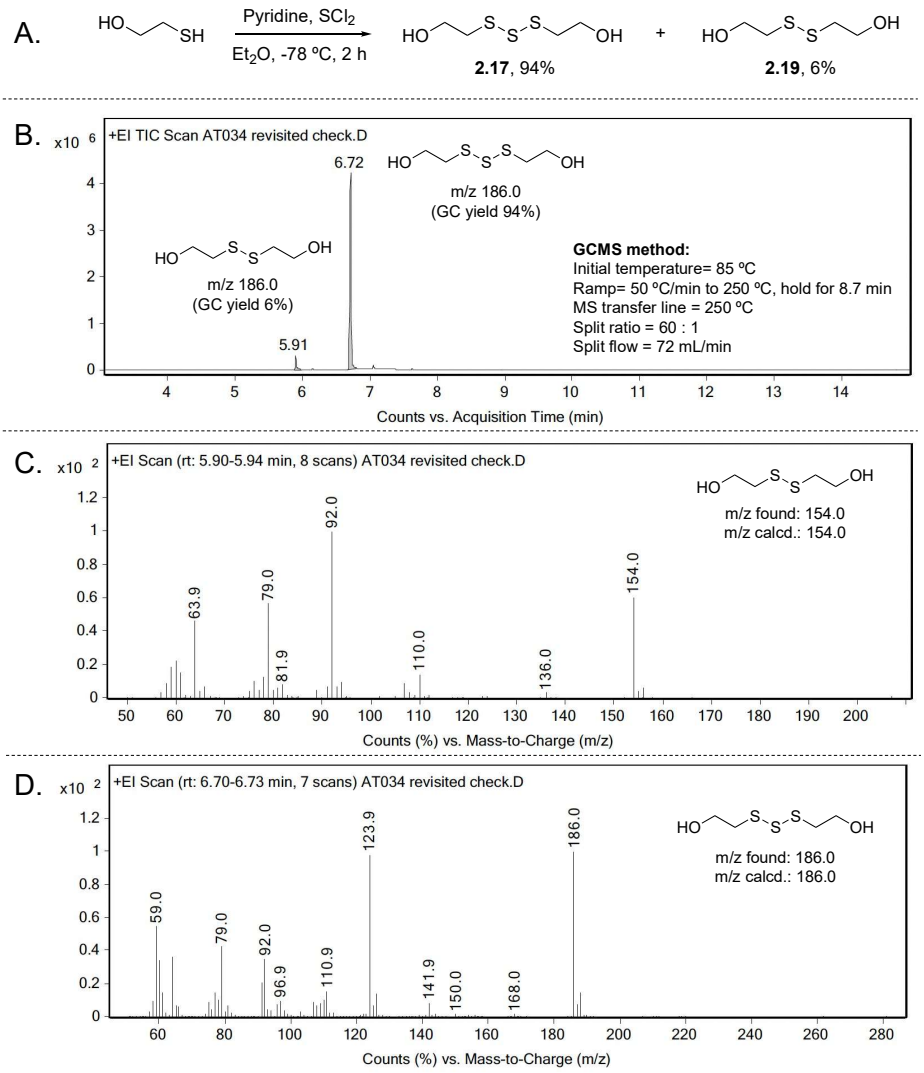

Figure 2.21: A. Synthesis of bis(2-hydroxyethyl) trisulfide using the sulfur dichloride method. B. GC-MS analysis of the product from the reaction A. B. MS spectrum of the peak at 5.9 min, indicating the mass fragments of bis(2-hydroxyethyl) disulfide. C. MS spectrum of the peak at 6.7 min, indicating the mass fragments of bis(2-hydroxyethyl) trisulfide.

Bis(2-hydroxyethyl) trisulfide was also prepared using the synthetic protocol reported by Ercole et al.[34] First, 2-mercaptoethanol was converted into disulfide **2.18** in a poor yield of 38%. Next, this disulfide **2.18** was reacted with 2-mercaptoethanol to obtain the target trisulfide **2.17** also in a poor yield of 39%. Both reactions (Figure 2.22) show a noticeable low yield for the product, but the target trisulfide could be prepared in decent purity. Trisulfide **2.17** can be obtained and this was further used for the synthesis of silyl protected trisulfide **2.20** which is shown in the next section.

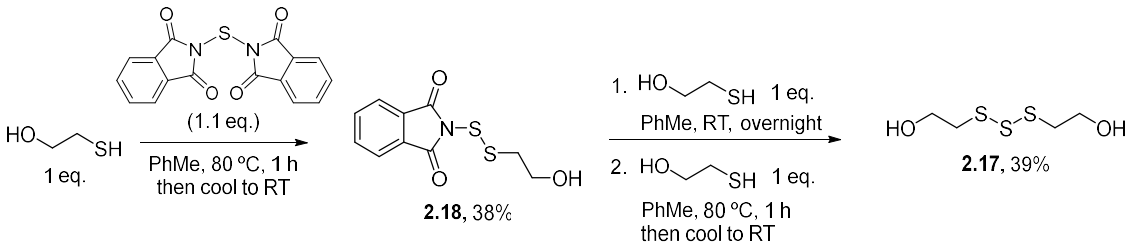

Figure 2.22: A two-step synthesis of bis(2-hydroxyethyl) trisulfide.

Synthesis of bis(2-trimethylsiloxyethyl) trisulfide

For investigating different substrate scope of S-S metathesis, and the tolerance of OH groups in trisulfide metathesis, we also prepared bis(2-trimethylsiloxyethyl) trisulfide (**2.20**). Silylation of **2.17** was carried out using chlorotrimetylsilane (Me_3SiCl) under basic conditions (Figure 2.23). After addition of the silylating agent, the reaction was allowed to proceed at room temperature for 3 hours. Isolation of the product was carried out by filtration using celite, followed by solvent removal under reduced pressure. The silyl protected trisulfide **2.20** was obtained in a very good yield (80%) as an oil. ^{1}H NMR analysis of the trisulfide product indicated a strong signal at δ 0.14 ppm, which strongly indicates the presence of 9 protons of trimethylsilyl group that typically appeared at δ close to 0 ppm[35], and two additional peaks of CH_2 proton at 3.02 and 3.89 ppm. In addition to this, three carbon peaks at δ 61.1, 41.0, and -0.3 ppm were also observed in ^{13}C NMR spectrum. Furthermore, GC-MS analysis showed a single peak with m/z 330.1, indicating the molecular ion $[M]^+$ for bis(2-trimethylsiloxyethyl) trisulfide (*m/z* calcd. for $C_{10}H_{26}O_2S_3Si_2^+$: 330.1 [*M*]$^+$). Elemental analysis also indicated the empirical formula of the target trisulfide.

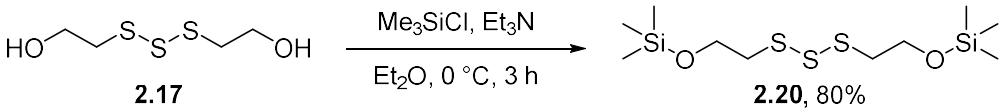

Figure 2.23: Synthesis of bis(2-trimethylsiloxyethyl) trisulfide.

Synthesis of bis(4-methoxybenzyl) trisulfide

Next, bis(4-methoxybenzyl) trisulfide (**2.21**) was prepared according to the general method reported by Harpp et al.[5] The synthesis of trisulfide **2.21** using *N,N'*-thiobisphthalimide has never been reported in the literature. 4-methoxybenzyl thiol and *N,N'*-thiobisphthalimide were reacted at 90 ºC for 3 hours in toluene (Figure 2.23). Because excess of the thiol was used in the synthesis, NMR analysis of the crude reaction mixture after 3 hours indicated a full consumption of the monosulfur transfer reagent **2.16**. The formation of bis(4-methoxybenzyl) trisulfide can be observed by ^{1}H NMR spectroscopy (δ benzylic proton = ~4.01 ppm, Figure 2.24A). ^{1}H NMR spectra comparison between the product and the starting materials is shown in Figure 2.24. The synthesis optimisation was not carried out for this trisulfide. Next, after purification by column chromatography trisulfide **2.21** was

obtained as an oil in a good yield of 79%. This oil was solidified to an off-white solid upon cooling at 12 – 14 ºC. Elemental analysis supported the empirical formula for the target trisulfide **2.21**. Unfortunately, an attempt to analyse this trisulfide by GC-MS failed as the compound was found to undergo decomposition under the GC-MS analysis condition (Figure 2.25).

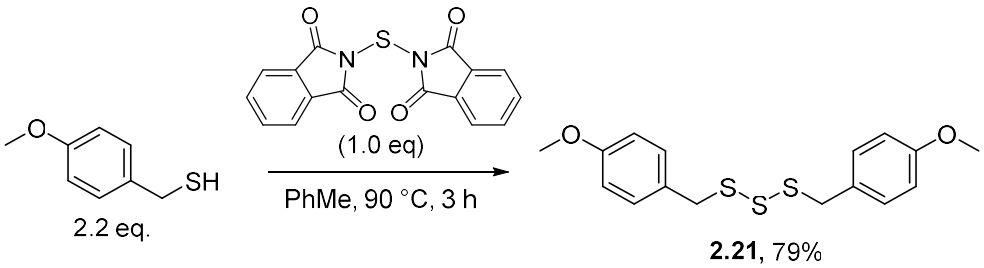

Figure 2.23: The synthesis of bis(4-methoxybenzyl) trisulfide.

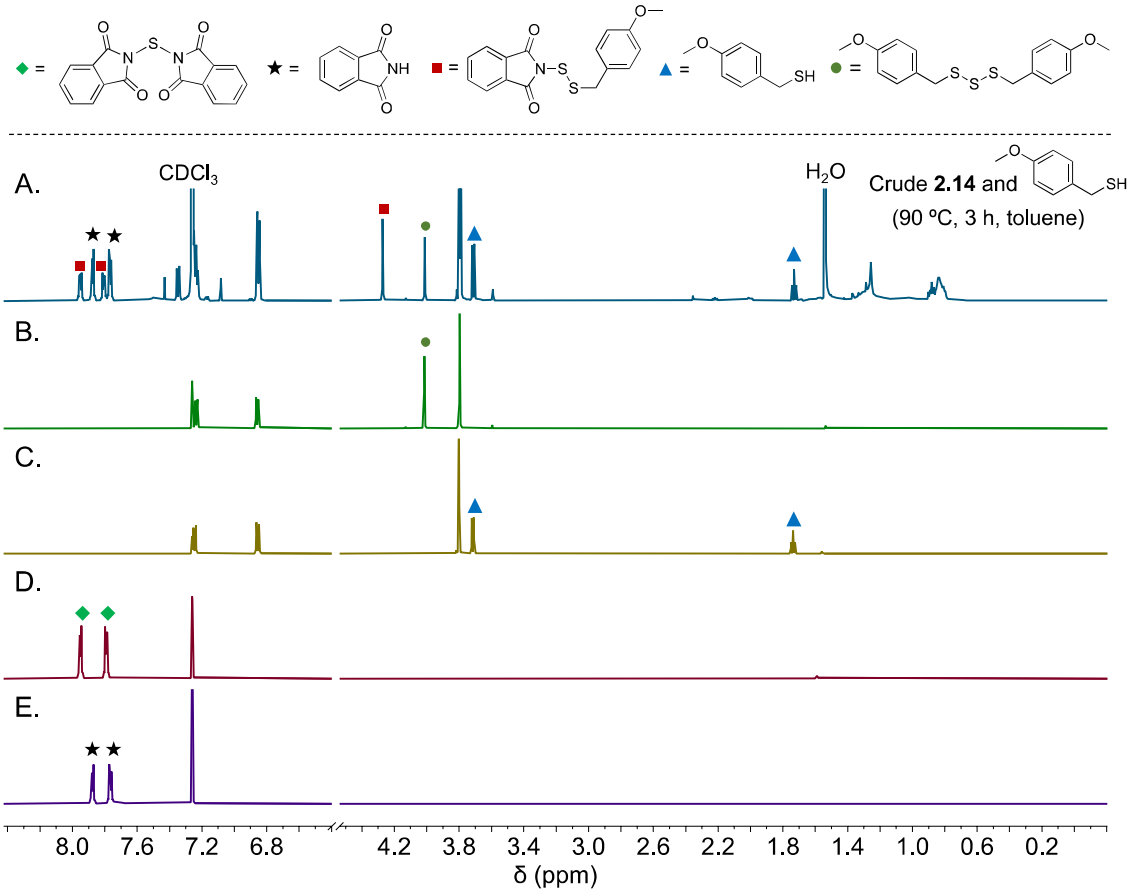

Figure 2.24: ^{1}H NMR studies of the reaction between *N,N'*-thiobisphthalimide (**2.14)** and 4-methoxybenzyl thiol at 90 ºC in toluene. ^{1}H NMR spectra of (A) the crude mixture after heating for 3 h heating, (B) bis(4-methoxybenzyl) trisulfide, (C) 4-methoxybenzyl thiol, (D) *N,N'*-thiobisphthalimide (**2.14**), and (E) phthalimide.

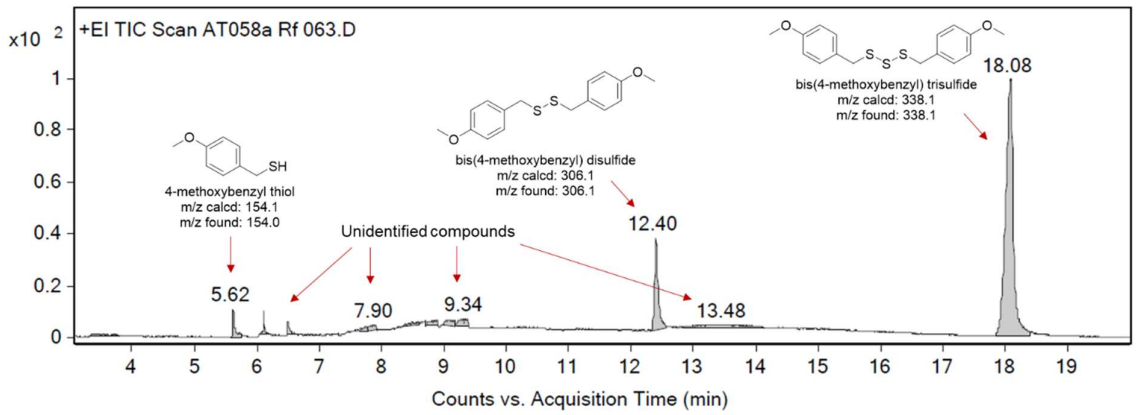

Figure 2.25: An attempt on the analysis of bis(4-methoxybenzyl) trisulfide by GC-MS. A peak at 18.08 min indicated bis(4-methoxybenzyl) trisulfide with m/z found 338.1, while the disulfide is observed at 12.40 min with m/z found 306.1. Other peaks were not identified.

Several trisulfides were prepared using several methods described above. This includes the preparation of new trisulfide compounds, diisobutyl trisulfide **2.4** and di-*n*-hexyl trisulfide **2.11**. Figure 2.26 summaries all trisulfides which were prepared and reported in this chapter. These compounds were critical in the study of the novel S-S metathesis reaction of trisulfides that is the focus of this thesis.

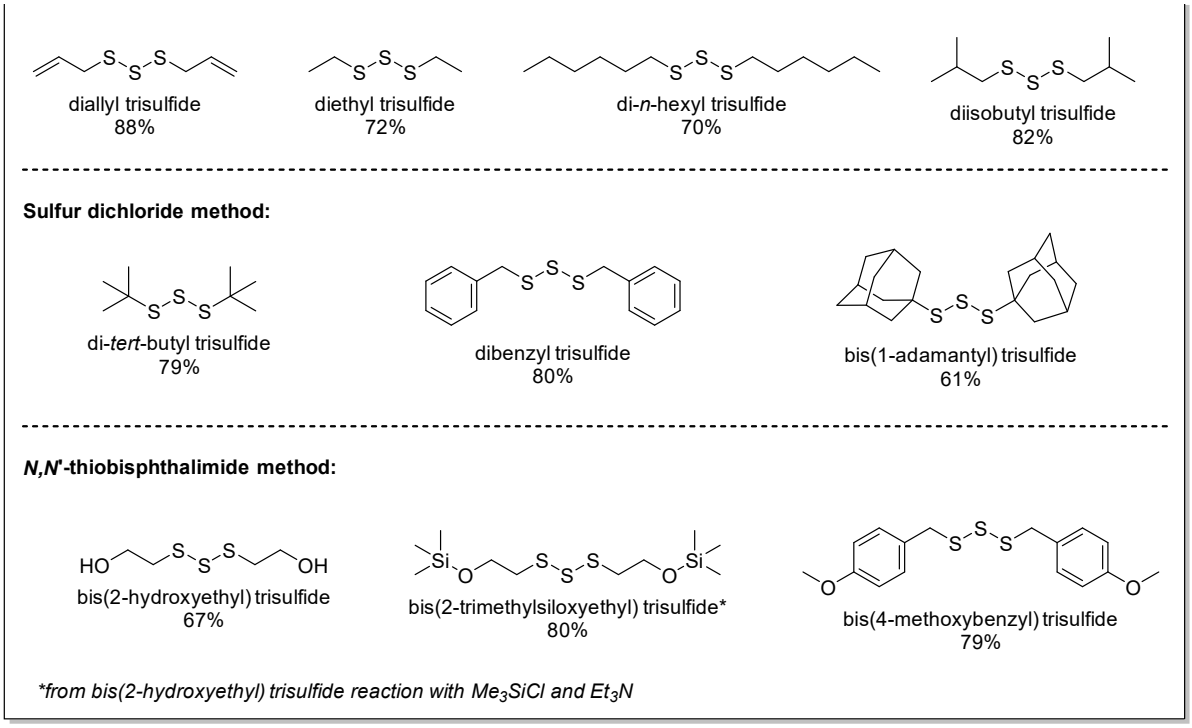

Figure 2.26: A summary of trisulfide syntheses reported in this chapter.

The synthesis of organic tetrasulfides

Three different tetrasulfides were also prepared: di-*n*-propyl tetrasulfide, dibenzyl tetrasulfide, bis(4-methoxybenzyl) tetrasulfide. These substrates were required so that S-S metathesis reactions of these unique compounds could be compared to trisulfides and disulfides. All tetrasulfides were synthesized from a thiol and sulfur monochloride (S_2Cl_2) with an amine as a base, e.g. pyridine, triethylamine, etc., in dry diethyl ether at a low reaction temperature (-78 ºC, acetone/dry ice bath) as shown in Figure 2.27. The reaction proceeds to the formation of alkyl- or arylchlorotrisulfide (RSSSCl) which is an intermediate. This intermediate further reacts with one equivalent of the thiol to form a tetrasulfide (Figure 2.2B, see the introduction section). This method was pioneered by Derbesy and Harpp[4], and it is a convenient method for the synthesis of organic tetrasulfides.

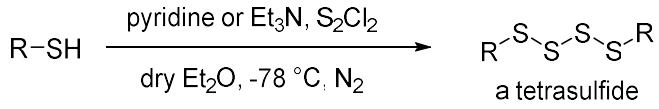

Figure 2.27: A general reaction for the synthesis of organic tetrasulfide

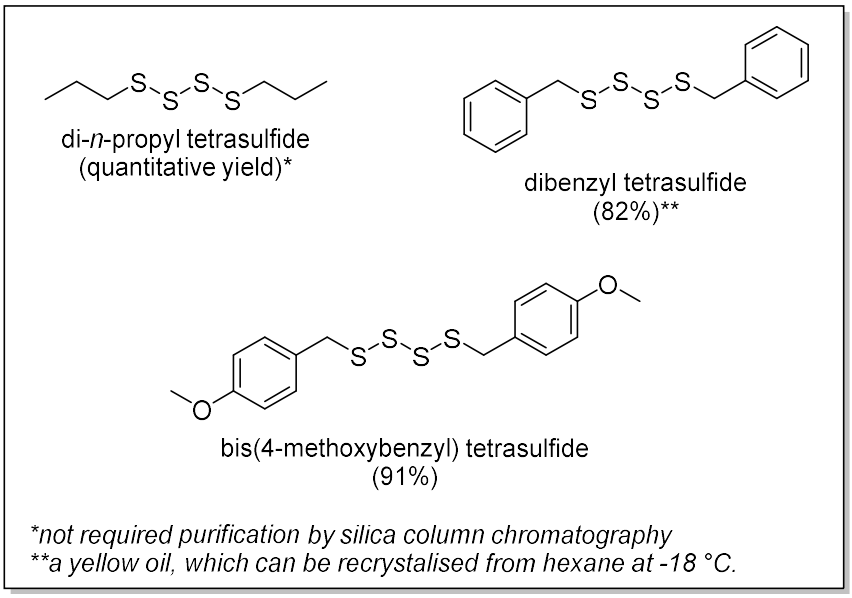

Figure 2.28: Organic tetrasulfides prepared from a thiol and sulfur monochloride.

Figure 2.28 summarises the synthesis and yields of three tetrasulfides. Overall, the synthesis of organic tetrasulfides is operationally simple and similar to that of the synthesis of organic trisulfides. It is relatively simple, as sulfur monochloride is more stable than sulfur dichloride. To access a tetrasulfide, sulfur monochloride was added to a stirred solution of a thiol and an amine (pyridine or triethylamine was used in this case) in anhydrous diethyl ether at -78 ºC. The reaction was stirred under a nitrogen atmosphere for a certain time. A slight excess of sulfur monochloride is typically used in the synthesis. To quench the remaining sulfur monochloride, water was then added

to the reaction mixture. Purification by chromatography on silica using either hexanes only or a mixture of ethyl acetate and hexanes afforded the tetrasulfides: dibenzyl tetrasulfide (yellow oil), bis(4-methoxybenzyl) tetrasulfide (yellow oil which solidifies into a yellow solid upon cooling in the fridge at around 4 – 5 °C). In the case of di-*n*-propyl tetrasulfide (yellow oil), this compound could be obtained in a quantitative yield without chromatographic purification.

2.4 Conclusion and Outlook

In conclusion, there are various methods available in literature for the synthesis of symmetrical trisulfides and tetrasulfides. For the synthesis of trisulfides, the method of choice depends on the starting material. Alkyl halides and sodium thiosulfate can be converted to the sodium *S*-alkyl thiosulfate, which is a precursor for making the trisulfide. The subsequent addition of sodium sulfide to the thiosulfate salt results in the formation of dialkyl trisulfide. A successful modification of this reaction through the addition of paraformaldehyde has led to the formation of highly pure trisulfide. However, this method was found to not suitable for the synthesis of dibenzyl trisulfide. This phenomenon will be studied in the future to understand the mechanism.

A direct conversion of thiols to their corresponding trisulfides can also be carried out using sulfur dichloride. The only problem arising from using this sulfur transfer reagent is that sulfur dichloride tends to decompose into sulfur monochloride; thus, this method frequently produces trisulfide with disulfide and tetrasulfide contaminants. The use of freshly distilled sulfur dichloride while maintaining the reaction at -78 °C is essential to minimise these side reactions. In addition, this method is efficient for the synthesis of trisulfides as it allows the reaction to take place within 1 – 2 hours. Despite of having this stability issue, sulfur dichloride is still a reagent of choice for the synthesis of organic trisulfides. Moreover, an amine such as pyridine and triethylamine can be used as a base for nucleophilic enhancement for the reaction. Additionally, diphenyl trisulfide was successfully synthesized but this trisulfide was not stable, which was an interesting discovery. This trisulfide was transformed to diphenyl disulfide after leaving at room temperature in dark condition for around 6 hours. This interesting and spontaneous desulfurization will be studied in the future.

N,N'-thiobisphthalimide was reported here as an alternative monosulfur transfer reagent in order to overcome the issue of using sulfur dichloride for the synthesis of trisulfide. This monosulfur transfer reagent can be conveniently synthesized from phthalimide and sulfur monochloride in DMF. This reagent here was used to synthesize bis(2-hydroxyethyl) trisulfide and bis(4-methoxybenzyl) trisulfide in a good to excellent yield in a one-pot reaction. Although a slight excess of thiol was used in the synthesis, after certain time the mixture also contains *N*-(thiosulfenyl) phthalimide as a by-product. The synthesis can also be done in two steps which was reported previously by Ercole et al.[34] However, this two-step reaction is not quite practical and time-consuming, particularly when the yield is comparable to the literature report. Bis(2-trimethylsiloxyethyl) trisulfide, a hydroxylated protected trisulfide, was also synthesized employing *N,N'*-thiobisphthalimide and β-

mercaptoethanol. Silylation of bis(2-hydroxyethyl) trisulfide using chlorotrimetylsilane (Me_3SiCl) gave the silyl protected trisulfide in a very good yield. This compound is purposely prepared for substrate investigations in the S-S metathesis study.

Lastly, several tetrasulfides were also synthesized for the investigation of S-S metathesis. The tetrasulfides can be accessed from thiols and sulfur monochloride in the presence of amine base such as pyridine and triethylamine in a one pot reaction. Owing to its stability, sulfur monochloride was used as the main reagent to make tetrasulfides.

2.5 References

(1) Milligan, B.; Saville, B.; Swan, J. M. 954. New syntheses of trisulphides. *J. Chem. Soc.* **1961**, (0), 4850-4853. DOI: 10.1039/JR9610004850.

(2) Milligan, B.; Saville, B.; Swan, J. M. 680. Trisulphides and tetrasulphides from Bunte salts. *J. Chem. Soc.* **1963**, 3608-3614. DOI: 10.1039/JR9630003608.

(3) Bhattacherjee, D.; Sufian, A.; Mahato, S. K.; Begum, S.; Banerjee, K.; De, S.; Srivastava, H. K.; Bhabak, K. P. Trisulfides over disulfides: highly selective synthetic strategies, anti-proliferative activities and sustained H_2S release profiles. *Chem. Commun.* **2019**, *55* (90), 13534-13537. DOI: 10.1039/C9CC05562B.

(4) Derbesy, G.; Harpp, D. N. A simple method to prepare unsymmetrical di- tri- and tetrasulfides. *Tetrahedron Lett.* **1994**, *35* (30), 5381-5384. DOI: 10.1016/S0040-4039(00)73505-2.

(5) Harpp, D. N.; Steliou, K.; Chan, T. H. Organic sulfur chemistry. 26. Synthesis and reactions of some new sulfur transfer reagents. *J. Am. Chem. Soc.* **1978**, *100* (4), 1222-1228. DOI: 10.1021/ja00472a032.

(6) Reeves, J. T.; Camara, K.; Han, Z. S.; Xu, Y.; Lee, H.; Busacca, C. A.; Senanayake, C. H. The Reaction of Grignard Reagents with Bunte Salts: A Thiol-Free Synthesis of Sulfides. *Org. Lett.* **2014**, *16* (4), 1196-1199. DOI: 10.1021/ol500067f.

(7) Distler, H. The Chemistry of Bunte Salts. *Angew. Chem., Int. Ed. Engl.* **1967**, *6* (6), 544-553. DOI: 10.1002/anie.196705441.

(8) Clayton, J.; Etzler, D. New Compounds. Hexadecyl Trisulfide and Hexadecyl Tetrasulfide. *J. Am. Chem. Soc.* **1947**, *69* (4), 974-975. DOI: 10.1021/ja01196a600.

(9) Lowry, T. M.; Jessop, G. CLXXXII.—The properties of the chlorides of sulphur. Part II. Molecular extinction coefficients. *J. Chem. Soc.* **1929**, (0), 1421-1435. DOI: 10.1039/JR9290001421.

(10) Chakravarti, G. C. CX.—Action of sulphur monochloride on mercaptans. *J. Chem. Soc., Trans.* **1923**, *123* (0), 964-968. DOI: 10.1039/CT9232300964.

(11) Derbesy, G. Synthesis and Oxidative Reactivity of Organopolysulphides. McGill University, Canada, 1994. https://escholarship.mcgill.ca/concern/theses/t148fk37t?locale=en.

(12) Zysman-Colman, E.; Harpp, D. N. Optimization of the Synthesis of Symmetric Aromatic Tri- and Tetrasulfides. *J. Org. Chem.* **2003**, *68* (6), 2487-2489. DOI: 10.1021/jo0265481.

(13) Brauer, G. *Handbook of Preparative Inorganic Chemistry*; Academic Press, 1963.

(14) Clayden, J.; Greeves, N.; Warren, S. *Organic chemistry*; Oxford University Press, USA, 2012.

(15) Nogueira, M. I.; Barbieri, C.; Vieira, R.; Marques, E.; Moreno, J. A practical device for histological fixative procedures that limits formaldehyde deleterious effects in laboratory environments. *J. Neurosci. Methods* **1997**, *72* (1), 65-70.

(16) Paananen, H.; Pakkanen, T. T. Kraft lignin reaction with paraformaldehyde. *Holzforschung* **2020**, *74* (7), 663-672. DOI: 10.1515/hf-2019-0147.

(17) Böhme, H.; Schneider, E. Struktur und Hydrolyse der Schwefelchloride. *Ber. dtsch. Chem. Ges. A/B* **1943**, *76* (5), 483-486. DOI: 10.1002/cber.19430760507.

(18) Rougee, M.; Bensasson, R.; Land, E. J.; Pariente, R. Deactivation of singlet molecular oxygen by thiols and related compounds, possible protectors against skin photosensitivity. *Photochem. Photobiol.* **1988**, *47* (4), 485-489. DOI: 10.1111/j.1751-1097.1988.tb08835.x.

(19) Devasagayam, T. P.; Sundquist, A. R.; Di Mascio, P.; Kaiser, S.; Sies, H. Activity of thiols as singlet molecular oxygen quenchers. *J. Photochem. Photobiol. B* **1991**, *9* (1), 105-116. DOI: 10.1016/1011-1344(91)80008-6.

(20) Clennan, E. L.; Stensaas, K. L. Recent progress in the synthesis, properties and reactions of trisulfanes and their oxides. *Org. Prep. Proced. Int.* **1998**, *30* (5), 551-600. DOI: 10.1080/00304949809355321.

(21) Harpp, D. N.; Ash, D. K.; Smith, R. A. Organic sulfur chemistry. 38. Desulfurization of organic trisulfides by tris(dialkylamino)phosphines. Mechanistic aspects. *J. Org. Chem.* **1980**, *45* (25), 5155-5160. DOI: 10.1021/jo01313a026.

(22) Xi, W.; Peng, H.; Aguirre-Soto, A.; Kloxin, C. J.; Stansbury, J. W.; Bowman, C. N. Spatial and Temporal Control of Thiol-Michael Addition via Photocaged Superbase in Photopatterning and Two-Stage Polymer Networks Formation. *Macromolecules* **2014**, *47* (18), 6159-6165. DOI: 10.1021/ma501366f.

(23) Northrop, B. H.; Frayne, S. H.; Choudhary, U. Thiol–maleimide “click” chemistry: evaluating the influence of solvent, initiator, and thiol on the reaction mechanism, kinetics, and selectivity. *Polym. Chem.* **2015**, *6* (18), 3415-3430. DOI: 10.1039/C5PY00168D.

(24) Pickering, T. L.; Saunders, K. J.; Tobolsky, A. V. Disproportionation of organic polysulfides. *J. Am. Chem. Soc.* **1967**, *89* (10), 2364-2367. DOI: 10.1021/ja00986a021.

(25) Harpp, D. N.; Smith, R. A. Reaction of trialkyl phosphites with organic trisulfides. Synthetic and mechanistic aspects. *J. Org. Chem.* **1979**, *44* (23), 4140-4144. DOI: 10.1021/jo01337a026.

(26) Sirakawa, K.; Aki, O.; Tsujikawa, T.; Tsuda, T. S-Alkylthioisothioureas. I. *Chem. Pharm. Bull.* **1970**, *18* (2), 235-242. DOI: 10.1248/cpb.18.235.

(27) Gorjian, H.; Khaligh, N. G. 3,4-Dichloro-1,2,5-thiadiazole: a commercially available electrophilic sulfur transfer agent and safe resource of ethanedinitrile. *J. Sulfur Chem.* **2022**, *43* (2), 169-179. DOI: 10.1080/17415993.2021.1991928.

(28) Pavelko, G. Correlation between thermochemical and antiscuff characteristics of organosulfur compounds. *J. Frict. Wear.* **2012**, *33*, 443-452. DOI: 10.3103/S1068366612060086.

(29) Павелко, Г. Ф.; Олейник, Д. М.; Багрий, Е. И. ОРГАНИЧЕСКИЕ СУЛЬФИДЫ – СИНТЕТИЧЕСКИЕ ПРИСАДКИ, СНИЖАЮЩИЕ ТРЕНИЕ И ИЗНОС [ORGANIC SULFIDES - SYNTHETIC ADDITIVES FOR DECREASING FRICTION AND WEAR]. *НЕФТЕХИМИЯ [PETROLEUM CHEMISTRY]* **1989**, *29* (4), 547-550.

(30) Sabet, A.; Kolvari, E.; koukabi, N.; Fakhraee, A.; Ramezanpour, M.; Bahmannia, G. Oxidative coupling of aromatic thiols to corresponding disulfides using magnetic particle-supported sulfonic acid catalyst and hydrogen peroxide under mild conditions. *J. Sulfur Chem.* **2015**, *36* (3), 300-307. DOI: 10.1080/17415993.2015.1024120.

(31) Wu, M.; Bhargav, A.; Cui, Y.; Siegel, A.; Agarwal, M.; Ma, Y.; Fu, Y. Highly Reversible Diphenyl Trisulfide Catholyte for Rechargeable Lithium Batteries. *ACS Energy Lett.* **2016**, *1* (6), 1221-1226. DOI: 10.1021/acsenergylett.6b00533.

(32) Kalnins, M. V. Reactions of phthalimide and potassium phthalimide with sulfur monochloride. *Can. J. Chem.,* **1966**, *44* (17), 2111-2113. DOI: 10.1139/v66-318.

(33) Dao, N. V.; Ercole, F.; Kaminskas, L. M.; Davis, T. P.; Sloan, E. K.; Whittaker, M. R.; Quinn, J. F. Trisulfide-Bearing PEG Brush Polymers Donate Hydrogen Sulfide and Ameliorate Cellular Oxidative Stress. *Biomacromolecules* **2020**, *21* (12), 5292-5305. DOI: 10.1021/acs.biomac.0c01347.

(34) Ercole, F.; Li, Y.; Whittaker, M. R.; Davis, T. P.; Quinn, J. F. H2S-Donating trisulfide linkers confer unexpected biological behaviour to poly(ethylene glycol)–cholesteryl conjugates. *J. Mater. Chem. B* **2020**, *8* (17), 3896-3907. DOI: 10.1039/C9TB02614B.

(35) Trofimov, B. A.; Markova, M. V.; Morozova, L. V.; Prozorova, G. F.; Korzhova, S. A.; Cho, M. D.; Annenkov, V. V.; Al'bina, I. M. Protected bis (hydroxyorganyl) polysulfides as modifiers of Li/S battery electrolyte. *Electrochim. Acta* **2011**, *56* (5), 2458-2463.

2.6 Experimental Details and Characterizations

General Considerations

Analytical thin-layer chromatography was conducted with commercial aluminium sheets coated with silica gel (Chem-supply, silica gel 60 F254). Compounds were either visualized under UV-light at 254 nm, or by dipping the plates in aqueous potassium permanganate or ceric ammonium molybdate solution followed by heating. Flash column chromatography was performed using either a glass chromatography column or a Biotage Selekt Flash Chromatography Instrument, with either silica gel (6 Å, 40 – 63 μm) or Biotage Sfär Silica (60 μm). Melting point (m.p.) was determined using either a Gallenkamp, or a DigiMelt 161 SRS (Stanford Research System), melting point apparatus using open ended capillary tubes.

Chemicals were purchased from commercial suppliers and used as received. Dry diethyl ether was obtained from solvent purification system and stored over 3Å molecular sieves. Pyridine and triethylamine were distilled and stored over 3Å molecular sieves and KOH pellets. Deionized water was used for chemical reactions. Brine refers to a saturated solution of sodium chloride. Anhydrous sodium sulfate (Na_2SO_4) or magnesium sulfate ($MgSO_4$) were used as drying agents after reaction workup, as indicated.

NMR (Nuclear Magnetic Resonance) Spectroscopy

^{1}H and ^{13}C NMR spectra were recorded on a Bruker Ultrashield Plus 600 MHz spectrometer at 600 MHz and 150 MHz respectively, or a Bruker Ascend 400 MHz spectrometer at 400 MHz and 100 MHz, respectively. All spectra were obtained at 298 K unless stated otherwise. Deuterated solvents were used as solvent and internal lock unless stated otherwise. Residual solvent peaks were used as an internal reference for ^{1}H NMR spectra [$CDCl_3$ δ 7.26 ppm; DMF-d_7 δ 8.03 ppm; Toluene-d_8 δ 7.09, 2.09 ppm] and for ^{13}C NMR spectra [$CDCl_3$ δ 77.16 ppm, DMF-d_7 δ 163.15 ppm; Toluene-d_8 δ 137.86 ppm].[1,2] Coupling constants (*J*) are quoted to the nearest 0.1 Hz. The following abbreviations, or combinations thereof, were used to describe NMR multiplicities: s = singlet, d = doublet, t = triplet, q = quartet, p = pentet, h = heptet, m = multiplet, ap. = apparent, br. = broad).

GC-MS (Gas Chromatography Mass Spectrometry)

GC-MS analysis was performed using an Agilent 5975C series GC-MS system. A 29.4 m x 250 μm x 0.25 μm, (5%-phenyl)-methylpolysiloxane column was used with a helium mobile phase. A 1 μL sample was injected with a split ratio of 60:1 and a gas flow rate of 1.2 mL/min. The following GC-MS methods were used for experiments as indicated:

GC-MS method **A**: Initial temperature 30 ºC. Hold at 30 ºC for 3 minutes. Ramp rate at 20 ºC/min to 250 ºC. Hold at 250 ºC for 6 minutes. Total run time was 20 minutes.

GC-MS method **B**: Initial temperature 85 ºC. Hold at 85 ºC for 3 minutes. Ramp rate at 50 ºC/min to 250 ºC. Hold at 250 ºC for 13.7 minutes. Total run time was 20 minutes.

GC-MS method **C**: Initial temperature 50 ºC. Hold at 50 ºC for 3 minutes. Ramp rate at 30 ºC/min to 250 ºC. Hold at 250 ºC for 20 minutes. Total run time of 29.667 minutes.

GC-MS method **D**: Initial temperature 85 ºC. Hold at 85 ºC for 3 minutes. Ramp rate at 10 ºC/min to 250 ºC. Hold at 250 ºC for 40 minutes. Total run time of 59.5 minutes.

FTIR (Fourier-transform infrared spectroscopy)

FTIR spectra were recorded between 4000 and 450 cm^{-1}, using either a Perkin Elmer Spectrum Two FT-IR Spectrometer equipped with a Universal ATR (Diamond Crystal), or a PerkinElmer Spectrum 100 FT-IR spectrometer equipped with ATR accessory (ZnSe crystal). Absorption maxima (ν_{max}) are reported in wavenumbers (cm^{-1}).

Elemental Analysis (CHNS)

Elemental analysis was performed by combustion analysis at the Chemical Analysis Facility at Macquarie University Analytical & Fabrication Facility. Elemental analysis was performed on Elementar vario MICRO (Elementar Analysensysteme GmbH). The instrument hardware was configured for the analysis of 4 elements (C, H, N and S). In a typical procedure, 1 – 2 mg of sample material was loaded into a tin foil boat and combusted at 1150 °C with oxygen dosing time of 80 s and total O_2 flow rate of 30 mL/min. Ultra-high purity grade helium (BOC, 99.999%) and oxygen (BOC, 99.995%) were employed as working fluids in all cases. Pure sulphanilamide was employed as a standard with quality control samples performed every 15-20 runs. The follow-up data analysis was performed using a custom peak picking and integration algorithm written in Python 3.11.

HRMS (High resolution mass spectrometry)

HRMS was recorded on a Waters Synapt HDMS Q-ToF by electrospray ionization (ESI). Where applicable, samples were dissolved in acetonitrile with silver nitrate 0.1% w/v, whereby $[M+Ag]^+$ values are quoted using ^{107}Ag.

Trisulfides synthesis from sodium thiosulfate and sodium sulfide

Trisulfide synthesis using a procedure by Bhattacherjee et al.[3] (method A)

General procedure

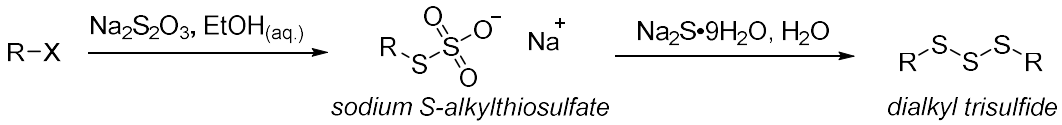

Synthesis of sodium S-alkylthiosulfate. To a 20 mL glass vial equipped with a stir bar was added sodium thiosulfate pentahydrate (2.98 g, 12 mmol, 1.2 eq.) and 10 mL of 30% v/v ethanol. The mixture was stirred until all sodium thiosulfate dissolved. The alkyl halide (10 mmol, 1.0 eq.) was added to the stirred solution giving a cloudy mixture, which was heated at 65 °C until a homogenous clear solution formed. After several minutes the mixture was homogeneous (***except for isobutyl bromide where the mixture became homogenous after around 6 hours***) and heating was continued for several hours. The solvent was then removed under reduced pressure to give a solid consisting of sodium *S*-alkylthiosulfate. The obtained thiosulfate salt was used without further purification.

Synthesis of dialkyl trisulfide. In a 100 mL round bottom flask, crude sodium S-alkyl thiosulfate (10 mmol, 1 eq., considering all alkyl bromide was converted to its thiosulfate salt) was dissolved in 25 mL of water and cooled to 0 ºC. To this stirred solution of sodium *S*-alkyl thiosulfate was added dropwise (~15 min) a pre-cooled solution of sodium sulfide nonahydrate (1.20 g, 5 mmol, 0.5 eq.) dissolved in 25 mL of water. Next, the mixture was stirred for 8 hours at 0 ºC using an ice bath. The product was then isolated by extraction using ethyl acetate (30 mL x 4). The extract was washed with brine (10 mL x 2). The combined organic layer was dried over anhydrous sodium sulfate and the solvent was evaporated under reduced pressure to afford crude trisulfide. NMR analysis of the crude trisulfide indicated the presence of disulfide as a minor product. No attempt for purification by column chromatography since the polarity of the obtained trisulfide and disulfide was similar. Only dibenzyl trisulfide that was purified by recrystallization from 100% hexane.

Diallyl trisulfide (2.2) – method A

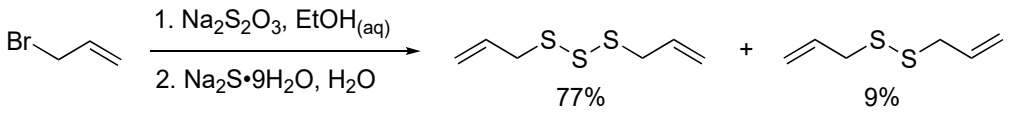

Diallyl trisulfide was synthesised following the general procedure using allyl bromide (864 µL, 10 mmol, 1.0 eq.). Heating at 65 ºC gave a clear yellow solution (around 5 minutes) and was continued for a total of 4 hours. Solvent removal under reduced pressure gave a pale-yellow solid of sodium *S*-allylthiosulfate. The solid was dissolved in water and reacted with sodium sulfide solution for a total of 8 hours (15 minutes for sodium sulfide addition). Following workup, diallyl trisulfide was obtained as a clear pale-yellow oil (766.0 mg, 86% yield, diallyl trisulfide ≥ 90% purity confirmed by ^{1}H NMR spectroscopy). The obtained spectral data is in agreement with the literature.[3, 4]

Sodium *S*-allylthiosulfate (2.1) – method A

^{1}H NMR (600 MHz, D_2O) δ 6.05 (ddtd, *J* = 17.05, 10.05, 7.06, 0.58 Hz, 1H), 5.40 – 5.32 (m, 1H), 5.23 (ddt, *J* = 9.89, 1.56, 0.77 Hz, 1H), 3.80 – 3.77 (m, 2H). **^{13}C NMR** (150 MHz, D_2O) δ 133.2, 118.4, 37.7.

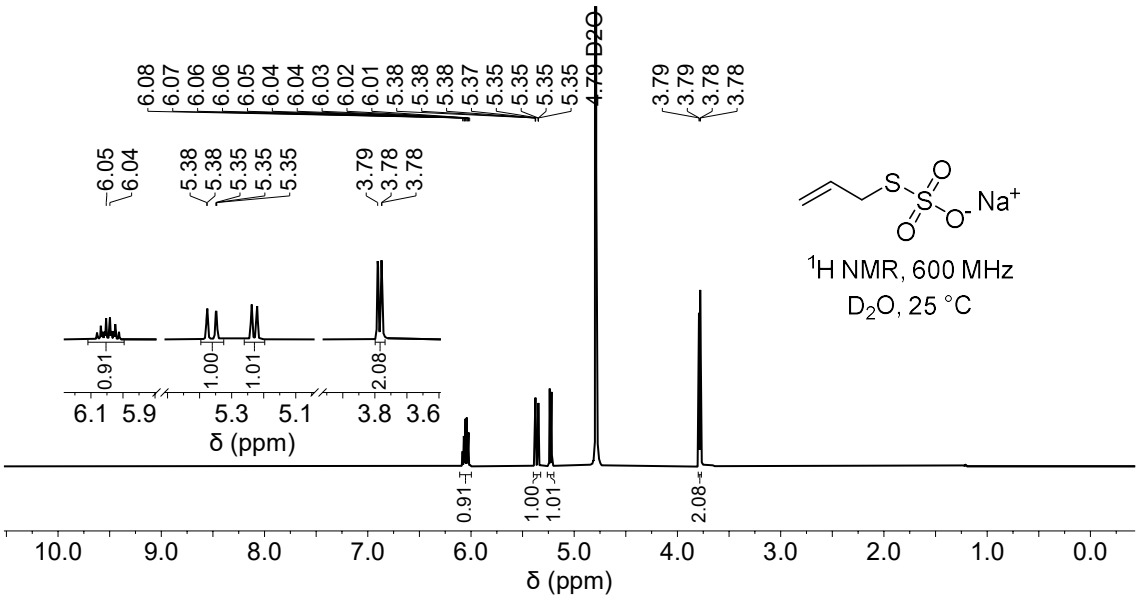

Figure S2.1: ^{1}H NMR spectrum of sodium *S*-allylthiosulfate

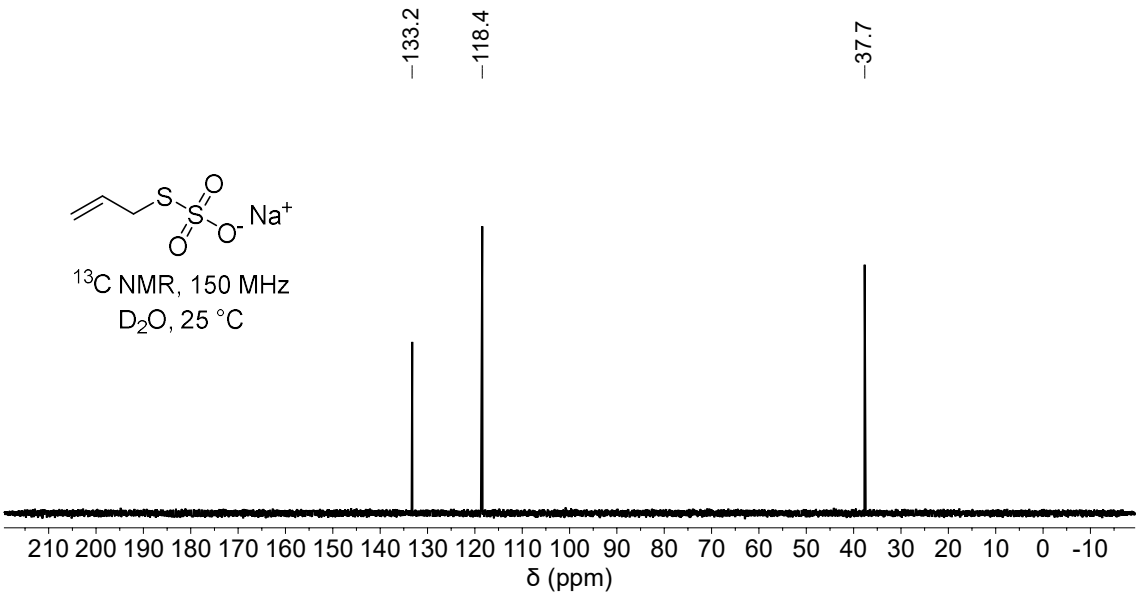

Figure S2.2: ^{13}C NMR spectrum of sodium *S*-allylthiosulfate

Diallyl trisulfide (2.2) – method A

^{1}H NMR (600 MHz, $CDCl_3$) δ 5.89 (ddt, *J* = 17.18, 9.97, 7.30 Hz, 1H), 5.28 – 5.18 (m, 2H), 3.51 (dt, *J* = 7.27, 1.03 Hz, 2H). **^{13}C NMR** (151 MHz, $CDCl_3$) δ 133.1, 119.5, 42.0.

Diallyl disulfide

^{1}H NMR (600 MHz, $CDCl_3$) δ 5.85 – 5.81 (m, 1H), 5.18 – 5.13 (m, 3H), 3.34 (dt, *J* = 7.34, 1.03 Hz, 4H). **^{13}C NMR** (151 MHz, $CDCl_3$) δ 133.8, 118.8, 42.6.

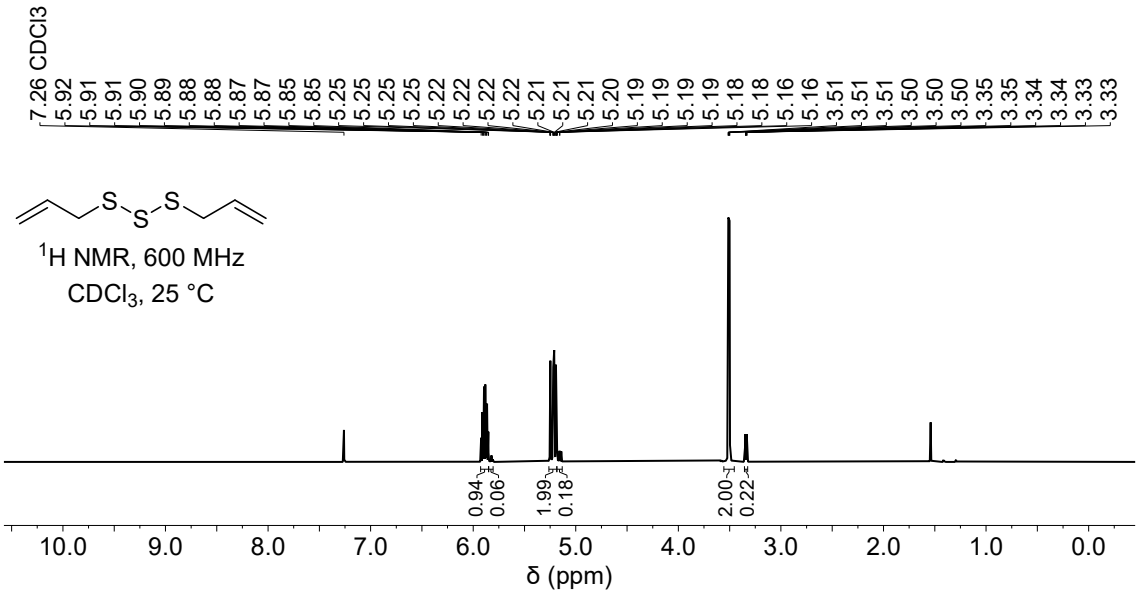

Figure S2.3: ^{1}H NMR spectrum of diallyl trisulfide (method A)

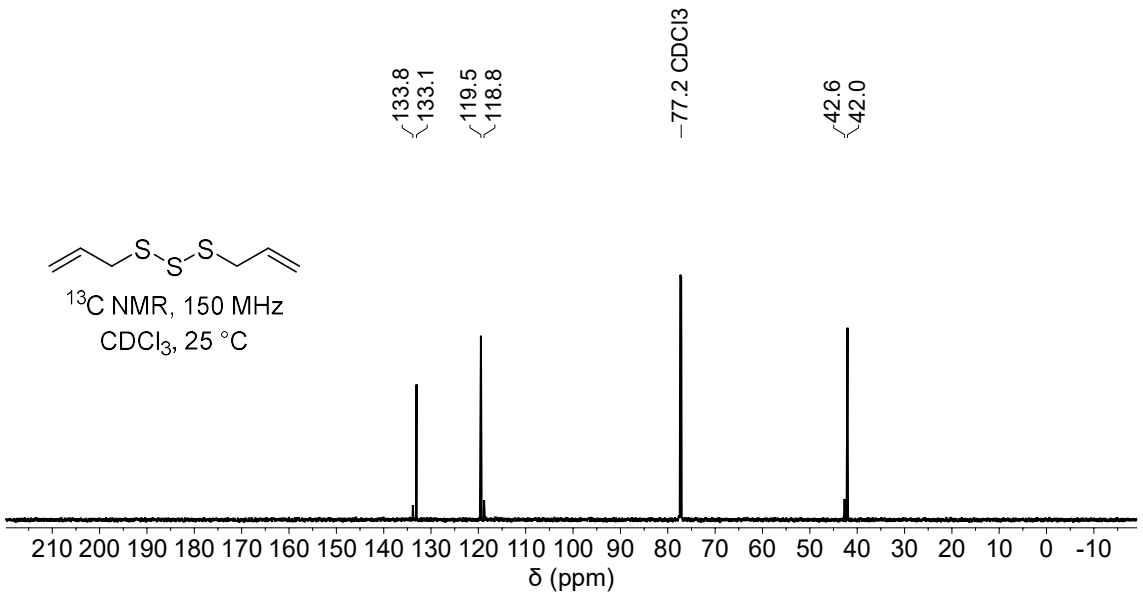

Figure S2.4:^{13}C NMR spectrum of diallyl trisulfide (method A)

Di-*iso*-butyl trisulfide (2.4) – method A

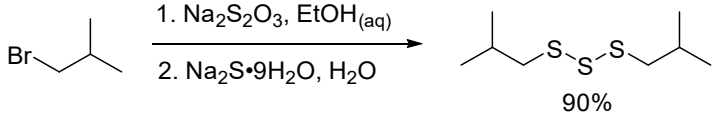

Di-*iso*-butyl trisulfide was synthesised following the general procedure using 1-bromo-2-methylpropane (1.087 mL, 10 mmol, 1.0 eq.). Heating at 65 ºC gave a clear solution (around 6 hours) and was continued for a total of 16 hours. Solvent removal under reduced pressure gave a white solid of sodium *S*-isobutylthiosulfate. The solid was dissolved in water and reacted with sodium sulfide solution for a total of 8 hours (15 minutes for sodium sulfide addition). Following workup, di-*iso*-butyl trisulfide was obtained as a beige oil (955.9 mg, 90% yield, ≥ 97% purity confirmed by ^{1}H NMR spectroscopy).

Sodium *S*-isobutyl thiosulfate (2.3) – method A

^{1}H NMR (600 MHz, D_2O) δ 3.03 (d, *J* = 6.89 Hz, 2H), 2.04 (n, *J* = 13.46, 6.73 Hz, 1H), 1.02 (d, *J* = 6.67 Hz, 6H). **^{13}C NMR** (151 MHz, D_2O) δ 43.6, 27.9, 21.0.

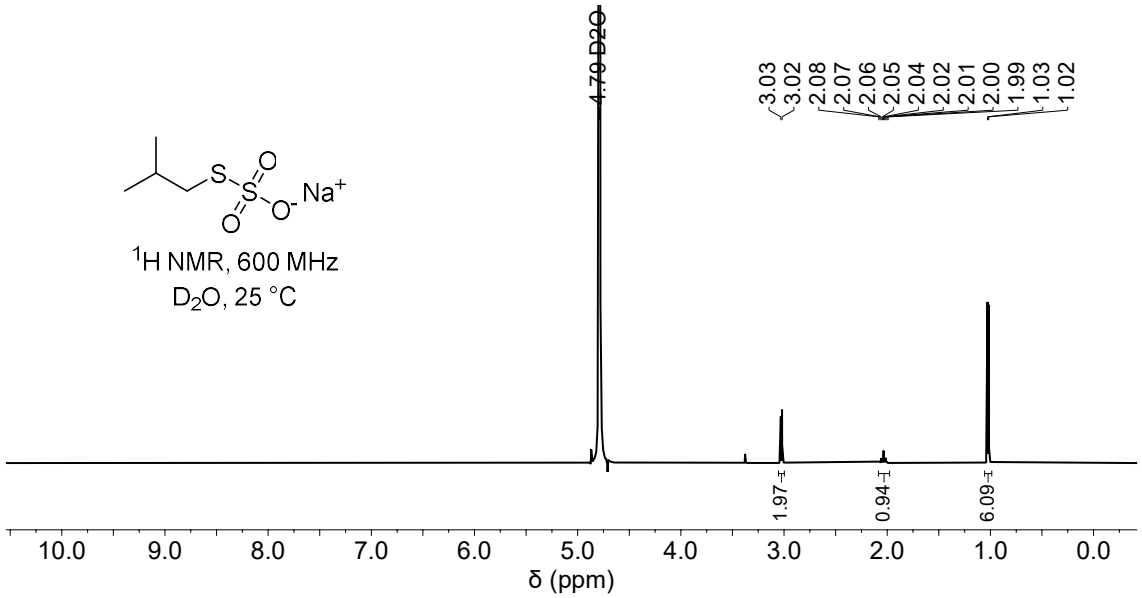

Figure S2.5: ^{1}H NMR spectrum of sodium *S*-isobutylthiosulfate

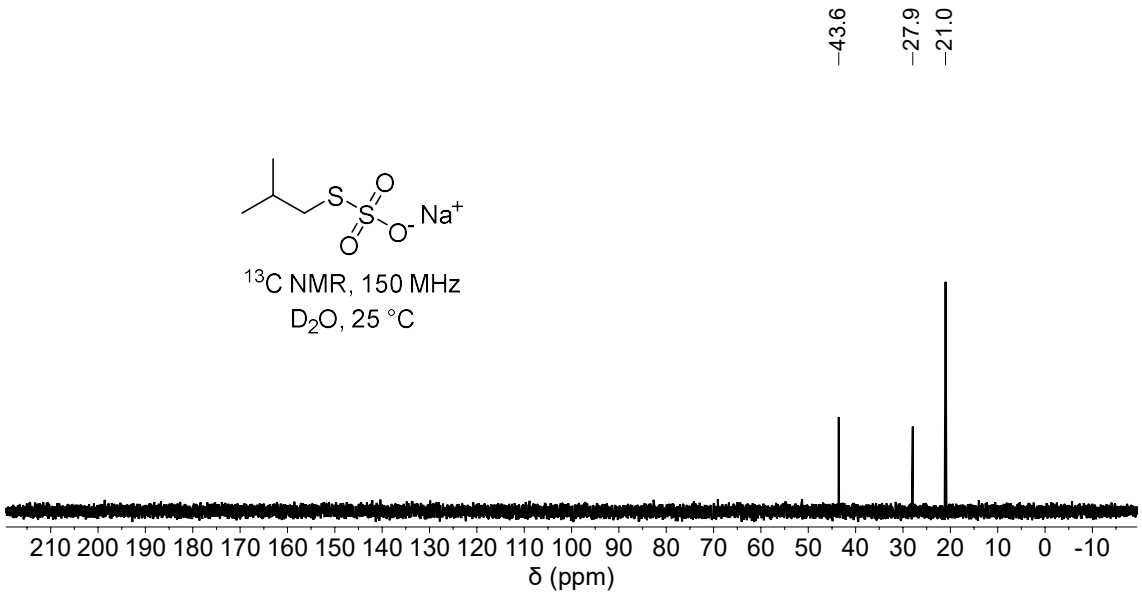

Figure S2.6: ^{13}C NMR spectrum of sodium *S*-isobutylthiosulfate

Di-*iso*-butyl trisulfide (2.4) – method A

^{1}H NMR (600 MHz, $CDCl_3$) δ 2.78 (d, *J* = 6.86 Hz, 4H), 2.04 (n, *J* = 13.44, 6.72 Hz, 2H), 1.02 (d, *J* = 6.69 Hz, 12H). **^{13}C NMR** (151 MHz, $CDCl_3$) δ 48.5, 28.1, 22.0.

Di-*iso*-butyl disulfide

^{1}H NMR (600 MHz, $CDCl_3$) δ 2.59 (d, *J* = 6.84 Hz, 4H), 1.98 – 1.90 (m, 2H), 1.00 (d, *J* = 6.68 Hz, 12H). **^{13}C NMR** (151 MHz, $CDCl_3$) δ 48.7, 28.3, 21.9.

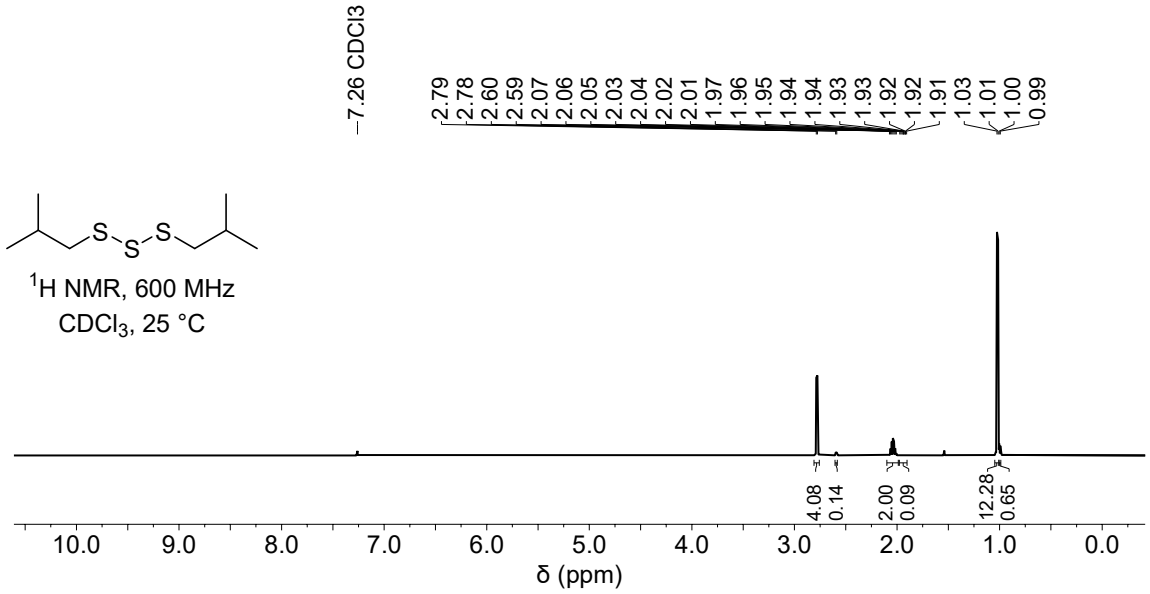

Figure S2.7: ^{1}H NMR spectrum of di-*iso*-butyl trisulfide

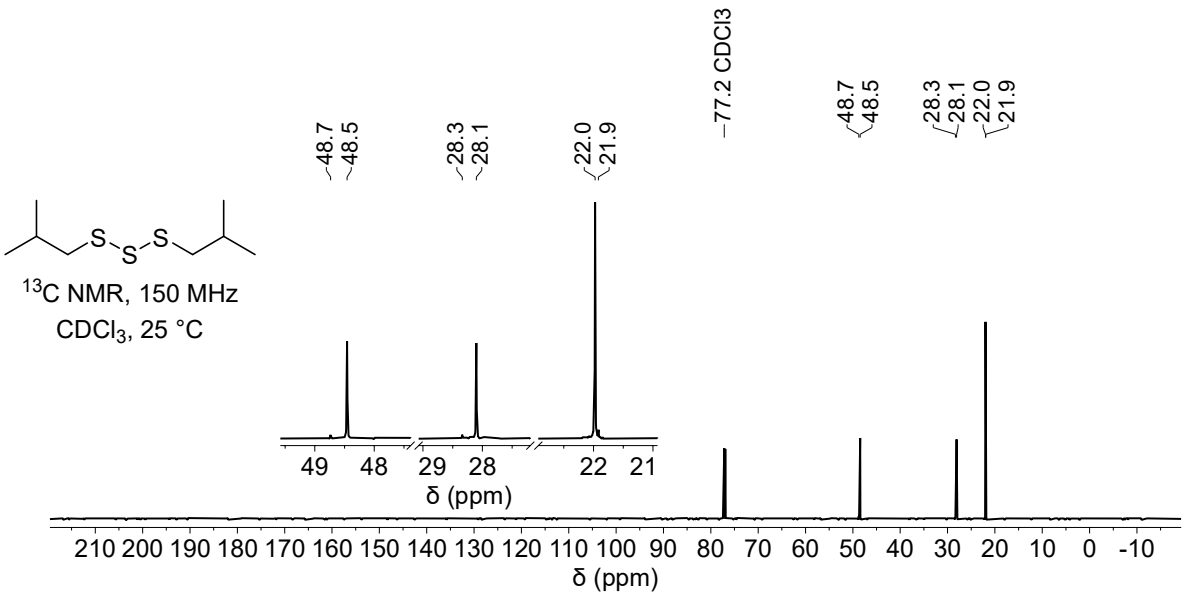

Figure S2.8: ^{13}C NMR spectrum of di-*iso*-butyl trisulfide

Dibenzyl trisulfide (2.6) – method A

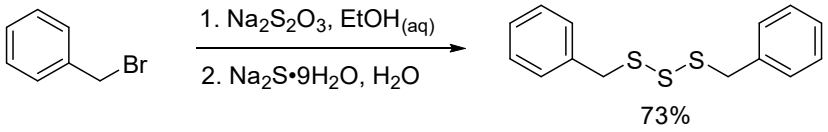

73%

Dibenzyl trisulfide was synthesised following the general procedure using benzyl bromide (1.19 mL, 10 mmol, 1.0 eq.). Heating at 65 ºC gave a clear solution (around 10 min) and was continued for a total of 4 hours. Solvent removal under reduced pressure gave a white solid of sodium *S*-benzylthiosulfate. The solid was dissolved in water and reacted with sodium sulfide solution for a total of 8 hours (15 minutes for sodium sulfide addition). Following workup, crude dibenzyl trisulfide was collected (1.27 g). This crude was dissolved in chloroform and filtered through silica gel (1 g). After solvent removal, the solid product was recrystallised from hexane to obtain dibenzyl trisulfide as a white solid in 73% yield (1.02 g, >99% purity confirmed by ^{1}H NMR spectroscopy). The obtained spectral data is in agreement with the literature.[3]

Sodium *S*-benzyl thiosulfate (2.5) – method A

^{1}H NMR (600 MHz, D_2O) δ 7.50 (d, *J* = 8.17 Hz, 2H), 7.45 (dd, *J* = 8.69, 6.74 Hz, 2H), 7.39 (t, *J* = 7.59 Hz, 1H), 4.38 (s, 2H). **^{13}C NMR** (151 MHz, D_2O) δ 136.8, 129.1, 128.9, 127.8, 39.0.

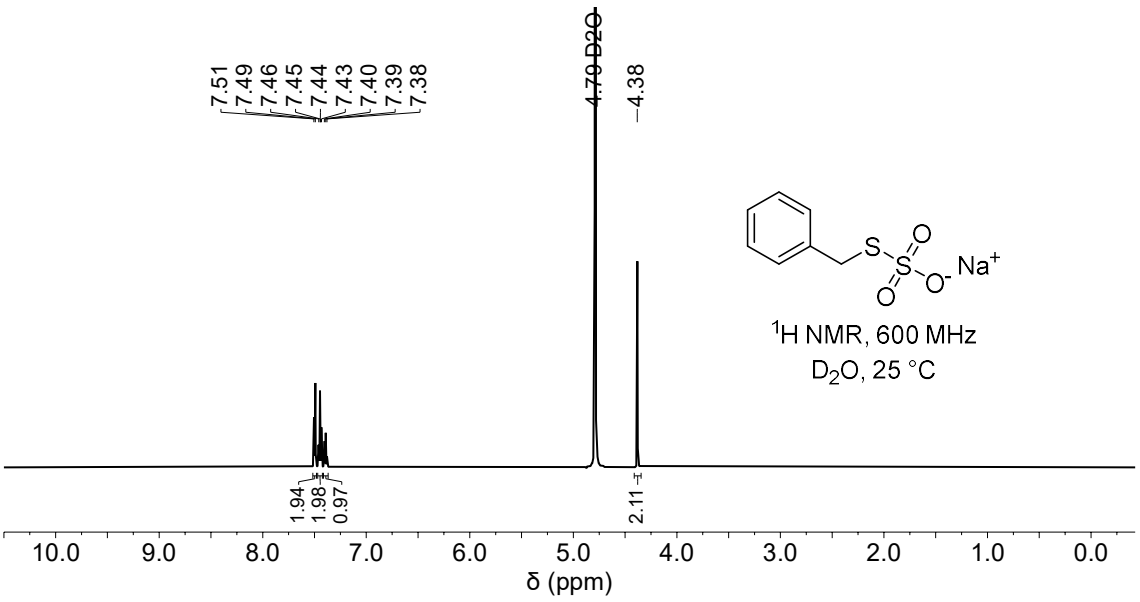

Figure S2.9: ^{1}H NMR spectrum of sodium *S*-benzyl thiosulfate

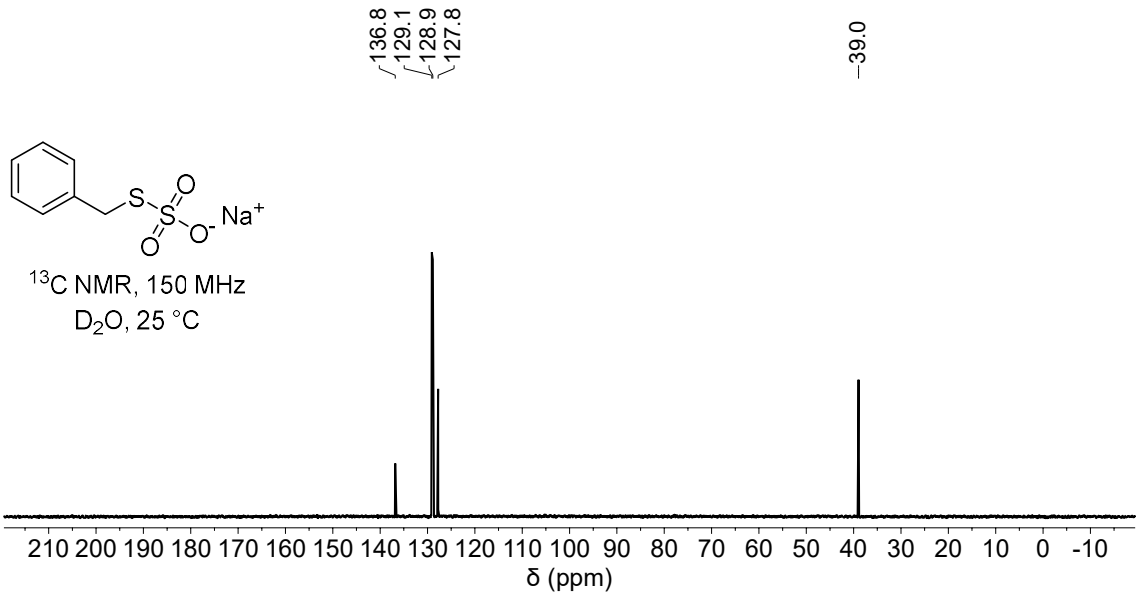

Figure S2.10: ^{13}C NMR spectrum of sodium *S*-benzylthiosulfate

Dibenzyl trisulfide (2.6) – method A

^{1}H NMR (600 MHz, $CDCl_3$) δ 7.38 – 7.31 (m, 8H), 7.31 – 7.26 (m, 2H), 4.04 (s, 4H). **^{13}C NMR** (151 MHz, $CDCl_3$) δ 136.7, 129.6, 128.8, 127.7, 43.3.

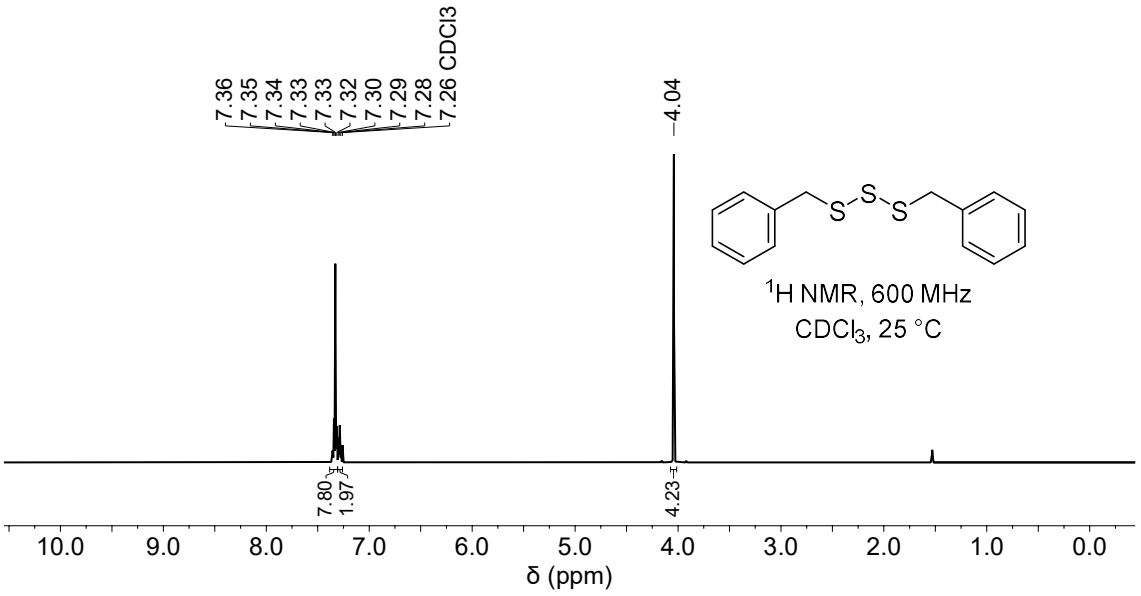

Figure S2.11: ^{1}H NMR spectrum of dibenzyl trisulfide

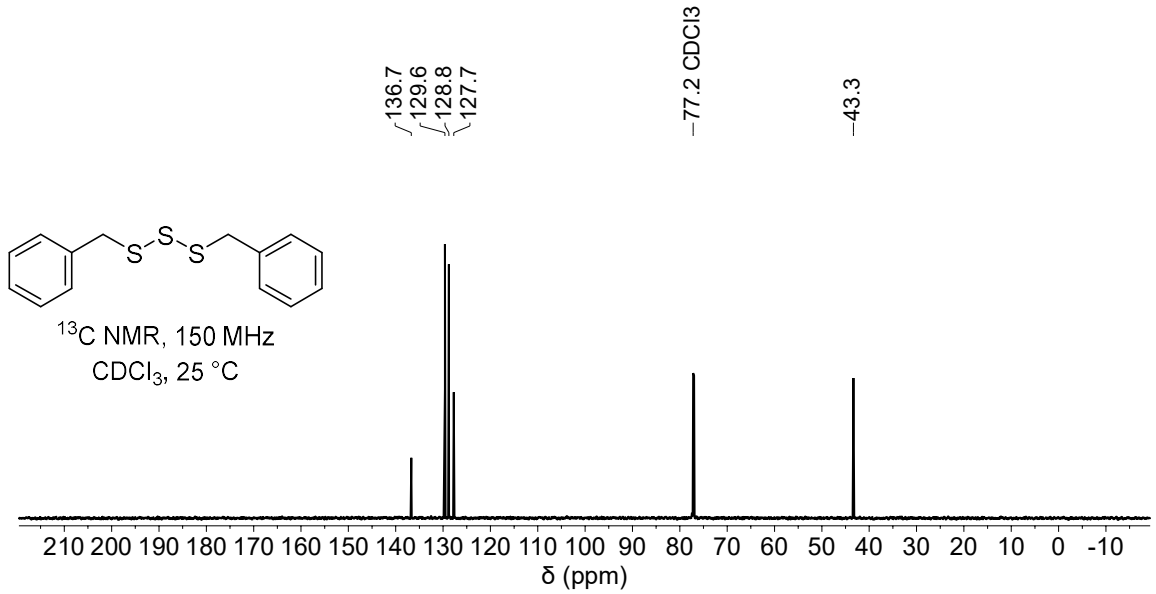

Figure S2.12: ^{13}C NMR spectrum of dibenzyl trisulfide

Trisulfide synthesis using a method from Milligan et al.[5] with modification (method B)

General procedure

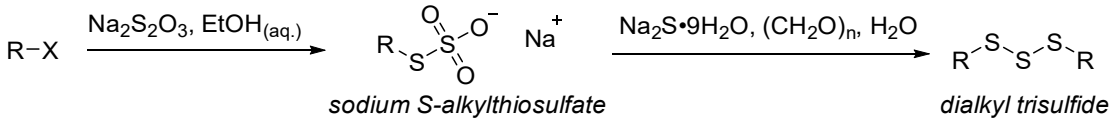

Synthesis of sodium *S*-alkylthiosulfate. To a 250 mL round bottom flask equipped with a stir bar was added sodium thiosulfate pentahydrate (27.3 g, 110 mmol, 1.1 eq.) and 100 mL of 50% v/v ethanol. The mixture was stirred until all sodium thiosulfate dissolved. The alkyl halide (100 mmol, 1.0 eq.) was added to the stirred solution giving a cloudy mixture, which was refluxed until a homogenous clear solution formed; refluxing was continued for several hours. The solvent was then removed under reduced pressure to give a solid consisting of sodium S-alkylthiosulfate. Methanol (75 mL) was added and the solid was crushed using a glass stir rod while heating the mixture at 60 ºC (water bath). The hot mixture was quickly filtered through a sintered glass funnel (porosity 3) and rinsed further with hot methanol (75 mL). This collects the sodium *S*-alkylthiosulfate, leaving behind excess sodium thiosulfate and sodium bromide. The filtrate was concentrated under reduced pressure to yield crude sodium S-alkyl thiosulfate (solid). (**Note**: *If the sodium S-alkylthiosulfate precipitates from the methanol filtrate, heat the methanol to redissolve*)

Synthesis of dialkyl trisulfide. The sodium *S*-alkylthiosulfate (~100 mmol) was dissolved in water (100 mL) and cooled to 0 ºC (ice bath) with stirring. Paraformaldehyde (7 g) was then added. A solution of sodium sulfide nonahydrate (12.01 g, 50 mmol, 0.5 eq.) in water (100 mL) was then added dropwise over 30 minutes to the cooled solution of sodium *S*-alkyl thiosulfate. The mixture was then stirred for several hours while maintaining the temperature at 0 °C. The product was extracted using diethyl ether (3 × 50 mL). The combined organic extracts were washed with water (2 × 25 mL) and saturated $NaCl_{(aq)}$ (50 mL). The organic layer was dried with $MgSO_4$, filtered through neutral alumina (10 g), and concentrated under reduced pressure to yield the dialkyl trisulfide.

Diallyl trisulfide (2.2) – method B

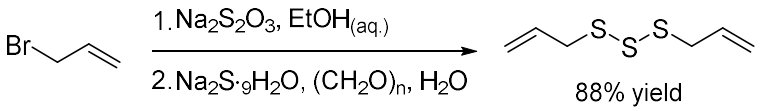

Diallyl trisulfide was synthesised following the general procedure (method B) using allyl bromide (12.1 g, 8.64 mL, 100 mmol, 1.0 eq.). Refluxing at 70 ºC gave a clear yellow solution (around 15 – 20 minutes) and was continued for an additional 2 hours. Methanol treatment and solvent removal gave a pale-yellow solid of sodium *S*-allylthiosulfate. The solid was dissolved in water and reacted with sodium sulfide solution for a total of 4 hours (30 minutes for sodium sulfide addition and 3.5 hours of additional stirring). Following workup, diallyl trisulfide was obtained as a clear pale-yellow oil (7.94 g, 88% yield, ≥ 99% purity confirmed by ^{1}H NMR spectroscopy and GC-MS). The obtained spectral data is in agreement with the literature.[3, 4]

^{1}H NMR (600 MHz, $CDCl_3$) δ 5.89 (ddt, *J* = 17.2, 10.0, 7.3 Hz, 2H), 5.23 (ap. dq, *J* = 16.9, 1.4 Hz, 2H), 5.20 (ap. dt, *J* = 9.9, 0.7 Hz, 2H), 3.51 (d, *J* = 7.3 Hz, 4H). **^{13}C NMR** (150 MHz, $CDCl_3$) δ 132.8, 119.2, 41.8. **IR** (ν_{max}, ATR): 3082, 3010, 2979, 2905, 1634, 1423, 1398, 1217, 984, 916, 721 cm^{-1}. **GC-MS** (EI, 70 eV) *m/z* (rel. intensity): *m/z* calcd. for $C_6H_{10}S_3^+$: 178.0 $[M]^+$, found: 178.0 (M^+, 7), 137.0 (2), 113.1 (91), 105.0 (6), 73.0 (100)

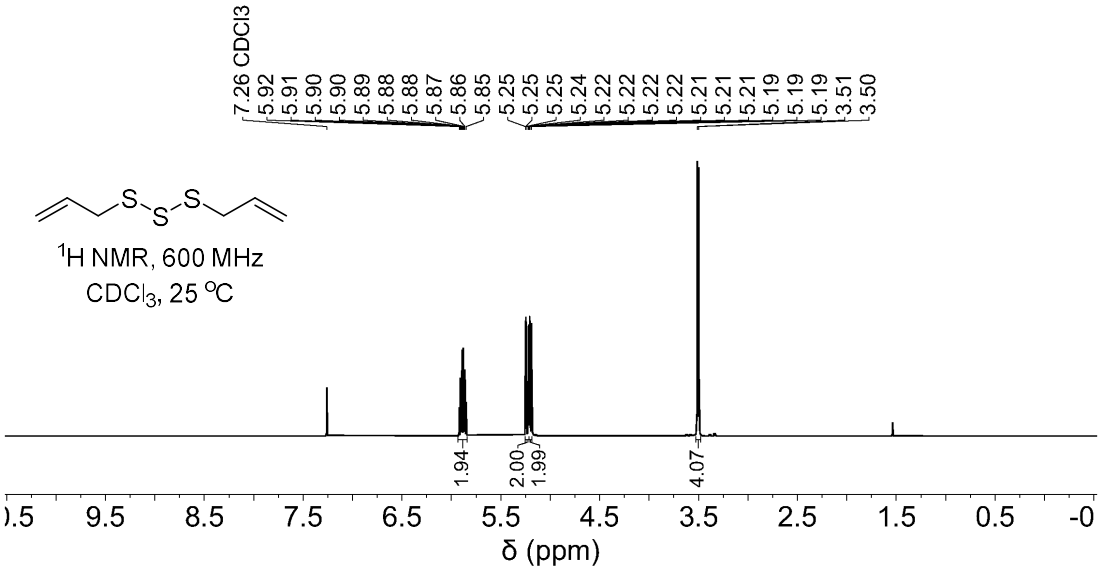

Figure S2.13: ^{1}H NMR spectrum of diallyl trisulfide

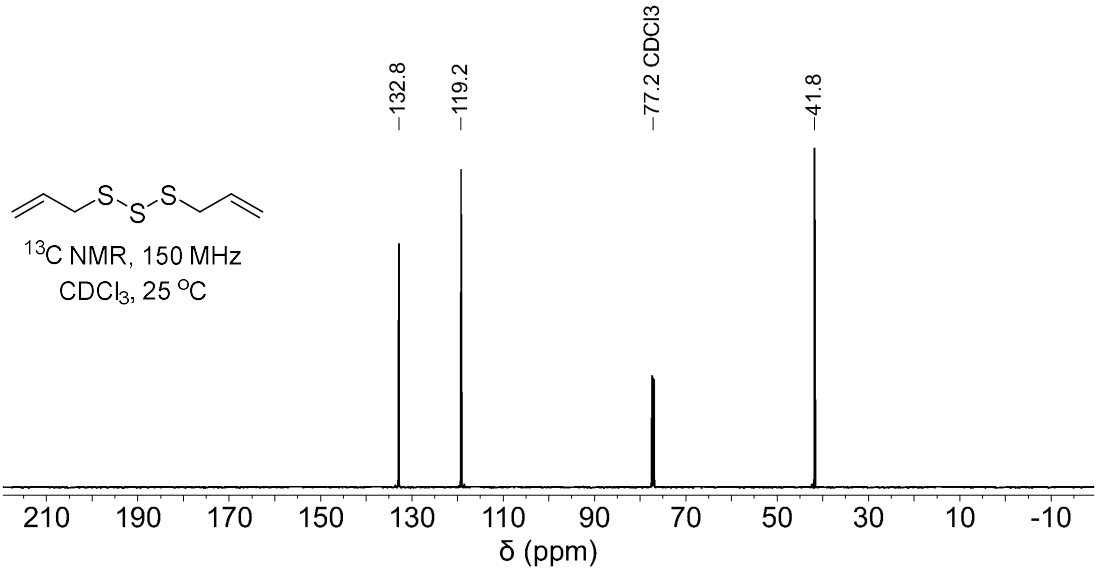

Figure S2.14: ^{13}C NMR spectrum of diallyl trisulfide

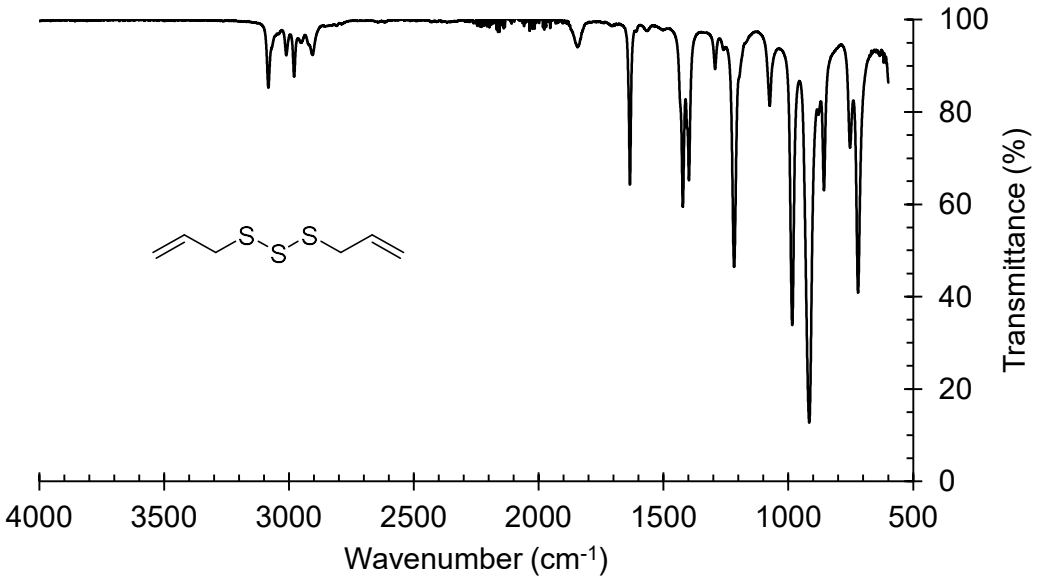

Figure S2.15: FTIR spectrum of diallyl trisulfide

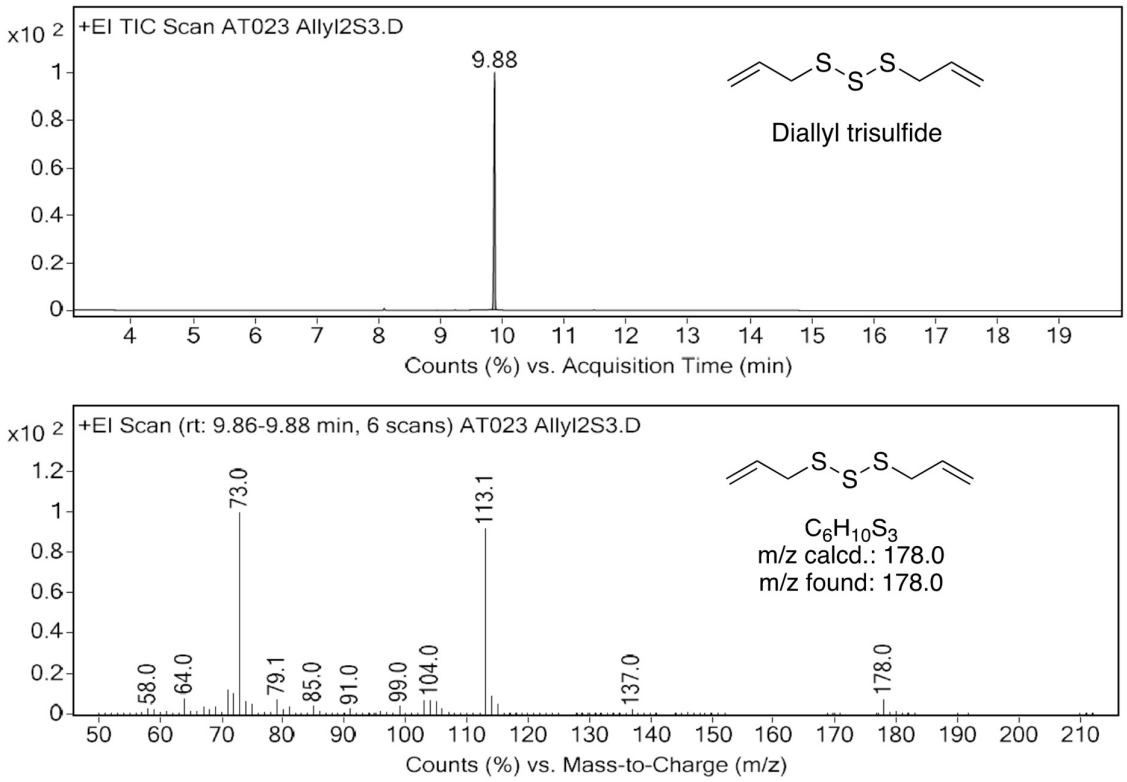

Figure S2.16: Gas chromatogram and mass spectrum of diallyl trisulfide. GC-MS method A. Retention time: 9.88 min ($Allyl_2S_3$)

Diethyl trisulfide (2.9) – method B

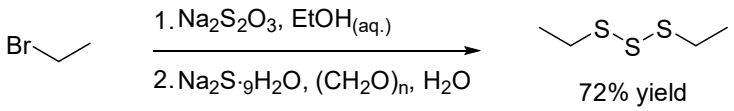

Diethyl trisulfide was synthesised following the general procedure (method B) using bromoethane (10.9 g, 7.46 mL, 100 mmol, 1.0 eq.). Refluxing at 70 ºC gave a clear solution (around 30 – 40 minutes) and was continued for an additional 2 hours. Methanol treatment and solvent removal gave a white solid of sodium *S*-ethylthiosulfate. The solid was dissolved in water and reacted with sodium sulfide solution for a total of 4 hours (30 minutes for sodium sulfide addition and 3.5 hours for an additional stirring). Following workup, diethyl trisulfide was obtained as a as a beige oil (5.57 g, 72% yield, ≥ 99% purity confirmed by ^{1}H NMR spectroscopy and GC-MS). The obtained spectral data is in agreement with the literature.[3]

^{1}H NMR (600 MHz, $CDCl_3$) δ 2.88 (q, *J* = 7.3 Hz, 4H), 1.37 (t, *J* = 7.4 Hz, 6H). **^{13}C NMR** (150 MHz, $CDCl_3$) δ 32.7, 14.3. **IR** (ν_{max}, ATR): 2969, 2925, 2868, 1446, 1417, 1373, 1252, 1049, 967, 758 cm^{-1}. **GC-MS** (EI, 70 eV) *m/z* (rel. intensity): *m/z* calcd. for $C_4H_{10}S_3^+$: 154.0 [M]$^+$, found: 154.0 (M+, 100), 125.0 (5), 122.0 (2), 93.0 (19), 61.1 (56).

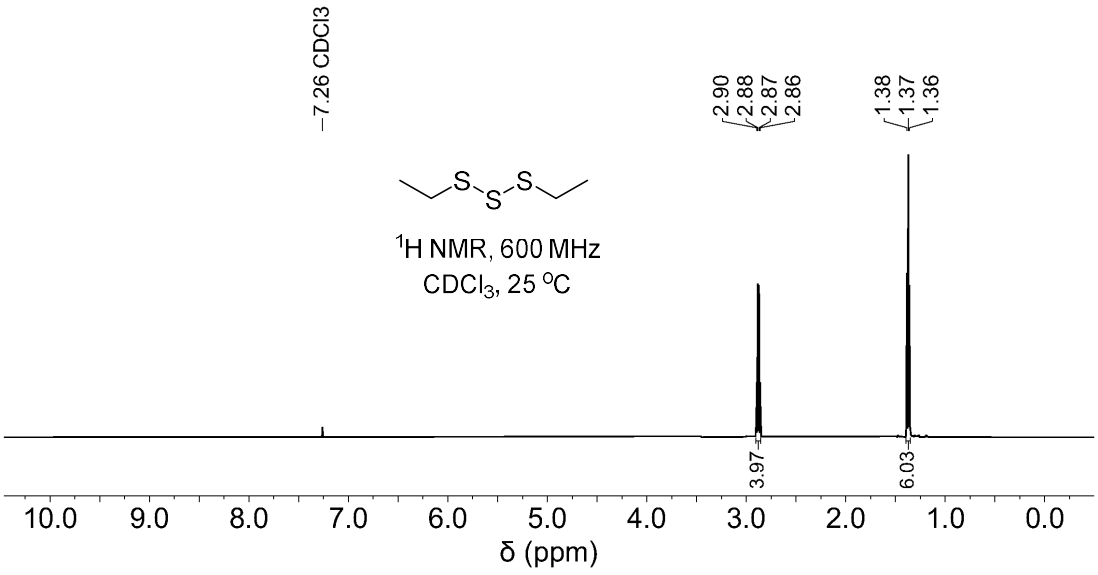

Figure S2.17: ^{1}H NMR spectrum of diethyl trisulfide

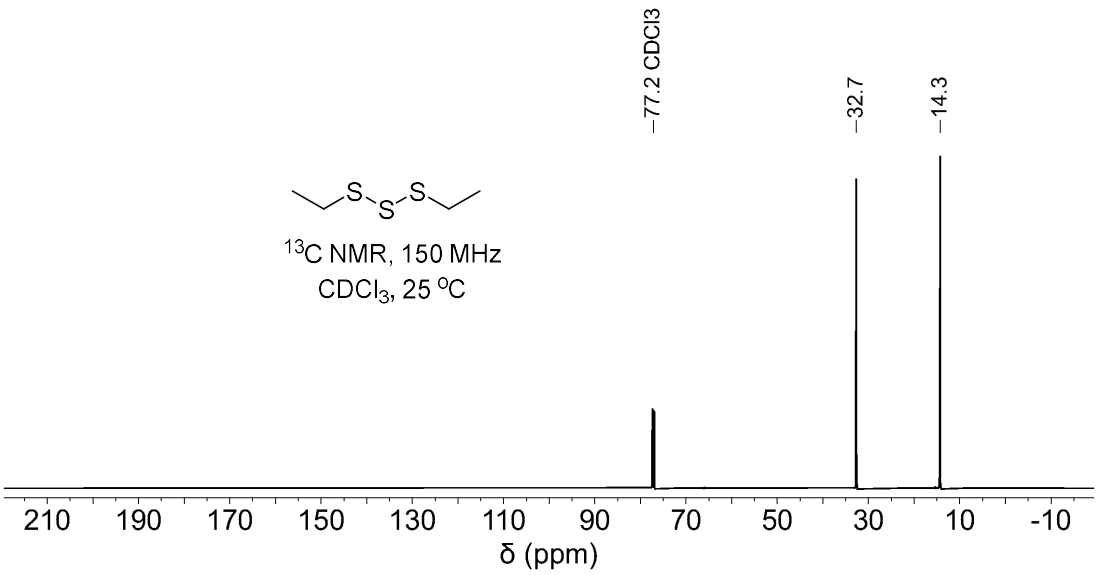

Figure S2.18: ^{13}C NMR spectrum of diethyl trisulfide

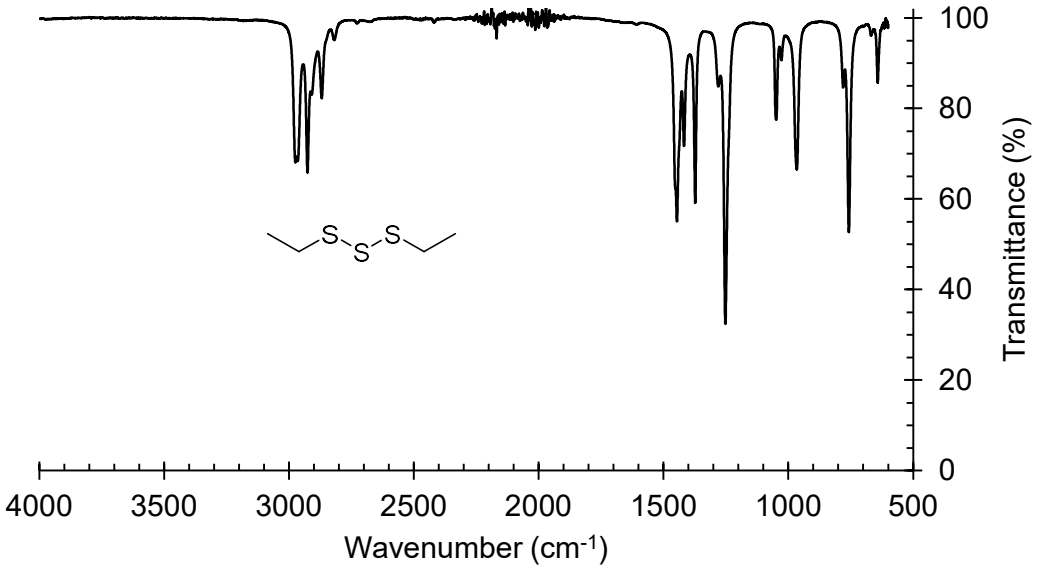

Figure S2.19: FTIR spectrum of diethyl trisulfide

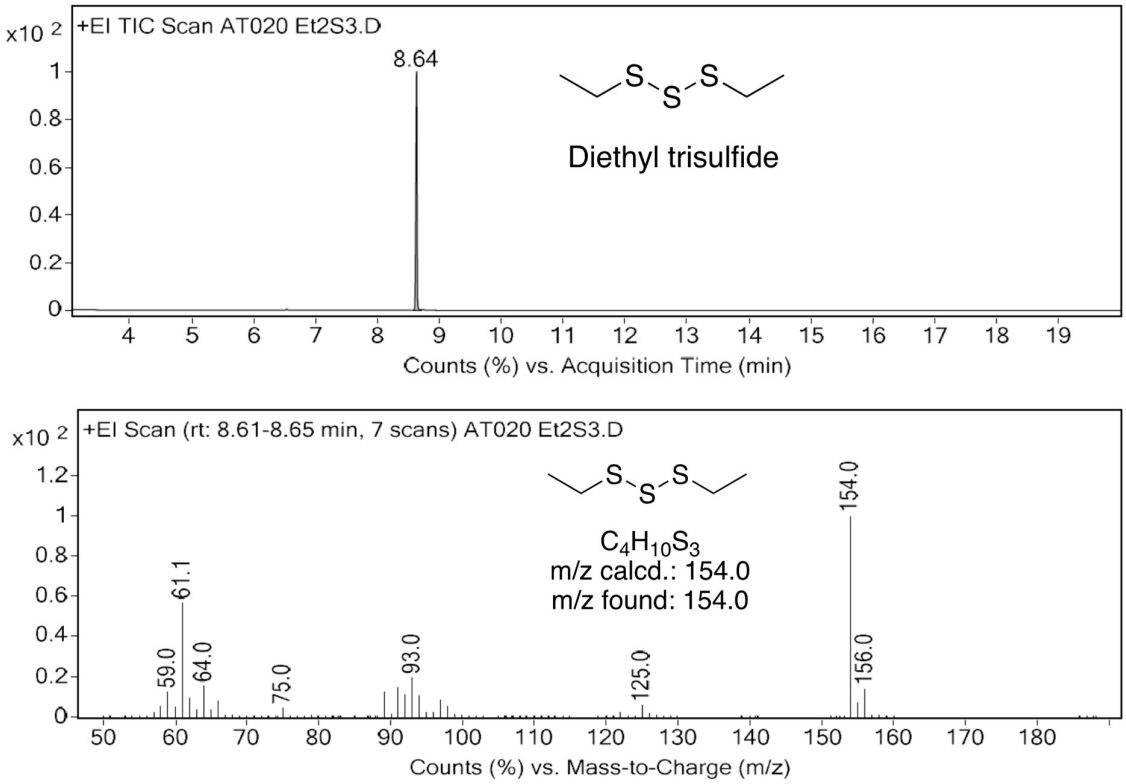

Figure S2.20: Gas chromatogram and mass spectrum of diethyl trisulfide. GC-MS method A. Retention time: 8.64 (Et_2S_3)

Di-*n*-hexyl trisulfide (2.11) – method B

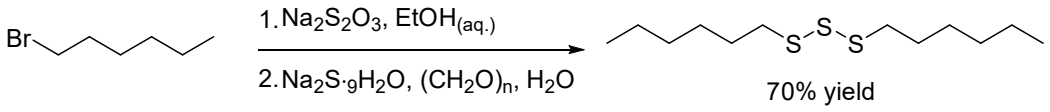

Di-*n*-hexyl trisulfide was synthesised following the general procedure using 1-bromohexane (16.5 g, 14.0 mL, 100 mmol, 1.0 eq.). Refluxing at 100 ºC gave a clear solution (around 40-50 minutes) and was continued for an additional 6 hours. Methanol treatment and solvent removal gave a white solid of sodium *S*-hexylthiosulfate. The solid was dissolved in water and reacted with sodium sulfide solution for a total of 4 hours (30 minutes for sodium sulfide addition and 3.5 hours for an additional stirring). Following workup, di-*n*-hexyl trisulfide was obtained as a beige oil (9.40 g, 70% yield, ≥ 99.9% purity confirmed by ^{1}H NMR spectroscopy and GC-MS).

^{1}H NMR (600 MHz, $CDCl_3$) δ 2.86 (t, *J* = 7.3 Hz, 4H), 1.73 (ap. p, *J* = 7.4 Hz, 4H), 1.40 (ap. p, *J* = 7.3 Hz, 4H), 1.36 – 1.26 (m, 8H), 0.89 (t, *J* = 7.0 Hz, 6H). **^{13}C NMR** (150 MHz, $CDCl_3$) δ 39.0, 31.5, 28.9, 28.3, 22.6, 14.1. **IR** (ν_{max}, ATR): 2955, 2925, 2856, 1460, 1413, 1378, 1284, 1256, 1206, 1112, 724 cm^{-1}. **GC-MS** (EI, 70 eV) *m/z* (rel. intensity): *m/z* calcd. for $C_{12}H_{26}S_3^+$: 266.1 $[M]^+$, found: 266.2 (M+, 71), 234.2 (13), 182.0 (9), 150.1 (10), 149.1 (2), 117.1 (100), 85.0 (38), 83.1 (50), 55.1 (46). **Elemental analysis (CHNS)**: $C_{12}H_{26}S_3$ requires C, 54.08%; H, 9.83%; N, 0%; S, 36.09%. Found C, 55.17%; H, 10.76%; N, 0%; S, 38.36%.

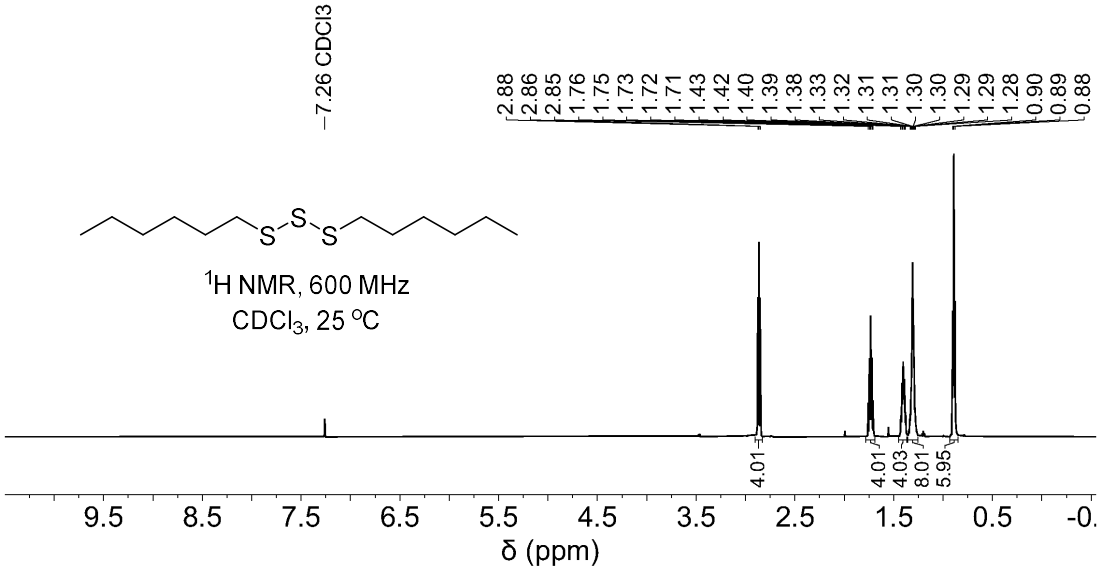

Figure S2.21: ^{1}H NMR spectrum of di-*n*-hexyl trisulfide

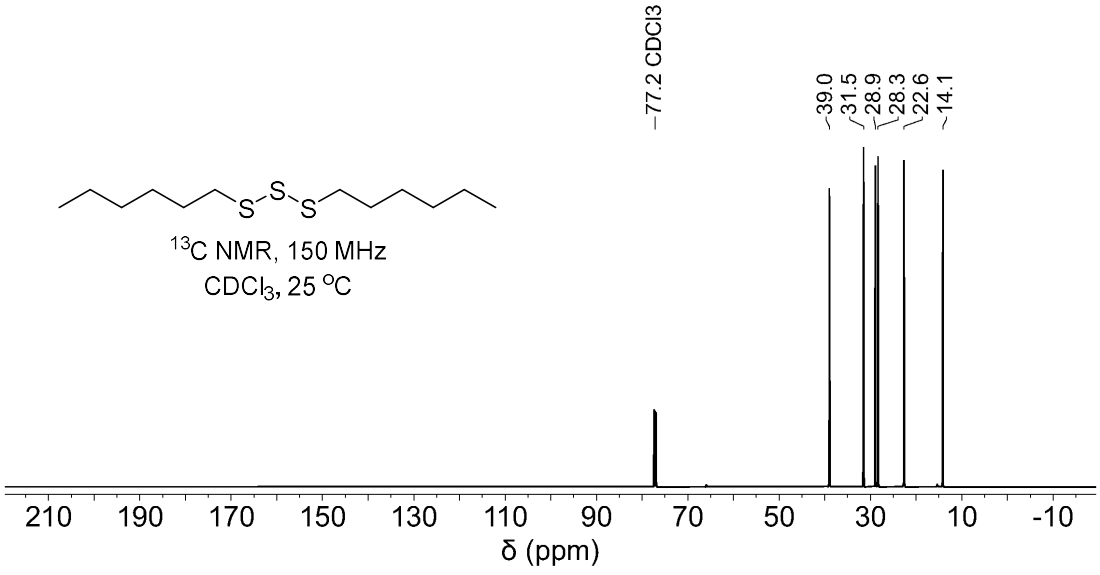

Figure S2.22: ^{13}C NMR spectrum of di-*n*-hexyl trisulfide

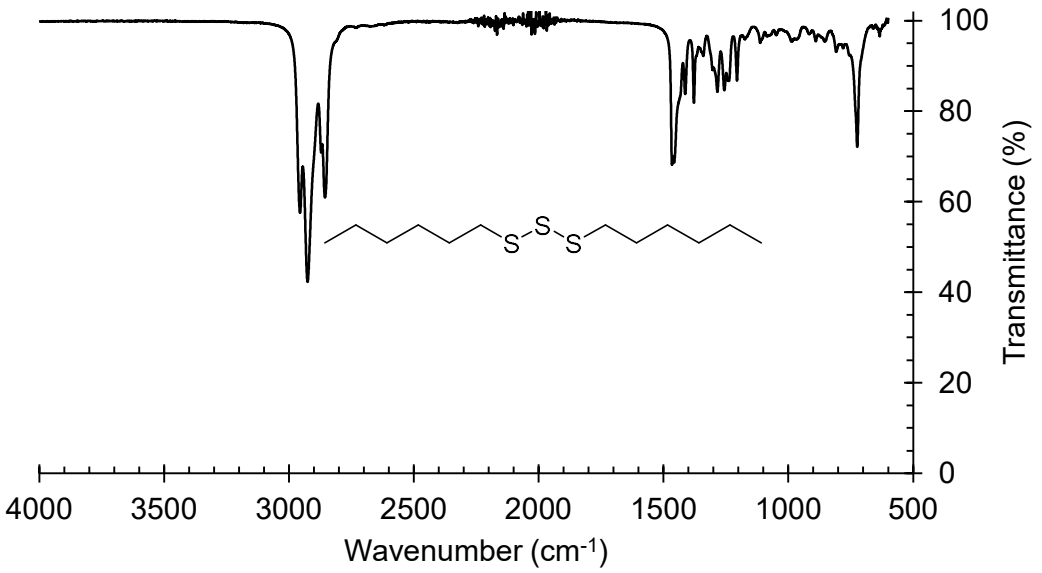

Figure S2.23: FTIR spectrum of di-*n*-hexyl trisulfide

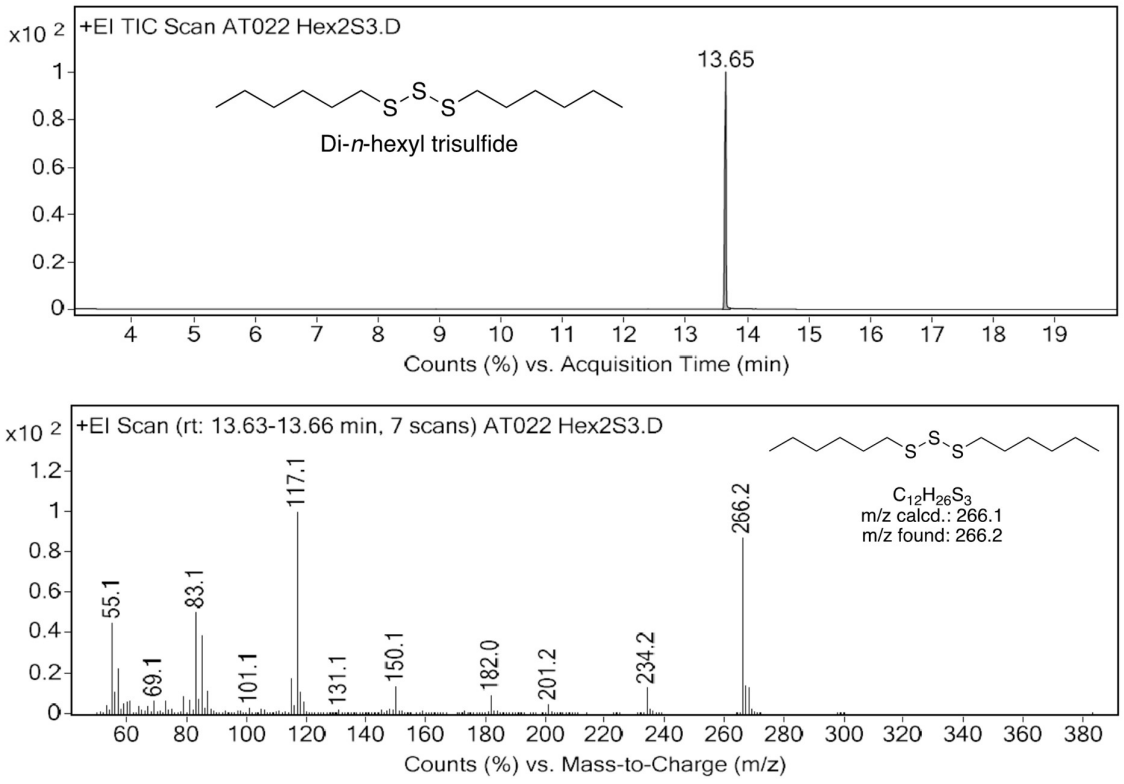

Figure S2.24: Gas chromatogram and mass spectrum of di-*n*-hexyl trisulfide. GC-MS method A. Retention time: 13.65 min ($^{n}Hex_2S_3$)

Di-iso-butyl trisulfide (2.4) – method B

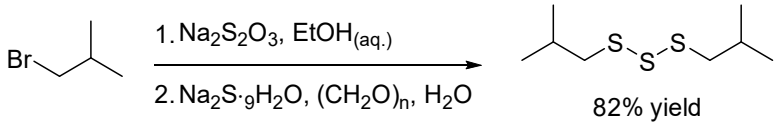

82% yield

Di-*iso*-butyl trisulfide was synthesised following the general procedure (method B) using 1-bromo-2-methylpropane (13.7 g, 10.87 mL, 100 mmol, 1.0 eq.). The mixture was refluxed (100 °C) for 24 h. Methanol treatment and solvent removal gave a white solid of sodium *S*-isobutylthiosulfate. The solid was dissolved in water and reacted with sodium sulfide solution for a total of 5.5 hours (30 minutes for sodium sulfide addition and 5 hours for an additional stirring). Following workup, di-*iso*-butyl trisulfide was obtained as a beige oil (8.58 g, 82% yield, ≥ 99.7% purity confirmed by ^{1}H NMR spectroscopy and GC-MS).

^{1}H NMR (600 MHz, $CDCl_3$) δ 2.78 (d, *J* = 6.9 Hz, 4H), 2.04 (ap. dh, *J* = 13.4, 6.7 Hz, 2H), 1.02 (d, *J* = 6.7 Hz, 12H). **^{13}C NMR** (150 MHz, $CDCl_3$) δ 48.4, 28.2, 22.0. **IR** (ν_{max}, ATR): 2956, 2927, 2869, 1463, 1382, 1365, 1318, 1239, 1167, 1070, 944, 923, 855, 800 cm^{-1}. **GC-MS** (EI, 70 eV) *m/z* (rel. intensity): *m/z* calcd. for $C_8H_{18}S_3^+$: 210.1 $[M]^+$, found: 210.1 (M+, 48), 178.1 (4), 154.0 (7), 89.1 (32), 57.1 (100). **Elemental analysis** (CHNS): $C_8H_{18}S_3$ requires C, 45.67%; H, 8.62%; N, 0%; S, 45.71%. Found C, 43.65%; H, 9.14%; N, 0%; S, 44.28%.

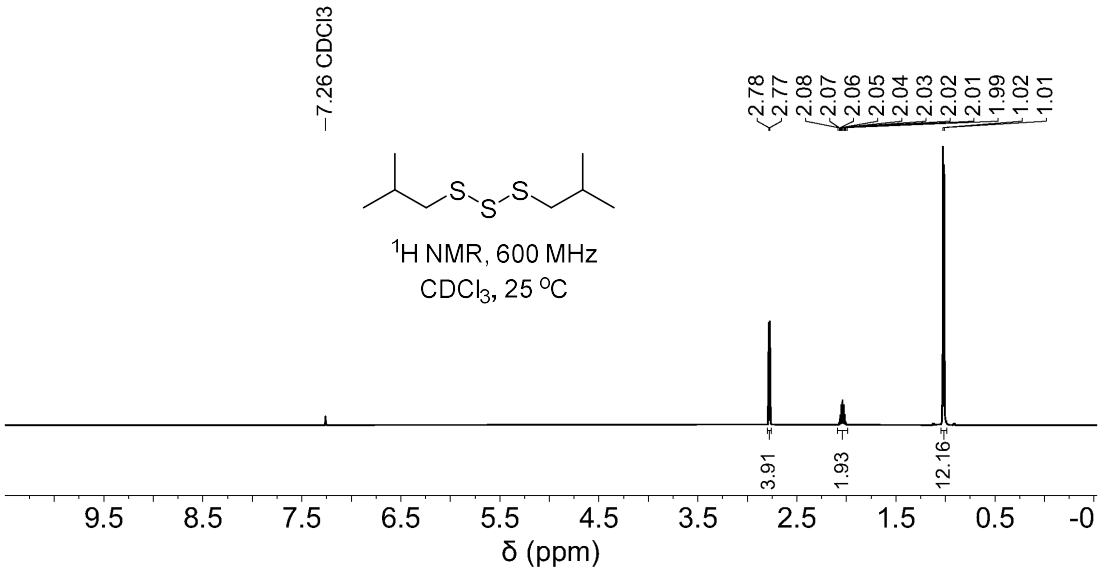

Figure S2.25: ^{1}H NMR spectrum of diisobutyl trisulfide

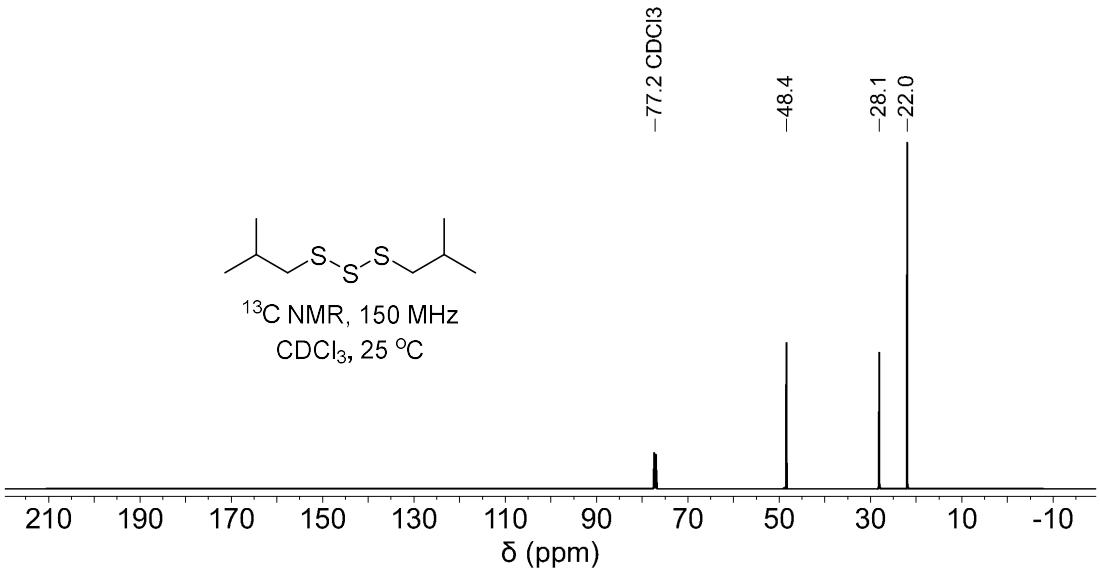

Figure S2.26: ^{13}C NMR spectrum of diisobutyl trisulfide

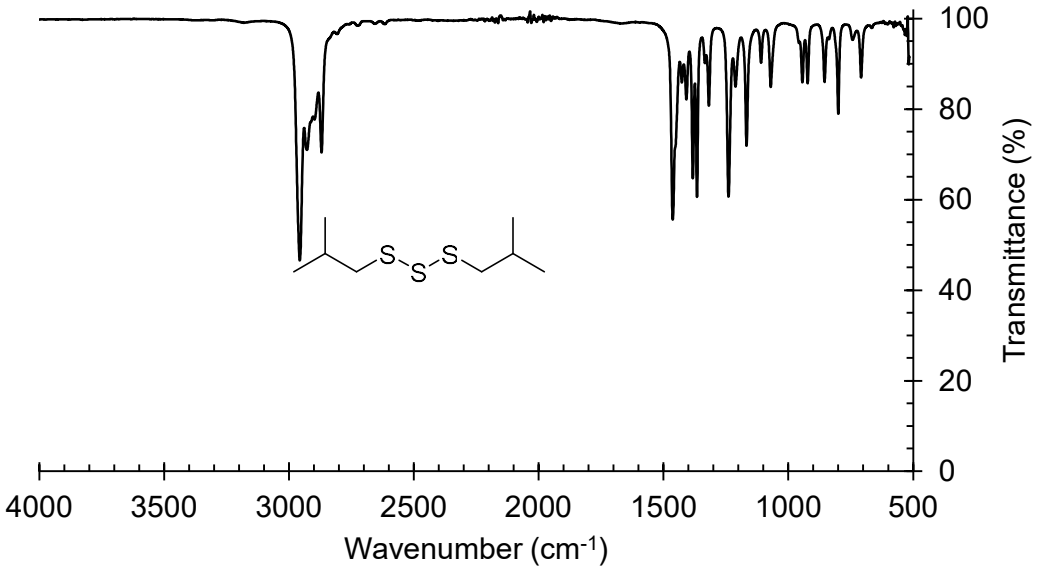

Figure S2.27: FTIR spectrum of diisobutyl trisulfide

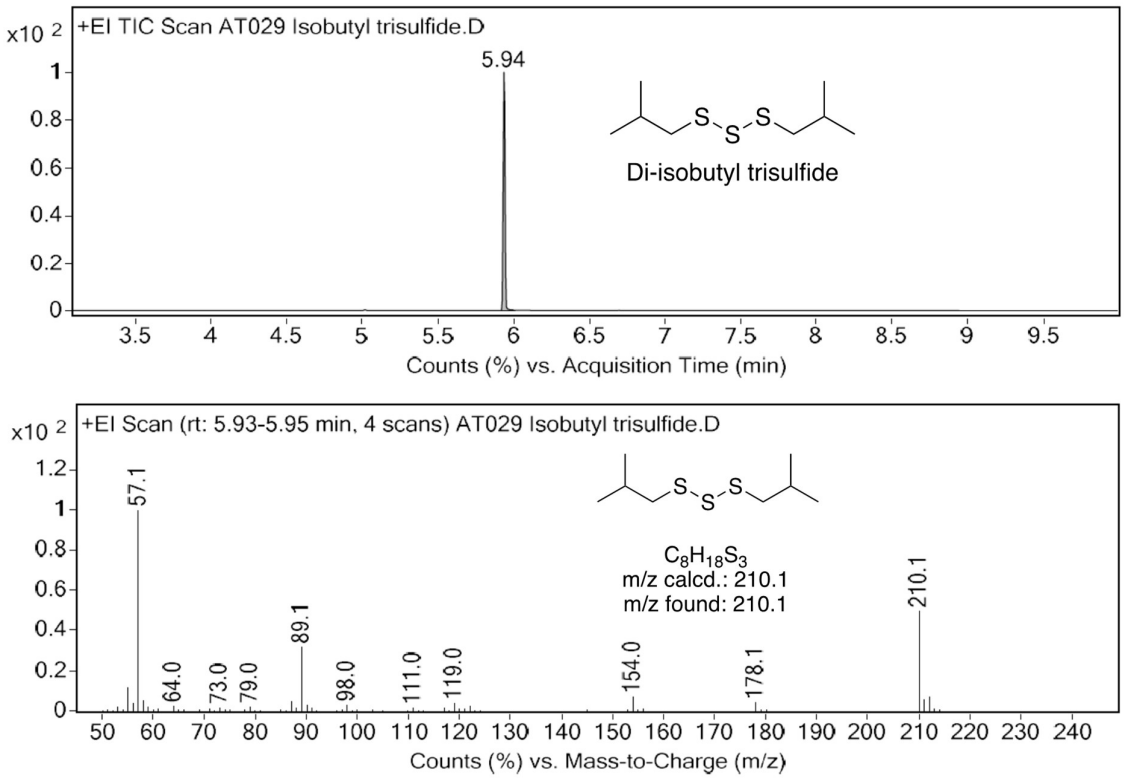

Figure S2.28: Gas chromatogram and mass spectrum of diisobutyl trisulfide. GC-MS method B with a hold time of 3.7 minutes at 250 ºC. Retention time: 5.94 min ($^{i}Bu_2S_3$)

An attempt on the synthesis of dibenzyl trisulfide via sodium *S*-benzyl thiosulfate in the presence of paraformaldehyde

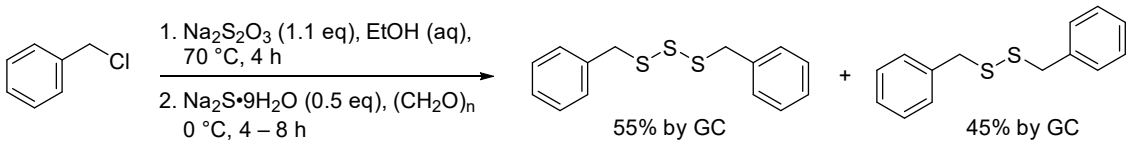

Dibenzyl trisulfide was synthesised following the general procedure (method B) benzyl chloride (11.5 mL, 100 mmol, 1.0 eq.). The mixture was heated (70 °C) for 4 h. Methanol treatment and solvent removal gave a white solid of sodium *S*-benzylthiosulfate. The solid was dissolved in water (200 mL). The solution was divided into two equal portions (each 100 mL, containing ~50 mmol of sodium *S*-benzylthiosulfate). One portion was reacted with sodium sulfide solution (25 mmol) for a total of 4 to 8 hours (30 minutes for sodium sulfide addition). g). After 4 h, ^{1}H NMR spectroscopy of the crude mixture revealed the composition of dibenzyl trisulfide to dibenzyl disulfide was 80% : 20% (4 : 1). Reaction was continued to 8 hours. Following workup, a mixture of dibenzyl trisulfide and dibenzyl disulfide was isolated as a white solid (4.70 g). GC-MS revealed the final composition of dibenzyl trisulfide to dibenzyl disulfide was 55% to 45%. The other portion of sodium *S*-benzyl thiosulfate was reacted with sodium sulfide (25 mmol) without the addition of paraformaldehyde. After 4 hours, the

crude was analysed by ^{1}H NMR spectroscopy. The peak at 4.03 and 3.60 ppm correspond to the benzylic proton of the trisulfide and the disulfide, respectively. Data was compared to the one reaction with paraformaldehyde.

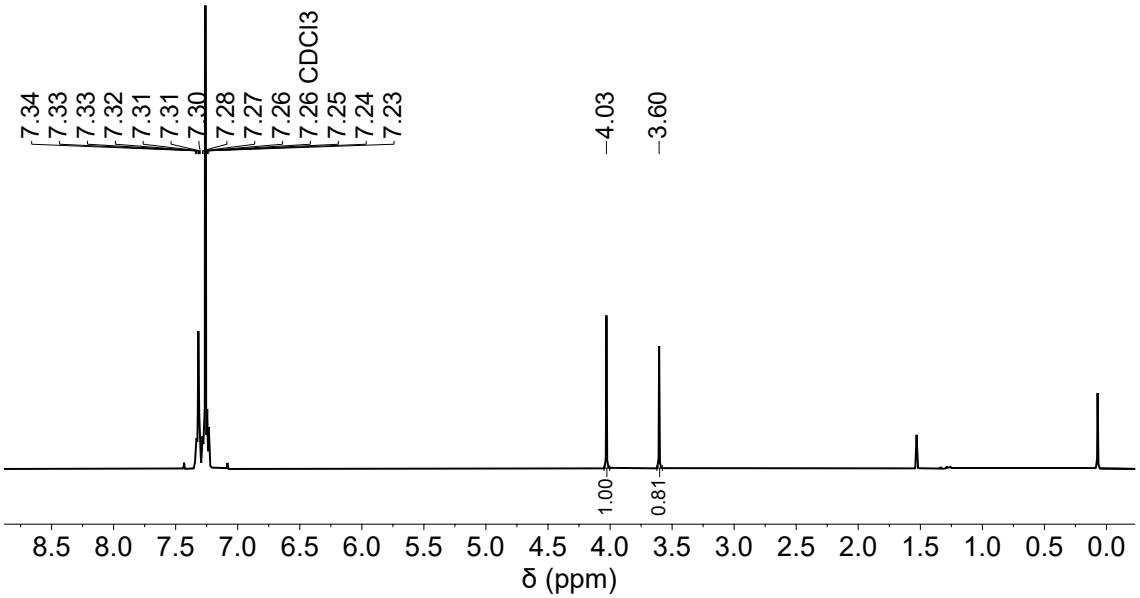

Figure S2.29: ^{1}H NMR spectrum (600 MHz) of a solid containing dibenzyl di- and trisulfide.

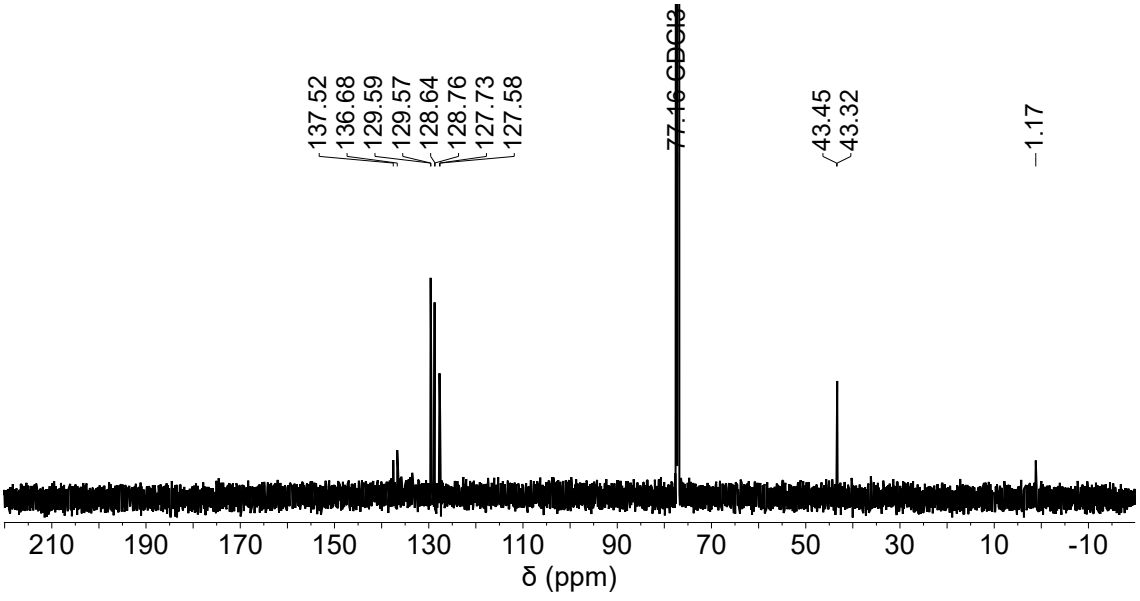

Figure S2.30: ^{13}C NMR spectrum (150 MHz) of a solid containing dibenzyl di- and trisulfide.

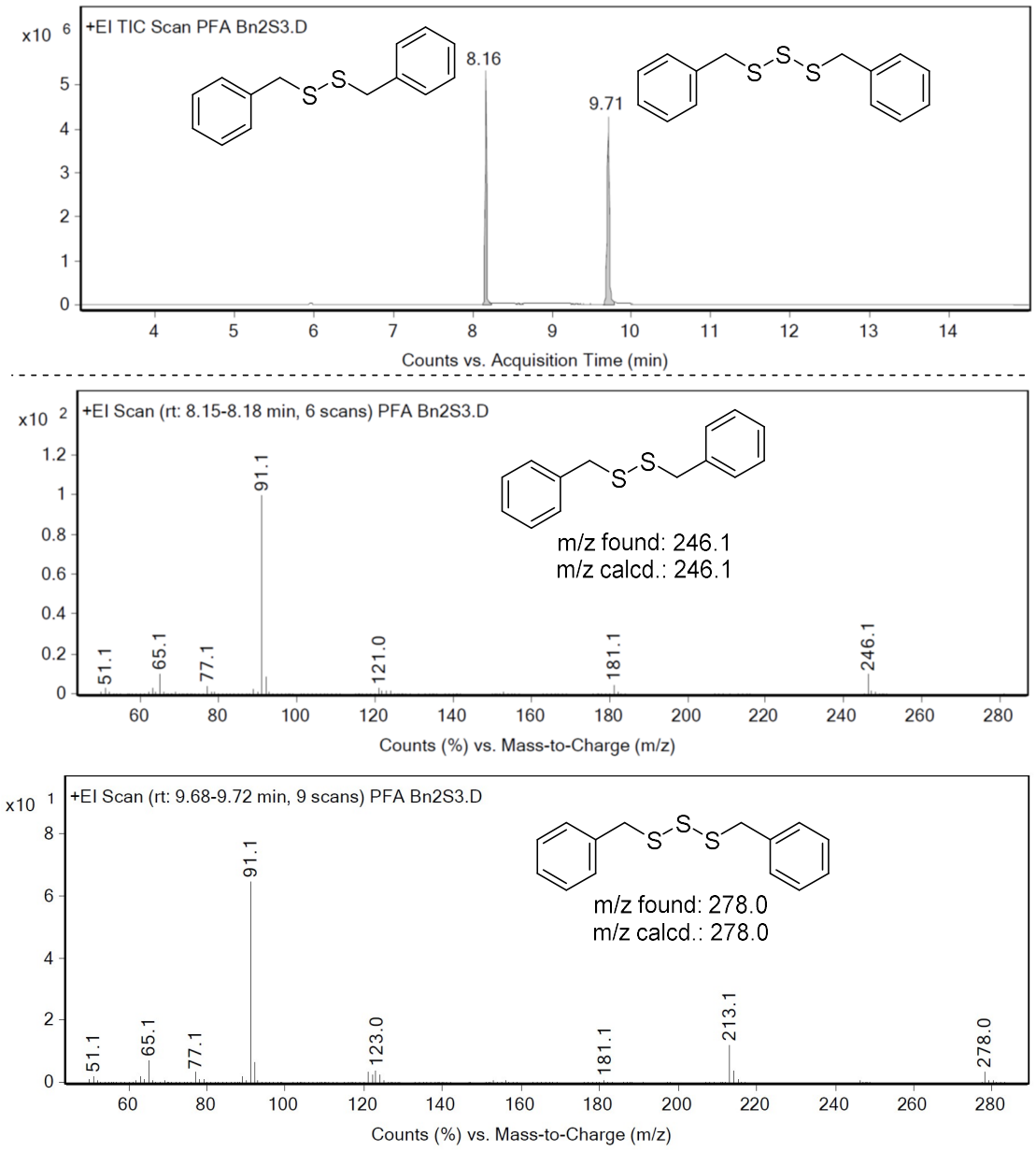

Figure S2.31: Gas chromatogram and mass spectra of dibenzyl disulfide and trisulfide. GC-MS method B with a hold time of 8.7 minutes at 250 ºC. Retention time: 8.16 min (Bn_2S_2) and 9.71 min (Bn_2S_3)

Trisulfides synthesis from a thiol and SCl_2

Sulfur dichloride (SCl_2) synthesis

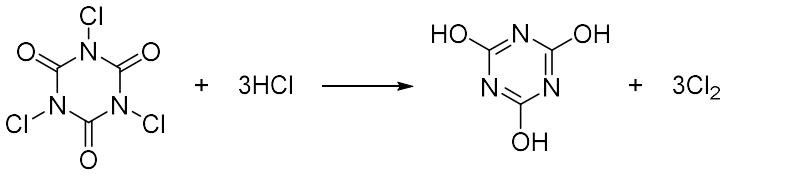

Step 1: $xS + Cl_2 \longrightarrow S_xCl_2$ (where x = 1 or 2)

Step 2: $S_xCl_2 + Cl_2 \longrightarrow SCl_2$ (where x = 1 or 2)

Generation of dry Cl_2: All glassware was dried prior to use. Trichloroisocyanuric acid (300 g, 1.3 mol) was added to a one-litre conical flask ***(Figure A: 2)*** connected to a vacuum adapter as a chlorine gas outlet, and a 500 mL pressure equalising dropping funnel containing hydrochloric acid (32%, 370 mL, 3.9 mol) ***(Figure A: 1)***. This amount of trichloroisocyanuric acid and hydrochloric acid provides 3.9 moles of Cl_2 (1.25 eq. to elemental sulfur). The resultant chlorine gas is dried by bubbling through concentrated sulfuric acid (100 mL) ***(Figure A: 3)*** and subsequently bubbled into the reaction ***(Figure A: 4/5)***.

Generation of S_xCl_2 (x = 1 or 2) from S and Cl_2: All glassware was dried prior to use. Elemental sulfur (100 g, 3.125 mol, 1 eq.) was added to a 500 mL two necked round bottom flask ***(Figure A: 5)***; the side neck served as chlorine gas inlet ***(Figure A: 4)***, while the main neck was connected to a distillation apparatus ***(Figure A: 8/9/10)***. The flask was heated using an oil bath at 150 ºC ***(Figure A: 6)*** which melts the sulfur; the oil bath was supported by a laboratory jack. A fast stream of dry chlorine gas was bubbled through the stirred molten sulfur resulting in an exothermic reaction (***oil bath temperature can climb to 180 ºC)***. The oil bath is lowered to allow the reaction to cool down or raised to heat up the reaction and maintain the melted state ***(this prevents blockages and pressure build-up)***. Unreacted chlorine gas is quenched by bubbling through 40% w/v $NaOH_{(aq)}$ (100 mL) ***(Figure A: 11)***. When the viscosity of the reaction noticeably decreases ***(Figure B)***, a spatula tip (~ 0.1 g) of iron powder is quickly added from the side neck ***(Figure A: 4)***, and then chlorine gas bubbling is resumed. As the reaction progresses, SCl_2 and S_2Cl_2, bp. 60 and 138 ºC respectively, form and distil into the receiving flask ***(Figure A: 10)*** giving a dark red liquid (205 g) ***(Figure C)***.

Generation of SCl_2 from S_xCl_2 (x = 1 or 2) and Cl_2: All glassware was dried prior to use; the reaction setup is analogous to the generation of S_xCl_2. S_xCl_2 (100 g) was cooled to 0 ºC, and dry chlorine gas (from trichloroisocyanuric acid (150 g, 0.65 mol) and hydrochloric acid (32%, 185 mL, 1.62 mol)) was bubbled through the stirred solution for one hour resulting in an exothermic reaction ***(efficient cooling is essential to prevent the distillation of S_xCl_2 (x = 1 or 2) at this stage, SCl_2 bp. 59 – 60 ºC)***. Chlorine gas bubbling was then stopped, PCl_5 (50 mg) was added to the reaction, and the mixture was distilled ***(Figure D)***. A fraction that distils at a constant temperature of 60 ºC was collected into a receiving flask cooled at 0 ºC ***(Figure E)***. The first 5 mL of distillate was discarded. The distillate, SCl_2 (80 g), was stored over PCl_5 (10 mg) and used within 30 minutes after distillation due to slow decomposition at room temperature giving S_2Cl_2 and chlorine gas.[6]

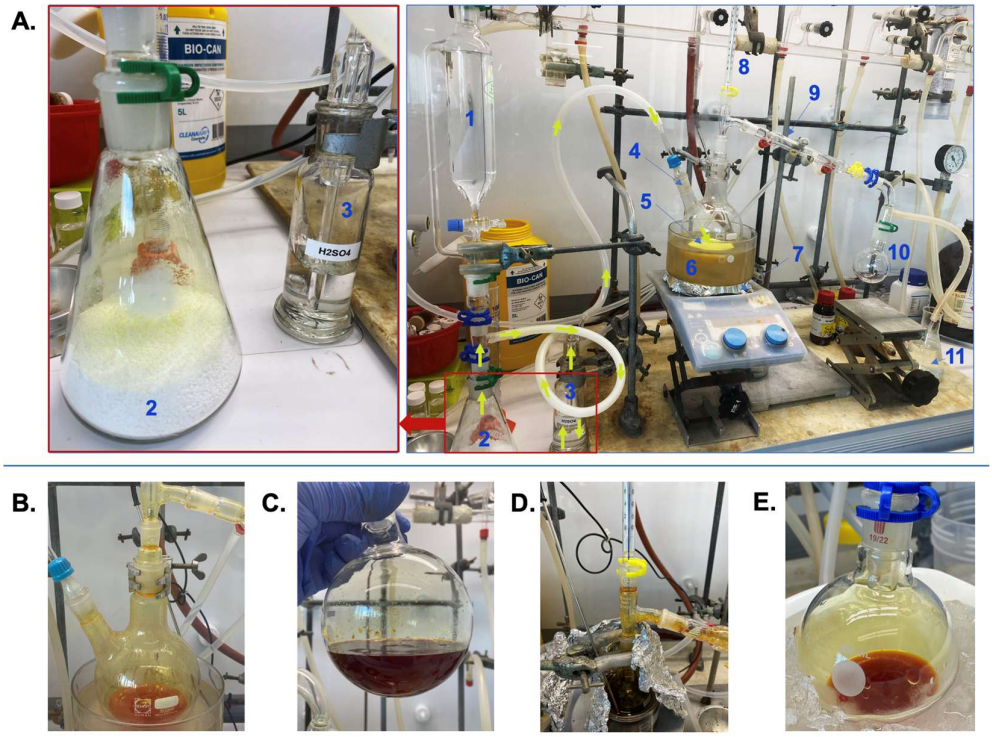

Figure S2.32: A. Images displaying setup for the synthesis of S_xCl_2 (x = 1 or 2). (1= HCl in a pressure equalizing dropping funnel, 2= trichloroisocyanuric acid in an Erlenmeyer flask, 3= concentrated H_2SO_4 bubbler for drying chlorine gas, 4= a pipette connected to sulfur from a side of a round bottom flask, 5= reaction mixture, 6= an oil bath, 7= a hot plate, 8= a thermometer, 9= a Liebig condenser, 10= a receiving flask, and 11= NaOH solution for quenching excess chlorine gas). The yellow arrows show the flow of chlorine gas. B. A flask containing a mixture of molten sulfur, chlorine gas, and S_xCl_2 (x = 1 or 2). The S_xCl_2 (x = 1 or 2) is then directly distilled to a receiving flask. C. S_xCl_2 (x = 1 or 2) collected in the receiving flask. D. After S_xCl_2 (x = 1 or 2) is saturated with chlorine, the product (mostly SCl_2) is distilled over PCl_5 to collect a fraction that boils at 59 ºC. E. SCl_2 is collected and ready to use.

Di-*tert*-butyl trisulfide (2.12)

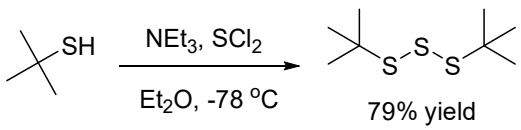

The compound was synthesised based on a literature method.[7] Freshly distilled sulfur dichloride (1.06 mL, 1.71 g, 16.6 mmol, 0.5 eq.) was added to dry Et_2O (50 mL) at -78 ºC, under an atmosphere of nitrogen with stirring. Triethylamine (4.6 mL, 33.3 mmol, 1 eq.) and *tert*-butyl thiol (3.75 mL, 33.3 mmol, 1 eq.) in dry Et_2O (50 mL) was added dropwise over 30 minutes. The reaction was stirred for an additional 30 minutes. The reaction was allowed to reach room temperature, after which it was diluted with ether (100 mL), washed with water (3 × 50 mL), saturated sodium carbonate (1 × 50 mL), and then saturated $NaCl_{(aq)}$ (1 × 50 mL). The organic layer was dried over magnesium sulfate, filtered, and concentrated under reduced pressure. The crude oil was purified by silica column chromatography using 100% hexanes as eluent to give di-*tert*-butyl trisulfide as a beige oil (2.78 g, 79% yield, ≥ 98.8% purity confirmed by ^{1}H NMR spectroscopy and GC). The obtained spectral data is in agreement with the literature.[7]

R_f= 0.71 (hexanes). **^{1}H NMR** (600 MHz, $CDCl_3$) δ 1.37 (s, 18H). **^{13}C NMR** (150 MHz, $CDCl_3$) δ 49.1, 30.0. **IR** (ν_{max}, ATR): 2960, 2921, 2895, 2860, 1471, 1455, 1390, 1363, 1162, 1019, 933, 802, 572. **GC-MS** (EI, 70 eV) *m/z* (rel. intensity): *m/z* calcd. for $C_8H_{18}S_3^+$: 210.1 $[M]^+$, found: 210.1 (M+, 15), 154.0 (28), 89.1 (4), 57.1 (100).

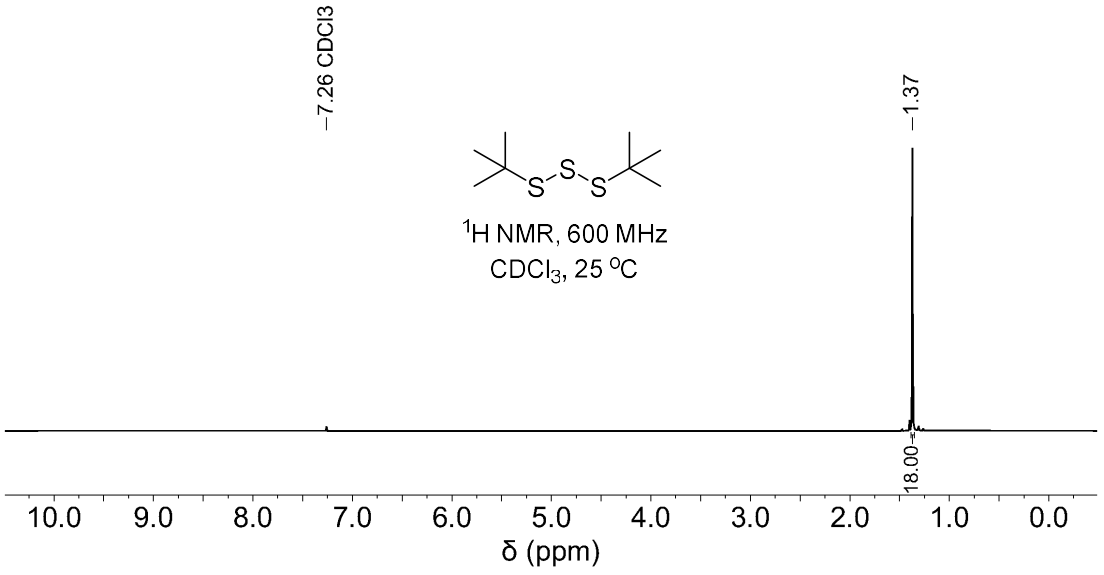

Figure S2.33: ^{1}H NMR spectrum of di-*tert*-butyl trisulfide

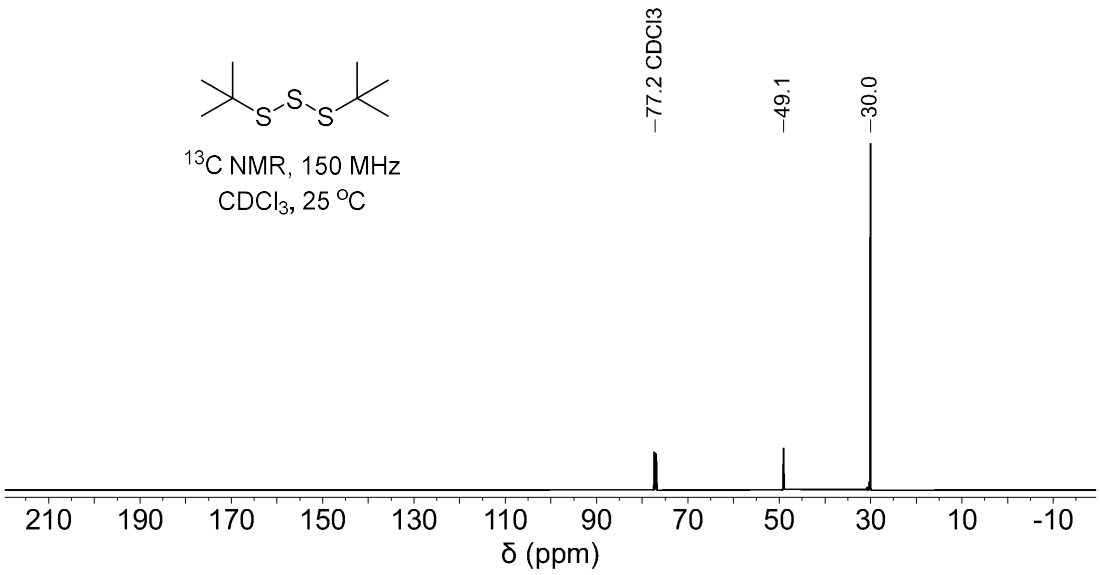

Figure S2.34: ^{13}C NMR spectrum of di-*tert*-butyl trisulfide

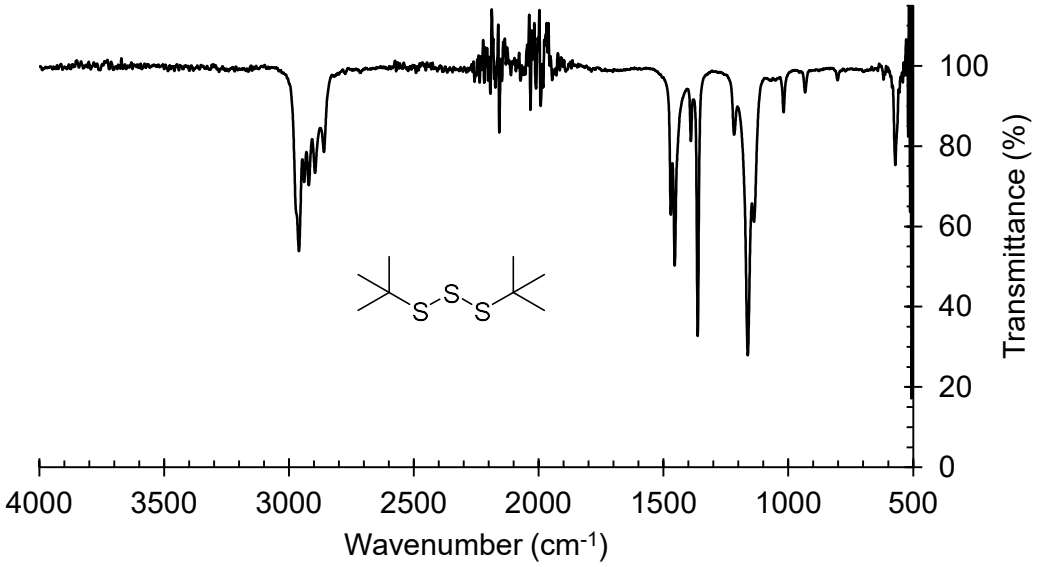

Figure S2.35: FTIR spectrum of di-*tert*-butyl trisulfide

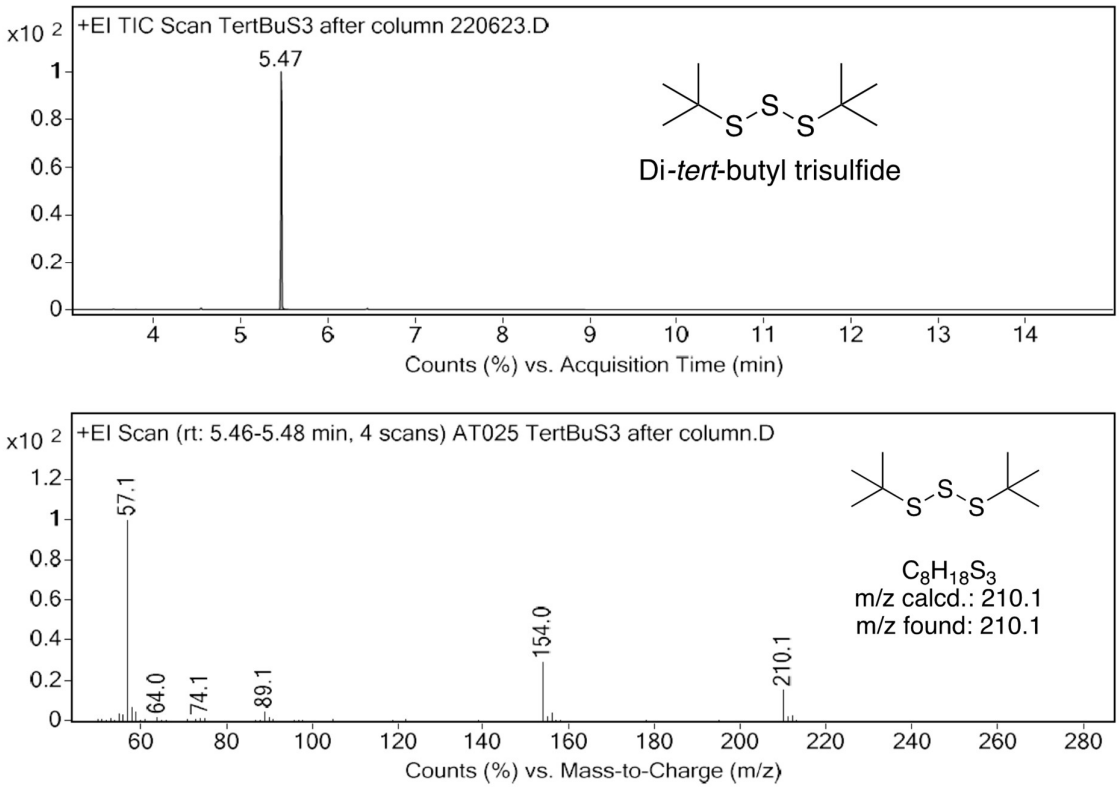

Figure S2.36: Gas chromatogram and mass spectrum of di-*tert*-butyl trisulfide. GC-MS method B with a hold time of 8.7 minutes at 250 ºC. Retention time: 5.47 min ($^{t}Bu_2S_3$)

Dibenzyl trisulfide (2.6)

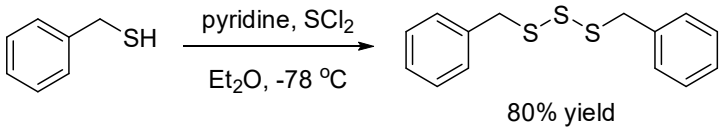

Freshly distilled sulfur dichloride (834 µL, 1.35 g, 13.1 mmol, 0.52 eq.) was added to dry Et_2O (50 mL) at -78 ºC, under an atmosphere of nitrogen with stirring. Pyridine (2.0 mL, 1.98 g, 25.0 mmol, 1 eq.) and benzyl thiol (2.93 mL, 3.11 g, 25.0 mmol, 1 eq.) in dry Et_2O (50 mL) was added dropwise over 30 minutes. The reaction was stirred for an additional 90 minutes. The reaction was allowed to reach room temperature, after which it was diluted with diethyl ether (100 mL), washed with water (4 × 25 mL), and then saturated $NaCl_{(aq)}$ (2 × 25 mL). The organic layer was dried over magnesium sulfate, filtered, and concentrated under reduced pressure to give an oil. The crude oil was purified by recrystallisation from hexane in a freezer at -25 ºC to give white needle-like crystals (2.77 g, 80% yield) which were suitable for X-ray analysis. The obtained spectral data is in agreement with the literature.[4]

^{1}H NMR (600 MHz, $CDCl_3$) δ 7.37 – 7.32 (m, 8H), 7.32 – 7.28 (m, 2H), 4.05 (s, 4H). **^{13}C NMR** (150 MHz, $CDCl_3$) δ 136.7, 129.6, 128.7, 127.7, 43.3. **IR** (ν_{max}, ATR): 3085, 3061, 3027, 2955, 2918, 1602, 1495, 1450, 1413, 1232, 1200, 1135, 1067, 1030, 858, 765, 692, 659. **GC-MS** (EI, 70 eV) *m/z* (rel. intensity): *m/z* calcd. for $C_{14}H_{14}S_3^+$: 278.0 $[M]^+$, found: 278.1 (M+, 3), 246.1 (2), 214.1 (4), 213.1 (15), 181.1 (2), 121.0 (7), 91.1 (100), 77.1 (5), 65.1 (12), 51.1 (3).

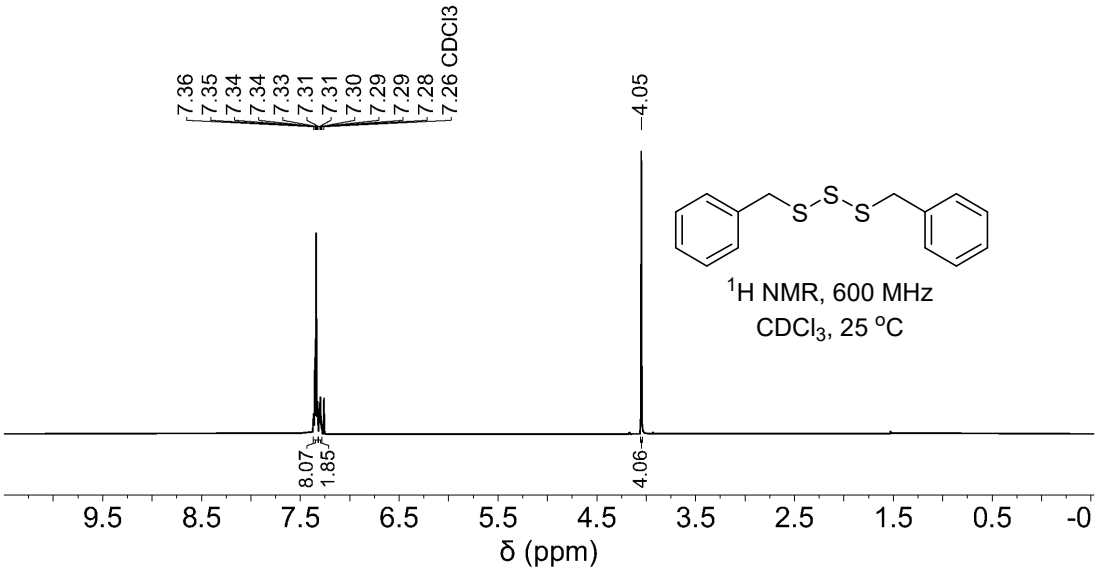

Figure S2.37: ^{1}H NMR spectrum of dibenzyl trisulfide

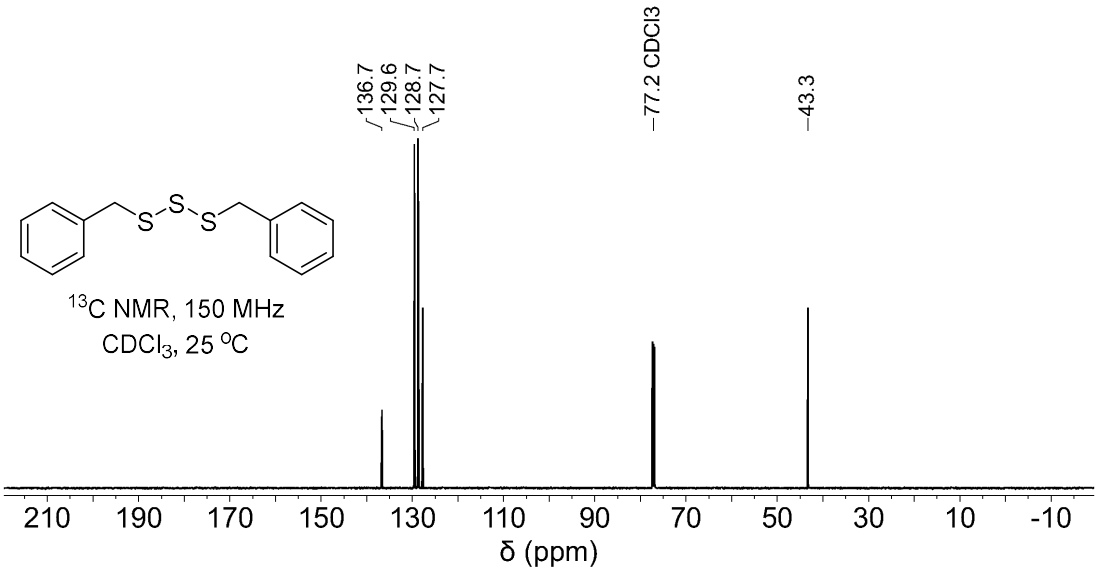

Figure S2.38: ^{13}C NMR spectrum of dibenzyl trisulfide

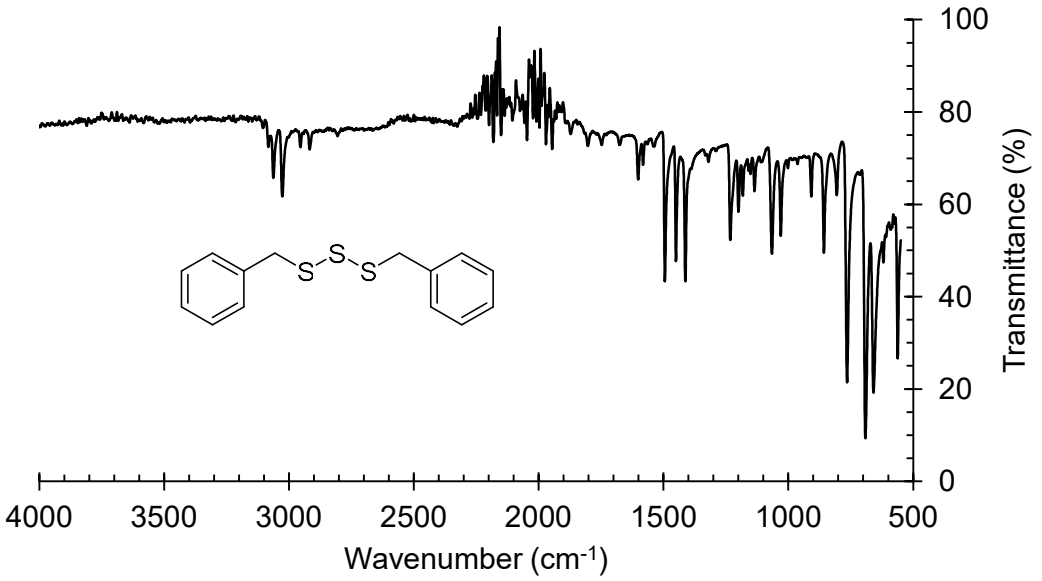

Figure S2.39: FTIR spectrum of dibenzyl trisulfide

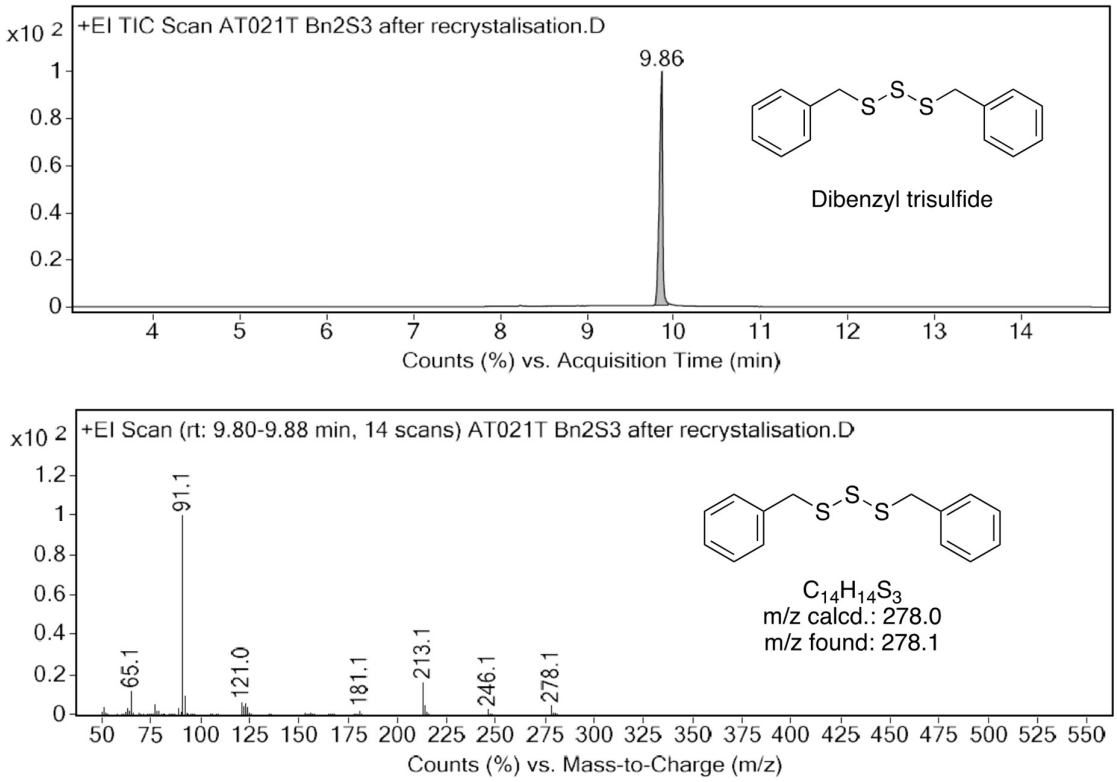

Figure S2.40: Gas chromatogram and mass spectrum of dibenzyl trisulfide. GC-MS method B with a hold time of 8.7 minutes at 250 ºC. Retention time: 9.86 min (Bn_2S_3)

Dibenzyl trisulfide crystal data

Single crystals were mounted in paratone-N oil on a nylon loop. X-ray diffraction data for dibenzyl trisulfide was collected at 100(2) K on the MX-2 beamline of the Australian Synchrotron.[8] Structures were solved by direct methods using SHELXT[9] and refined with SHELXL[10] and ShelXle[11] as a graphical user interface. All non-hydrogen atoms were refined anisotropically and hydrogen atoms were included as invariants at geometrically estimated positions.

Thermal ellipsoid plot

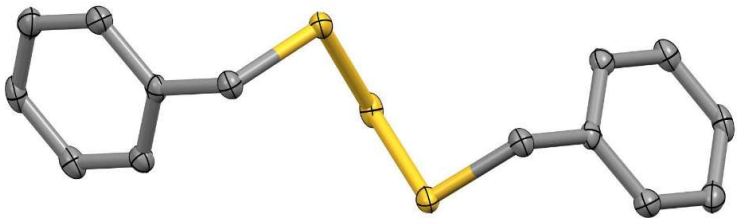

The asymmetric unit of dibenzyl trisulfide with all non-hydrogen atoms shown as ellipsoids at the 50% probability level.

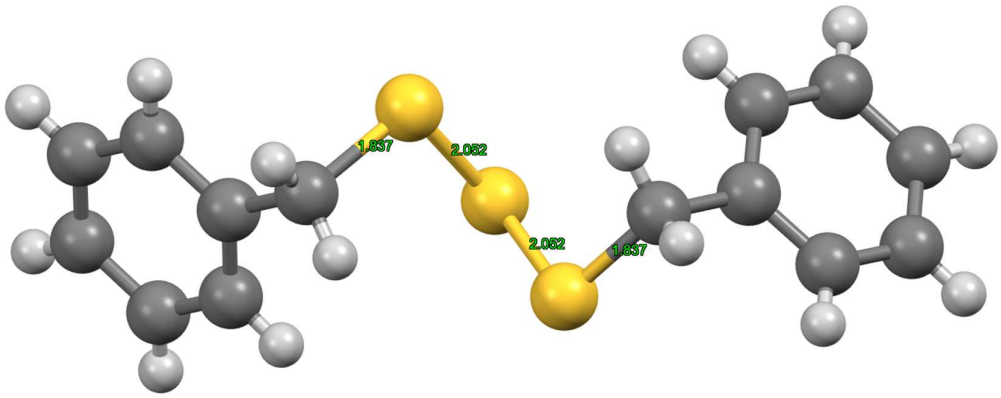

Bond length for S–S was found to be 2.052 Å and for C–S was 1.837 Å.

Dibenzyl trisulfide X-ray experimental data

Compound	**Bn_2S_3**
CCDC number	N/A
Empirical formula	$C_{14}H_{14}S_3$
Formula weight	278.43
Crystal system	Monoclinic
Space group	C2
a (Å)	11.882(2)
b (Å)	4.7830(10)
c (Å)	12.029(2)
α (º)	90
β (º)	103.36(3)
γ (º)	90
Volume (Å^3)	665.1(2)
Z	2
Density (calc.) (Mg/m^3)	1.390
Absorption coefficient (mm^{-1})	0.531
F(000)	292
Crystal size (mm^3)	0.35 x 0.10 x 0.09
θ range for data collection (º)	1.740 to 27.878
Reflections collected	5144
Observed reflections [R(int)]	1603 [0.1228]
Goodness-of-fit on F^2	1.089
R_1 [I>2σ(I)]	0.0592
wR_2 (all data)	0.1328
Largest diff. peak and hole (e.Å-3)	0.912 and -0.714
Data / restraints / parameters	1603 / 1 / 79

Bis(1-adamantyl) trisulfide (2.13)

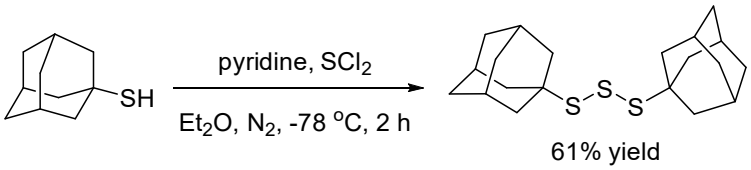

Freshly distilled sulfur dichloride (334 µL, 0.54 g, 2.6 mmol, 0.52 eq.) was added to dry Et_2O (25 mL) at -78 ºC, under an atmosphere of nitrogen with stirring. Pyridine (805 µL, 0.79 g, 10.0 mmol, 1 eq.) and 1-adamantane thiol (1.68 g, 10.0 mmol, 1 eq.) in dry Et_2O (25 mL) was added dropwise over 30 minutes. The reaction was stirred for an additional 90 minutes. The reaction was allowed to reach room temperature, after which it was diluted with ether (50 mL), washed with water (2 × 25 mL), and then saturated $NaCl_{(aq)}$ (25 mL). The organic layer was dried over magnesium sulfate, filtered, and concentrated under reduced pressure to give a white solid 1680 mg. The solid was dissolved in chloroform and recrystallised through methanol addition as antisolvent to give high purity bis(adamantyl) trisulfide (white solid, 1124.4 mg, 61% yield).

m.p. 213.0 – 214.3 ºC. **^{1}H NMR** (600 MHz, $CDCl_3$) δ 2.09 (br. s, 6H), 1.92 (d, *J* = 2.8 Hz, 12H), 1.69 (br. s, 12H). **^{13}C NMR** (150 MHz, $CDCl_3$) δ 50.8, 42.7, 36.3, 30.0. **FTIR** (ν_{max}, ATR): 2899, 2845, 1447, 1340, 1294, 1040, 975, 685. **GC-MS** (EI, 70 eV) *m/z* (rel. intensity): *m/z* calcd. for $C_{20}H_{30}S_3^+$: 366.2[*M*]$^+$, found: 366.2 (M^+, 4), 334.2 (1), 168.1 (1), 135.1 (100). **Elemental analysis** (CHNS): $C_{20}H_{30}S_3$ requires C, 65.52%; H, 8.25%; N, 0%; S, 26.23%. Found C, 65.74%; H, 8.72%; N, 0%; S, 27.92%.

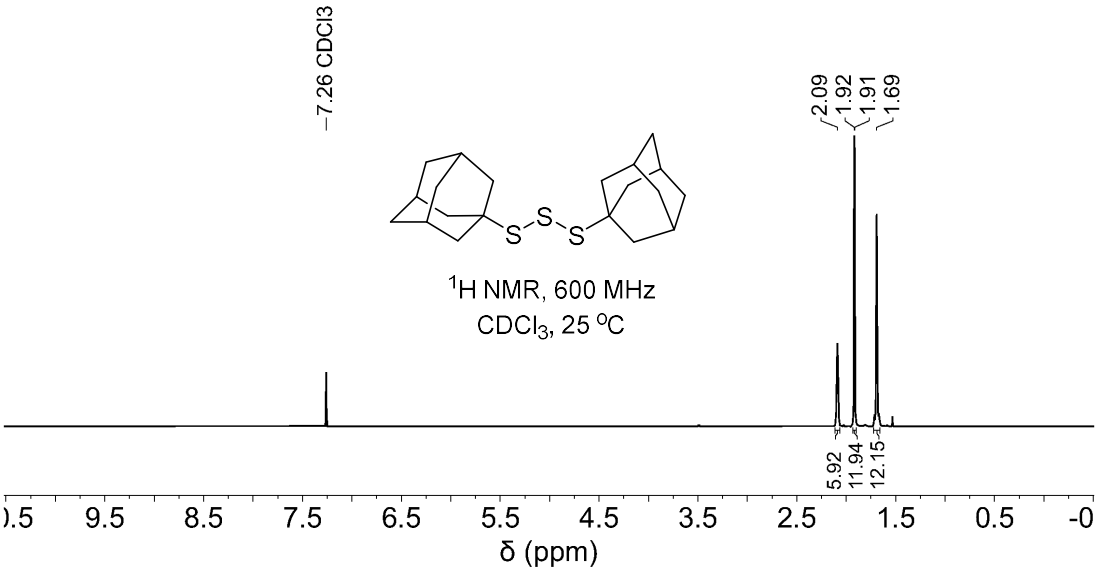

Figure S2.41: ^{1}H NMR spectrum of bis(adamantyl) trisulfide

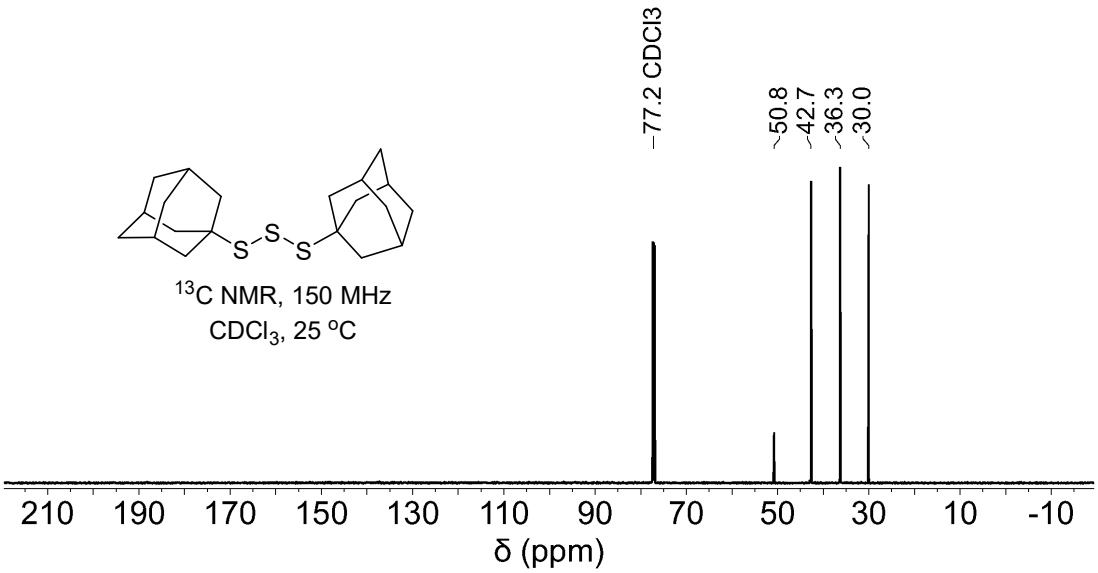

Figure S2.42: ^{13}C NMR spectrum of bis(adamantyl) trisulfide

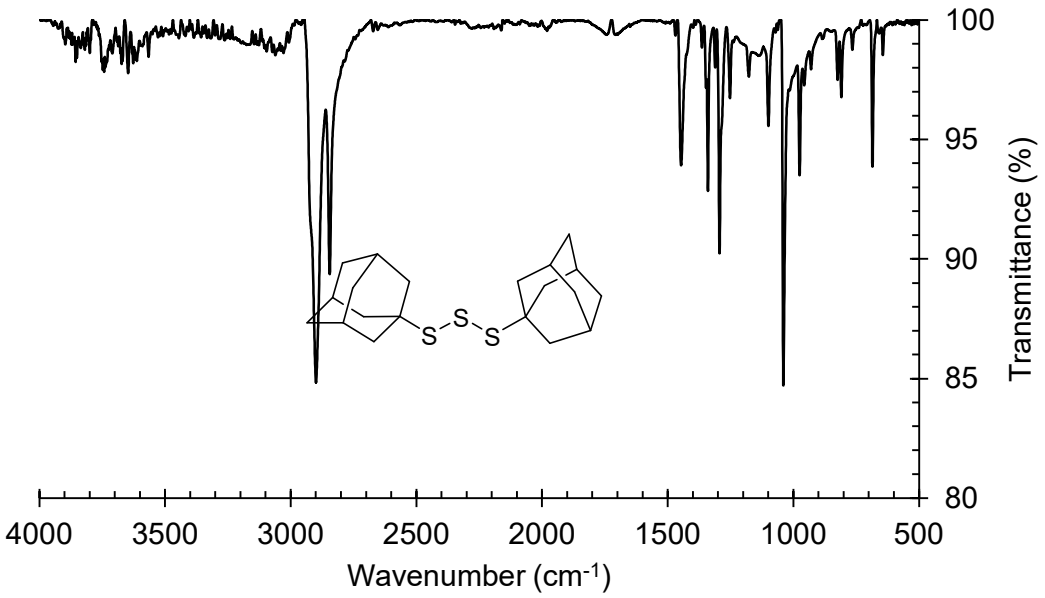

Figure S2.43: FTIR spectrum of bis(1-adamantyl) trisulfide

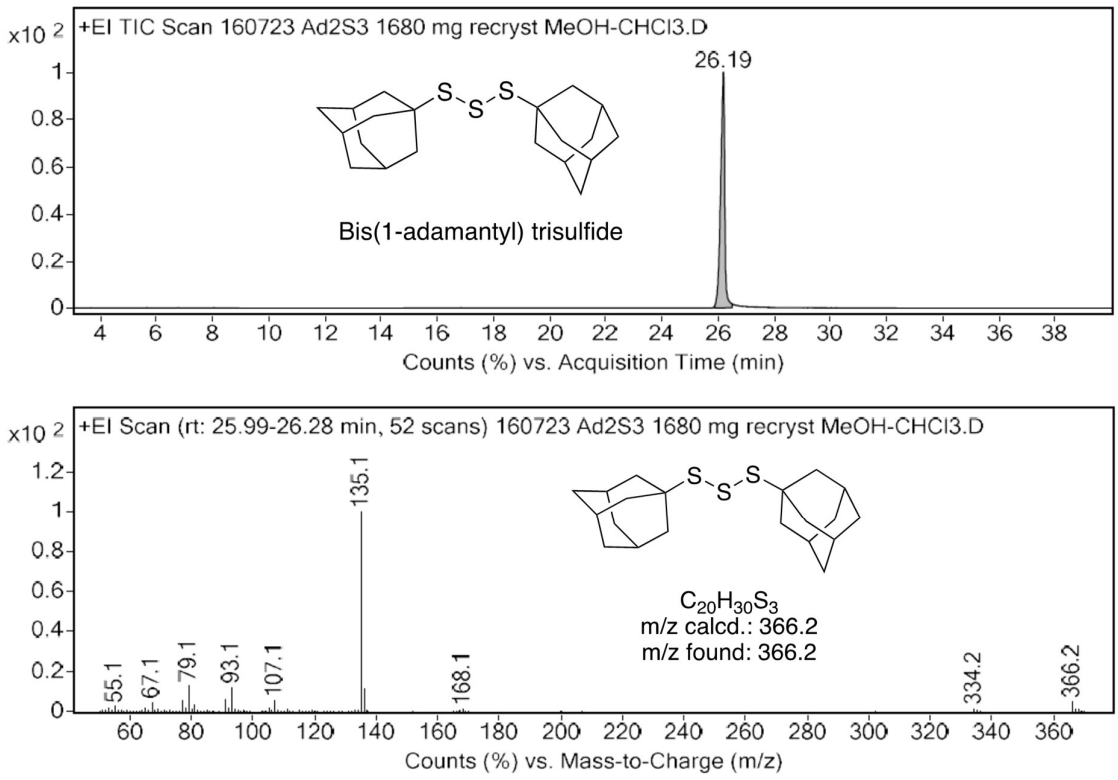

Figure S2.44: Gas chromatogram and mass spectrum of bis(1-adamantyl) trisulfide. GC-MS method B with a hold time of 33.7 minutes at 250 ºC. Retention time: 26.19 min (Ad_2S_3)

Diphenyl trisulfide synthesis

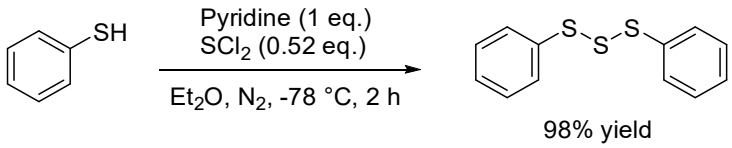

The compound was synthesised based on a literature method.[12] A solution of thiophenol (2.05 mL, 20 mmol, 1 eq.) and pyridine (1.61 mL, 20 mmol, 1 eq.) in 50 mL of dry diethyl ether was allowed to stir under nitrogen at -78 °C (dry ice/acetone bath). A solution of sulfur dichloride (667 μL, 10.5 mmol, 0.52 eq.) in 50 mL of ether was added dropwise to the thiol solution over 0.5 h. The reaction mixture was allowed to stir at -78 °C for an additional 1.5 h. After that, the reaction mixture was quenched with water (25 mL). The organic layer was washed with water (3 × 25 mL) or until the aqueous layer became clear. The organic layer was dried over $MgSO_4$. The dried organic layer was vacuum filtered and the solvent was removed under reduced pressure to obtain diphenyl trisulfide as a yellow oil (2.45 g, 98% yield).

^{1}H NMR (600 MHz, $CDCl_3$) δ 7.51 (m, 4H), 7.31 (dd, *J* = 8.37, 6.97 Hz, 4H), 7.23 (m, 2H). **^{13}C NMR** (150 MHz, $CDCl_3$) δ 137.2, 129.2, 127.7, 127.3. **GC-MS** (EI, 70 eV) m/z (rel. intensity) m/z calcd. for $C_{12}H_{10}S_3^+$: 250.0[*M*]$^+$, found: 250.0 (M^+, 57), 218.0 (6), 186.1 (14), 154.1 (1), 141.0 (82), 109.0 (68), 77.1 (40), 65.1 (30), 51.1 (22)

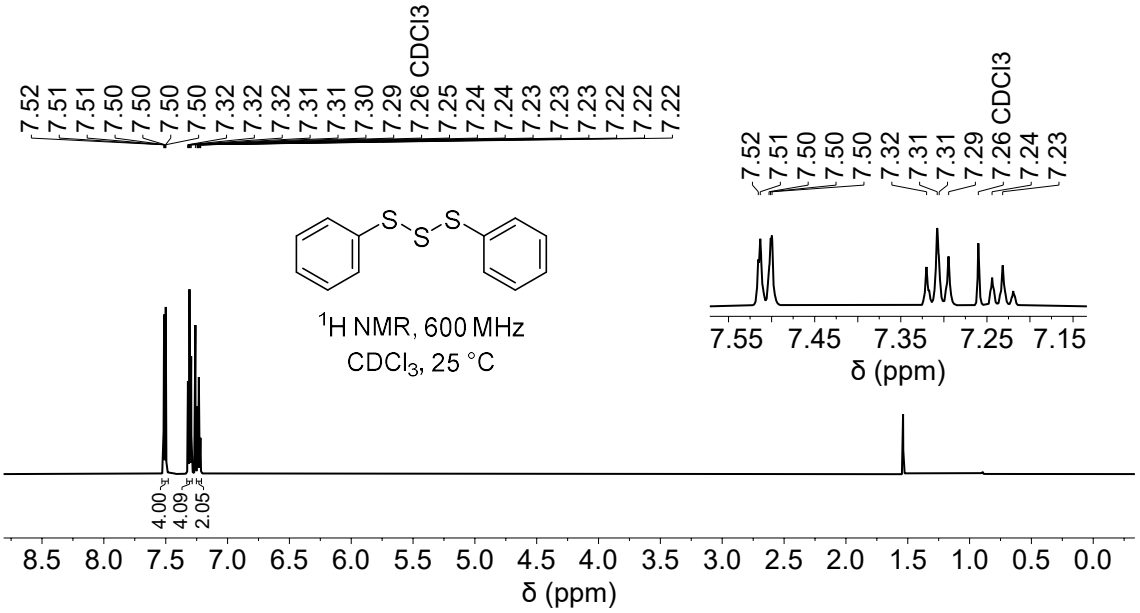

Figure S2.45: ^{1}H NMR spectrum of diphenyl trisulfide

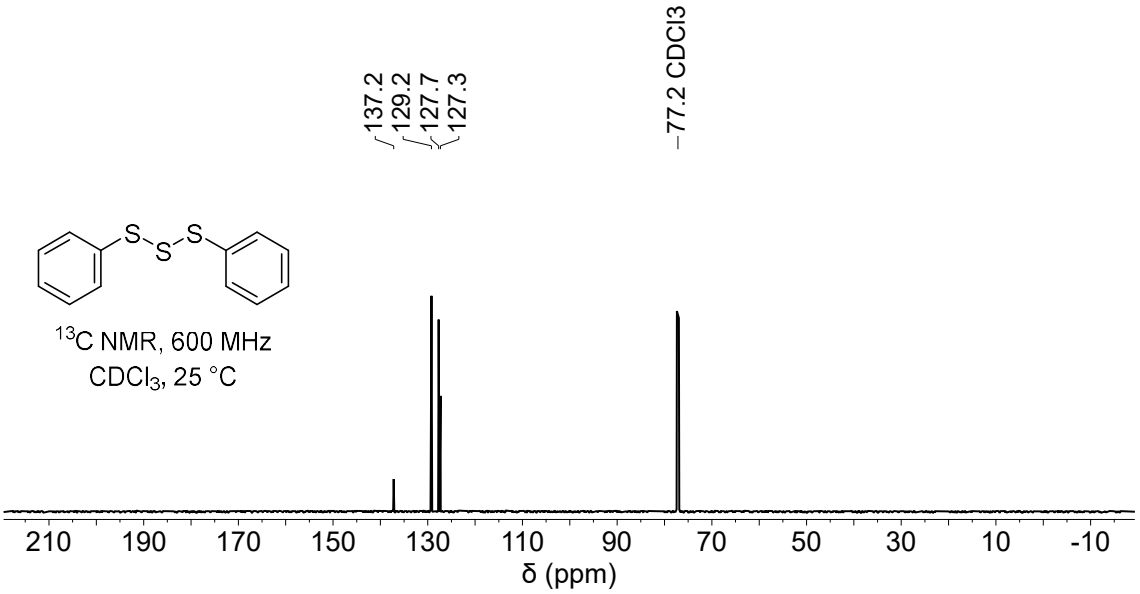

Figure S2.46: ^{13}C NMR spectrum of diphenyl trisulfide

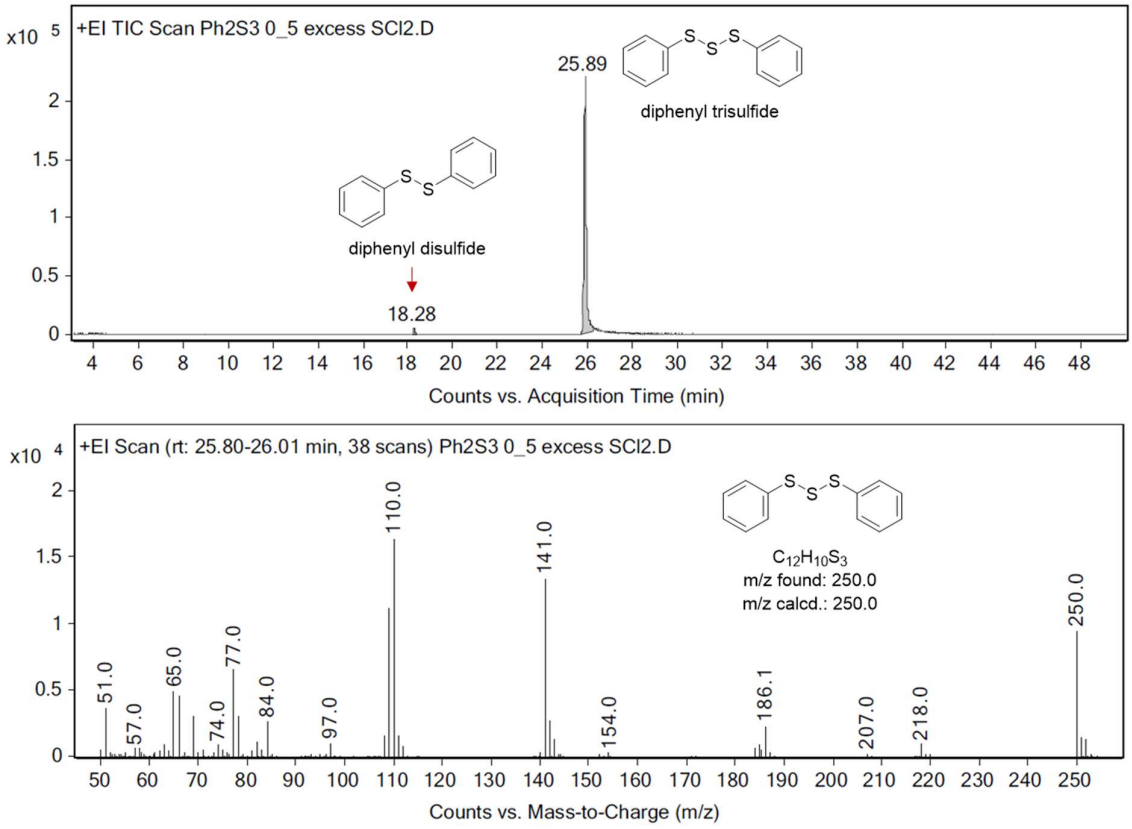

Figure S2.47: Gas chromatogram and mass spectrum of diphenyl trisulfide. GC-MS method adapted from Wu et al.[13]: initial temp. 60 °C, ramp at 8 °C/min to 180 °C, then hold for 35 min. MS transfer line was set at 180 °C. Split ratio and split flow were set at 100:1 and 120 mL/min, respectively. Retention time: 18.28 (Ph_2S_2) and 25.89 min (Ph_2S_3).

Characterization of commercial diphenyl disulfide from TCI

^{1}H NMR (600 MHz, $CDCl_3$) δ 7.51(m, 4H), 7.31 (t, *J* = 7.71 Hz, 4H), 7.24 (t, *J* = 7.37 Hz, 2H).

^{13}C NMR (151 MHz, $CDCl_3$) δ 137.2, 129.2, 127.7, 127.3.

GC-MS (EI, 70 eV) m/z (rel. intensity) m/z calcd. for $C_{12}H_{10}S_2^+$: 218.0[*M*]$^+$, found: 218.1 (M^+, 100), 186.1 (11), 185.0 (22), 154.1 (21), 141.0 (5), 109.0 (97), 77.1 (10), 65.1 (31), 51.1 (10)

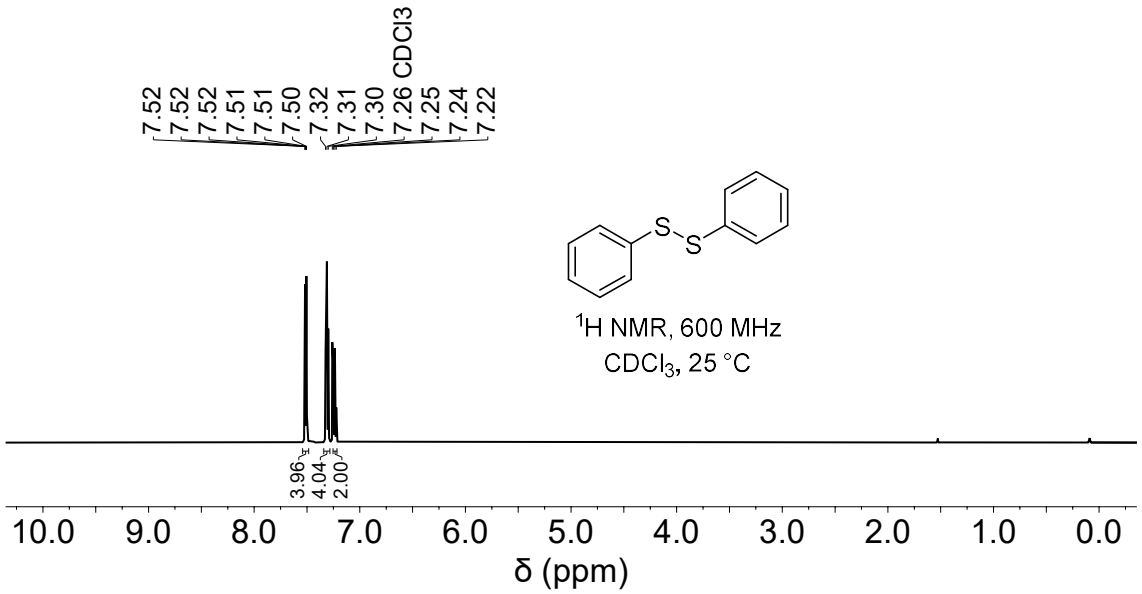

Figure S2.48: ^{1}H NMR spectrum of diphenyl disulfide (TCI)

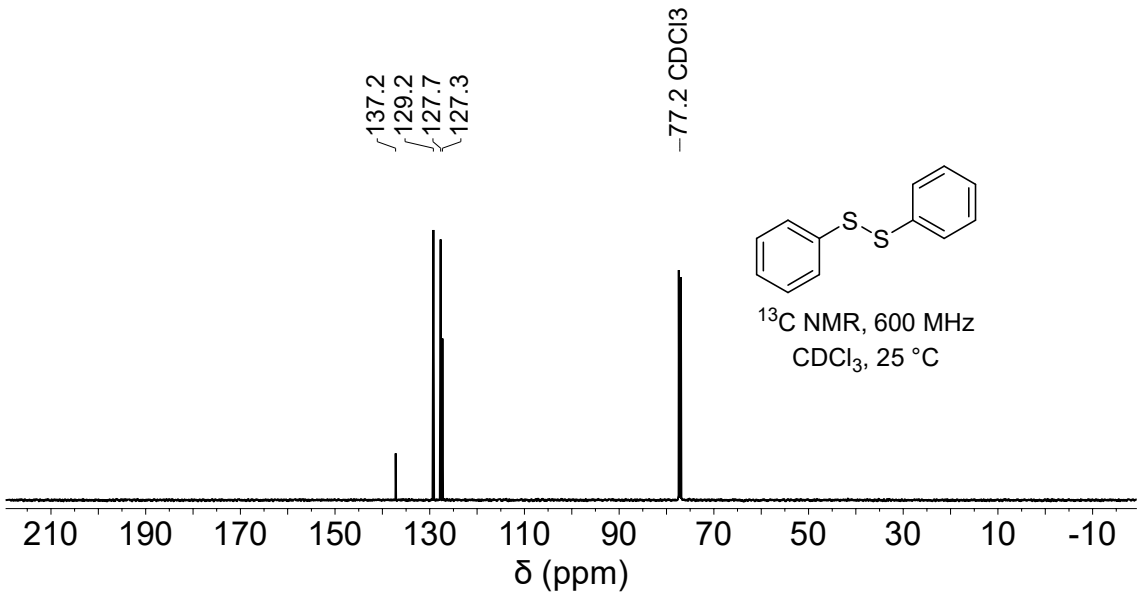

Figure S2.49: ^{13}C NMR spectrum of diphenyl disulfide (TCI)

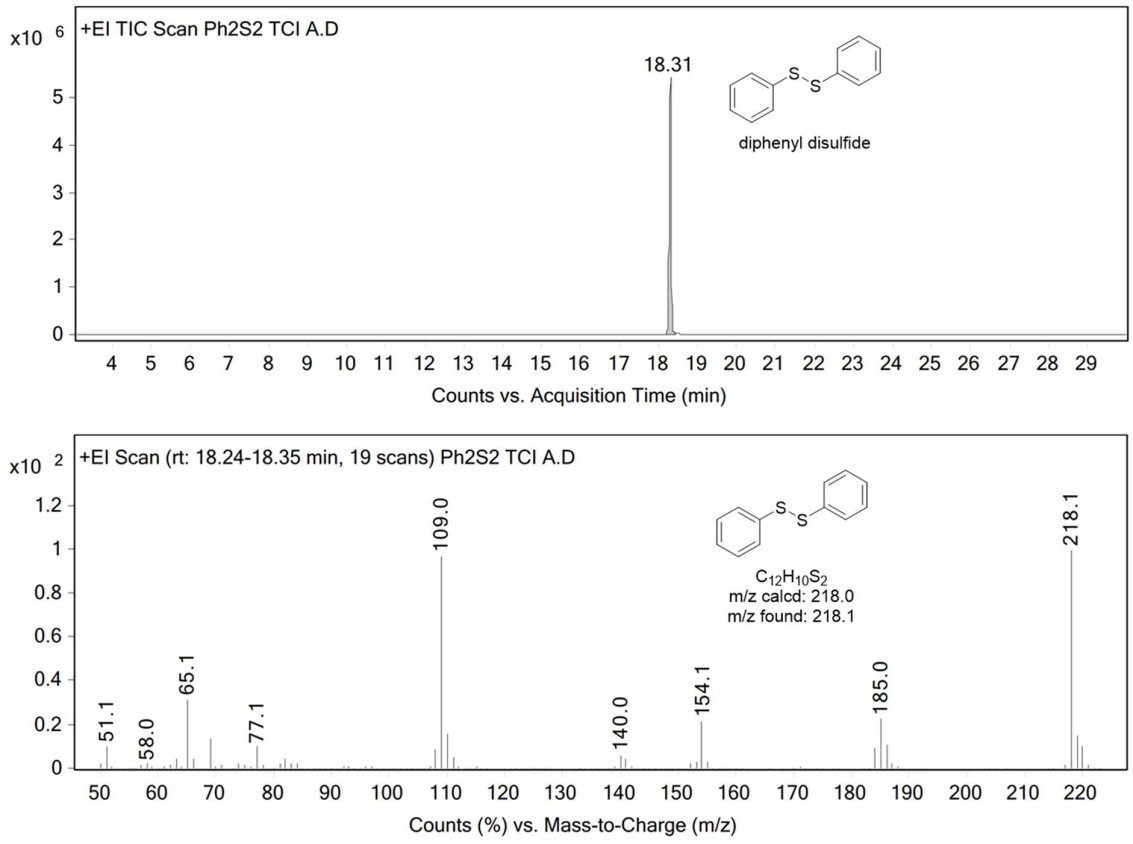

Figure S2.50: Gas chromatogram and mass spectrum of diphenyl trisulfide. GC-MS method adapted from Wu et al.[13]: initial temp. 60 °C, ramp at 8 °C/min to 180 °C, then hold for 35 min. MS transfer line was set at 180 °C. Split ratio and split flow were set at 100:1 and 120 mL/min, respectively. Retention time: 18.31 (Ph_2S_2).

Trisulfides synthesis from *N,N'*-thiobisphthalimide

N,N'-thiobisphthalimide

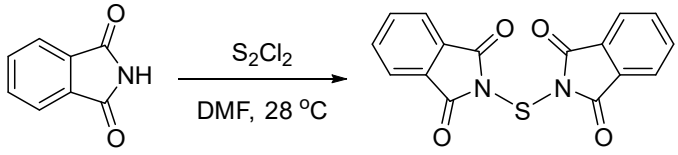

62% yield

The compound was synthesised based on a literature method.[15, 16] Phthalimide (14.7 g, 100 mmol, 1.0 eq.) was added to a dry round bottom flask and dissolved in anhydrous dimethylformamide (80 mL) under a nitrogen atmosphere. The stirred solution was heated to 28 ºC, and S_2Cl_2 (8.0 mL, 100 mmol, 1.0 eq.) was added dropwise via syringe over 5 minutes. The yellow mixture was stirred at 28 ºC for 20 hours; after 20-30 minutes a precipitate appeared. The suspension was filtered, and the

solids washed with MeOH. The solids were dried under vacuum giving *N,N*'-thiobisphthalimide as a white solid (10.055 g, 62% yield). The obtained spectral data is in agreement with the literature.[17]

^{1}H NMR (600 MHz, $CDCl_3$) δ 7.97 – 7.93 (m, 2H), 7.81 – 7.77 (m, 2H). **^{13}C NMR** (150 MHz, $CDCl_3$) δ 166.2, 135.3, 131.6, 124.8.

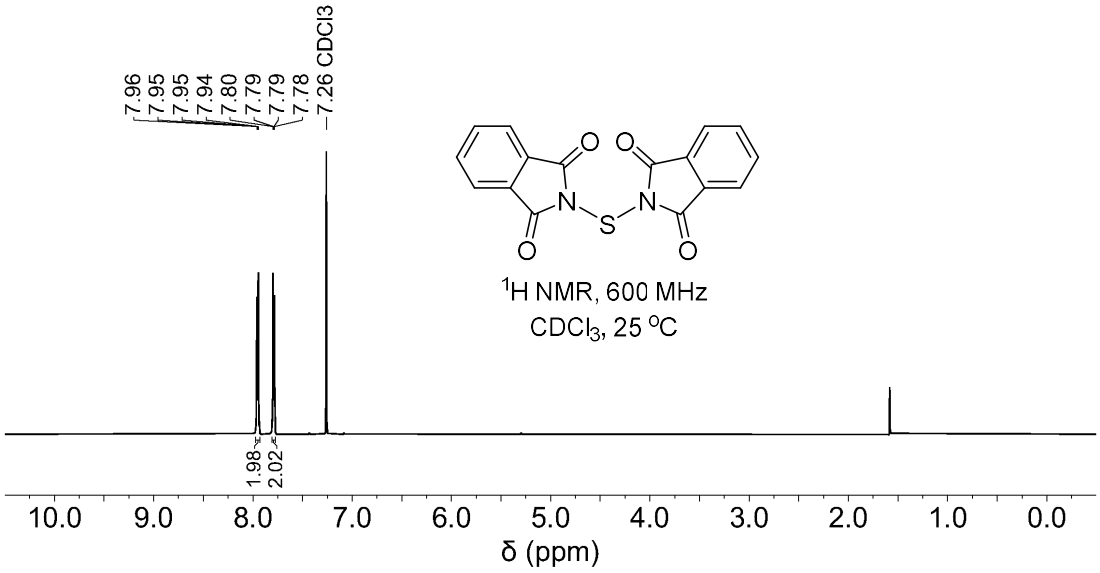

Figure S2.51: ^{1}H NMR spectrum of *N,N*'-thiobisphthalimide

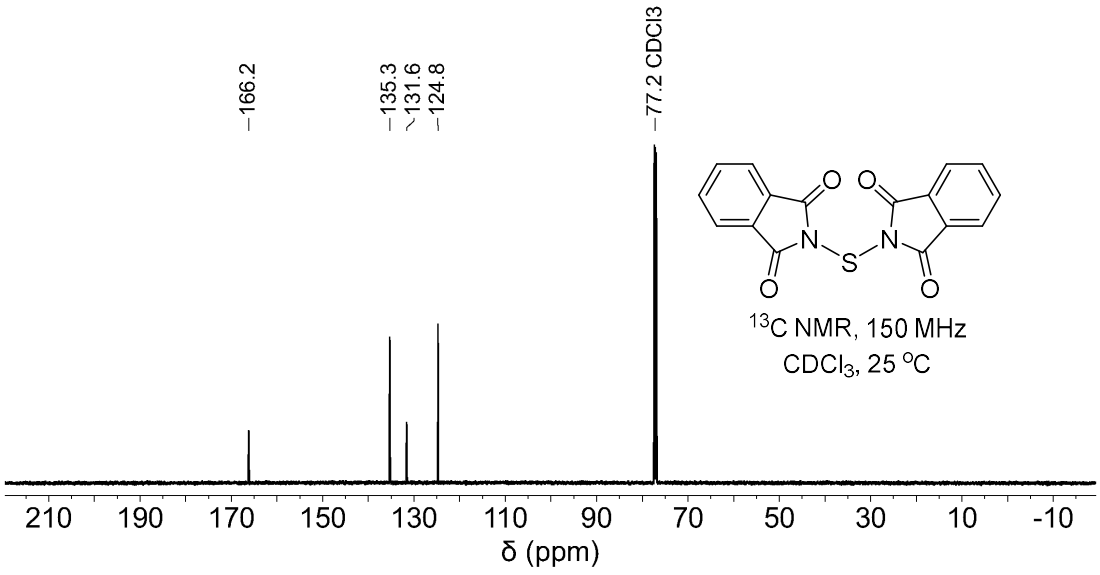

Figure S2.52: ^{13}C NMR spectrum of *N,N*'-thiobisphthalimide

Bis(2-hydroxyethyl) trisulfide (2.16)

From 2-mercaptoethanol and *N,N'*-thiobisphthalimide

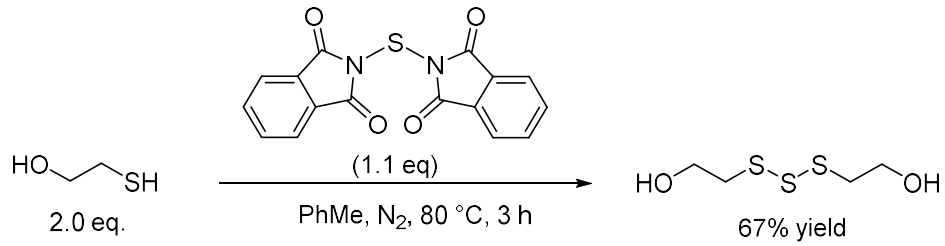

Bis(2-hydroxyethyl) trisulfide was prepared by the general method described by Harpp et al.[18] with a slight modification. To a 100 mL round bottom flask was added *N,N*'-thiobisphthalimide (540 mg, 1.67 mmol, 1.1 equiv.) and toluene (30 mL). To this suspension, 2-mercaptoethanol (211.2 µL, 3.0 mmol, 2.0 equiv.) was added in one portion and the mixture was heated to 80 ºC. TLC analysis (50% EtOAc in hexanes) revealed complete consumption of *N,N*'-thiobisphthalimide after 3 hours of reaction (the trisulfide products formed with R_f= 0.22). After that, the mixture was allowed to cool to room temperature. The mixture was filtered, and the residue was washed with DCM (3 × 10 mL). The combined filtrate and washings were evaporated to give a white waxy solid. Next, to this waxy solid was added DCM (20 mL) and silica gel (~3 grams). The solvent was removed under reduced pressure and the resulting free-flowing residue (for dry loading) was purified by flash column chromatography (ethyl acetate/hexane 1:1). Bis(2-hydroxyethyl) trisulfide (187.3 mg, 67%) was isolated as a viscous beige oil. Along with the trisulfide product, *N*-(2-hydroxyethyl thiosulfenyl) phthalimide (R_f = 0.44, 50% EtOAc in hexanes) and phthalimide (R_f = 0.72, 50% EtOAc in hexanes) were isolated as pure compounds.

^{1}H NMR ($CDCl_3$, 600 MHz): δ 2.25 (br. s, 2H, OH), 3.09 (t, *J* = 5.7 Hz, 4H), 3.98 (t, *J* = 5.7 Hz, 4H). **^{13}C NMR** (CDCl3, 150 MHz): δ 41.9, 59.7. **GC-MS** (EI, 70 eV) m/z (rel. intensity) m/z calcd for $C_4H_{10}S_3^+$: 186.0[*M*]$^+$, found: 186.0 (M^+, 100), 168.0 (2), 141.9 (10), 124.0 (98), 110.9 (14), 92.0 (34), 79.0 (36), 59.0 (54).

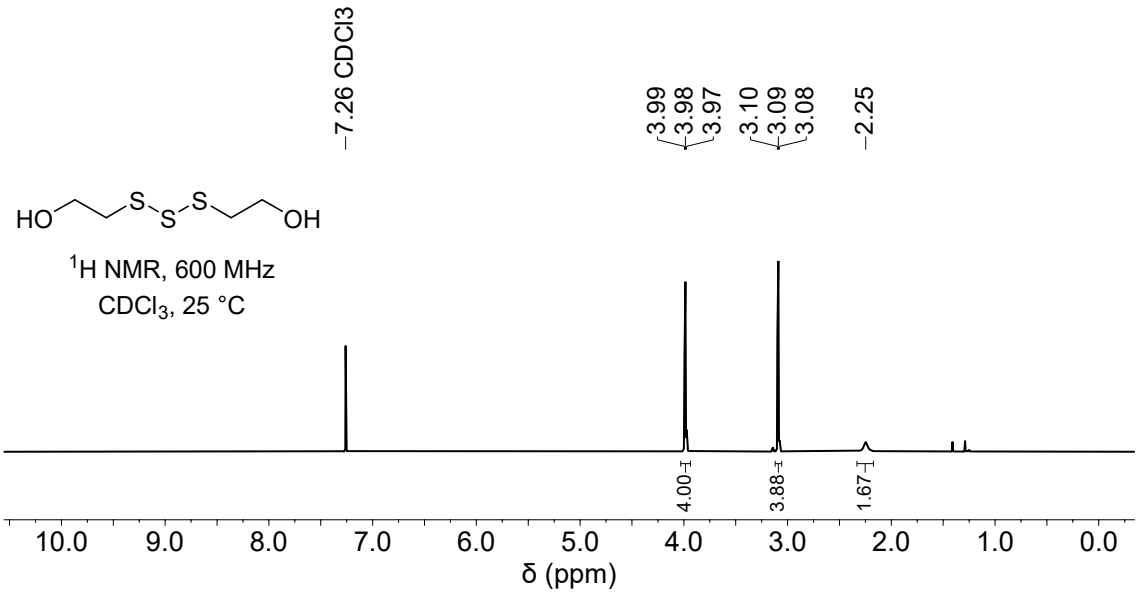

Figure S2.53: ^{1}H NMR spectrum of bis(2-hydroxyethyl) trisulfide

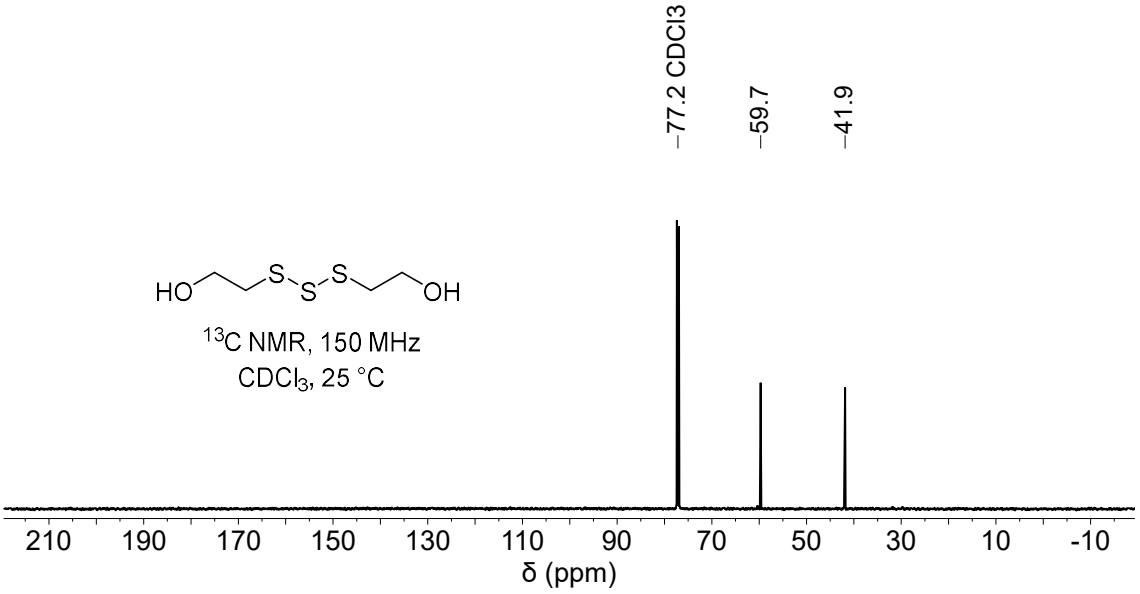

Figure S2.54: ^{13}C NMR spectrum of bis(2-hydroxyethyl) trisulfide

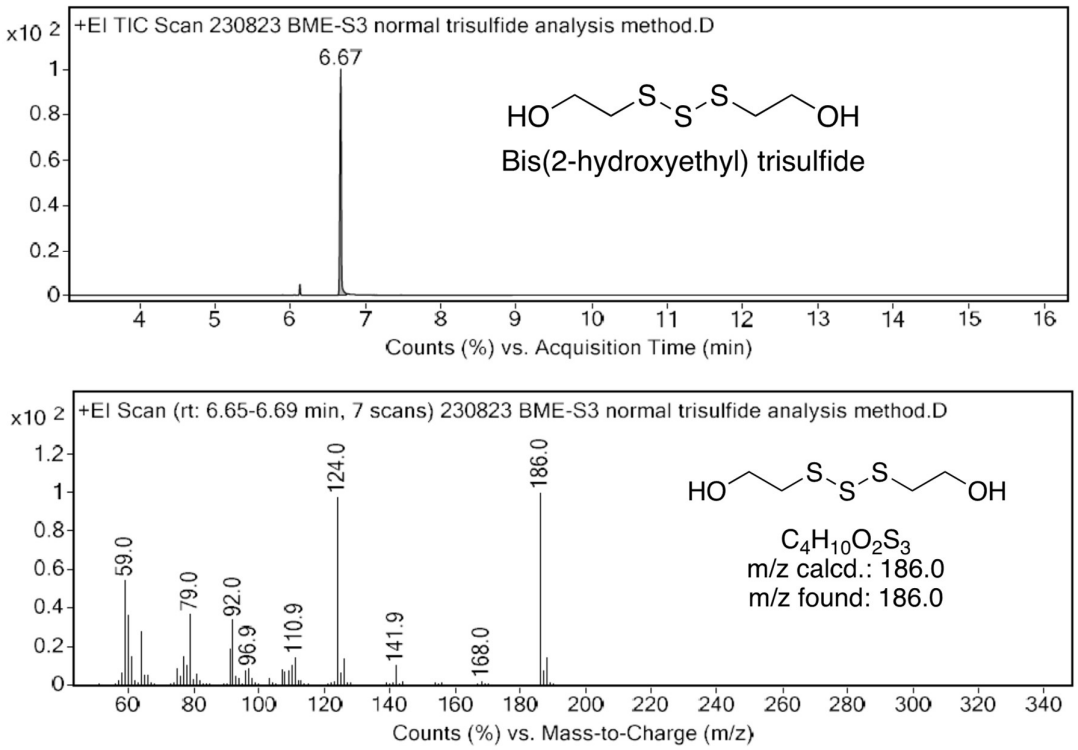

Figure S2.55: Gas chromatogram and mass spectrum of bis(2-hydroxyethyl) trisulfide. GC-MS method B with a hold time of 10 minutes at 250 ºC. Retention time: 6.67 min (bis(2-hydroxyethyl) trisulfide)

***N*-(2-hydroxyethyl thiosulfenyl) phthalimide**

R_f = 0.44 (50% EtOAc in hexane)

^{1}H NMR (600 MHz, $CDCl_3$) δ 7.94 (dd, *J* = 5.50, 3.07 Hz, 2H), 7.80 (dd, *J* = 5.53, 3.04 Hz, 2H), 4.07 (q, *J* = 5.85 Hz, 2H), 3.23 (t, *J* = 5.78 Hz, 2H), 1.87 (t, *J* = 6.10 Hz, 1H).

^{13}C NMR (151 MHz, $CDCl_3$) δ 167.9, 135.0, 132.3, 124.3, 60.9, 43.5.

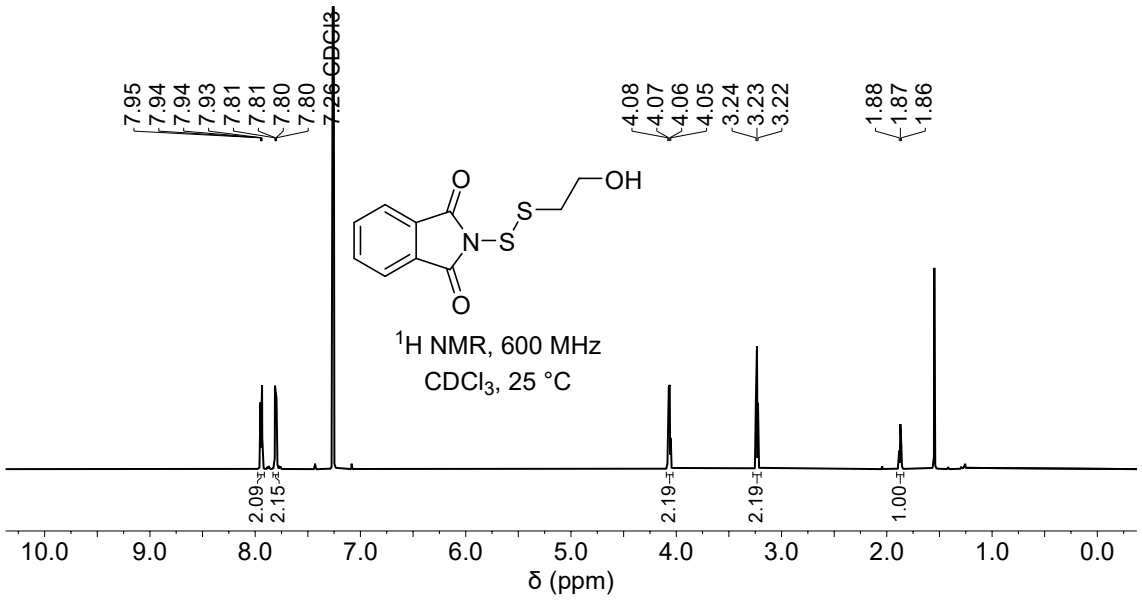

Figure S2.56: ^{1}H NMR spectrum of *N*-(2-hydroxyethyl thiosulfenyl) phthalimide

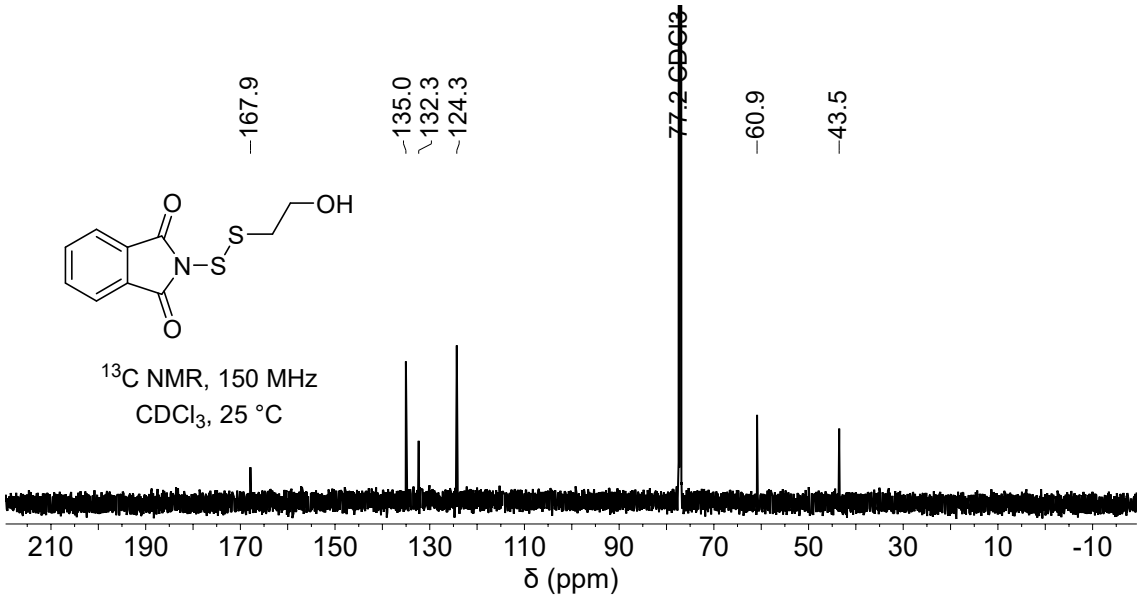

Figure S2.57: ^{13}C NMR spectrum of *N*-(2-hydroxyethyl thiosulfenyl) phthalimide

Phthalimide

R_f = 0.72 (50% EtOAc in hexane)

^{1}H NMR (600 MHz, $CDCl_3$) δ 7.88 (dd, *J* = 5.44, 3.06 Hz, 2H), 7.77 (dd, *J* = 5.50, 3.04 Hz, 2H).

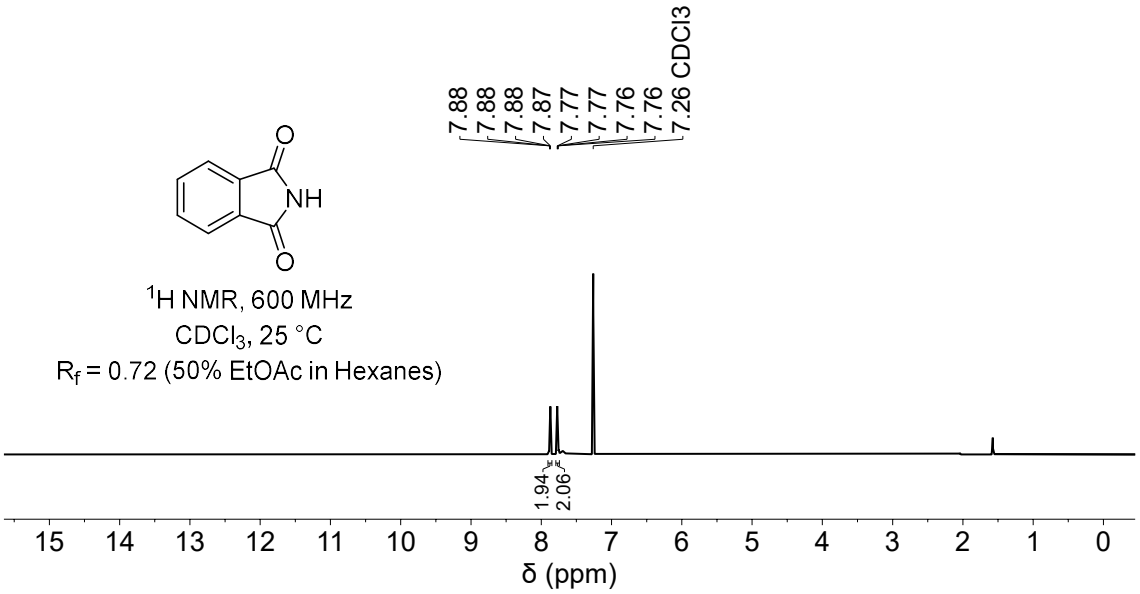

Figure S2.58: ^{1}H NMR spectrum of phthalimide (R_f = 0.72, 50% EtOAc in hexane)

Phthalimide (Sigma Aldrich)

^{1}H NMR (600 MHz, $CDCl_3$) δ 7.88 (dd, *J* = 5.47, 3.06 Hz, 2H), 7.77 (dd, *J* = 5.50, 3.03 Hz, 2H).

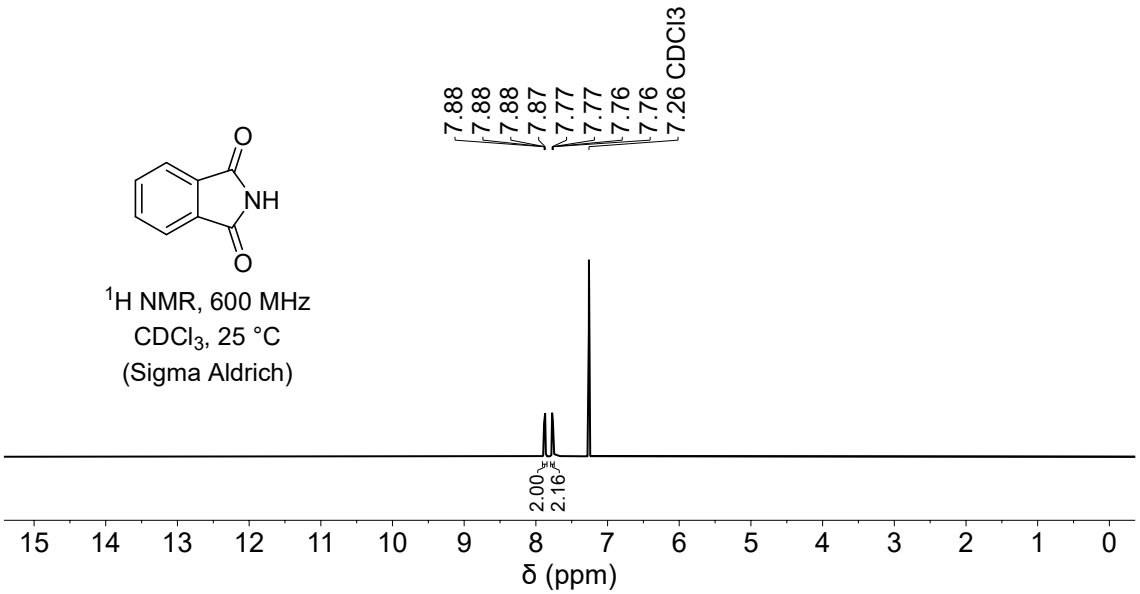

Figure S2.59: ^{1}H NMR spectrum of phthalimide (Sigma Aldrich)

From 2-mercaptoethanol and SCl_2

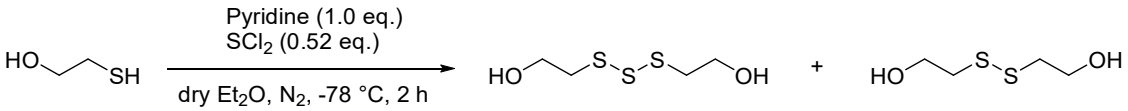

Under nitrogen atmosphere, to a dried 25 mL round bottom flask was added dry ether (5 mL) and freshly distilled sulfur dichloride (100 µL, 1.57 mmol, 0.52 equiv.) cooled to -78 ºC (dry ice/acetone bath). To this solution was added dropwise via a syringe a solution of 2-mercaptoethanol (210 µL, 2.98 mmol, 1 equiv.) and pyridine (240 µL, 2.98 mmol, 1 equiv.) in dry diethyl ether (5 mL). After the addition was complete (20 minutes), the solution was stirred for an additional 1.5 hours at -78 ºC, after which the mixture was diluted with ether (30 mL) and washed with water (2 × 10 mL) and brine (2 × 10 mL). The organic layer was dried over magnesium sulfate, filtered, and concentrated under reduced pressure to give a viscous yellow oil. TLC shows one spot with R_f = 0.22 (50% EtOAc in hexane). Purification by silica column chromatography gave a viscous oil (277.9 mg). However, GC-MS analysis revealed that the product consists of bis(2-hydroxyethyl) trisulfide (94%) and bis(2-hydroxyethyl) disulfide (6%).

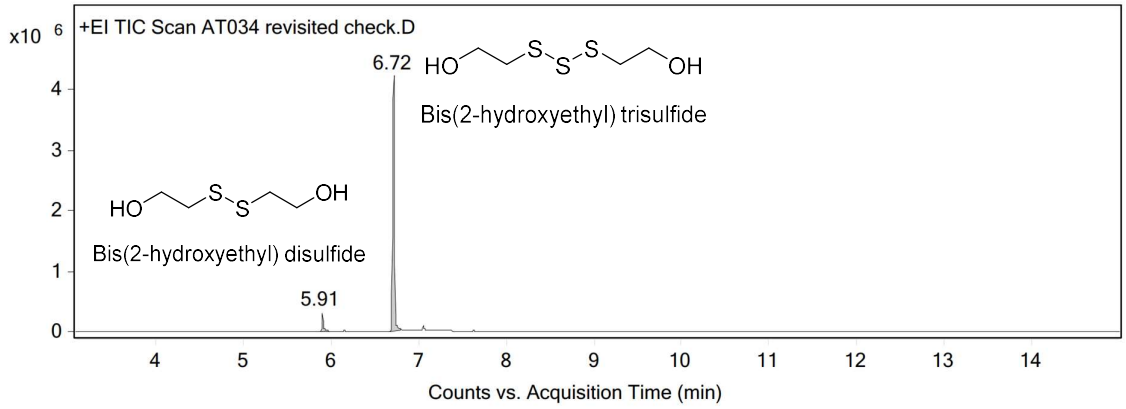

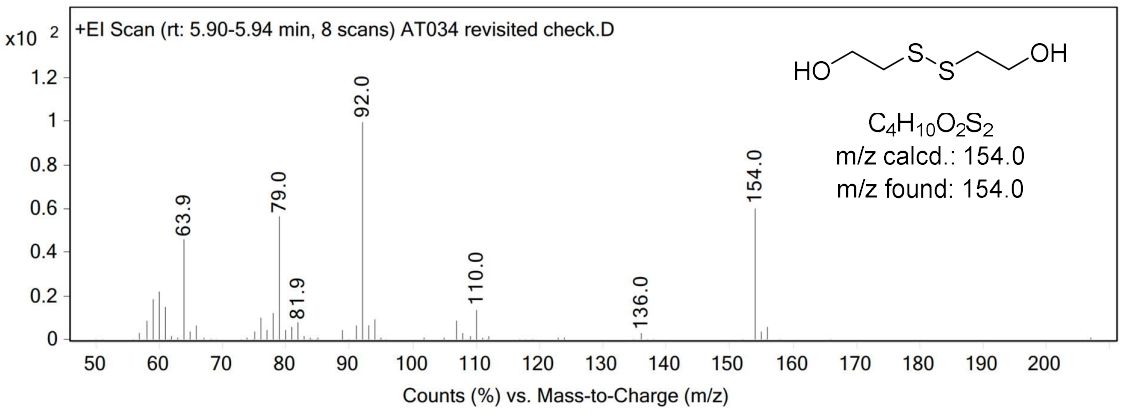

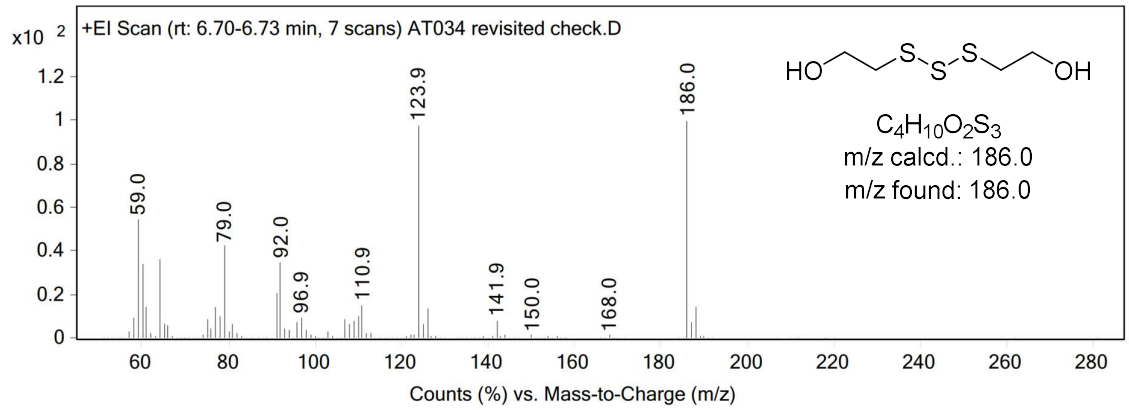

Figure S2.60: Gas chromatogram and mass spectrum of bis(2-hydroxyethyl) trisulfide prepared from the reaction between 2-mercaptoethanol and SCl_2. GC-MS method B with a hold time of 10 minutes at 250 ºC. Retention time: 5.91 min (bis(2-hydroxyethyl) disulfide), 6.72 min (bis(2-hydroxyethyl) trisulfide).

Bis(2-hydroxyethyl) trisulfide synthesized from the protocol reported by Ercole et al.[15] (This experiment was conducted by Dr. Harshal D. Patel of Flinders University)

***N*-(2-hydroxyethyl thiosulfenyl)phthalimide**

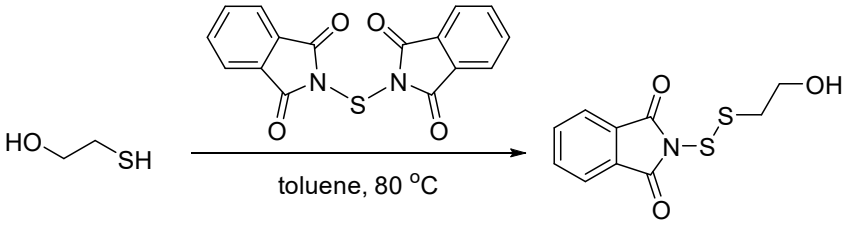

38% yield

The compound was synthesised based on a literature method.[15] *N,N*'-thiobisphthalimide (2.53 g, 7.81 mmol, 1.1 eq.) and 2-mercaptoethanol (0.50 mL, 7.1 mmol, 1.0 eq.) in 40 mL toluene were heated at 80 ºC for 1 hour with stirring. After cooling to room temperature, the mixture was filtered through cotton wool and the solids washed with DCM. The solvent was removed under reduced pressure and the crude mixture purified by column chromatography using DCM with a gradient to gradient to EtOAc/DCM (20/80), giving the product as a white solid (0.692 g, 38% yield). The obtained spectral data is in agreement with the literature.[15]

R_f = 0.25 (EtOAc/DCM 5:95). **^{1}H NMR** (400 MHz, $CDCl_3$) δ 7.97 – 7.91 (m, 2H), 7.83 – 7.78 (m, 2H), 4.06 (t, *J* = 5.8 Hz, 2H), 3.23 (t, *J* = 5.8 Hz, 2H), 1.93 (s, 1H). **^{13}C NMR** (100 MHz, $CDCl_3$) δ 167.9, 135.0, 132. 3, 124.3, 60.9, 43.5.

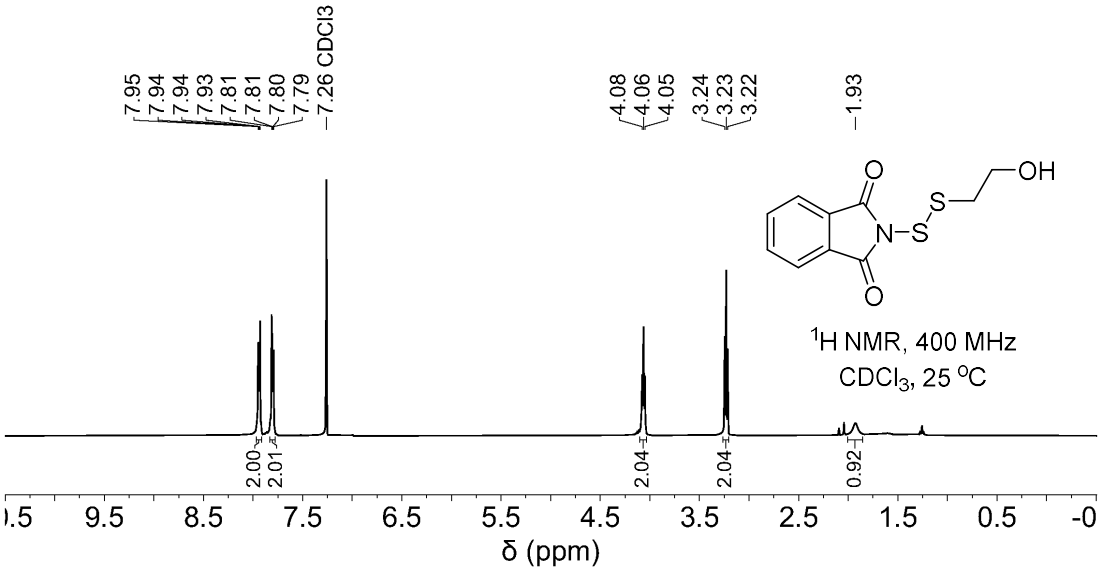

Figure S2.61: ^{1}H NMR spectrum of *N*-(2-hydroxyethyl thiosulfenyl) phthalimide

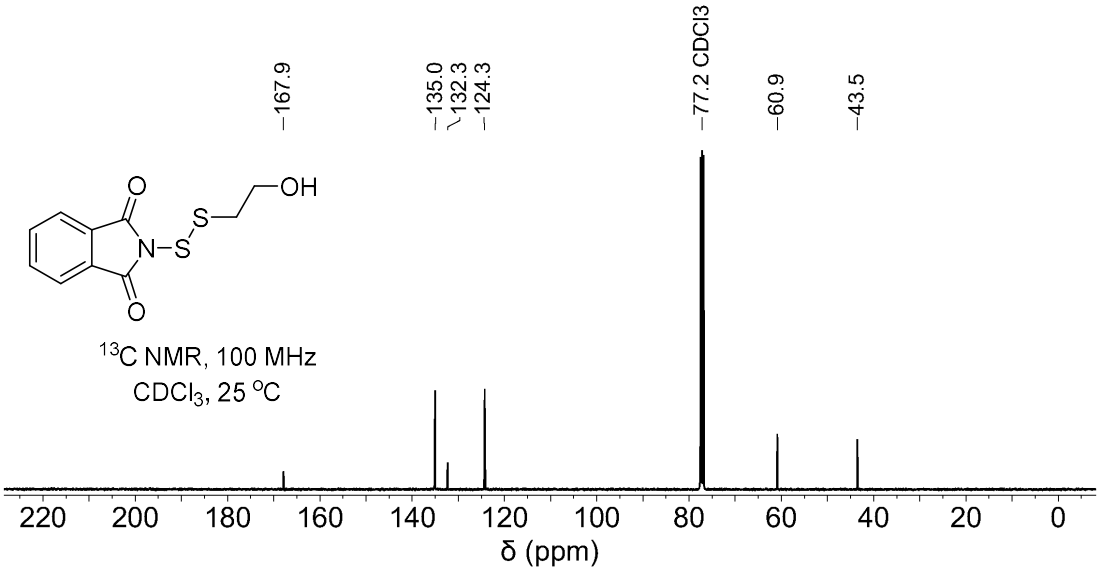

Figure S2.62: ^{13}C NMR spectrum of *N*-(2-hydroxyethyl thiosulfenyl) phthalimide

Bis(2-hydroxyethyl) trisulfide

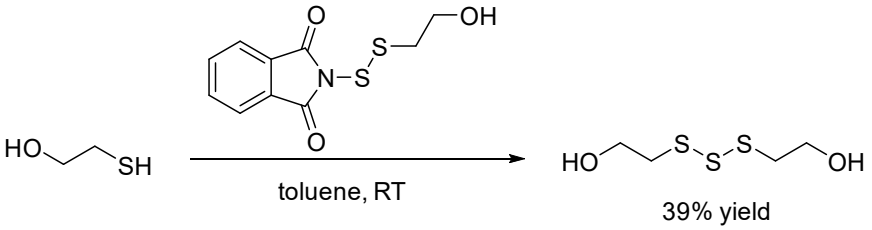

The compound was synthesised based on a literature method.[15] *N*-(2-hydroxyethyl thiosulfenyl) phthalimide (649 mg, 2.54 mmol, 1.0 eq.) and 2-mercaptoethanol (0.18 mL, 2.5 mmol, 1.0 eq.) in 15 mL toluene were stirred at room temperature overnight. The mixture was filtered through cotton wool, the solids washed with DCM, and the solvent removed under reduced pressure. To the crude, 2-mercaptoethanol (0.18 mL, 2.5 mmol, 1.0 eq.) and 15 mL toluene was added, and the mixture stirred at 80 ºC for 1 hour. After cooling to room temperature, the mixture was filtered through cotton wool, the solids washed with DCM, and the solvent removed under reduced pressure. The crude was purified by column chromatography using DCM with a gradient to gradient to EtOAc/DCM (50/50), giving the product as beige oil (184 mg, 39% yield). The obtained spectral data is in agreement with the literature.[15]

R_f = 0.40 (EtOAc/DCM 50:50). **^{1}H NMR** (600 MHz, $CDCl_3$) δ 3.98 (t, *J* = 5.7 Hz, 6H), 3.09 (t, *J* = 5.7 Hz, 6H), 2.25 (br. s, 2H). **^{13}C NMR** (150 MHz, $CDCl_3$) δ 59.7, 41.9.

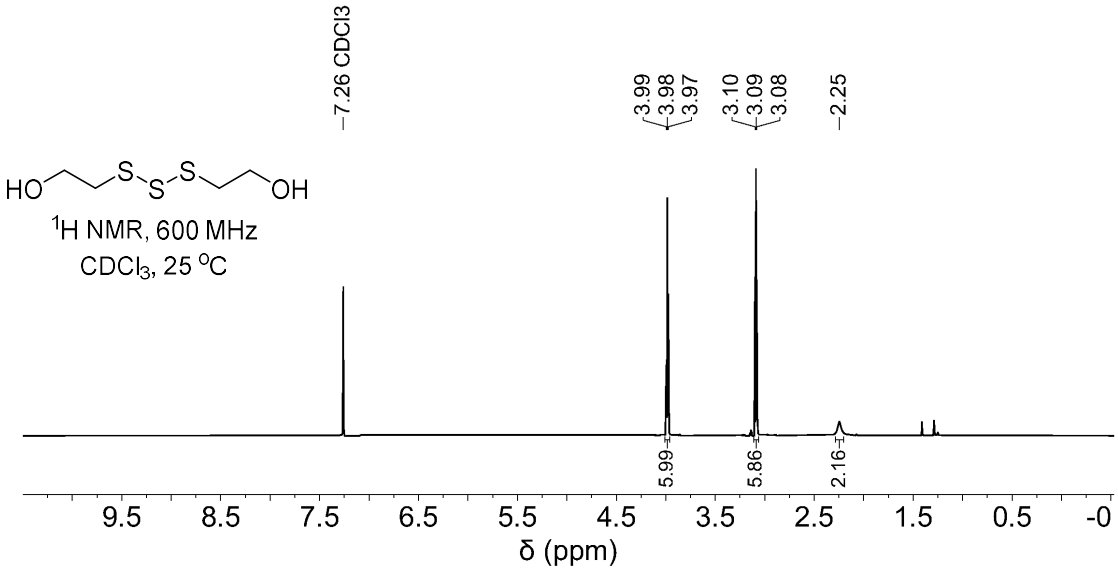

Figure S2.63: ^{1}H NMR spectrum of bis(2-hydroxyethyl) trisulfide

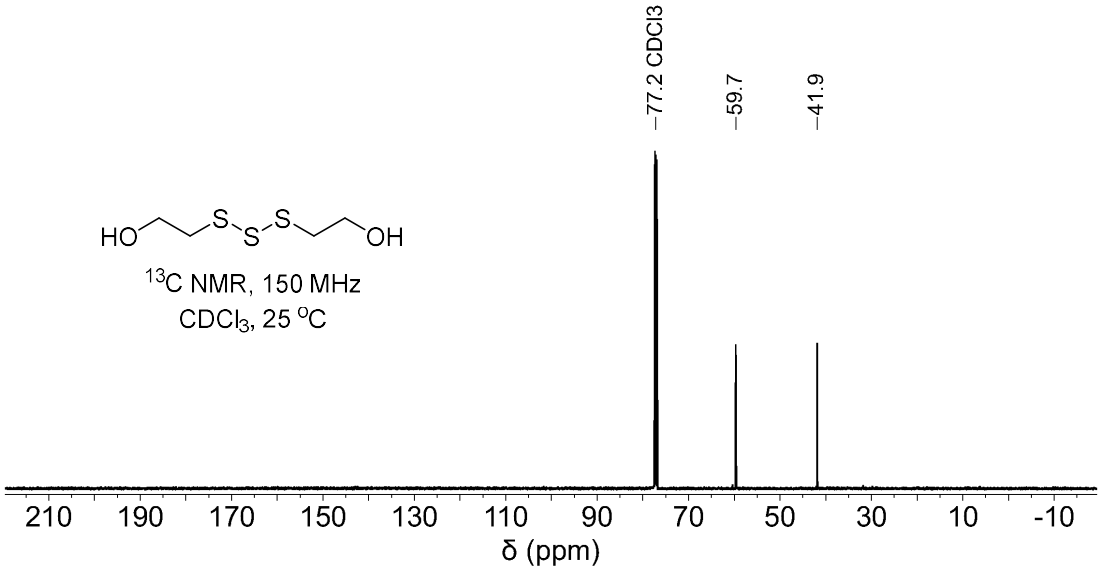

Figure S2.64: ^{13}C NMR spectrum of bis(2-hydroxyethyl) trisulfide

Bis(2-trimethylsiloxyethyl) trisulfide synthesis

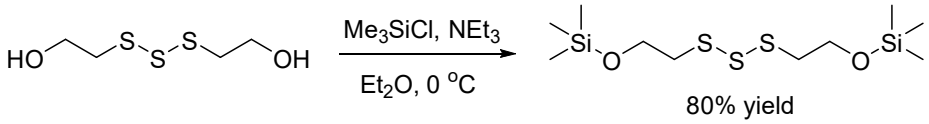

To a stirred solution of bis(2-hydroxyethyl) trisulfide (184 mg, 0.99 mmol, 1.0 eq.) and NEt_3 (0.30 mL, 2.2 mmol, 2.2 eq.) in 6 mL anhydrous Et_2O at 0 ºC, was added Me_3SiCl (0.28 mL, 2.2 mmol, 2.2 eq.) dropwise. The reaction was allowed to reach room temperature and stirred for an additional 3 hours. The mixture was filtered through celite washing with Et_2O, and the solvent removed under reduced pressure to give bis(2-trimethylsiloxyethyl) trisulfide as a pale brown oil (262 mg, 80% yield).

^{1}H NMR (600 MHz, $CDCl_3$) δ 3.89 (t, *J* = 6.8 Hz, 4H), 3.02 (t, *J* = 6.8 Hz, 4H), 0.14 (s, 18H). **13C NMR** (150 MHz, $CDCl_3$) δ 61.1, 41.0, -0.3. **FTIR** (neat, cm^{-1}): 2956, 2862, 1250, 1081, 870, 835, 746, 708, 690, 478. **GC-MS** (EI, 70 eV) *m/z* (rel. intensity): *m/z* calcd for $C_{10}H_{26}O_2S_3Si_2^+$: 330.1[*M*]$^+$, found: 330.1 (M+, 14), 298.1 (1), 182.0 (4), 151.0 (9), 133.0 (15), 117.1 (27), 103.1 (34), 91.0 (6), 73.1 (100), 59.0 (12). **Elemental analysis** (CHNS): $C_{10}H_{26}O_2S_3Si_2$ requires C, 36.32%; H, 7.93%; N, 0%; S, 29.09% (O, 9.68%; Si, 16.99%). Found C, 36.57%; H, 7.71%; N, 0.12%; S, 29.57%.

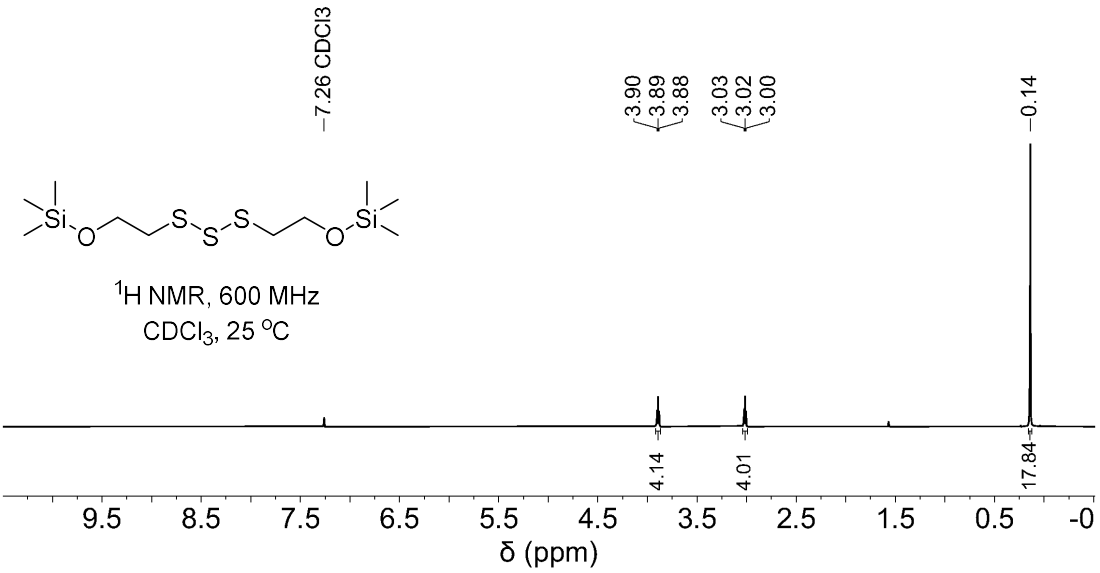

Figure S2.65: ^{1}H NMR spectrum of bis(2-trimethylsiloxyethyl) trisulfide

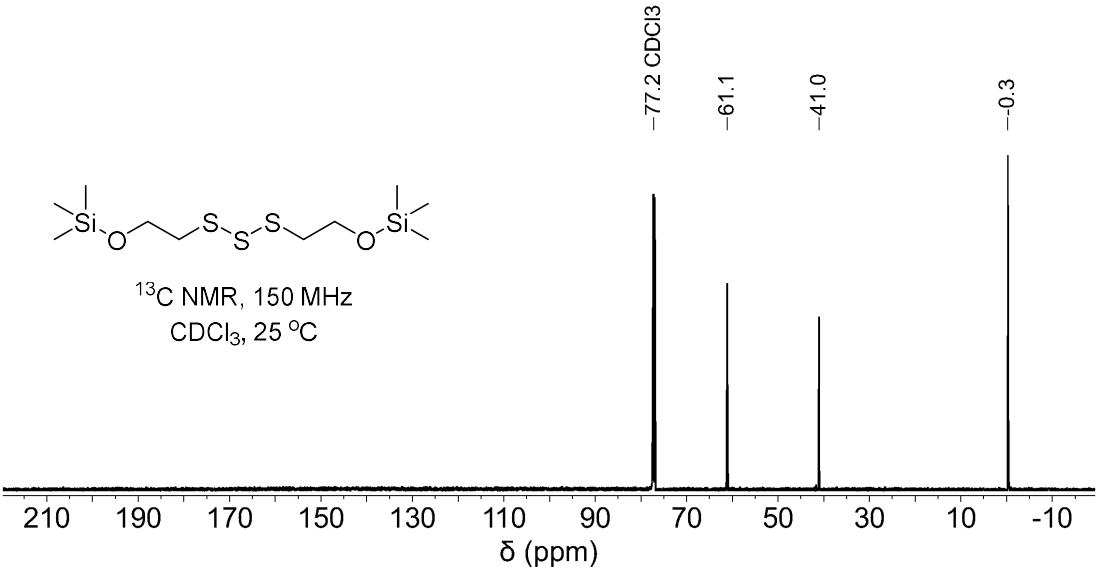

Figure S2.66: ^{13}C NMR spectrum of bis(2-trimethylsiloxyethyl) trisulfide

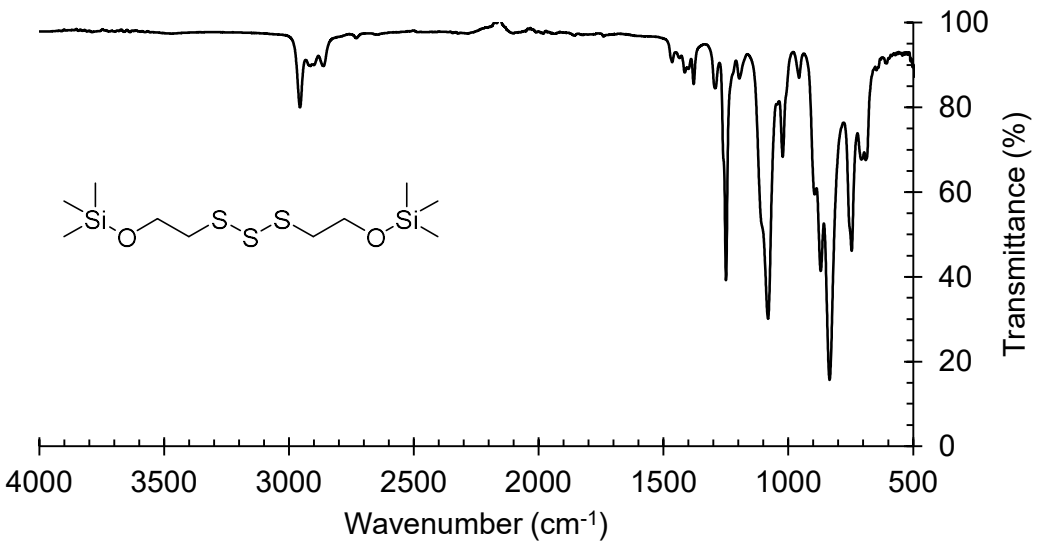

Figure S2.67: FTIR spectrum of bis(2-trimethylsiloxyethyl) trisulfide

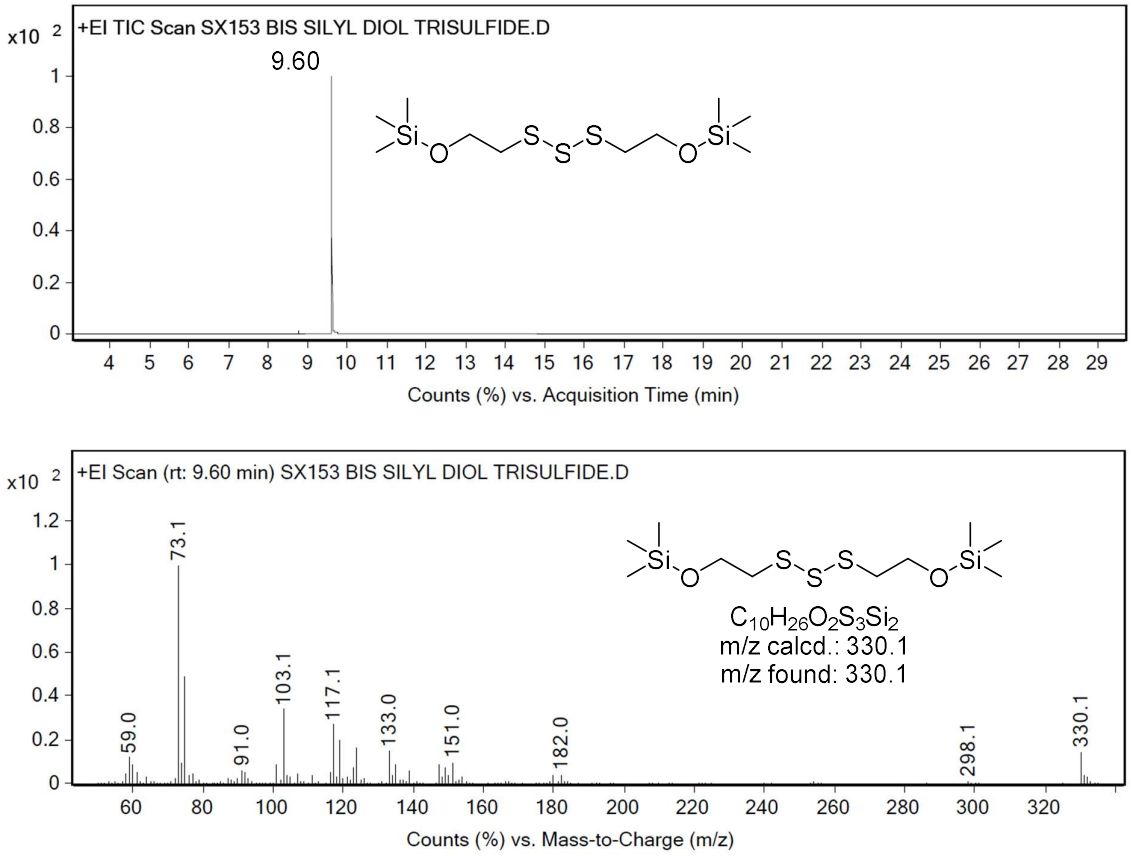

Figure S2.68: Gas chromatogram and mass spectrum of bis(2-trimethylsiloxyethyl) trisulfide. GC-MS method C. Retention time: 9.604 min (bis(2-trimethylsiloxyethyl) trisulfide).

Bis(4-methoxybenzyl) trisulfide synthesis

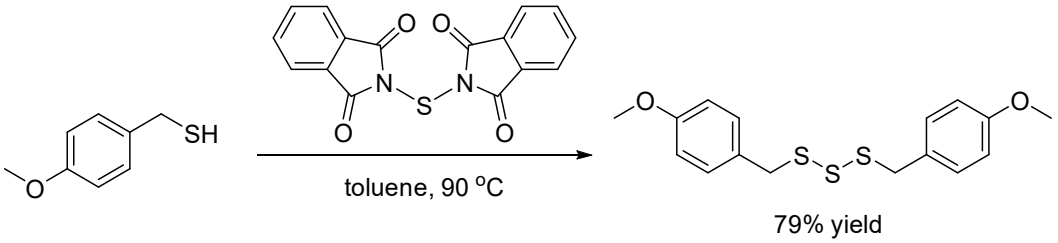

Bis(4-methoxybenzyl)trisulfide was prepared by a modified general method described by Harpp et al.[17] *N,N'*-thiobisphthalimide (104.5 mg, 0.32 mmol, 0.45 eq.) and toluene (25 mL) were added to a 100 mL round bottom flask equipped with a magnetic stir bar, giving a suspension. 4-methoxybenzyl thiol (100 µL, 0.72 mmol, 1.0 eq.) was added in one portion and the mixture heated to 90 ºC for 3 hours. NMR analysis of the crude mixture indicated the formation of the trisulfide product (δ -C**H**$_2$-S ~4.01 ppm). The mixture was allowed to cool to room temperature and the solvent was removed under reduced pressure. The crude solid was dissolved in dichloromethane (10 mL) and then silica gel (1 g) was added to the mixture. After solvent removal, the dry loaded sample underwent flash column chromatography (ethyl acetate/hexane 1:9 to 1:1 v/v) to yield bis(4-methoxybenzyl) trisulfide (79% yield, 86.8 mg) as a beige oil which solidified to an off-white solid upon cooling at 12 – 14 ºC.

m.p = 57.5 – 60.0 ºC. **R$_f$** = 0.63 (EtOAc/Hexanes 20:80). **^{1}H NMR** (600 MHz, $CDCl_3$) δ 7.23 (d, *J* = 8.5 Hz, 4H), 6.86 (d, *J* = 8.6 Hz, 4H), 4.01 (s, 4H), 3.80 (s, 6H). **^{13}C NMR** (150 MHz, $CDCl_3$) δ 159.3, 130.7, 128.6, 114.2, 55.4, 42.8. **FTIR** (neat, cm^{-1}): 1607, 1510, 1245, 1174, 1025, 822, 653, 543. **HRMS** (ESI): *m/z* calcd for $C_{16}H_{18}O_2S_3$+Ag$^+$: 444.9515 [M+Ag]$^+$, found: 444.9522. **Elemental analysis** (CHNS): $C_{16}H_{18}O_2S_3$ requires C, 56.77%; H, 5.36%; N, 0%; S, 28.41% (O, 9.45%). Found C, 57.16%; H, 5.39%; N, 0%; S, 30.08%.

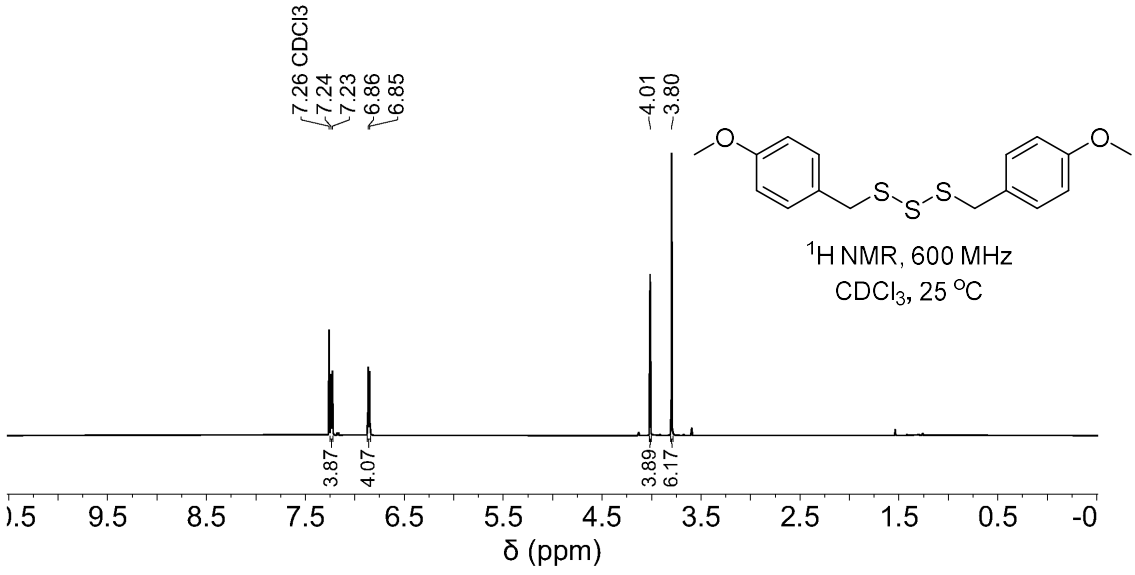

Figure S2.69: ^{1}H NMR spectrum of bis(4-methoxybenzyl) trisulfide

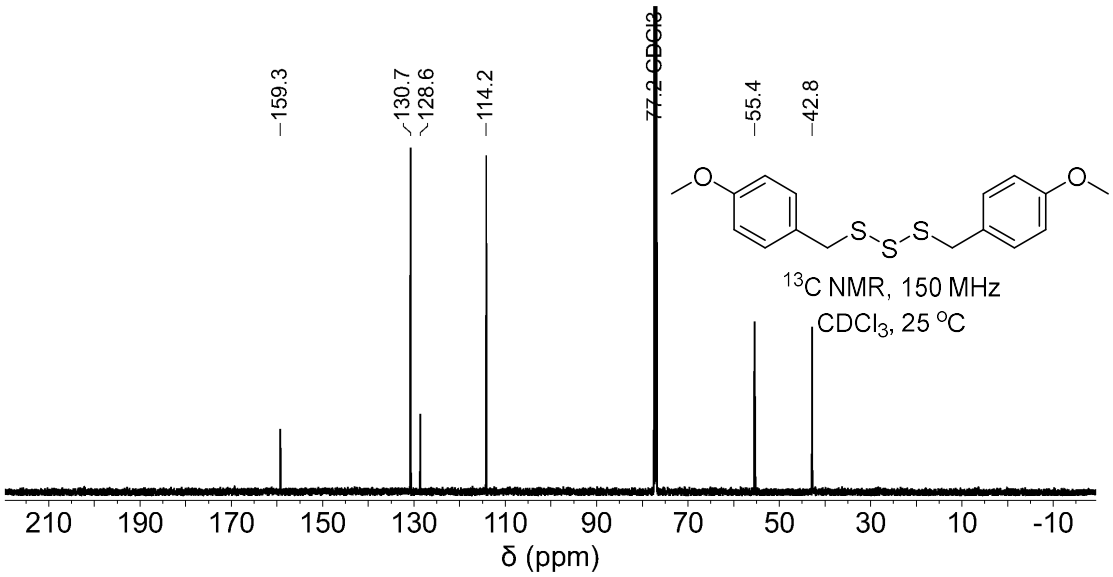

Figure S2.70: ^{13}C NMR spectrum of bis(4-methoxybenzyl) trisulfide

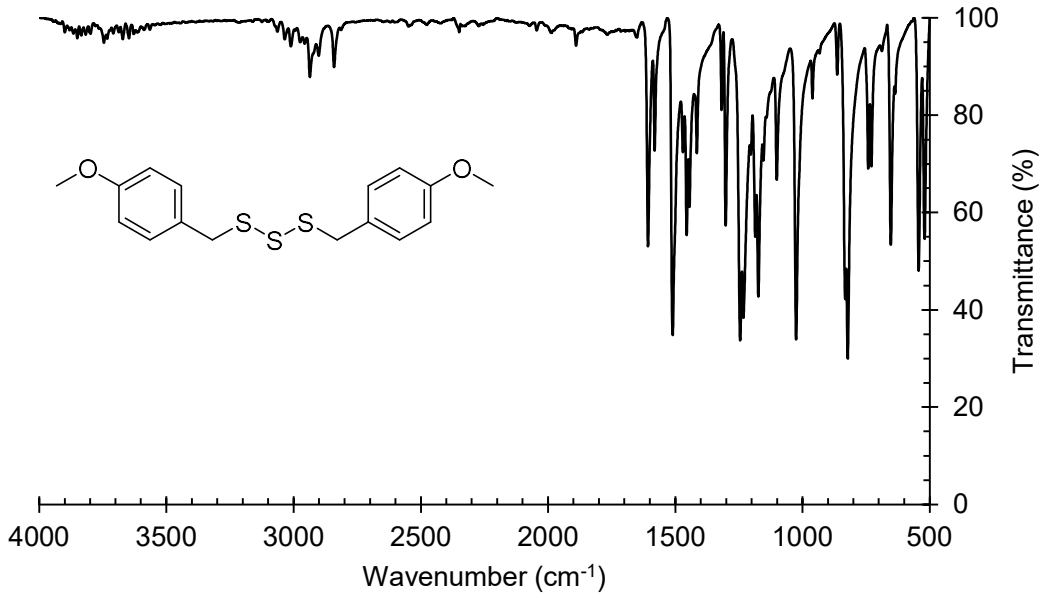

Figure S2.71: FTIR spectrum of bis(4-methoxybenzyl) trisulfide

Tetrasulfide synthesis

Di-*n*-propyl tetrasulfide

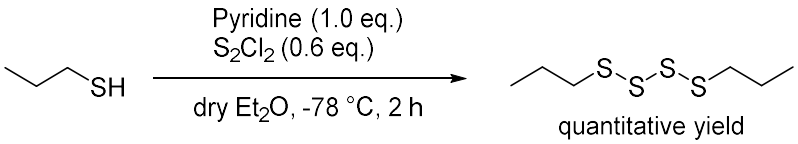

A stirred solution of ^{n}PrSH (0.19 mL, 2.1 mmol, 1.0 eq.), pyridine (0.17 mL, 2.1 mmol, 1.0 eq.), and 20 mL anhydrous Et_2O was cooled to -78 ºC. S_2Cl_2 (0.10 mL, 1.3 mmol, 0.6 eq.) was added dropwise and the reaction stirred for 2 hours. Water was then added to the reaction, and the reaction was allowed to warm to room temperature. The reaction was transferred to a separating funnel, and the organic layer washed twice with water. The combined aqueous layers were extracted twice with DCM. The combined organic extracts were dried with $MgSO_4$, filtered through cotton wool, and concentrated under reduced pressure to give the product as a yellow oil (223 mg, 100% yield).

Di-*n*-propyl tetrasulfide, $^{n}Pr_2S_4$

^{1}H NMR (600 MHz, $CDCl_3$) δ 2.93 (t, *J* = 7.1 Hz, 4H), 1.81 (ap. h, *J* = 7.3 Hz, 4H), 1.03 (t, *J* = 7.3 Hz, 6H). **^{13}C NMR** (150 MHz, $CDCl_3$) δ 41.5, 22.5, 13.2.

^{1}H NMR (600 MHz, Toluene-d_8) δ 2.57 (t, J = 7.3 Hz, 4H), 1.56 (ap. h, J = 7.3 Hz, 4H), 0.77 (t, J = 7.3 Hz, 6H). **^{13}C NMR** (150 MHz, Toluene-d_8) δ 41.8, 23.0, 13.4.

^{1}H NMR (600 MHz, DMF-d_7) δ 3.02 (t, *J* = 7.1 Hz, 4H), 1.80 (ap. h, *J* = 7.3 Hz, 4H), 1.02 (t, *J* = 7.3 Hz, 6H). **^{13}C NMR** (150 MHz, DMF-d_7) δ 42.1, 23.3, 13.5.

FTIR (neat, cm^{-1}): 2960, 2928, 2871, 1454, 1376, 1289, 1230, 780.

GC-MS (EI, 70 eV) *m/z* (rel. intensity): *m/z* calcd for $C_6H_{14}S_4^{+}$: 214.0[*M*]$^{+}$, found: 214.0 (M+, 100), 182.0 (12), 150.0 (18), 108.0 (80), 73.0 (44), 64.0 (22).

Elemental analysis (CHNS): $C_6H_{14}S_4$ requires C, 33.61%; H, 6.58%; N, 0%; S, 59.81%. Found C, 33.10%; H, 6.48%; N, 0%; S, 59.90%.

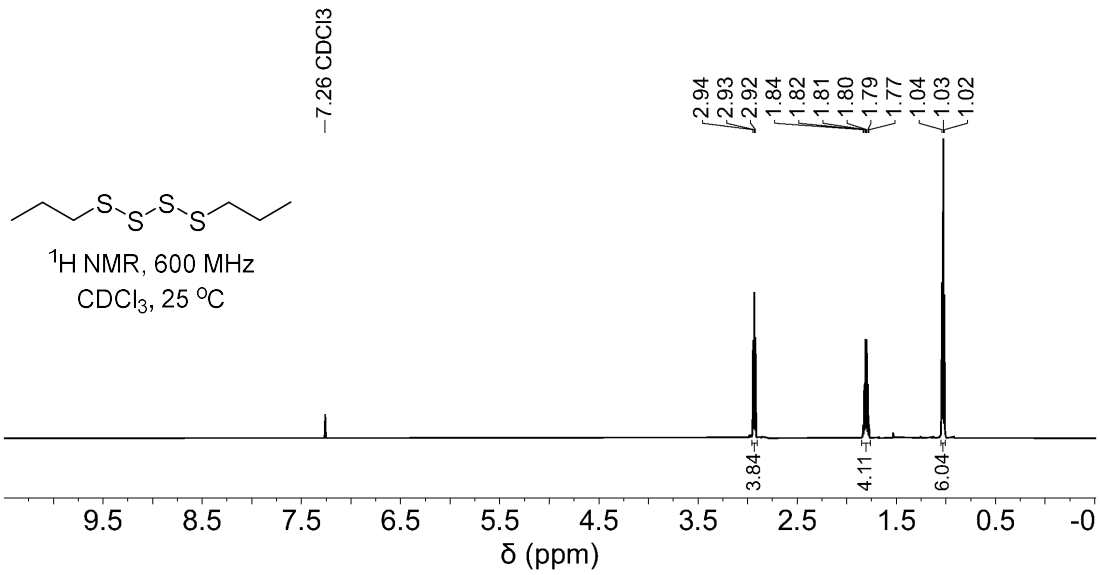

Figure S2.72: ^{1}H NMR spectrum of di-*n*-propyl tetrasulfide in $CDCl_3$

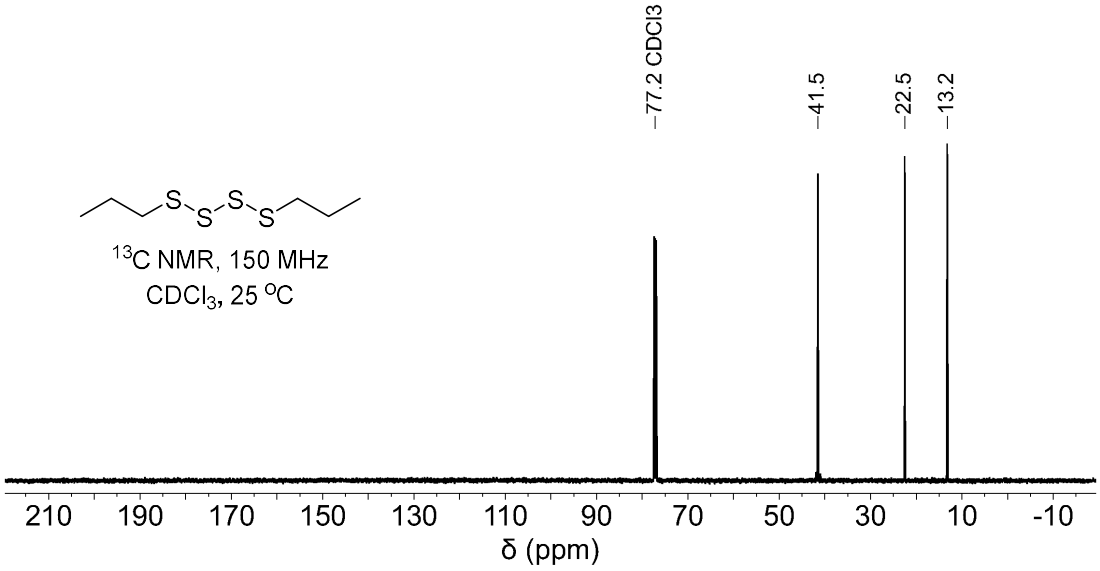

Figure S2.73: ^{13}C NMR spectrum of di-*n*-propyl tetrasulfide in $CDCl_3$

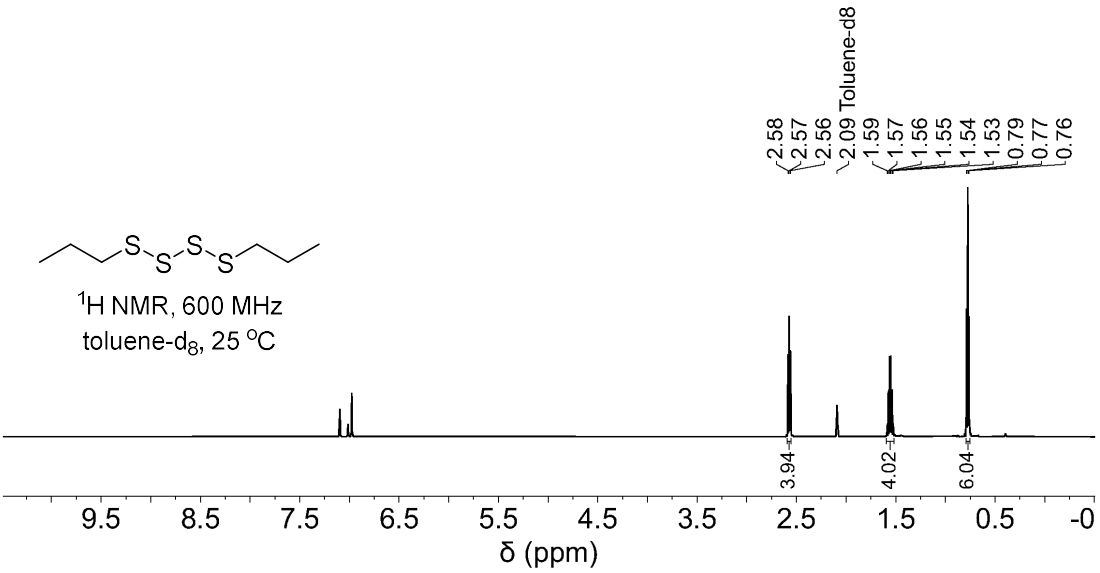

Figure S2.74: ^{1}H NMR spectrum of di-*n*-propyl tetrasulfide in toluene-d_8

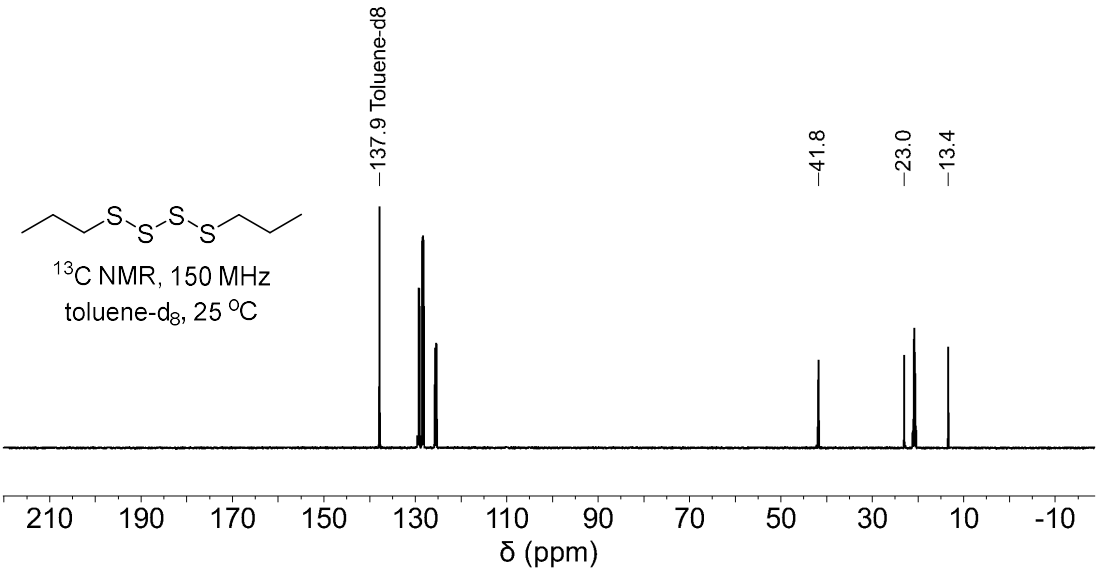

Figure S2.75: ^{13}C NMR spectrum of di-*n*-propyl tetrasulfide in toluene-d_8

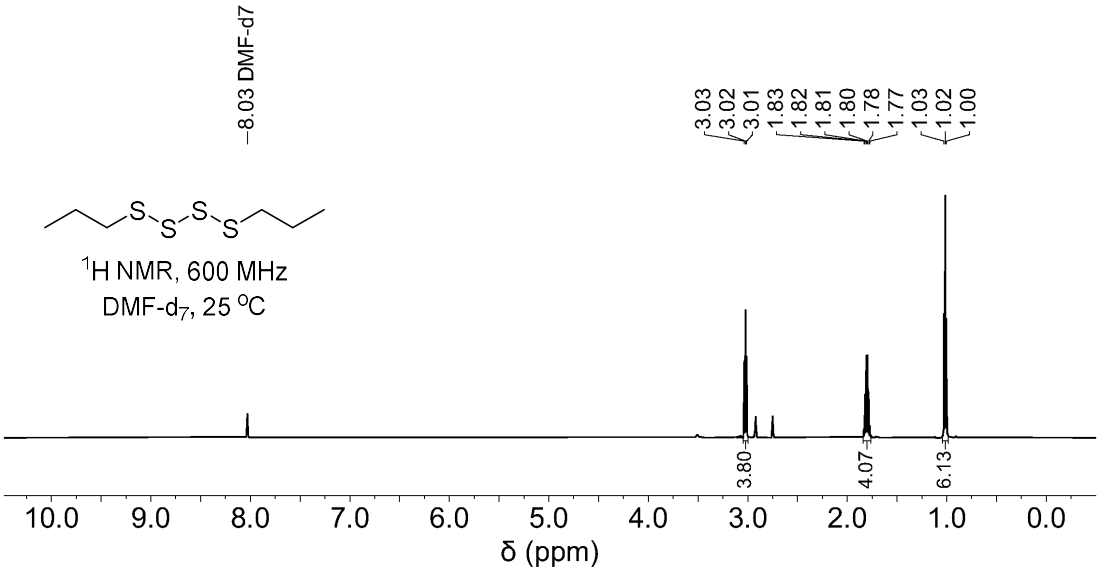

Figure S2.76: ^{1}H NMR spectrum of di-*n*-propyl tetrasulfide in DMF-d_7

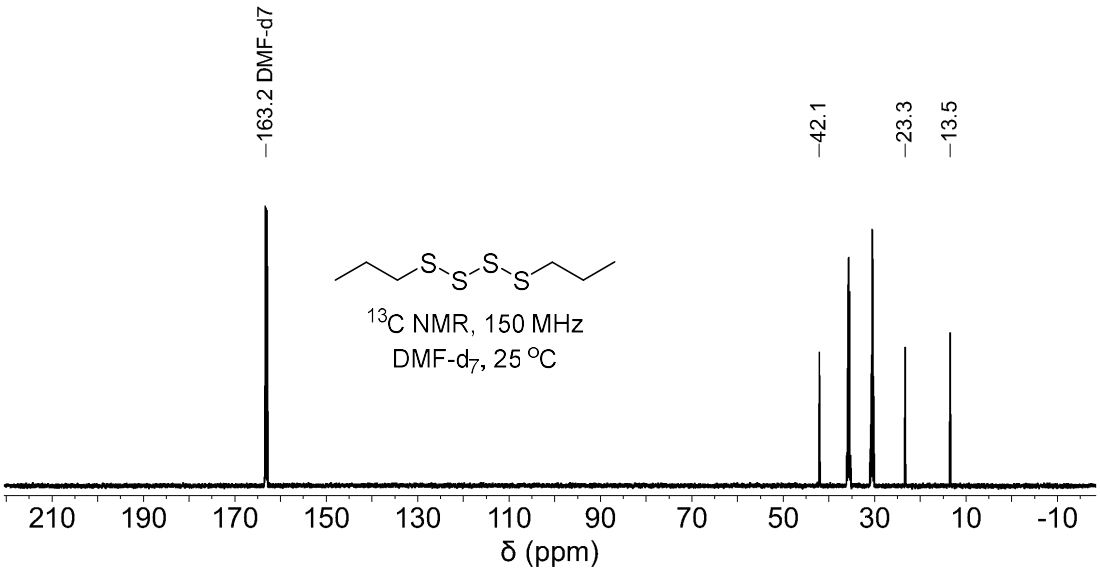

Figure S2.77: ^{13}C NMR spectrum of di-*n*-propyl tetrasulfide in DMF-d_7

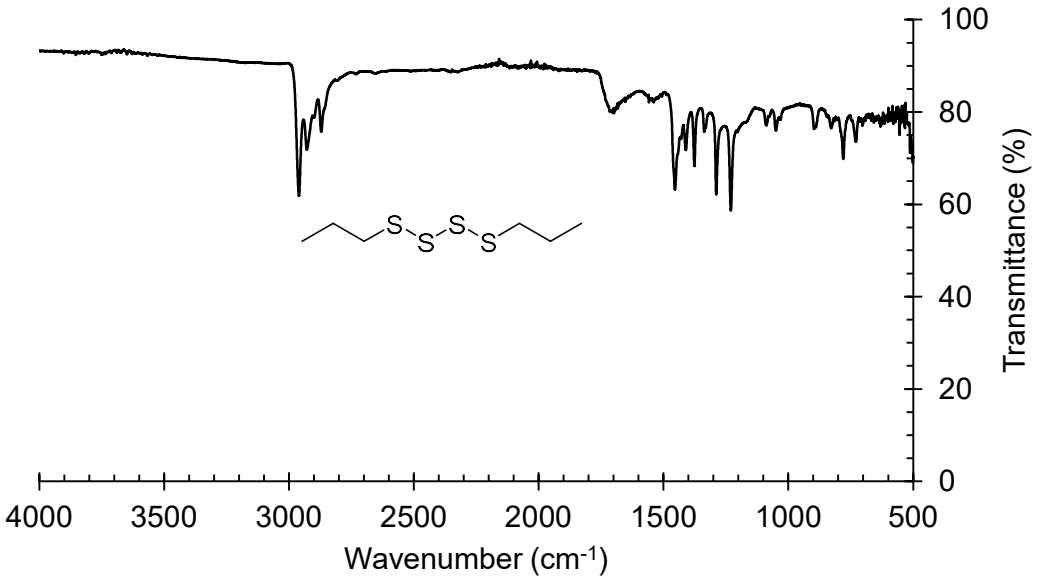

Figure S2.78: FTIR spectrum of di-*n*-propyl tetrasulfide

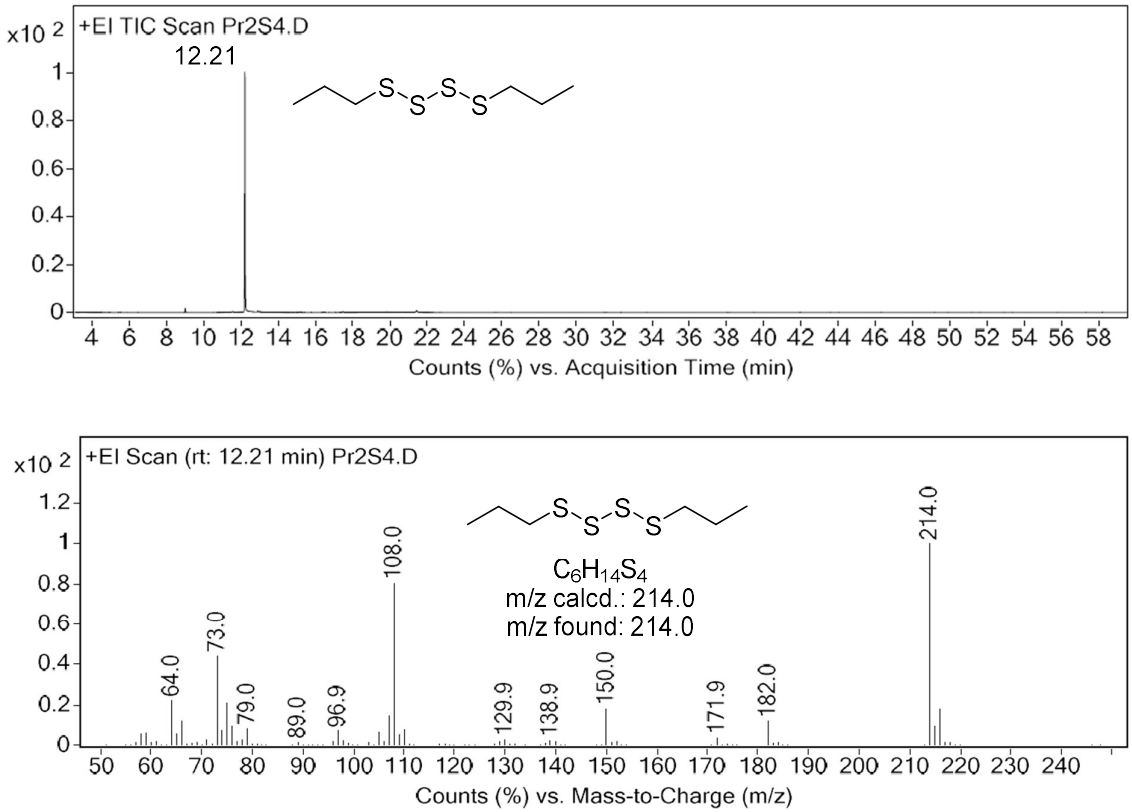

Figure S2.79: Gas chromatogram and mass spectrum of di-*n*-propyl tetrasulfide. GC-MS method D. Retention time: 12.208 min ($^{n}Pr_2S_4$).

Dibenzyl Tetrasulfide Synthesis

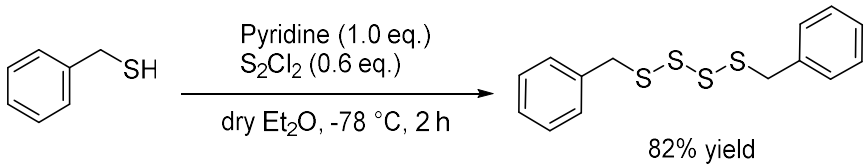

The compound was synthesised according to the literature procedure.[18] A stirred solution of benzyl thiol (0.75 mL, 6.4 mmol, 1.0 eq.), pyridine (0.52 mL, 6.4 mmol, 1.0 eq.), and 65 mL anhydrous Et_2O was cooled to -78 °C. S_2Cl_2 (0.31 mL, 3.9 mmol, 0.6 eq.) was added dropwise and the reaction stirred for 2 hours. Water was then added to the reaction, and the reaction was allowed to warm to room temperature. The reaction was transferred to a separating funnel, and the organic layer washed twice with water. The combined aqueous layers were extracted twice with DCM. The combined organic extracts were dried with $MgSO_4$, filtered through cotton wool, and concentrated under reduced pressure. The crude material was purified by column chromatography using hexanes only to give the product as a yellow oil (817 mg, 82% yield). The obtained spectral data is in agreement with the literature.[18] Crystals suitable for X-ray analysis were grown from hexanes at –18 °C. Benzylic tetrasulfide samples were analysed and tested in the crossover reaction following their synthesis; when older samples were dissolved in DMF-d_7 the formation of other benzylic polysulfides was observed.

Dibenzyl tetrasulfide, Bn_2S_4

R_f = 0.12 (Hexanes)

^{1}H NMR (600 MHz, $CDCl_3$) δ 7.36 – 7.32 (m, 8H), 7.31 – 7.27 (m, 2H), 4.16 (s, 4H). **^{13}C NMR** (150 MHz, $CDCl_3$) δ 136.4, 129.6, 128.8, 127.8, 43.8.

^{1}H NMR (600 MHz, Toluene-d_8) δ 7.06 – 7.03 (m, 8H), 7.02 – 6.99 (m, 2H), 3.77 (s, 4H). **^{13}C NMR** (150 MHz, Toluene-d_8) δ 137.0, 130.1, 129.1, 128.1, 44.1.

^{1}H NMR (600 MHz, DMF-d_7) δ 7.44 – 7.37 (m, 8H), 7.35 – 7.32 (m, 2H), 4.30 (s, 4H). **^{13}C NMR** (150 MHz, DMF-d_7) δ 137.9, 130.7, 129.8, 128.8, 44.1.

HRMS (ESI): *m/z* calcd for $C_{14}H_{14}S_4$+Ag^+: 416.9024 $[M+Ag]^+$, found: 416.9029.

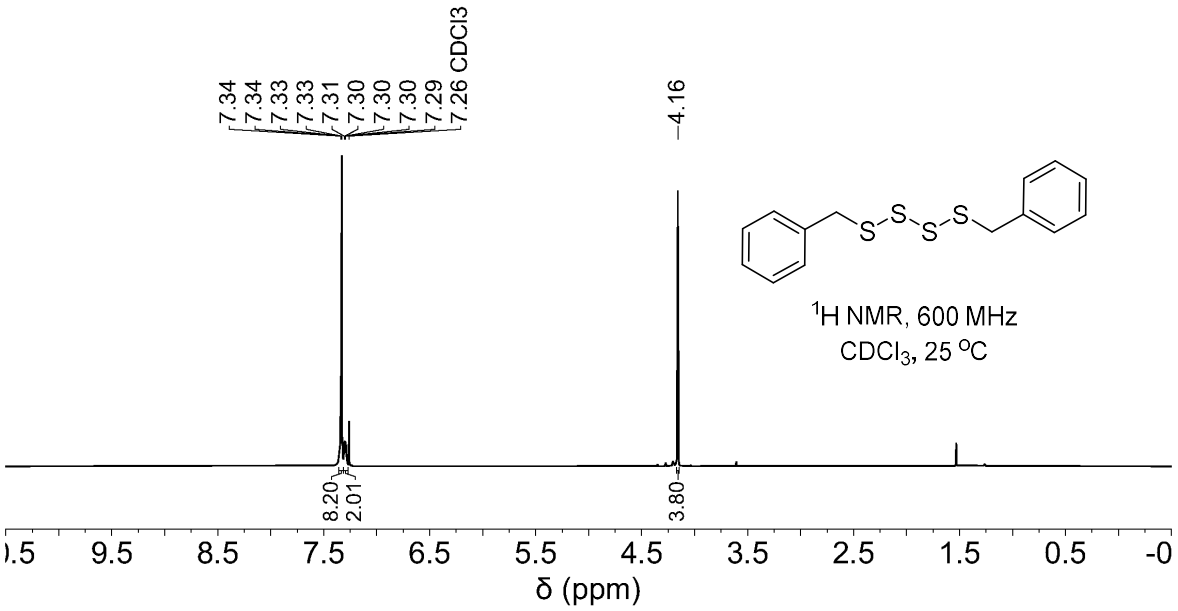

Figure S2.80: ^{1}H NMR spectrum of dibenzyl tetrasulfide in $CDCl_3$

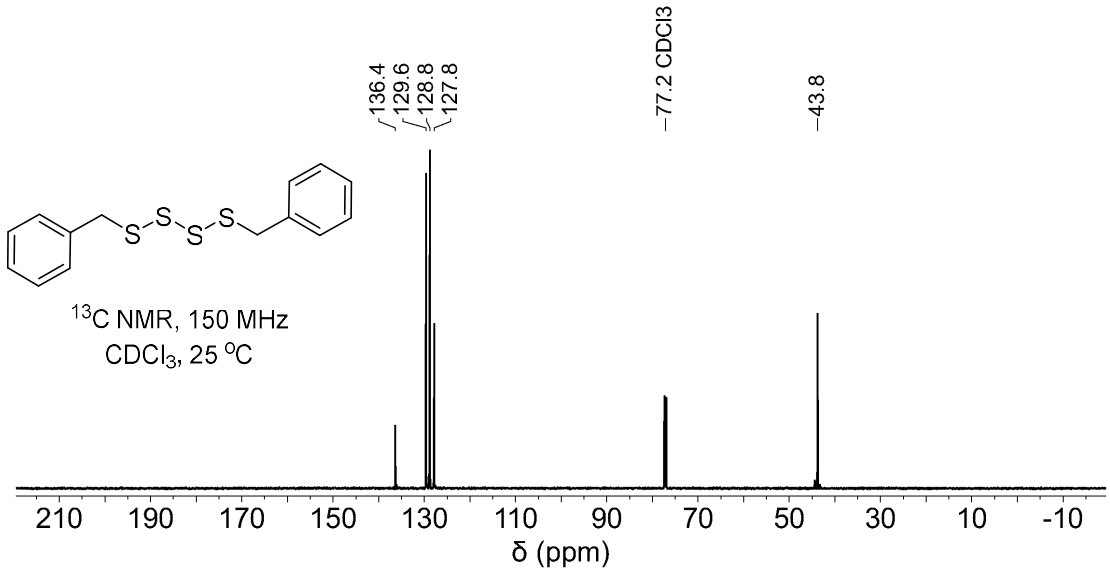

Figure S2.81: ^{13}C NMR spectrum of dibenzyl tetrasulfide in $CDCl_3$

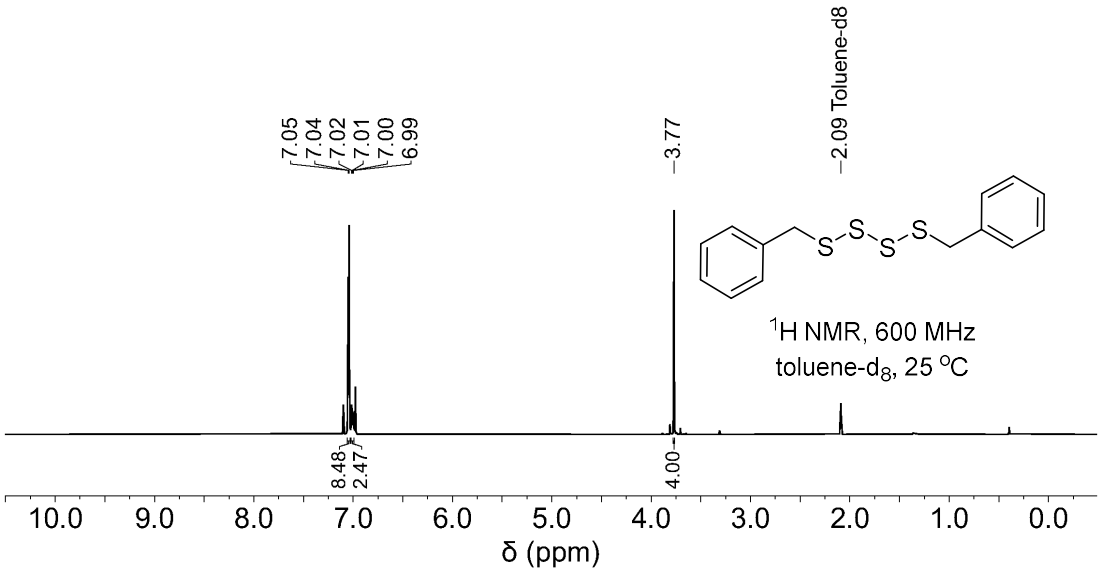

Figure S2.82: ^{1}H NMR spectrum of dibenzyl tetrasulfide in toluene-d_8

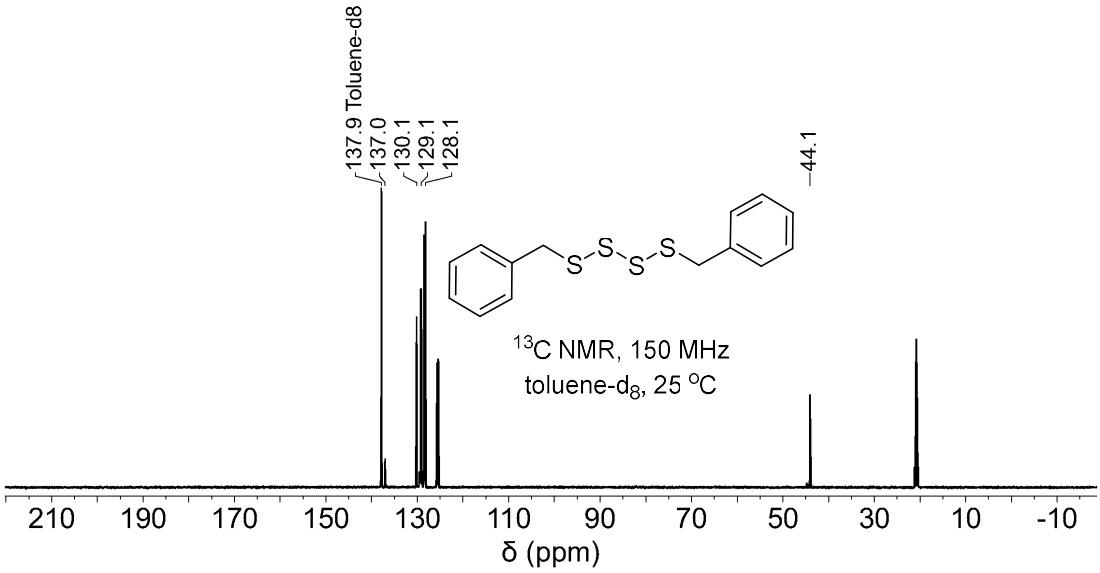

Figure S2.83: ^{13}C NMR spectrum of dibenzyl tetrasulfide in toluene-d_8

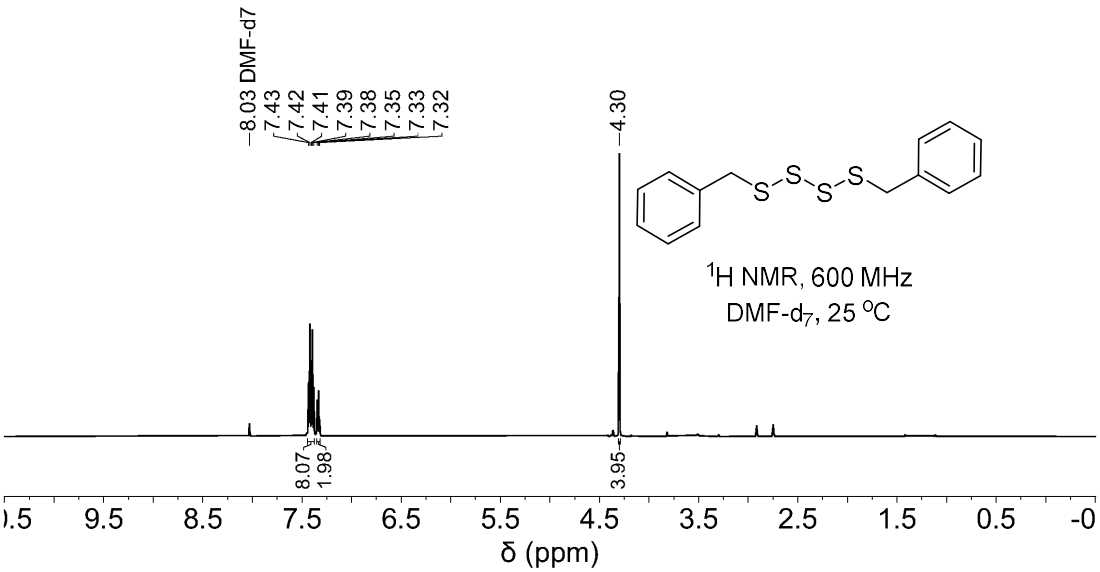

Figure S2.84: ^{1}H NMR spectrum of dibenzyl tetrasulfide in DMF-d_7

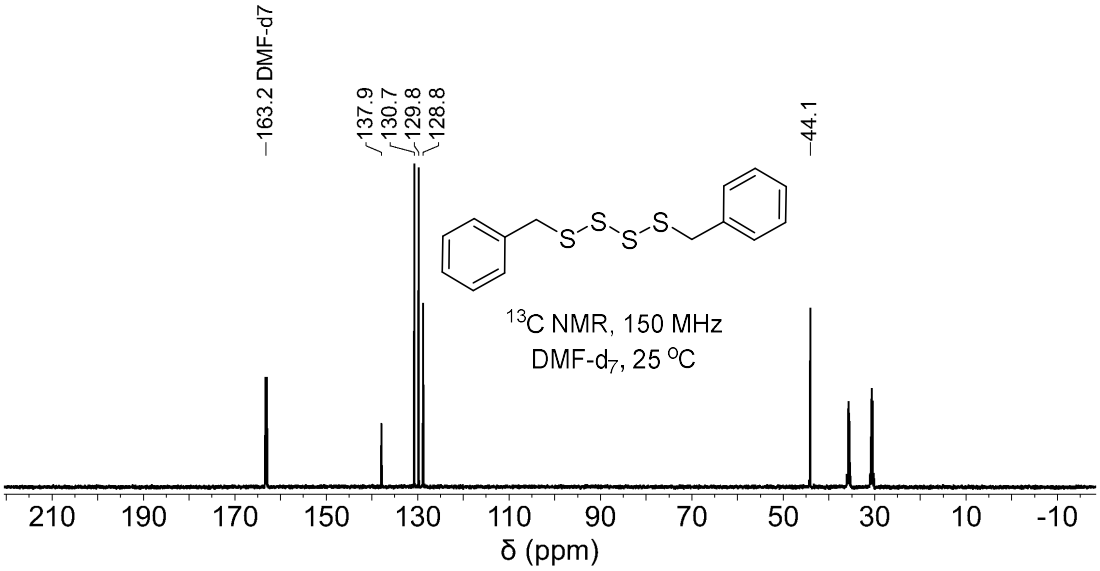

Figure S2.85: ^{13}C NMR spectrum of dibenzyl tetrasulfide in DMF-d_7

Bis(4-methoxybenzyl) tetrasulfide synthesis

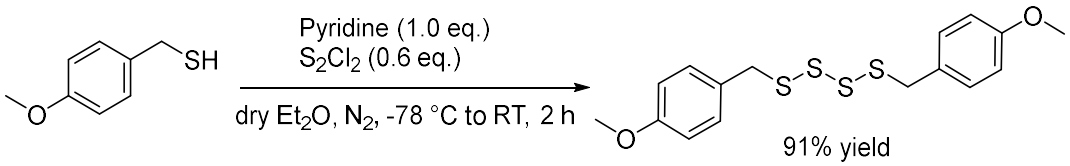

The synthesis of bis(4-methoxybenzyl) tetrasulfide was adapted from the method described by Bolton et al.[18] with a slight modification. Under nitrogen atmosphere, to a dry 100 mL round bottom flask equipped with a magnetic stir bar was added dry ether (20 mL), pyridine (116 µL, 1.44 mmol, 1 eq.), and 4-methoxybenzyl thiol (200 µL, 1.44 mmol, 1 eq.) and the mixture was cooled to -78 ºC (dry ice/acetone). Sulfur monochloride (70 µL, 0.87 mmol, 0.6 eq.) was added dropwise via syringe to the cooled mixture over 20 minutes. During the addition of sulfur monochloride, the mixture turned from cloudy white to yellow. The reaction was stirred at -78 ºC for a total of 2 hours. After that, water (30 mL) was added to quench the reaction and the mixture was allowed to warm to room temperature. The mixture was diluted with dichloromethane (30 mL). The organic layer was collected, and the aqueous layer was extracted with dichloromethane (2 x 30 mL). The combined organic layers were washed with saturated $NaCl_{(aq)}$ (2 x 25 mL), dried over magnesium sulfate, filtered, and evaporated under reduced pressure to give a crude product as a yellow oil. Purification of this oil with flash column chromatography (ethyl acetate/hexane 1:9 to 1:1) yield bis(4-methoxybenzyl) tetrasulfide as a yellow oil (242.1 mg, 91%) which solidify when store in the fridge (4 – 5 ºC). The obtained NMR data in $CDCl_3$ is in agreement with the literature.[19] Benzylic tetrasulfide samples were analysed and tested in the crossover reaction following their synthesis; when older samples were dissolved in DMF-d_7 the formation of other benzylic polysulfides was observed.

Bis(4-methoxybenzyl) tetrasulfide, $(4\text{-MeOBn})_2S_4$

^{1}H NMR ($CDCl_3$, 600 MHz) δ 7.25 (d, *J* = 8.6 Hz, 4H), 6.86 (d, *J* = 8.6 Hz, 4H), 4.13 (s, 4H), 3.81 (s, 6H). **^{13}C NMR** ($CDCl_3$, 150 MHz): δ 43.4, 55.4, 114.2, 128.3, 130.8, 159.4.

^{1}H NMR (600 MHz, Toluene-d_8) δ 7.01 (d, *J* = 8.6 Hz, 4H), 6.65 (d, *J* = 8.6 Hz, 4H), 3.86 (s, 4H), 3.29 (s, 6H). **^{13}C NMR** (150 MHz, Toluene-d_8) δ 160.1, 131.3, 128.8, 114.7, 55.0, 43.8.

^{1}H NMR (600 MHz, DMF-d_7) δ 7.35 (d, *J* = 8.7 Hz, 4H), 6.97 (d, *J* = 8.6 Hz, 4H), 4.27 (s, 4H), 3.82 (s, 6H). **^{13}C NMR** (150 MHz, DMF-d_7) δ 160.5, 131.9, 129.6, 115.2, 56.0, 43.7.

HRMS (ESI): *m/z* calcd for $C_{16}H_{18}O_2S_4$+Ag^+: 476.9236 $[M+Ag]^+$, found: 476.9247.

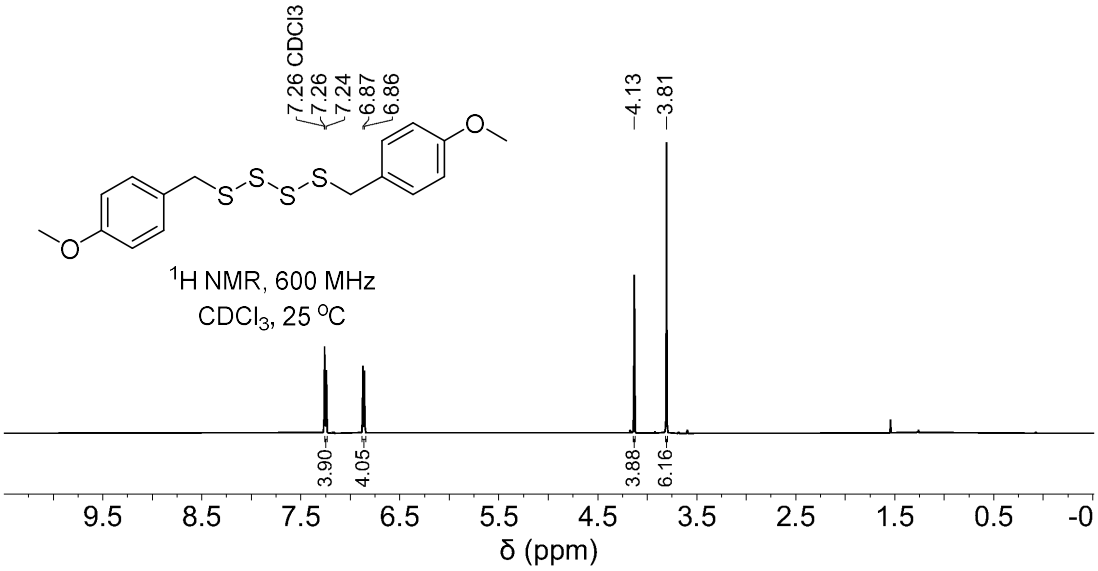

Figure S2.86: ^{1}H NMR spectrum of bis(4-methoxybenzyl) tetrasulfide in $CDCl_3$

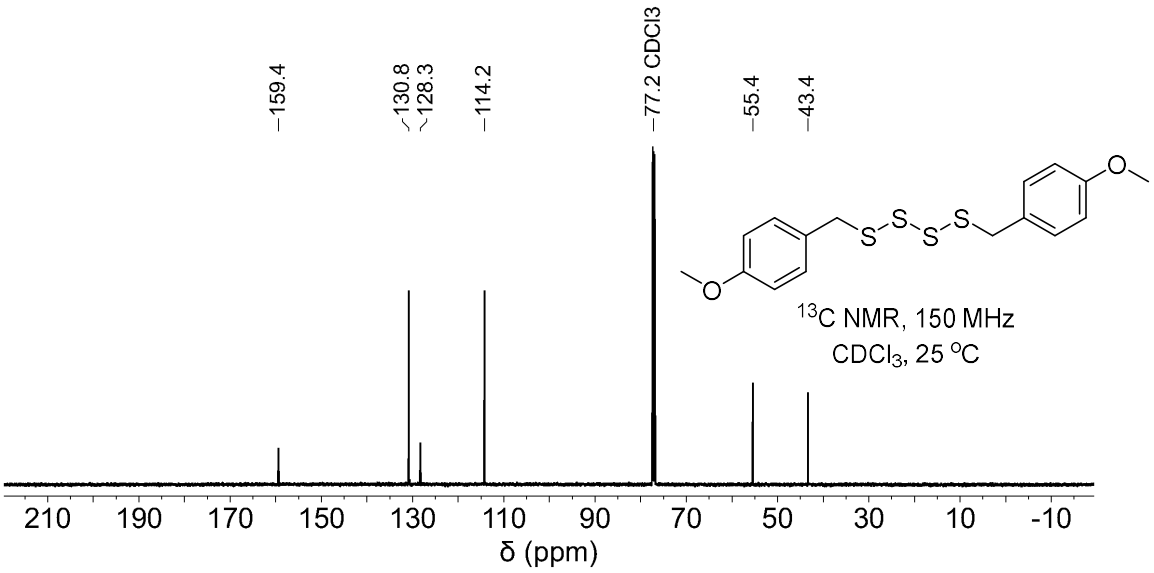

Figure S2.87: ^{13}C NMR spectrum of bis(4-methoxybenzyl) tetrasulfide in $CDCl_3$

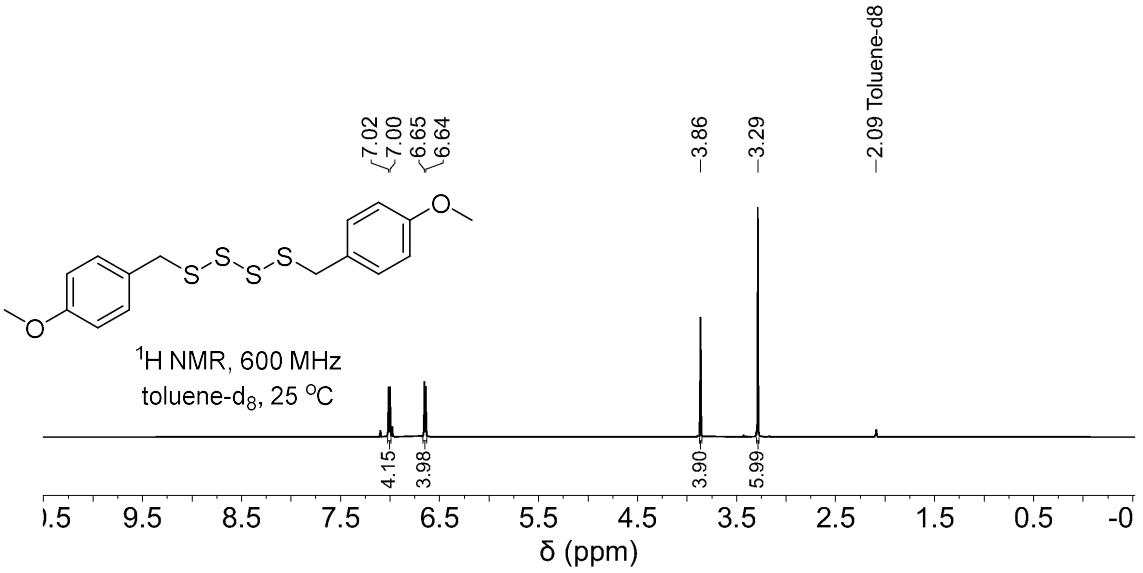

Figure S2.88: ^{1}H NMR spectrum of bis(4-methoxybenzyl) tetrasulfide in toluene-d_8

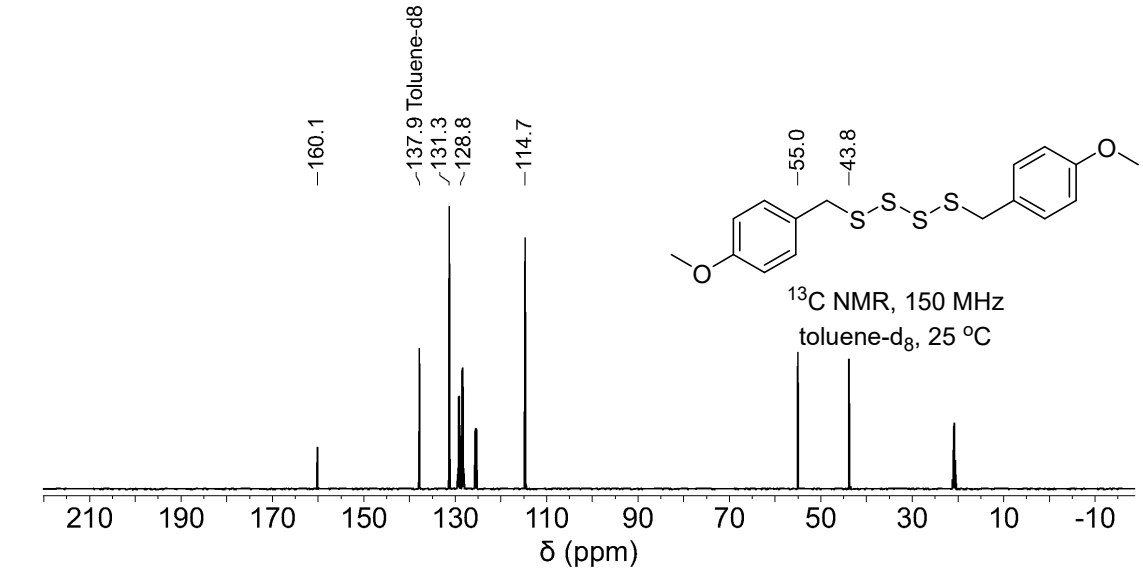

Figure S2.89: ^{13}C NMR spectrum of bis(4-methoxybenzyl) tetrasulfide in toluene-d_8

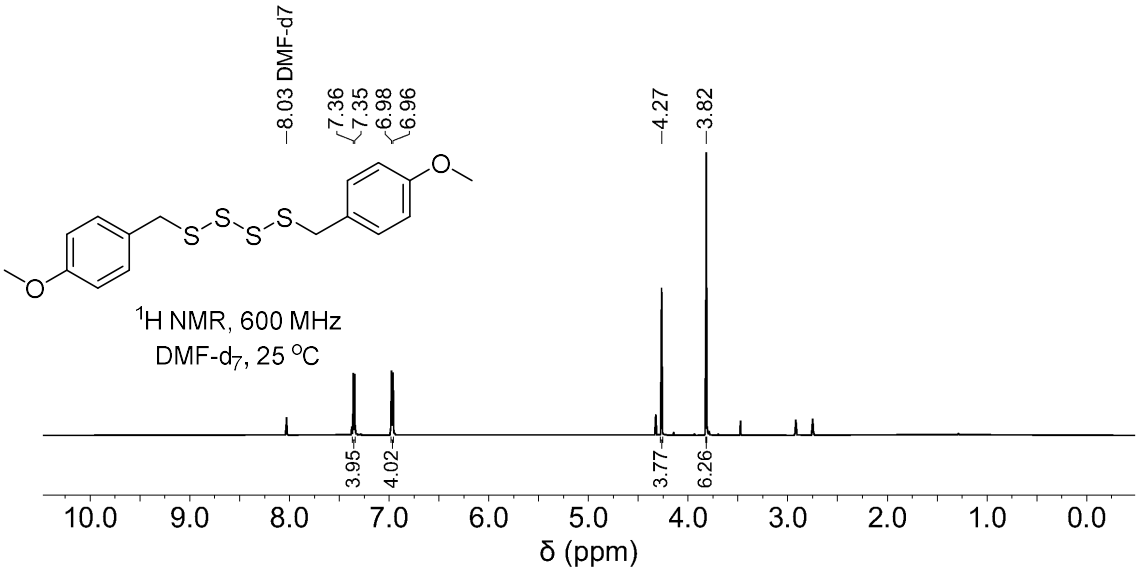

Figure S2.90: ^{1}H NMR spectrum of bis(4-methoxybenzyl) tetrasulfide in DMF-d_7

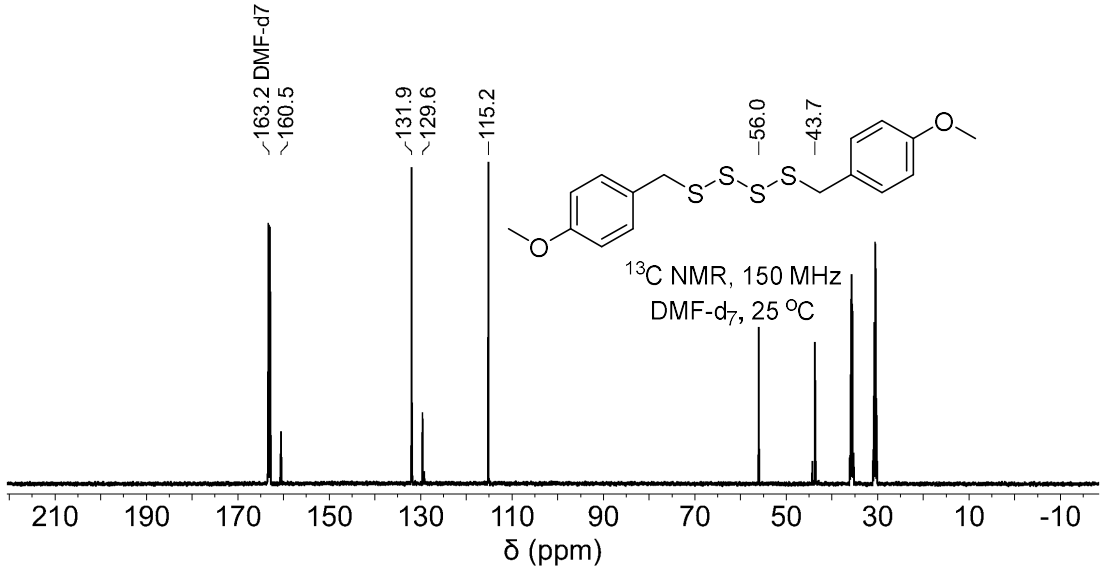

Figure S2.91: ^{13}C NMR spectrum of bis(4-methoxybenzyl) tetrasulfide in DMF-d_7

2.7 References for Experimental Details and Characterizations

1. Gottlieb, H. E.; Kotlyar, V.; Nudelman, A. NMR Chemical Shifts of Common Laboratory Solvents as Trace Impurities. *J. Org. Chem.* **1997**, *62* (21), 7512-7515. DOI: 10.1021/jo971176v.
2. The MERCK Index: An Encyclopedia of Chemical, Drugs and Biologicals. 11th ed.; S. Budavari Ed.; Merck & Co., Inc., 1989.
3. Bhattacherjee, D.; Sufian, A.; Mahato, S. K.; Begum, S.; Banerjee, K.; De, S.; Srivastava, H. K.; Bhabak, K. P. Trisulfides over disulfides: highly selective synthetic strategies, anti-proliferative activities and sustained H_2S release profiles. *Chem. Commun.* **2019**, *55* (90), 13534-13537. DOI: 10.1039/C9CC05562B.
4. Higuchi, O.; Tateshita, K.; Nishimura, H. Antioxidative Activity of Sulfur-Containing Compounds in Allium Species for Human Low-Density Lipoprotein (LDL) Oxidation in Vitro. *J. Agric. Food Chem.* **2003**, *51* (24), 7208-7214. DOI: 10.1021/jf034294u.
5. Milligan, B.; Saville, B.; Swan, J. M. 680. Trisulphides and tetrasulphides from Bunte salts. *J. Chem. Soc.* **1963**, 3608-3614. DOI: 10.1039/JR9630003608.
6. Stone, B. D.; Nielsen, M. L. The Reaction of Sulfur Dichloride with Methylamine1. *J. Am. Chem. Soc.* **1959**, *81* (14), 3580-3584. DOI: 10.1021/ja01523a025.
7. Chauvin, J.-P. R.; Griesser, M.; Pratt, D. A. The antioxidant activity of polysulfides: it's radical! *Chem. Sci.* **2019**, *10* (19), 4999-5010. DOI: 10.1039/C9SC00276F.
8. Aragão, D.; Aishima, J.; Cherukuvada, H.; Clarken, R.; Clift, M.; Cowieson, N. P.; Ericsson, D. J.; Gee, C. L.; Macedo, S.; Mudie, N. MX2: a high-flux undulator microfocus beamline serving both the chemical and macromolecular crystallography communities at the Australian Synchrotron. *J. Synchrotron Radiat.* **2018**, *25* (3), 885-891. DOI: 10.1107/S1600577518003120.
9. Sheldrick, G. M. SHELXT–Integrated space-group and crystal-structure determination. *Acta Crystallogr. Sect. A.* **2015**, *71* (1), 3-8. DOI: 10.1107/S2053273314026370.
10. Sheldrick, G. Crystal structure refinement with SHELXL. *Acta Crystallogr. Sect. C.* **2015**, *71* (1), 3-8. DOI: 10.1107/S2053229614024218.
11. Hubschle, C. B.; Sheldrick, G. M.; Dittrich, B. ShelXle: a Qt graphical user interface for SHELXL. *J. Appl. Crystallogr.* **2011**, *44* (6), 1281-1284. DOI: 10.1107/S0021889811043202.
12. Zysman-Colman, E.; Harpp, D. N. Optimization of the Synthesis of Symmetric Aromatic Tri- and Tetrasulfides. *J. Org. Chem.* **2003**, *68* (6), 2487-2489. DOI: 10.1021/jo0265481.
13. Wu, M.; Bhargav, A.; Cui, Y.; Siegel, A.; Agarwal, M.; Ma, Y.; Fu, Y. Highly Reversible Diphenyl Trisulfide Catholyte for Rechargeable Lithium Batteries. *ACS Energy Lett.* **2016**, *1* (6), 1221-1226. DOI: 10.1021/acsenergylett.6b00533.
14. Kalnins, M. V. Reactions of phthalimide and potassium phthalimide with sulfur monochloride. *Can. J. Chem.,* **1966**, *44* (17), 2111-2113. DOI: 10.1139/v66-318.
15. Ercole, F.; Li, Y.; Whittaker, M. R.; Davis, T. P.; Quinn, J. F., H_2S-Donating trisulfide linkers confer unexpected biological behaviour to poly(ethylene glycol)–cholesteryl conjugates. *J. Mater. Chem. B*, **2020**, *8*, 3896-3907

16. Dao, N. V.; Ercole, F.; Urquhart, M. C.; Kaminkas, L. M.; Nowell, C. J.; Davis, T. P.; Sloan, E. K.; Whittaker, M. R.; Quinn, J. F., Trisulfide linked cholesteryl PEG conjugate attenuates intracellular ROS and collagen-1 production in a breast cancer co-culture model. *Biomater. Sci.*, **2021**, *9*, 835-846.
17. Harpp, D. N.; Steliou, K.; Chan, T. H. Organic sulfur chemistry. 26. Synthesis and reactions of some new sulfur transfer reagents. *J. Am. Chem. Soc.* **1978**, *100* (4), 1222-1228. DOI: 10.1021/ja00472a032.
18. Bolton, S. G.; Cerda, M. M.; Gilbert, A. K.; Pluth, M. D. Effects of sulfane sulfur content in benzyl polysulfides on thiol-triggered H_2S release and cell proliferation. *Free Radic. Biol. Med.* **2019**, *131*, 393-398. DOI: 10.1016/j.freeradbiomed.2018.12.025.
19. Zhang, J.; Studer, A. Decatungstate-catalyzed radical disulfuration through direct C-H functionalization for the preparation of unsymmetrical disulfides. *Nat. Commun.* **2022**, *13* (1), 3886. DOI: 10.1038/s41467-022-31617-5.

CHAPTER 3: THE EFFECTS OF SOLVENTS ON THE TRISULFIDES METATHESIS

3.1 Acknowledgement

Dr. Harshal Patel for the investigation of trisulfide S-S metathesis and the applications of this chemistry for the synthesis of methyl benzyl trisulfide and the modification of a trisulfide natural product, calicheamicin γ_1. James Smith for the study of calicheamicin γ_1 crossover reactions. Ryan Shapter for the permission of using the data for the S-S metathesis studies involving acetic acid and several solvents.

3.2 Introduction

UV and thermal induced S-S metathesis in trisulfides

In 1953, ultraviolet irradiation of dimethyl trisulfide was reported by Birch and co-workers.[1] They found that the UV irradiation to the trisulfide gave a mixture of di-, tri-, and tetrasulfide. A decade later, the same investigation was done by Milligan and co-workers[2]. They also confirmed the same result. The first UV light induced trisulfide metathesis was probably reported by Milligan and co-worker where they studied the reaction between dimethyl and diethyl trisulfide under UV irradiation. As expected, they found the trisulfide exchange products and decomposition products were formed.

In the early 1966, the thermal S-S exchange reaction between two symmetrical trisulfides was then reported by Trivette and Coran.[3] They aimed to understand the S-S metathesis mechanism by studying the kinetic exchange between the trisulfide models i.e., diethyl trisulfide (**1**) and di-*n*-propyl trisulfide (**2**) over the temperature range 132 – 148 ºC. The results showed that after many hours of reaction time, ethyl *n*-propyl trisulfide (**3**) was formed as the major product (Figure 3.1). In a control experiment, the mixture of both trisulfide **1** and **2** was left at room temperature in the dark for at least a month and the result showed that no S-S exchange had occurred. It should be noted that benzene or a mixture of benzene and nitrobenzene (3:2, v/v) were used as the solvents for this reaction. The thermal S-S exchange between trisulfide **1** and **2** was found to be reversible based on the statistical distribution of the product in which the value of equilibrium constant (*K*) is approximately 4 (Equation 3.1). In terms of the mechanism, a free-radical chain mechanism was thought to be involved in this thermal S-S metathesis reaction.

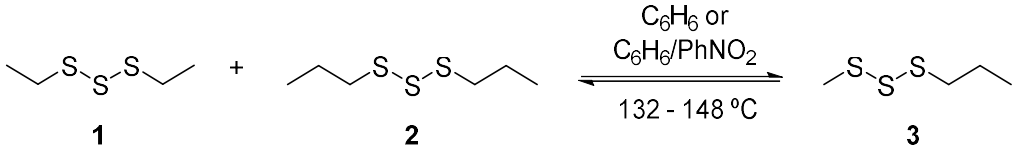

Figure 3.1: A thermal S-S metathesis between diethyl trisulfide and di-*n*-propyl trisulfide reported by Trivette and Coran.[3]

$$K = \frac{[EtS_3Pr]^2}{[Et\ _3Et][PrS_3Pr]} \qquad \text{(Equation 3.1)}$$

In 1966, Tobolsky's lab[4] demonstrated that a slow S-S exchange can occur between dimethyl trisulfide molecules upon heating at 80 °C (Figure 3.2). Even though neat dimethyl trisulfide was heated for almost 3 days, only 11% of the trisulfide was converted to the disulfide (5%) and dimethyl tetrasulfide (6%). Prolonged heating for more than 9 days leads to the formation of trace amounts of dimethyl pentasulfide (Me_2S_5) and dimethyl hexasulfide (Me_2S_6). When the trisulfide was dissolved in benzene or nitrobenzene and heated at such temperature for around 6 days, the S-S metathesis took place even more slowly, giving only a small percentage (< 4%) of dimethyl di- and tetrasulfide.

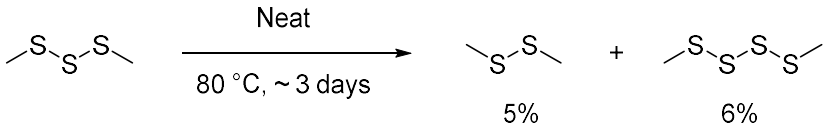

Figure 3.2: A thermal S-S metathesis reaction between dimethyl trisulfide molecules at 80 °C reported by Tobolsky.[4]

Recently, in 2019, Pratt's lab[5] reported the S-S exchange between two symmetrical tetrasulfides i.e., di-*iso*-propyl tetrasulfide (**4**) and di-*tert*-butyl tetrasulfide (**5**) in chlorobenzene at 100 °C for 2 hours. The finding was that S-S metathesis occurs on those tetrasulfides, giving *iso*-propyl *tert*-butyl tetrasulfide (**6**) as the product (Figure 3.3A). Additionally, they found that the reaction did not occur for the trisulfide analogues, di-isopropyl trisulfide (**4a**) and di-*tert*-butyl trisulfide (**5a**) (Figure 3.3B). The S-S bond energy in the trisulfides is stronger than that of the tetrasulfide. The sterically bulky R groups present in the trisulfides (i.e., *iso*-propyl and *tert*-butyl) could also lead to a slower reaction in the case of the trisulfide. The thermal trisulfide metathesis in Pratt's report[5] and in Trivette's report[3] showed that the steric hindrance clearly affected the S-S metathesis reaction.

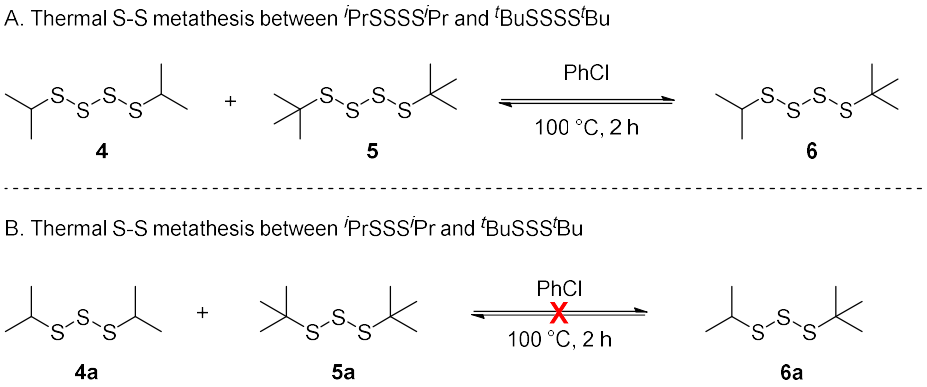

Figure 3.3: A. Thermal S-S metathesis of tetrasulfide between di-*iso*-propyl tetrasulfide and di-*tert*-butyl tetrasulfide in chlorobenzene as a solvent at 100 °C. B. Thermal S-S metathesis in the trisulfide analogues does not occur at such condition as reported by Pratt[5]

Solvent induced S-S metathesis in trisulfides at room temperature

In 2020, Tonkin and co-workers[6] studied the effect of nucleophiles such as *tert*-butyl phosphine and amines (i.e., pyridine, triethylamine, 2,6-lutidine, and ethyl nicotinate) to repair an inverse vulcanized polymer made from dicyclopentadiene, an unsaturated triglyceride, and sulfur. These nucleophiles were found to break and reform the S-S bond in the polymer surface (Figure 3.4). When the two polymer pieces were treated with those nucleophiles and joined together, both sulfur polymer surfaces adhere to each other and becomes one solid polymer (Figure 3.5). Further investigation on the reactivity of these nucleophiles towards small molecules trisulfides shed light on the sulfur rank required to induce S-S metathesis with these nucleophiles. Tonkin and co-workers[6] also reported that the phosphine rapidly induced S-S metathesis between dimethyl trisulfide and di-*n*-propyl trisulfide. Notably, triethylamine and pyridine selectively generated the trisulfide crossover product $MeS_3{}^nPr$ (Figure 3.6C-D), while the phosphine gave a mixture of disulfide, trisulfide, phosphine sulfide, and phosphine oxide (Figure 3.6A).

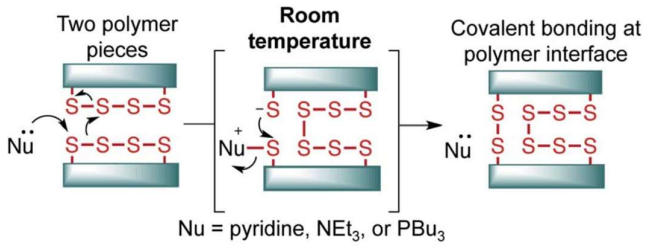

Figure 3.4: An illustration of the inverse vulcanized polymer repair by nucleophiles (pyridine, triethylamine, and *tert*-butyl phosphine).[6] This image was reproduced from ref. 6, under a Creative Commons licence: CC BY 3.0.

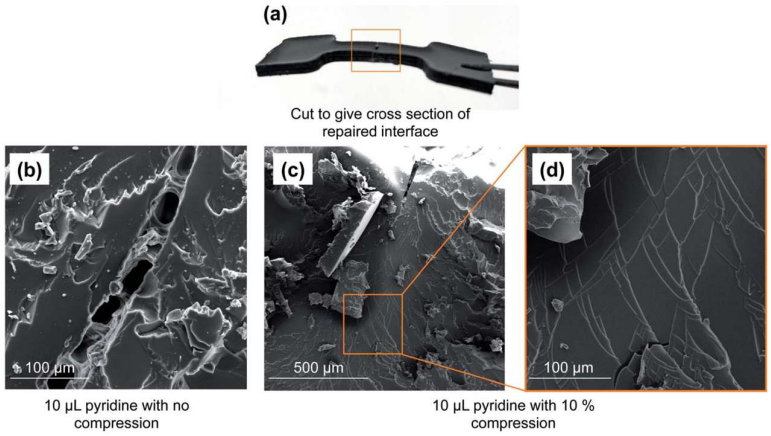

Figure 3.5: (A) A sulfur co-polymer specimen made by the reaction of sulfur (50%), an unsaturated triglyceride (35%), and dicyclopentadiene (15%). SEM cross section of the polymer treated with pyridine (B) without any compression, (C) 10% compression, and (D) Zoomed SEM image in the treated area showing full repaired interface.[6] This image was reproduced from ref. 6, under a Creative Commons licence: CC BY 3.0.

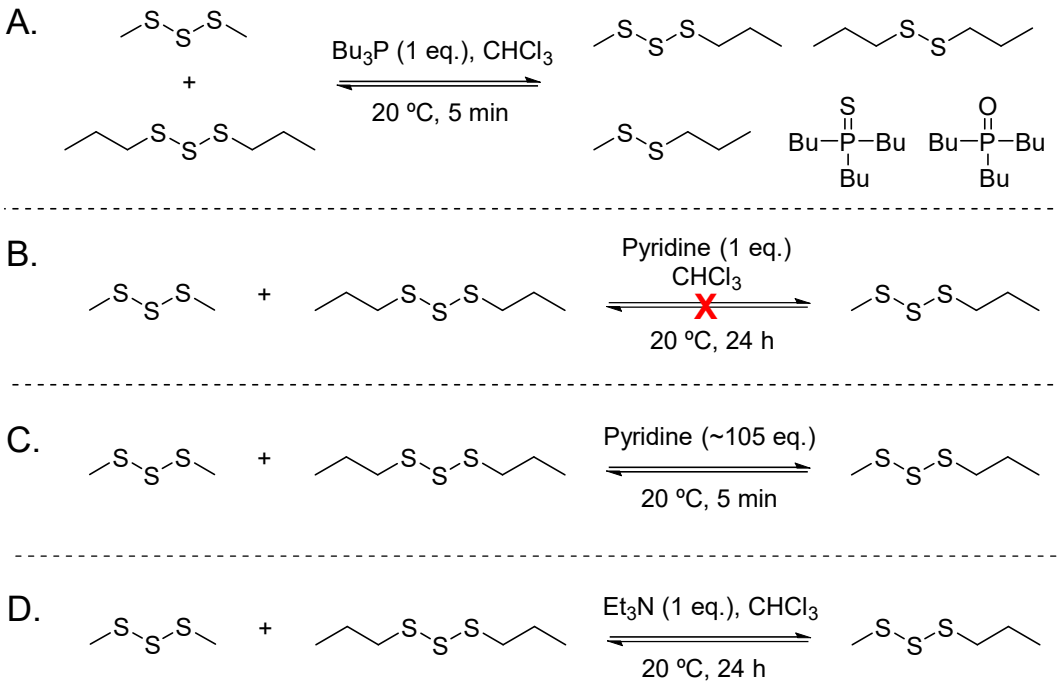

Figure 3.6: S-S metathesis reaction between dimethyl trisulfide and di-*n*-propyl trisulfide in (A) 1 eq. of tributyl phosphine dissolved in chloroform (a mixture of disulfide and trisulfide was observed by GC), (B) 1 eq. of pyridine dissolved in chloroform (no product observed by GC), (C) excess pyridine promotes rapid S-S metathesis of the trisulfides (D) 1 eq. of triethylamine dissolved in chloroform causes S-S metathesis over 24 hours.[6]

It is important to note that it only required 1 eq. for either the phosphine or triethylamine to induce the metathesis reaction in chloroform, even though a slow trisulfide S-S metathesis reaction was observed in the presence of triethylamine. Excess pyridine (~105 eq.) was required to ensure the metathesis reaction to occur rapidly, while no reaction between the trisulfides was observed after 24 h in 1 eq. of pyridine (Figure 3.6B). There was no data given for the reaction in excess triethylamine. In the presence of tributyl phosphine, the trisulfides transformed into a mixture of disulfide, trisulfide, phosphine sulfide, and phosphine oxide within a short period of time.

The similar reactions were also reported by Harpp and co-workers[7-10] and Taylor and co-workers[11-14] in which a phosphine (R_3P, where R= alkyl, aryl, alkoxy, or dialkylamino) reacts with trisulfide compounds to undergo desulfurization to disulfide and subsequently to monosulfide (thioether). Typically, the rate of desulfurization of a disulfide to the corresponding thioether is very slow. Furthermore, the rate of desulfurization depends on the nucleophilicity of phosphines.[7] In the case of reaction in Figure 3.6A above, no tetrasulfide was observed which suggest a rapid desulfurization occurs rapidly in the reaction.

Figure 3.7A illustrates the S-S metathesis of trisulfides **7** and **8** in the presence of triphenylphosphine to yield unsymmetrical trisulfide **9**, followed by desulfurization of the trisulfide mixture. The first trisulfide exchange reaction was reported to complete around 15 h and the second

desulfurization reaction completed after 5 days. Desulfurization could take place either at a terminal or central sulfur atom of the trisulfide giving disulfide and tetrasulfide via anion exchange from the resulting phosphonium salts **10** and **11** (Figure 3.7B). This process also depends on the solvent polarity (e.g., MeCN, THF, C_6H_6).[7] Similar to the reaction in Figure 3.7A, Harpp and co-workers[7] reported that when acetonitrile-d_3 was used in place of benzene the complete S-S exchange occurred within 7 minutes and the complete desulfurization occurred within 24 h.

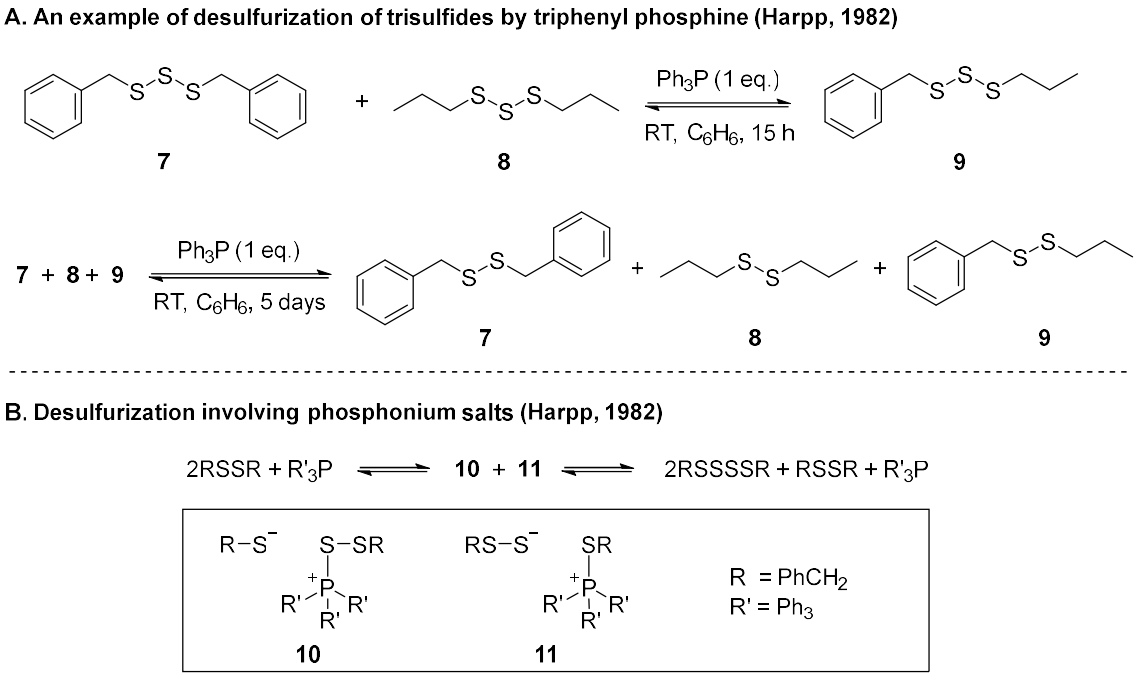

Figure 3.7: A. Desulfurization of dibenzyl and di-*n*-propyl trisulfide by triphenyl phosphines (Ph_3P). B. Anion exchange of phosphonium salts.[7]

Recently, a collaborative study between Hasell lab at the University of Liverpool and Chalker lab at Flinders University led to the discovery of an unusual reactivity of trisulfides in amide solvents such as DMF, NMP, and DMAc.[15] The discovery started when Hasell lab found that the weight-average molecular weight (M_w) of a polysulfide made by inverse vulcanization was reduced after treatment with DMF. It has been thought that the amide solvents were able to coordinate and break S-S bond in the polysulfide system. To test whether S-S metathesis reaction can occur in a polysulfide system with sulfur rank ≥ 3, two symmetrical trisulfide models, i.e., dimethyl and di-*n*-propyl trisulfide, were reacted together in the presence of the amide solvents. Results showed that these solvents had induced S-S metathesis between the trisulfides, leading to the formation of methyl *n*-propyl trisulfide ($MeS_3{}^nPr$) (Figure 3.8A). Equilibrium for this reaction was established within 1 hour and no product other than $MeS_3{}^nPr$ was formed after longer reaction time (24 hours). Changing the solvent to THF (Figure 3.8B), which was used as a negative control because the sulfur polymer is practically insoluble in THF, the metathesis reaction did not occur after 1 hour. However, a very small portion of $MeS_3{}^nPr$ was observed after the reaction proceeded for 24 hours in THF. This indicates

that the metathesis can occur but the rate was much slower compared to those in amide-containing solvents. Overall, this discovery showed an unusual reactivity of the trisulfides in amide solvents. Unlike pyridine which is a strong nucleophile, amides such as DMF, NMP and DMAc, are only weak nucleophiles.

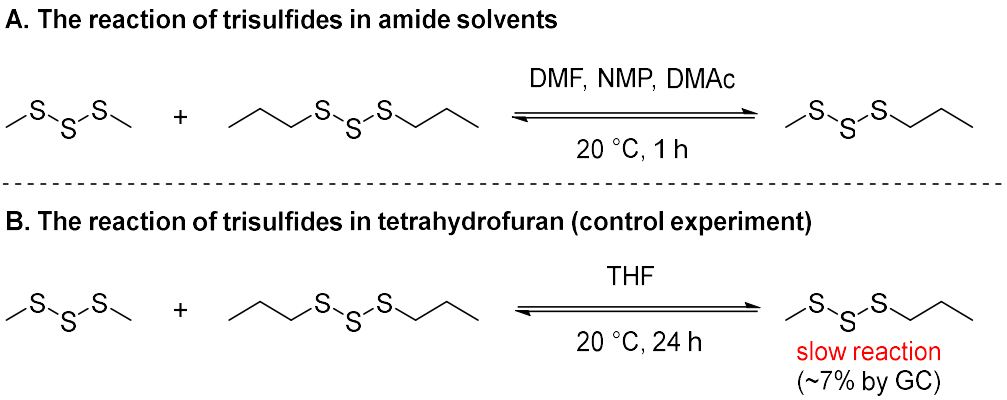

Figure 3.8: S-S metathesis between dimethyl trisulfide and di-*n*-propyl trisulfide. A. S-S metathesis between the trisulfides in the presence of amides solvents. B. A control reaction using THF as the solvent.[15]

Recent studies on the room temperature solvents induced S-S metathesis

In the previous studies by Trivette, Tobolsky and Pratt,[3-5] S-S metathesis of trisulfides were generally carried out at elevated temperature and in relatively non-polar solvents such as benzene and chlorobenzene. To date, there have been no systematic studies on the effect of polar solvents such as amides, ureas, or alcohols on the trisulfide S-S metathesis, and no conclusive information has been determined regarding the mechanism of the reaction in Figure 3.8.

In this Chapter, we explored various solvents (from non-polar to highly polar) to see which solvents induce the trisulfide S-S metathesis reaction at room temperature. In previous unpublished studies in the Chalker Lab[15, 16], several common laboratory solvents such as amide-containing solvents (i.e., DMF, NMP, DMAc), DMSO, MeCN, acetone, THF, and alcohols (i.e., methanol, ethanol, and isopropanol) were tested for S-S metathesis between dimethyl trisulfide and di-*n*-propyl trisulfide. In terms of the reaction rate, these solvents were divided into two main categories: solvents that promoted rapid S-S metathesis and solvents that promoted slow S-S metathesis (Figure 3.9). These categories are based on the amount of $MeS_3{}^nPr$ product formed in the reaction. Moreover, although in general amide-containing solvents promoted rapid S-S metathesis for the trisulfides, it was found that TEMPO, a common radical scavenger, suppressed the reaction, giving no $MeS_3{}^nPr$ product even after 24 hours.[15] Since then, TEMPO was thought to inhibit the reaction by quenching the thiyl ($RS^\bullet$) or perthiyl ($RSS^\bullet$) radical that could be generated during the reaction. However, alternative mechanism of TEMPO inhibition through redox process is discussed in Chapter 4 of this thesis.

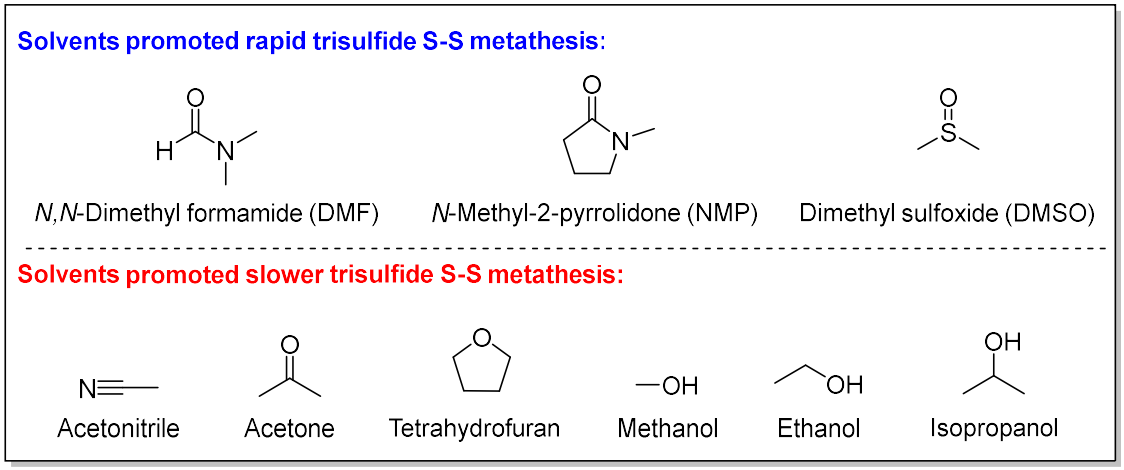

Figure 3.9: Solvents used in the trisulfide S-S metathesis study in an Honours project at Flinders University (Ryan Shapter, unpublished)[16]

The previous works on the S-S metathesis by Shapter[16] as well as Hasell and co-workers[15] did not consider several factors which may affect the S-S metathesis reaction such as the presence of oxygen, ambient light, the effect of water in the solvents, and steric and electronic influence of various substrates (e.g., R groups in the trisulfides). These factors were examined in this Chapter for the first time to address the research gaps arising from the previous works, with an aim to reveal some insight into the mechanism of this unusual reaction. This Chapter specifically elaborates the effect of solvents with different polarity on the S-S metathesis between trisulfides. In addition, the room temperature solvent induced S-S metathesis in trisulfides has been reported only for the reaction between trisulfides with short alkyl chains i.e., dimethyl trisulfide and di-*n*-propyl trisulfide (Figure 3.8).[15, 16] Therefore, various trisulfides were synthesized (previously described in Chapter 2) and used in this S-S metathesis study to more thoroughly assess the substrate scope. Furthermore, other types of solvents such as ureas (i.e., TMU, DMPU, and DMI), phosphoramides (i.e., HMPA and TPPO), and other highly polar compounds were employed to evaluate their performances in the trisulfide metathesis.

This Chapter also demonstrated several new applications of this S-S metathesis chemistry in the field of dynamic combinatorial chemistry and synthetic organic chemistry. These two applications are anticipated to be useful for the development of drug target discovery by using trisulfide based dynamic combinatorial library and synthetic strategies for making unsymmetrical trisulfides or trisulfide substrate modification. Additionally, several S-S metathesis studies employing disulfides and tetrasulfides in the presence of DMF were provided for comparison in the last section of this Chapter. These reactions revealed unexpected differences in S-S metathesis reactivity between di-, tri-, and tetrasulfides.

3.3 Results and Discussion

Solvents promoted rapid S-S metathesis of Me_2S_3 and $^nPr_2S_3$

To begin with, the trisulfide metathesis reaction in Figure 3.8A was re-examined to assess the reproducibility. The reaction between the trisulfides was tested using nitrogen degassed anhydrous DMF. Reagents and the solvent were purposely degassed to remove any oxygen and other volatile impurities which could potentially affect the reaction. Dimethylamine (b.p. ~7 °C at 1 atm), for instance, is a common impurity present in DMF.[17] This impurity can be easily removed by purging with an inert gas, i.e., nitrogen or argon gas. In this way, DMF can be assessed as the solvent for the S-S metathesis without contaminant amines. (Amine solvents were also assessed as nucleophilic solvents, as described later in this chapter). In previous work[15], it was reported that the reaction reached equilibrium within 1 h in DMF. It should be noted that the equilibrium here was determined as the area percentage of the metathesis product, i.e., $MeS_3{}^nPr$, which has reached nearly 50% by GC-MS. In other words, the ratio of products at equilibrium was Me_2S_3 : $MeS_3{}^nPr$: $^nPr_2S_3$ equal to 1 : 2 : 1. The result showed that the trisulfide metathesis equilibrium can be achieved within 5 min (Figure 3.10B). In fact, even after 5 seconds the reaction had almost reached equilibrium (Figure 3.10A). The same results were also reported by Shapter[16] for the reaction with non-degassed trisulfide reagents and solvents in his unpublished Honours research. Hence, the result suggested that oxygen does not affect the S-S metathesis.

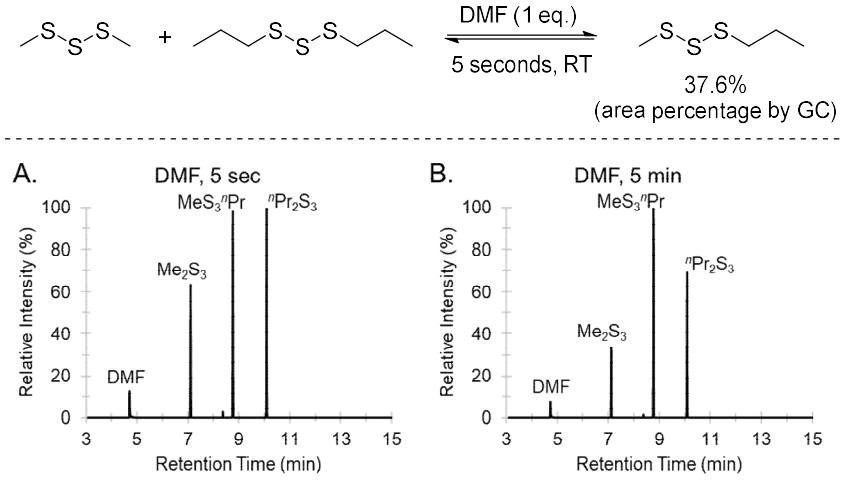

Figure 3.10: Rapid S-S metathesis between Me_2S_3 and $^nPr_2S_3$ in the presence of DMF (1.0 eq.). GC traces of the reaction after (A) 5 seconds and (B) 5 minutes.

Moreover, we also found similar observations when the trisulfide models were reacted with the following solvents: *N*-methyl-2-pyrrolidone (NMP), dimethyl acetamide (DMAc), *N,N'*-dimethylpropylene urea (DMPU), tetramethylurea (TMU), and dimethyl sulfoxide (DMSO). These solvents were able to facilitate the rapid S-S metathesis reaction within 5 seconds (Figure 3.11). In addition, other solvents such as phosphoramides, i.e., hexamethylphosphoramide (HMPA) and

tri(pyrrolidin-1-yl)phosphine oxide (TPPO), and another cyclic urea 1,3-dimethyl-2-imidazolidinone (DMI) were also found to induce rapid trisulfide metathesis. Although these solvents were not tested for 5 seconds, equilibrium was achieved within 5 minutes. Data shown in Table 3.1 below provides information about the percentage of the product for those rapid metathesis reactions. In subsequent reactions, most of the S-S metathesis investigations were using DMF as the solvent, but Figure 3.11 highlights other polar, aprotic solvents that promote the key reaction.

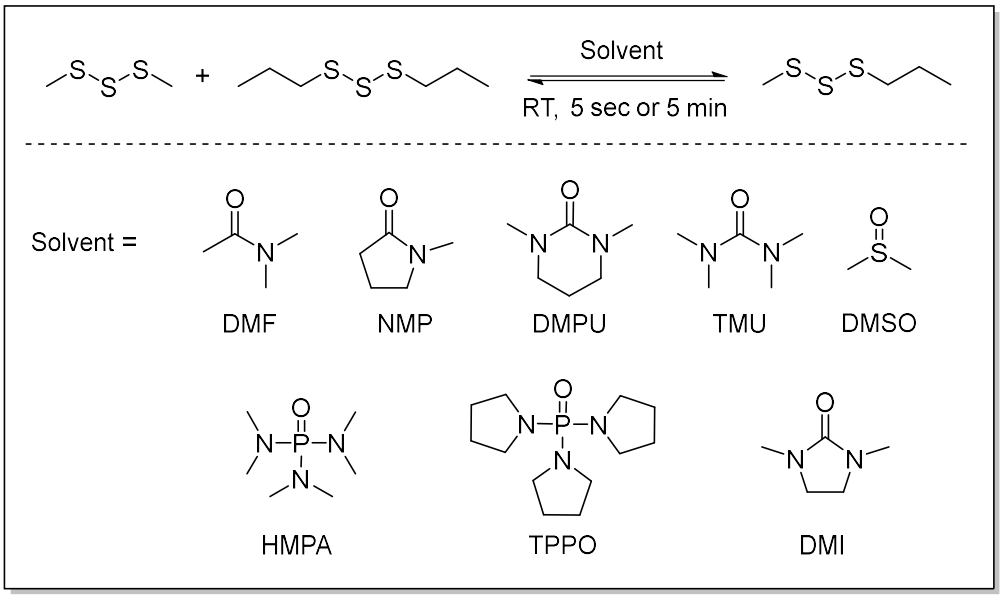

Figure 3.11: Solvents that promoted a rapid trisulfide metathesis.

The S-S bond in the trisulfide could potentially be cleaved on exposure to light. Indeed, several studies reported that light induces S-S metathesis in polysulfide systems.[18-21] For instance, Otsuka reported UV light (maximum peak intensity at 365 nm in the range of 312 – 577 nm, 400 W) induced disulfide S-S metathesis.[20] Zysman-Colman and Harpp[21] reported that several aromatic trisulfides (ArS_3Ar, Ar=Ph, *p*-MePh, *p*-BrPh, *p*-NO_2Ph) can undergo decomposition into a series of polysulfides (ArS_nAr, where n= 2 – 6) when exposed to light within few hours. In the previous studies by Shapter,[16] it was found that DMF induced the S-S metathesis reaction between Me_2S_3 and $^nPr_2S_3$ in the dark. This reaction was repeated and also carried out in under nitrogen atmosphere as an added control. Yet, the reaction of trisulfides in DMF either in the dark or in ambient light proceeded with no difference (Figure 3.12): both reactions resulted in rapid S-S metathesis. This result suggests that ambient light was not required to initiate the S-S metathesis.

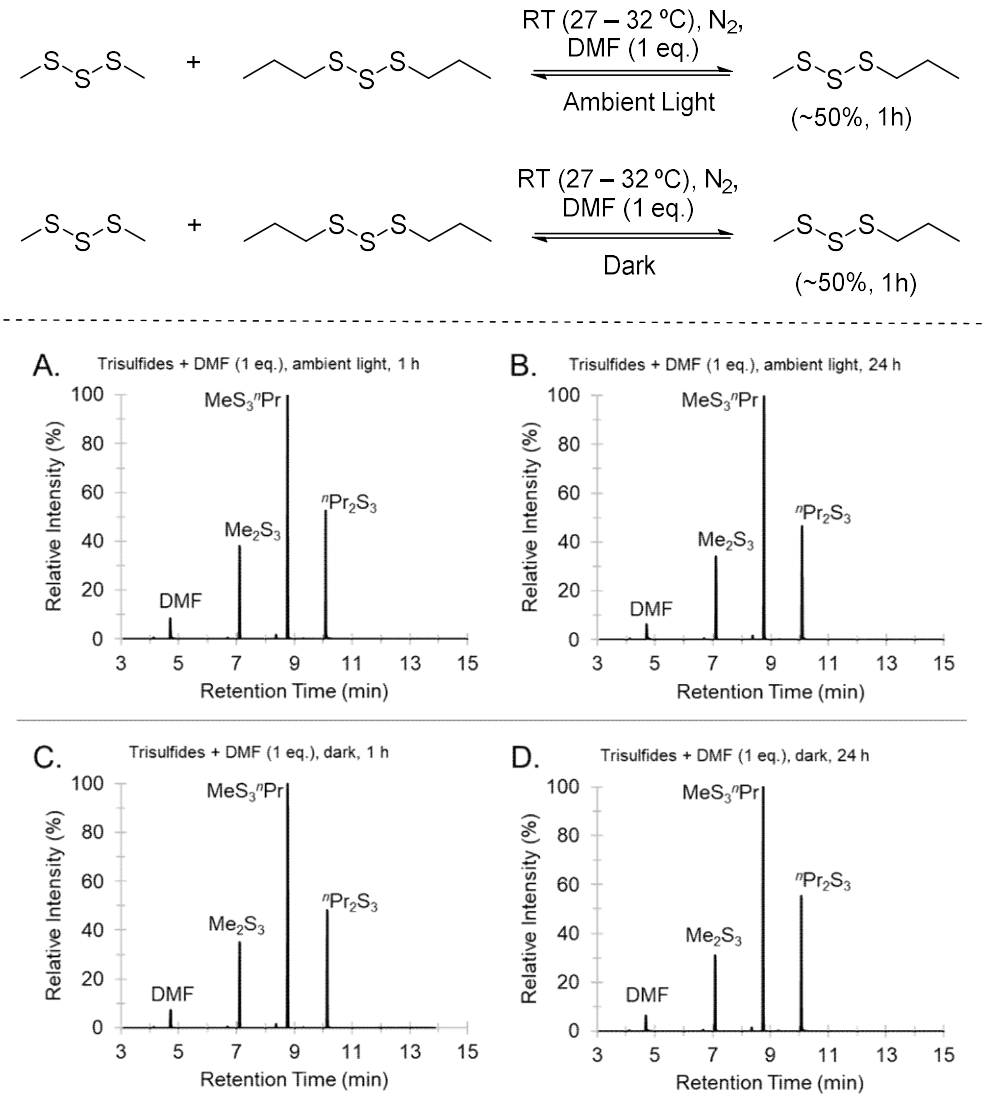

Figure 3.12: Trisulfide S-S metathesis reactions under ambient light and in the dark. GC traces of the reaction under ambient light for (A) 1 h and (B) 24 h, and dark for (C) 1 h and (D) 24 h. No difference was observed, indicating light is not required for this reaction.

When using an equimolar ratio between the trisulfides (Me_2S_3 and $^nPr_2S_3$) and DMF, the S-S metathesis occurs rapidly and reaches equilibrium in a matter of seconds. We next considered what would happen if a catalytic amount of DMF (10 mol%) was used in the reaction. If DMF is merely a nucleophilic catalyst in the reaction, lower amounts of DMF should still initiate the metathesis. However, 10 mol% of DMF was not sufficient to rapidly induce the S-S metathesis. And even after 72 hours, the equilibrium reaction between the trisulfides had not been established (Figure 3.13). This result suggests that the amount of DMF is important in this reaction, with more DMF resulting in more rapid equilibration of the trisulfide products. This result may also indicate that the polarity of the reaction medium is also important for facilitating this S-S metathesis reaction.

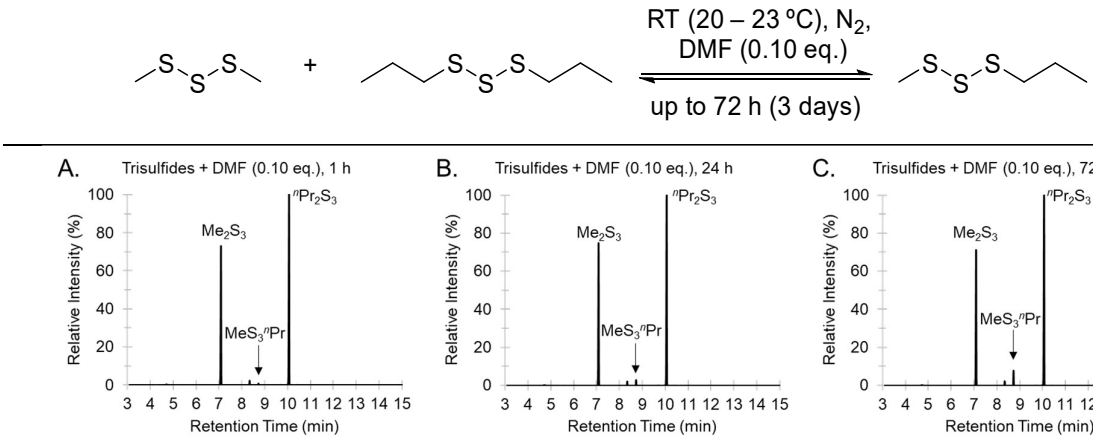

Figure 3.13: GC traces for the crossover reaction between Me_2S_3 and $^nPr_2S_3$ with a catalytic amount of DMF (0.1 eq.) after (A) 1 h, (B) 24 h, and (C) 72 hours (3 days) at room temperature (20 – 23 ºC).

From this finding, a thorough investigation of the S-S metathesis between the trisulfide models was then carried out to find the suitable amount of the amide solvent for the rapid S-S metathesis reaction. Both degassed Me_2S_3 and $^nPr_2S_3$ (1 eq. each) were reacted in DMF at various percentages (% v/v) at room temperature. After 2 min, each sample was removed, diluted with chloroform, and analysed by GC-MS. As shown in Figure 3.14, results showed that a minimum of 50% DMF is required for the rapid S-S metathesis (equilibrium reached < 5 minutes). This minimal amount of DMF was then generally used for further investigations of the trisulfide metathesis.

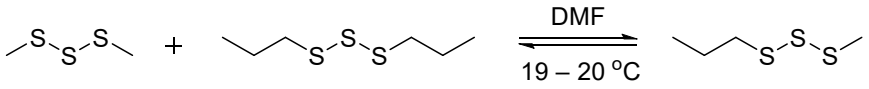

DMF% v/v	DMF (µL)	Mixed trisulfides (µL)	% area $MeS_3{}^nPr$ by GC after 2 minutes
5.0	40	760	0
7.5	60	740	0
10	80	720	0.1
12.5	100	700	0.4
15	120	680	0.9
20	160	640	4.8
21.9	-	-	*DMF = Me_2S_3 = Pr_2S_3 = 1 eq.*
25	200	600	17.1
30	240	560	22.9
35	280	520	35.2
50	400	400	45.9
73.7	-	-	*DMF = 10 eq., Me_2S_3 = Pr_2S_3 = 1 eq.*
75	600	200	47.7
87.5	700	100	46.9
95	760	40	39.7

Figure 3.14: S-S metathesis of trisulfides in DMF at various percentages (% v/v). The reaction has reached equilibrium at 50% DMF within 2 minutes (highlighted green).

To prove that the key to rapid S-S metathesis in trisulfides is the requirement of a polar amide solvent such as DMF, a control reaction was carried out between the trisulfides (neat) without any addition of solvent (Figure 3.15A and 3.15B). The result showed no reaction was observed between the trisulfides at room temperature after 24 h. When the reaction proceeded for 7 days, only a tiny portion of $MeS_3{}^nPr$ product (~5% area by GC) was formed. This result suggests that the metathesis reaction between neat trisulfides can still occur, but the reaction is much, much slower than the metathesis reaction in DMF.

Next, the temperature of a neat reaction was increased to 80 °C. Even with heating, the crossover product only formed at a very small portion after 24 h (< 2% area by GC, Figure 3.15C and 3.15D). This result was consistent with the study reported by Tobolsky[4] where dimethyl trisulfide, upon heating at 80 °C for several hours, only transformed into disulfide and tetrasulfide in a small proportion (~2%). In addition to this, Tobolsky reported that the use of nonpolar solvent such as benzene in the thermal treatment of dimethyl trisulfide did not promote the disproportionation of the trisulfide into its corresponding disulfide and polysulfides. More importantly, a key difference between S-S metathesis in DMF and thermally-induced S-S metathesis is the formation of disulfide and tetrasulfides in the latter case. In contrast, amide solvents such as DMF only promote the formation of trisulfides in the S-S metathesis reaction: disulfides and tetrasulfides are not formed.

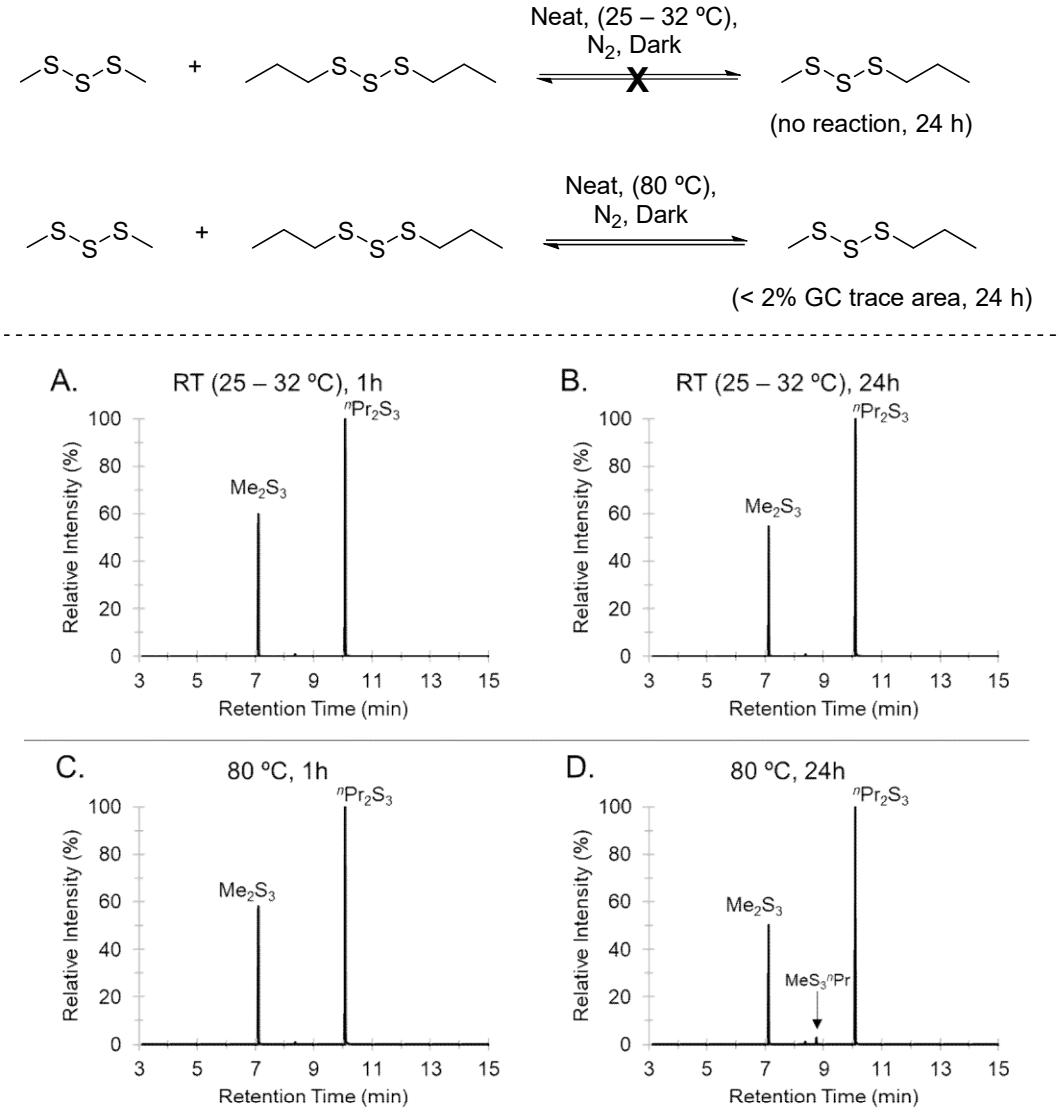

Figure 3.15: Control reactions between the trisulfides at room temperature and elevated temperature (80 °C). GC traces for the trisulfides after stirring (A) 1 h and (B) 24 h at room temperature, and after heating (C) 1 h and (D) 24 h at 80 °C. In these reactions, which do not include solvent, the S-S metathesis reaction does not occur or it is very slow.

Solvent mixture in S-S metathesis between Me_2S_3 and $^nPr_2S_3$

The dielectric constant (ε_0), or relative permittivity, of a solvent is often correlated with the solvent polarity. However, there are many factors such as hydrogen bonding, temperature, and electron pair donor-electron pair acceptor (EPD-EPA) interaction which have to be considered in order to understand the polarity of an individual solvent.[22] Therefore, it is not easy to make a correlation between the dielectric constant and solvent polarity. Despite of this, the solvent dielectric constant and solvent polarity are often discussed in a correlative fashion.

When two solvents with different values of dielectric constant are mixed, the resulting dielectric constant of the mixed solvents will change depending on the composition of each solvent and the temperature. For example, DMF (ε_0 = 37.06) and PhCl (ε_0 =5.66) at 25 °C when mixed at mol fraction of DMF (χ_{DMF}) 0.47, the combined static dielectric constant for this binary solvent is 20.47 or about half ε_0 value of pure liquid DMF at 25 °C.[23] The binary solvent polarity will change depending on the relative amount of each solvent.

As pure DMF promotes rapid trisulfide S-S metathesis, we wondered if mixed solvent systems showed any clear trend in the reaction rate. Our hypothesis was that by decreasing the polarity of the solvent, the rate of S-S metathesis will also decrease. DMF and PhCl were used as the solvent models, as a polar and non-polar solvent, respectively. The trisulfides were reacted mixtures of DMF and PhCl (v/v) at 1, 5, and 10% DMF. The trisulfide metathesis reaction almost reached equilibrium within 1 h in 10% DMF (Figure 3.16C). At 5% DMF, only a slight amount of $MeS_3{}^nPr$ was formed after 1 h (Figure 3.16B). No S-S exchange was observed after 1 h for the reaction in 1% DMF (Figure 3.16A). These results clearly show that low polarity of solvents reduces the rate of the S-S metathesis reaction.

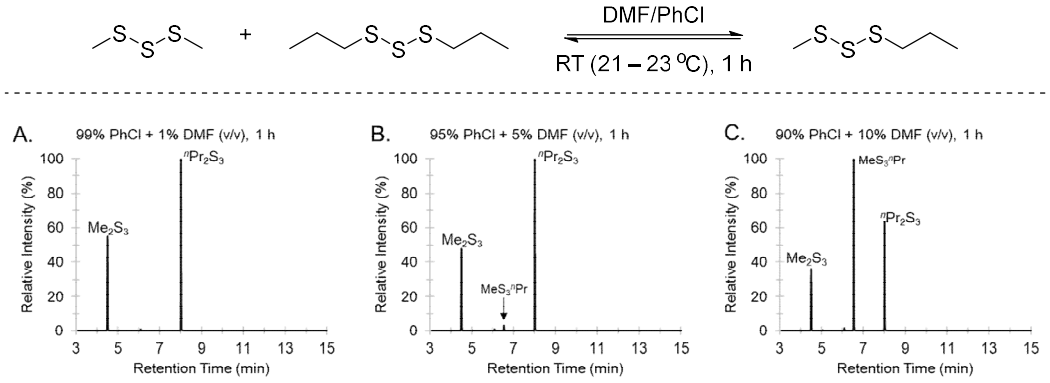

Figure 3.16: GC traces for crossover reaction between dimethyl trisulfide (Me_2S_3) and di-*n*-propyl trisulfide ($^nPr_2S_3$) in DMF/PhCl at varying concentration (1 – 10% v/v DMF content) after 1 hour at room temperature (21 – 23 °C). The trisulfides in (A) 1% DMF, (B) 5% DMF, (C) 10% DMF after 1 h.

Solvent effects in the S-S metathesis reaction between Me_2S_3 and $^nPr_2S_3$

The previous results suggested that solvent polarity or high dielectric constant (ε_0) may be important in inducing the trisulfide metathesis. Therefore, we tested the reaction between the trisulfide models and a variety of solvents to see which promote the crossover and see if there is a general trend. Table 3.1. shows the list of solvents tested for the trisulfide S-S metathesis.

Table 3.1: S-S metathesis reaction between Me_2S_3 and $^nPr_2S_3$ in various of solvents at room temperature for 72 h. (see Table S3 for data beyond 72 hours)

Solvent	Dielectric constant (e_0)[a]	Polarity[b] E_T^N	% crossover product ($MeS_3{}^nPr$) by GC					Notes
			5 sec	5 min	1 h	24 h	72 h	
Formamide	109.57[24]	0.775	-	-	1	10.5	-	1 eq.[e]
			-	-	0.4	27.5	-	10 eq.
4-Methyl-1,3-dioxolan-2-one (Propylene carbonate)	64.40[25] (at 20°C)	0.472	-	0.2	2.1	6.7	19.2	1 eq.[e]
			-	13.1	26.5	33.9	36.6	10 eq.
Dimethyl sulfoxide (DMSO)	46.60[26]	0.444	46.9	50.2	49.0	-	-	1 eq.
Tri(pyrrolidin-1-yl)phosphine oxide (TPPO)	45.08[27]	-	-	49	48.5	47.5	-	1 eq.
			-	51.3	51.6	50.4	-	10 eq.
Furan-2-carbaldehyde (Furfural)	41.80[28]	0.426	-	-	0	0	-	1 eq.
			-	0	0.4	1.2	-	10 eq.
e-caprolactone	39.43[29]	-	-	1	6.1	10.6	32.9	1 eq.
			-	0	5.7	16.3	34.2	10 eq.
Dimethylacetamide (DMAc)	37.80[30]	0.377	9.4	45.4	46.1	-	-	1 eq.
1,3-Dimethyl-2-imidazolidinone (DMI)	37.47[31]	0.364	-	49	48.8	47.9	-	1 eq.
			-	52.5	52.1	51.1	-	10 eq.
Dihydrolevoglucosenone (Cyrene™)	37.30[30]	-	-	-	0	0	-	1 eq.
Dimethyl formamide (DMF)	37.06[23]	0.386	37.6	51.4	48.9	-	-	1 eq.
N,N′-dimethylpropyleneurea (DMPU)	36.12[32]	0.352	46.8	44.7	44.9	-	-	1 eq
			-	0.4	3.4	-	20[d]	10 eq.[c]
Nitromethane	35.99[33]	0.481	-	-	0	0	-	1 eq.[e]
				0.3	11.2	22.4	25.6	10 eq.
Acetonitrile (ref.[16])	35.87[34]	0.460	-	-	0.8	22.3	46.3	1 eq.[c]
Nitrobenzene	34.30[35] (at 20 °C)	0.324	-	0	0	36.7	38.6	10 eq.
Methanol (ref.[16])	33.00[36]	0.762	-	-	0	3.8	16.6	1 eq.[c]
Methanol (this work)			-	-	0	0	-	1 eq.
			-	0.2	0.4	0.3	-	10 eq.
Hexamethylphosphoramide (HMPA)	32.70[37]	0.315	-	46.6	46.7	46.2	-	1 eq.
			-	46.6	46.8	46.6	-	10 eq.
N-methyl-2-pyrrolidone (NMP)	32.16[31]	0.355	42	51.2	48.9	-	-	1 eq.
Ethanol (ref.[16])	25.33[38]	0.654	-	-	0	1.4	11.3	1 eq.[c]
1,1,3,3-tetramethylurea (TMU)	23.60[39]	0.315	-	-	0	1.3	8.5	1 eq.[c]
			2.7	42.4	46.4	-	-	1 eq.
Acetone (ref.[16])	20.80[36]	0.355	-	-	0.1	5.3	37.9	1 eq.[c]
2-propanol (ref. [16])	19.20[40]	0.546	-	-	0	0.9	5.9	1 eq.[c]
1,1,1,3,3,3-hexafluoro-2-propanol (HFIP)[e]	16.75[41]	0.969	-	-	0	0.7	1.5	1 eq.[c]
2-methylpropan-2-ol (*tert*-butanol)	12.20[42]	0.389	-	-	0	0.2	1.0	1 eq.[c]
Pyridine	12.00[43]	0.302	4.6[f]	28.6	50.1	48.4	-	10 eq.
Tetrahydrofuran (THF, ref.[16])	7.54[44]	0.207	-	0	7	15	20	1 eq.[c]
Acetic acid	6.60[45]	0.648	-	-	0	0	0.2	1 eq.
Ethyl acetate	6.01[46]	0.228	-	-	0	0.1	0.6	1 eq.
n-Butylamine	4.62[47]	0.213	-	32	41.2	14.3[g]	-	10 eq.
Diethylamine	3.33[48]	0.145	-	0.5	1.2	36[h]	-	10 eq.
Carbon disulfide	2.64[49]	0.065	-	-	0	0	0.3	1 eq.
Triethylamine	2.46[48]	0.043	-	-	0	0	0.1	10 eq.

Toluene	2.38[50]	0.099	-	-	0	0.1	0.5	1 eq.
1,4-dioxane	2.23[51]	0.164	-	-	0	0	0.6	1 eq.
Hexanes (*n*-hexane)	1.89[52]	0.009	-	-	0	0	0.3	1 eq.

[a] measured at 25 °C unless otherwise stated.
[b] E_T^N represent solvent polarity that correlates with chemical kinetics and equilibria according to Reichardt (1979).[53]
[c] used as a non-dried and as received solvent, thus it may contain high level ppm of water and impurities.
[d] data obtained after 40 h, old sample of DMPU was used and possibly very wet.
[e] at this condition, the mixture was heterogeneous.
[f] area percentage by GC measured after 1 min of reaction
[g] Me_2S_2 (7.9%), $MeS_2{}^nPr$ (25.6%), Me_2S_3 (9.7%), $^nPr_2S_2$ (14.6%), Me_2S_4 (2.4%), $^nPr_2S_3$ (14.6%), $^nPr_2S_4$ (1.1%) were observed by GC after 24 h of reaction.
[h] Me_2S_2 (0.3%), $MeS_2{}^nPr$ (0.3%), and $^nPr_2S_2$ (0.3%) were observed by GC after 24 h of reaction.

Table 3.1 shows that the most efficient reactions are still in the solvents with high dielectric constant or high polarity. In some cases, several high polar solvents show slow reaction. Take formamide as an example, although it has the highest polarity amongst the tested solvents, a significant proportion of $MeS_3{}^nPr$ can be observed only after 24 h of reaction. This low crossover percentage may be because formamide is hydrated or the NH_2 group is a good hydrogen bond donor. Furfural and dihydrolevoglucosenone, despite of being a relatively high polarity solvent, also did not induce a rapid S-S metathesis in the trisulfides. Meanwhile, ureas such as DMPU and TMU, which have a slightly lower polarity compared to furfural and dihydrolevoglucosenone, were also found to induce a rapid S-S metathesis and facilitate the equilibrium similar to that of DMF, NMP, and DMAc. Finally, most low polar solvents that have ε_0 value < 10 did not induce S-S metathesis, except for those nucleophilic amines. For ease of understanding, the effect of solvents in the trisulfide S-S metathesis is summarized in Figure 3.17. There are three main categories of solvents based on their ability to facilitate the S-S metathesis to reach equilibrium: rapid, moderate, and slow or not established.

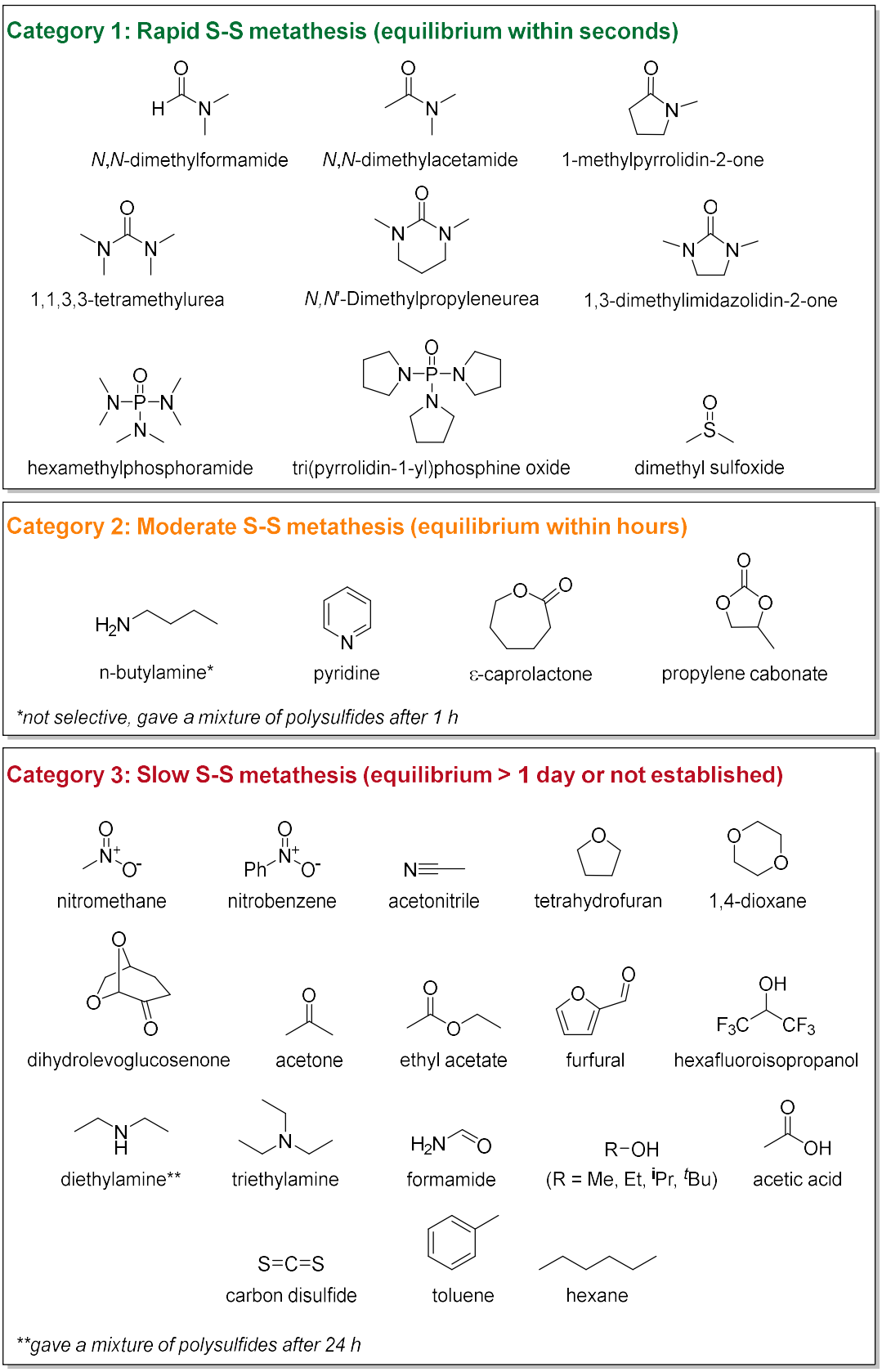

Figure 3.17: Solvent effect in the trisulfide S-S metathesis.

Amides, ureas, phosphoramides, and dimethyl sulfoxide are generally categorized as the solvents that rapidly induce the S-S metathesis between Me_2S_3 and $^{n}Pr_2S_3$ at room temperature. However, attention should be given to the water content of the solvents, especially the amides and ureas. The S-S metathesis reaction is greatly affected by the presence of water. In the non-dried and as received solvent (e.g., DMF, DMPU, or TMU – *not anhydrous quality*), the formation of $MeS_3{}^{n}Pr$ was slow. Even after 24 hours of reaction, we found that the area percentage of the metathesis product observed by GCMS was not significant (Table 3.1). In Table 3.1, for example, non-dried TMU (used as received from the chemical supplier) only gave around 1% of $MeS_3{}^{n}Pr$ after 24 hours while the dry TMU was able to closely reach the metathesis equilibrium within 5 min (42% area $MeS_3{}^{n}Pr$ detected by GC). Since water has ε_0 value of around 78, the binary mixture of water-amide, or water-urea should result in a slightly higher dielectric constant compared to just the pure amide solvent. In other words, the binary solvent of water-amide becomes more polar. But again, we found no correlation between a high polarity solvent and rapid trisulfide S-S metathesis. Further exploration of the effect of water on the trisulfide metathesis in DMF is discussed in the next section. For phosphoramides and dimethyl sulfoxide, the effect of water has not been investigated because the study was merely focused on the amide solvents. Additionally, both phosphoramides and dimethyl sulfoxide are slightly more nucleophilic compared to those amides.

The second category is the solvents that promoted moderate S-S metathesis. Propylene carbonate, ε-caprolactone, and other amines are the solvents that fall in this category. Propylene carbonate is a very polar solvent and notable in its sustainability metrics, according to the GlaxoSmithKline sustainability guide.[54] At equimolar ratio to the trisulfide (1 eq.), propylene carbonate was found to slowly induce S-S metathesis. This reactivity was also similar to that of ε-caprolactone. There was no significant difference in the rate of the S-S metathesis reaction when using 1 eq. of those solvents. For propylene carbonate, the use of 10 eq. of this solvent could noticeably enhance the metathesis reaction, whereas for ε-caprolactone the reaction was slightly improved. We also observed that when the trisulfides were mixed with 1 eq. of dry propylene carbonate, the mixture became heterogenous. This solubility issue could be the cause of the slow S-S metathesis reaction.

Furthermore, pyridine and *n*-butylamine were included in this second category. Despite the greater nucleophilicity of amines compared to the amides, these solvents promoted slower S-S metathesis than amide-containing solvents such as DMF. Unlike other amines such as Et_2NH and *n*-$BuNH_2$ that yield polysulfides at longer reaction time (24 h), interestingly pyridine gives only $MeS_3{}^{n}Pr$ as the metathesis product. The reaction of trisulfides in *n*-$BuNH_2$ is noticeably fast and unselective. This primary amine likely induced S-S metathesis via a nucleophilic attack and gave a mixture of disulfide, trisulfide, and tetrasulfide (Figure 3.18). We also noticed that the rate of trisulfide S-S metathesis within the first 5 min in wet *n*-$BuNH_2$ is slightly slower than in dry *n*-$BuNH_2$. In general, the rate of trisulfide S-S metathesis in these amines is shown as follows: pyridine ≈ *n*-$BuNH_2$ > Et_2NH > Et_3N.

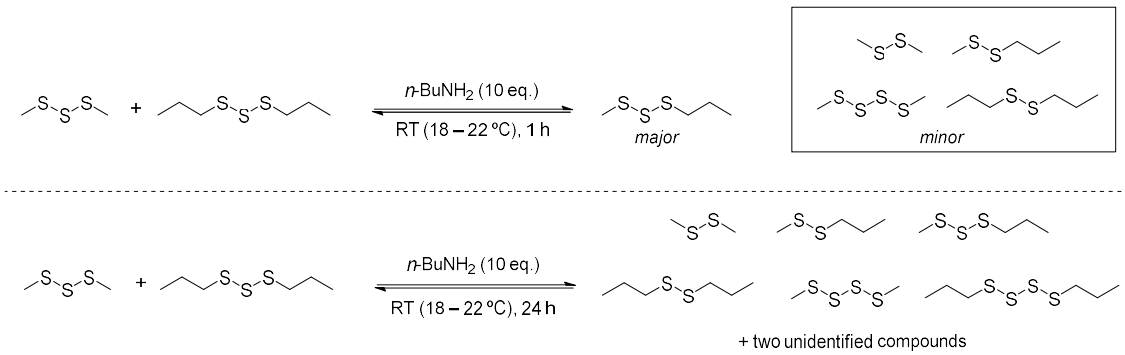

Figure 3.18: S-S metathesis reaction between dimethyl trisulfide and di-*n*-propyl trisulfide in *n*-butylamine after 1 h and 24 h.

The third category comprises the solvents that promoted slow trisulfide S-S metathesis reactions. These solvents can induce the S-S metathesis but the equilibrium is established over more than 24 h or even not established at all. Formamide and nitromethane can induce the trisulfide metathesis reaction when these solvents are dry and used in excess (10 eq.). A heterogeneous mixture was observed when the trisulfides were mixed either with 1 eq. of formamide or nitromethane. And again, this could account for the low percentage of the crossover product. Similar to the reaction in formamide, we also observed the same solubility problem for the reaction in 1,1,1,3,3,3-hexafluoro-2-propanol (HFIP) that also gave a very small portion of the crossover product (< 1% area of $MeS_3{}^nPr$ by GC).

Furthermore, acetonitrile, acetone, THF, methanol, ethanol, and isopropanol have been reported previously for the trisulfide S-S metathesis.[15, 16] Among these solvents, only acetonitrile promoted the trisulfide S-S metathesis and reached equilibrium after 48 hours. It took around 168 hours (7 days) to reach equilibrium in acetone. THF and alcohols, overall, result in similar reactivity in the metathesis reaction. In this work, we also tested *tert*-butanol but there was no significant different to other alcohols.

Another solvent of interest is nitrobenzene. This solvent was used to investigate the trisulfide metathesis because of its high polarity, which is similar to acetonitrile and nitromethane. In the S-S metathesis reaction, dry nitrobenzene gave a similar behaviour to acetonitrile. Within the first hour of reaction, no $MeS_3{}^nPr$ was observed by GC but then the reaction was reached equilibrium after 24 h. Lastly, we found that ethers, acetic acid, ethyl acetate, carbon disulfide and hexanes do not induce S-S metathesis.

The effect of water and acid on the trisulfide S-S metathesis

From the previous findings, we discovered that dry solvents were required for this trisulfide metathesis reaction. Any presence of water in the solvent, whether it is simply non-dried or a solvent that is purposely spiked with water, was found to significantly decrease the rate of trisulfide metathesis reaction. Because the level of water in the solvent was not determined (typically by Karl

Fischer titration), here the trisulfide S-S metathesis reaction was studied using the dry solvents that were spiked with water. By doing so, the amount of water in a tested solvent is can be quantified. This is important to provide quantitative information about the water tolerance.

In the initial investigation, we revisited the work by Shapter[16] where he reported that non-dried and as received isopropanol and methanol can induce S-S metathesis between Me_2S_3 and $^{n}Pr_2S_3$, although the yield of $MeS_3{}^{n}Pr$ was not significant (1% for isopropanol and 4% for methanol). And because we learned that dry solvents could improve the S-S metathesis, we attempted to do the trisulfide S-S metathesis reaction in dry methanol and isopropanol with the hope that the equilibrium could be achieved. Alcohols are hygroscopic, so both alcohols were rigorously dried using CaH_2 and 3A molecular sieves.[17] The trisulfides were reacted in both dry alcohols for 24 h. For a comparison, 1 eq. of methanol and isopropanol were used in the reaction. Results showed that both dry alcohols do not improve the rate of S-S metathesis. No $MeS_3{}^{n}Pr$ was observed by GC for the reaction in methanol (Figure 3.19A) and in isopropanol (Figure 3.19B) under this condition.

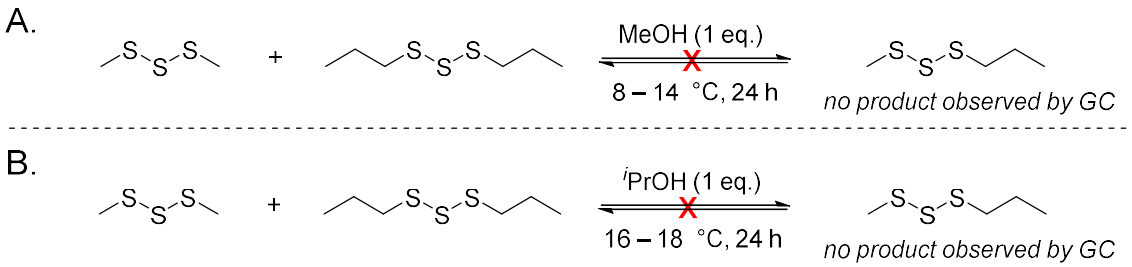

Figure 3.19: S-S metathesis between Me_2S_3 and $^{n}Pr_2S_3$ in dry (A) methanol and (B) isopropanol. No $MeS_3{}^{n}Pr$ was observed after 24 h of reaction.

Previous studies by Shapter[16] also showed that the addition of acetic acid (10 mol%) to DMF could inhibit the reaction. The addition of acetic acid in DMF or other amide solvents will neutralise any trace amine present in the amide solvents. Thus, the S-S metathesis reaction could take place solely because of the amide solvent and not be caused by contaminant amine nucleophiles. Shapter[16] found that the S-S metathesis reaction between Me_2S_3 and $^{n}Pr_2S_3$ in acidic DMF is significantly reduced (Figure 3.20). Interestingly, a different result was found when NMP was used in the reaction, where no inhibition in the first hour of reaction was observed. In our report, acetic acid alone cannot induce rapid S-S metathesis. The mixture of acetic acid (ε_0 = 6.60) and DMF (ε_0 = 37.06) would lead to the lower combined dielectric constant which could be the cause of this phenomenon. It might also be that the protons from the acid hydrogen bond to a reactive intermediate and lower its reactivity (see Chapter 4).

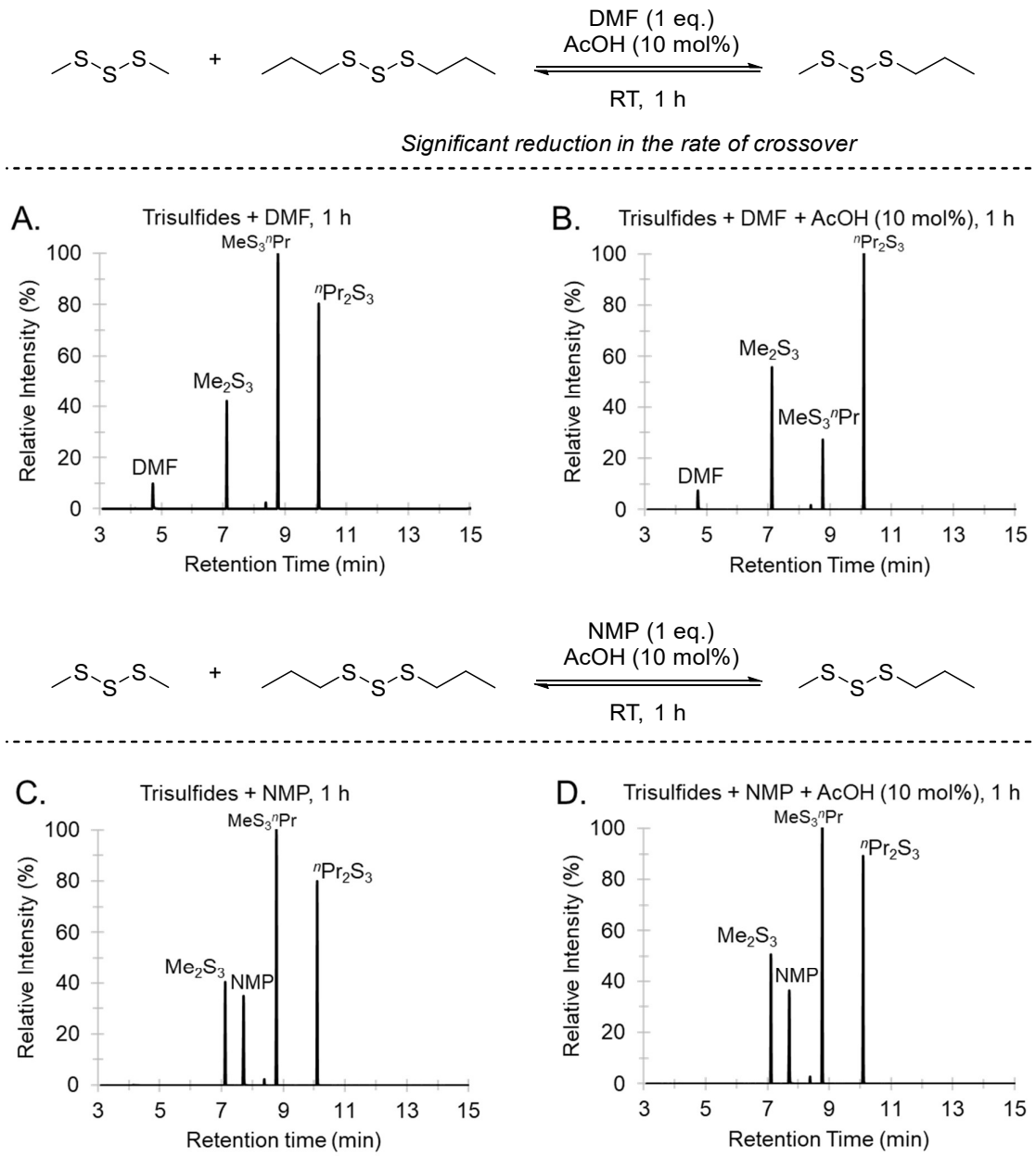

Figure 3.20: Trisulfide S-S metathesis inhibition by acetic acid. (A, B) GC traces of the reaction between the trisulfides and DMF without and with 10 mol% AcOH. (C, D) GC traces of the reaction between the trisulfides and NMP without and with 10 mol% AcOH. Data reused from ref.[16] with the permission from the author.

As water can cause the inhibition in the trisulfide metathesis, we then carried out experiments involving DMF and water. Figure 3.21 showed the effect of water on the trisulfide metathesis in DMF. Since water content was not determined quantitatively in the non-dried and as received solvent, we purposely added water to the dry DMF. To do this, dry DMF was spiked with water from 2.5 to 5.0% (w/w). After the addition of water to DMF, the solvent was allowed to stir for about 5 minutes before the trisulfides were added. The results showed that water significantly affects the rate of S-S

metathesis when 1 equiv. of DMF was used, while in 10 equiv. of DMF water did not seem to have a big influence on the S-S metathesis rate. The reaction was not monitored at a time period below 1 h. However, the result clearly highlighted that water slows the S-S metathesis, but some water can be tolerated when excess DMF is used. In addition to this, we have learned that water and protons (H^+) are two factors that significantly affect the trisulfide S-S metathesis reaction, which is an important consideration when formulating mechanistic hypotheses of this process.

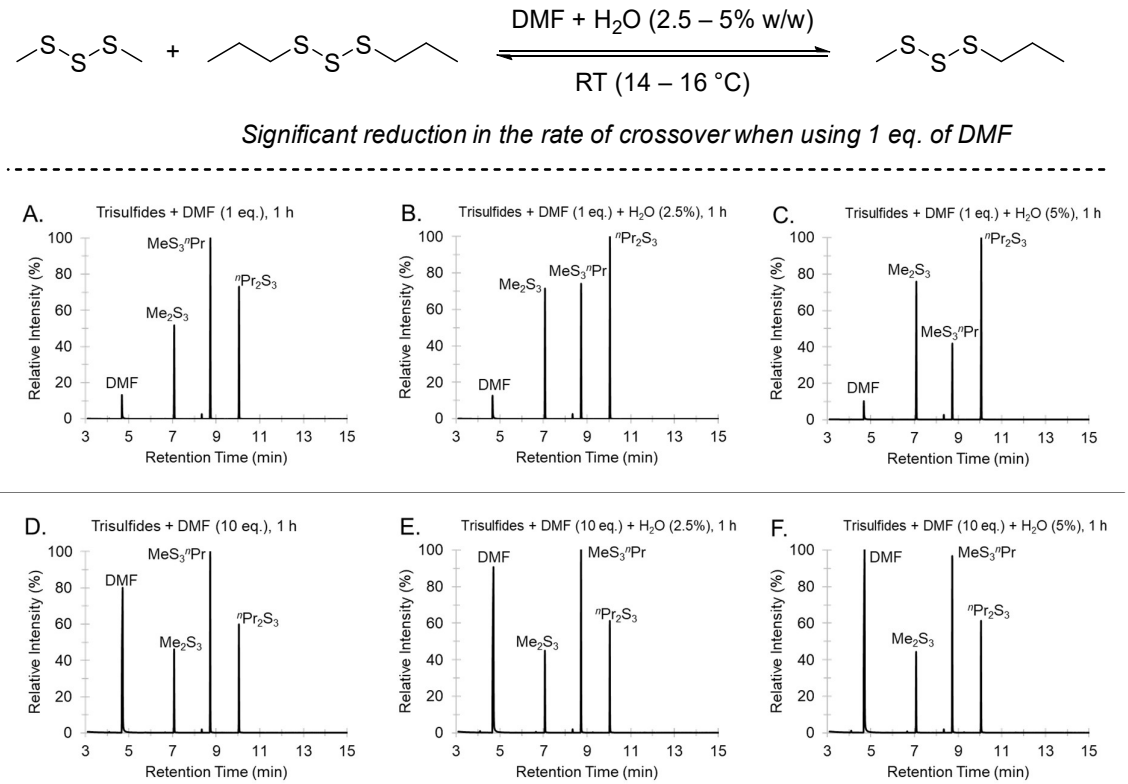

Figure 3.21: GC traces for the crossover reaction between the trisulfides over 1 hour at room temperature (14 – 16 °C). For 1 eq. each, after 1 h: (A) The trisulfide and DMF (100% w/w). (B) The trisulfides and DMF (97.5% w/w). (C) The trisulfides and DMF (95% w/w). For 10 eq. DMF, after 1 h: (D) The trisulfide and DMF (100% w/w). (E) The trisulfides and DMF (97.5% w/w). (F) The trisulfides and DMF (95% w/w). GCMS method A (see general consideration in Section 3.5). Retention time: DMF (4.70 min), Me_2S_3 (7.10 min), $^nPr_2S_2$ (8.36 min, impurity from dipropyl trisulfide), $MeS_3{}^nPr$ (8.75 min), and $^nPr_2S_3$ (10.09 min).

S-S metathesis involving various trisulfides

The trisulfide S-S metathesis reaction was most efficient in dry, polar, aprotic solvents (Figure 3.17). For subsequent studies, DMF was used as it is commonly available and widely used as a polar, aprotic solvent. The studies discussed previously focused on the S-S metathesis between dimethyl trisulfide and di-*n*-propyl trisulfide. Thus, in order to obtain a more comprehensive understanding of the S-S metathesis reaction, we used various trisulfides (previously discussed in Chapter 2) and

tested their reactions with dimethyl trisulfide. A summary of the S-S metathesis reaction between dimethyl trisulfide and various trisulfides is shown in Figure 3.22, providing some insight into the substrate scope of this reaction.

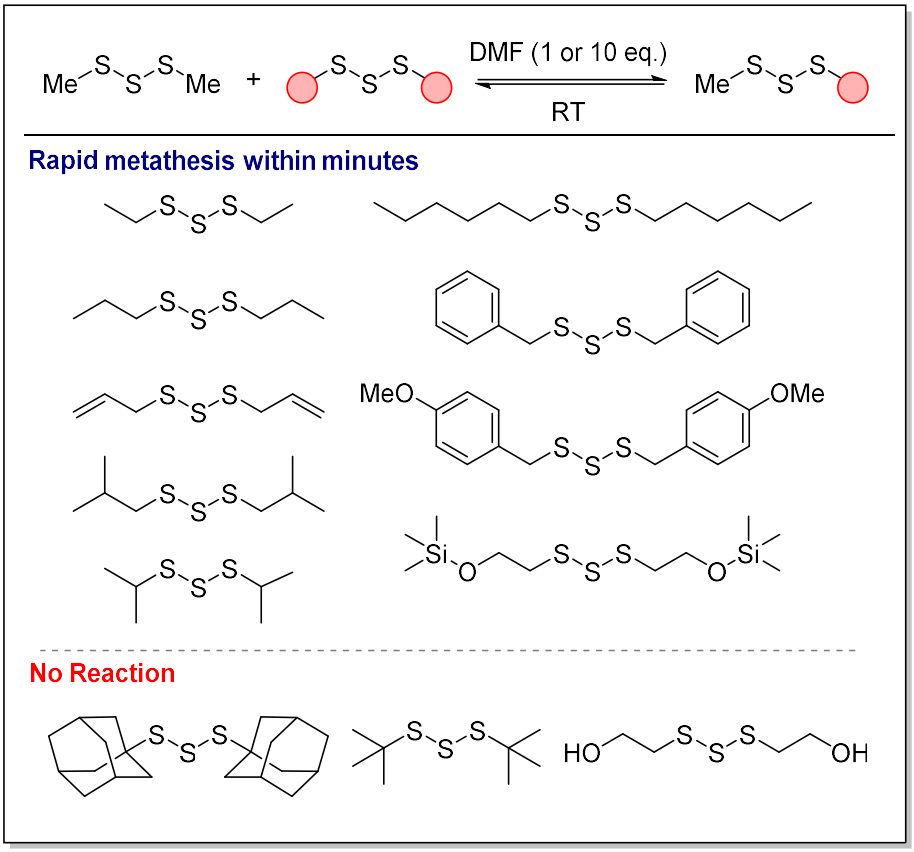

Figure 3.22: Trisulfide substrate scope.

The S-S metathesis reaction involving various trisulfides was carried out using either 1 or 10 equiv. of DMF. Most trisulfides can react rapidly with dimethyl trisulfide in DMF to yield their unsymmetrical trisulfides. While other trisulfides that possess bulkier groups such as adamantyl trisulfide (Ad_2S_3), *tert*-butyl trisulfide ($^tBu_2S_3$), or hydroxylated trisulfide ($HO(CH_2)_2S_3(CH_2)_2OH$) did not react with dimethyl trisulfide (Me_2S_3). In the case of the reaction between Ad_2S_3 and Me_2S_3, even heating these trisulfides up to 80 °C did not facilitate the S-S metathesis reaction. This result clearly shows that steric hindrance is important factor for the trisulfide S-S metathesis.

At an equimolar ratio in DMF, diallyl trisulfide ($Allyl_2S_3$) reacted with Me_2S_3 to yield allyl methyl trisulfide ($AllylS_3Me$). Our initial hypothesis was that the S-S metathesis may proceed through a radical mechanism.[15] Thiyl or perthiyl radicals could induce addition reactions or polymerization if alkenes are employed in the reaction.[55] However, we observed no addition to the alkene in this reaction. The trisulfide S-S metathesis reaction in DMF gives $AllS_3Me$ selectively. No reaction occurs between the neat trisulfides. Next, we found no issue in the reaction of diethyl trisulfide (Et_2S_3) or di-

n-hexyl trisulfide ($^{n}Hex_2S_3$) with Me_2S_3 where the S-S metathesis reactions occur rapidly within minutes, giving ethyl methyl trisulfide (EtS_3Me) or methyl *n*-hexyl trisulfide ($^{n}HexS_3Me$), respectively.

Furthermore, dibenzyl trisulfide (Bn_2S_3) reacted with Me_2S_3 or $^{n}Pr_2S_3$ in DMF to yield benzyl methyl trisulfide (BnS_3Me) or benzyl *n*-propyl trisulfide ($BnS_3{}^{n}Pr$), respectively. Due to the poor solubility of Bn_2S_3 in Me_2S_3 or $^{n}Pr_2S_3$, neat reactions were not possible to carry out at room temperature. Therefore, those trisulfides were dissolved in a non-polar solvent that does not promote S-S metathesis, i.e., diethyl ether, for a control experiment. We found that neither BnS_3Me nor $BnS_3{}^{n}Pr$ product were observed in the control experiments.

The S-S metathesis reaction between bis(*p*-methoxybenzyl) trisulfide and dimethyl trisulfide was tested next. This reaction was monitored by ^{1}H NMR spectroscopy due to the sample degradation by GC (see Chapter 2 for bis(*p*-methoxybenzyl) trisulfide synthesis and characterization). Upon reaction in DMF-d_7 (Figure 3.23), new peaks were formed at 4.20 and 2.58 ppm, which correspond to the crossover product methyl *p*-methoxybenzyl trisulfide (*p*-$MeOBnS_3Me$). An attempt was also made for the reaction between dibenzyl trisulfide and *p*-methoxybenzyl trisulfide. For this reaction, ^{1}H NMR analysis showed new peaks at 4.13 and 4.19 ppm were observed which corresponds to the methyl benzyl *p*-methoxybenzyl trisulfide (*p*-$MeOBnS_3Bn$) crossover product (Figure 3.24). The formation of new peaks in the ^{1}H NMR spectra for both reactions indicate that the S-S metathesis took place. Equilibrium for these both reactions were achieved within 1 h of reaction.

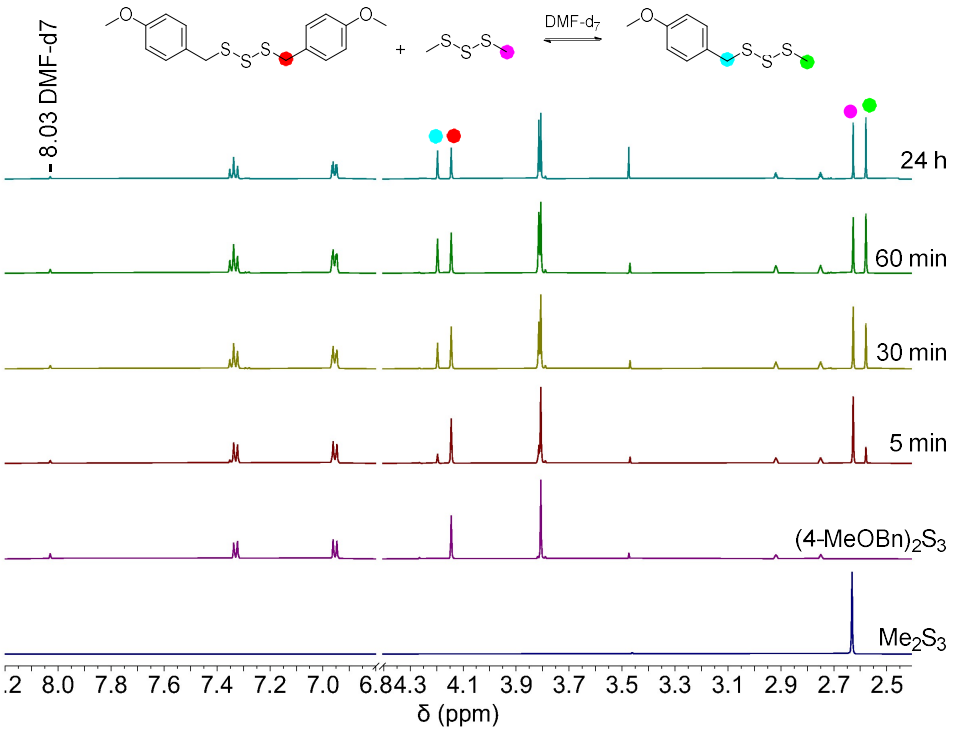

Figure 3.23: Stacked ^{1}H NMR spectra of bis(4-methoxybenzyl) trisulfide and dimethyl trisulfide mixture in DMF-d_7.

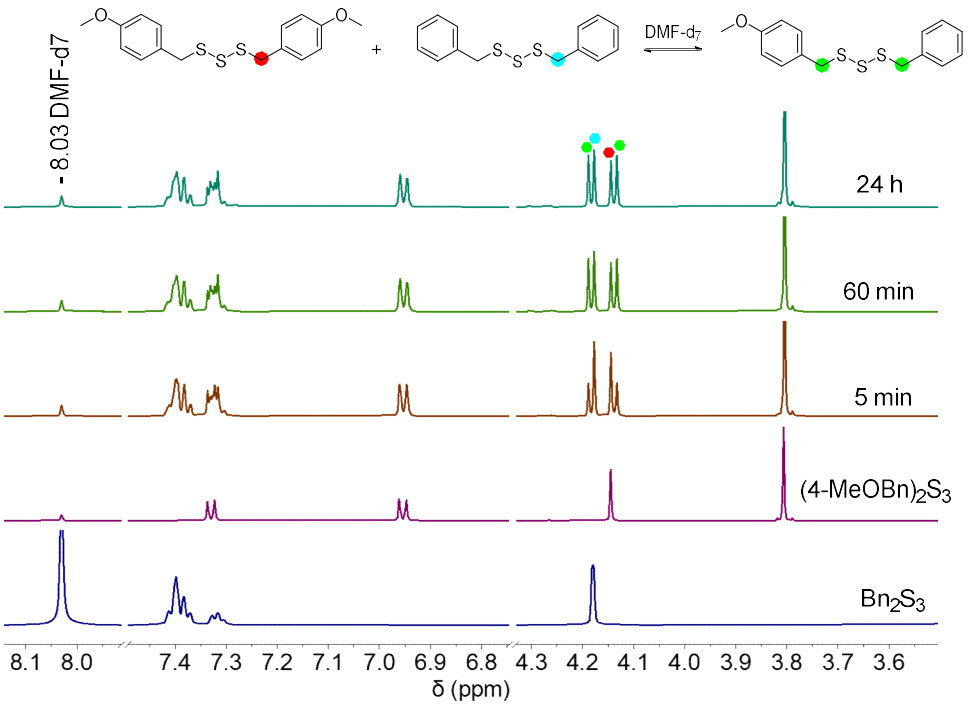

Figure 3.24: Stacked ^{1}H NMR spectra of bis(4-methoxybenzyl) trisulfide and dibenzyl trisulfide mixture in DMF-d_7.

For slightly bulkier trisulfides, i.e., di-*iso*-butyl trisulfide ($^{i}Bu_2S_3$) and di-*iso*-propyl trisulfide ($^{i}Pr_2S_3$), the S-S metathesis involving an equimolar ratio of the bulkier trisulfides with Me_2S_3 in the presence of DMF was generally slower compared to that of trisulfides with the primary alkyl groups. When using 10 eq. of DMF, the metathesis rate had improved significantly.

Unlike the other trisulfides, Ad_2S_3 and $^{t}Bu_2S_3$ did not give any S-S metathesis product when they reacted with Me_2S_3 in DMF. For Ad_2S_3, a two-phase mixture was observed when this bulky trisulfide was mixed with Me_2S_3. At room temperature (17 – 29 °C), even when 100 equiv. of DMF was used the trisulfide mixture created a white suspension. GC-MS analysis for this suspension after 24 h shows only the starting trisulfides. An attempt was made to continue the reaction between Ad_2S_3 and Me_2S_3 at elevated temperature (80 °C) for an additional 24 h. Results showed no adamantyl methyl trisulfide (AdS_3Me) formed under this reaction condition. For $^{t}Bu_2S_3$, the reaction of this trisulfide with either Me_2S_3 or $^{n}Pr_2S_3$ in DMF did not give any S-S metathesis products. Thermal treatment of neat $^{t}Bu_2S_3$ and Me_2S_3 at 150 – 170 °C showed slower S-S metathesis. This illustrates the nature of *tert*-butyl substituent. Hence, the trisulfide S-S metathesis reaction in DMF is influenced by the bulk of the organic part of the molecule.

Lastly, we found an interesting result when bis(2-hydroxyethyl) trisulfide was reacted with dimethyl trisulfide in DMF. The S-S metathesis reaction did not occur. However, when the hydroxylated trisulfide was protected, i.e., bis(2-trimethylsiloxyethyl) trisulfide, and reacted with dimethyl trisulfide in DMF, the S-S metathesis took place rapidly and gave methyl 2-

trimethylsiloxyethyl trisulfide as the crossover product. The hydroxyl group of bis(2-hydroxyethyl) trisulfide seems to provide a proton source which could interact and inhibit the S-S metathesis reaction, which could provide a clue to the mechanism, which is discussed in more detail in Chapter 4.

S-S metathesis involving a cyclic trisulfide: Norbonane trisulfide

We also explored the S-S metathesis reaction involving norbornane trisulfide. The trisulfide was kindly provided by Jasmine Pople, a PhD candidate in our group. The synthesis protocol to make this cyclic trisulfide was previously reported.[56] Since the trisulfide was stored in the fridge for nearly 6 months, it was then purified by silica column chromatography (R_f = 0.58, 100% hexane) to remove polymeric impurities. The obtained NMR spectra agreed with the literature report.[56] With the cyclic trisulfide in hand, the S-S metathesis of this cyclic trisulfide and dimethyl trisulfide was carried out in either 1 or 10 eq. DMF (Figure 3.25). GC-MS analysis revealed that the reaction gave dimethyl disulfide, dimethyl tetrasulfide, and other unknown compounds.

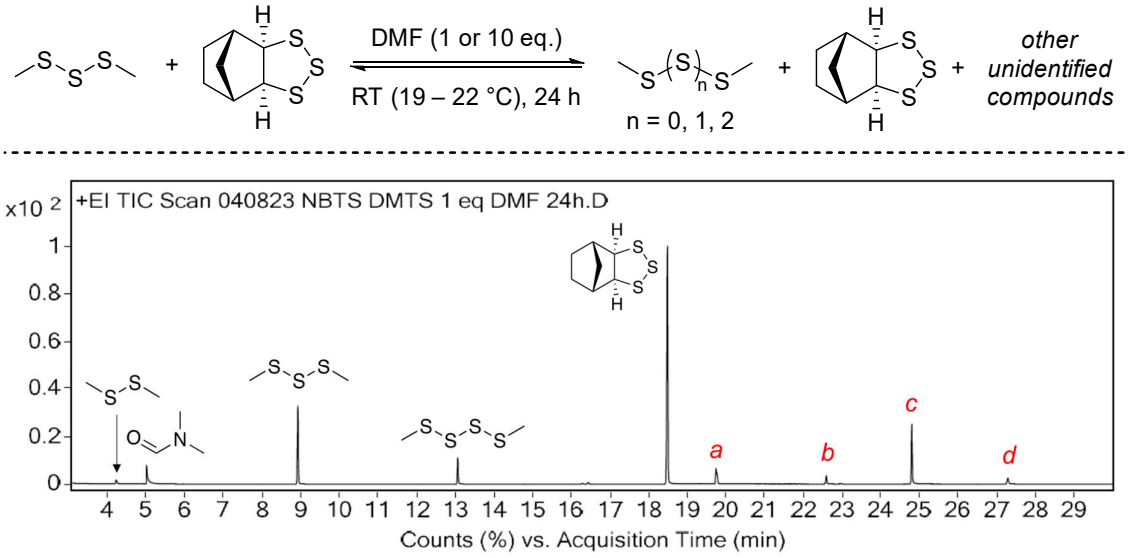

Figure 2.25: An attempt on the S-S metathesis reaction between dimethyl trisulfide and norbornane trisulfide in DMF (1 eq.). A GC trace for the reaction showing the formation of dimethyl disulfide and dimethyl tetrasulfide and other unidentified compounds after 24 h.

The unknown compounds were probably norbornane polysulfide derivatives. The result was different to the other linear trisulfides. Because this reaction gave a mixture of polysulfides, the mechanism might be different too in comparison to the linear trisulfide metathesis reaction. Bartlett and Gosh[57] demonstrated that norbornane trisulfide and pentasulfide formed an equilibrium ratio 3.5 : 1 in polar solvents such as DMF and DMSO. They also showed that sulfur was obtained from the mixture by a careful preparative TLC. Whether or not the cyclic pentasulfide may form during the dissolution of norbornane trisulfide in DMF, it still remains unclear which species contribute to the

reaction to occur. However, looking at the products (dimethyl disulfide and tetrasulfide) and a control experiment of norbornane trisulfide in DMF (Figure S3.82), it is more likely that a trace of sulfur plays a role in the reaction as sulfur may be generated during the dissolution of the trisulfide in DMF.

Applications of DMF induced S-S metathesis chemistry

With a better understanding of the trisulfide S-S metathesis, in terms of substrate scope and solvent effects, we then used this chemistry for several applications. In these applications, DMF was used as the solvent. First, we used this chemistry by manipulating the S-S metathesis equilibrium to prepare unsymmetrical trisulfide, i.e., benzyl methyl trisulfide. Second, we used this S-S metathesis chemistry for the production of dynamic combinatorial library (DCL) from 8 different trisulfides. Lastly, another interesting exploration of this S-S metathesis chemistry is the direct modification of an antitumor natural product containing trisulfide, calicheamicin γ_1.

Synthesis of benzyl methyl trisulfide via S-S metathesis chemistry

The reaction between two unsymmetrical trisulfides, i.e., Me_2S_3 and $^{n}Pr_2S_3$, in DMF leads to the selective formation of unsymmetrical trisulfide, $MeS_3{}^{n}Pr$, which is in equilibrium with the starting materials. We next wanted to demonstrate that this equilibrium composition can be manipulated by using excess of one of the trisulfides, to favour the formation of an unsymmetrical trisulfide product. Accordingly, benzyl methyl trisulfide (BnS_3Me) was obtained as a pale-yellow oil in excellent yield (92%) from the reaction between benzyl trisulfide and excess dimethyl trisulfide (50 eq.) in DMF for around 5 h (Figure 3.26). The excess dimethyl trisulfide can be recovered in 81% yield by distillation (70°C, 0.44 mbar). This result provides evidence that the S-S metathesis reaction is indeed under equilibrium control, and that unsymmetric trisulfides can be isolated in good yields.

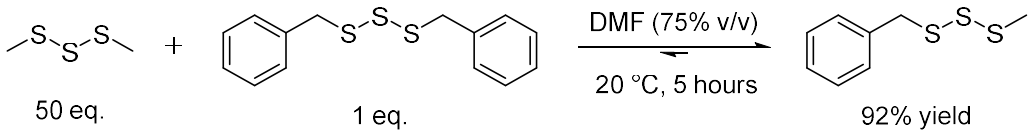

Figure 3.26: The synthesis of benzyl methyl trisulfide via S-S metathesis chemistry in DMF.

The synthesis of an unsymmetrical trisulfide is typically complicated and only few literature reports on the construction of unsymmetrical trisulfides are available. The current strategies for making unsymmetrical trisulfides are via a coupling reaction between a thiol and an electrophilic disulfurating reagent or a sulfenylating compound and a nucleophilic disulfurating reagent.[58-64] Very recently, Liang and co-workers demonstrated the preparation of unsymmetrical trisulfide via iodine catalysed coupling of *S*-substituted sulfenylthiosulphates, alkyl electrophiles and thiourea.[65] Although this method can be used for making unsymmetrical trisulfides with a broad range of functional groups, the complexity of the synthesis is a drawback. The synthesis of unsymmetrical trisulfide via trisulfide

S-S metathesis in DMF demonstrates a simple, quick, and selective protocol for obtaining an unsymmetrical trisulfide. The excess reagent needs to be separated from the product, but distillation is possible for the example in Figure 3.26.

An attempt to see whether BnS_3Me can reversibly form its parent symmetrical trisulfides, i.e., dimethyl trisulfide and dibenzyl trisulfide, in DMF was carried out. In a test, BnS_3Me was dissolved in DMF-d_7 and the reaction was monitored by ^{1}H NMR spectroscopy. Result showed that equilibrium had been achieved within 10 minutes (Figure 3.27A). Both dimethyl trisulfide and dibenzyl trisulfide were identified in solution through comparison with analytically pure samples in DMF-d_7. This reaction also provides convincing evidence that the S-S metathesis is reversible. In relation to this reaction, we also tested the metathesis reaction of benzyl *tert*-butyl trisulfide ($BnS_3{}^tBu$) in DMF. Accordingly, $BnS_3{}^tBu$ was dissolved in DMF-d_7 but no reaction was observed at room temperature or even at 100 °C after 11 hours (Figure 3.27B). This result indicates that even a *single* bulky group is sufficient to prevent S-S metathesis.

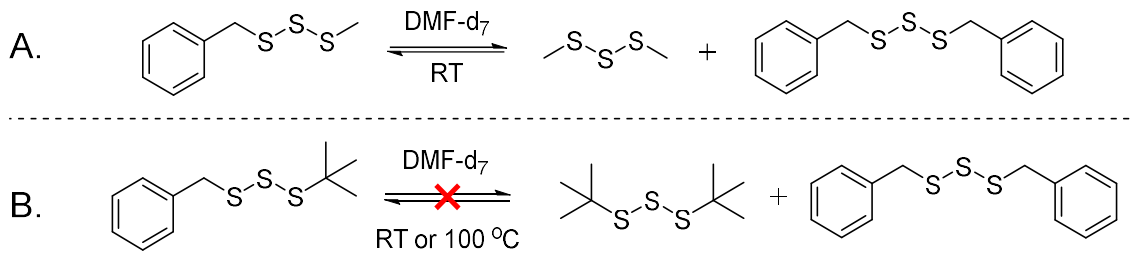

Figure 3.27: S-S metathesis reaction of (A) benzyl methyl trisulfide and (B) benzyl *tert*-butyl trisulfide in DMF-d_7

Further investigations were carried out to see whether dimethyl trisulfide could induce S-S metathesis of $BnS_3{}^tBu$. The equimolar mixture of Me_2S_3 and $BnS_3{}^tBu$ was heated at 100 °C for 1 h. Under this reaction condition, no metathesis products were observed by GC-MS (Figure 3.28A). Next, when the mixture was dissolved in DMF-d_7 and heated to 100 °C, the reaction had reached equilibrium within 30 minutes (Figure 3.28B). ^{1}H NMR analysis showed that this reaction gave a mixture of trisulfide compounds, i.e., Bn_2S_3, $MeS_3{}^tBu$, BnS_3Me. Due to the low abundance of Bn_2S_3, it was difficult to observe this trisulfide by GC-MS. Another interesting finding was that $^tBu_2S_3$ was not observed by GC-MS. This suggested that the S-S metathesis reaction of Me_2S_3 and $BnS_3{}^tBu$ in DMF does not favour the formation of the bulkiest parent trisulfide ($^tBu_2S_3$). Importantly, only trisulfides (and no di- or tetrasulfides) were formed—even at 100 ºC.

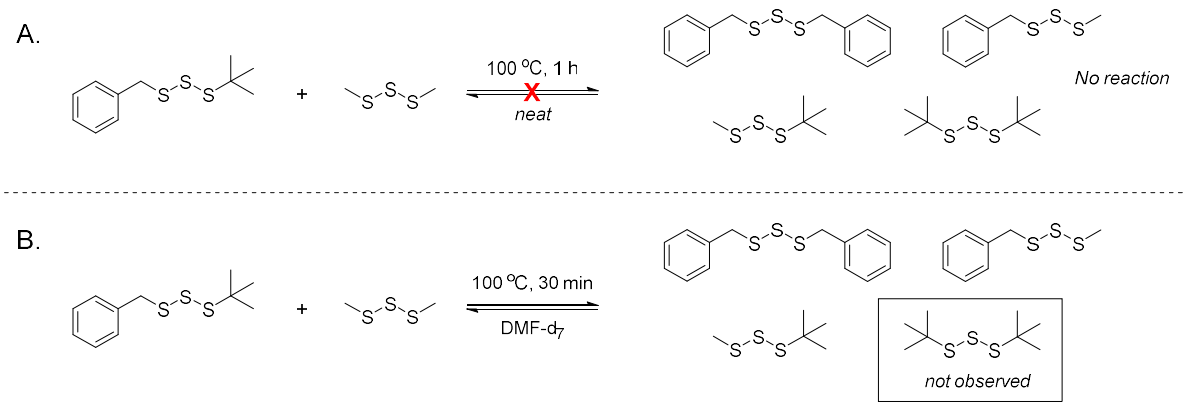

Figure 3.28: Benzyl *tert*-butyl trisulfide ($BnS_3{}^tBu$) and dimethyl trisulfide (Me_2S_3) at 100 °C: (A) No reaction after 1 h (neat). (B) S-S metathesis reaction occurs in the presence of DMF-d_7 and equilibrium established within 30 minutes.

Dynamic Combinatorial Library in trisulfide system

The production of dynamic combinatorial library in trisulfide system was studied using this S-S metathesis chemistry. Eight different trisulfides: Me_2S_3, Et_2S_3, $^nPr_2S_3$, $^iPr_2S_3$, $^iBu_2S_3$, $^tBu_2S_3$, $^nHex_2S_3$, and Bn_2S_3 were reacted simultaneously in DMF. All possible combinations of the trisulfide products were listed in Table 3.2. Within 5 min of reaction, GC-MS revealed that these 8 parent trisulfides had been transformed into 29 trisulfides (Figure 3.29A and 3.29C). In a control experiment, no reaction was observed for the reaction of these parent trisulfides when no solvent was used (Figure 3.29B). All possible combinations of trisulfides formed, but no reaction was observed with the bulky $^tBu_2S_3$. This result was consistent with the previous result on the S-S metathesis attempt between $^tBu_2S_3$ and Me_2S_3, which resulted in no reaction. As anticipated, we also found that di-*iso*-propyl trisulfide reacted slowly in this complex mixture. Furthermore, when the mixture was allowed to react for 24 h some disulfides from benzyl group were present. This indicates that benzyl trisulfide is more reactive than the other trisulfides or can participate in other mechanisms. Wang and co-workers[66] found that dibenzyl trisulfide undergoes self-reaction to form its disulfide after treated with DMF at 40 °C for 24 h. This reaction has not been fully explained. Overall, it should be noted that this alternative reaction pathway involving the dibenzyl trisulfide substrate only occurs with prolonged reaction times.

m/z = 126.0								
m/z = 154.0	m/z= 140.0							
m/z = 182.0	m/z= 154.0	m/z= 168.0						
m/z = 210.1	m/z= 168.0	m/z= 182.0	m/z= 196.0					
m/z = 182.0	m/z= 154.0	m/z= 168.0	m/z= 182.0	m/z= 196.0				
m/z= 210.1	m/z= 168.0	m/z= 182.0	m/z= 196.0	m/z= 210.1	m/z= 196.0			
m/z= 266.1	m/z= 196.0	m/z= 210.1	m/z= 224.1	m/z= 238.1	m/z= 224.1	m/z= 238.1		
m/z= 278.0	m/z= 202.0	m/z= 216.0	m/z= 230.0	m/z= 244.0	m/z= 230.0	m/z= 244.0	m/z= 272.1	

Trisulfides containing tert-butyl group were expected to not form in the mixture.

Table 3.2: All possible combinations of trisulfide products from the eight trisulfides in DMF

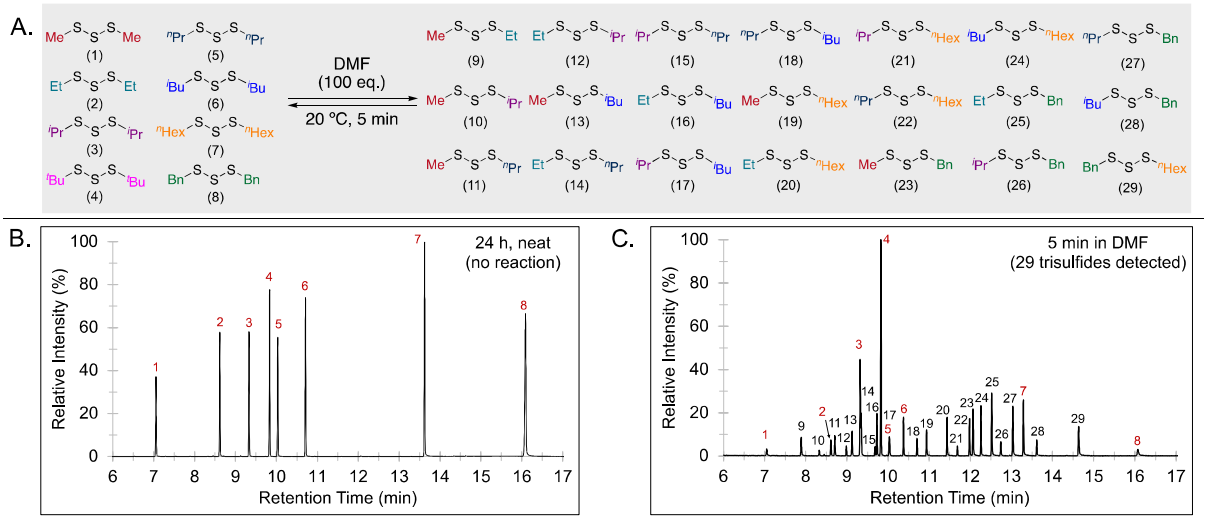

Figure 3.29: A. Dynamic combinatorial library (DCL) production from 8 different trisulfides to 29 trisulfides within a 5-minute reaction at room temperature. B. GC trace for 8 parent trisulfides after 24 h mixing – no reaction. C. GC trace for a mixture of 8 trisulfides in DMF (100 eq.) – a quick formation of trisulfide DCL. Red numbers indicate the parent trisulfides: (1) dimethyl trisulfide, (2) diethyl trisulfide, (3) di-*iso*-propyl trisulfide, (4) di-*tert*-butyl trisulfide, (5) di-*n*-propyl trisulfide, (6) di-*iso*-butyl trisulfide, (7) di-*n*-hexyl trisulfide, (8) dibenzyl trisulfide.

Direct modification of a natural product containing trisulfide: Calicheamicin γ_1

The trisulfide S-S metathesis induced by DMF is rapid and highly selective for trisulfide products. We next explored this chemistry for a late-stage modification of natural product containing trisulfide moiety. Trisulfide compounds such as diallyl trisulfide, epidithiodioxopiperazines, the calicheamicin class of enediyne compounds including calicheamicin γ_1 and shishijimicin have been known to have an antifungal, antibacterial and antitumor properties.[67] Such properties are related to the trisulfide

moiety which serve as a reductant-labile sulfide. Calicheamicin γ_1 for instance, after being attacked by a nucleophile such as a thiol (thiol-trisulfide exchange), undergoes an intermolecular cyclization (Bergman or Myers–Saito cyclization mechanism) to generate a reactive *para*-1,4-diradical, which then abstracts hydrogen atoms from the DNA backbone and results in DNA cleavage.[68] If the methyl group in the trisulfide moiety can be manipulated or installed with other groups, the reactivity might change.[69] Clinically, calicheamicin is attached to an antibody through an S-S linkage, so selective manipulation of the trisulfide is important in medicine. Additionally, we wanted to see if the trisulfide metathesis was compatible with calicheamicin's potentially labilie ene-diyne, α,β-unsaturated ketone, and thioester groups.

In the previous study, we found that unsymmetrical trisulfides such as benzyl methyl trisulfide (BnS_3Me) can be transformed into its parent trisulfides by dissolving it in DMF. Because calicheamicin γ_1 is an unsymmetrical trisulfide, the calicheamicin γ_1 molecules are possible to react by itself to form a dimer, di-calicheamicin γ_1 in the presence of DMF. Indeed, we discovered dimerization of calicheamicin γ_1 occurred in DMF-d_7 at 40 °C (Figure 3.30). LC-MS analysis confirmed the formation of di-calicheamicin γ_1 ($[M+2H]^{2+}$ calcd.: 1305.8016, found 1305.7841). In addition, ^{1}H NMR analysis revealed the formation of a new peak at 2.62 ppm which corresponds to dimethyl trisulfide (Me_2S_3), the by-product of calicheamicin γ_1 dimerization.

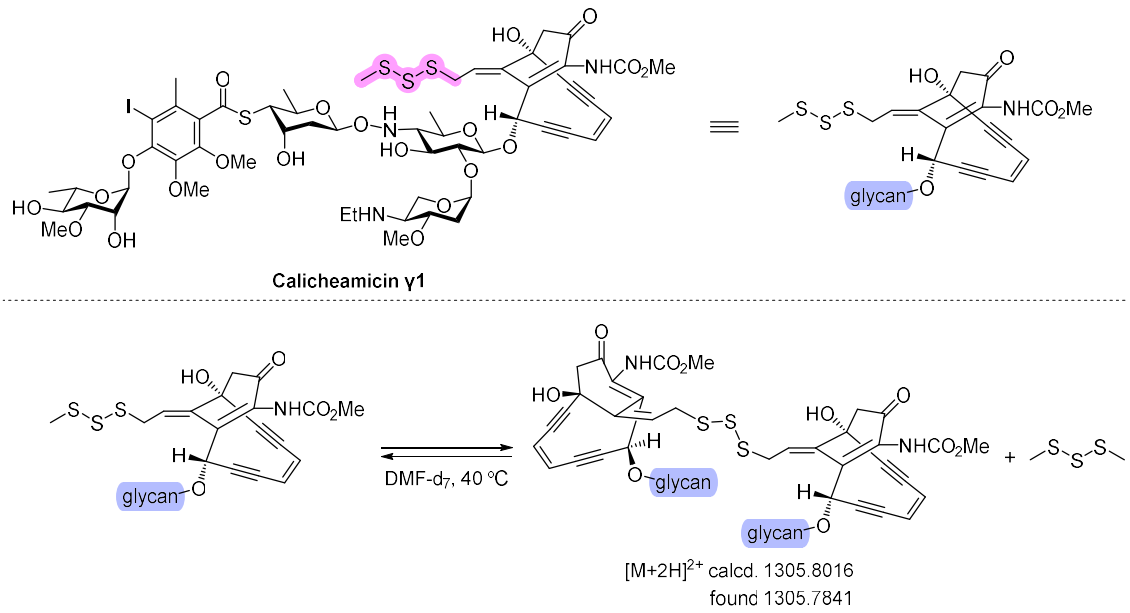

Figure 3.30: Dimerization of calicheamicin γ_1 in DMF-d_7 at 40°C

Next, the modification of calicheamicin γ_1 was demonstrated using excess dibenzyl trisulfide in DMF-d_7 as the solvent (Figure 3.31). The S-S metathesis reaction was monitored by ^{1}H NMR spectroscopy (Figure 3.32). The most noticeable change was the formation of a new peak at 2.56 ppm which corresponds to the methyl protons of benzyl methyl trisulfide (BnS_3Me). After a 10-minute

reaction in DMF-d_7, the intensity of methyl protons of the trisulfide in calicheamicin γ_1 (~2.60 ppm) had decreased significantly. After the solvent, excess dibenzyl trisulfide, and benzyl methyl trisulfide by-product removal, Bn-calicheamicin trisulfide obtained from the reaction was isolated as a white solid. LC-MS analysis confirmed that the compound was Bn-calicheamicin trisulfide ($[M+H]^+$ calcd.: 1444.4395, found: 1444.4395). There was no evidence by ^{1}H NMR spectroscopy or LC-MS that any reaction had occurred at the ene-diyne, thioester, or α,β-unsaturated ketone, which indicates the exquisite selectivity of this reaction.

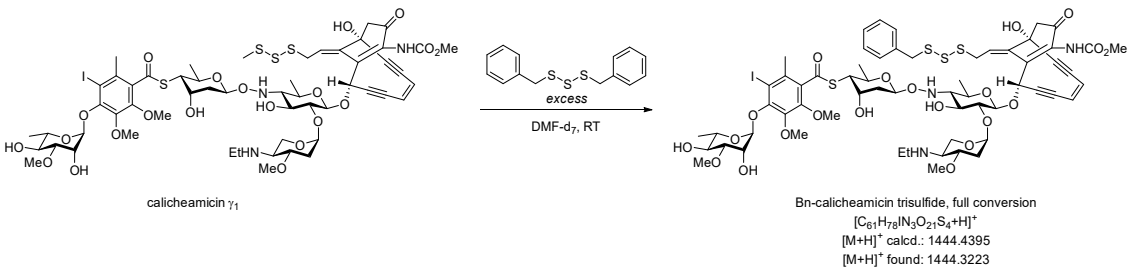

Figure 3.31: Trisulfide modification in calicheamicin γ_1 using dibenzyl trisulfide in DMF-d_7

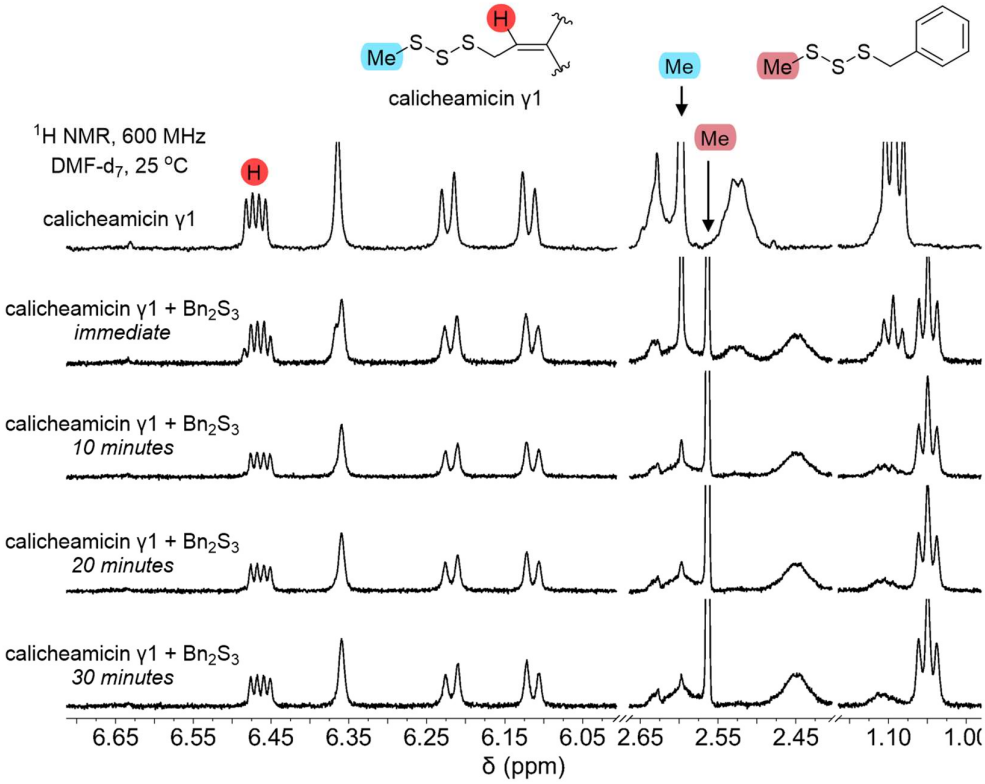

Figure 3.32: Stacked ^{1}H NMR spectra in regions of interest in DMF-d_7, from top to bottom: calicheamicin γ_1, calicheamicin γ_1 and Bn_2S_3 (t = 0), calicheamicin γ_1 and Bn_2S_3 after 10 minutes, calicheamicin γ_1 and Bn_2S_3 after 20 minutes, calicheamicin γ_1 and Bn_2S_3 after 30 minutes.

The modification of the trisulfide in calicheamicin γ_1 was also carried out using di-*n*-propyl trisulfide ($^{n}Pr_2S_3$). With the similar approach to the modification using Bn_2S_3, excess $^{n}Pr_2S_3$ was reacted with calicheamicin γ_1 in DMF-d_7 at 40 °C and the reaction was monitored by ^{1}H NMR spectroscopy. After 30 minutes, the excess reagent and solvent were removed. Analysis by LC-MS showed that *n*-propyl calicheamicin γ_1 trisulfide ([M+H]+ calcd. 1396.3129; found 1396.4498.) was formed. Figure 3.33 shows the transformation of calicheamicin γ_1 to calicheamicin *n*-propyl trisulfide.

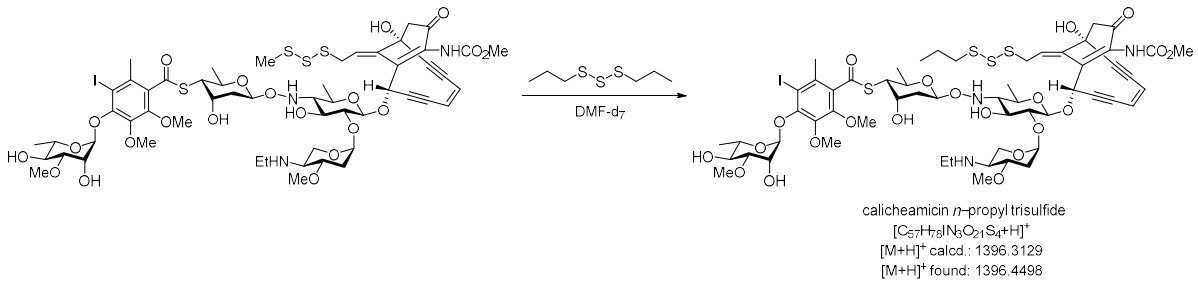

Figure 3.33: Trisulfide modification in calicheamicin γ_1 using di-*n*-propyl trisulfide in DMF-d_7

Lastly, we attempted to react calicheamicin γ_1 with *n*-propanethiol (^{n}PrSH). If a thiol is involved in the reaction, it may induce S-S scrambling, intermolecular cyclization or other reactions.[68] Myers and co-workers found that the reaction between calicheamicin γ_1 with glutathione resulted in the formation of calicheamicin γ_1 glutathione disulfide as the major product. Another relevant study to our experiment was reported by Ellestad and co-workers[70] where they investigated the reactions of trisulfide moiety in calicheamicin γ_1 using methanethiol (MeSH). The reaction of calicheamicin γ_1 with excess MeSH in acetonitrile gave selectively calicheamicin γ_1 methyl disulfide (Figure 3.34A). The mechanism probably proceeds via the formation of a disulfide and perthiolate in the first step which could then lead to a rapid equilibrium.[68, 70] In addition to this, they also reported that there was no reaction in DCM but the reaction occurred in MeOH to give only the dihydrothiophene derivate (Figure 3.35D). Similarly, we observed calicheamicin γ_1 *n*-propyl disulfide as the major product for the reaction of calicheamicin γ_1 with ^{n}PrSH (Figure 3.34B). LC-MS for the reaction in Figure 3.34B showed multiple peaks which indicate the major disulfide product is formed with a number of other products in a complex mixture. Some other potential products are shown in Figure 3.35.

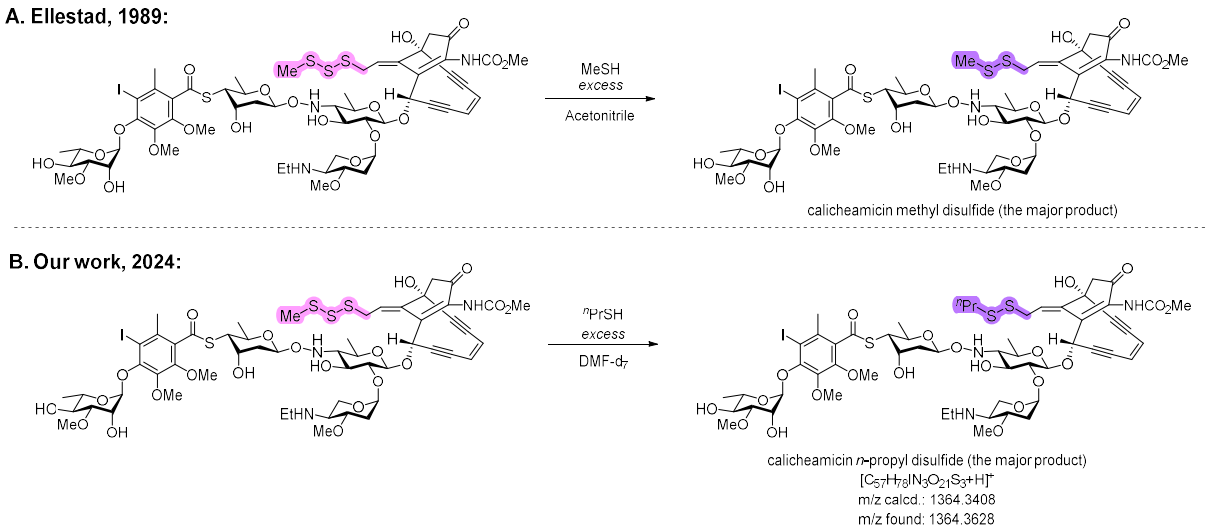

Figure 3.34: A. Calicheamicin modification by methanethiol in acetonitrile reported by Ellestad and co-workers[70]. B. Calicheamicin modification by *n*-propanethiol in DMF-d_7 reported by our lab.

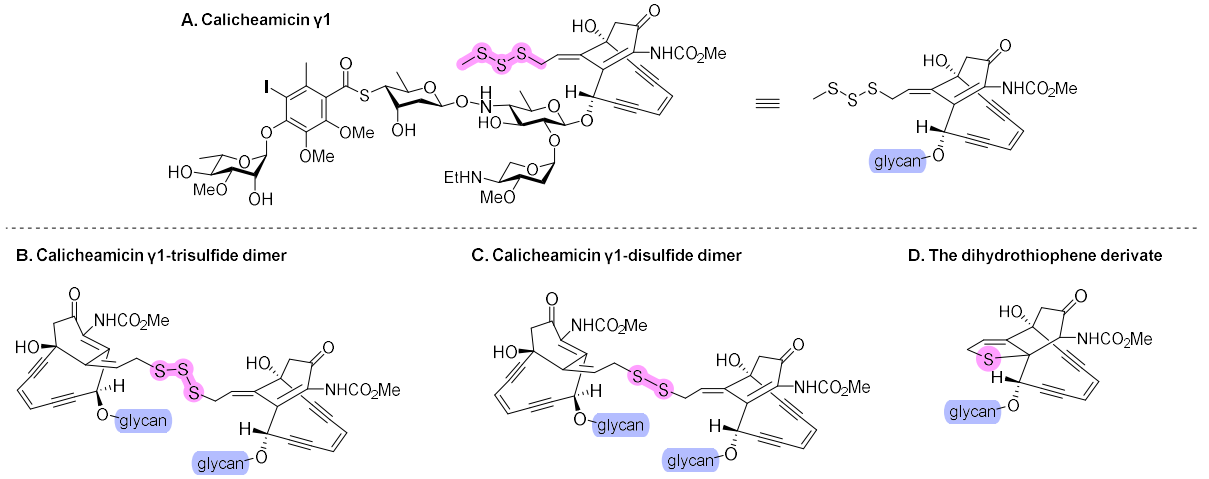

Figure 3.35: Other possible products from the reaction between *n*-propane thiol and calicheamicin γ_1. Other products with low molecular weights such as Me_2S_3, $MeS_3{}^nPr$, $^nPr_2S_2$, and other dialkyl polysulfides are not shown here.

S-S metathesis involving disulfides and tetrasulfides

With a growing understanding of the solvent and substrate effects of the trisulfide metathesis, we also investigated the S-S metathesis for the corresponding organic disulfides and tetrasulfides for comparison. The dynamic covalent chemistry involving disulfide bonds is crucial for many applications in various fields such as polymer chemistry[71, 72] and protein chemistry[73, 74]. In polymer chemistry, for example, the importance of disulfide metathesis can be seen in the application of reprocessable polymers and self-healing polymeric materials. For tetrasulfide metathesis, it has been shown to be useful as an intermediate in catalysis for the efficient synthesis of unsymmetrical disulfide.[75] Thus, if these chemistries are thoroughly understood there will be many opportunities to

use them as a synthetic tool for many chemistry applications. We were also curious if the trisulfide chemistry is unique to trisulfides, or if the same phenomenon occurs with disulfides and tetrasulfides.

Disulfide metathesis

In comparison to dialkyl trisulfides, the disulfide analogues have a stronger S-S bond strength while the tetrasulfide analogues have a weaker central S-S bond.[5] Because of these differences, we wanted to see if either di- or tetrasulfides could undergo metathesis in DMF. Hasell and Chalker[15] had shown that the S-S metathesis reaction occurred between dimethyl trisulfide and di-*n*-propyl trisulfide in the presence of DMF at equimolar ratio (1 eq. each), whereas the disulfide analogues, i.e., dimethyl disulfide and di-*n*-propyl disulfide showed no reaction. Surprisingly, we observed a different result when excess DMF (10 eq.) was used in the reaction between those disulfides. The S-S metathesis product, methyl *n*-propyl disulfide was formed. The reaction was much slower than trisulfide metathesis, but it did occur. Figure 3.36 showed the comparison for these S-S metathesis reaction using different amount of DMF. This result again suggests that an adequate amount of DMF is required to induce S-S metathesis, and that this effect can be extended to disulfide metathesis.

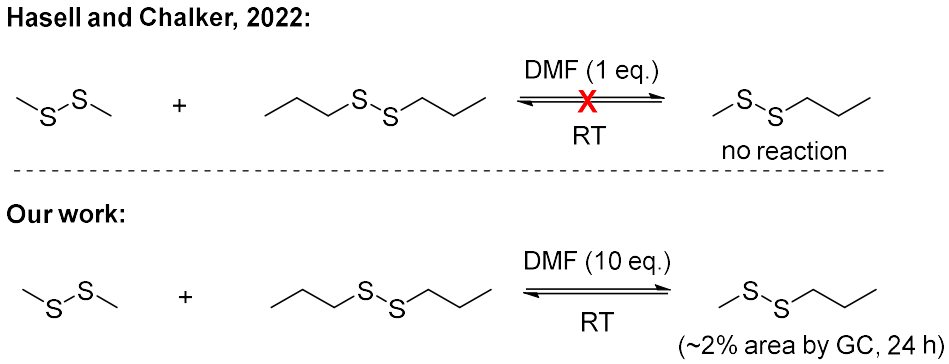

Figure 3.36: S-S metathesis between dimethyl disulfide and di-*n*-propyl disulfide using different amount of DMF

From the above result, we then investigated on the S-S metathesis reaction between dimethyl disulfide and various commercial disulfides. A summary of the disulfide S-S metathesis reactions is shown in Figure 3.37. In general, disulfide metathesis reactions do not occur in excess DMF (10 eq.) at room temperature over the course of 1 hour. However, surprisingly a rapid S-S metathesis was observed for the reaction between dimethyl disulfide and dibenzyl disulfide, giving benzyl methyl disulfide within 5 minutes. This was a very interesting result because it is a reagent-free S-S metathesis process. The disulfide metathesis reactions typically occurs in the presence of a phosphine[76], a thiolate[77], or a base[78]. Another reagent-free method for the disulfide metathesis has been reported by Fritz and co-workers[79] where the ultrasound energy has been shown to induce S-S metathesis between disulfides.

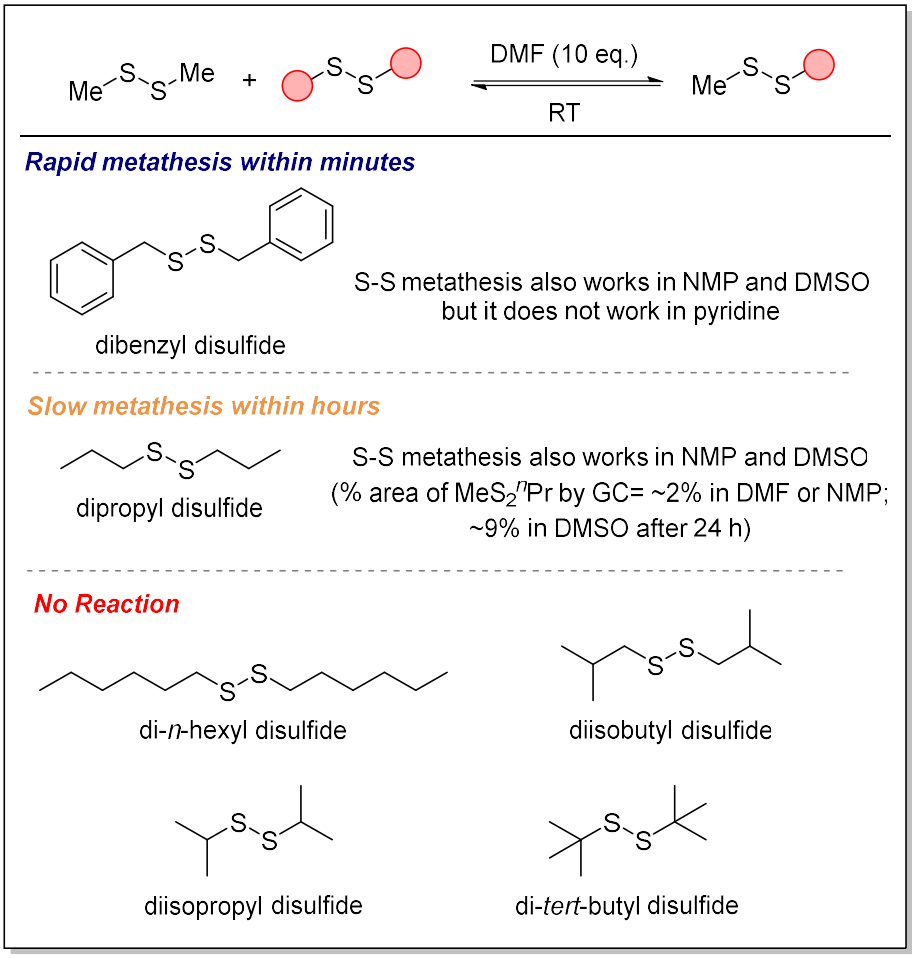

Figure 3.37: Substrate scope for disulfide metathesis

Our initial investigation was to evaluate the reaction between dimethyl disulfide and di-*n*-propyl disulfide. The objective was to see the reaction's outcome when excess DMF is used. As shown in Figure 3.37, the use of 10 eq. of DMF in the reaction between dimethyl and di-*n*-propyl disulfide was crucial to induce the metathesis reaction even though only a very small portion of methyl *n*-propyl disulfide was observed by GC within a few minutes. We found that longer reaction time did not improve the reaction (2% of $MeS_2{}^nPr$ by GC after 24 h). There was no difference when NMP was used as the solvent for the reaction (3% of $MeS_2{}^nPr$ by GC after 24 h). There was a slight improvement when DMSO was employed in the disulfide metathesis reaction. This solvent could induce S-S metathesis with around 9% product observed by GC after 24 h.

Next, the rapid S-S metathesis between dimethyl disulfide and dibenzyl disulfide was not anticipated. It was thought that the reaction would be the same as the other disulfide. Yet, DMF efficiently induces the rapid and clean disulfide S-S metathesis reaction within minutes. A similar observation was also found when NMP and DMSO were used in the reaction. In contrast, the disulfides did not undergo S-S metathesis in the presence of pyridine. A similar result was also reported by Tonkin and co-workers[6] where no reaction was observed between dimethyl disulfide and di-*n*-propyl disulfide in pyridine. They also reported that the computational calculations for the

trisulfide metathesis is kinetically more favourable (around 7 orders of magnitude faster) than the disulfide exchange. Furthermore, the disulfide S-S metathesis was also rapid for the reaction between di-*n*-propyl disulfide and dibenzyl disulfide. We observed no reaction between di-*tert*-butyl disulfide and dibenzyl disulfide. The steric factor indeed plays a crucial role in both disulfide and trisulfide S-S metathesis.

Lastly, despite of using 10 eq. of DMF we observed no reaction between dimethyl disulfide and several disulfides, i.e., di-*n*-hexyl disulfide, diisobutyl disulfide, diisopropyl disulfide, and di-*tert*-butyl disulfide. This observation indicates that, in general, disulfides do not undergo spontaneous S-S exchange in DMF. However, a notable exception is dibenzyl disulfide, which does undergo very rapid S-S metathesis with dimethyl disulfide in DMF.

Tetrasulfide metathesis

In Chapter 2, three tetrasulfides, i.e., di-*n*-propyl, dibenzyl, and bis(4-methoxybenzyl) tetrasulfide, were synthesized and used for the S-S metathesis study. Since di-*n*-propyl tetrasulfide is the only compound that can be detected by GC-MS, all S-S metathesis reactions were carried out in DMF-d_7 and monitored by ^{1}H NMR spectroscopy. In this experiment, the main goal was to see if the S-S metathesis reaction between the organic tetrasulfides occurs and if DMF promotes that reaction. Due to the weaker S-S bond in tetrasulfide, our hypothesis was that the tetrasulfide S-S metathesis reaction would occur. Two reactions were prepared in NMR tubes: (1) dibenzyl tetrasulfide and di-*n*-propyl tetrasulfide, (2) bis(4-methoxybenzyl) tetrasulfide and di-*n*-propyl tetrasulfide. DMF-d_7 was then added to each NMR tube and the reaction was monitored immediately. Remarkably, tetrasulfide S-S metathesis reactions did not occur at all for both mixtures (Figure 3.38).

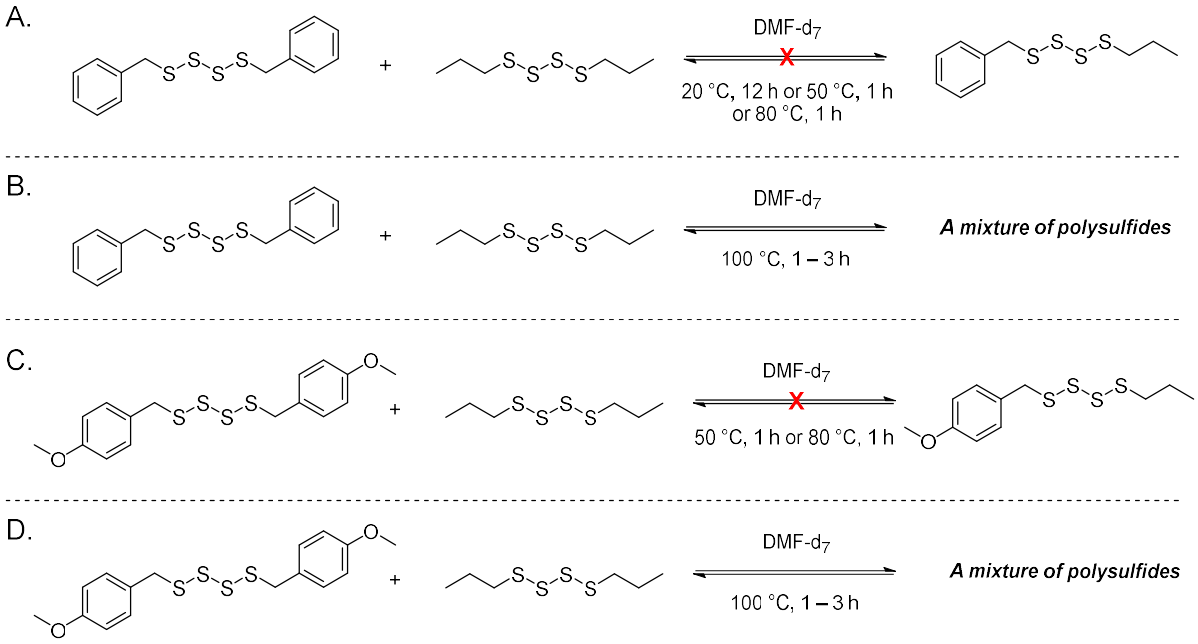

Figure 3.38: Tetrasulfide S-S metathesis of (A) Dibenzyl tetrasulfide and di-*n*-propyl tetrasulfide in DMF-d_7 at 20 °C for 12 h, 50 °C for 1 h, and 80 °C for 1 h gave no reaction. (B) Dibenzyl tetrasulfide and di-*n*-propyl tetrasulfide in DMF-d_7 at 100 °C for 1 to 3 h gave a mixture of polysulfides. (C) Bis(4-methoxybenzyl) tetrasulfide and di-*n*-propyl tetrasulfide in DMF-d_7 at 50 °C for 1 h and 80 °C for 1 h gave no reaction. (D) Bis(4-methoxybenzyl) tetrasulfide and di-*n*-propyl tetrasulfide in DMF-d_7 100 °C for 1 to 3 h gave a mixture of polysulfides.

Figure 3.39 showed ^{1}H NMR analyses for tetrasulfide metathesis reactions in DMF-d_7. It was evident that the reaction started to occur at relatively high temperature, i.e., 100 °C and not at room temperature. This is most likely caused by a thermal cleavage of the central S-S bond of the tetrasulfide due to a weak S-S bond. The same temperature was also reported by Pratt and co-workers[5] in which the tetrasulfide exchange between diisopropyl tetrasulfide and di-*tert*-butyl tetrasulfide had occurred in chlorobenzene at 100 °C (Figure 3.3). Due to the complexity to identify the mixture of polysulfides, we did not further analyse or make any attempt to isolate the products. Moreover, in control experiments, both tetrasulfide reactions were monitored in toluene-d_8, a solvent that does not induce S-S metathesis for trisulfides. The experiments aimed to see whether the reactions that occurred at 100 °C are due to the effect of heat or the effect of DMF. The same procedures were applied to monitor the reactions by ^{1}H NMR spectroscopy. The results were similar to that of reactions in DMF-d_7 at 100 °C where new peaks started to appear when heated to that temperature for 1 h (see page S135).

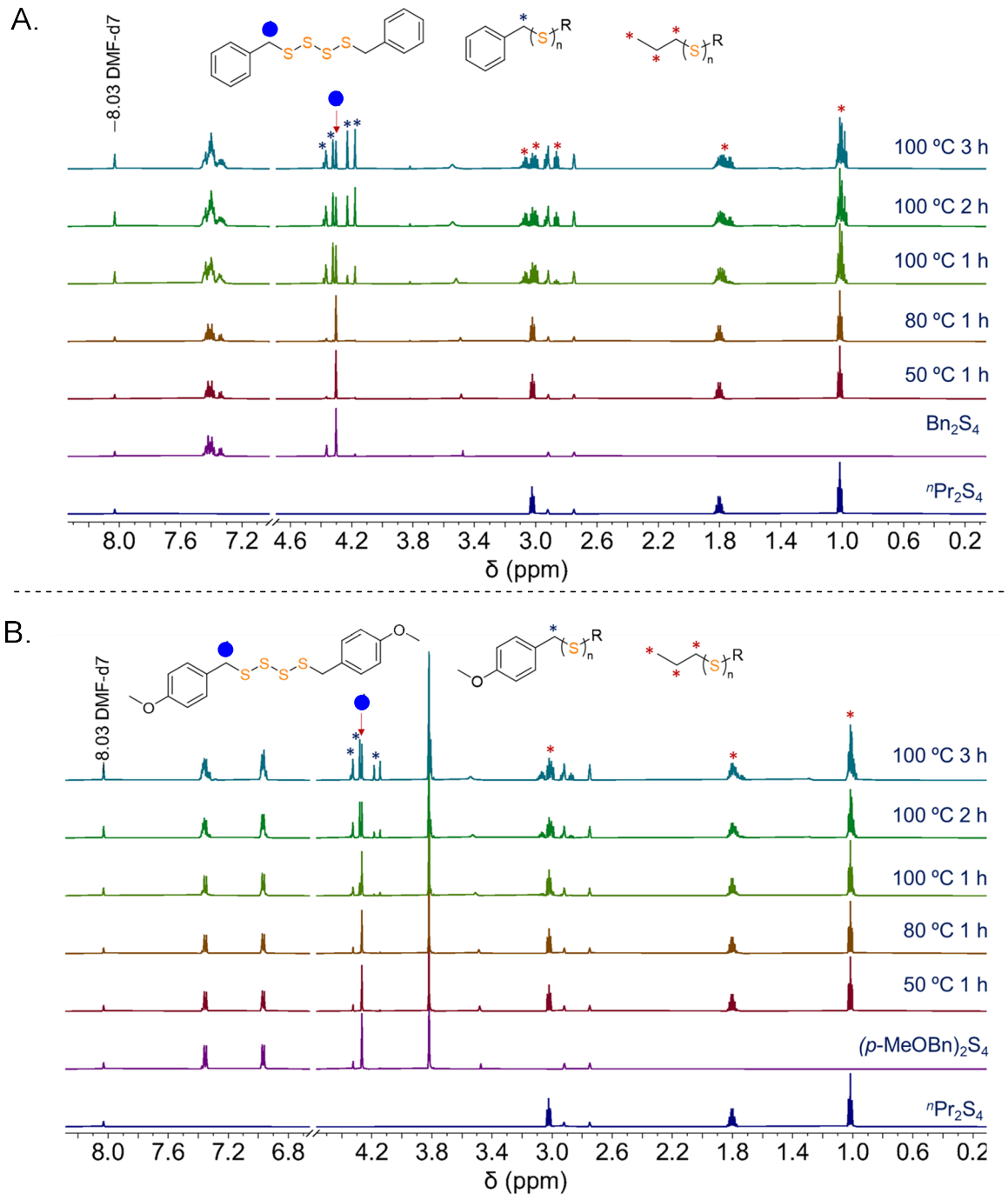

Figure 3.39: A. Stacked ^{1}H NMR spectra of dibenzyl tetrasulfide and di-*n*-propyl tetrasulfide mixture in DMF-d_7 at elevated temperature. B. Stacked ^{1}H NMR spectra of bis(4-methoxybenzyl) tetrasulfide and di-*n*-propyl tetrasulfide mixture in DMF-d_7 at elevated temperature. The blue asterisks (*) indicate the benzylic protons of products formed at 100 ºC. The red asterisks (*) indicate the methylene and methyl protons of products formed at 100 ºC.

The trisulfide S-S metathesis in DMF, or amide solvents in general, highlighted a unique, selective, rapid and reversible chemical reaction. From the disulfide and tetrasulfide metathesis experiments, we found that DMF cannot induce S-S metathesis reaction for most disulfides, except for the exception of dibenzyl disulfide, and DMF did not promote S-S metathesis for the tetrasulfides tested. The tetrasulfide experiments were especially surprising because they contain the weakest S-S bond of all substrates tested. These results suggest that trisulfide metathesis is unique and occurs through a mechanism that can only happen with this type of substrate.

3.4 Conclusion and Outlook

The trisulfide S-S metathesis reaction can be rapidly induced by solvents that contain amides, ureas, phosphoramides, or sulfoxides. While phosphoramides and DMSO are more nucleophilic, amides and ureas are exceptional because they are not considered strong nucleophiles. Other solvents such as propylene carbonate and caprolactone can induce S-S metathesis in the trisulfide system. However, the rate was relatively slow compared to those amides, ureas, phosphoramides and DMSO. Despite having a high polarity or dielectric constant, solvents such as formamide, HFIP, alcohols, nitro compounds, acetone and propylene carbonates slowly induced S-S metathesis. In addition to this, dihydrolevoglucosenone (or Cyrene)[80], a highly polar aprotic bio-based solvent, did not induce the trisulfide S-S metathesis. For common non-polar solvents that have lower dielectric constant (typically < 10) most of them did not promote rapid S-S metathesis or the equilibrium was not established during the tested times. Lastly, although amines are a good nucleophile, their ability to induce S-S metathesis is relatively poor compared to those amides. Therefore, no correlations can be established between the high polar compounds and the trisulfide S-S metathesis. These results may point to a novel mechanism for trisulfide metathesis.

Water present in the solvent was found to significantly reduce the rate of S-S metathesis in amides and ureas. However, around 5% water (w/w) can be tolerated when excess of amide solvent (i.e., 10 equiv. of DMF relative to the trisulfide substrates) was used. Furthermore, the presence of acid in the DMF solvent has been shown previously to decrease the rate of S-S metathesis, which is consistent with the absence of metathesis in acetic acid. These results are important in understanding the mechanism of the reaction, as any mechanism must account for the reduction in rate due to the addition of water or acids.

To demonstrate that the reactivity of DMF is not specific only to dimethyl trisulfide and di-*n*-propyl trisulfide, several trisulfide compounds were synthesized and tested for their reaction with dimethyl trisulfide (Figure 3.21). The S-S metathesis reaction was done rapidly for trisulfides with primary alkyl, allyl or benzyl groups. For secondary alkyl such as di-*iso*-propyl trisulfide, the rate of reaction was slower compared to the primary one. The S-S metathesis reaction does not work for tertiary butyl, adamantyl, or if the trisulfide contains hydroxyl group. When the hydroxy group of the trisulfide is protected, the S-S metathesis occurs normally. Thus, it is clear that the steric hindrance and hydroxyl group are key factors which influence trisulfide S-S metathesis in DMF.

For a successful S-S metathesis, amide and urea solvents must be dried and used in excess (e.g., 10 equiv.). Light was not required to accelerate the reaction. We also found that the reaction tolerates oxygen and can be run in open air. All of these observations are important in developing a hypothesis of the reaction mechanism.

In terms of applications, the chemistry of this trisulfide S-S metathesis in DMF was useful for the production of a dynamic combinatorial library (DCL) and selective synthesis of an unsymmetrical trisulfide. These two examples are important in the field of chemical biology[81] and synthetic organic chemistry.[65, 82] In chemical biology, trisulfide S-S metathesis could be of potential use in protein-directed dynamic combinatorial chemistry as a tool to recognize protein ligands which is crucial in enzyme inhibition and drug discovery. Although trisulfide examples shown in this Chapter are not peptide-based trisulfides, the concept of DCL can be adapted later for the relevant applications. Another important consideration is that the solvents used in the process involving the component of DCL must be biocompatible. While the use of DMF or DMSO is restricted to be used for cell lines in *in vitro* studies[83], other biocompatible solvents can be studied further to evaluate their reactivity on the trisulfide S-S metathesis. In synthetic organic chemistry, this chemistry allows for the rapid and selective synthesis of an unsymmetrical trisulfide directly from its trisulfides.

Several surprising results were found for the S-S metathesis involving disulfides and tetrasulfides. While DMF has been found to induce most of the trisulfides used in this study, this amide solvent did not successfully induce the S-S metathesis reactions for most tested disulfides as anticipated; however, an exception was found for dibenzyl disulfide. This disulfide was found to react with dimethyl and di-*n*-propyl disulfide to give the metathesis products. Because only dibenzyl disulfide is reactive, in the future study this compound could possibly be employed as a catalyst for the disulfide metathesis. Next, the tetrasulfides, which we thought would be more reactive than disulfides or trisulfides due to their weaker S-S bonds, were surprisingly found to be inert in DMF-d_7, giving no S-S metathesis reaction at room temperature. This was unexpected and prompted further investigation about the unique reactivity of trisulfides in these solvents.

Lastly, several results from the experiments in this chapter provided some clues to the mechanism of S-S metathesis reaction in DMF. First, the presence of water or acid (H^+) can significantly reduce the rate of S-S metathesis reaction. Second, steric hindrance is another factor which contributes to the reactivity of S-S metathesis. With this information, the mechanism of this chemistry was investigated and presented in Chapter 4.

3.5 References

(1) Birch S. F.; Cullum T. V.; Dean R. A. The Preparation and Properties of Dialkyl Di- and Poly-sulphides. Some Disproportionation Reactions *J. Inst. Petrol.* **1953**, *39*, 206.

(2) Milligan, B.; Rivett, D.; Savige, W. The photolysis of dialkyl sulphides, disulphides, and trisulphides. *Aust. J. Chem.* **1963**, *16* (6), 1020-1029. DOI: 10.1071/CH9631020.

(3) Trivette Jr, C.; Coran, A. Polysulfide Exchange Reactions. I. Kinetics and Mechanism of the Thermal Exchange between Diethyl Trisulfide and Di-n-propyl Trisulfide. *J. Org. Chem.* **1966**, *31* (1), 100-104. DOI: 10.1021/jo01339a020.

(4) Pickering, T. L.; Saunders, K. J.; Tobolsky, A. V. Disproportionation of organic polysulfides. *J. Am. Chem. Soc.* **1967**, *89* (10), 2364-2367. DOI: 10.1021/ja00986a021.

(5) Chauvin, J.-P. R.; Griesser, M.; Pratt, D. A. The antioxidant activity of polysulfides: it's radical! *Chem. Sci.* **2019**, *10* (19), 4999-5010. DOI: 10.1039/C9SC00276F.

(6) Tonkin, S. J.; Gibson, C. T.; Campbell, J. A.; Lewis, D. A.; Karton, A.; Hasell, T.; Chalker, J. M. Chemically induced repair, adhesion, and recycling of polymers made by inverse vulcanization. *Chem. Sci.* **2020**, *11* (21), 5537-5546. DOI: 10.1039/D0SC00855A.

(7) Harpp, D. N.; Smith, R. A. Organic sulfur chemistry. 42. Sulfur-sulfur bond cleavage processes. Selective desulfurization of trisulfides. *J. Am. Chem. Soc.* **1982**, *104* (22), 6045-6053. DOI: 10.1021/ja00386a034.

(8) Harpp, D. N.; Ash, D. K.; Smith, R. A. Organic sulfur chemistry. 38. Desulfurization of organic trisulfides by tris(dialkylamino)phosphines. Mechanistic aspects. *J. Org. Chem.* **1980**, *45* (25), 5155-5160. DOI: 10.1021/jo01313a026.

(9) Harpp, D. N.; Adams, J.; Gleason, J. G.; Mullins, D.; Steliou, K. A useful polymeric desulfurization reagent. *Tetrahedron Lett.* **1978**, *19* (42), 3989-3992. DOI: 10.1016/S0040-4039(01)95119-6.

(10) Harpp, D. N.; Ash, D. K. Desulphurisation of aliphatic trisulphides, a mechanistic dichotomy. *J. Chem. Soc. D* **1970**, (13), 811-812. DOI: 10.1039/C29700000811.

(11) Safe, S.; Taylor, A. Sporidesmins. Part XI. The reaction of triphenylphosphine with epipolythiodioxopiperazines. *J. Chem. Soc. C* **1971**, (0), 1189-1192. DOI: 10.1039/J39710001189.

(12) Rahman, R.; Safe, S.; Taylor, A. Sporidesmins. Part IX. Isolation and structure of sporidesmin E. *J. Chem. Soc. C* **1969**, (12), 1665-1668. DOI: 10.1039/J39690001665.

(13) Safe, S.; Taylor, A. Stereochemistry of the reaction of epipolythiadioxopiperazines with triphenylphosphine. *J. Chem. Soc. D* **1969**, (24), 1466b-1467. DOI: 10.1039/C2969001466B.

(14) Brewer, D.; Rahman, R.; Safe, S.; Taylor, A. A new toxic metabolite of Pithomyces chartarum related to the sporidesmins. *Chem. Commun. (London)* **1968**, (24), 1571-1571. DOI: 10.1039/C19680001571.

(15) Yan, P.; Zhao, W.; Tonkin, S. J.; Chalker, J. M.; Schiller, T. L.; Hasell, T. Stretchable and Durable Inverse Vulcanized Polymers with Chemical and Thermal Recycling. *Chem. Matter.* **2022**, *34* (3), 1167-1178. DOI: 10.1021/acs.chemmater.1c03662.

(16) Shapter, R. Investigating reactions of trisulfide system. Undergraduate thesis, Flinders University, Bedford Park, South Australia, 2021.

(17) Armarego, W. L. F.; Chai, C. L. L. *Purification of laboratory chemicals*, 6th ed.; Elsevier/Butterworth-Heinemann, 2009.

(18) Guryanova, E.; Vasilyeva, V.; Kuzina, L. Sulfur Exchange in Polysulfides and in Various Vulcanization Accelerators. In *Conference of the Academy of Sciences of the USSR on the Peaceful Uses of Atomic Energy, July 1-5, 1955*, United States Atomic Energy Commission: Vol. 1.

(19) Steudel, R. The Chemistry of Organic Polysulfanes R− S n− R (n> 2). *Chem. Rev.* **2002**, *102* (11), 3905-3946.

(20) Otsuka, H.; Nagano, S.; Kobashi, Y.; Maeda, T.; Takahara, A. A dynamic covalent polymer driven by disulfide metathesis under photoirradiation. *Chem. Comm.* **2010**, *46* (7), 1150-1152. DOI: 10.1039/b916128g.

(21) Zysman-Colman, E.; Harpp, D. N. Optimization of the Synthesis of Symmetric Aromatic Tri- and Tetrasulfides. *J. Org. Chem.* **2003**, *68* (6), 2487-2489. DOI: 10.1021/jo0265481.

(22) Reichardt, C. Classification of Solvents. In *Solvents and Solvent Effects in Organic Chemistry*, Reichardt, C. Ed.; Wiley, 2002; pp 57-91.

(23) Pawar, V. P.; Mehrotra, S. C. Dielectric relaxation study of chlorobenzene-dimethylformamide mixtures using time domain reflectometry. *J. Mol. Liq.* **2002**, *95* (1), 63-74. DOI: 10.1016/S0167-7322(01)00282-3.

(24) Hernández-Luis, F.; Galleguillos-Castro, H.; Esteso, M. A. Activity coefficients of NaF in aqueous mixtures with ε-increasing co-solvent: formamide–water mixtures at 298.15K. *Fluid Ph. Equilib.* **2005**, *227* (2), 245-253. DOI: 10.1016/j.fluid.2004.09.038.

(25) Cavell, E. A. S. Dielectric relaxation in non-aqueous solutions. Part 5.—Propylene carbonate (4-methyl-1,3-dioxolan-2-one). *J. Chem. Soc., Faraday Trans. 2* **1974**, *70* (0), 78-84. DOI: 10.1039/F29747000078.

(26) Ritzoulis, G. Excess properties of the binary liquid systems dimethylsulfoxide + isopropanol and propylene carbonate + isopropanol. *Can. J. Chem.* **1989**, *67* (6), 1105-1108. DOI: 10.1139/v89-166.

(27) Ozari, Y.; Jagur-Grodzinski, J. Donor strength of N-substituted phosphoramides. *J. Chem. Soc., Chem. Commun.* **1974**, (8), 295-296. DOI: 10.1039/C39740000295.

(28) Lomba, L.; Giner, B.; Bandrés, I.; Lafuente, C.; Pino, M. a. R. Physicochemical properties of green solvents derived from biomass. *Green Chem.* **2011**, *13* (8), 2062-2070. DOI: 10.1039/C0GC00853B.

(29) Fornefeld-Schwarz, U. M.; Svejda, P. Refractive Indices and Relative Permittivities of Liquid Mixtures of γ-Butyrolactone, γ-Valerolactone, δ-Valerolactone, or ε-Caprolactone + Benzene, + Toluene, or + Ethylbenzene at 293.15 K and 313.15 K and Atmospheric Pressure. *J. Chem. Eng. Data* **1999**, *44* (3), 597-604. DOI: 10.1021/je980288w.

(30) Cseri, L.; Szekely, G. Towards cleaner PolarClean: efficient synthesis and extended applications of the polar aprotic solvent methyl 5-(dimethylamino)-2-methyl-5-oxopentanoate. *Green Chem.* **2019**, *21* (15), 4178-4188. DOI: 10.1039/C9GC01958H.

(31) Uosaki, Y.; Kawamura, K.; Moriyoshi, T. Static Relative Permittivities of Water + 1-Methyl-2-pyrrolidinone and Water + 1,3-Dimethyl-2-imidazolidinone Mixtures under Pressures up to 300 MPa at 298.15 K. *J. Chem. Eng. Data* **1996**, *41* (6), 1525-1528. DOI: 10.1021/je960236b.

(32) Rosenfarb, J.; Huffman, H. L., Jr.; Caruso, J. A. Dielectric constants, viscosities, and related physical properties of several substituted liquid ureas at various temperatures. *J. Chem. Eng. Data* **1976**, *21* (2), 150-153. DOI: 10.1021/je60069a034.

(33) D'Aprano, A.; Sesta, B.; Princi, A. Ion-ion and ion-solvent interactions of lithium picrate and lithium perchlorate in pure nitromethane and in 15-crown-5 + nitromethane mixtures at 25°C. *J. Electroanal. Chem.* **1993**, *361* (1), 135-141. DOI: 10.1016/0022-0728(93)87047-Y.

(34) Kuila, D. K.; Lahiri, S. C. Comparison of the Macroscopic Molecular Properties in Understanding the Structural Aspects of Mixed Aquo–Organic Binary Mixtures. *Z. Phys. Chem.* **2004**, *218* (7), 803-828. DOI: 10.1524/zpch.218.7.803.35726.

(35) Jannelli, L.; Lopez, A.; Saiello, S. Excess volumes and dielectric constants of benzonitrile + nitrobenzene and acetonitrile + nitrobenzene systems. *J. Chem. Eng. Data* **1983**, *28* (2), 169-173. DOI: 10.1021/je00032a011.

(36) Campbell, A. N.; Kartzmark, E. M. Thermodynamic and other properties of methanol + acetone, carbon disulphide + acetone, carbon disulphide + methanol, and carbon disulphide + methanol + acetone. *J. Chem. Thermodynamics* **1973**, *5* (2), 163-172. DOI: 10.1016/S0021-9614(73)80076-X.

(37) Kumbharkhane, A. C.; Helambe, S. N.; Doraiswamy, S.; Mehrotra, S. C. Dielectric relaxation study of hexamethylphosphoramide-water mixtures using time domain reflectometry. *J. Chem. Phys.* **1993**, *99* (4), 2405-2409. DOI: 10.1063/1.465255.

(38) Krasnoperova, A. P.; Asheko, A. A. Dielectric constant and characteristic features of the structure of methanol and ethanol. *J. Struct. Chem.* **1978**, *18* (5), 760-762. DOI: 10.1007/BF00746119.

(39) Okpala, C.; Guiseppi-Elie, A.; Maharajh, D. M. Several properties of 1,1,3,3-tetramethylurea-water systems. *J. Chem. Eng. Data* **1980**, *25* (4), 384-386. DOI: 10.1021/je60087a007.

(40) Celiano, A. V.; Gentile, P. S.; Cefola, M. Dielectric Constants of Binary Systems. *J. Chem. Eng. Data* **1962**, *7* (3), 391-391. DOI: 10.1021/je60014a023.

(41) Evans, D. F.; McElroy, M. I. The conductance of electrolytes in acetone-2-propanol and acetone-1,1,1,3,3,3-hexafluoro-2-propanol mixtures at 25°C1. *J. Solution Chem.* **1975**, *4* (5), 413-430. DOI: 10.1007/BF00645574.

(42) Kaatze, U.; Schumacher, A.; Pottel, R. The Dielectric Properties of tert.-Butanol/Water Mixtures as a Function of Composition. *Ber. Bunsenges. Physik. Chem.* **1991**, *95* (5), 585-592. DOI: 10.1002/bbpc.19910950508.

(43) Ahire, S.; Chaudhari, A.; Lokhande, M.; Mehrotra, S. C. Complex Permittivity Spectra of Binary Pyridine–Amide Mixtures Using Time–Domain Reflectometry. *J. Solution Chem.* **1998**, *27* (11), 993-1008. DOI: 10.1023/A:1022648204099.

(44) Kolling, O. W. Dielectric characterization of binary solvents containing acetonitrile. *Anal. Chem.* **1987**, *59* (4), 674-677. DOI: 10.1021/ac00131a029.

(45) Kaatze, U.; Menzel, K.; Pottel, R. Broad-band dielectric spectroscopy on carboxylic acid/water mixtures. Dependence upon composition. *J. Phys. Chem.* **1991**, *95* (1), 324-331. DOI: 10.1021/j100154a059.

(46) Thenappan, T.; Devaraj, A. P. Dielectric studies on binary polar mixtures of propanoic acid with esters. *J. Mol. Liq.* **2006**, *123* (2), 72-79. DOI: 10.1016/j.molliq.2005.04.010.

(47) Kinart, C. M.; Kinart, W. J.; Chęcińska-Majak, D. Relative Permittivity, Viscosity, and Speed of Sound for 2-Methoxyethanol + Butylamine Mixtures. *J. Chem. Eng. Data* **2003**, *48* (4), 1037-1039. DOI: 10.1021/je030127e.

(48) Kinart, C. M.; Kinart, W. J.; Checinska-Majak, D.; Bald, A. Densities and relative permittivities for mixtures of 2-methoxyethanol with DEA and TEA, at various temperatures. *J. Therm. Anal. Calorim.* **2004**, *75* (1), 347-354. DOI: 10.1023/B:JTAN.0000017355.26845.a4.

(49) Gee, N.; Freeman, G. R. Relative permittivities of 10 organic liquids as functions of temperature. *J. Chem. Thermodynamics* **1993**, *25* (4), 549-554. DOI: 10.1006/jcht.1993.1163.

(50) Ritzoulis, G.; Papadopoulos, N.; Jannakoudakis, D. Densities, viscosities, and dielectric constants of acetonitrile + toluene at 15, 25, and 35 .degree.C. *J. Chem. Eng. Data* **1986**, *31* (2), 146-148. DOI: 10.1021/je00044a004.

(51) Ghanadzadeh Gilani, A.; Ghanadzadeh Gilani, H.; Ansari, M. Dielectric analysis of binary systems of primary diols with 1-hexanol and 1,4-dioxane at various temperatures. *J. Mol. Liq.* **2014**, *196*, 270-279. DOI: 10.1016/j.molliq.2014.03.041.

(52) Iglesias, T. P.; Forniés-Marquina, J. M.; De Cominges, B. Excess permittivity behaviour of some mixtures n-alcohol + alkane: an interpretation of the underlying molecular mechanism. *Mol. Phys.* **2005**, *103* (19), 2639-2646. DOI: 10.1080/00222930500190384.

(53) Reichardt, C. Empirical Parameters of Solvent Polarity as Linear Free-Energy Relationships. *Angew. Chem., Int. Ed. Engl.* **1979**, *18* (2), 98-110. DOI: 10.1002/anie.197900981.

(54) Alder, C. M.; Hayler, J. D.; Henderson, R. K.; Redman, A. M.; Shukla, L.; Shuster, L. E.; Sneddon, H. F. Updating and further expanding GSK's solvent sustainability guide. *Green Chem.* **2016**, *18* (13), 3879-3890. DOI: 10.1039/C6GC00611F.

(55) Chubachi, S.; Chatterjee, P. K.; Tobolsky, A. V. Reaction of dimethyl tetrasulfide with unsaturated compounds. *J. Org. Chem.* **1967**, *32* (5), 1511-1517. DOI: 10.1021/jo01280a046.

(56) Pople, J. M.; Nicholls, T. P.; Pham, L. N.; Bloch, W. M.; Lisboa, L. S.; Perkins, M. V.; Gibson, C. T.; Coote, M. L.; Jia, Z.; Chalker, J. M. Electrochemical synthesis of poly (trisulfides). *J. Am. Chem. Soc.* **2023**, *145* (21), 11798-11810. DOI: 10.1021/jacs.3c03239

(57) Bartlett, P. D.; Ghosh, T. Sulfuration of the norbornene double bond. *J. Org. Chem.* **1987**, *52* (22), 4937-4943. DOI: 10.1021/jo00231a020

(58) Park, C.-M.; Johnson, B. A.; Duan, J.; Park, J.-J.; Day, J. J.; Gang, D.; Qian, W.-J.; Xian, M. 9-Fluorenylmethyl (Fm) disulfides: biomimetic precursors for persulfides. *Org. Lett.* **2016**, *18* (5), 904-907. DOI: 10.1021/acs.orglett.5b03557

(59) Xu, S.; Wang, Y.; Radford, M. N.; Ferrell, A. J.; Xian, M. Synthesis of unsymmetric trisulfides from 9-fluorenylmethyl disulfides. *Org. Lett.* **2018**, *20* (2), 465-468. DOI: 10.1021/acs.orglett.7b03846

(60) Lach, S.; Witt, D. Efficient synthesis of functionalized unsymmetrical dialkyl trisulfanes. *Synlett* **2013**, *24* (15), 1927-1930. DOI: 10.1055/s-0033-1338966

(61) Ali, D.; Hunter, R.; Kaschula, C. H.; De Doncker, S.; Rees-Jones, S. C. Unsymmetrical organotrisulfide formation via low-temperature disulfanyl anion transfer to an organothiosulfonate. *J. Org. Chem.* **2019**, *84* (5), 2862-2869. DOI: 10.1021/acs.joc.8b03262

(62) Xiao, X.; Xue, J.; Jiang, X. Polysulfurating reagent design for unsymmetrical polysulfide construction. *Nat. Commun.* **2018**, *9* (1), 2191. DOI: 10.1038/s41467-018-04306-5

(63) Wang, W.; Lin, Y.; Ma, Y.; Tung, C.-H.; Xu, Z. Cu-catalyzed electrophilic disulfur transfer: synthesis of unsymmetrical disulfides. *Org. Lett.* **2018**, *20* (13), 3829-3832. DOI: 10.1021/acs.orglett.8b01418

(64) Lach, S.; Sliwka-Kaszynska, M.; Witt, D. Novel and efficient synthesis of unsymmetrical trisulfides. *Synlett* **2010**, *2010* (19), 2857-2860. DOI: 10.1055/s-0030-1259033

(65) Liang, S.; Ma, L.; Guo, Z.; Liu, F.; Lin, Z.; Yi, W. Synthesis of Unsymmetrical Trisulfides from S-Substituted Sulphenylthiosulphates. *Angew. Chem. Int. Ed.* **2024**, *63* (28), e202404139. DOI: 10.1002/anie.202404139.

(66) Wang, F.; Chen, Y.; Rao, W.; Ackermann, L.; Wang, S.-Y. Efficient preparation of unsymmetrical disulfides by nickel-catalyzed reductive coupling strategy. *Nat. Commun.* **2022**, *13* (1), 2588. DOI: 10.1038/s41467-022-30256-0.

(67) Pluth, M. D.; Bailey, T. S.; Hammers, M. D.; Hartle, M. D.; Henthorn, H. A.; Steiger, A. K. Natural products containing hydrogen sulfide releasing moieties. *Synlett* **2015**, *26* (19), 2633-2643. DOI: 10.1055/s-0035-1560638

(68) Myers, A. G.; Cohen, S. B.; Kwon, B. M. A Study of the Reaction of Calicheamicin .gamma.1 with Glutathione in the Presence of Double-Stranded DNA. *J. Am. Chem. Soc.* **1994**, *116* (4), 1255-1271. DOI: 10.1021/ja00083a012.

(69) Ben-Zvi, B.; Lian, C.; Brusco, M. F.; Diao, T. Tunable and Photoactivatable Mimics of Calicheamicin γ1 for DNA Cleavage. *J. Am. Chem. Soc.* **2024**. DOI: 10.1021/jacs.4c07754.

(70) Ellestad, G. A.; Hamann, P. R.; Zein, N.; Morton, G. O.; Siegel, M. M.; Pastel, M.; Borders, D. B.; McGahren, W. J. Reactions of the trisulfide moiety in calicheamicin. *Tetrahedron Lett.* **1989**, *30* (23), 3033-3036. DOI: 10.1016/S0040-4039(00)99395-X.

(71) Guo, H.; Han, Y.; Zhao, W.; Yang, J.; Zhang, L. Universally autonomous self-healing elastomer with high stretchability. *Nat. Commun.* **2020**, *11* (1), 2037. DOI: 10.1038/s41467-020-15949-8.

(72) Lei, Z. Q.; Xiang, H. P.; Yuan, Y. J.; Rong, M. Z.; Zhang, M. Q. Room-Temperature Self-Healable and Remoldable Cross-linked Polymer Based on the Dynamic Exchange of Disulfide Bonds. *Chem. Mater.* **2014**, *26* (6), 2038-2046. DOI: 10.1021/cm4040616.

(73) Alegre-Cebollada, J.; Kosuri, P.; Rivas-Pardo, J. A.; Fernández, J. M. Direct observation of disulfide isomerization in a single protein. *Nat. Chem.* **2011**, *3* (11), 882-887. DOI: 10.1038/nchem.1155.

(74) Canal-Martín, A.; Pérez-Fernández, R. Protein-Directed Dynamic Combinatorial Chemistry: An Efficient Strategy in Drug Design. *ACS Omega* **2020**, *5* (41), 26307-26315. DOI: 10.1021/acsomega.0c03800.

(75) Wu, Z.; Pratt, D. A. Radical Substitution Provides a Unique Route to Disulfides. *J. Am. Chem. Soc.* **2020**, *142* (23), 10284-10290. DOI: 10.1021/jacs.0c03626.

(76) Caraballo, R.; Rahm, M.; Vongvilai, P.; Brinck, T.; Ramström, O. Phosphine-catalyzed disulfide metathesis. *Chem.Commun.* **2008**, (48), 6603-6605. DOI: 10.1039/B815710C.

(77) Singh, R.; Whitesides, G. M. Comparisons of rate constants for thiolate-disulfide interchange in water and in polar aprotic solvents using dynamic proton NMR line shape analysis. *J. Am. Chem. Soc.* **1990**, *112* (3), 1190-1197. DOI: 10.1021/ja00159a046.

(78) Belenguer, A. M.; Friščić, T.; Day, G. M.; Sanders, J. K. M. Solid-state dynamic combinatorial chemistry: reversibility and thermodynamic product selection in covalent mechanosynthesis. *Chem. Sci.* **2011**, *2* (4), 696-700. DOI: 10.1039/C0SC00533A.

(79) Fritze, U. F.; von Delius, M. Dynamic disulfide metathesis induced by ultrasound. *Chem. Commun.* **2016**, *52* (38), 6363-6366. DOI: 10.1039/C6CC02034H.

(80) Sherwood, J.; Constantinou, A.; Moity, L.; McElroy, C. R.; Farmer, T. J.; Duncan, T.; Raverty, W.; Hunt, A. J.; Clark, J. H. Dihydrolevoglucosenone (Cyrene) as a bio-based alternative for dipolar aprotic solvents. *Chem. Commun.* **2014**, *50* (68), 9650-9652. DOI: 10.1039/C4CC04133J

(81) Ramström, O.; Lehn, J.-M. In Situ Generation and Screening of a Dynamic Combinatorial Carbohydrate Library against Concanavalin A. *ChemBioChem* **2000**, *1* (1), 41-48. DOI: 10.1002/1439-7633(20000703)1:1<41::AID-CBIC41>3.0.CO;2-L.

(82) Ali, D.; Amer, Y.; Petersen, W. F.; Kaschula, C. H.; Hunter, R. A Review of Heterolytic Synthesis Methodologies for Organotri-and Organotetrasulfane Synthesis. *SynOpen* **2021**, *5* (01), 49-64. DOI: 10.1055/s-0040-1706018.

(83) Ilieva, Y.; Dimitrova, L.; Zaharieva, M. M.; Kaleva, M.; Alov, P.; Tsakovska, I.; Pencheva, T.; Pencheva-El Tibi, I.; Najdenski, H.; Pajeva, I. Cytotoxicity and microbicidal activity of commonly used organic solvents: A comparative study and application to a standardized extract from Vaccinium macrocarpon. *Toxics* **2021**, *9* (5), 92.

3.6 Experimental Details and Characterizations

General Considerations

Analytical thin-layer chromatography was conducted with commercial aluminium sheets coated with silica gel (Chem-supply, silica gel 60 F254). Compounds were either visualized under UV-light at 254 nm, or by dipping the plates in aqueous potassium permanganate or ceric ammonium molybdate solution followed by heating.

Chemicals were purchased from commercial suppliers and used as received. Dry diethyl ether was obtained from solvent purification system and stored over 3Å molecular sieves. Pyridine and triethylamine were distilled and stored over 3Å molecular sieves and KOH pellets. N-butylamine was dried over KOH pellets and stored over 3Å molecular sieves. Deionized water was used for chemical reactions. Brine refers to a saturated solution of sodium chloride. Anhydrous sodium sulfate (Na_2SO_4) or magnesium sulfate ($MgSO_4$) were used as drying agents after reaction workup, as indicated.

Solvent drying

Where dry solvents are used, reactions are conducted under an atmosphere of nitrogen with dry glassware. Solvents were dried at least 48 hours prior to use if dried over molecular sieves. Reagents and solvents were degassed using nitrogen gas prior to use. Glass vials for chemical reaction were dried in an oven prior to use.

TMU and methanol were dried and distilled from CaH_2 and then stored over 3 Å molecular sieves. DMPU, EtOAc, and 1,3-dimethyl-2-imidazolidinone (DMI), were dried directly using 3 Å molecular sieves. Hexamethylphosphoramide (HMPA) and tri(pyrrolidin-1-yl)phosphine oxide (TPPO) were dried directly using 4 Å molecular sieves. DMF was dried and distilled from CaH_2 and then stored over 4 Å molecular sieves. Anhydrous DMF was also purchased from Sigma Aldrich and used as received. Anhydrous DMF was also obtained from solvent purification system (LC Technology Solution Inc.) and stored over 4 Å molecular sieves. NMP was dried over CaH_2 at 100 °C overnight. The solvent was allowed to cool to room temperature, distilled under vacuum, and stored over 3 Å molecular sieves under N_2. Dry diethyl ether was obtained from a solvent purification system. Isopropanol was dried and distilled over calcium hydride. The solvent was stored over 3 Å molecular sieves. Furfural was purified by passing through neutral alumina (chromatographic grade) and stored over 3Å molecular sieves prior to use. Pyridine, triethylamine, and diethylamine, were distilled from KOH pellets and stored over KOH pellets and 3Å molecular sieves. *n*-Butylamine was stored over KOH pellets and 3Å molecular sieves.

NMR (Nuclear Magnetic Resonance) Spectroscopy

^{1}H and ^{13}C NMR spectra were recorded on a Bruker Ultrashield Plus 600 MHz spectrometer at 600 MHz and 150 MHz respectively, or a Bruker Ascend 400 MHz spectrometer at 400 MHz and 100 MHz, respectively. All spectra were obtained at 298 K unless stated otherwise. Deuterated solvents were used as solvent and internal lock unless stated otherwise. Residual solvent peaks were used as an internal reference for ^{1}H NMR spectra [$CDCl_3$ δ 7.26 ppm; DMF-d_7 δ 8.03 ppm; Toluene-d_8 δ 7.09, 2.09 ppm] and for ^{13}C NMR spectra [$CDCl_3$ δ 77.16 ppm, DMF-d_7 δ 163.15 ppm; Toluene-d_8 δ 137.86 ppm].[1,2] Coupling constants (*J*) are quoted to the nearest 0.1 Hz. The following abbreviations, or combinations thereof, were used to describe NMR multiplicities: s = singlet, d = doublet, t = triplet, q = quartet, p = pentet, h = heptet, m = multiplet, ap. = apparent, br. = broad).

GC-MS (Gas Chromatography Mass Spectrometry)

GC-MS analysis was performed using an Agilent 5975C series GCMS system. A 29.4 m x 250 µm x 0.25 µm, (5%-phenyl)-methylpolysiloxane column was used with a helium mobile phase. A 1 µL sample was injected with a split ratio of 60:1 and a gas flow rate of 1.2 mL/min.

GC-MS method **A**: Initial temperature 30 ºC. Hold at 30 ºC for 3 minutes. Ramp rate at 20 ºC/min to 250 ºC. Hold at 250 ºC for 6 minutes. Total run time was 20 minutes.

GC-MS method **B**: Initial temperature 85 ºC. Hold at 85 ºC for 3 minutes. Ramp rate at 60 ºC/min to 250 ºC. Hold at 250 ºC for 2 minutes. Total run time of 7.75 minutes.

GC-MS method **C**: Initial temperature 70 ºC. Hold at 70 ºC for 3 minutes. First ramp rate at 20 ºC/min to 135 ºC. Hold at 135 ºC for 0 minutes. Second ramp rate at 20 ºC/min to 250 ºC. Hold at 250 ºC for 3 minutes. Total run time was 15 minutes.

GC-MS method **D**: Initial temperature 30 ºC. Hold at 30 ºC for 3 minutes. First ramp rate at 20 ºC/min to 50 ºC. Hold at 50 ºC for 0 minutes. Second ramp rate at 20 ºC/min to 170 ºC. Hold at 170 ºC for 0 minutes. Third ramp rate at 50 ºC/min to 250 ºC. Hold at 250 ºC for 38.4 minutes. Total run time was 50 minutes.

GC-MS method **E**: Initial temperature 85 ºC. Hold at 85 ºC for 3 minutes. Ramp rate at 50 ºC/min to 250 ºC. Hold at 250 ºC for 8.7 minutes. Total run time of 15 minutes.

GC-MS method **F**: Initial temperature 85 ºC. Hold at 85 ºC for 3 minutes. Ramp rate at 50 ºC/min to 250 ºC. Hold at 250 ºC for 10 minutes. Total run time of 16.3 minutes.

GC-MS method **G**: Initial temperature 50 ºC. Hold at 50 ºC for 3 minutes. Ramp rate at 30 ºC/min to 250 ºC. Hold at 250 ºC for 20 minutes. Total run time of 29.667 minutes.

GC-MS method **H**: Initial temperature 30 ºC. Hold at 30 ºC for 3 minutes. Ramp rate at 10 ºC/min to 250 ºC. Hold at 250 ºC for 5 minutes. Total run time was 30 minutes.

GC-MS method **I**: Initial temperature 30 ºC. Hold at 30 ºC for 3 minutes. Ramp rate at 20 ºC/min to 250 ºC. Hold at 250 ºC for 16 minutes. Total run time was 30 minutes.

GC-MS method **J**: Initial temperature 85 ºC. Hold at 85 ºC for 3 minutes. Ramp rate at 50 ºC/min to 250 ºC. Hold at 250 ºC for 13.7 minutes. Total run time was 20 minutes.

FTIR (Fourier-transform infrared spectroscopy)

FTIR spectra were recorded between 4000 and 450 cm^{-1}, using either a Perkin Elmer Spectrum Two FT-IR Spectrometer equipped with a Universal ATR (Diamond Crystal), or a PerkinElmer Spectrum 100 FT-IR spectrometer equipped with ATR accessory (ZnSe crystal). Absorption maxima (ν_{max}) are reported in wavenumbers (cm^{-1}).

Elemental Analysis (CHNS)

Elemental analysis was performed by combustion analysis at the Chemical Analysis Facility at Macquarie University Analytical & Fabrication Facility. Elemental analysis was performed on Elementar vario MICRO (Elementar Analysensysteme GmbH). The instrument hardware was configured for the analysis of 4 elements (C, H, N and S). In a typical procedure, 1 – 2 mg of sample material was loaded into a tin foil boat and combusted at 1150 °C with oxygen dosing time of 80 s and total O_2 flow rate of 30 mL/min. Ultra-high purity grade helium (BOC, 99.999%) and oxygen (BOC, 99.995%) were employed as working fluids in all cases. Pure sulphanilamide was employed as a standard with quality control samples performed every 15-20 runs. The follow-up data analysis was performed using a custom peak picking and integration algorithm written in Python 3.11.

Liquid chromatography mass spectrometry (LC-MS)

LC-MS was performed using an Waters Acquity UPLC System coupled to a PDA Detector (214 nm detection), and a Waters Synapt HDMS mass spectrometer in positive mode for m/z measurements. LC separation was performed by reverse-phase chromatography using an a Phenomenex kinetex 2.6 um XB-C18 100A 50 x 2.1mm column at 45 °C. Samples were prepared in acetonitrile; sample injection volume was 1 µL. Mobile phase A was water with 0.01% trifluoroacetic acid, mobile phase B was acetonitrile with 0.01% trifluoroacetic acid. The following elution system, with a flow rate of 0.3 mL min^{-1}, was used: 95:5 (A:B) for 1 minute, gradient to 5:95 (A:B) over 4 minutes, and hold at 5:95 (A:B) for 3 minutes.

Solvents that promote rapid crossover of Me_2S_3 and $^nPr_2S_3$

Me_2S_3 and $^nPr_2S_3$ crossover in *N,N*-dimethylformamide (DMF), *N*-methyl-2-pyrrolidone (NMP), *N,N*-dimethyl acetamide (DMAc), *N,N'*-dimethylpropyleneurea (DMPU), 1,1,3,3-tetramethylurea (TMU), and dimethyl sulfoxide (DMSO)

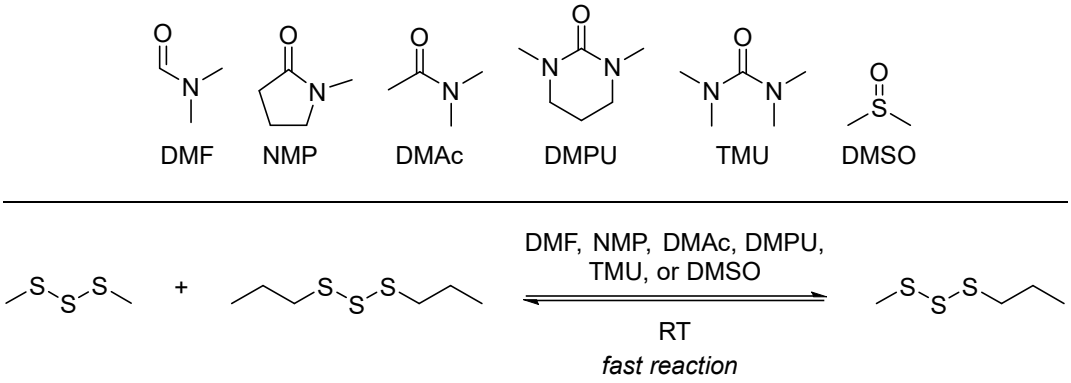

Dimethyl trisulfide (126 µL, 1.20 mmol, 1.0 eq.) and di-*n*-propyl trisulfide (203 µL, 1.20 mmol, 1.0 eq.) were added to a 2 mL glass vial equipped with a stirrer bar, followed by the solvent (1.20 mmol, 1.0 eq.). The solvents tested were *N,N*-dimethylformamide (DMF) (93 µL, 1.20 mmol, 1.0 eq.), *N*-methyl-2-pyrrolidone (NMP) (115.8 µL, 1.20 mmol, 1.0 eq.), *N,N*-dimethyl acetamide (DMAc) (111.2 µL, 1.20 mmol, 1.0 eq.), *N,N'*-dimethylpropyleneurea (DMPU) (145 µL, 1.20 mmol, 1.0 eq.), 1,1,3,3-tetramethylurea (TMU) (144 µL, 1.20 mmol, 1.0 eq.), and dimethyl sulfoxide (DMSO) (85.2 µL, 1.20 mmol, 1.0 eq.). The reaction was stirred at room temperature (9 – 14 ºC). A 10 µL aliquot was removed and diluted to 1 mL with chloroform for GC-MS analysis after 5 seconds and 5 minutes of reaction time. In these solvents, reactions had reached or almost reached equilibrium within 5 minutes.

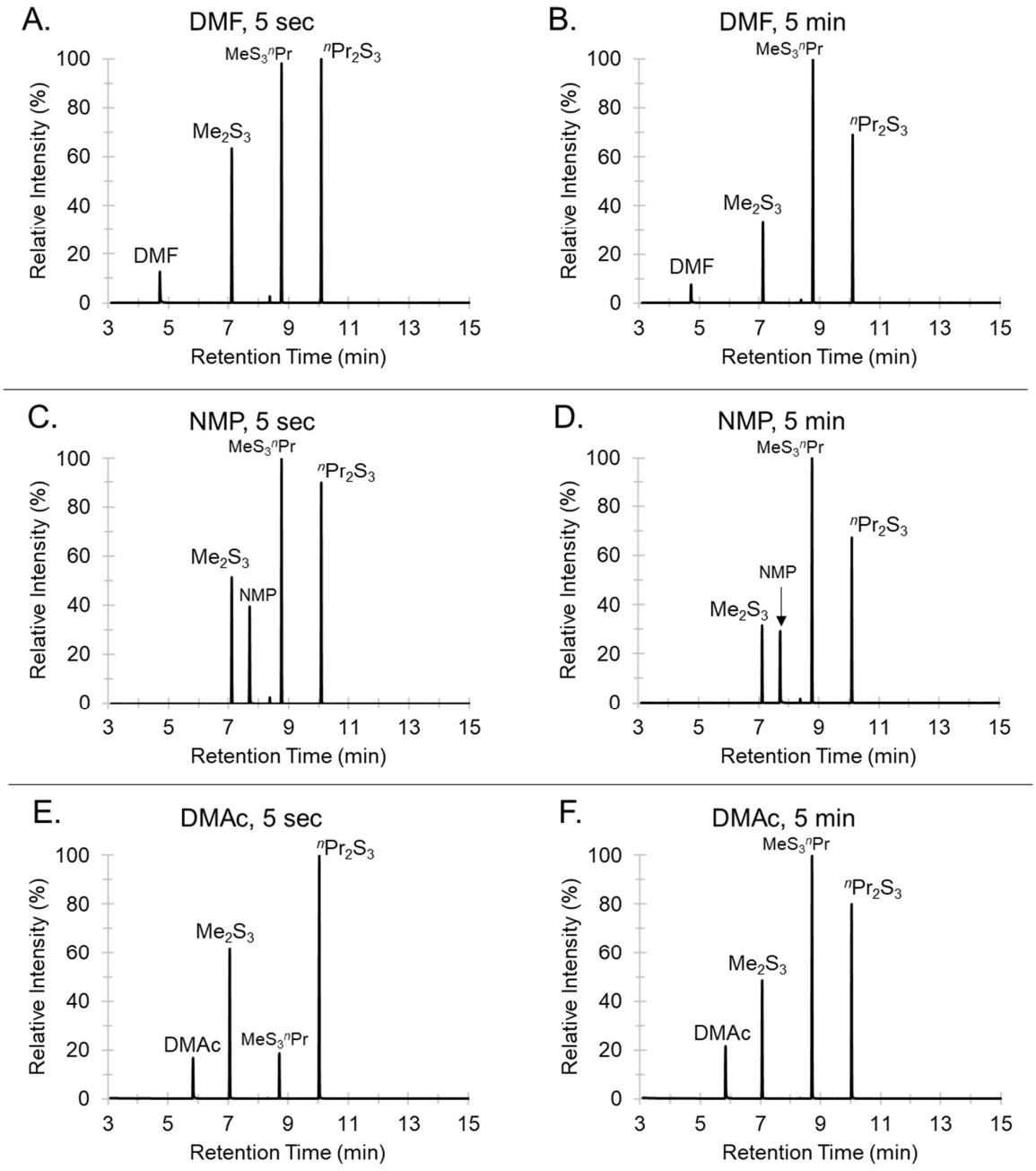
A.
DMF, 5 sec
B.
DMF, 5 min
C.
NMP, 5 sec
D.
NMP, 5 min
E.
DMAc, 5 sec
F.
DMAc, 5 min
Relative Intensity (%)
Retention Time (min)
DMF
DMAc
NMP
Me2S3
MeS3nPr
nPr2S3

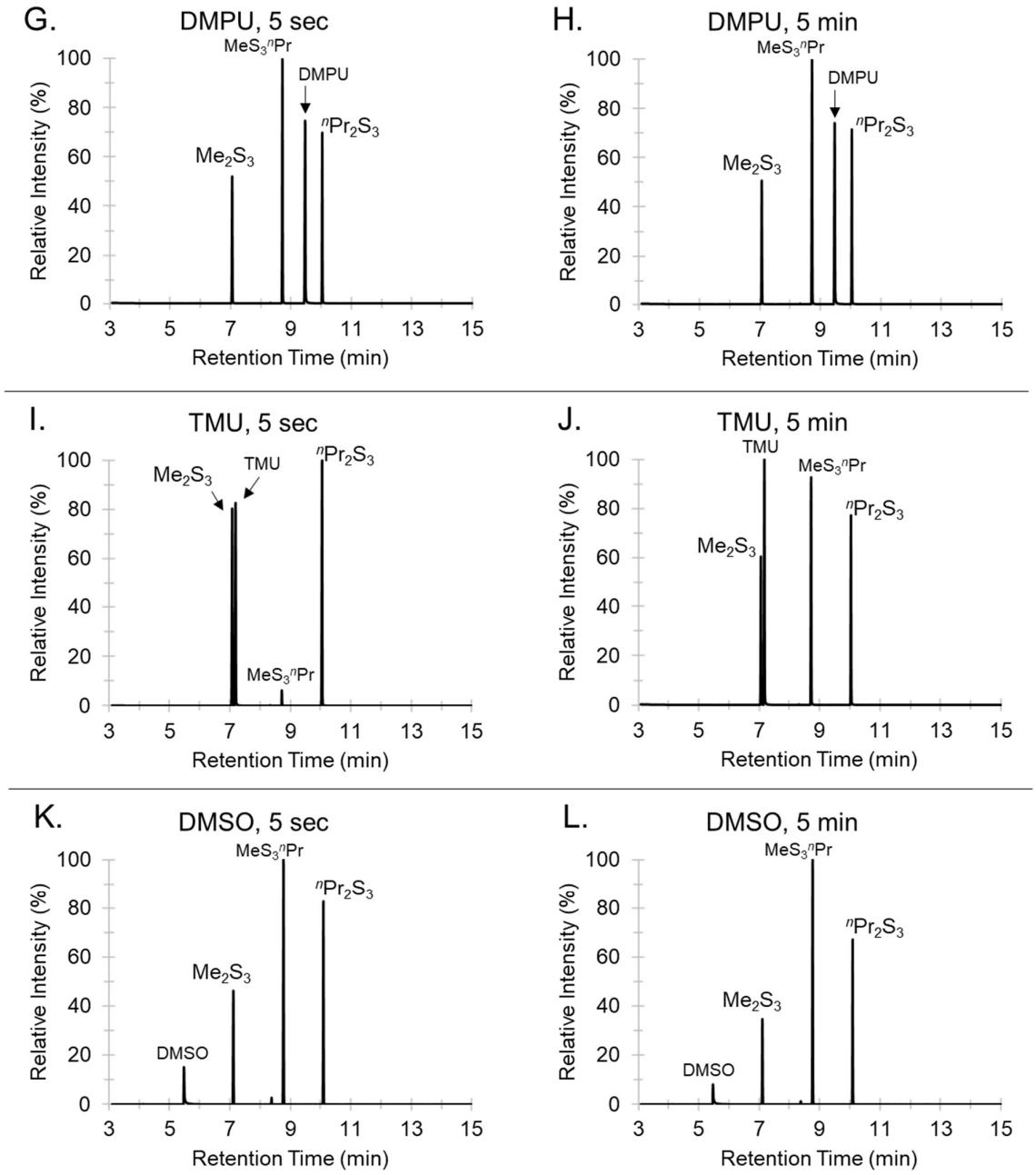

Figure S3.1: GC traces for the crossover reaction between dimethyl trisulfide (Me_2S_3) and di-*n*-propyl trisulfide ($^nPr_2S_3$) with the selected solvent at room temperature (9 – 14 ºC) after 5 seconds and 5 minutes. (A, B) DMF, (C, D) NMP, (E, F) DMAc, (G, H) DMPU, (I, J) TMU, or (K, L) DMSO. GC-MS method A. Retention time: DMF (4.70 min), DMSO (5.46 min), DMAc (5.85 min), Me_2S_3 (7.10 min), TMU (7.18 min), NMP (7.71 min), $^nPr_2S_2$ (8.36 min, impurity from $^nPr_2S_3$), $MeS_3{}^nPr$ (8.75 min), DMPU (9.47 min), and $^nPr_2S_3$ (10.09 min).

Me_2S_3 and $^nPr_2S_3$ crossover in 1,3-dimethyl-2-imidazolidinone (DMI), hexamethylphosphoramide (HMPA), and tri(pyrrolidin-1-yl)phosphine oxide (TPPO)

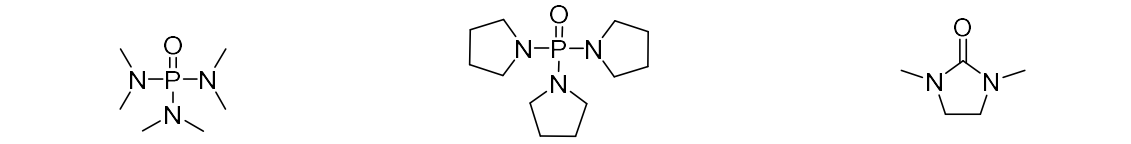

Hexamethylphosphoramide (HMPA) | Tri(pyrrolidin-1-yl)phosphine oxide (TPPO) | 1,3-Dimethyl-2-imidazolidinone (DMI)

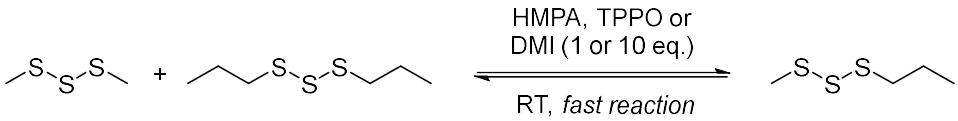

Dimethyl trisulfide (42 µL, 0.4 mmol, 1 eq.) and di-*n*-propyl trisulfide (67.8 µL, 0.4 mmol, 1 eq.) were added to a 2 mL glass vial equipped with a stirrer bar, followed by the solvent (0.4 mmol for 1 eq. or 4.0 mmol for 10 eq.). The solvents tested were HMPA (69.6 µL, 0.4 mmol, 1 eq. or 696 µL, 4.0 mmol, 10 eq.), TPPO (91.9 µL, 0.4 mmol, 1 eq. or 919 µL, 4.0 mmol, 10 eq.), and DMI (43.2 µL, 0.4 mmol, 1 eq. or 432.4 µL, 4.0 mmol, 10 eq.). The mixture was stirred at room temperature (12 – 26 ºC) for 24 h. After 5 minutes, 1 hours and 24 hours, a 10 µL of aliquot from was removed and diluted to 1 mL with chloroform for GCMS analysis. In these solvents, reactions had reached or almost reached equilibrium in 5 minutes.

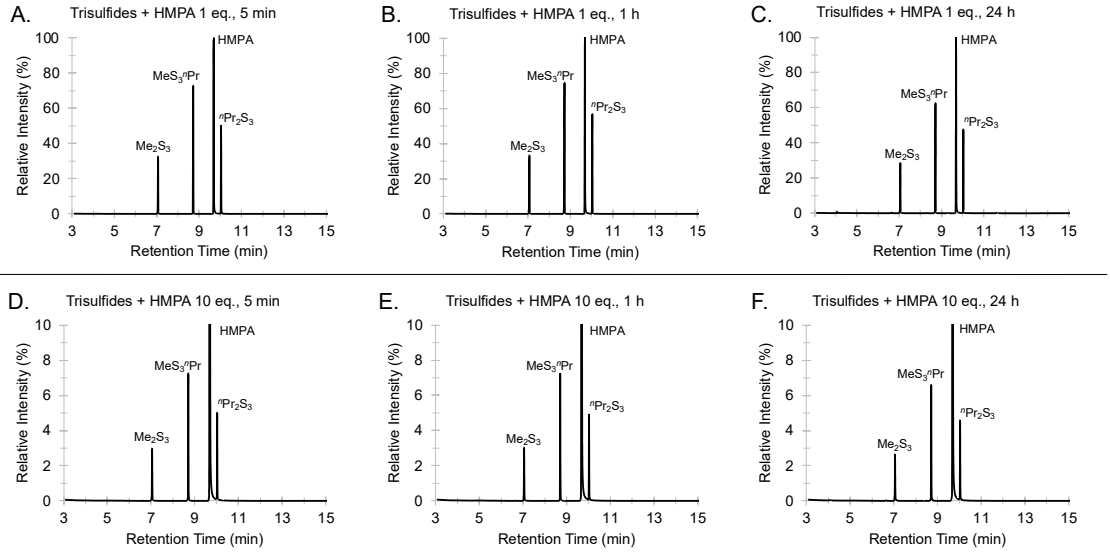

Figure S3.2: GC traces for the crossover reactions between dimethyl trisulfide (Me_2S_3) and di-*n*-propyl trisulfide ($^nPr_2S_3$) in HMPA at room temperature (12 – 26 ºC). (A, B, C) The trisulfides (1 eq. each) and HMPA (1 eq.) after 5 min, 1 h, and 24 h. (D, E, F) The trisulfides (1 eq. each) and HMPA (10 eq.) after 5 min, 1 h, and 24 h. After 5 min, 47% $MeS_3{}^nPr$ (1 eq. of HMPA) and 47% $MeS_3{}^nPr$ (10 eq. of HMPA) were formed. GCMS method A. Retention time: Me_2S_3 (7.05 min), $MeS_3{}^nPr$ (8.71 min), HMPA (9.68 min), and $^nPr_2S_3$ (10.03 min).

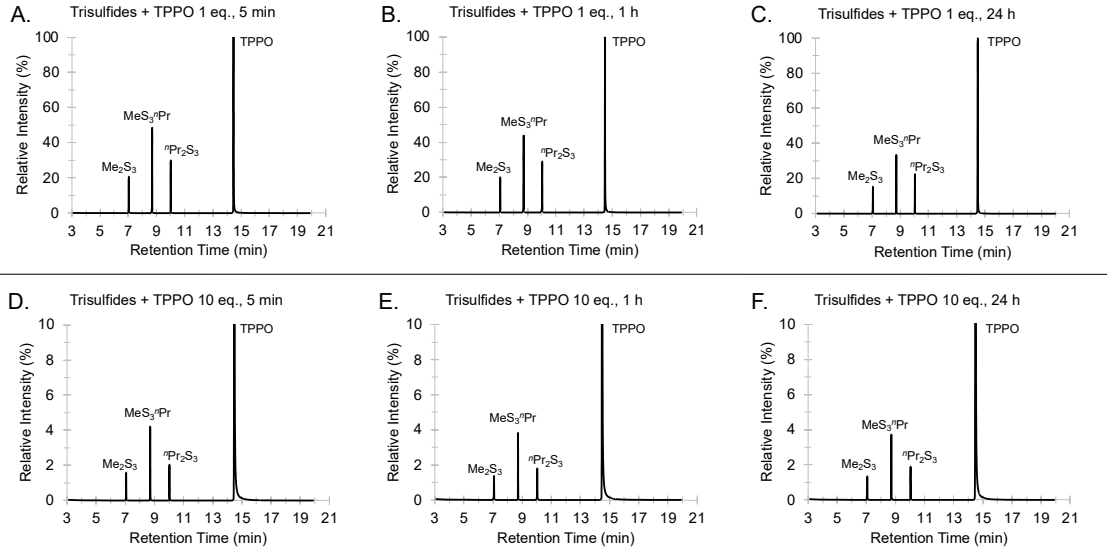

Figure S3.3: GC traces for the crossover reactions between dimethyl trisulfide (Me_2S_3) and di-*n*-propyl trisulfide ($^nPr_2S_3$) in TPPO at room temperature (12 – 26 ºC). (A, B, C) The trisulfides (1 eq. each) and TPPO (1 eq.) after 5 min, 1 h, and 24 h. (D, E, F) The trisulfides (1 eq. each) and TPPO (10 eq.) after 5 min, 1 h, and 24 h. After 5 min, 49% $MeS_3{}^nPr$ (1 eq. of TPPO) and 51% $MeS_3{}^nPr$ (10 eq. of TPPO) were produced. GCMS method A. Retention time: Me_2S_3 (7.05 min), $MeS_3{}^nPr$ (8.71 min), $^nPr_2S_3$ (10.03 min), and HMPA (14.49 min).

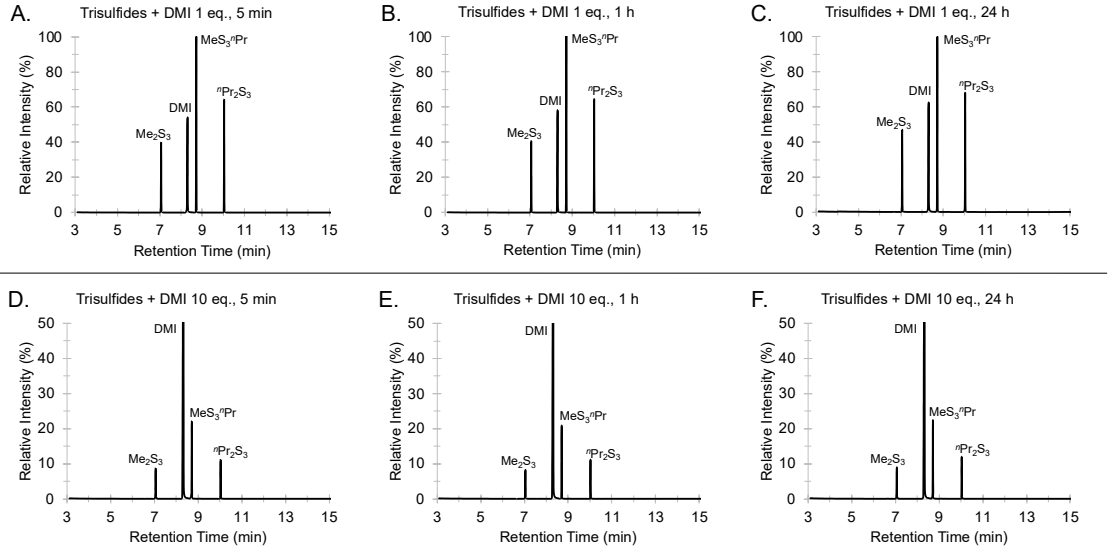

Figure S3.4: GC traces for the crossover reactions between dimethyl trisulfide (Me_2S_3) and di-*n*-propyl trisulfide ($^nPr_2S_3$) in DMI at room temperature (12 – 26 ºC). (A, B, C) The trisulfides (1 eq. each) and DMI (1 eq.) after 5 min, 1 h, and 24 h. (D, E, F) The trisulfides (1 eq. each) and DMI (10 eq.) after 5 min, 1 h, and 24 h. After 5 min, 49% $MeS_3{}^nPr$ (1 eq. of DMI) and 52% $MeS_3{}^nPr$ (10 eq. of DMI) were produced. GCMS method A. Retention time: Me_2S_3 (7.05 min), DMI (8.30 min), $MeS_3{}^nPr$ (8.71 min), and $^nPr_2S_3$ (10.03 min).

Me_2S_3 and $^nPr_2S_3$ crossover in *N,N*-dimethylformamide (DMF), under ambient light or in darkness

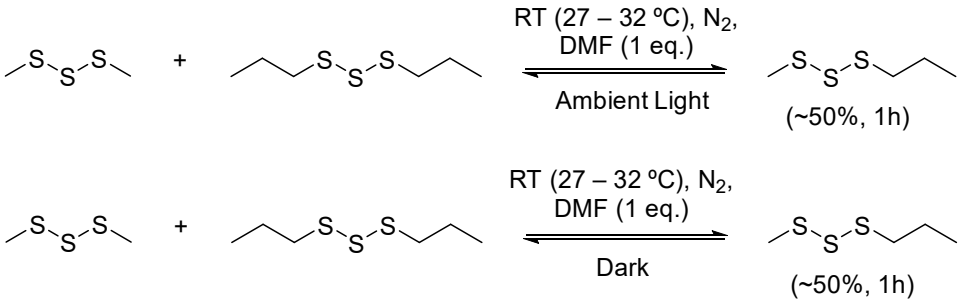

Dimethyl trisulfide (126 µL, 1.20 mmol, 1.0 eq.) and di-*n*-propyl trisulfide (203 µL, 1.20 mmol, 1.0 eq.) were added to a 5 mL glass vial equipped with a stir bar, followed by DMF (93 µL, 1.2 mmol, 1.0 eq.), and sealed with a rubber septum. The mixture was then stirred at room temperature (27 – 32 ºC) under ambient lighting. A duplicate experiment was carried out between the trisulfides in DMF in darkness by covering the reaction vial with aluminium foil to exclude light. After 1 h and 24 h, a 10 µL aliquot was removed from the reaction and diluted to 1 mL with chloroform for GC-MS analysis. Control experiments were performed, duplicating the reaction setup for both ambient light and darkness, with the exclusion of DMF. The reaction reached equilibrium within 1 hour if conducted in the presence of DMF in both ambient light and darkness; when DMF was excluded the reaction did not occur.

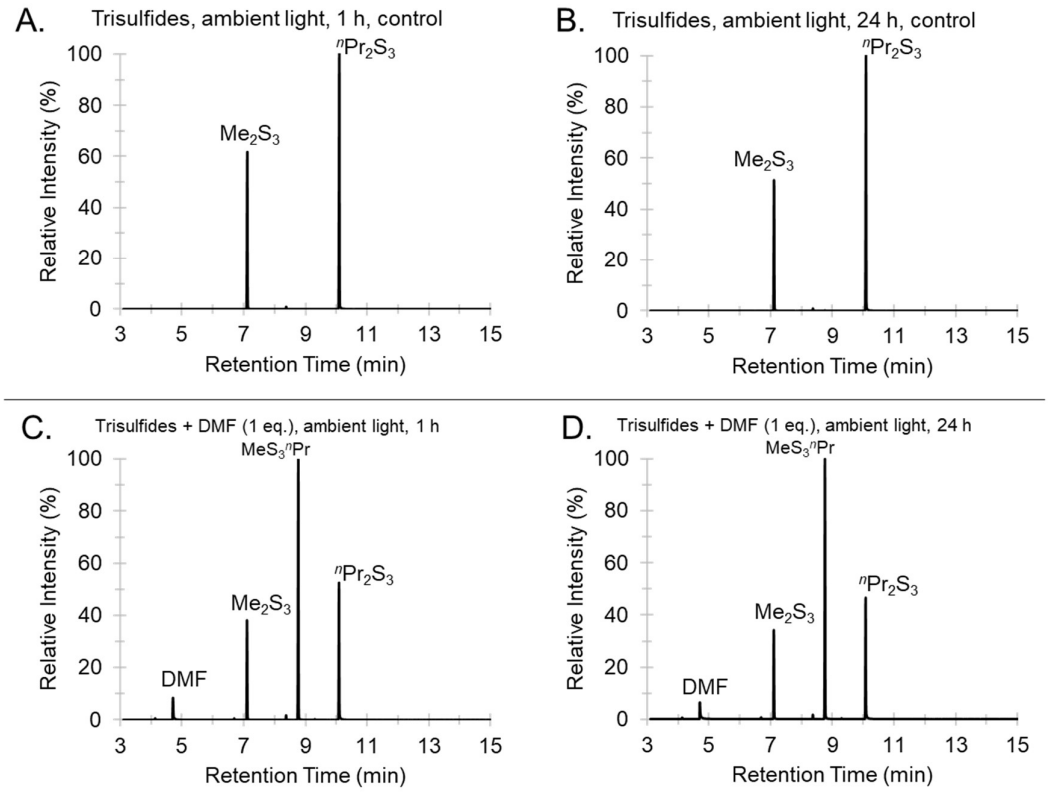

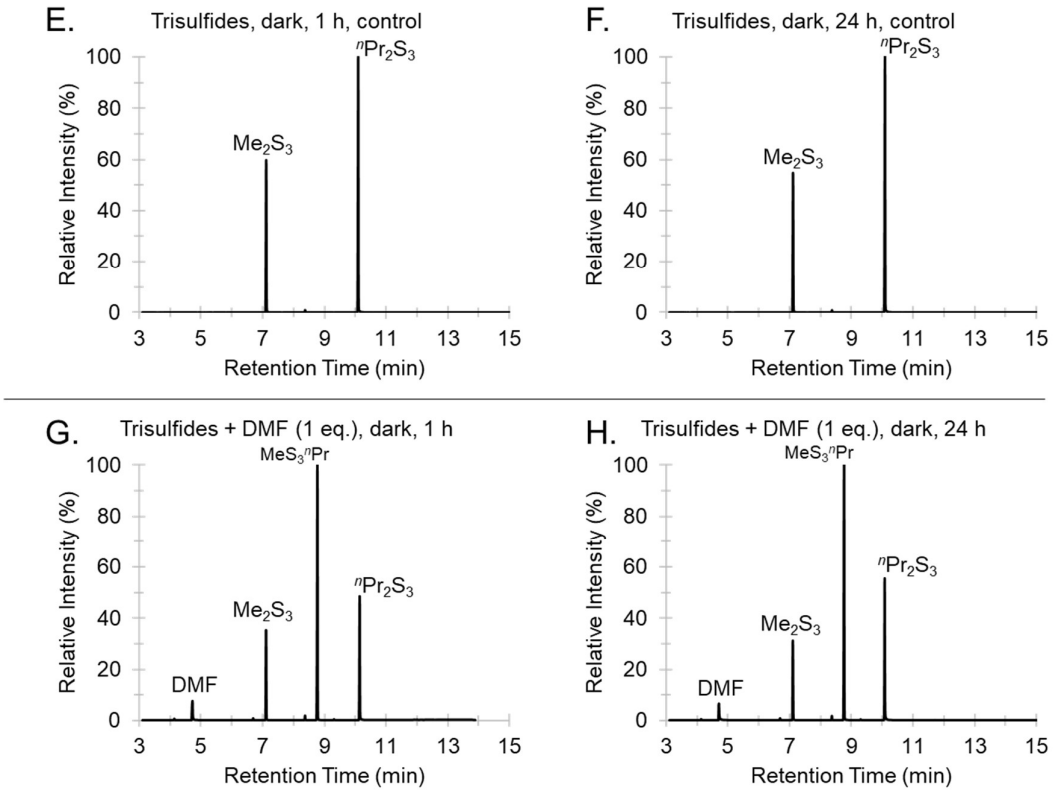

Figure S3.5: GC traces for the crossover reaction between dimethyl trisulfide (Me_2S_3) and di-*n*-propyl trisulfide ($^{n}Pr_2S_3$) over 24 hours at room temperature (27-32 °C). (A, B) The trisulfides (1 eq. each) under ambient light after 1 h and 24 h. (C, D) The trisulfides (1 eq. each) and DMF (1 eq.) under ambient light after 1 h and 24h. (E, F) The trisulfides (1 eq. each) under darkness after 1 h and 24 h. (G, H) The trisulfides (1 eq. each) and DMF (1 eq.) under darkness after 1 h and 24 h. GC-MS method A. Retention time: DMF (4.70 min), Me_2S_3 (7.10 min), $^{n}Pr_2S_2$ (8.36 min, impurity from $^{n}Pr_2S_3$), $MeS_3{}^{n}Pr$ (8.75 min), and $^{n}Pr_2S_3$ (10.09 min).

Me_2S_3 and $^{n}Pr_2S_3$ crossover using 10 mol% *N,N*-dimethyl formamide (DMF)

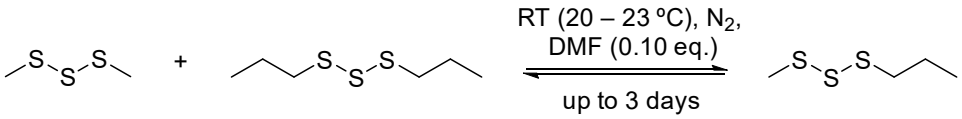

Dimethyl trisulfide (126 µL, 1.2 mmol) and di-*n*-propyl trisulfide (203 µL, 1.2 mmol) were added to a 1.5 mL GCMS glass vial equipped with a stir bar, followed by DMF (9.3 µL, 0.12 mmol, 0.10 eq., 10 mol%), and sealed with the lid. The vial was covered with aluminium foil to exclude light. The mixture was stirred at room temperature (20 – 23 ºC) under a nitrogen atmosphere. A 10 µL aliquot was removed from the reaction and diluted to 1 mL with chloroform after 1 h, 24 h, and 72 h, for GCMS analysis.

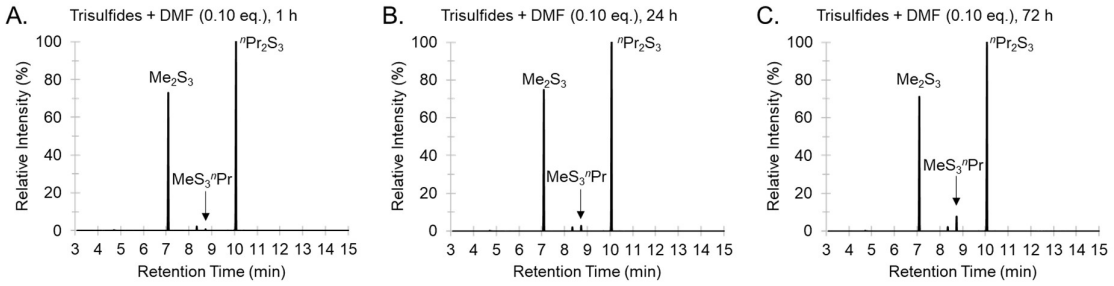

Figure S3.6: GC traces for the crossover reaction between dimethyl trisulfide (Me_2S_3) and di-*n*-propyl trisulfide ($^{n}Pr_2S_3$) with a catalytic amount of *N*,*N*-dimethylformamide (0.1 eq., 10 mol%) over 72 hours (3 days) at room temperature (20 – 23 ºC) with the exclusion of light. GCMS method A. Retention time: DMF (4.70 min), Me_2S_3 (7.10 min), $^{n}Pr_2S_2$ (8.36 min, impurity from dipropyl trisulfide), $MeS_3{}^{n}Pr$ (8.75 min), and $^{n}Pr_2S_3$ (10.09 min).

Me_2S_3 and $^{n}Pr_2S_3$ crossover at varying *N,N*-dimethylformamide (DMF) concentrations

(This experiment was conducted by Dr. Harshal D. Patel)

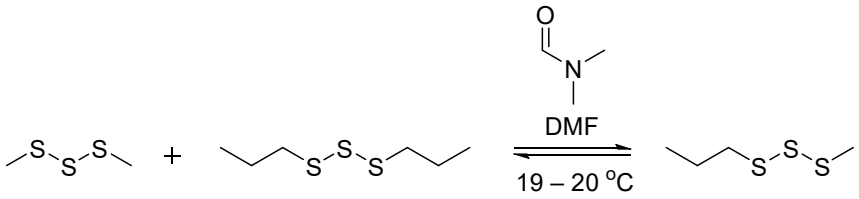

A freshly prepared, degassed mixture of dimethyl trisulfide (1.0 eq.) and di-*n*-propyl trisulfide (1.0 eq.) was added to a stirred solution of degassed, anhydrous *N,N*-dimethylformamide (DMF). The same batch of *N,N*-dimethylformamide and the mixed trisulfides were used to collect the following data. The progress of the reaction was monitored by GC-MS. 10 µL samples were taken from the reaction mixture and "quenched" by diluting with 990 µL of $CHCl_3$, which adequately slows the reaction prior to GC-MS analysis. Samples were taken at regular time intervals $T \pm 2$ seconds. T (0) was measured from the freshly prepared trisulfides mixture without *N,N*-dimethylformamide, via a 1 µL trisulfides sample in 1 mL $CHCl_3$. The table below shows the volumes of *N,N*-dimethylformamide and the trisulfides in the solution, as well as the corresponding DMF% v/v.

Table S3.1: Ratio of DMF to trisulfides used in crossover experiments

DMF% v/v	DMF (µL)	Trisulfide mixture (µL)	$MeS_3{}^nPr$ % after 2 minutes
5	40	760	0
7.5	60	740	0
10	80	720	0.1
12.5	100	700	0.4
15	120	680	0.9
20	160	640	4.8
21.9	-	-	*DMF = Me_2S_3 = Pr_2S_3 = 1 eq.*
25	200	600	17.1
30	240	560	22.9
35	280	520	35.2
50	400	400	45.9
73.7	-	-	*DMF = 10 eq. and Me_2S_3 = Pr_2S_3 = 1 eq.*
75	600	200	47.7
87.5	700	100	46.9
95	760	40	39.7

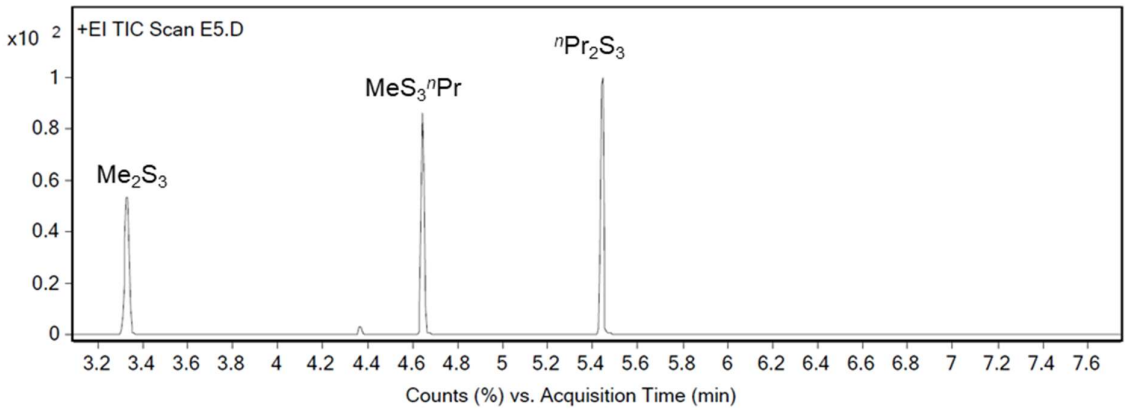

Figure S3.7: Exemplar gas chromatogram of the reaction between Me_2S_3 and Pr_2S_3 in DMF. GC-MS method B. Retention time: Me_2S_3 (3.327 min), $^nPr_2S_2$ (4.363 min, impurity from dipropyl trisulfide), $MeS_3{}^nPr$ (4.638 min), and $^nPr_2S_3$ (5.433 min).

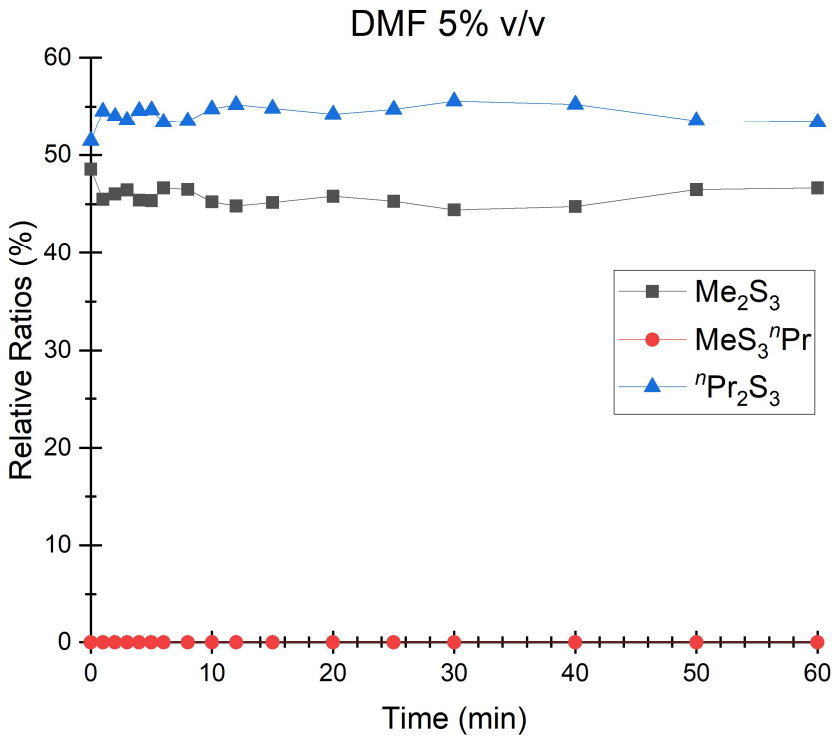

Figure S3.8: GC-MS relative ratios of Me_2S_3, $^nPr_2S_3$, and $MeS_3{}^nPr$ at 5% v/v of DMF.

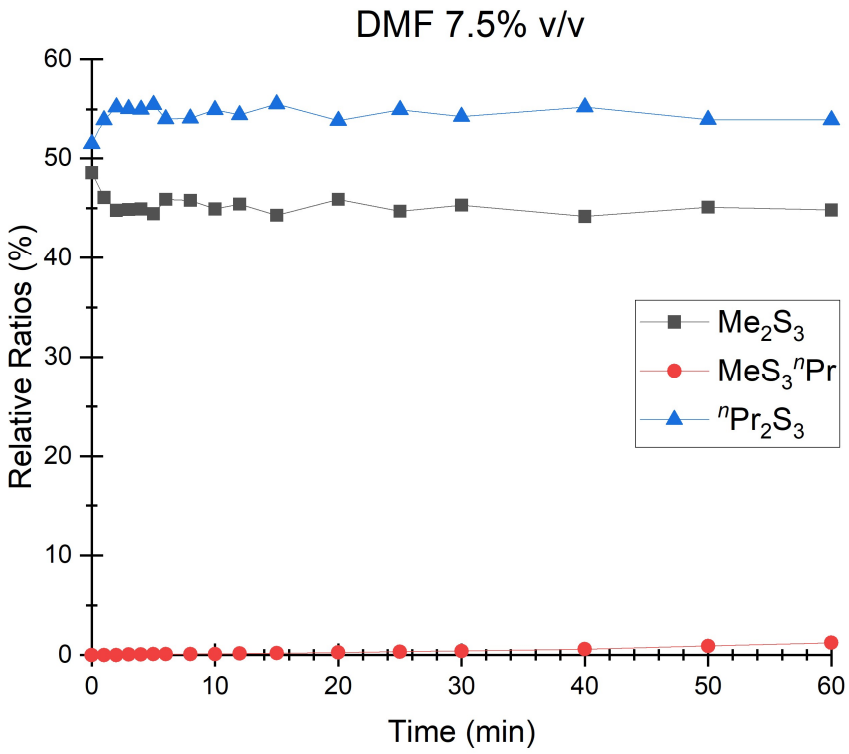

Figure S3.9: GC-MS relative ratios of Me_2S_3, $^nPr_2S_3$, and $MeS_3{}^nPr$ at 7.5% v/v of DMF.

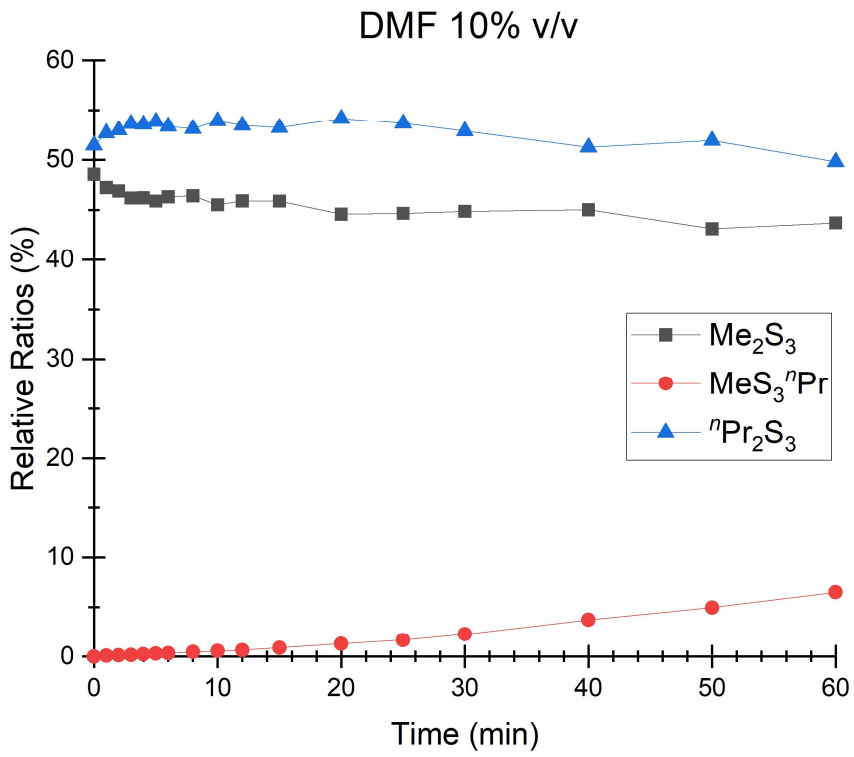

Figure S3.10: GC-MS relative ratios of Me_2S_3, $^nPr_2S_3$, and $MeS_3{}^nPr$ at 10% v/v of DMF.

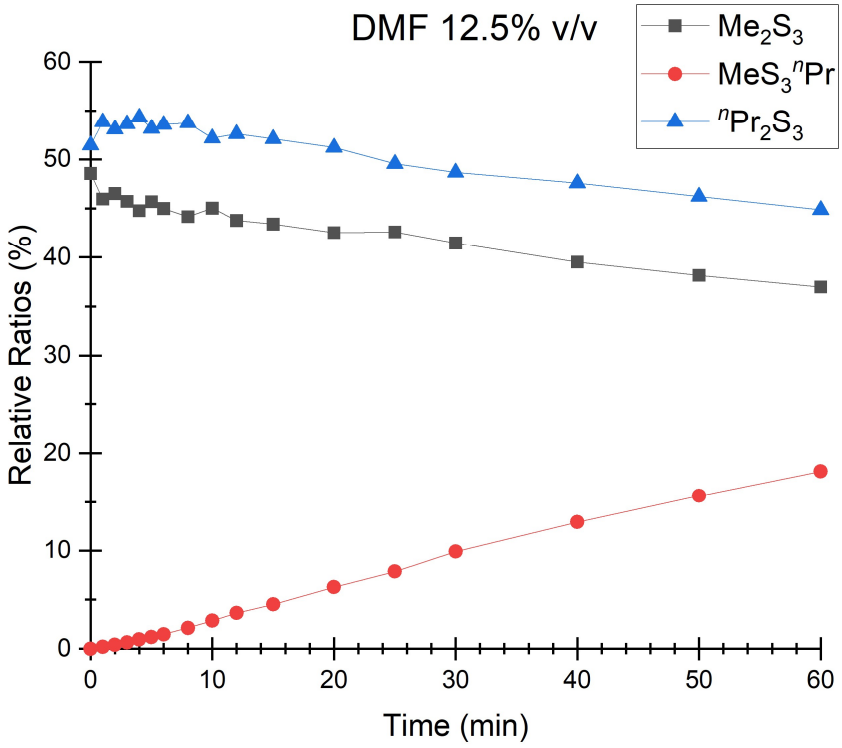

Figure S3.11: GC-MS relative ratios of Me_2S_3, $^nPr_2S_3$, and $MeS_3{}^nPr$ at 12.5% v/v of DMF.

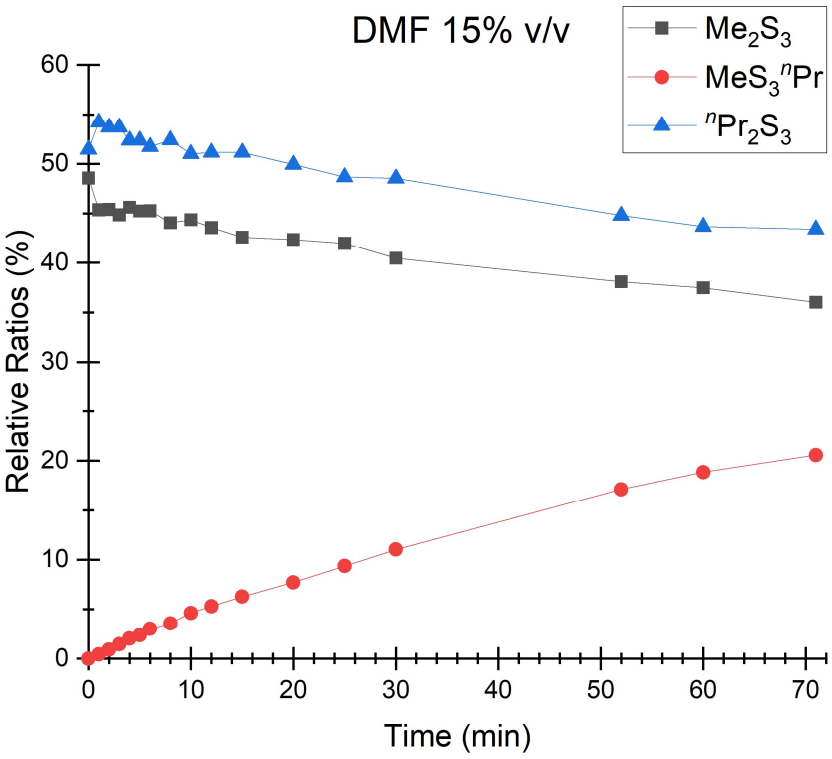

Figure S3.12: GC-MS relative ratios of Me_2S_3, $^nPr_2S_3$, and $MeS_3{}^nPr$ at 15% v/v of DMF.

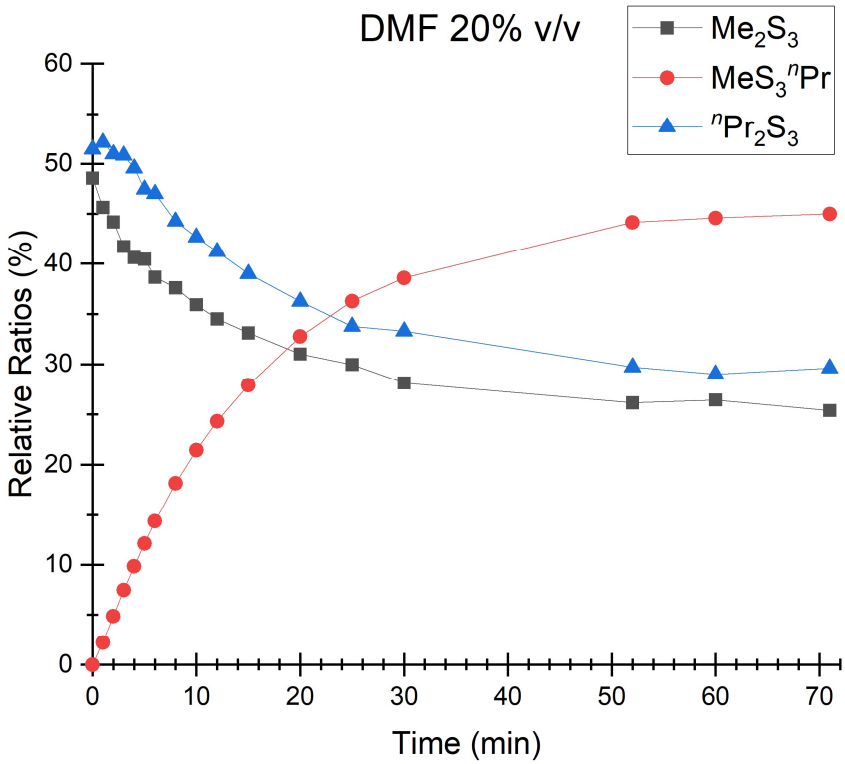

Figure S3.13: GC-MS relative ratios of Me_2S_3, $^nPr_2S_3$, and $MeS_3{}^nPr$ at 20% v/v of DMF.

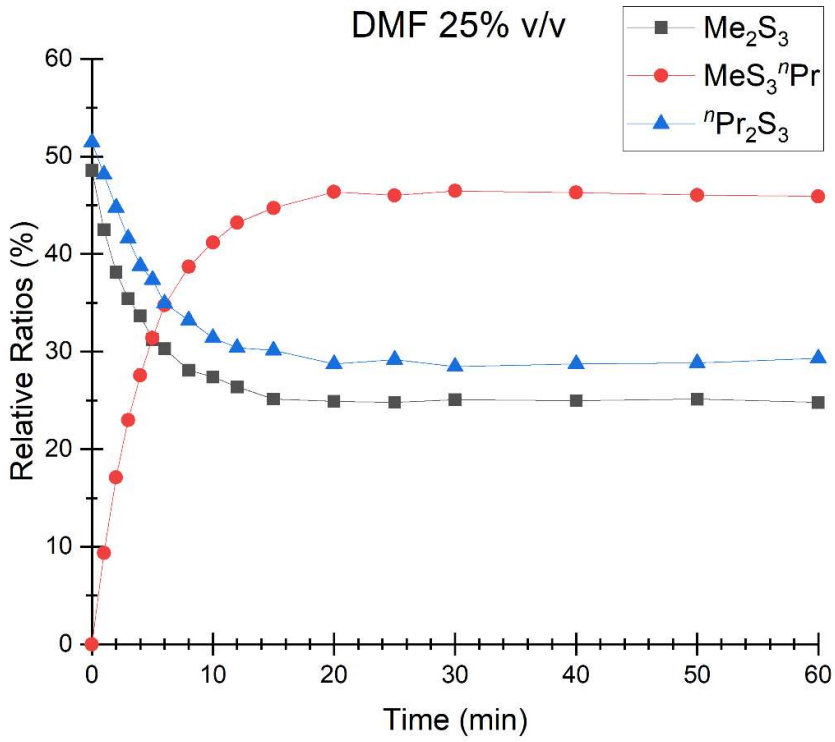

Figure S3.14: GC-MS relative ratios of Me_2S_3, $^nPr_2S_3$, and $MeS_3{}^nPr$ at 25% v/v of DMF.

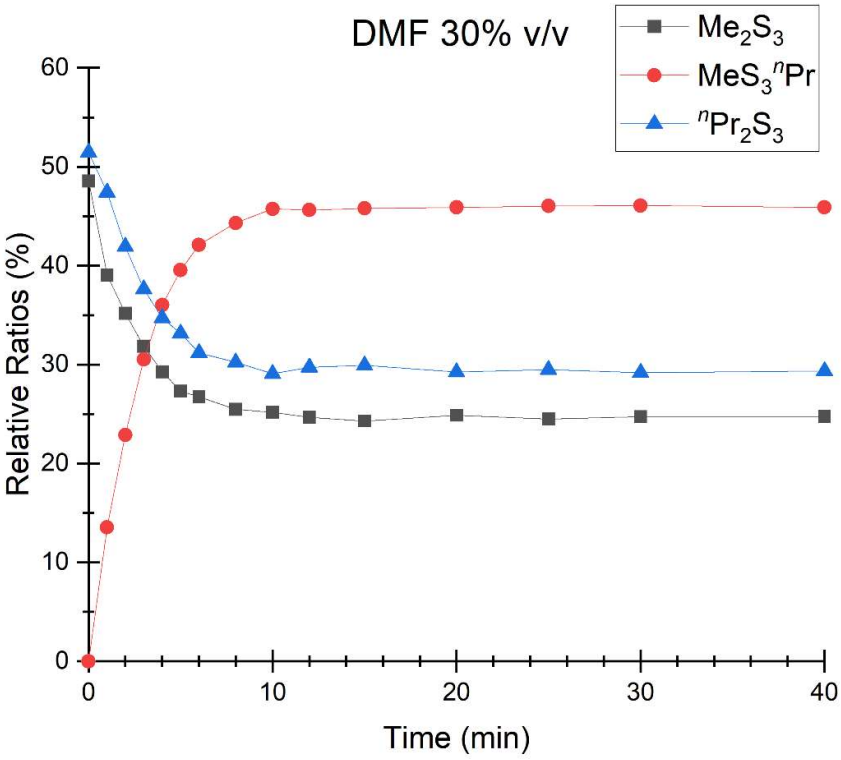

Figure S3.15: GC-MS relative ratios of Me_2S_3, $^nPr_2S_3$, and $MeS_3{}^nPr$ at 30% v/v of DMF.

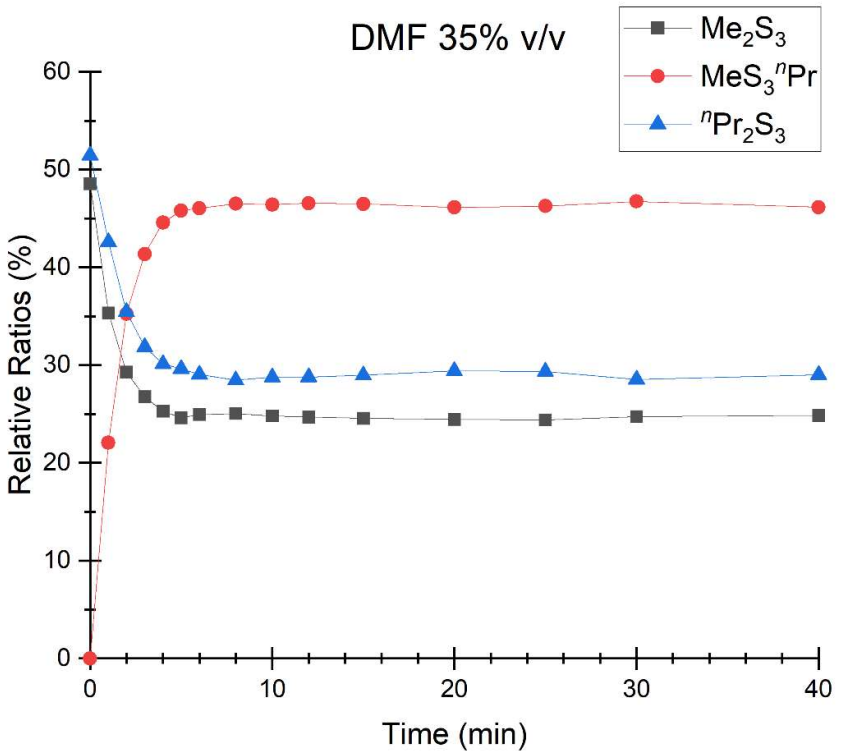

Figure S3.16: GC-MS relative ratios of Me_2S_3, $^nPr_2S_3$, and $MeS_3{}^nPr$ at 35% v/v of DMF.

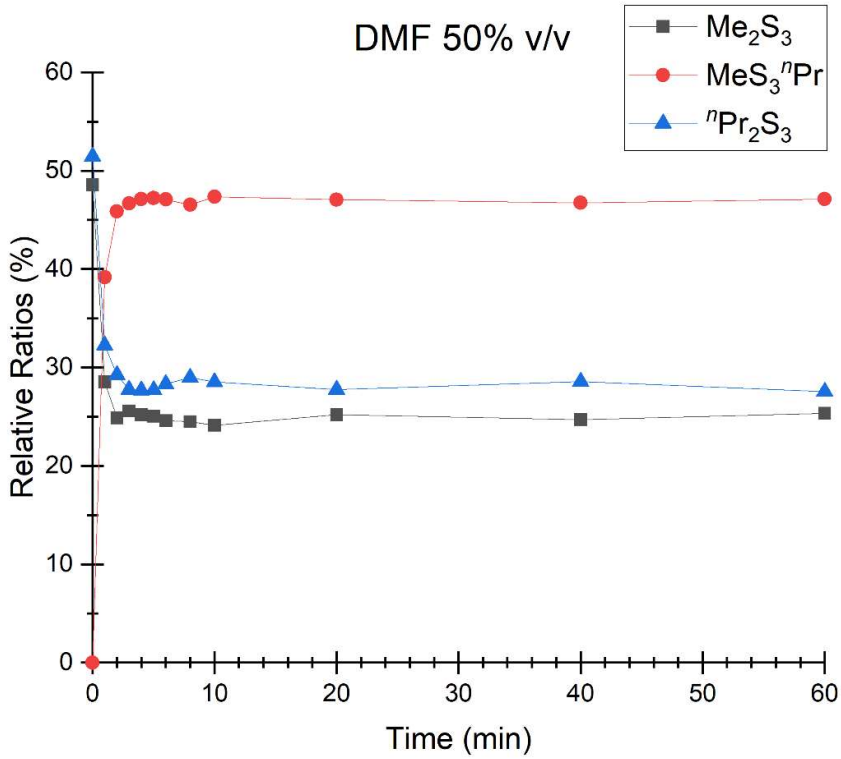

Figure S3.17: GC-MS relative ratios of Me_2S_3, $^nPr_2S_3$, and $MeS_3{}^nPr$ at 50% v/v of DMF.

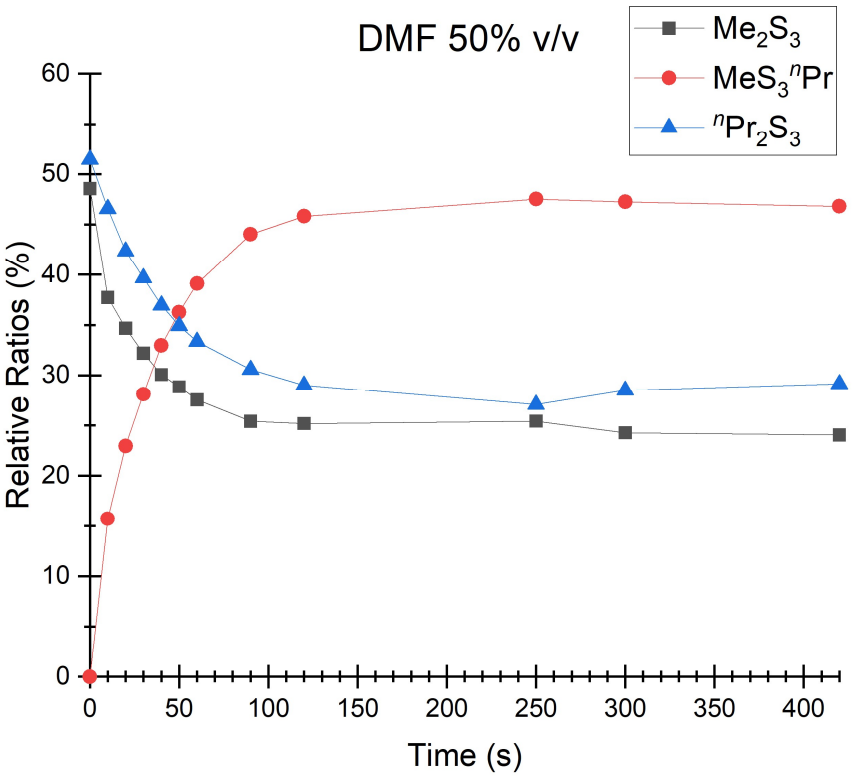

Figure S3.18: GC-MS relative ratios of Me_2S_3, $^nPr_2S_3$, and $MeS_3{}^nPr$ at 50% v/v of DMF.

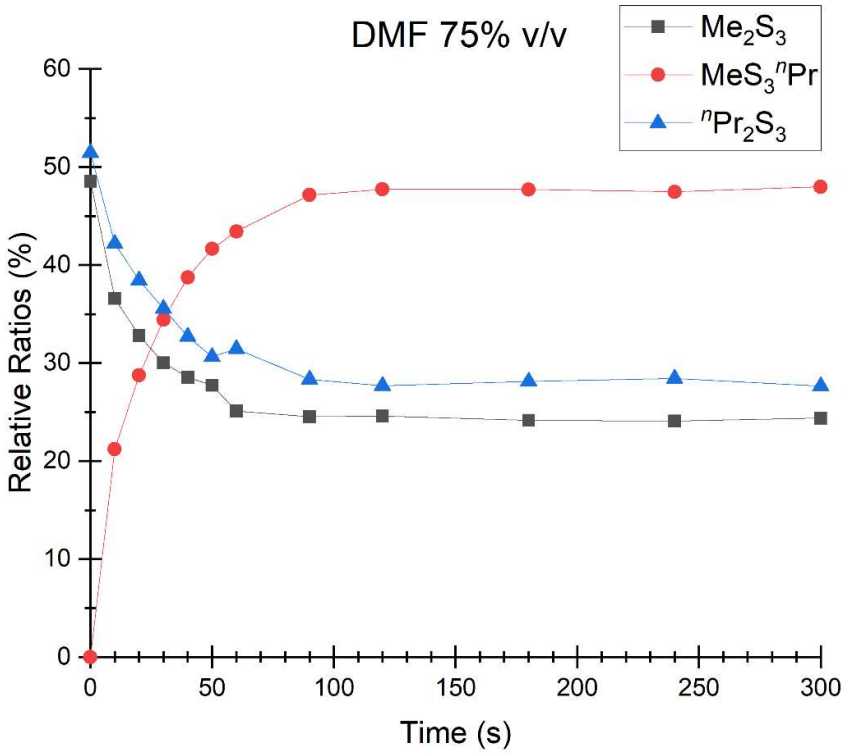

Figure S3.19: GC-MS relative ratios of Me_2S_3, $^nPr_2S_3$, and $MeS_3{}^nPr$ at 75% v/v of DMF.

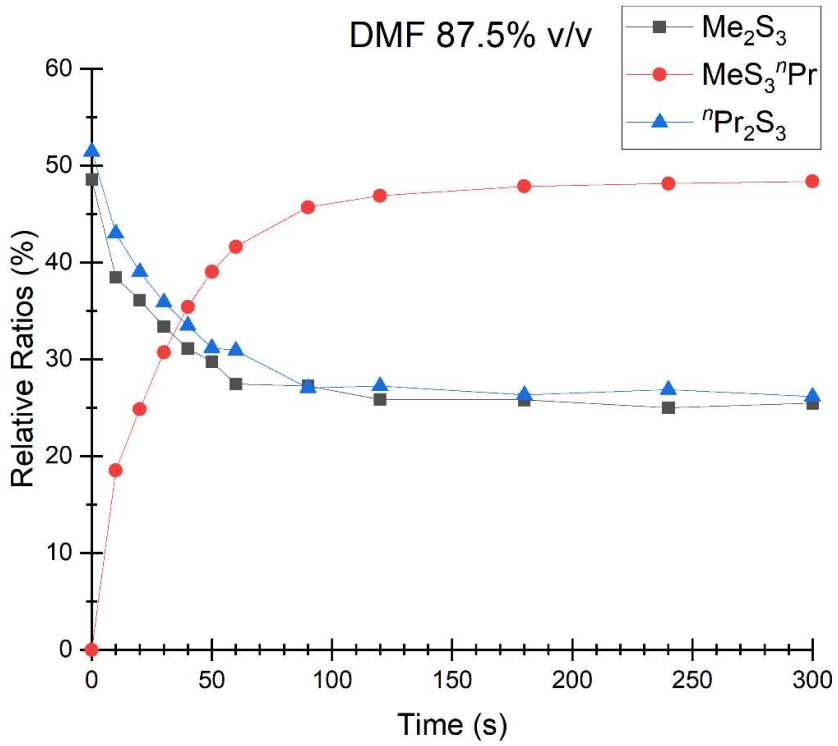

Figure S3.20: GC-MS relative ratios of Me_2S_3, $^nPr_2S_3$, and $MeS_3{}^nPr$ at 87.5% v/v of DMF.

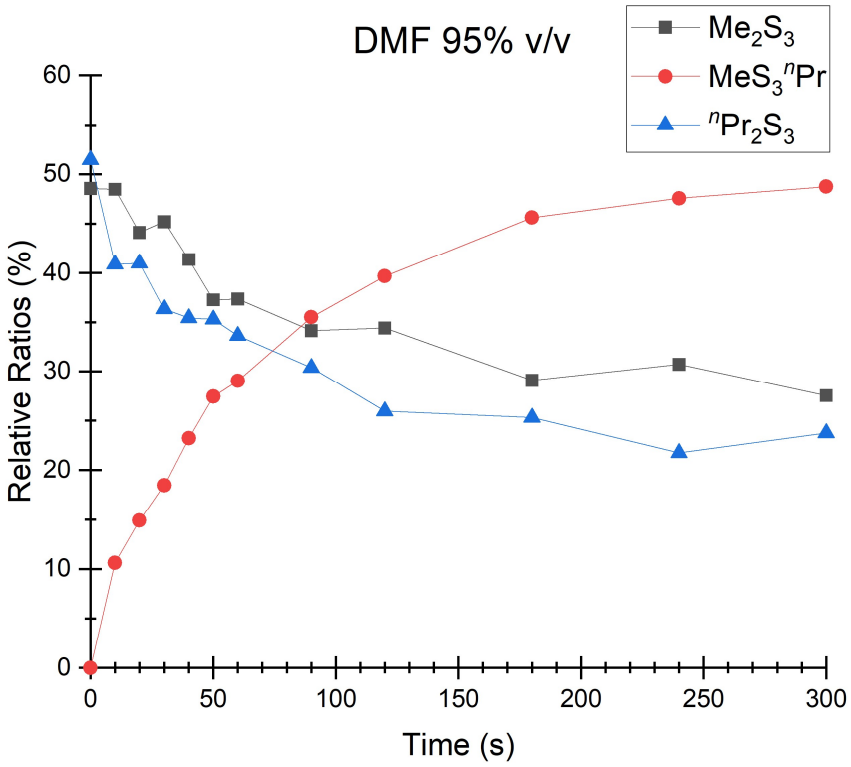

Figure S3.21: GC-MS relative ratios of Me_2S_3, $^nPr_2S_3$, and $MeS_3{}^nPr$ at 95% v/v of DMF.

Table S3.2: GC integrated abundance of Me_2S_3, $^nPr_2S_3$, and $MeS_3{}^nPr$, used to create graphs in Figures S3.8 – S3.21.

Equimolar Trisulfide mix	**Integrated Abundance**		
	Me_2S_3	**$MeS_3{}^nPr$**	**$^nPr_2S_3$**
	1884615	0	1996651

Equimolar Trisulfide mix	**Relative Ratios**		
	Me_2S_3	**$MeS_3{}^nPr$**	**$^nPr_2S_3$**
	48.6	0.0	51.4

DMF 5% v/v	**Integrated Abundance**		
Time (minutes)	**Me_2S_3**	**$MeS_3{}^nPr$**	**$^nPr_2S_3$**
0	1884615	0	1996651
1	16211590	0	19423775
2	19503225	0	22850514
3	18703095	0	21561157
4	17783470	0	21366482
5	16804838	0	20237933
6	18436015	0	21083093
8	19426284	0	22354977
10	17931247	0	21706118
12	14172873	0	17443697
15	15897561	0	19294384
20	19742524	0	23351922
25	19513604	0	23562091
30	13898479	0	17380208
40	15743695	0	19426081
50	23643561	0	27227513
60	17634505	0	20157237

DMF 5% v/v	**Relative Ratios**		
Time (minutes)	**Me_2S_3**	**$MeS_3{}^nPr$**	**$^nPr_2S_3$**
0	48.6	0.0	51.4
1	45.5	0.0	54.5
2	46.0	0.0	54.0
3	46.5	0.0	53.5
4	45.4	0.0	54.6
5	45.4	0.0	54.6
6	46.7	0.0	53.3
8	46.5	0.0	53.5
10	45.2	0.0	54.8
12	44.8	0.0	55.2
15	45.2	0.0	54.8
20	45.8	0.0	54.2
25	45.3	0.0	54.7
30	44.4	0.0	55.6
40	44.8	0.0	55.2
50	46.5	0.0	53.5
60	46.7	0.0	53.3

DMF 7.5% v/v	**Integrated Abundance**		
Time (minutes)	**Me_2S_3**	**$MeS_3{}^nPr$**	**$^nPr_2S_3$**
0	1884615	0	1996651
1	20462868	0	23953530
2	13279077	0	16375309
3	18953327	27887	23260124
4	14434120	23096	17669350
5	14184572	25147	17701118
6	18819751	38037	22152264
8	17887487	38725	21138332
10	14836954	35509	18148584
12	16520837	52875	19796913
15	16070251	66011	20150310
20	19111646	103843	22434663

DMF 7.5% v/v	**Relative Ratios**		
Time (minutes)	**Me_2S_3**	**$MeS_3{}^nPr$**	**$^nPr_2S_3$**
0	48.6	0.0	51.4
1	46.1	0.0	53.9
2	44.8	0.0	55.2
3	44.9	0.1	55.1
4	44.9	0.1	55.0
5	44.5	0.1	55.5
6	45.9	0.1	54.0
8	45.8	0.1	54.1
10	44.9	0.1	55.0
12	45.4	0.1	54.4
15	44.3	0.2	55.5
20	45.9	0.2	53.9

25	18032826	135799	22167450
30	17368902	154320	20804224
40	13244114	176457	16556398
50	16589344	335907	19845702
60	15624493	430652	18799850

25	44.7	0.3	55.0
30	45.3	0.4	54.3
40	44.2	0.6	55.2
50	45.1	0.9	54.0
60	44.8	1.2	53.9

DMF 10% v/v	**Integrated Abundance**		
Time (minutes)	**Me_2S_3**	**$MeS_3{}^nPr$**	**$^nPr_2S_3$**
0	1884615	0	1996651
1	17648192	33871	19682120
2	15536299	43106	17546970
3	17295385	65911	20082677
4	15611615	74396	18093462
5	17749375	111157	20813644
6	16548726	117354	19061957
8	18027281	175247	20628354
10	17387369	216194	20588675
12	13783917	191789	16052105
15	16869728	324027	19562473
20	16750013	485771	20330013
25	14999158	560475	18019864
30	15495850	778770	18253533
40	20128184	1659761	22913802
50	16019251	1839547	19286327
60	16631953	2472442	18937310

DMF 10% v/v	**Relative Ratios**		
Time (minutes)	**Me_2S_3**	**$MeS_3{}^nPr$**	**$^nPr_2S_3$**
0	48.6	0.0	51.4
1	47.2	0.1	52.7
2	46.9	0.1	53.0
3	46.2	0.2	53.6
4	46.2	0.2	53.6
5	45.9	0.3	53.8
6	46.3	0.3	53.4
8	46.4	0.5	53.1
10	45.5	0.6	53.9
12	45.9	0.6	53.5
15	45.9	0.9	53.2
20	44.6	1.3	54.1
25	44.7	1.7	53.7
30	44.9	2.3	52.9
40	45.0	3.7	51.3
50	43.1	5.0	51.9
60	43.7	6.5	49.8

DMF 12.5% v/v	**Integrated Abundance**		
Time (minutes)	**Me_2S_3**	**$MeS_3{}^nPr$**	**$^nPr_2S_3$**
0	1884615	0	1996651
1	20405391	87538	23903124
2	17198556	151347	19617303
3	16044173	224655	18818133
4	17913309	378237	21722527
5	15622207	398596	18177657
6	15267417	497560	18174240
8	16833883	804541	20483494
10	18081217	1136379	20944456
12	18675227	1540687	22451533
15	15672783	1625668	18822841
20	14099183	2077207	16972423
25	13184707	2431843	15333648
30	17878410	4265526	20981667

DMF 12.5% v/v	**Relative Ratios**		
Time (minutes)	**Me_2S_3**	**$MeS_3{}^nPr$**	**$^nPr_2S_3$**
0	48.6	0.0	51.4
1	46.0	0.2	53.8
2	46.5	0.4	53.1
3	45.7	0.6	53.6
4	44.8	0.9	54.3
5	45.7	1.2	53.2
6	45.0	1.5	53.5
8	44.2	2.1	53.7
10	45.0	2.8	52.1
12	43.8	3.6	52.6
15	43.4	4.5	52.1
20	42.5	6.3	51.2
25	42.6	7.9	49.5
30	41.5	9.9	48.7

40	15795831	5165800	19028096
50	14867340	6094507	18010506
60	14449048	7096862	17543286

40	39.5	12.9	47.6
50	38.1	15.6	46.2
60	37.0	18.2	44.9

DMF 15% v/v	**Integrated Abundance**		
Time (minutes)	**Me_2S_3**	**$MeS_3{}^nPr$**	**$^nPr_2S_3$**
0	1884615	0	1996651
1	15310644	141751	18291956
2	14467937	288519	17107998
3	15270113	493757	18284633
4	17930989	797029	20583136
5	14482416	759393	16767630
6	18696975	1239391	21372984
8	14052274	1134925	16712522
10	18152298	1887077	20879833
12	16423142	1995785	19276192
15	14988958	2201786	17992860
20	12871716	2341678	15168069
25	14477138	3228586	16789274
30	14043972	3827188	16842781
52	16502374	7414857	19410474
60	16016240	8057590	18670253
71	10979705	6276191	13237452

DMF 15% v/v	**Relative Ratios**		
Time (minutes)	**Me_2S_3**	**$MeS_3{}^nPr$**	**$^nPr_2S_3$**
0	48.6	0.0	51.4
1	45.4	0.4	54.2
2	45.4	0.9	53.7
3	44.8	1.5	53.7
4	45.6	2.0	52.4
5	45.2	2.4	52.4
6	45.3	3.0	51.7
8	44.1	3.6	52.4
10	44.4	4.6	51.0
12	43.6	5.3	51.1
15	42.6	6.3	51.1
20	42.4	7.7	49.9
25	42.0	9.4	48.7
30	40.5	11.0	48.5
52	38.1	17.1	44.8
60	37.5	18.9	43.7
71	36.0	20.6	43.4

DMF 20% v/v	**Integrated Abundance**		
Time (minutes)	**Me_2S_3**	**$MeS_3{}^nPr$**	**$^nPr_2S_3$**
0	1884615	0	1996651
1	10858385	525771	12404952
2	14353898	1575065	16563420
3	11508930	2058157	14027137
4	10573394	2561090	12902818
5	11860551	3556206	13910903
6	12973941	4813828	15781007
8	13575527	6556200	15977146
10	12045583	7193021	14312811
12	12591933	8871187	15033546
15	11368720	9580942	13384133
20	11693629	12344492	13657883
25	9346742	11309020	10534652
30	10061415	13790602	11904805
52	7093915	11976271	8064260
60	8131696	13712763	8918389

DMF 20% v/v	**Relative Ratios**		
Time (minutes)	**Me_2S_3**	**$MeS_3{}^nPr$**	**$^nPr_2S_3$**
0	48.6	0.0	51.4
1	45.6	2.2	52.1
2	44.2	4.8	51.0
3	41.7	7.5	50.8
4	40.6	9.8	49.6
5	40.4	12.1	47.4
6	38.6	14.3	47.0
8	37.6	18.2	44.2
10	35.9	21.4	42.7
12	34.5	24.3	41.2
15	33.1	27.9	39.0
20	31.0	32.7	36.2
25	30.0	36.3	33.8
30	28.1	38.6	33.3
52	26.1	44.1	29.7
60	26.4	44.6	29.0

71	8000182	14183520	9342812

71	25.4	45.0	29.6

DMF 25% v/v	**Integrated Abundance**		
Time (minutes)	**Me_2S_3**	**$MeS_3{}^nPr$**	**$^nPr_2S_3$**
0	1884615	0	1996651
1	11177788	2461463	12669201
2	11259602	5046273	13222415
3	11305843	7336264	13273534
4	8950456	7324862	10314377
5	10344192	10402320	12373090
6	11195146	12846090	12916172
8	8714162	12004427	10311667
10	9385879	14108014	10760109
12	7805513	12783541	8991978
15	6844289	12171861	8198922
20	5373001	10006733	6198659
25	6602790	12241951	7765243
30	5845791	10829721	6633297
40	6842169	12690047	7872944
50	7655034	14032207	8785500
60	7600520	14076343	8986618

DMF 25% v/v	**Relative Ratios**		
Time (minutes)	**Me_2S_3**	**$MeS_3{}^nPr$**	**$^nPr_2S_3$**
0	48.6	0.0	51.4
1	42.5	9.4	48.2
2	38.1	17.1	44.8
3	35.4	23.0	41.6
4	33.7	27.5	38.8
5	31.2	31.4	37.4
6	30.3	34.8	34.9
8	28.1	38.7	33.2
10	27.4	41.2	31.4
12	26.4	43.2	30.4
15	25.1	44.7	30.1
20	24.9	46.4	28.7
25	24.8	46.0	29.2
30	25.1	46.5	28.5
40	25.0	46.3	28.7
50	25.1	46.0	28.8
60	24.8	45.9	29.3

DMF 30% v/v	**Integrated Abundance**		
Time (minutes)	**Me_2S_3**	**$MeS_3{}^nPr$**	**$^nPr_2S_3$**
0	1884615	0	1996651
1	12124513	4208390	14716644
2	4686311	3049441	5587138
3	9244904	8858319	10923651
4	7412120	9117321	8791993
5	7423261	10747260	9006351
6	6575259	10364523	7671827
8	7121192	12387405	8451095
10	5397219	9807606	6237386
12	7532007	13933016	9071711
15	7596638	14319285	9355281
20	7453830	13752519	8766156
25	7303840	13719326	8786100
30	6878128	12813460	8117949
40	7776808	14419219	9222281

DMF 30% v/v	**Relative Ratios**		
Time (minutes)	**Me_2S_3**	**$MeS_3{}^nPr$**	**$^nPr_2S_3$**
0	48.6	0.0	51.4
1	39.0	13.6	47.4
2	35.2	22.9	41.9
3	31.8	30.5	37.6
4	29.3	36.0	34.7
5	27.3	39.5	33.1
6	26.7	42.1	31.2
8	25.5	44.3	30.2
10	25.2	45.7	29.1
12	24.7	45.6	29.7
15	24.3	45.8	29.9
20	24.9	45.9	29.2
25	24.5	46.0	29.5
30	24.7	46.1	29.2
40	24.8	45.9	29.4

DMF 35% v/v	**Integrated Abundance**

DMF 35% v/v	**Relative Ratios**

Time (minutes)	Me_2S_3	$MeS_3{}^nPr$	$^nPr_2S_3$
0	1884615	0	1996651
1	9364421	5853524	11295231
2	8915346	10729072	10796036
3	6644026	10261493	7902186
4	6442668	11360385	7676499
5	6300029	11717367	7575968
6	6651328	12279157	7741782
8	5895795	10950209	6702511
10	5260142	9841340	6101980
12	5937371	11197802	6917706
15	5886707	11145173	6945482
20	6506236	12279913	7833524
25	6574842	12463633	7903169
30	5136349	9707583	5926459
40	6759231	12545902	7882062

Time (minutes)	Me_2S_3	$MeS_3{}^nPr$	$^nPr_2S_3$
0	48.6	0.0	51.4
1	35.3	22.1	42.6
2	29.3	35.2	35.5
3	26.8	41.4	31.9
4	25.3	44.6	30.1
5	24.6	45.8	29.6
6	24.9	46.0	29.0
8	25.0	46.5	28.5
10	24.8	46.4	28.8
12	24.7	46.6	28.8
15	24.6	46.5	29.0
20	24.4	46.1	29.4
25	24.4	46.3	29.3
30	24.7	46.7	28.5
40	24.9	46.1	29.0

DMF 50% v/v	**Integrated Abundance**		
Time (minutes)	**Me_2S_3**	**$MeS_3{}^nPr$**	**$^nPr_2S_3$**
0	1884615	0	1996651
1	4558088	6255803	5154378
2	4170413	7680299	4899382
3	4638702	8462673	5028552
4	3755465	7020334	4125643
5	3742881	7061173	4145959
6	4408723	8443864	5080073
8	4751437	9023262	5618175
10	3847304	7548374	4545713
20	3269129	6107058	3599518
40	3572321	6759907	4128460
60	3278628	6093581	3560672

DMF 50% v/v	**Relative Ratios**		
Time (minutes)	**Me_2S_3**	**$MeS_3{}^nPr$**	**$^nPr_2S_3$**
0	48.6	0.0	51.4
1	28.5	39.2	32.3
2	24.9	45.9	29.2
3	25.6	46.7	27.7
4	25.2	47.1	27.7
5	25.0	47.2	27.7
6	24.6	47.1	28.3
8	24.5	46.5	29.0
10	24.1	47.4	28.5
20	25.2	47.1	27.7
40	24.7	46.7	28.5
60	25.4	47.1	27.5

DMF 50% v/v	**Integrated Abundance**		
Time (seconds)	**Me_2S_3**	**$MeS_3{}^nPr$**	**$^nPr_2S_3$**
0	1884615	0	1996651
10	5379379	2241061	6636277
20	6024141	3989925	7361857
30	5165853	4511419	6367206
40	4588293	5031183	5641476
50	4094039	5147601	4954729
60	4305955	6112158	5216643

DMF 50% v/v	**Relative Ratios**		
Time (seconds)	**Me_2S_3**	**$MeS_3{}^nPr$**	**$^nPr_2S_3$**
0	48.6	0.0	51.4
10	37.7	15.7	46.5
20	34.7	23.0	42.4
30	32.2	28.1	39.7
40	30.1	33.0	37.0
50	28.8	36.3	34.9
60	27.5	39.1	33.4

90	3850819	6674181	4634711
120	3668713	6675479	4225121
250	1995230	3730527	2125175
300	2980726	5803921	3500513
420	3769482	7342775	4572695

90	25.4	44.0	30.6
120	25.2	45.8	29.0
250	25.4	47.5	27.1
300	24.3	47.2	28.5
420	24.0	46.8	29.2

DMF 75% v/v	**Integrated Abundance**		
Time (seconds)	**Me_2S_3**	**$MeS_3{}^nPr$**	**$^nPr_2S_3$**
0	1884615	0	1996651
10	3570613	2071363	4117415
20	3364275	2948379	3944078
30	2358483	2705550	2792974
40	1560434	2117676	1786803
50	1380734	2073912	1525076
60	2526974	4372038	3167357
90	1542701	2966856	1783106
120	1587186	3079953	1787150
180	1798090	3551395	2093292
240	2377923	4684431	2807109
300	1839395	3621198	2086006

DMF 75% v/v	**Relative Ratios**		
Time (seconds)	**Me_2S_3**	**$MeS_3{}^nPr$**	**$^nPr_2S_3$**
0	48.6	0.0	51.4
10	36.6	21.2	42.2
20	32.8	28.7	38.5
30	30.0	34.4	35.5
40	28.6	38.8	32.7
50	27.7	41.6	30.6
60	25.1	43.4	31.5
90	24.5	47.1	28.3
120	24.6	47.7	27.7
180	24.2	47.7	28.1
240	24.1	47.5	28.4
300	24.4	48.0	27.6

DMF 87.5% v/v	**Integrated Abundance**		
Time (seconds)	**Me_2S_3**	**$MeS_3{}^nPr$**	**$^nPr_2S_3$**
0	1884615	0	1996651
10	1453451	700964	1624793
20	1165942	802653	1259720
30	1210501	1113115	1300853
40	1371517	1562027	1476251
50	1163622	1526878	1219336
60	1330391	2018236	1498564
90	849644	1425647	843451
120	1158909	2101648	1221543
180	988491	1833469	1009136
240	876168	1687202	940975
300	907559	1723143	932092

DMF 87.5% v/v	**Relative Ratios**		
Time (seconds)	**Me_2S_3**	**$MeS_3{}^nPr$**	**$^nPr_2S_3$**
0	48.6	0.0	51.4
10	38.5	18.5	43.0
20	36.1	24.9	39.0
30	33.4	30.7	35.9
40	31.1	35.4	33.5
50	29.8	39.1	31.2
60	27.4	41.6	30.9
90	27.2	45.7	27.0
120	25.9	46.9	27.3
180	25.8	47.9	26.3
240	25.0	48.1	26.9
300	25.5	48.4	26.2

DMF 95% v/v	**Integrated Abundance**		
Time (seconds)	**Me_2S_3**	**$MeS_3{}^nPr$**	**$^nPr_2S_3$**
0	1884615	0	1996651

DMF 95% v/v	**Relative Ratios**		
Time (seconds)	**Me_2S_3**	**$MeS_3{}^nPr$**	**$^nPr_2S_3$**
0	48.6	0.0	51.4

10	447202	98009	377275	10	48.5	10.6	40.9
20	472973	159631	439785	20	44.1	14.9	41.0
30	369421	150904	297175	30	45.2	18.5	36.4
40	507080	284456	433918	40	41.4	23.2	35.4
50	601492	442582	569616	50	37.3	27.4	35.3
60	417943	324778	376331	60	37.3	29.0	33.6
90	347978	361897	309597	90	34.1	35.5	30.4
120	302903	349398	228417	120	34.4	39.7	25.9
180	359712	564445	313299	180	29.1	45.6	25.3
240	336285	521208	237995	240	30.7	47.6	21.7
300	319690	566192	275658	300	27.5	48.7	23.7

Me_2S_3 and $^nPr_2S_3$ crossover at 80 ºC (neat, no light)

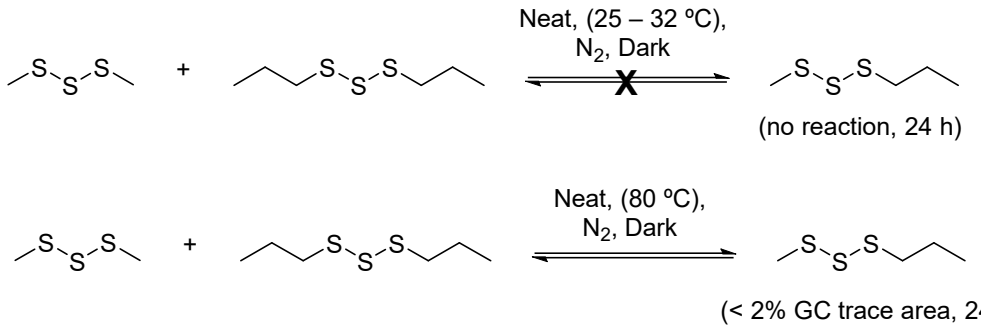

Dimethyl trisulfide (126 µL, 1.20 mmol, 1.0 eq.) and di-n-propyl trisulfide (203 µL, 1.20 mmol, 1.0 eq.) were added to two separate 5 mL glass vials equipped with a stir bar, sealed with rubber septum, and covered with aluminium foil. Both reactions were conducted in the dark under an atmosphere of nitrogen. One reaction was stirred at room temperature (25 – 32 ºC), and the other at 80 ºC. At 1 hour and 24 hours, a 10 µL reaction aliquot was diluted to 1 mL with chloroform for GC-MS analysis. More crossover product, $MeS_3{}^nPr$, was observed in the reaction heated at 80 ºC, however, the formation of $MeS_3{}^nPr$ is still slow (< 2% of the total GC trace area). The thermal disproportionation of Me_2S_3 at 80 ºC has been previously studied.[3] The thermal exchange reaction between diethyl trisulfide (Et_2S_3) and di-*n*-propyl trisulfide ($^nPr_2S_3$) at > 130 ºC has been previously studied.[4] For the reaction of neat trisulfides at room temperature, after 7 days the area percentage of $MeS_3{}^nPr$ was found to be ~5% by GC-MS.

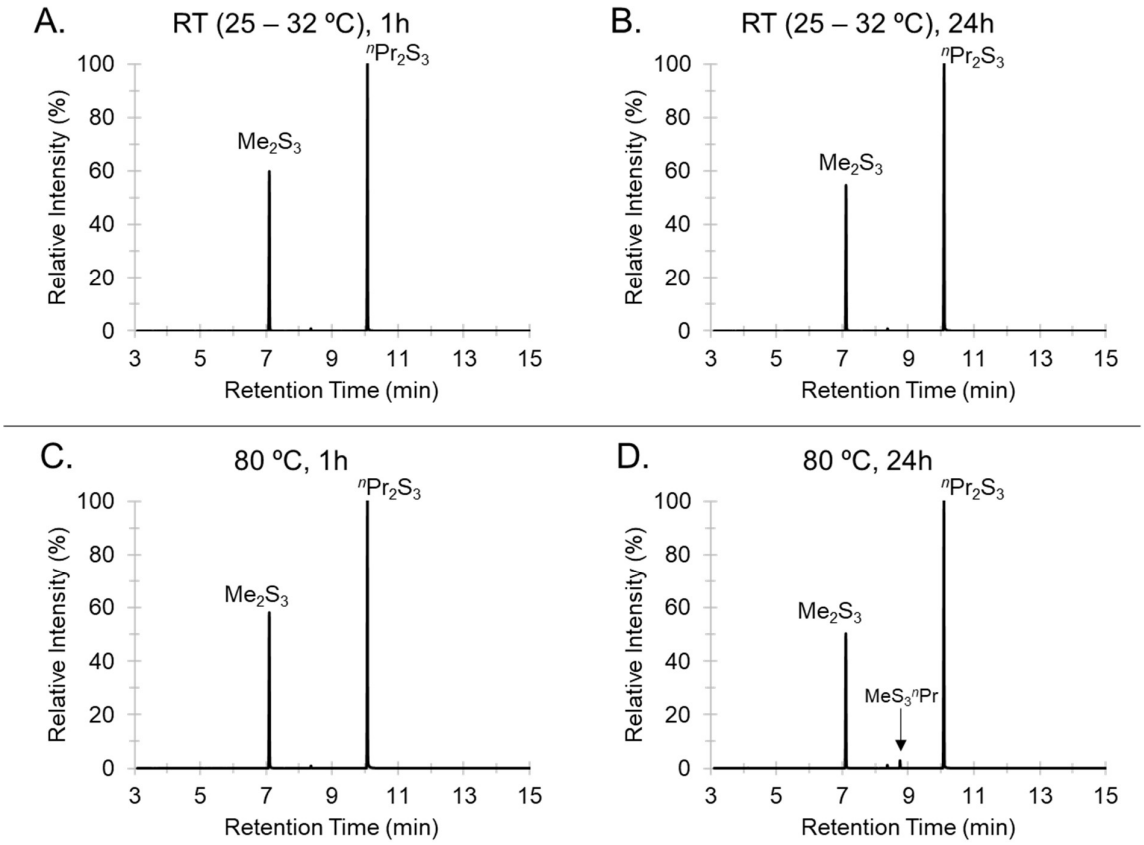

Figure S3.22: GC traces for the crossover reaction between dimethyl Me_2S_3 and $^{n}Pr_2S_3$, without solvent. (A, B) The trisulfides (1 eq. each) at room temperature (25 – 32 ºC) after 1 h and 24 h. (C, D) The trisulfides (1 eq. each) at 80 °C after 1 h and 24 h. GC-MS method A. Retention time: Me_2S_3 (7.10 min), $^{n}Pr_2S_2$ (8.36 min, impurity from $^{n}Pr_2S_3$), $MeS_3{}^{n}Pr$ (8.75 min), and $^{n}Pr_2S_3$ (10.09 min).

Me_2S_3 and $^{n}Pr_2S_3$ crossover in DMF/chlorobenzene mixtures

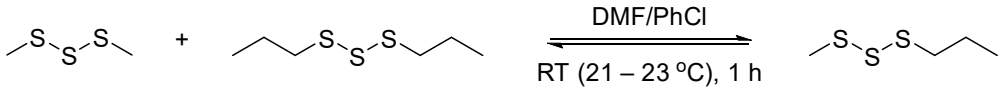

Dimethyl trisulfide (42 µL, 0.4 mmol) and di-*n*-propyl trisulfide (68 µL, 0.4 mmol) were added to a glass vial containing 2 mL of the mixed solvent. The solvents used were made up to 2 mL with varying ratios of DMF to PhCl giving a total of three reactions at: 1%, 5%, and 10% v/v DMF/PhCl. Reactions were stirred for 1 hour at room temperature (21 – 23 °C). A 10 µL reaction aliquot was diluted to 1 mL using chloroform for GC-MS analysis after 5 minutes and 1 hour of reaction time.

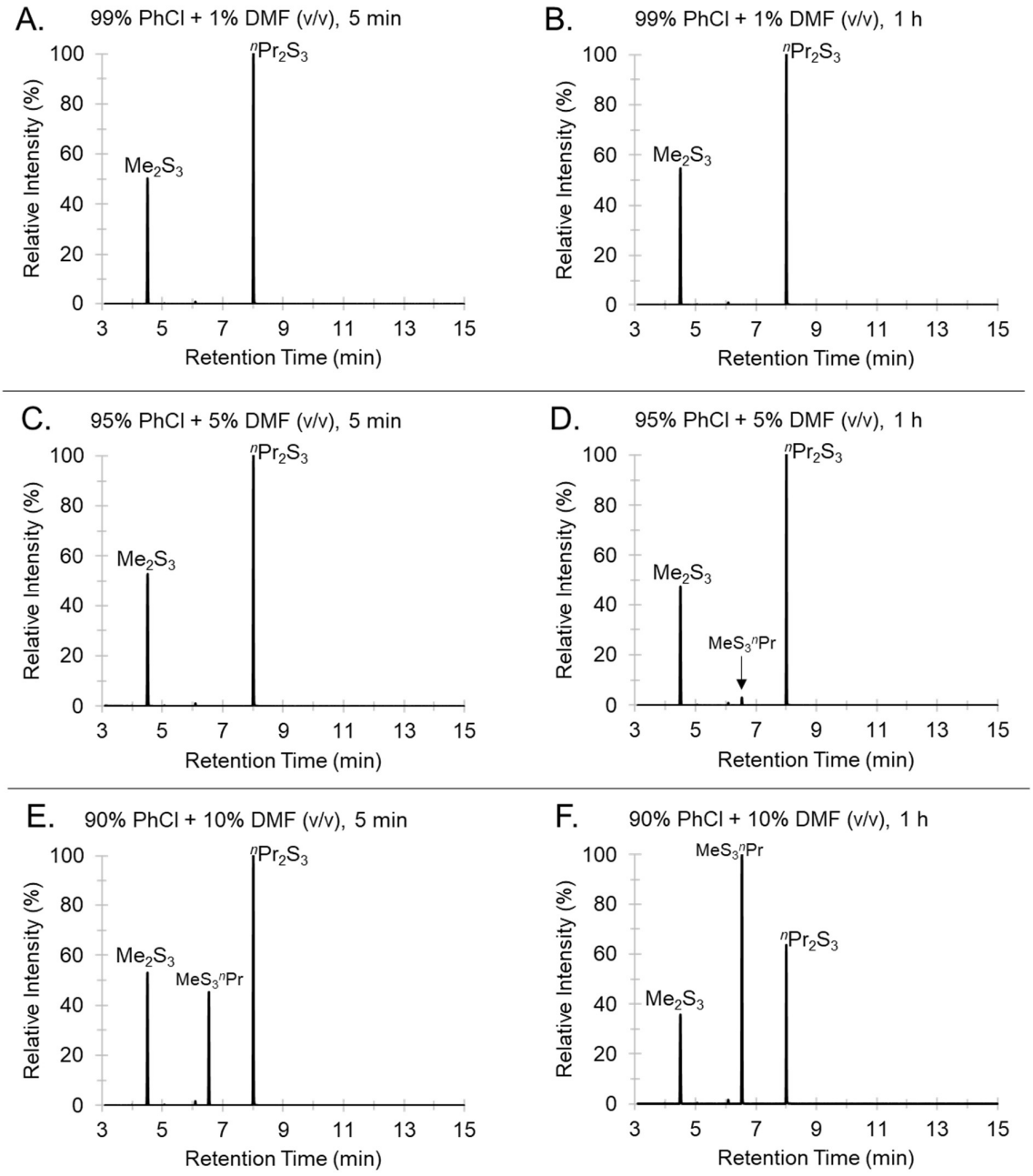

Figure S3.23: GC traces for crossover reaction between dimethyl trisulfide (Me_2S_3) and di-*n*-propyl trisulfide ($^nPr_2S_3$) in DMF/PhCl at varying concentration (1 – 10% v/v DMF content) after 1 hour at room temperature (21 – 23 °C). (A, B) The trisulfides in 1% DMF after 5 min and 1 h. (C, D) The trisulfides in 5% DMF after 5 min and 1 h. (E, F) The trisulfides in 10% DMF after 5 min and 1 h. GC-MS method C. Retention time: Me_2S_3 (4.50 min), $^nPr_2S_2$ (6.08 min) – impurity from dipropyl trisulfide, $MeS_3{}^nPr$ (6.54 min), and $^nPr_2S_3$ (8.01 min).

Solvents that promote slower crossover of Me_2S_3 and $^nPr_2S_3$

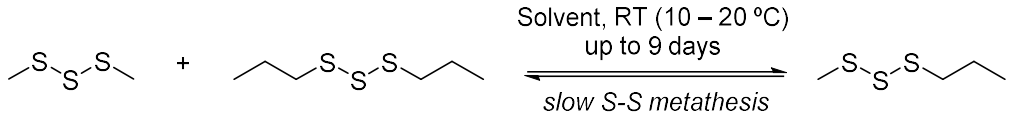

Dimethyl trisulfide (1.0 eq.) and di-*n*-propyl trisulfide (1.0 eq.) were added to a 2 mL glass vial equipped with a magnetic stir bar, followed by a selected solvent (1.0 eq. or 10 eq.). The mixture was then stirred for several days. After reaching allocated reaction time, a 10 µL aliquot was removed and diluted to 1 mL with chloroform for GC-MS analysis.

GC traces of the crossover reaction in dry formamide

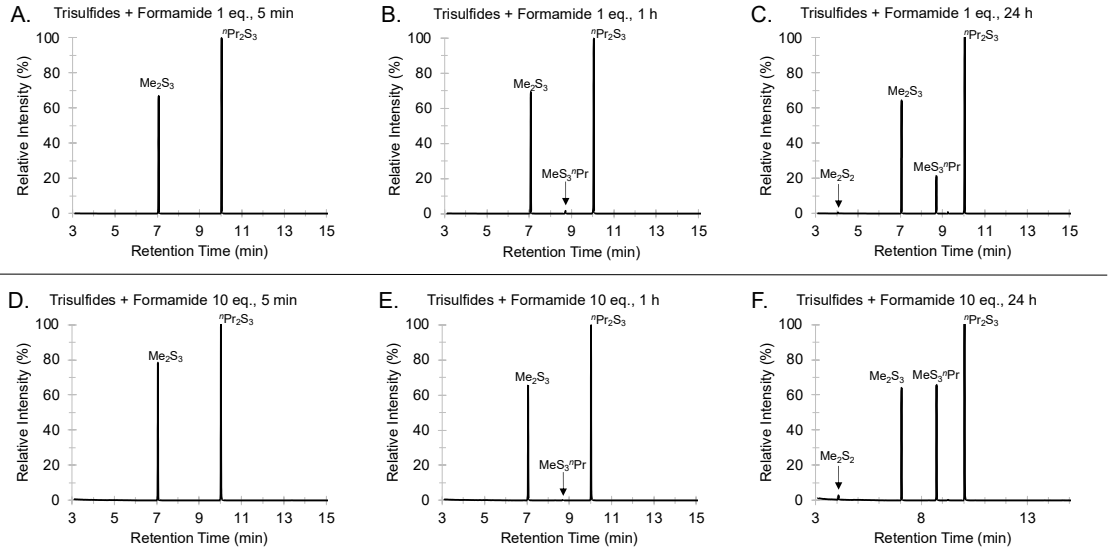

Figure S3.24: GC traces for the room temperature (12 – 26 ºC) crossover reactions between dimethyl trisulfide (42 µL, 0.4 mmol, 1 eq.) and di-*n*-propyl trisulfide (67.8 µL, 0.4 mmol, 1 eq.), and formamide (16 µL, 0.4 mmol, 1 eq. or 159 µL, 4.0 mmol, 10 eq.). (A, B, C) GC traces after 5 min, 1 h, and 24 h using 1 eq. of formamide. (D, E, F) GC traces after 5 min, 1 h, and 24 h using 10 eq. of formamide. After 24 h, 11% $MeS_3{}^nPr$ (1 eq. of formamide) and 28% $MeS_3{}^nPr$ (10 eq. of formamide) were formed. The GCMS method A. Retention time: Me_2S_3 (7.06 min), $MeS_3{}^nPr$ (8.71 min), and $^nPr_2S_3$ (10.03 min). It should be noted that a two-phases (heterogenous) solution was observed in a mixture of the trisulfides and 1 eq. of formamide.

GC traces of the crossover reaction in 4-Methyl-1,3-dioxolan-2-one (propylene carbonate)

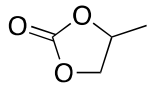

(4-Methyl-1,3-dioxolan-2-one)

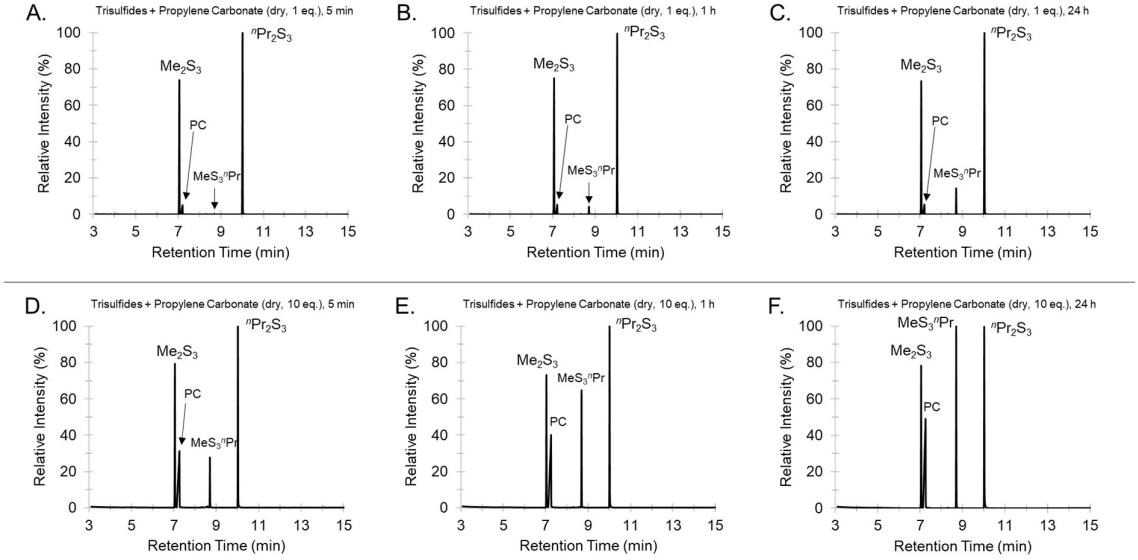

Figure S3.25: GC traces of the room temperature (24 – 27 ºC) reaction between dimethyl trisulfide, di-*n*-propyl trisulfide, and propylene carbonate. (A, B, C) The trisulfides (42 µL, 0.4 mmol, 1 eq. for dimethyl trisulfide and 68 µL, 0.4 mmol, 1 eq. for di-*n*-propyl trisulfide) with dry propylene carbonate (34 µL, 0.4 mmol, 1 eq.) after 5 min, 1 h, and 24 h (*this forms a heterogenous mixture*). (D, E, F) The trisulfides (42 µL, 0.4 mmol, 1 eq. for dimethyl trisulfide and 68 µL, 0.4 mmol, 1 eq. for di-*n*-propyl trisulfide) with dry propylene carbonate (340 µL, 4.0 mmol, 10 eq.) after 5 min, 1 h, and 24 h. GC-MS method A. Retention time: Me_2S_3 (7.10 min), propylene carbonate (PC) (7.22 min), $MeS_3{}^nPr$ (8.75 min), and $^nPr_2S_3$ (10.09 min).

GC traces of the crossover reaction in furan-2-carbaldehyde (furfural)

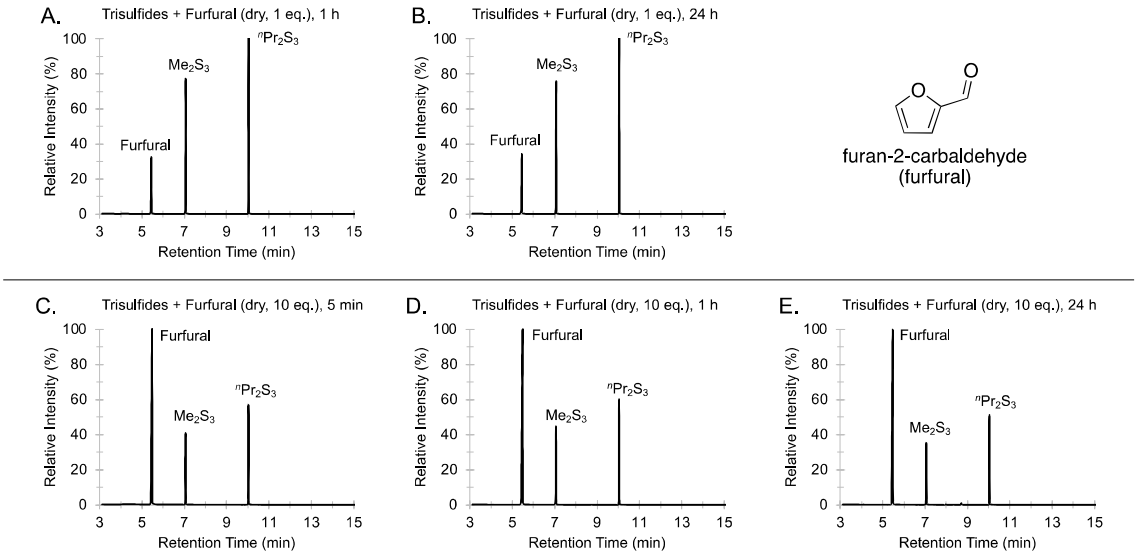

Figure S3.26: GC traces of the room temperature (8 – 12 ºC) reaction between dimethyl trisulfide, di-*n*-propyl trisulfide, and dry furfural. (A, B) Trisulfides (42 µL, 0.4 mmol, 1 eq. for dimethyl trisulfide and 68 µL, 0.4 mmol, 1 eq. for di-*n*-propyl trisulfide) with dry furfural (33.2 µL, 0.4 mmol, 1 eq.) after 1 h and 24 h, (C, D, E) Trisulfides (42 µL, 0.4 mmol, 1 eq. for dimethyl trisulfide and 68 µL, 0.4 mmol, 1 eq. for di-*n*-propyl trisulfide) with dry furfural (332 µL, 4.0 mmol, 10 eq.) after 5 min, 1 h, and 24 h. GC-MS method A. Retention time: furfural (5.45 min), Me_2S_3 (7.10 min), $^{n}Pr_2S_2$ (8.36 min, impurity from dipropyl trisulfide), $MeS_3{}^{n}Pr$ (8.75 min), and $^{n}Pr_2S_3$ (10.09 min).

GC traces of the crossover reaction in ε-caprolactone

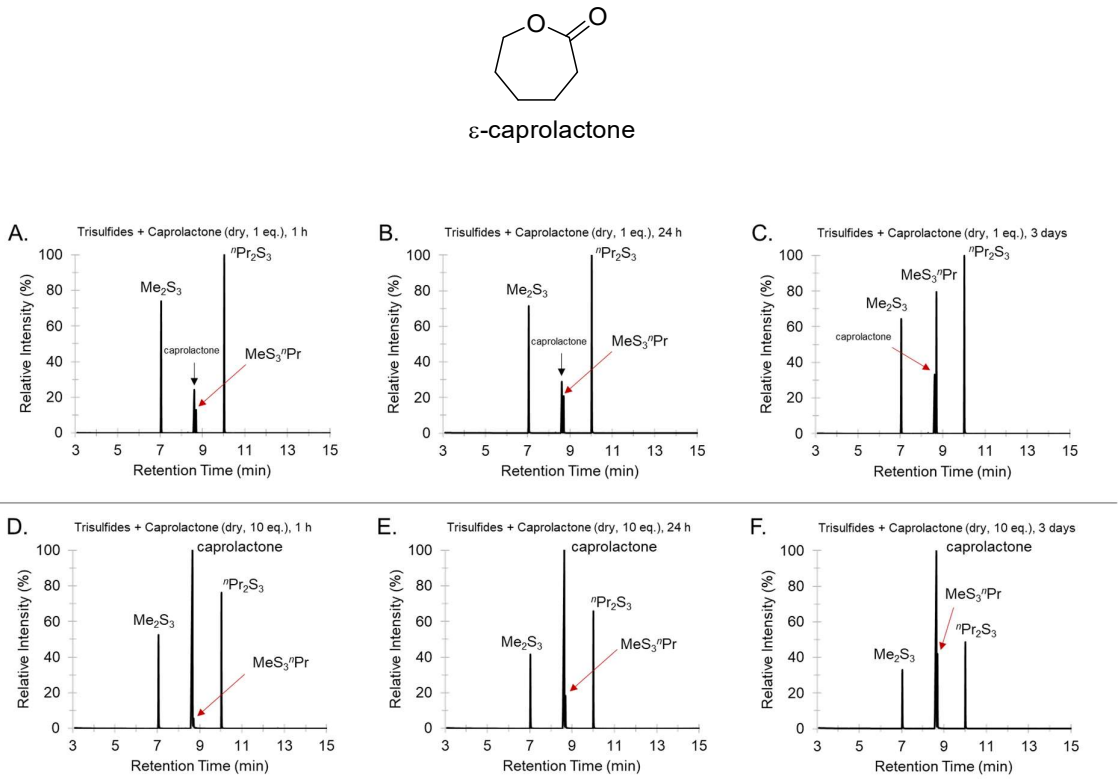

Figure S3.27: GC traces of the room temperature (12 – 18 ºC) reaction between dimethyl trisulfide, di-*n*-propyl trisulfide, and ε-caprolactone. (A, B, C) The trisulfides (42 µL, 0.4 mmol, 1 eq. for dimethyl trisulfide and 68 µL, 0.4 mmol, 1 eq. for di-*n*-propyl trisulfide) with dry ε-caprolactone (44.2 µL, 0.4 mmol, 1 eq.) after 1 h, 24 h, and 3 days. (D, E, F) The trisulfides (42 µL, 0.4 mmol, 1 eq. for dimethyl trisulfide and 68 µL, 0.4 mmol, 1 eq. for di-*n*-propyl trisulfide) with dry ε-caprolactone (442 µL, 4.0 mmol, 10 eq.) after 1 h, 24 h, and 3 days. GC-MS method A. Retention time: Me_2S_3 (7.10 min), ε-caprolactone (8.63 min), $MeS_3{}^nPr$ (8.75 min), and $^nPr_2S_3$ (10.09 min).

GC traces of the crossover reaction in dihydrolevoglucosenone (Cyrene™)

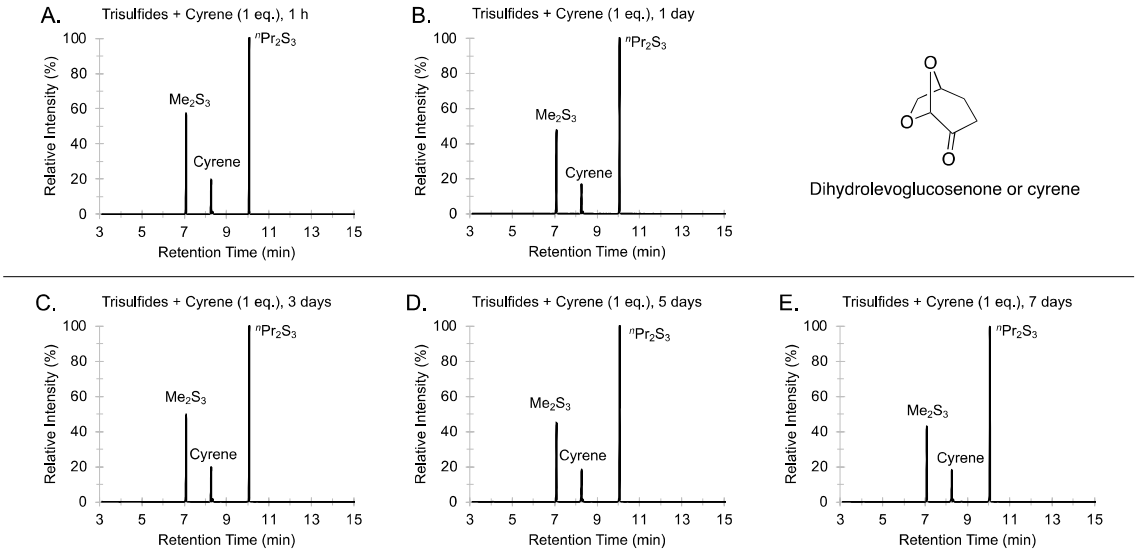

Figure S3.28: GC traces of the room temperature (15 – 24 ºC) reaction between dimethyl trisulfide (Me_2S_3) (126.2 µL, 1.2 mmol, 1 eq.), di-*n*-propyl trisulfide ($^{n}Pr_2S_3$) (203.4 µL, 1.2 mmol, 1 eq.), and dihydrolevoglucosenone (cyrene) (123 µL, 1.2 mmol, 1 eq.) after (A) 1 hour, (B) 1 day, (C) 3 days, (D) 5 days, and (E) 7 days. GC-MS method A. Retention time: Me_2S_3 (7.10 min), cyrene (8.26 min), $^{n}Pr_2S_2$ (8.36 min, impurity from dipropyl trisulfide), $MeS_3{}^{n}Pr$ (8.75 min), and $^{n}Pr_2S_3$ (10.09 min).

GC traces of the crossover reaction in nitromethane

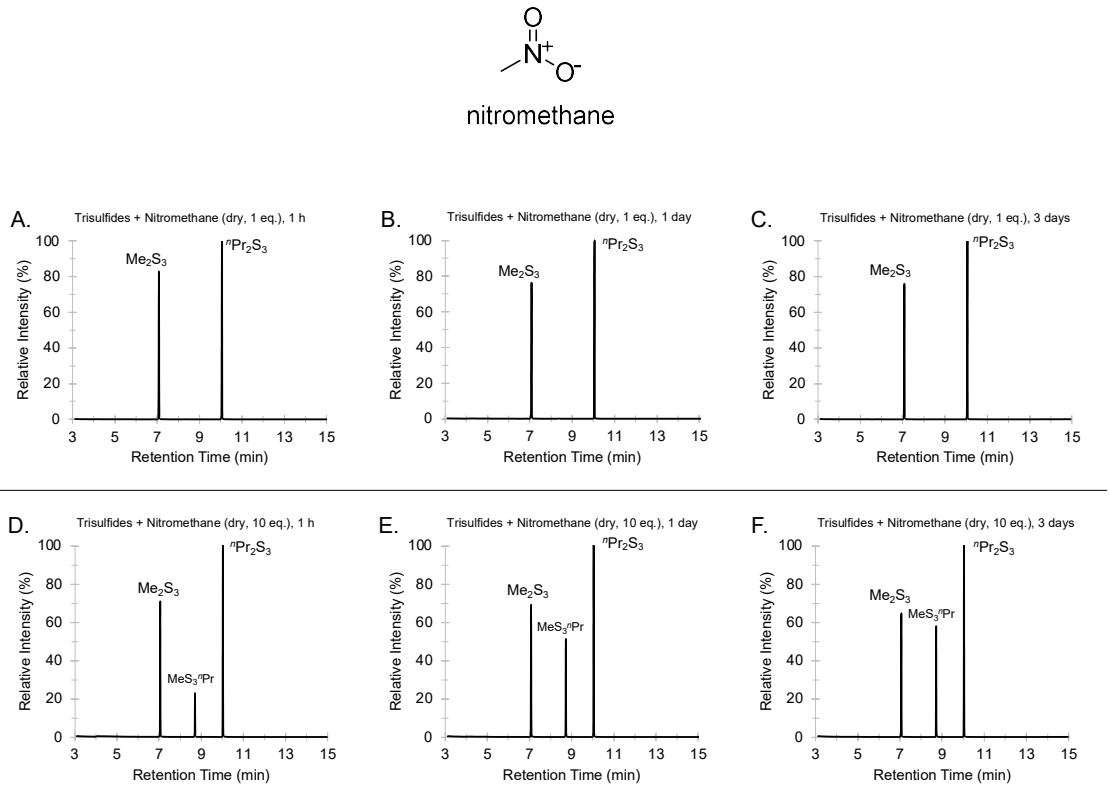

Figure S3.29: GC traces of the room temperature (15 – 19 ºC) reaction between dimethyl trisulfide, di-*n*-propyl trisulfide, and dry nitromethane. (A, B, C) Trisulfides (42 µL, 0.4 mmol, 1 eq. for dimethyl trisulfide and 68 µL, 0.4 mmol, 1 eq. for di-*n*-propyl trisulfide) with dry nitromethane (21.6 µL, 0.4 mmol, 1 eq.) after 1 h, 1 day, and 3 days. (D, E, F) Trisulfides (42 µL, 0.4 mmol, 1 eq. for dimethyl trisulfide and 68 µL, 0.4 mmol, 1 eq. for di-*n*-propyl trisulfide) with dry nitromethane (216 µL, 4.0 mmol, 10 eq.) 1 h, 1 day, and 3 days. GC-MS method A. Retention time: Me_2S_3 (7.10 min), $MeS_3{}^nPr$ (8.75 min), and ${}^nPr_2S_3$ (10.09 min).

GC traces of the crossover reaction in acetonitrile

(Data was obtained from Ryan Shapter – see ref.5)

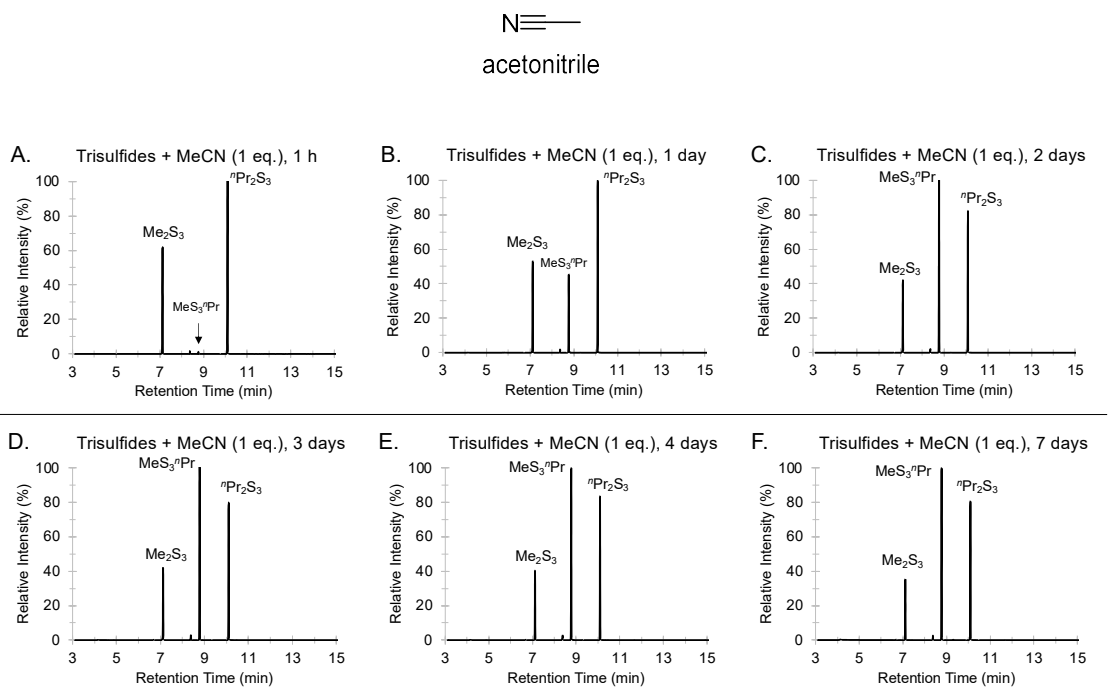

Figure S3.30: GC traces of the room temperature (20 °C) crossover reaction between dimethyl trisulfide (Me_2S_3) (126.2 µL, 1.2 mmol, 1 eq.), di-*n*-propyl trisulfide ($^{n}Pr_2S_3$) (203.4 µL, 1.2 mmol, 1 eq.), and acetonitrile (62.6 µL, 1.2 mmol, 1.2 eq.) after (A) 1 hour, (B) 1 day (C) 2 days, (D) 3 days, (E) 4 days, and (F) 7 days (1 week). GC-MS method A. Retention time: Me_2S_3 (7.10 min), $^{n}Pr_2S_2$ (8.36 min, impurity from dipropyl trisulfide), $MeS_3{}^{n}Pr$ (8.75 min), and $^{n}Pr_2S_3$ (10.09 min).

GC traces of the crossover reaction in nitrobenzene

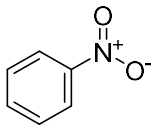

nitrobenzene

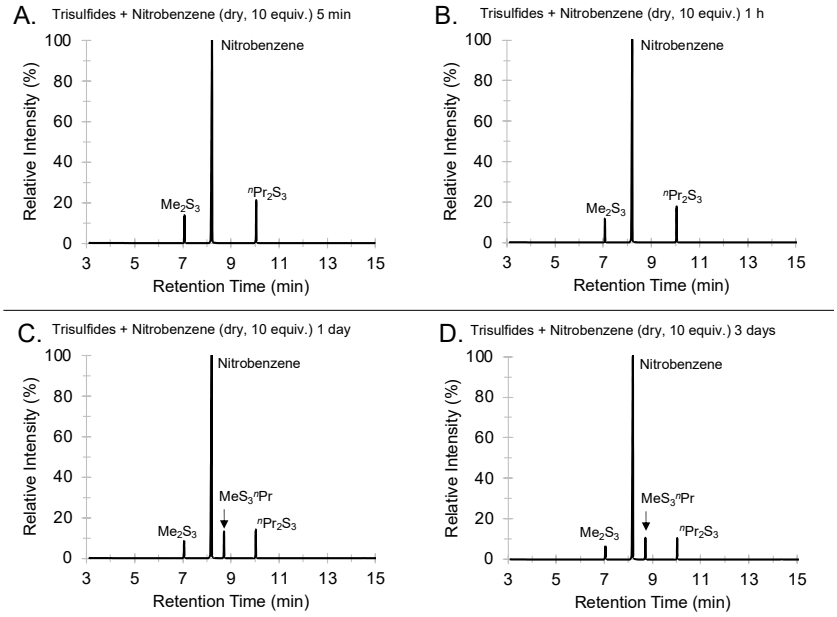

Figure S3.31: GC traces of the room temperature (18 – 21 ºC) reaction between dimethyl trisulfide (Me_2S_3) (42 µL, 0.4 mmol, 1 eq.) and di-*n*-propyl trisulfide (68 µL, 0.4 mmol, 1 eq.) in dry nitrobenzene (411.8 µL, 4.0 mmol, 10 eq.) after (A) 5 min, (B) 1 hour, (C) 1 day, and (D) 3 days. GC-MS method A. Retention time: Me_2S_3 (7.10 min), nitrobenzene (8.20 min), $MeS_3{}^{n}Pr$ (8.75 min), and ${}^{n}Pr_2S_3$ (10.09 min).

GC traces of the crossover reaction in methanol

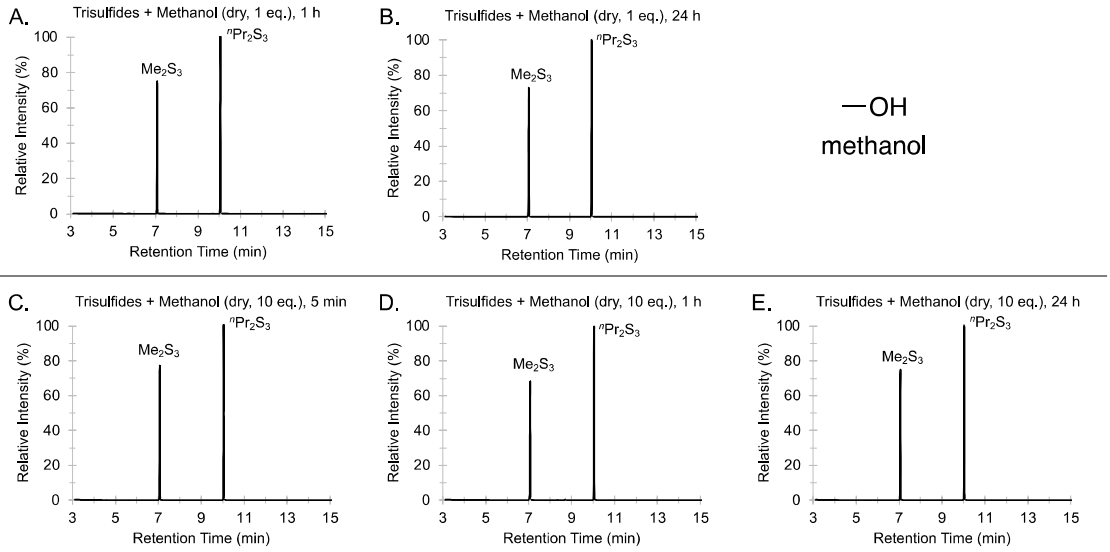

Figure S3.32: GC traces of the room temperature (8 – 14 ºC) reaction between dimethyl trisulfide (Me_2S_3) (42 µL, 0.4 mmol, 1 eq.), di-*n*-propyl trisulfide ($^nPr_2S_3$) (68 µL, 0.4 mmol, 1 eq.), and dry methanol (16.2 µL, 0.4 mmol for 1 eq. or 162 µL, 4.0 mmol for 10 eq.). (A, B) The trisulfides with dry methanol (1 eq. each) after 1 and 24 h. (C, D, E) The trisulfides (1 eq. each) with dry methanol (10 eq.) after 5 min, 1 h, and 24 h. GC-MS method A. Retention time: Me_2S_3 (7.10 min), $^nPr_2S_2$ (8.36 min, impurity from dipropyl trisulfide), $MeS_3{}^nPr$ (8.75 min), and $^nPr_2S_3$ (10.09 min).

GC traces of the crossover reaction in ethanol

(Data was obtained from Ryan Shapter – see ref.5)

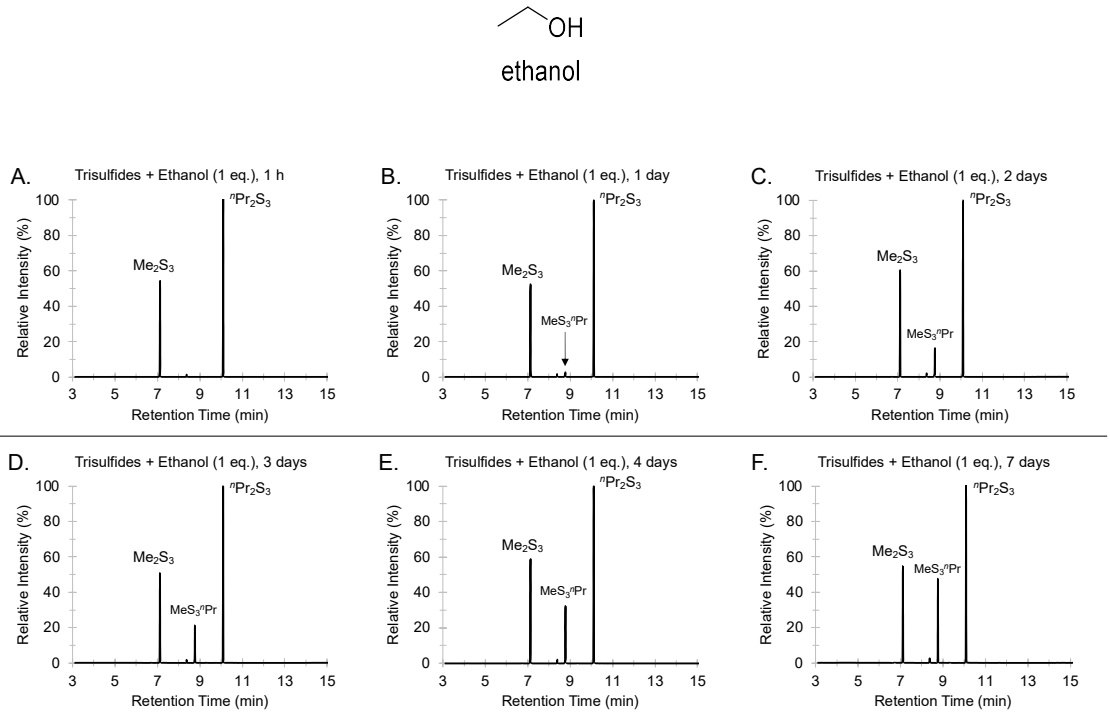

Figure S3.33: GC traces of the room temperature reaction between dimethyl trisulfide (Me_2S_3) (126.2 µL, 1.2 mmol, 1 eq.), di-*n*-propyl trisulfide ($^{n}Pr_2S_3$) (203.4 µL, 1.2 mmol, 1 eq.), and ethanol (70 µL, 1.2 mmol, 1 eq.) after (A) 1 hour, (B) 1 day (C) 2 days, (D) 3 days, (E) 4 days, and (F) 7 days (1 week). GC-MS method A. Retention time: Me_2S_3 (7.10 min), $^{n}Pr_2S_2$ (8.36 min, impurity from dipropyl trisulfide), $MeS_3{}^{n}Pr$ (8.75 min), and $^{n}Pr_2S_3$ (10.09 min).

GC traces of the crossover reaction in acetone

(Data was obtained from Ryan Shapter – see ref.5)

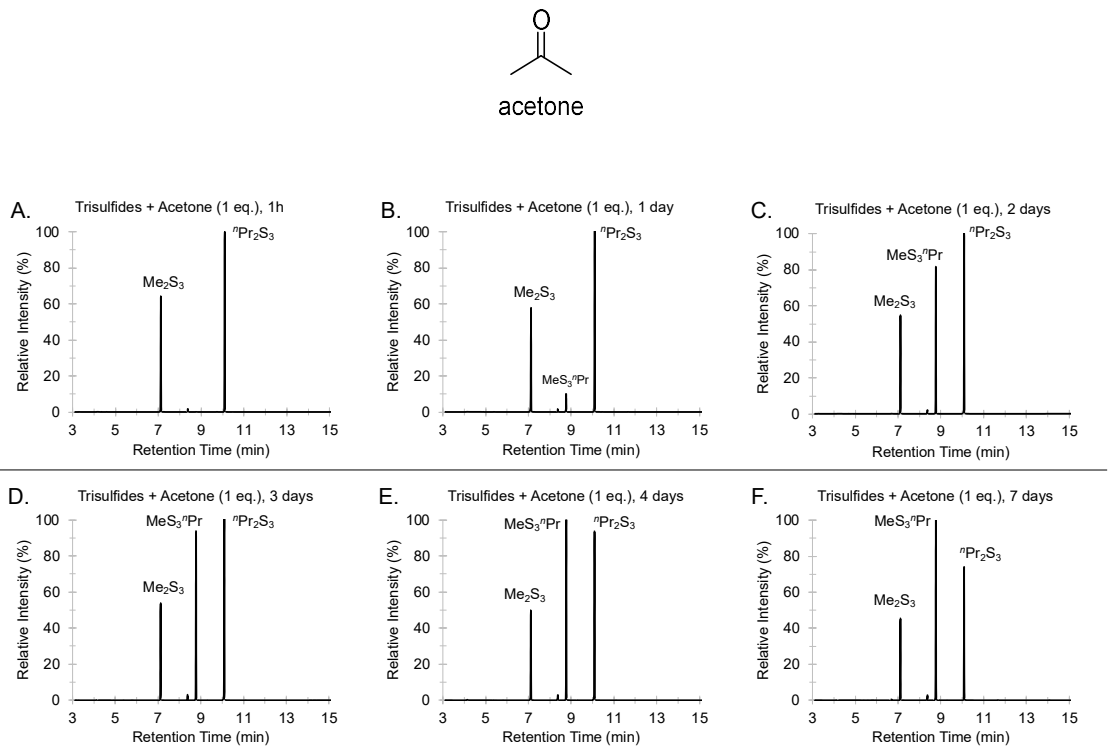

Figure S3.34: GC traces of the room temperature reaction between dimethyl trisulfide (Me_2S_3) (126.2 µL, 1.2 mmol, 1 eq.), di-*n*-propyl trisulfide ($^{n}Pr_2S_3$) (203.4 µL, 1.2 mmol, 1 eq.), and acetone (88 µL, 1.2 mmol, 1 eq.) after (A) 1 hour, (B) 1 day (C) 2 days, (D) 3 days, (E) 4 days, and (F) 7 days (1 week). GC-MS method A. Retention time: Me_2S_3 (7.10 min), $^{n}Pr_2S_2$ (8.36 min, impurity from dipropyl trisulfide), $MeS_3{}^{n}Pr$ (8.75 min), and $^{n}Pr_2S_3$ (10.09 min).

GC traces of the crossover reaction in isopropanol

(Data was obtained from Ryan Shapter – see ref.5)

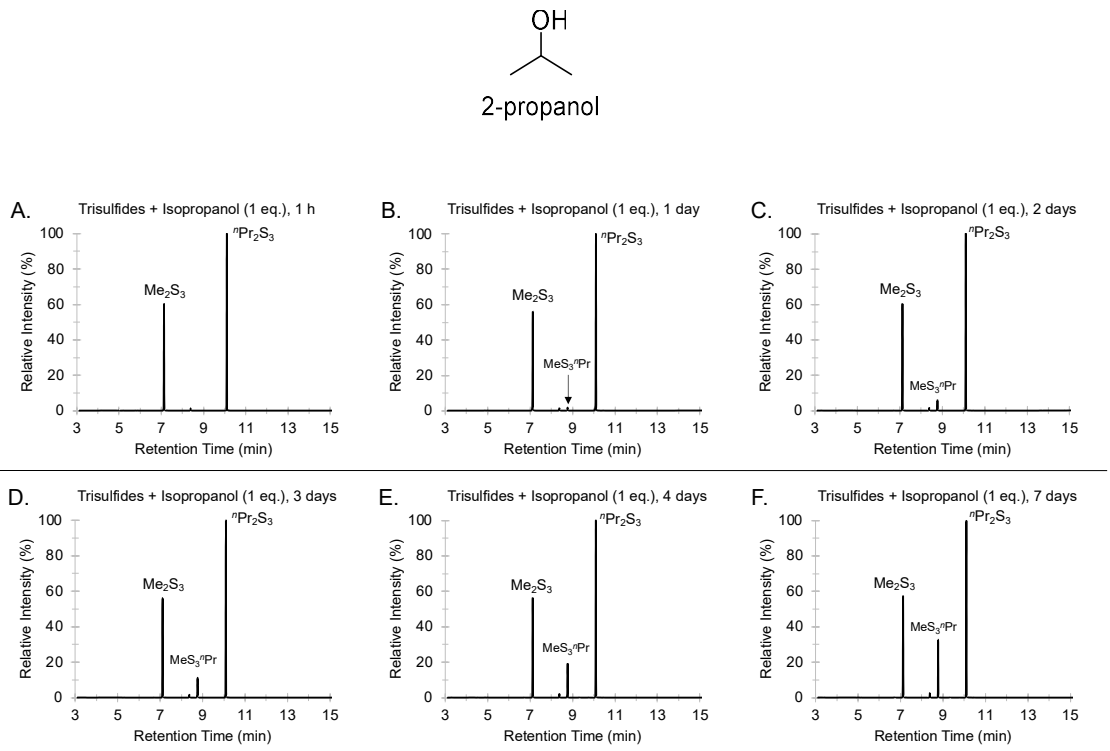

Figure S3.35: GC traces of the room temperature reaction between dimethyl trisulfide (Me_2S_3) (126.2 µL, 1.2 mmol, 1 eq.), di-*n*-propyl trisulfide ($^{n}Pr_2S_3$) (203.4 µL, 1.2 mmol, 1 eq.), and isopropanol (91.8 µL, 1.2 mmol, 1 eq.) after (A) 1 hour, (B) 1 day (C) 2 days, (D) 3 days, (E) 4 days, and (F) 7 days (1 week). GC-MS method A. Retention time: Me_2S_3 (7.10 min), $^{n}Pr_2S_2$ (8.36 min, impurity from dipropyl trisulfide), $MeS_3{}^{n}Pr$ (8.75 min), and $^{n}Pr_2S_3$ (10.09 min).

GC traces of the crossover reaction in 1,1,1,3,3,3-hexafluoro-2-propanol (HFIP)

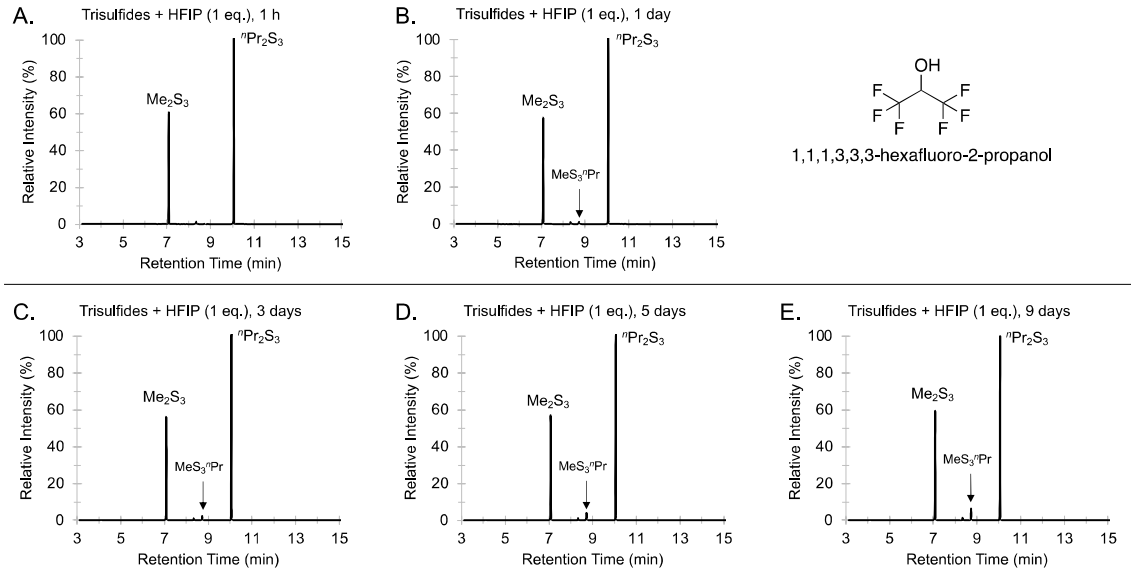

Figure S3.36: GC traces of the room temperature (10 – 18 ºC) reaction between dimethyl trisulfide (Me_2S_3) (126.2 µL, 1.2 mmol, 1 eq.), di-*n*-propyl trisulfide ($^nPr_2S_3$) (203.4 µL, 1.2 mmol, 1 eq.), and 1,1,1,3,3,3-hexafluoro-2-propanol (HFIP) (126.4 µL, 1.2 mmol, 1 eq.) after (A) 1 hour, (B) 1 day (C) 3 days, (D) 5 days, and (E) 9 days (*This forms a heterogenous mixture)*. GC-MS method A. Retention time: Me_2S_3 (7.10 min), $^nPr_2S_2$ (8.36 min, impurity from dipropyl trisulfide), $MeS_3{}^nPr$ (8.75 min), and $^nPr_2S_3$ (10.09 min).

GC traces of the crossover reaction in tert-butanol

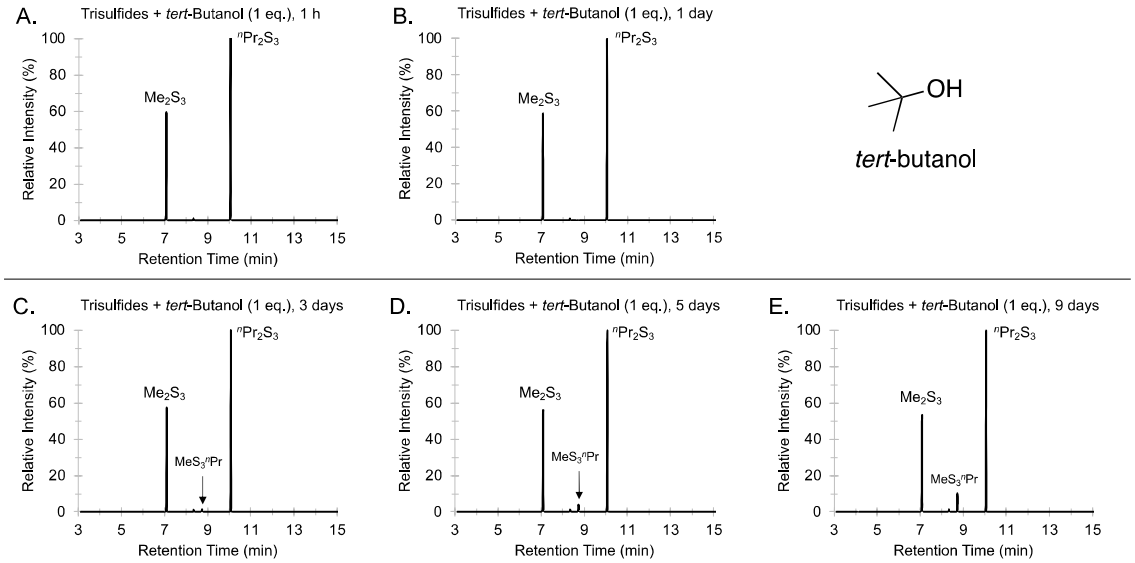

Figure S3.37: GC traces of the room temperature (10 – 18 ºC) reaction between dimethyl trisulfide (126.2 µL, 1.2 mmol, 1 eq.), di-*n*-propyl trisulfide (203.4 µL, 1.2 mmol, 1 eq.), and *tert*-butanol (114.8 µL, 1.2 mmol, 1 eq.) after (A) 1 hour, (B) 1 day (C) 3 days, (D) 5 days, and (E) 9 days. GCMS method A. Retention time: Me_2S_3 (7.10 min), $^{n}Pr_2S_2$ (8.36 min, impurity from dipropyl trisulfide), $MeS_3{}^{n}Pr$ (8.75 min), and $^{n}Pr_2S_3$ (10.09 min).

GC traces of the crossover reaction in tetrahydrofuran

(Data was obtained from Ryan Shapter – see ref.5)

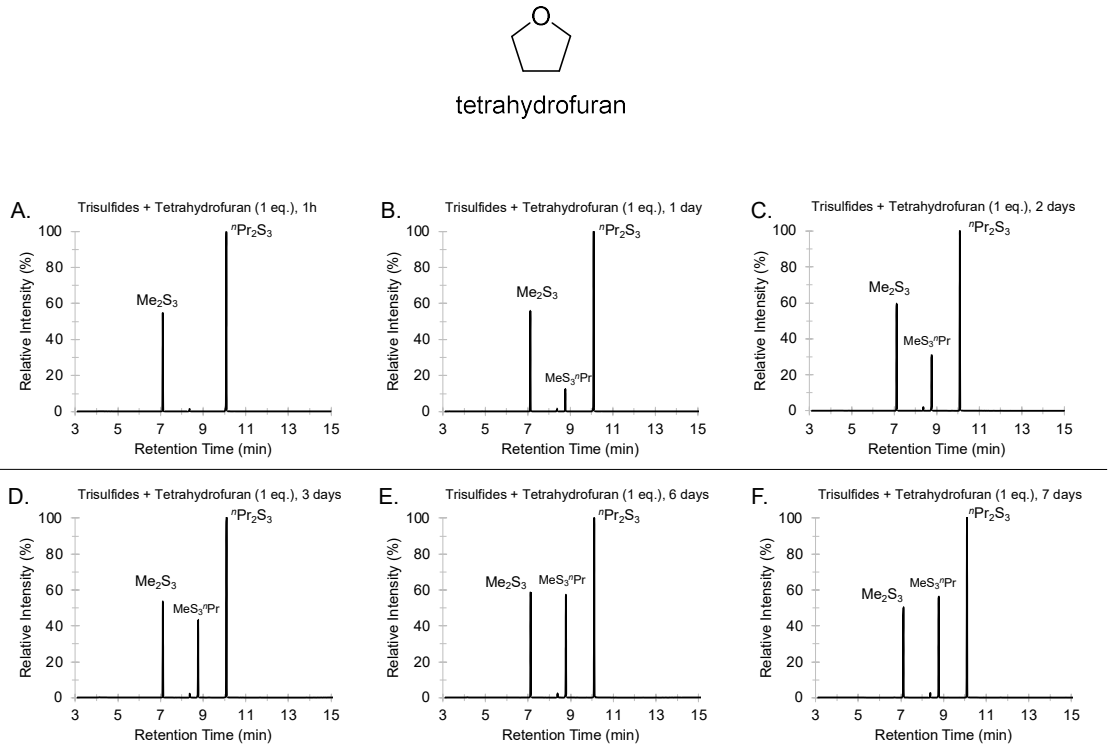

Figure S3.38: GC traces of the room temperature reaction between dimethyl trisulfide (Me_2S_3) (126.2 µL, 1.2 mmol, 1 eq.), di-*n*-propyl trisulfide ($^{n}Pr_2S_3$) (203.4 µL, 1.2 mmol, 1 eq.), and tetrahydrofuran (97.4 µL, 1.2 mmol, 1 eq.) after (A) 1 hour, (B) 1 day (C) 2 days, (D) 3 days, (E) 6 days, and (F) 7 days (1 week). GC-MS method A. Retention time: Me_2S_3 (7.10 min), $^{n}Pr_2S_2$ (8.36 min, impurity from dipropyl trisulfide), $MeS_3{}^{n}Pr$ (8.75 min), and $^{n}Pr_2S_3$ (10.09 min).

GC traces of the crossover reaction in acetic acid

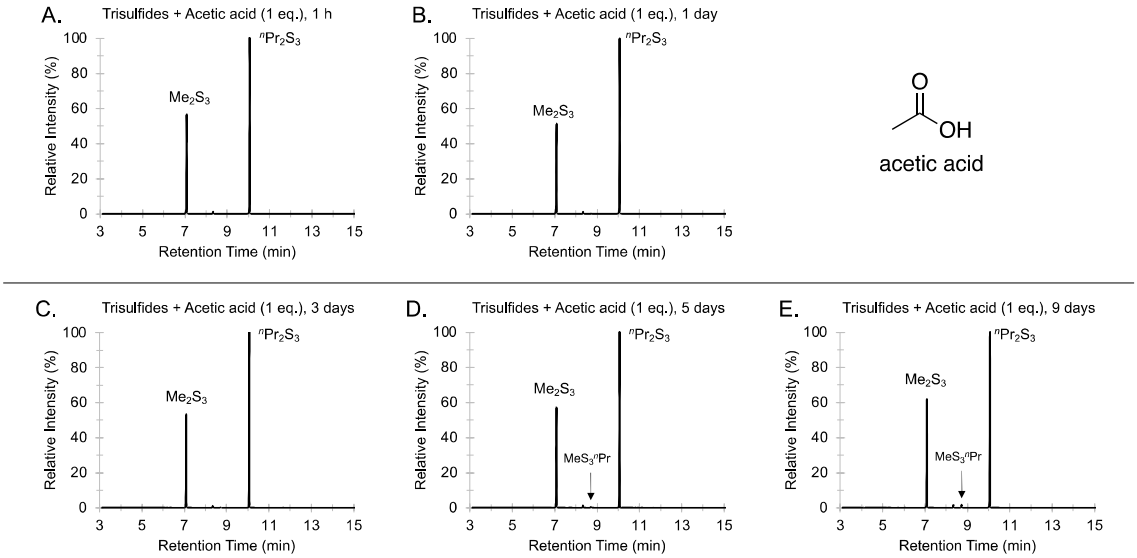

Figure S3.39: GC traces of the room temperature (10 – 18 ºC) reaction between dimethyl trisulfide (126.2 µL, 1.2 mmol, 1 eq.), di-*n*-propyl trisulfide (203.4 µL, 1.2 mmol, 1 eq.), and acetic acid (71.8 µL, 1.2 mmol, 1 eq.) after (A) 1 hour, (B) 1 day, (C) 3 days, (D) 5 days, and (E) 9 days. GCMS method A. Retention time: Me_2S_3 (7.10 min), $^{n}Pr_2S_2$ (8.36 min, impurity from dipropyl trisulfide), $MeS_3{}^{n}Pr$ (8.75 min), and $^{n}Pr_2S_3$ (10.09 min).

GC traces of the crossover reaction in ethyl acetate

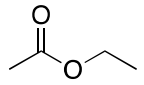

ethyl acetate

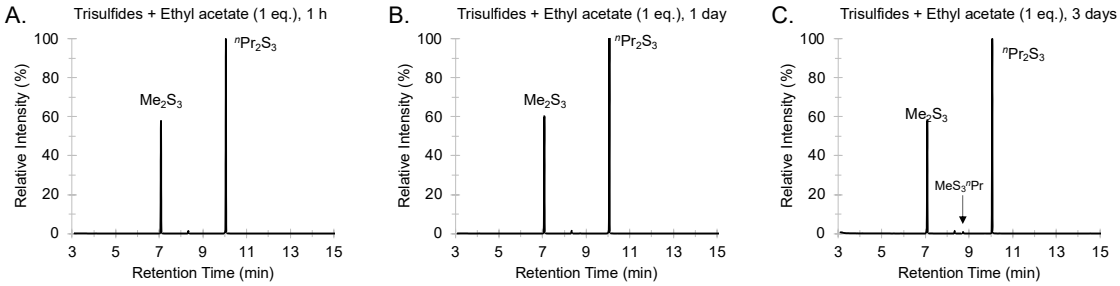

Figure S3.40: GC traces of the room temperature (15 – 18 ºC) reaction between dimethyl trisulfide (126.2 µL, 1.2 mmol, 1 eq.), di-*n*-propyl trisulfide (203.4 µL, 1.2 mmol, 1 eq.), and dry ethyl acetate (117.2 µL, 1.2 mmol, 1 eq.) after (A) 1 hour, (B) 1 day, and (C) 3 days. GC-MS method A. Retention time: Me_2S_3 (7.10 min), $^{n}Pr_2S_2$ (8.36 min, impurity from dipropyl trisulfide), $MeS_3{}^{n}Pr$ (8.75 min), and $^{n}Pr_2S_3$ (10.09 min).

GC traces of the crossover reaction in carbon disulfide

S=C=S

carbon disulfide

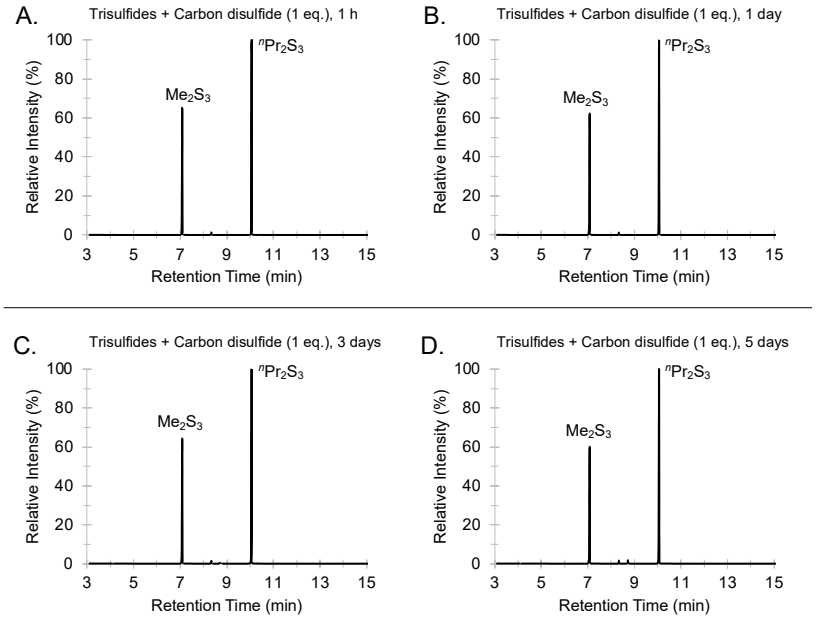

Figure S3.41: GC traces of the room temperature (12 – 18 ºC) reaction between dimethyl trisulfide (Me_2S_3) (126.2 µL, 1.2 mmol, 1 eq.), di-*n*-propyl trisulfide ($^{n}Pr_2S_3$) (203.4 µL, 1.2 mmol, 1 eq.), and carbon disulfide (72.2 µL, 1.2 mmol, 1 eq.) after (A) 1 hour, (B) 1 day, (C) 3 days, and (D) 5 days. GC-MS method A. Retention time: Me_2S_3 (7.10 min), $^{n}Pr_2S_2$ (8.36 min, impurity from dipropyl trisulfide), $MeS_3{}^{n}Pr$ (8.75 min), and $^{n}Pr_2S_3$ (10.09 min)

GC traces of the crossover reaction in toluene

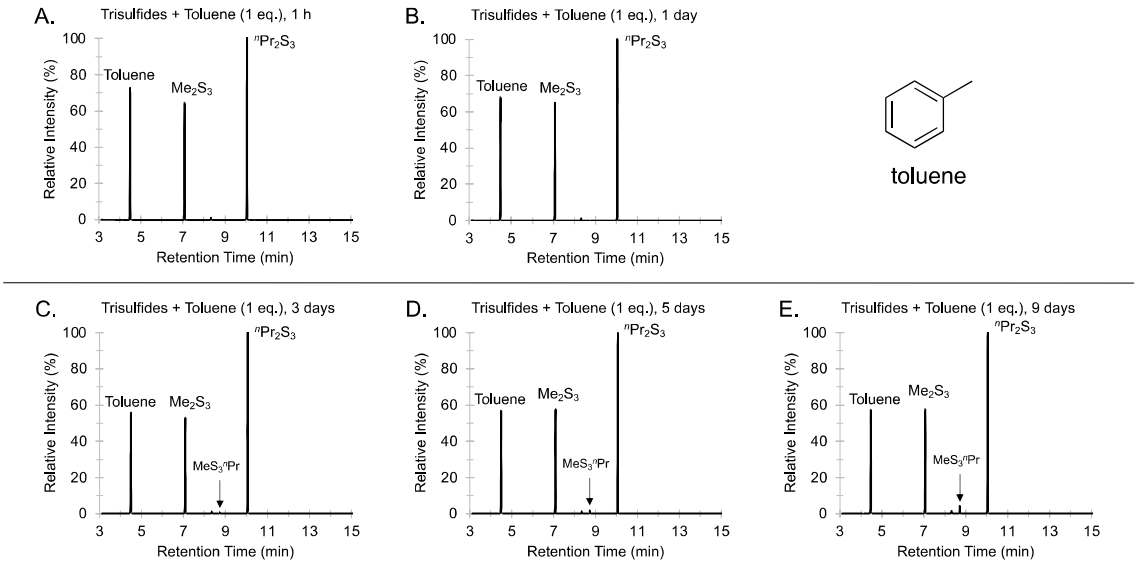

Figure S3.42: GC traces of the room temperature (10 – 18 ºC) reaction between dimethyl trisulfide (Me_2S_3) (126.2 µL, 1.2 mmol, 1 eq.), di-*n*-propyl trisulfide ($^{n}Pr_2S_3$) (203.4 µL, 1.2 mmol, 1 eq.), and toluene (127.8 µL, 1.2 mmol, 1 eq.) after (A) 1 hour, (B) 1 day (C) 3 days, (D) 5 days, and (E) 9 days. GC-MS method A. Retention time: toluene (4.48 min), Me_2S_3 (7.10 min), $^{n}Pr_2S_2$ (8.36 min, impurity from dipropyl trisulfide), $MeS_3{}^{n}Pr$ (8.75 min), and $^{n}Pr_2S_3$ (10.09 min).

GC traces of the crossover reaction in 1,4-dioxane

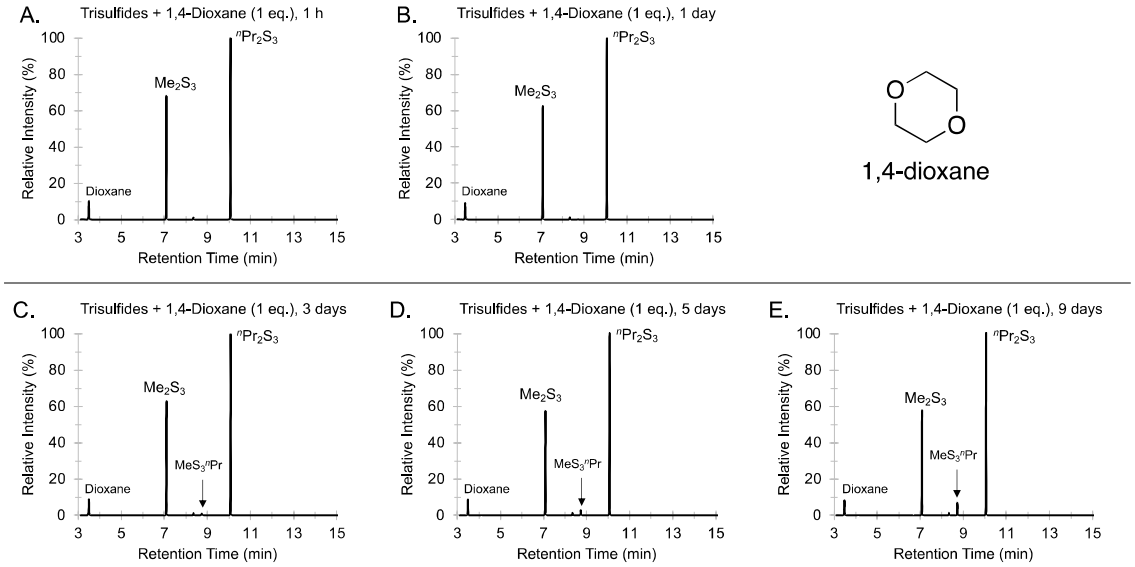

Figure S3.43: GC traces of the room temperature (10 – 18 ºC) reaction between dimethyl trisulfide (Me_2S_3) (126.2 µL, 1.2 mmol, 1 eq.), di-*n*-propyl trisulfide ($^nPr_2S_3$) (203.4 µL, 1.2 mmol, 1 eq.), and 1,4-dioxane (102.2 µL, 1.2 mmol, 1 eq.) after (A) 1 hour, (B) 1 day, (C) 3 days, (D) 5 days, and (E) 9 days. GC-MS method A. Retention time: 1,4-dioxane (3.47 min), Me_2S_3 (7.10 min), $^nPr_2S_2$ (8.36 min, impurity from dipropyl trisulfide), $MeS_3{}^nPr$ (8.75 min), and $^nPr_2S_3$ (10.09 min).

GC traces of the crossover reaction in hexanes

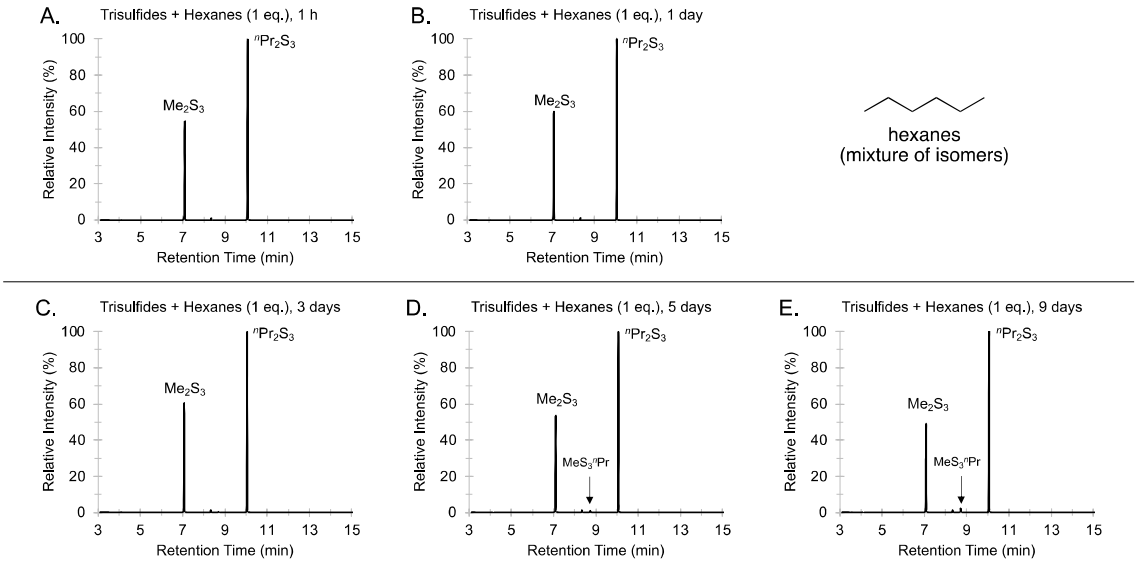

Figure S3.44: GC traces of the room temperature (10 – 18 ºC) reaction between dimethyl trisulfide (Me_2S_3) (126.2 µL, 1.2 mmol, 1 eq.), di-*n*-propyl trisulfide ($^nPr_2S_3$) (203.4 µL, 1.2 mmol, 1 eq.), and hexanes (157 µL, 1.2 mmol, 1 eq.) after (A) 1 hour, (B) 1 day (C) 3 days, (D) 5 days, and (E) 9 days. GC-MS method A. Retention time: Me_2S_3 (7.10 min), $^nPr_2S_2$ (8.36 min, impurity from dipropyl trisulfide), $MeS_3{}^nPr$ (8.75 min), and $^nPr_2S_3$ (10.09 min).

Table S3.3: S-S metathesis reaction between Me_2S_3 and $^nPr_2S_3$ in various of solvents at room temperature

Solvent	% crossover product (methyl *n*-propyl trisulfide) by GC											
	5 sec	5 min	1h	1 day	2 days	3 days	4 days	5 days	6 days	7 days	8 days	9 days
Formamide (dry, 1 eq.)[b]	-	-	1	10.5	-	-	-	-	-	-	-	-
Formamide (dry, 10 eq.)	-	-	0.4	27.5	-	-	-	-	-	-	-	-
Propylene carbonate (4-Methyl-1,3-dioxolan-2-one) (dry, 1 eq.)[b]	-	0.2	2.1	6.7	-	19.2	-	-	-	-	-	-
Propylene carbonate (4-Methyl-1,3-dioxolan-2-one) (dry, 10 eq.)	-	13.1	26.5	33.9	-	36.6	-	-	-	-	-	-
Dimethyl sulfoxide (1 eq.) ref. 5	46.9	50.2	49		-	-	-	-	-	-	-	-
Tri(pyrrolidin-1-yl)phosphine oxide (dry, 1 eq.)	-	49	48.5	47.5	-	-	-	-	-	-	-	-
Tri(pyrrolidin-1-yl)phosphine oxide (dry, 10 eq.)	-	51.3	51.6	50.4	-	-	-	-	-	-	-	-
Furan-2-carbaldehyde (furfural, dry, 1 eq.)	-	-	0	0	-	-	-	-	-	-	-	-
Furan-2-carbaldehyde (furfural, dry, 10 eq.)	-	-	0.4	1.2	-	-	-	-	-	-	-	-
ε-caprolactone (dry, 1 eq.)	-	1	6.1	10.6	-	32.9	-	-	-	-	-	-
ε-caprolactone (dry, 10 eq.)	-	*nd*	5.7	16.3	-	34.2	-	-	-	-	-	-
Dimethyl acetamide (dry, 1 eq.)	9.4	45.4	46.1		-	-	-	-	-	-	-	-
1,3-Dimethyl-2-imidazolidinone (dry, 1 eq.)	-	49	48.8	47.9	-	-	-	-	-	-	-	-
1,3-Dimethyl-2-imidazolidinone (dry, 10 eq.)	-	52.5	52.1	51.1	-	-	-	-	-	-	-	-
Dihydrolevoglucosenone (cyrene)[a]	-	-	0	0	-	0	-	<0.1	-	<0.1	-	0.1
Dimethyl formamide (dry, 1 eq.)	37.6	51.4	48.9		-	-	-	-	-	-	-	-
N,N'-dimethylpropyleneurea (10 eq.)[a]	-	0.4	3.4	-	20[c]	-	-	-	-	-	-	-
N,N'-dimethylpropyleneurea (dry, 1 eq.)	47.1	47.1	46.5	-	-	-	-	-	-	-	-	-
Nitromethane (dry, 1 eq.)[b]	-	-	0	0	-	0.1	-	-	-	-	-	-
Nitromethane (dry, 10 eq.)	-	0.3	11.2	22.4	25.6	-	-	-	-	-	-	-
Acetonitrile (1 eq.)[a] ref. 5	-	-	0.8	22.3	47.7	46.3	46.9	-	-	47.9	-	-
Nitrobenzene (dry, 10 eq.)	-	0	0	36.7	-	38.6	-	-	-	-	-	-
Methanol (1 eq.)[a] ref. 5	-	-	0	3.8	13.9	16.6	19.3	-	-	22.7	-	-
Methanol (dry, 1 eq.)	-	-	0	0	-	-	-	-	-	-	-	-
Methanol (dry, 10 eq.)	-	0.2	0.4	0.3	-	-	-	-	-	-	-	-
Hexamethylphosphoramide (dry, 1 eq.)	-	46.6	46.7	46.2	-	-	-	-	-	-	-	-
Hexamethylphosphoramide (dry, 10 eq.)	-	46.6	46.8	46.6	-	-	-	-	-	-	-	-
N-methyl-2-pyrrolidone (dry, 1 eq.)	42	51.2	48.9		-	-	-	-	-	-	-	-
Ethanol (1 eq.)[a] ref. 5	-	-	0	1.4	7.8	11.3	15.4	-	-	22.4	-	-
1,1,3,3-tetramethylurea (1 eq.)	-	-	0	1.3	-	8.5	-	23.4	-	-	-	-
1,1,3,3-tetramethylurea (dry, 1 eq.)	2.7	42.4	46.4	-	-	-	-	-	-	-	-	-
Acetone (1 eq.)[a] ref. 5	-	-	0.1	5.3	33.9	37.9	41.3	-	-	46.1	-	-
iso-propanol (1 eq.) ref. 5	-	-	0	0.9	3.2	5.9	9.7	-	-	17	-	-
1,1,1,3,3,3-hexafluoro-2-propanol (1 eq.)	-	-	0	0.7	-	1.5	-	2.5	-	-	-	3.8
tert-butanol *(1 eq.)*[a]	-	-	0	0.2	-	1	-	2.4	-	-	-	5.7
Pyridine (dry, 10 eq.)	4.6[d]	28.6	50.1	48.4	-	-	-	-	-	-	-	-
Tetrahydrofuran (1 eq.)[a] ref. 5	-	-	0	7	15	20	-	-	25	26	-	-
Acetic acid (1 eq.)	-	-	0	0	-	0.2	-	0.4	-	-	-	0.9
Ethyl acetate (dry, 1 eq.)	-	-	0	0.1	-	0.6	-	-	-	-	-	-
n-Butylamine (dry, 10 eq.)	-	32	41.2	14.3[e]								
Diethylamine (dry, 10 eq.)	-	0.5	1.2	36[f]	-	-	-	-	-	-	-	-
Carbon disulfide (dry, 1 eq.)	-	-	0	0	-	0.3	-	0.9	-	-	-	-
Triethylamine (dry, 10 eq.)	-	0	0	1	-	-	-	-	-	-	-	-
Toluene (dry, 1 eq.)	-	-	0	0.1	-	0.5	-	1.2	-	-	-	2.5
1,4-dioxane (dry, 1 eq.)	-	-	0	0	-	0.6	-	1.6	-	-	-	4.1
Hexanes (dry, 1 eq.)	-	-	0	0	-	0.3	-	0.7	-	-	-	2

[a] used as a non-dried and as received solvent, thus it may contain high level ppm of water and impurities.

[b] at this condition, the mixture was heterogeneous.

[c] data obtained after 40 h, old sample of DMPU was used and possibly very wet.

[d] area percentage by GC measured after 1 min of reaction

[e] Me_2S_2 (7.9%), $MeS_2{}^nPr$ (25.6%), Me_2S_3 (9.7%), $^nPr_2S_2$ (14.6%), Me_2S_4 (2.4%), $^nPr_2S_3$ (14.6%), $^nPr_2S_4$ (1.1%) were observed by GC after 24 h of reaction.

[f] Me_2S_2 (0.3%), $MeS_2{}^nPr$ (0.3%), and $^nPr_2S_2$ (0.3%) were observed by GC after 24 h of reaction.

Crossover in amine solvents

Me_2S_3 and $^nPr_2S_3$ crossover in diethylamine

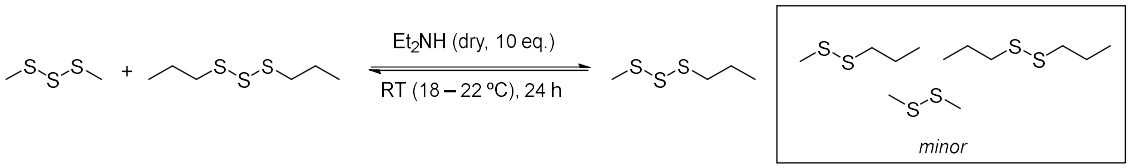

Dimethyl trisulfide (42 µL, 0.4 mmol, 1 eq.) and di-*n*-propyl trisulfide (67.8 µL, 0.4 mmol, 1 eq.) were added to a 2 mL glass vial equipped with a stirrer bar, followed by dry diethylamine (414 µL, 4.0 mmol, 10 eq.). The mixture was stirred at room temperature (18 – 22 ºC) for 24 h. After 5 minutes, 1 hours and 24 hours, a 10 µL of aliquot from was removed and diluted to 1 mL with chloroform for GC-MS analysis. Small quantities of disulfide products i.e. dimethyl disulfide (0.3%), methyl *n*-propyl disulfide (0.3%), and dipropyl disulfide (0.3%) were observed after a 24-hour reaction whereas methyl *n*-propyl trisulfide ($MeS_3{}^nPr$) was the major product (35.6%).

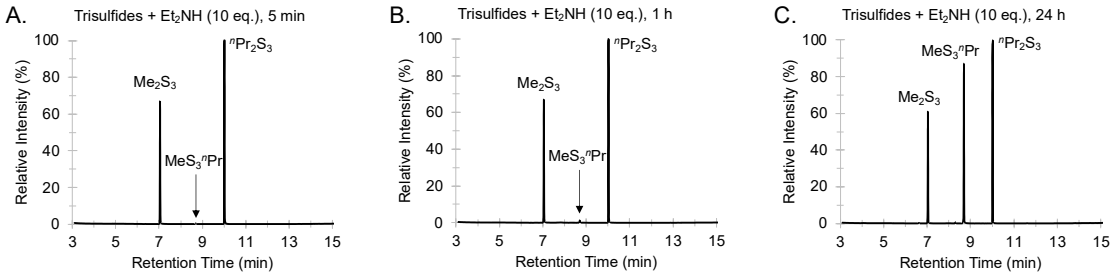

Figure S3.45: GC traces for the crossover reactions between dimethyl trisulfide (Me_2S_3) and di-*n*-propyl trisulfide ($^nPr_2S_3$) in diethylamine. GC-MS method A. Retention time: Me_2S_2 (4.07 min), $MeS_2{}^nPr$ (6.63 min), Me_2S_3 (7.05 min), $^nPr_2S_2$ (8.31 min), $MeS_3{}^nPr$ (8.71 min), and $^nPr_2S_3$ (10.03 min).

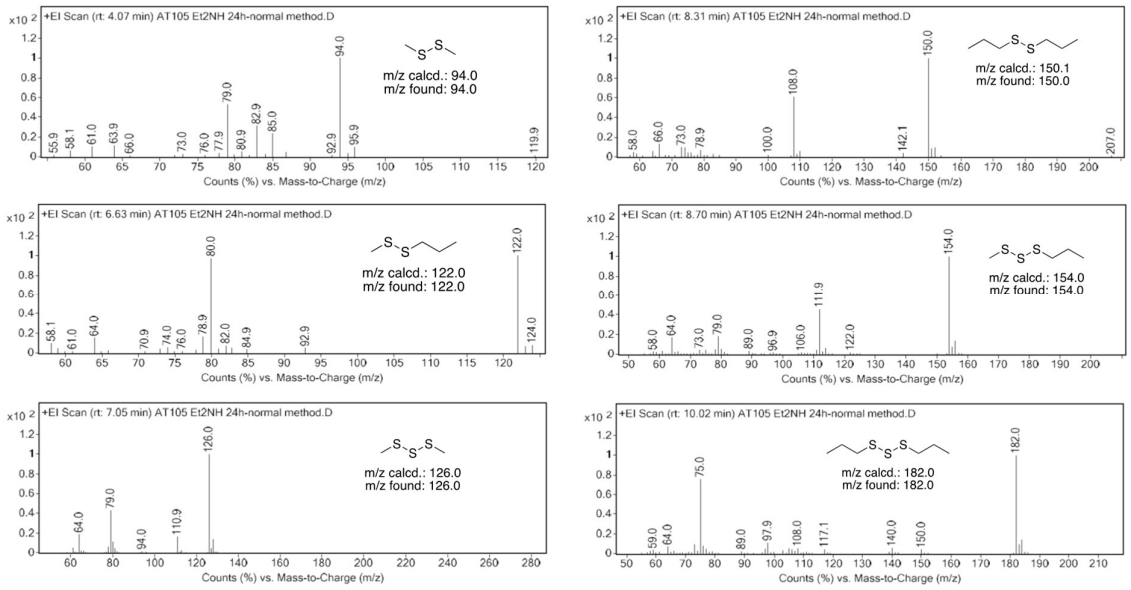

Figure S3.46: Mass spectra of the peaks observed for the crossover reaction between dimethyl trisulfide (Me_2S_3) and di-*n*-propyl trisulfide ($^nPr_2S_3$) in diethylamine after 24 hours.

Me_2S_3 and $^nPr_2S_3$ crossover in *n*-butylamine

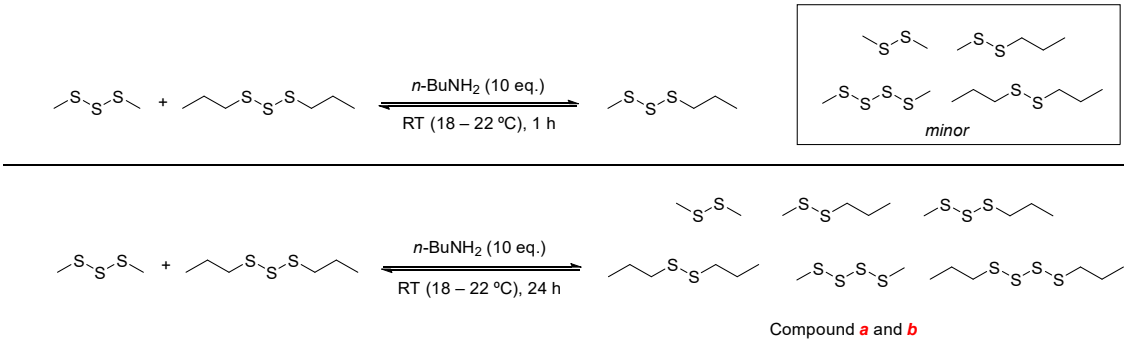

Dimethyl trisulfide (42 µL, 0.4 mmol, 1 eq.) and di-*n*-propyl trisulfide (67.8 µL, 0.4 mmol, 1 eq.) were added to a 2 mL glass vial equipped with a stirrer bar, followed by *n*-butylamine (414 µL, 4.0 mmol, 10 eq.). The mixture was stirred at room temperature (18 – 22 ºC) for 24 h. After 5 minutes, 1 hours and 24 hours, a 10 µL of aliquot from was removed and diluted to 1 mL with chloroform for GC-MS analysis. After 1 h, methyl *n*-propyl trisulfide ($MeS_3{}^nPr$) was the major product. Longer reaction time had led to the formation of other polysulfides and yielded methyl *n*-propyl disulfide ($MeS_2{}^nPr$) as the major product.

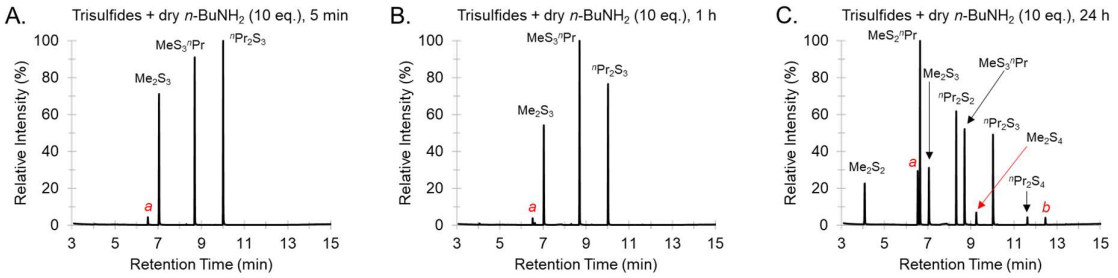

Figure S3.47: GC traces for the crossover reactions between dimethyl trisulfide (Me_2S_3) and di-*n*-propyl trisulfide ($^nPr_2S_3$) in *n*-butylamine after (A) 5 min, (B) 1 h, and (C) 24 h. GC-MS method A. Retention time: Me_2S_2 (4.07 min), $MeS_2{}^nPr$ (6.63 min), Me_2S_3 (7.05 min), $^nPr_2S_2$ (8.31 min), $MeS_3{}^nPr$ (8.70 min), Me_2S_4 (9.24 min), $^nPr_2S_3$ (10.02 min), and $^nPr_2S_4$ (11.61 min). Peak a (6.53 min) and b (12.45 min) indicate two unknown compounds.

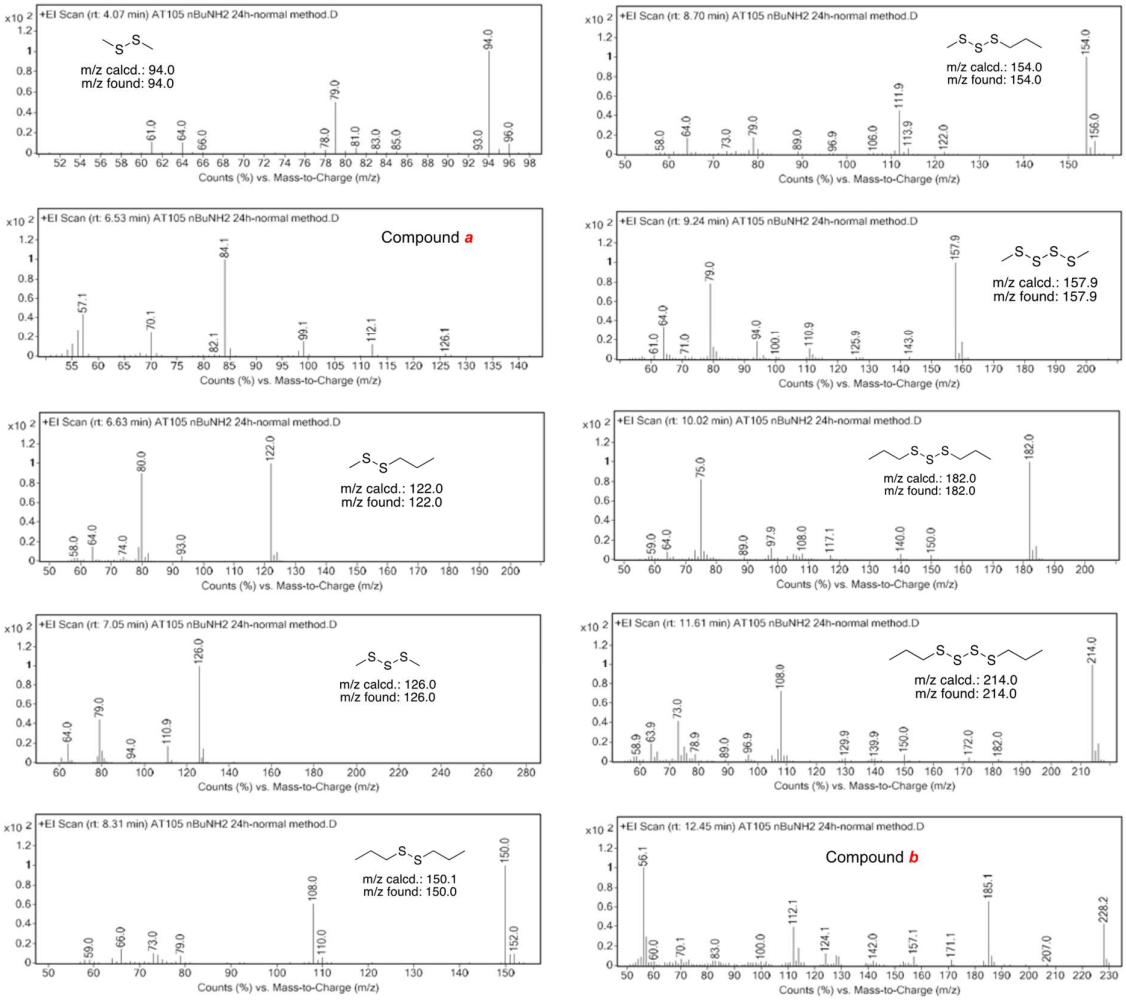

Figure S3.48: Mass spectra of the peaks observed for the crossover reaction between dimethyl trisulfide (Me_2S_3) and di-*n*-propyl trisulfide ($^nPr_2S_3$) in dry *n*-butylamine after 24 hours.

Me_2S_3 and $^nPr_2S_3$ crossover in triethylamine

(This experiment was performed by Dr. Harshal D. Patel)

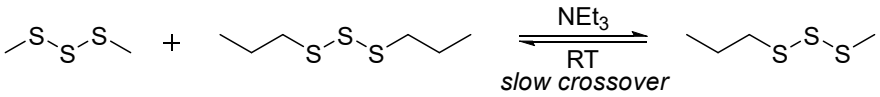

713 µL of degassed triethylamine was added to a vial under an atmosphere of nitrogen. A mixture of nitrogen degassed dimethyl trisulfide (97.3 µL, 925 µmol, 1.0 eq.) and di-*n*-propyl trisulfide (156 µL, 925 µmol, 1.0 eq.) was added, and the reaction monitored by GC-MS over time: 1 min and 15 min. GC-MS samples were prepared by taking a 10 µL aliquot from the reaction mixture and "quenching" by diluting with 990 µL of $CHCl_3$, which adequately slows the reaction prior to GC-MS analysis. The crossover reaction occurs slowly in triethylamine.

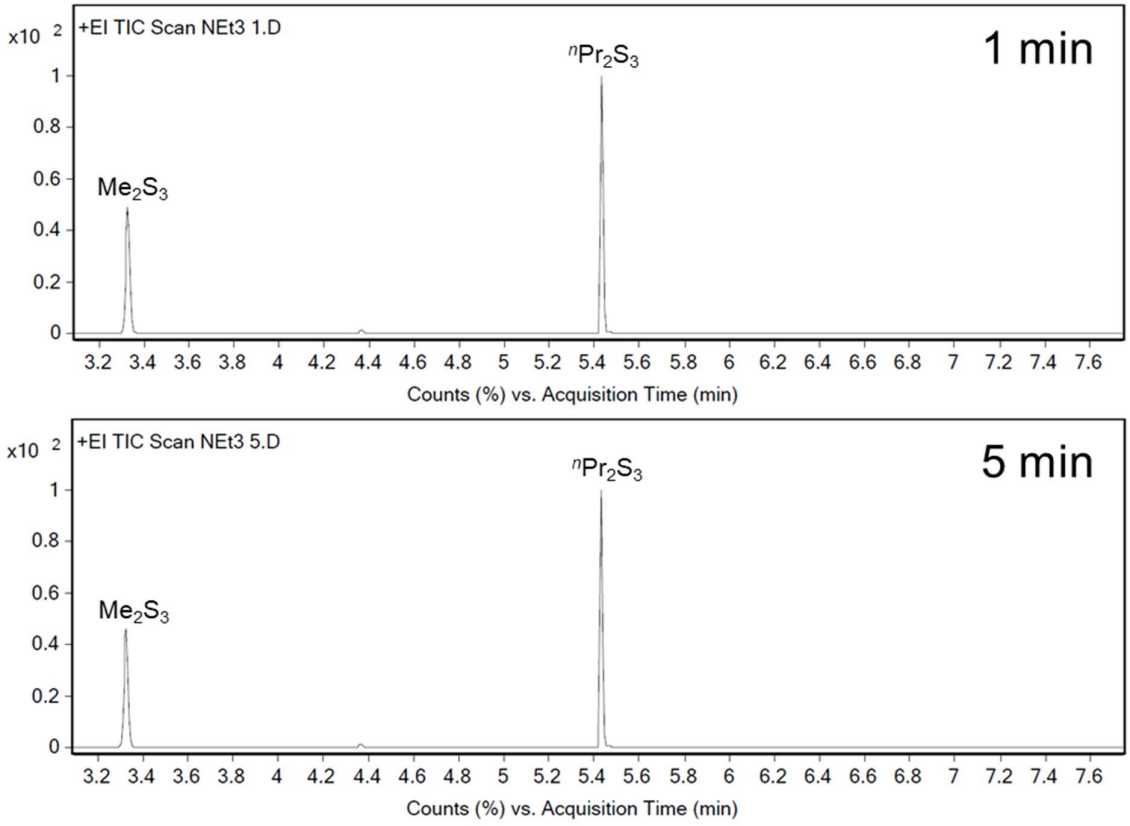

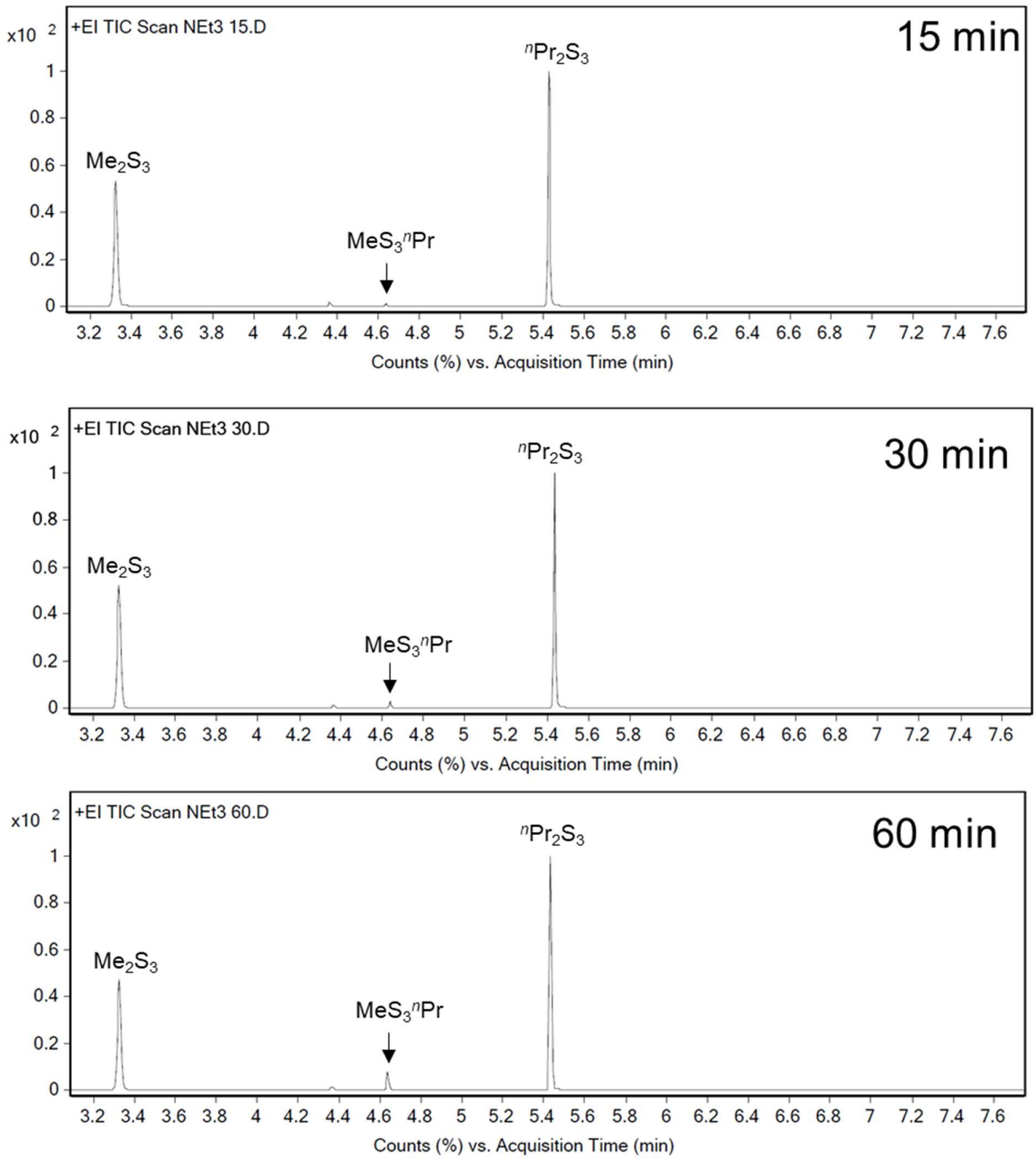

Figure S3.49: Gas chromatogram of the reaction between Me_2S_3 and $^{n}Pr_2S_3$ in NEt_3 after 1, 5, 15, 30, and 60 minutes. GC-MS method B. Me_2S_3 (3.33 min), $MeS_3{}^{n}Pr$ (4.64 min), and $^{n}Pr_2S_3$ (5.43 min).

Me_2S_3 and $^nPr_2S_3$ crossover in pyridine

(This experiment was performed by Dr. Harshal D. Patel)

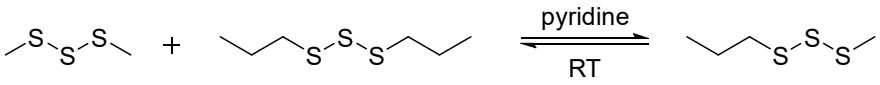

713 µL pyridine was added to a vial under an atmosphere of nitrogen. A mixture of nitrogen degassed dimethyl trisulfide (97.3 µL, 925 µmol, 1.0 eq.) and di-*n*-propyl trisulfide (156 µL, 925 µmol, 1.0 eq.) were added, and the reaction monitored by GC-MS over time: 1 min and 15 min. GC-MS samples were prepared by taking a 10 µL aliquot from the reaction mixture and "quenching" by diluting in 990 µL of $CHCl_3$, which adequately slows the reaction prior to GC-MS analysis. The crossover reaction occurs in pyridine.

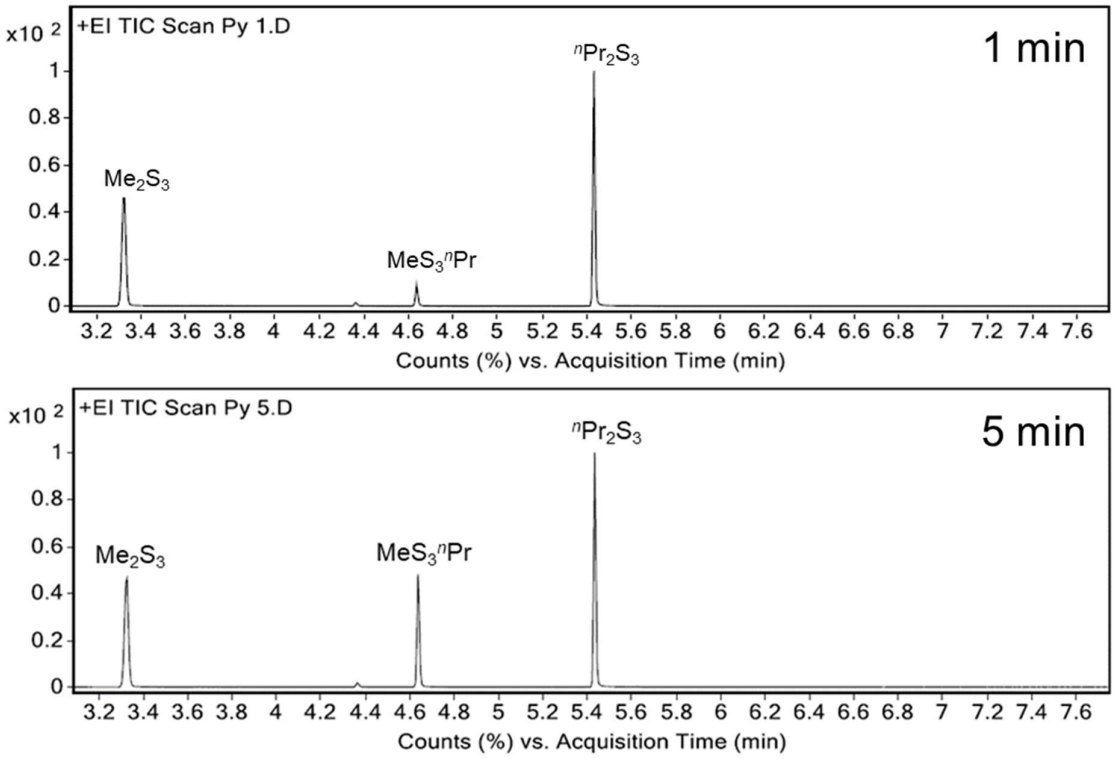

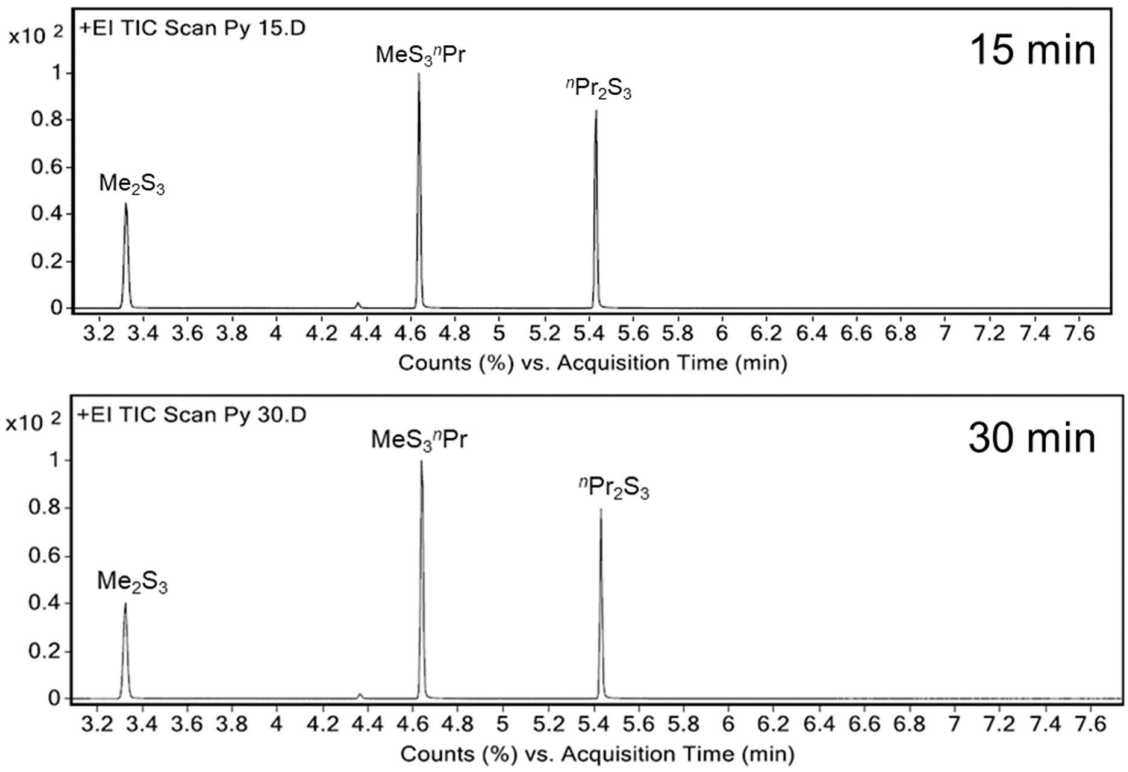

Figure S3.50: Gas chromatogram of the reaction between Me_2S_3 and $^nPr_2S_3$ in pyridine after 30 minutes. GC-MS method B. Retention time: Me_2S_3 (3.327 min), $MeS_3{}^nPr$ (4.638 min), and $^nPr_2S_3$ (5.433 min).

Influence of water on crossover of Me_2S_3 and $^nPr_2S_3$

Me_2S_3 and $^nPr_2S_3$ crossover in wet *N,N*-dimethylformamide (DMF)

Dimethyl trisulfide (42 µL, 0.4 mmol) and di-*n*-propyl trisulfide (68 µL, 0.4 mmol) were added to a 2 mL glass vial followed by the solvent specified below. The reaction was stirred for 1 hour at room temperature (14 – 16 ºC), after which a 10 µL reaction aliquot was diluted to 1 mL with chloroform for GC-MS analysis. Six reactions were carried out using the following solvents: 31 µL dry DMF (1 eq.) (100% DMF), 310 µL dry DMF (10 eq.) (100% DMF), 31 µL dry DMF (1 eq.) spiked with 0.77 µL water (97.5% DMF and 2.5% H_2O), 310 µL dry DMF (10 eq.) spiked with 7.7 µL water (97.5% DMF and 2.5% H_2O), 31 µL dry DMF (1 eq.) spiked with 1.54 µL water (95% DMF and 5% H_2O), or 310 µL dry DMF (10 eq.) spiked with 15.4 µL water (95% DMF and 5% H_2O). A control reaction was carried out as above in the absence of additional solvent and monitored over 24 hours.

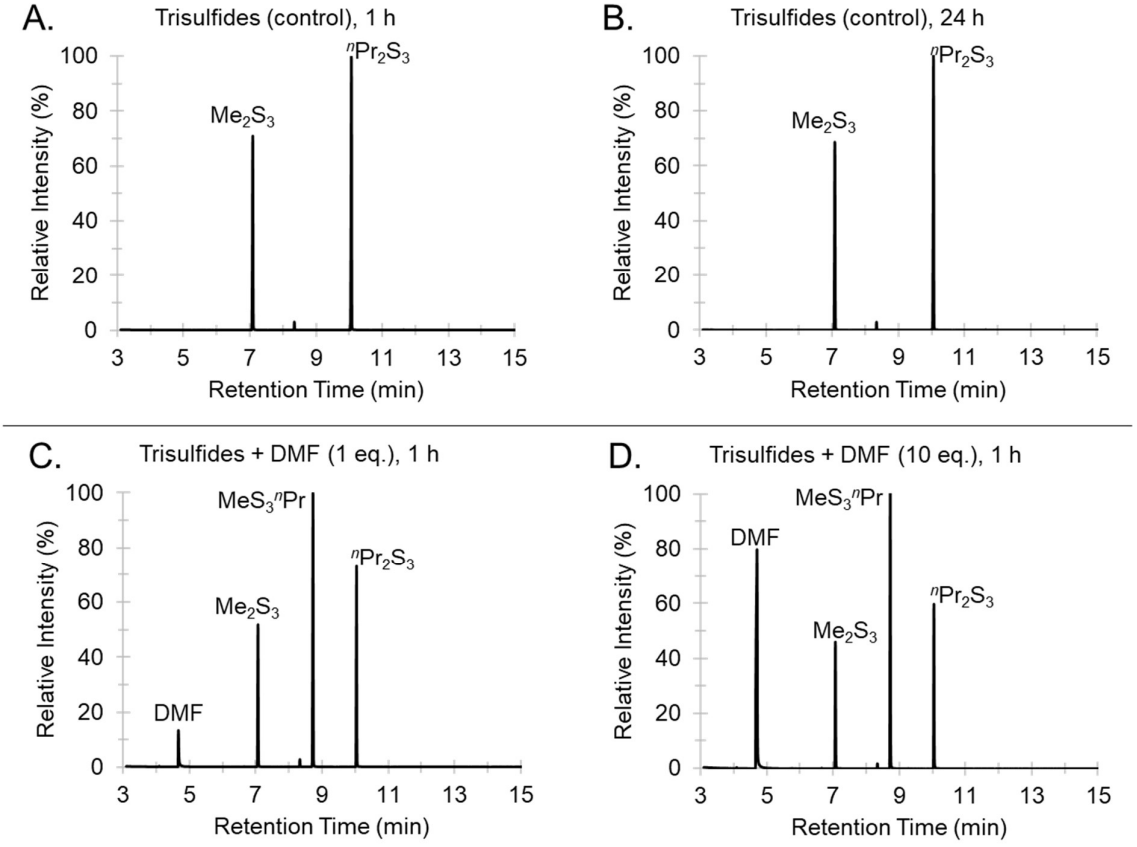

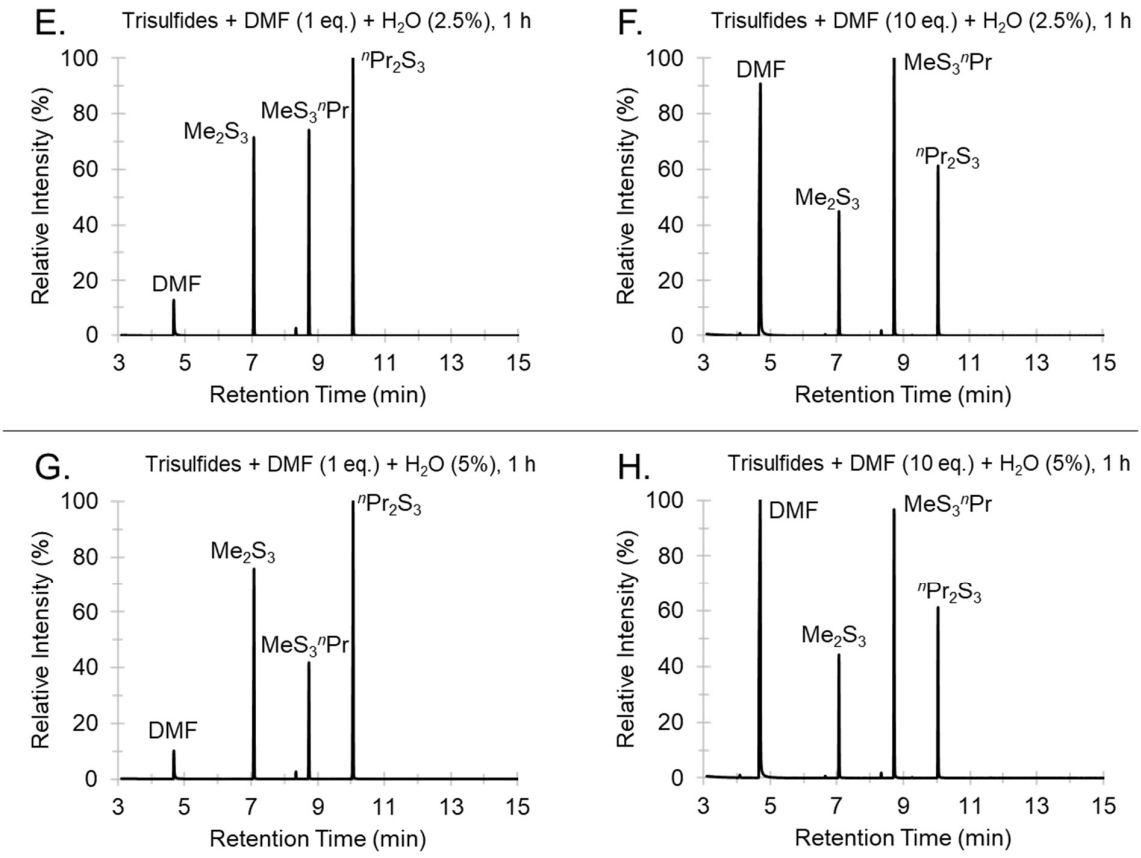

Figure S3.51: GC traces for the crossover reaction between dimethyl trisulfide (Me_2S_3) and di-*n*-propyl trisulfide ($^nPr_2S_3$) over 1 hour at room temperature (14 – 16 °C). (A, B) The trisulfides (1 eq. each) without additional solvent after 1 h and 24 h – control experiment. (C, D) The trisulfide (1 eq. each) and dry DMF (1 eq. and 10 eq., 100% DMF) after 1 h. (E, F) The trisulfides (1 eq. each) and dry DMF (1 eq. and 10 eq.) with the addition of H_2O (2.5% w/w) after 1 h. (G, H) The trisulfides (1 eq. each) and dry DMF (1 eq. and 10 eq.) with the addition of H_2O (5% w/w) after 1 h. GC-MS method A. Retention time: DMF (4.70 min), Me_2S_3 (7.10 min), $^nPr_2S_2$ (8.36 min, impurity from dipropyl trisulfide), $MeS_3{}^nPr$ (8.75 min), and $^nPr_2S_3$ (10.09 min).

GC traces of the crossover reaction in 1,1,3,3-tetramethylurea (wet, non-dried and used as received)

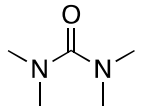

1,1,3,3-tetramethylurea

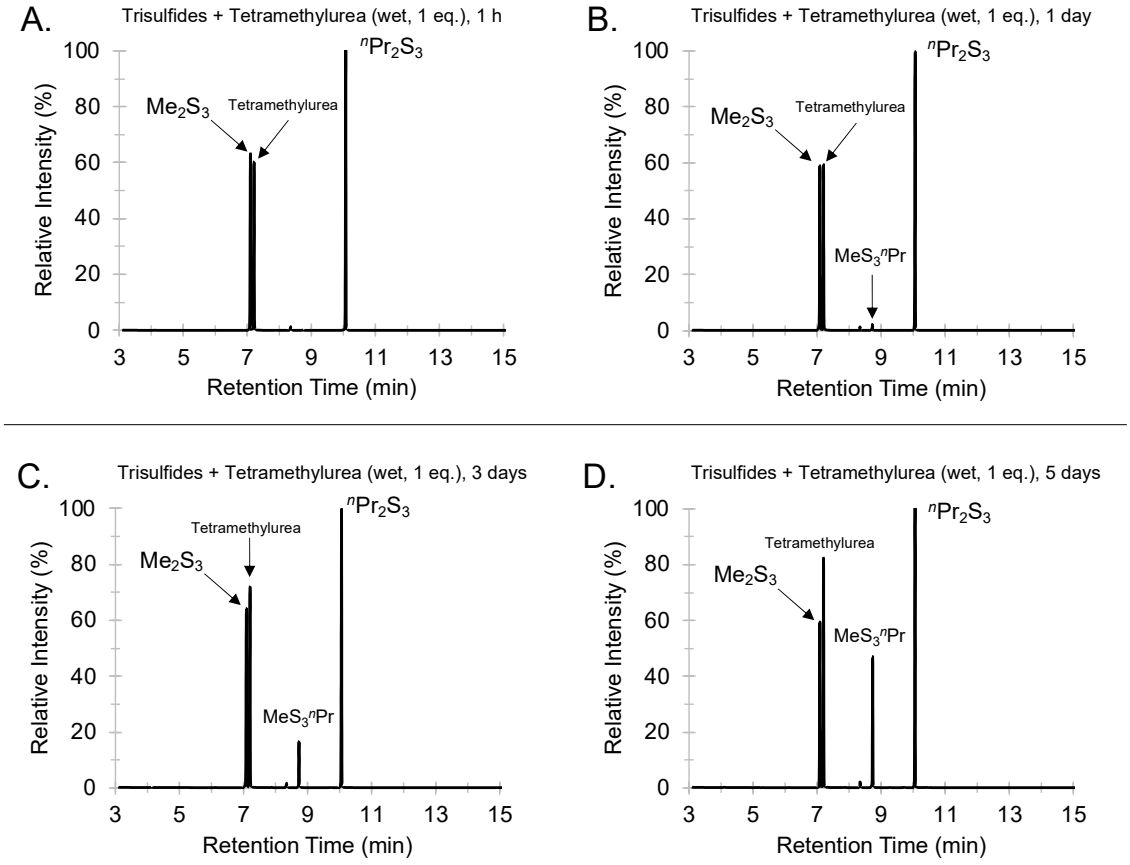

Figure S3.52: GC traces of the room temperature (12 – 18 ºC) reaction between dimethyl trisulfide (Me_2S_3) (126.2 µL, 1.2 mmol, 1 eq.), di-*n*-propyl trisulfide ($^{n}Pr_2S_3$) (203.4 µL, 1.2 mmol, 1 eq.), and 1,1,3,3-tetramethylurea (144 µL, 1.2 mmol, 1 eq.) after (A) 1 hour, (B) 1 day, (C) 3 days, and (D) 5 days. GC-MS method A. Retention time: Me_2S_3 (7.10 min), 1,1,3,3-tetramethylurea (7.19 min), $^{n}Pr_2S_2$ (8.36 min, impurity from dipropyl trisulfide), $MeS_3{}^{n}Pr$ (8.75 min), and $^{n}Pr_2S_3$ (10.09 min).

GC traces of the crossover reaction in *N,N'*-dimethylpropyleneurea (DMPU) (10 eq., wet, non-dried and used as received)

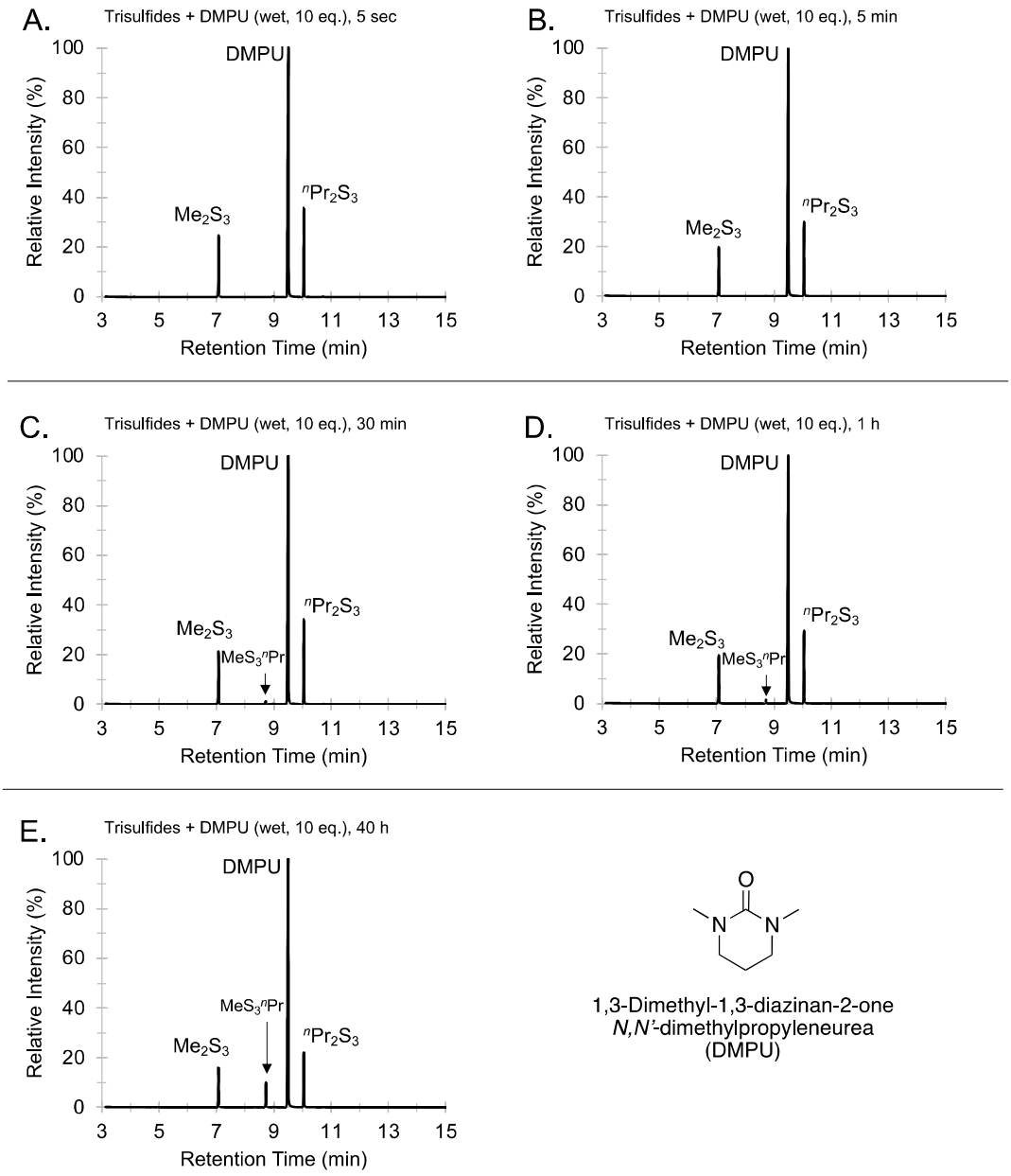

Figure S3.53: GC traces of the room temperature (8 – 14 ºC) reaction between dimethyl trisulfide (Me_2S_3) (42 µL, 0.4 mmol, 1 eq.), di-*n*-propyl trisulfide ($^nPr_2S_3$) (68 µL, 0.4 mmol, 1 eq.), and *N,N'*-dimethylpropyleneurea (482 µL, 4.0 mmol, 10 eq.) after (A) 5 sec, (B) 5 min, (C) 30 min, (D) 1 hour, and (E) 40 h. GC-MS method A. Retention time: Me_2S_3 (7.10 min), $MeS_3{}^nPr$ (8.75 min), DMPU (9.47 min), and $^nPr_2S_3$ (10.09 min).

Trisulfide Crossover: Substrate Scope

Dimethyl trisulfide (Me_2S_3) and diethyl trisulfide (Et_2S_3) crossover

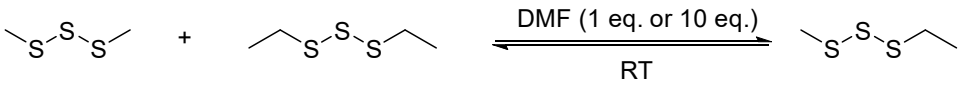

Dimethyl trisulfide (42 µL, 0.4 mmol, 1 eq.), diethyl trisulfide (61.7 mg, 0.4 mmol, 1 eq.) and *N*,*N*-dimethylformamide (31 µL, 0.4 mmol, 1 eq. or 310 µL, 4.0 mmol, 10 eq.) were added to a 2 mL glass vial equipped with a stir bar and sealed with a lid. The mixture was stirred at room temperature for 24 hours. After 1 and 24 h, a 10 µL aliquot was removed and diluted to 1 mL with chloroform for GC-MS analysis. A control experiment was carried out without *N*,*N*-dimethylformamide.

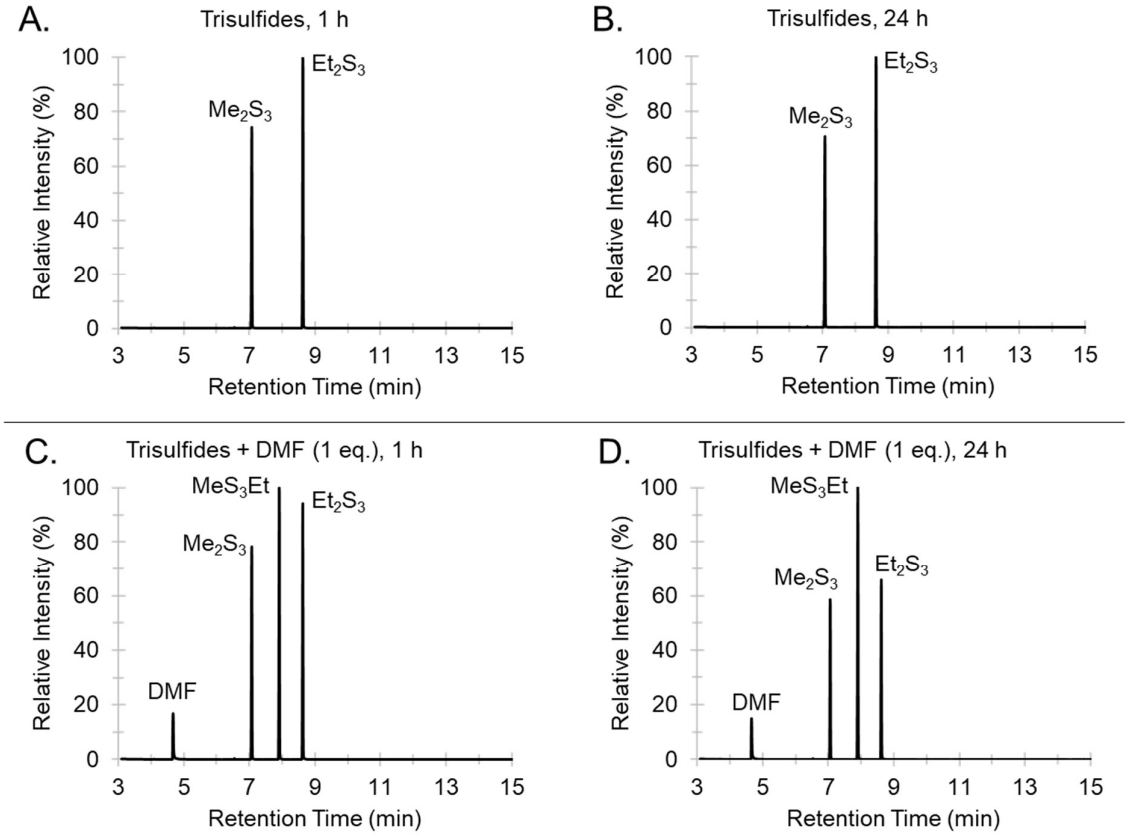

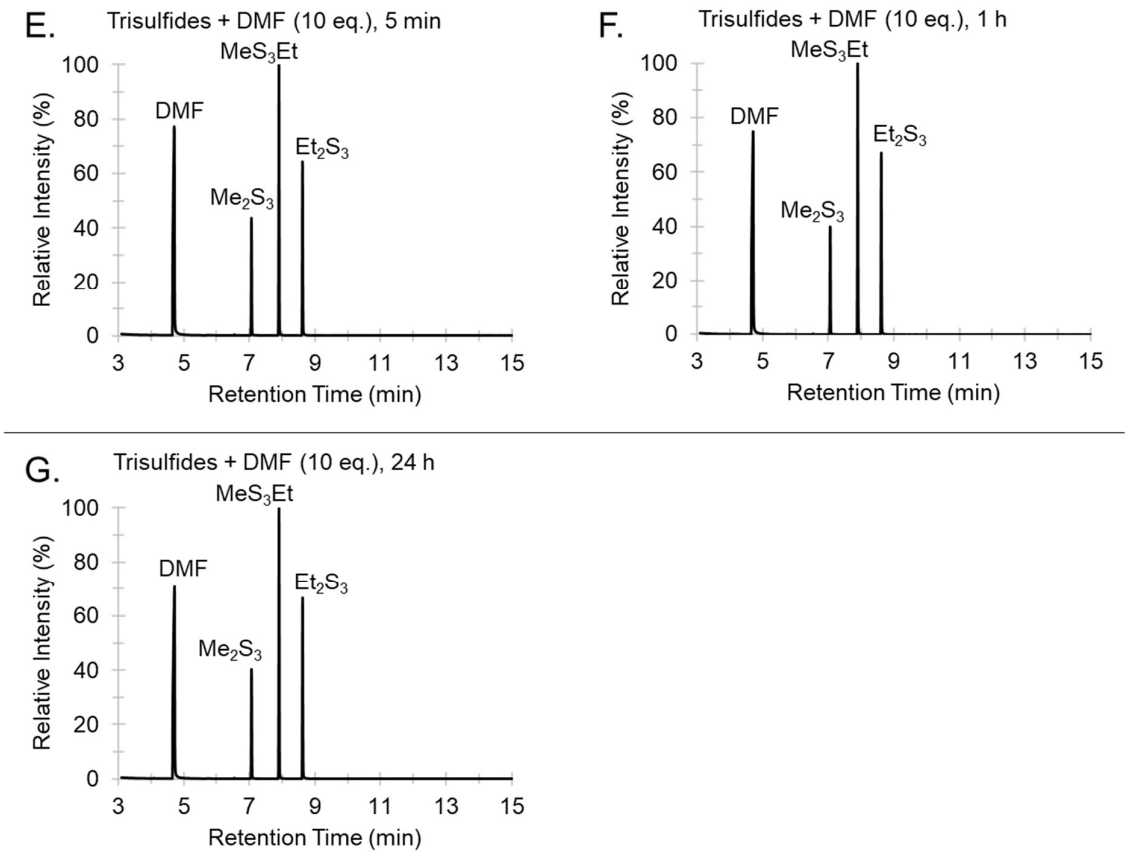

Figure S3.54: GC-MS traces for crossover reaction between dimethyl trisulfide (Me_2S_3) and diethyl trisulfide (Et_2S_3) with DMF over 1 hour at room temperature (10 – 12 °C). (A, B) The trisulfides (1 eq. each) after 1 h and 24 h (no solvent). (C, D) The trisulfides (1 eq.) and DMF (1 eq.) after 1 h and 24 h. (E, F, G) The trisulfides (1 eq. each) and DMF (10 eq.) after 5 min, 1 h and 24 h. GC-MS method A. Retention time: DMF (4.70 min), Me_2S_3 (7.10 min), EtS_3Me (7.90 min), and Et_2S_3 (8.62 min).

Dimethyl trisulfide (Me_2S_3) and di-*n*-hexyl trisulfide ($^nHex_2S_3$) crossover

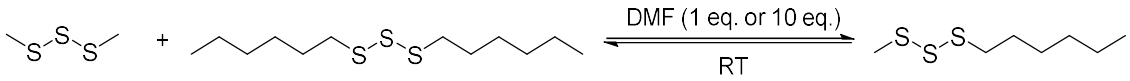

Dimethyl trisulfide (42 µL, 0.4 mmol, 1 eq.), di-*n*-hexyl trisulfide (106.6 mg, 0.4 mmol, 1 eq.) and *N*,*N*-dimethylformamide (31 µL, 0.4 mmol, for 1 eq., or 310 µL, 4.0 mmol, for 10 eq.) were added to a 2 mL glass vial equipped with a stir bar and sealed with a lid. The mixture was stirred at room temperature (10 – 12 ºC) for 24 hours. After 1 h and 24 h, a 10 µL aliquot was removed and diluted to 1 mL with chloroform for GC-MS analysis. A control experiment was also carried out without *N*,*N*-dimethylformamide.

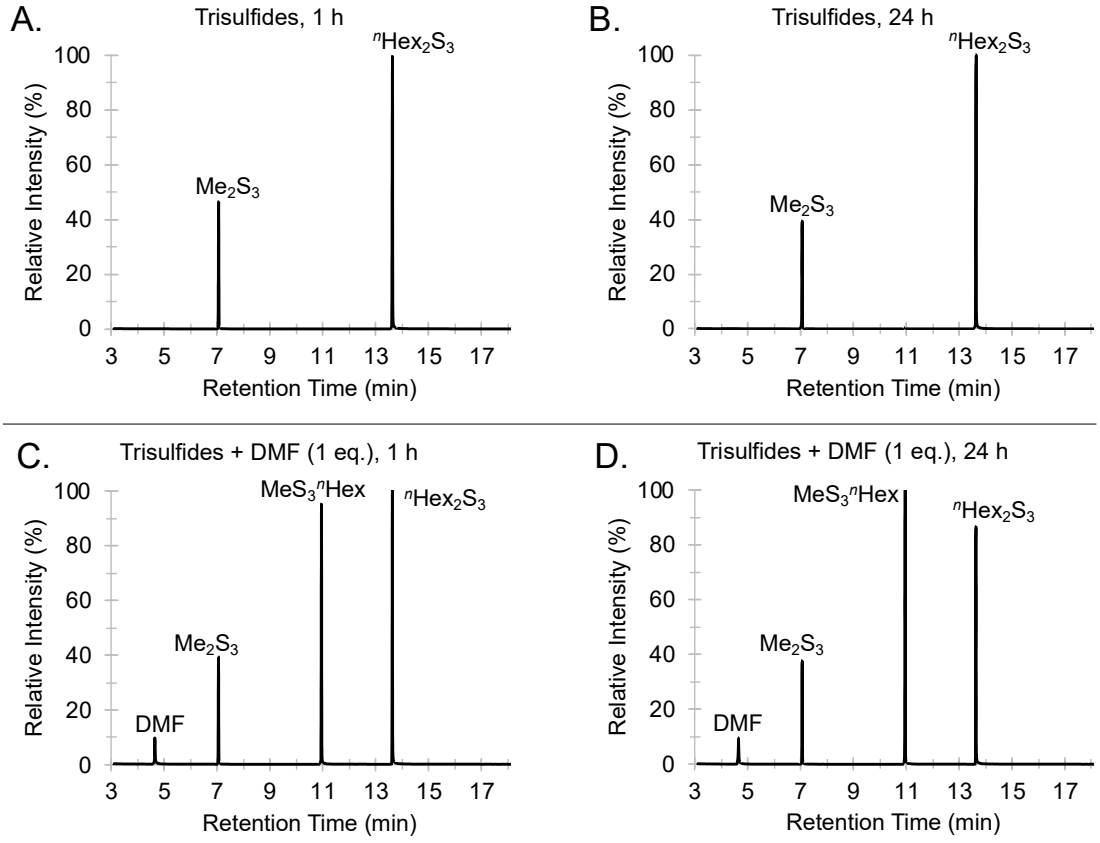

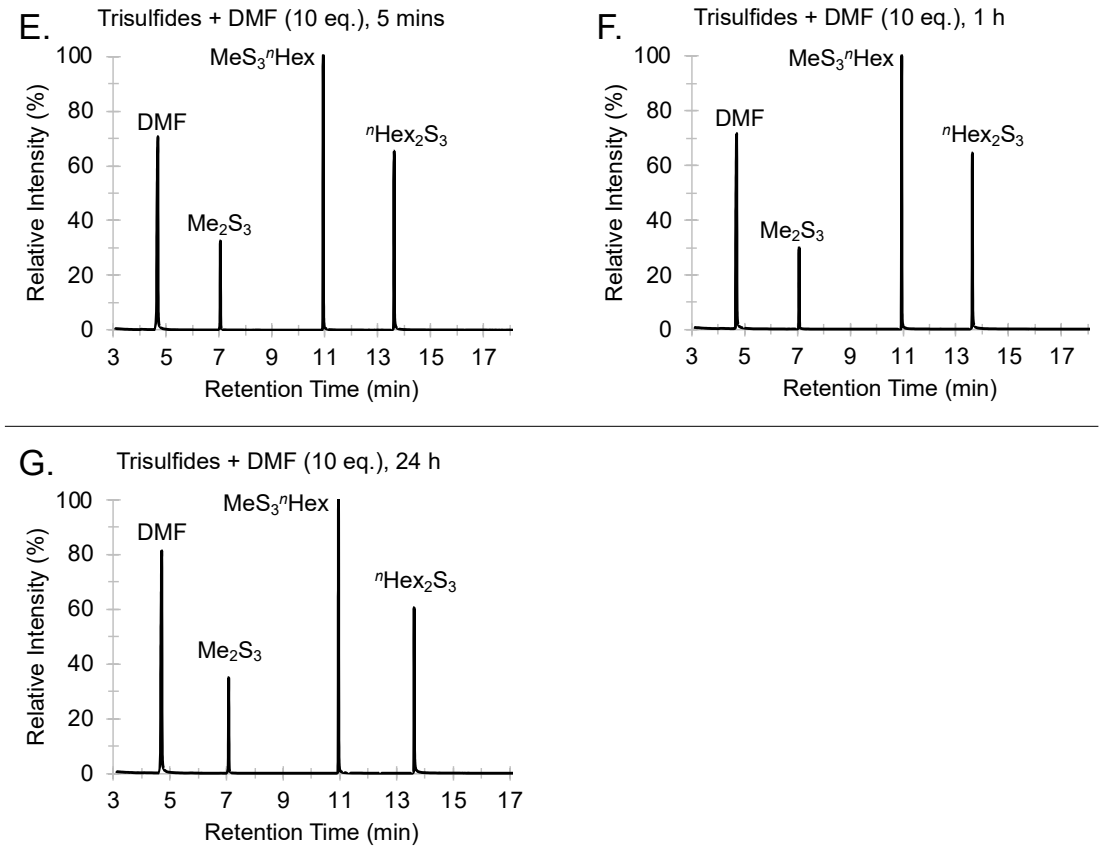

Figure S3.55: GC-MS traces for crossover reaction between dimethyl trisulfide (Me_2S_3) and di-*n*-hexyl trisulfide ($^{n}Hex_2S_3$) with DMF over 24 hours at room temperature (10 – 12 °C). (A, B) The trisulfides (1 eq. each) after 1 h and 24 h (no solvent). (C, D) The trisulfides (1 eq.) and DMF (1 eq.) after 1 h and 24 h. (E, F, G) The trisulfides (1 eq. each) and DMF (10 eq.) after 5 min, 1 h and 24 h. GC-MS method A. Retention time: DMF (4.70 min), Me_2S_3 (7.10 min), $^{n}HexS_3Me$ (10.95 min), and $^{n}Hex_2S_3$ (13.63 min).

Dimethyl trisulfide (Me_2S_3) and diallyl trisulfide ($Allyl_2S_3$) crossover

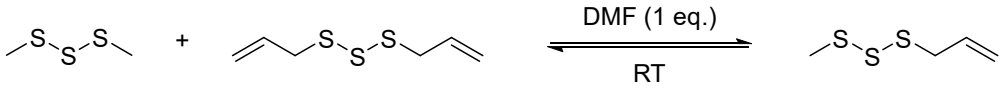

Dimethyl trisulfide (126 µL, 1.2 mmol, 1 eq.), diallyl trisulfide (214 mg, 1.2 mmol, 1 eq.), and *N*,*N*-dimethylformamide (93 µL, 1.2 mmol, 1 eq.) were added in a 2 mL glass vial equipped with a stir bar and sealed with a lid. The mixture was stirred at room temperature (13 – 17 ºC). After 1 h and 24 h, a 10 µL aliquot was removed and diluted to 1 mL with chloroform for GC-MS analysis. A control experiment was carried out between the trisulfides without DMF.

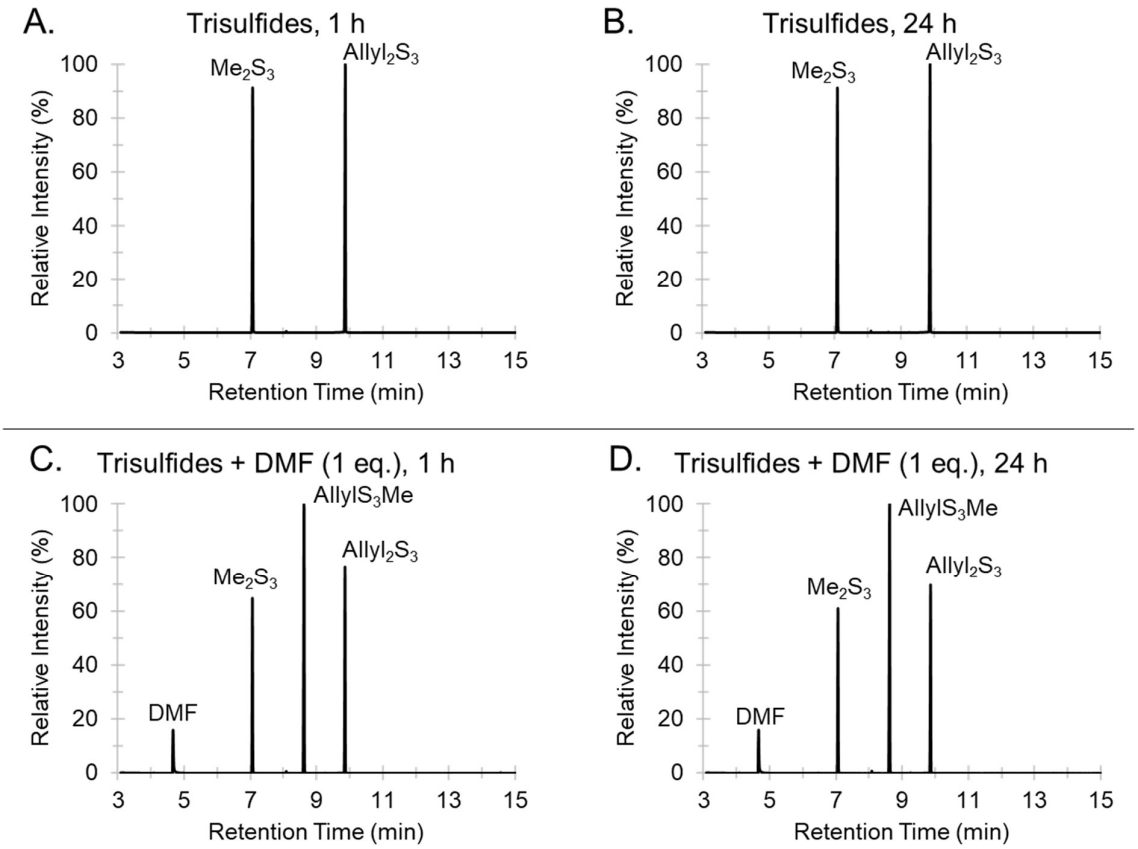

Figure S3.56: GC-MS traces for crossover reaction between dimethyl trisulfide (Me_2S_3) and diallyl trisulfide ($Allyl_2S_3$) with *N*,*N*-dimethylformamide (DMF) over 24 hours at room temperature (13 – 17 °C). (A, B) The trisulfides (1 eq. each) after 1 h and 24 h (no solvent). (C, D) The trisulfides (1 eq. each) and DMF (1 eq.) after 1 h and 24 h. The reaction reached equilibrium after 1 hour with the yield of the crossover product, $AllylMeS_3$. GC-MS method A. Retention time: DMF (4.67 min), Me_2S_3 (7.07 min), $AllylS_3Me$ (8.63 min), and $Allyl_2S_3$ (9.87 min).

Dimethyl trisulfide (Me_2S_3) and dibenzyl trisulfide (Bn_2S_3) crossover

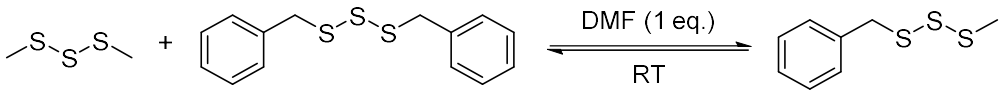

Dimethyl trisulfide (42 µL, 0.4 mmol, 1 eq.), dibenzyl trisulfide (111.3 mg, 0.4 mmol, 1 eq.), and *N*,*N*-dimethylformamide (31 µL, 0.4 mmol, 1 eq.) were added to a 2 mL glass vial equipped with a stir bar and sealed with a lid. The mixture was stirred at room temperature (13 – 15 ºC). After 1 and 24 h, a 10 µL aliquot was removed and diluted to 1 mL with chloroform for GC-MS analysis. A control experiment was attempted without the presence of *N*,*N*-dimethylformamide; however, the mixture was heterogeneous and, thus, the trisulfides (0.4 mmol each, 1 eq. each) were dissolved in diethyl ether for this control experiment (200 µL, 3.13 mmol, 7.8 eq.).

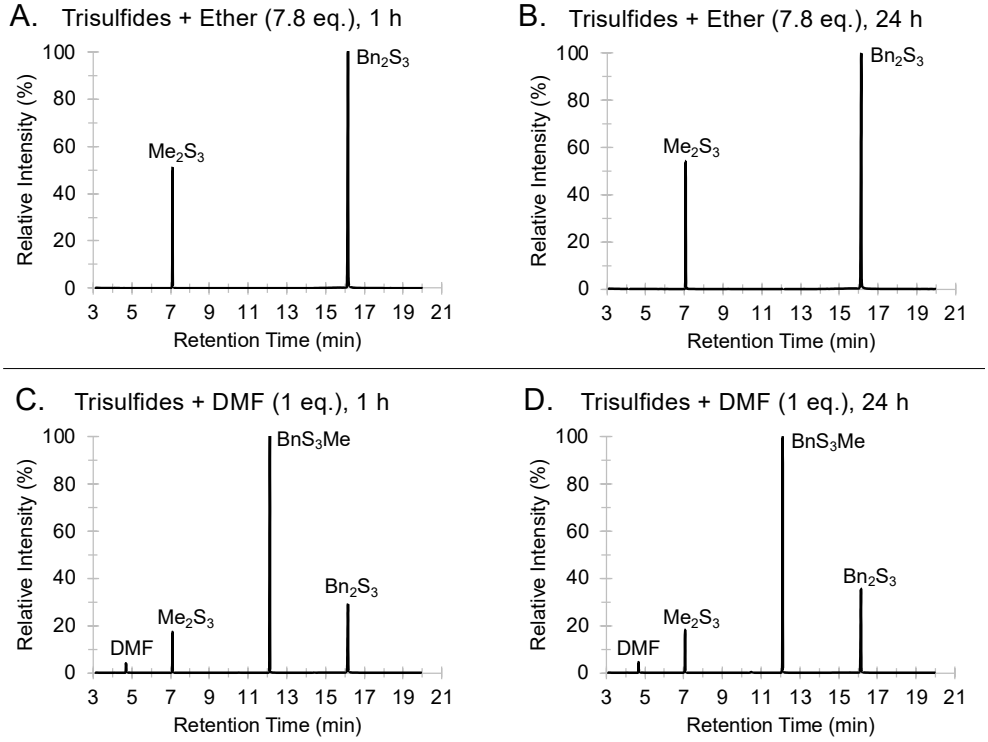

Figure S3.57: GC-MS traces for crossover reaction between dimethyl trisulfide (Me_2S_3) and dibenzyl trisulfide (Bn_2S_3) with *N*,*N*-dimethylformamide (DMF) over 24 hours at room temperature (13 – 15 °C). (A, B) The trisulfides (1 eq. each) and diethyl ether (7.8 eq.) after 1 h and 24 h (non-polar solvent negative control). (C, D) The trisulfides (1 eq. each) and DMF (1 eq.) after 1 h and 24 h. GC-MS method A. Retention time: DMF (4.67 min), Me_2S_3 (7.07 min), BnS_3Me (12.10 min), and Bn_2S_3 (16.14 min).

Di-*n*-propyl trisulfide ($^{n}Pr_2S_3$) and dibenzyl trisulfide (Bn_2S_3) crossover

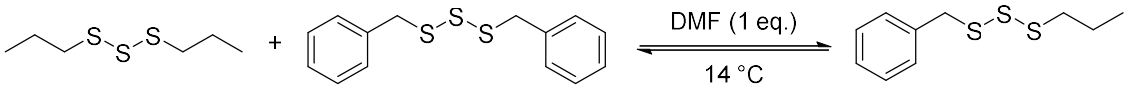

Di-*n*-propyl trisulfide (68 µL, 0.4 mmol, 1 eq.), dibenzyl trisulfide (111.3 mg, 0.4 mmol, 1 eq.) and *N*,*N*-dimethylformamide (31 µL, 0.4 mmol, 1 eq.) were added to a 2 mL glass vial equipped with a stir bar and sealed with a lid. The mixture was stirred at room temperature (13 – 15 ºC) for 24 hours. After 1 h and 24 h, a 10 µL aliquot was removed and diluted to 1 mL with chloroform for GC-MS analysis. A control experiment was also attempted without the presence of *N*,*N*-dimethylformamide; however, the trisulfides mixture was heterogenous. The control experiment was then carried out by dissolving the trisulfides (0.4 mmol each, 1 eq. each) with diethyl ether (200 µL, 3.13 mmol, 7.8 eq.).

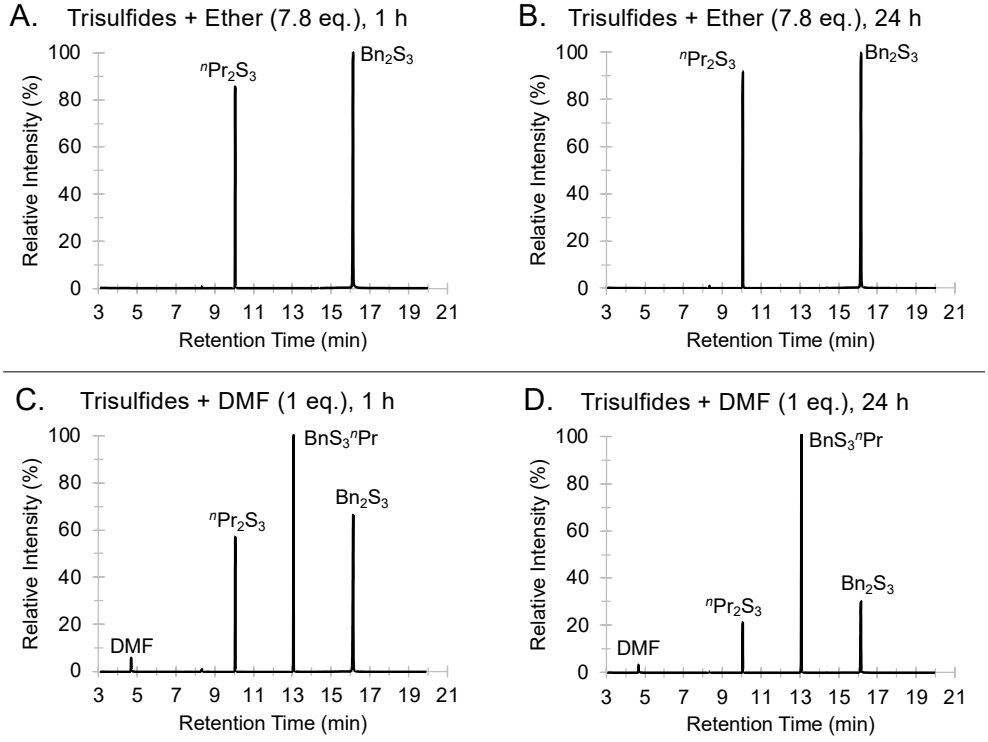

Figure S3.58: GC-MS traces for crossover reaction between di-*n*-propyl trisulfide ($^{n}Pr_2S_3$) and dibenzyl trisulfide (Bn_2S_3) with *N*,*N*-dimethylformamide (DMF) over 24 hours at room temperature (13 – 15 °C). (A, B) The trisulfides (1 eq. each) and diethyl ether (7.8 eq.) after 1 h and 24 h. (C, D) The trisulfides (1 eq. each) and DMF (1 eq.) after 1 h and 24 h. GC-MS method A. Retention time: DMF (4.67 min), $^{n}Pr_2S_3$ (10.05 min), $BnS_3{}^{n}Pr$ (13.07 min), and Bn_2S_3 (16.14 min).

Bis(4-methoxybenzyl) trisulfide and dimethyl trisulfide crossover

(This experiment was performed by Dr. Harshal D. Patel)

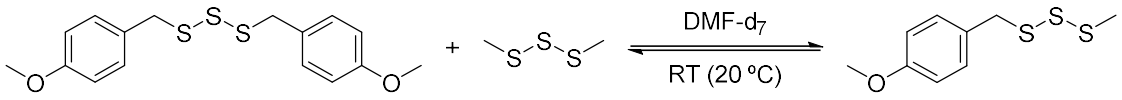

Bis(4-methoxybenzyl) trisulfide (10 mg, 30 µmol) was dissolved in DMF-d_7 (600 µL) in an NMR tube at room temperature (20 °C). Dimethyl trisulfide (3.11 µL, 29.5 µmol) was added and ^{1}H NMR spectra recorded at 5 min, 30 min, 1 h, and 24 h. New peaks at 4.20 ppm and 2.58 ppm were formed after 5 minutes reaction corresponding to the unsymmetrical crossover product. Equilibrium was reached within 1 hour.

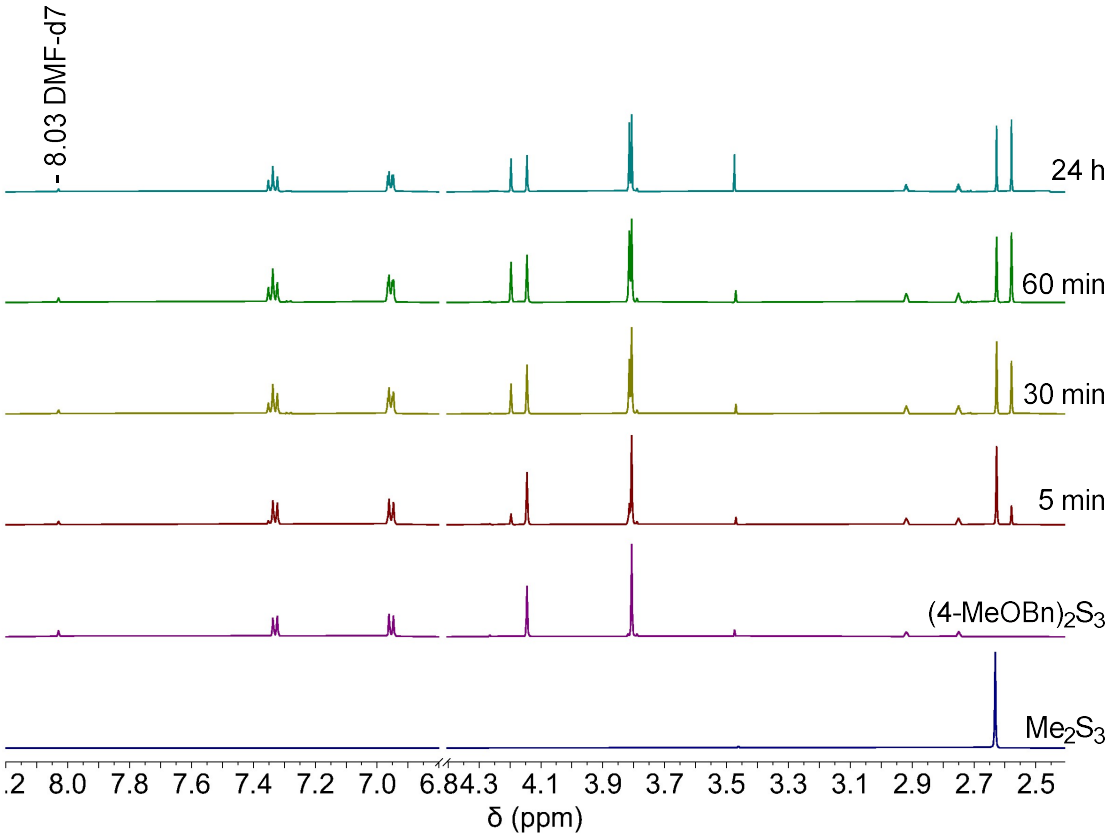

Figure S3.59: Stacked ^{1}H NMR spectra of bis(4-methoxybenzyl) trisulfide and dimethyl trisulfide mixture in DMF-d_7.

Bis(4-methoxybenzyl) trisulfide and dibenzyl trisulfide crossover

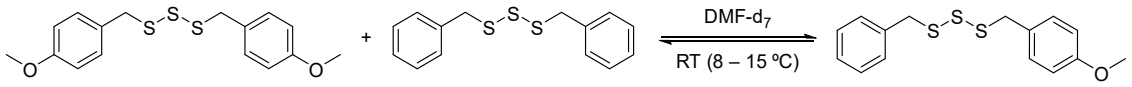

Bis(4-methoxybenzyl) trisulfide (9.5 mg, 28 µmol) and dibenzyl trisulfide (7.8 mg, 28 µmol) were added to a GC vial and dissolved in DMF-d_7 (600 µL) at room temperature (20 ºC). This mixture was quickly transferred to an NMR tube and ^{1}H NMR spectra recorded at 5 min, 1 h, 12 h, and 24 h. New peaks at 4.19 ppm and 4.13 ppm, corresponding to the crossover product, were formed after 5 minutes reaction. Equilibrium was reached after 1 hour.

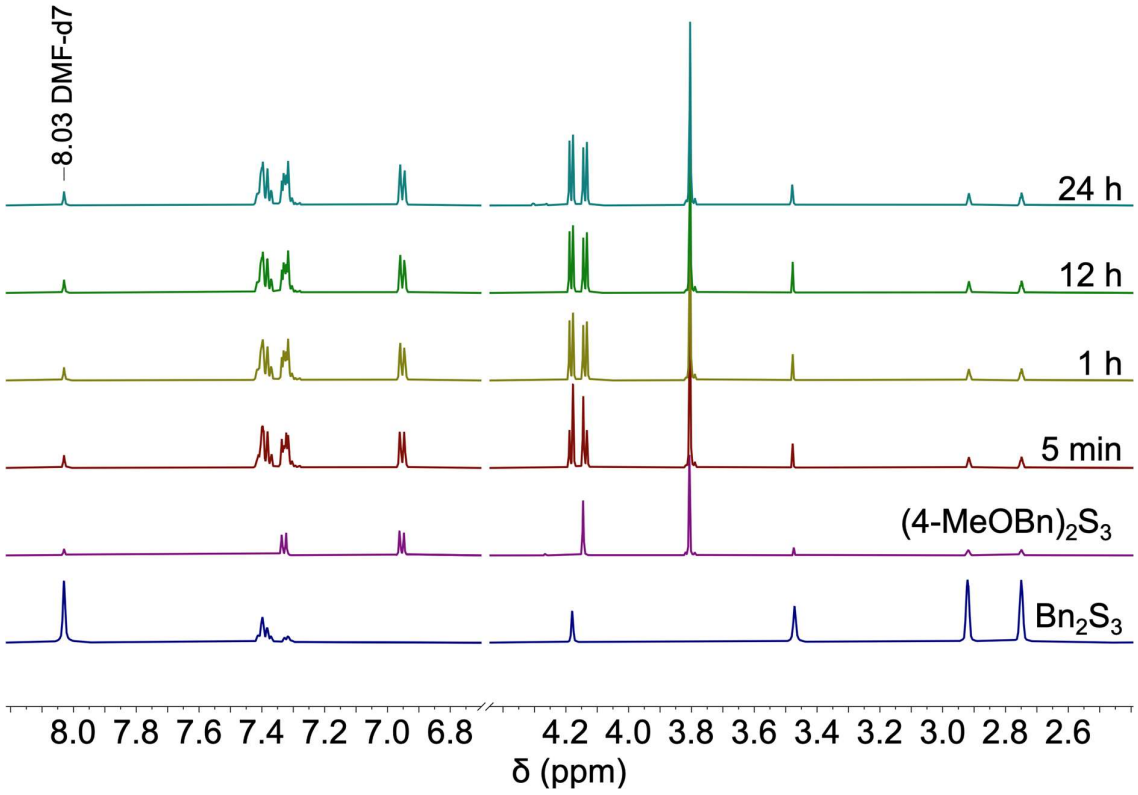

Figure S3.60: Stacked ^{1}H NMR spectra of bis(4-methoxybenzyl) trisulfide and dibenzyl trisulfide mixture in DMF-d_7.

Dimethyl trisulfide and di-isobutyl trisulfide crossover

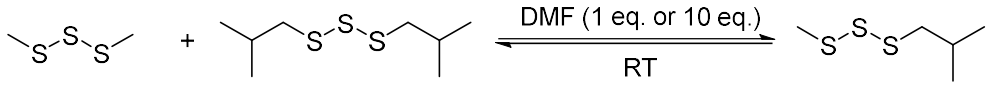

Dimethyl trisulfide (42 µL, 0.4 mmol, 1 eq.), di-isobutyl trisulfide (84.1 mg, 0.4 mmol, 1 eq.) and *N*,*N*-dimethylformamide (31 µL, 0.4 mmol, for 1 eq., or 310 µL, 4.0 mmol, for 10 eq.) were added to a 2 mL glass vial equipped with a stir bar and sealed with a lid. The mixture was stirred at room temperature (9 – 12 ºC) for 24 hours. After 1 and 24 h, a 10 µL aliquot was removed and diluted to 1 mL with chloroform for GC-MS analysis. A control experiment was carried out without *N*,*N*-dimethylformamide.

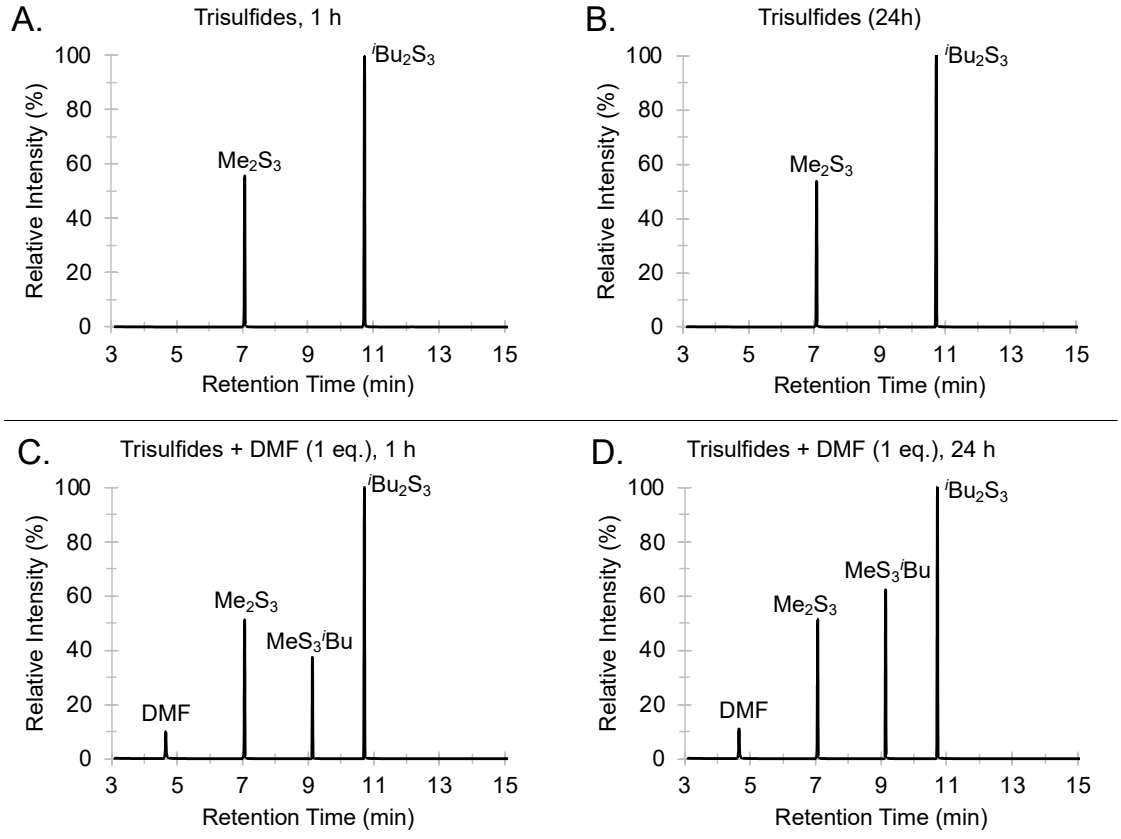

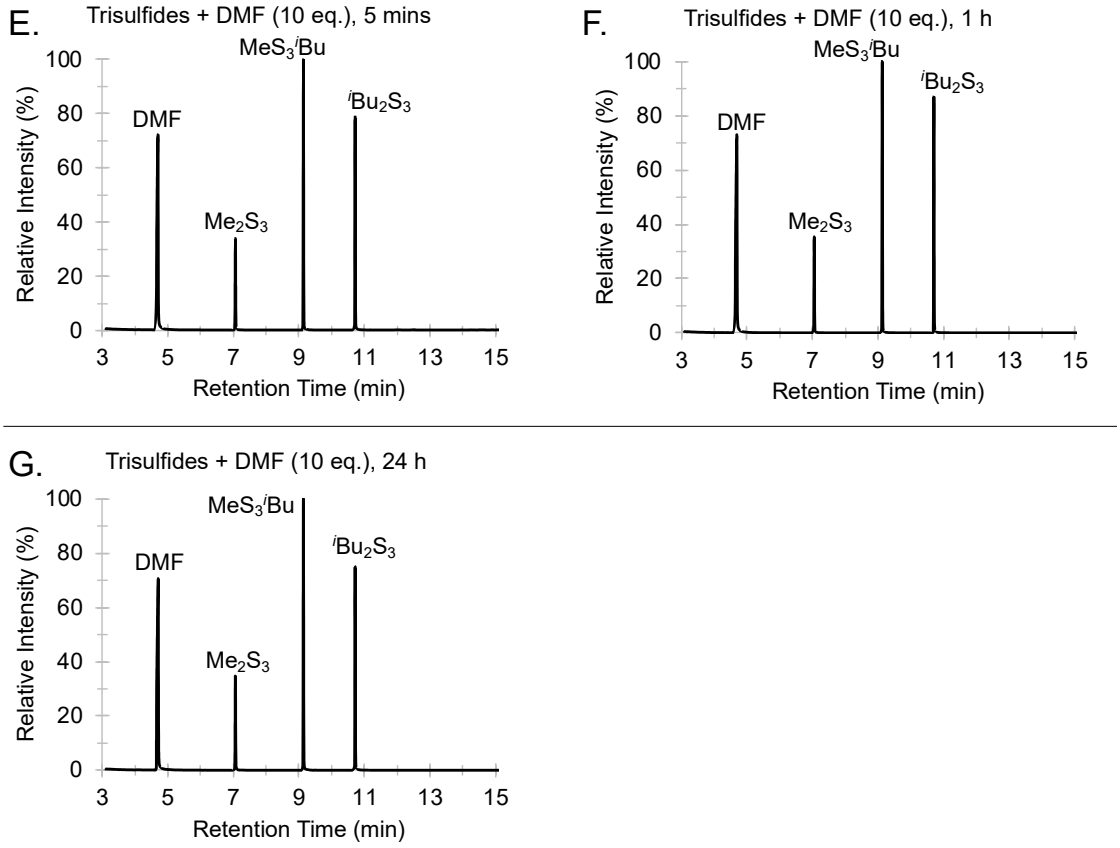

Figure S3.61: GC-MS traces for crossover reaction between dimethyl trisulfide (Me_2S_3) and di-isobutyl trisulfide ($^{i}Bu_2S_3$) with DMF over 1 hour at room temperature (9 – 12 °C). (A, B) The trisulfides (1 eq. each) after 1 h and 24 h (no solvent). (C, D) The trisulfides (1 eq.) and DMF (1 eq.) after 1 h and 24 h. (E, F, G) The trisulfides (1 eq. each) and DMF (10 eq.) after 5 min, 1 h and 24 h. GC-MS method A. Retention time: DMF (4.70 min), Me_2S_3 (7.10 min), $^{i}BuS_3Me$ (9.14 min), and $^{i}Bu_2S_3$ (10.71 min).

Dimethyl trisulfide and di-isopropyl trisulfide crossover

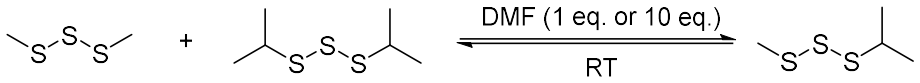

Dimethyl trisulfide (42 µL, 0.4 mmol, 1 eq.), di-isopropyl trisulfide (70.2 µL, 0.4 mmol, 1 eq.) and *N*,*N*-dimethylformamide (31 µL, 0.4 mmol, 1 eq., or 310 µL, 4.0 mmol, 10 eq.) were added to a 2 mL glass vial equipped with a stir bar and sealed with a lid. The mixture was stirred at room temperature (14 – 16 ºC) for 24 hours. After 1 h and 24 h, a 10 µL aliquot was removed and diluted to 1 mL with chloroform for GC-MS analysis. A control experiment was carried out without *N*,*N*-dimethylformamide.

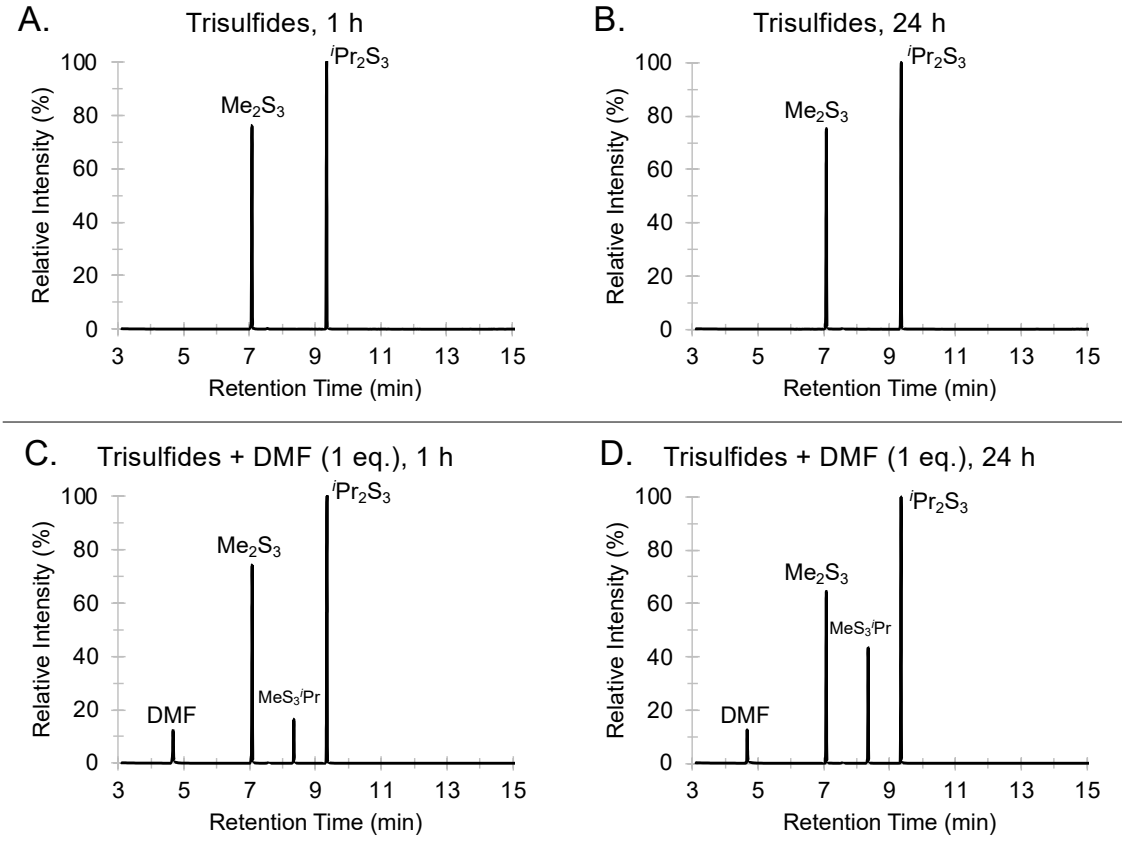

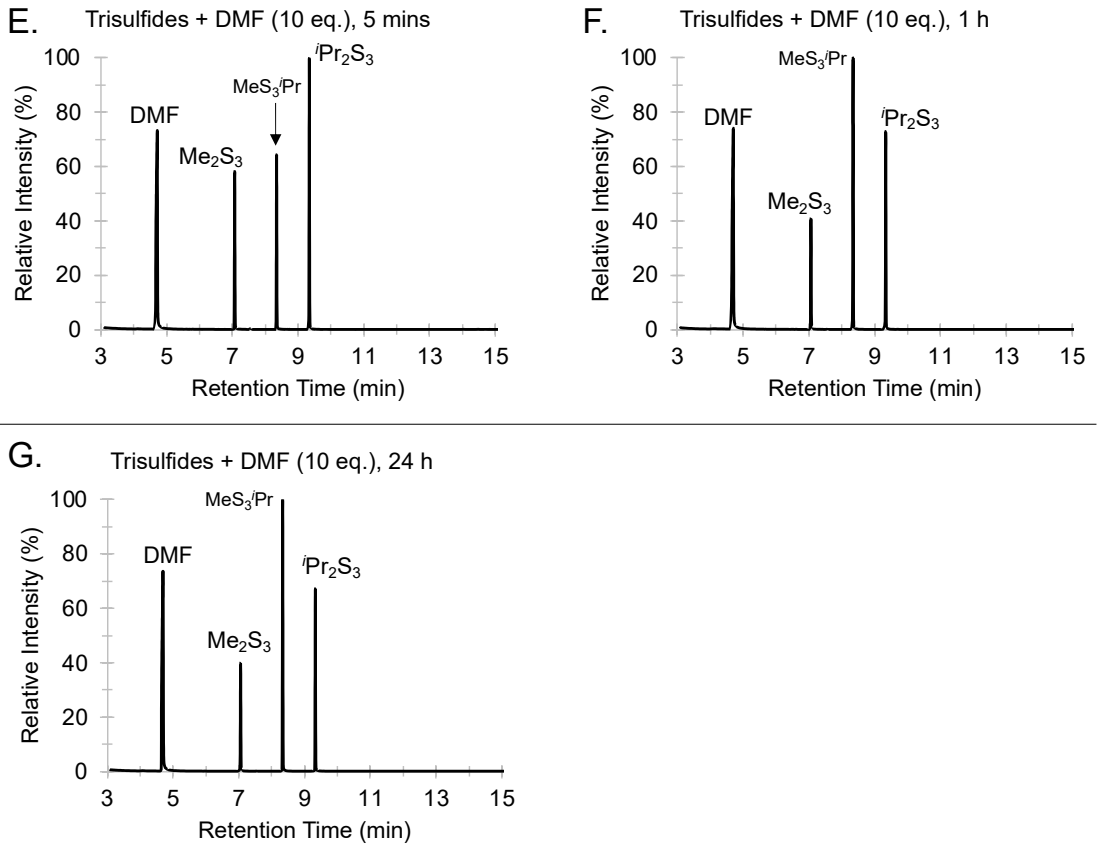

Figure S3.62: GC-MS traces for crossover reaction between dimethyl trisulfide (Me_2S_3) and di-isopropyl trisulfide ($^{i}Pr_2S_3$) with DMF over 1 hour at room temperature (14 – 16 °C). (A, B) The trisulfides (1 eq. each) after 1 h and 24 h (no solvent). (C, D) The trisulfides (1 eq. each) and DMF (1 eq.) after 1 h and 24 h. (E, F, G) The trisulfides (1 eq. each) and DMF (10 eq.) after 5 min, 1 h, and 24 h. GC-MS method A. Retention time: DMF (4.70 min), Me_2S_3 (7.10 min), $MeS_3{}^{i}Pr$ (8.34 min), and $^{i}Pr_2S_3$ (9.34 min).

Bis(adamantyl) trisulfide and dimethyl trisulfide (Me_2S_3) crossover

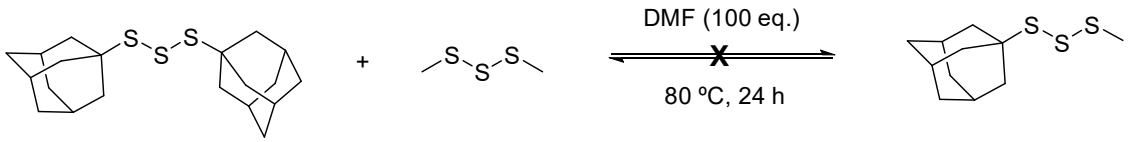

No reaction was observed between equimolar amounts of bis(1-adamantyl) trisulfide and dimethyl trisulfide at room temperature (17 – 29 ºC) in excess DMF over 24 h. The bis(1-adamantyl) trisulfide was also not completely soluble under these conditions. Therefore, the stirred mixture was heated at 80 ºC for 24 h. Heating at this temperature gave the clear mixture, indicating that bis(1-adamantyl) trisulfide was completely dissolved in this condition. After 1 and 24 h, a 10 µL aliquot was removed and diluted to 1 mL with chloroform for GC-MS analysis. No crossover reaction was observed under these conditions either.

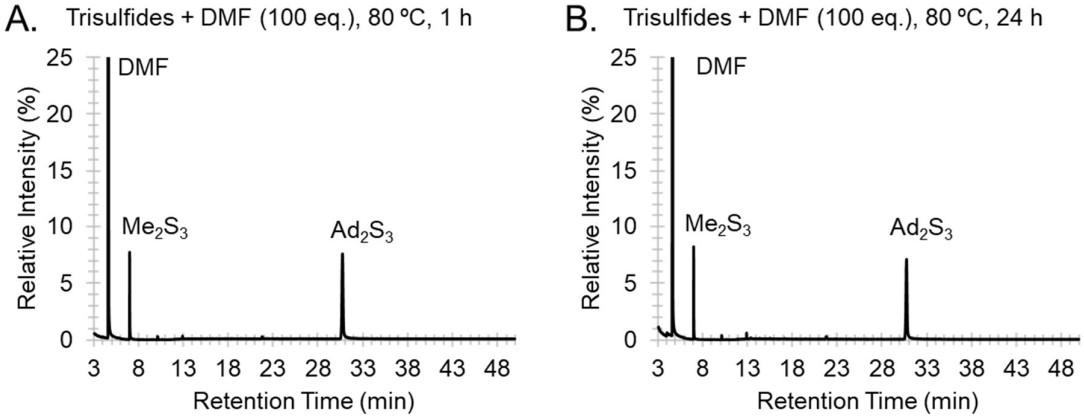

Figure S3.63: GC-MS traces for crossover reaction between bis(1-adamantyl) trisulfide (Ad_2S_3) and dimethyl trisulfide (Me_2S_3) in DMF at 80 ºC. The trisulfides (1 eq. each) in DMF (100 eq.) at 80 ºC after (A) 1 h and (B) 24 hours. GC-MS method D. Retention time: DMF (4.70 min), Me_2S_3 (7.03 min), and Ad_2S_3 (30.76 min).

Dimethyl trisulfide (Me_2S_3) and di-*tert*-butyl trisulfide ($^tBu_2S_3$) crossover

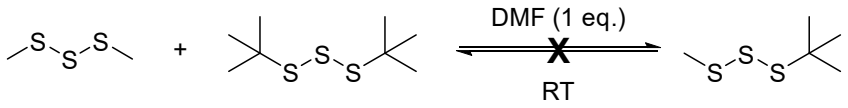

Dimethyl trisulfide (42 µL, 0.4 mmol, 1 eq.), di-*tert*-butyl trisulfide (84.2 mg, 0.4 mmol, 1 eq.) and *N*,*N*-dimethylformamide (31 µL, 0.4 mmol, for 1 eq., or 310 µL, 4.0 mmol, for 10 eq.) were added to a 2 mL glass vial was added equipped with a stir bar and sealed with a lid. The mixture was stirred at room temperature (10 – 12 ºC) for 24 hours. After 1 h and 24 h, a 10 µL aliquot was removed and diluted to 1 mL with chloroform for GC-MS analysis. A control experiment was carried out without *N*,*N*-dimethylformamide.

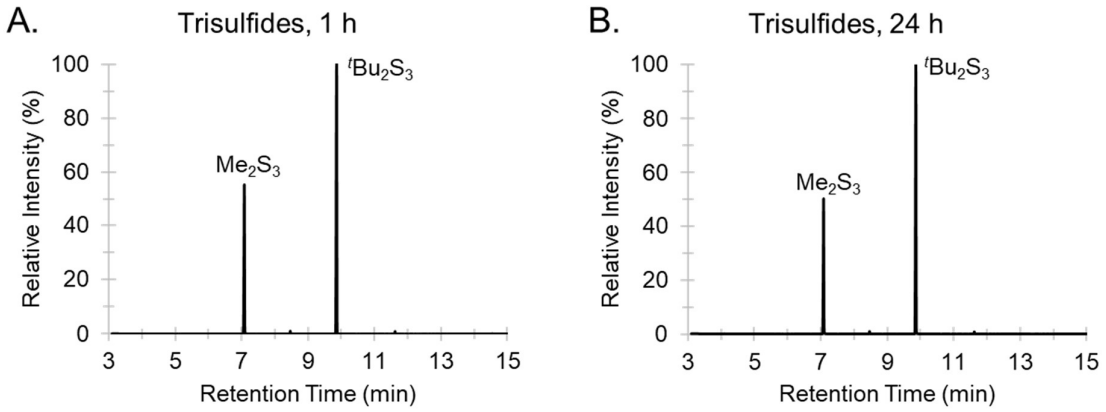

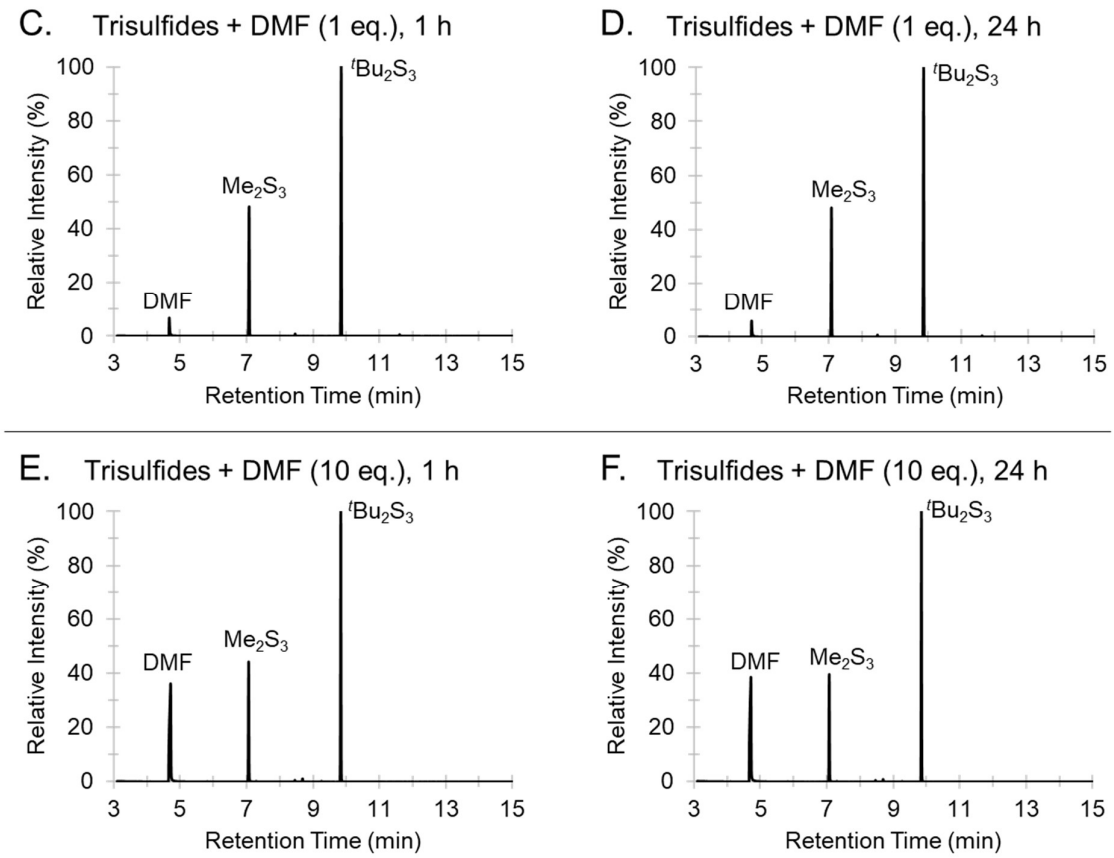

Figure S3.64: GC-MS traces for crossover reaction between dimethyl trisulfide (Me_2S_3) and di-*tert*-butyl trisulfide ($^tBu_2S_3$) with *N*,*N*-dimethylformamide (DMF) over 24 hours at room temperature (10 – 12 °C). (A, B) The trisulfides (1 eq. each) after 1 h and 24 h (no solvent). (C, D) The trisulfides (1 eq. each) and DMF (1 eq.) after 1 h and 24 h. (E, F) The trisulfides (1 eq. each) and DMF (10 eq.) after 1 h and 24 h. No crossover product formed in these experiments. GC-MS method A. Retention time: DMF (4.67 min), Me_2S_3 (7.07 min), and $^tBu_2S_3$ (9.85 min).

Me_2S_3 and $^tBu_2S_3$ thermal crossover (neat)

(This experiment was performed by Dr. Harshal D. Patel)

Me_2S_3 (29 µL, 270 µmol, 1.0 eq.) and $^tBu_2S_3$ (57 mg, 270 µmol, 1.0 eq.) were heated together at either 150 ºC or 170 ºC. Samples were taken at regular intervals for analysis by GC-MS (1 µL trisulfides sample diluted in 1 mL $CHCl_3$). The crossover product, *t*-BuS_3Me, was observable by GC-MS.

$MeS_3{}^tBu$

GC-MS (EI, 70 eV) *m/z* (rel. intensity): *m/z* calcd. for $C_5H_{12}S_3^+$: 168.0[*M*]$^+$, found: 168.0 (M+, 25), 111.9 (16), 89.0 (7), 79.0 (6), 64.0 (7), 57.1 (100).

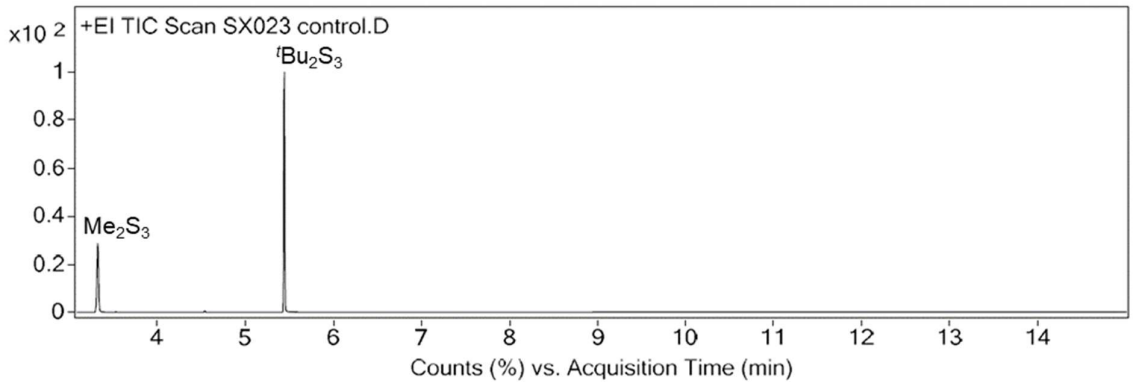

Figure S3.65: Gas chromatogram of the reaction between Me_2S_3 and $^tBu_2S_3$, prior to heating. GC-MS method E. Retention time: Me_2S_3 (3.333 min), $^tBu_2S_3$ (5.450 min).

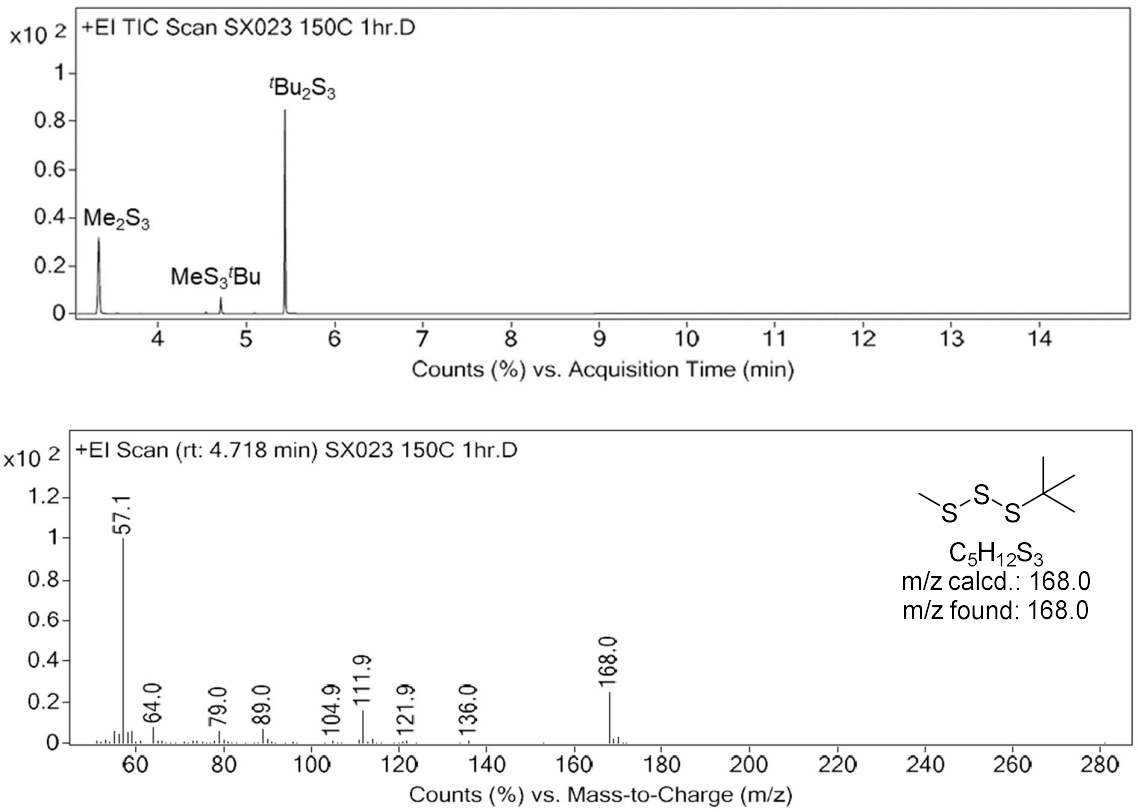

Figure S3.66: Gas chromatogram of the reaction between Me_2S_3 and $^tBu_2S_3$ after heating for 1 hour at 150 ºC, and the mass spectrum of the $MeS_3{}^tBu$ peak. GC-MS method E. Retention time: Me_2S_3 (3.333 min), MeS_3t-Bu (4.718 min), t-Bu_2S_3 (5.450 min).

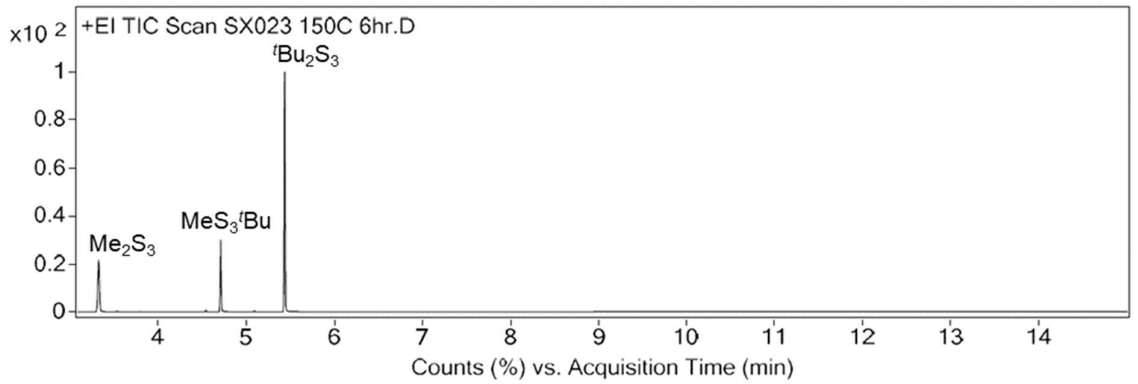

Figure S3.67: Gas chromatogram of the reaction between Me_2S_3 and $^tBu_2S_3$ after heating for 6 hours at 150 ºC. GC-MS method E. Retention time: Me_2S_3 (3.333 min), $MeS_3{}^tBu$ (4.718 min), $^tBu_2S_3$ (5.450 min).

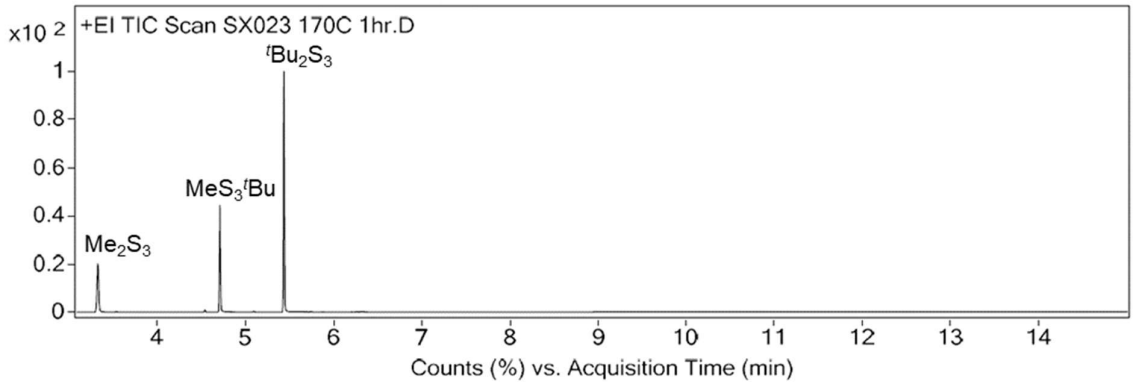

Figure S3.68: Gas chromatogram of the reaction between Me_2S_3 and *t*-Bu_2S_3 after heating for 1 hour at 170 ºC. GC-MS method F. Retention time: Me_2S_3 (3.333 min), MeS_3*t*-Bu (4.718 min), *t*-Bu_2S_3 (5.450 min).

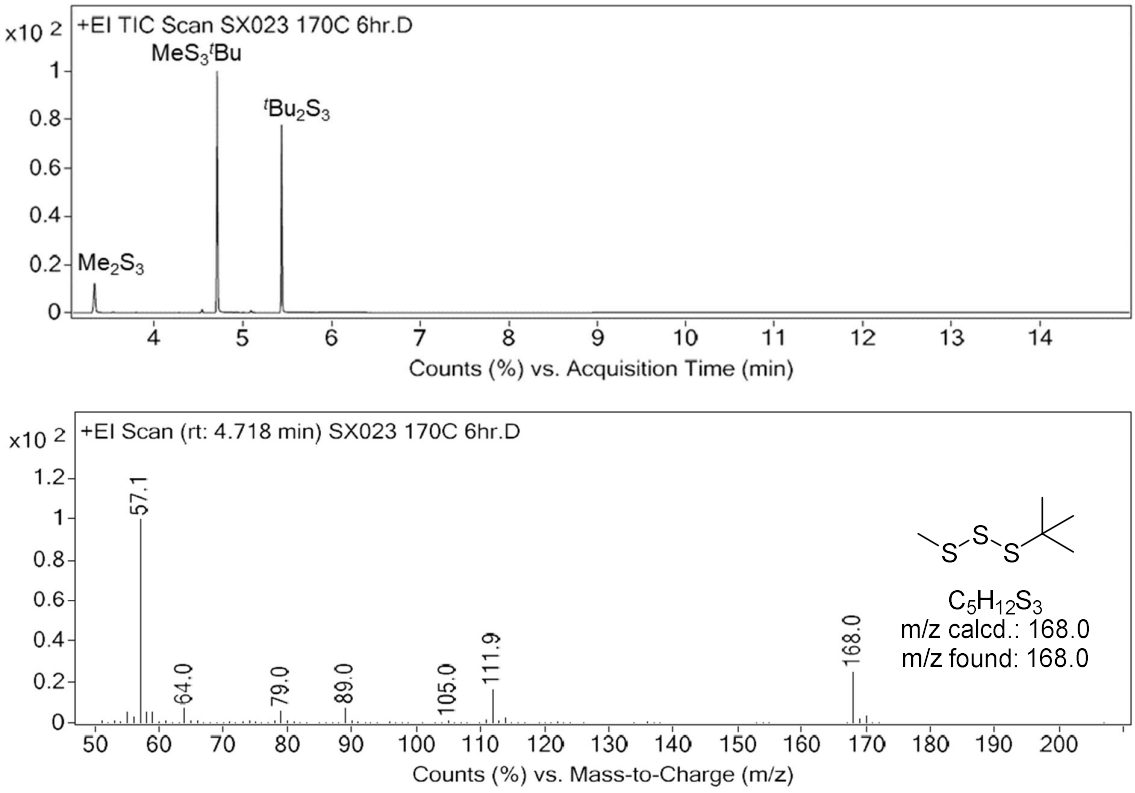

Figure S3.70: Gas chromatogram of the reaction between Me_2S_3 and *t*-Bu_2S_3 after heating for 6 hours at 170 °C, and the mass spectrum of the MeS_3*t*-Bu peak. GC-MS method E. Retention time: Me_2S_3 (3.333 min), MeS_3*t*-Bu (4.718 min), *t*-Bu_2S_3 (5.450 min).

Bis(2-hydroxyethyl) trisulfide and dimethyl trisulfide (Me_2S_3) crossover

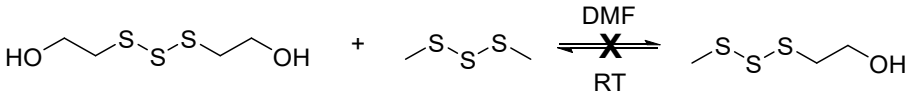

Bis(2-hydroxyethyl) trisulfide (30 mg, 161 μmol, 1 eq.), dimethyl trisulfide (16.9 μL, 20.3 mg, 1 eq.), and *N*,*N*-dimethylformamide (12.6 μL, 11.8 mg, 161 μmol, for 1 eq., or 125 μL, 1.61 mmol, for 10 eq.) were added to a 1.5 mL GC vial equipped with a stir bar and sealed with a lid. A control experiment was carried out between the trisulfides without *N*,*N*-dimethylformamide. After 1 h and 24 h of stirring at room temperature (8 – 15 ºC), a 5 μL aliquot was removed and diluted to 1 mL with chloroform for GC-MS analysis for the reaction in DMF. For the control experiment, a 2.5 μL aliquot was removed and diluted to 1 mL with chloroform for GC-MS analysis.

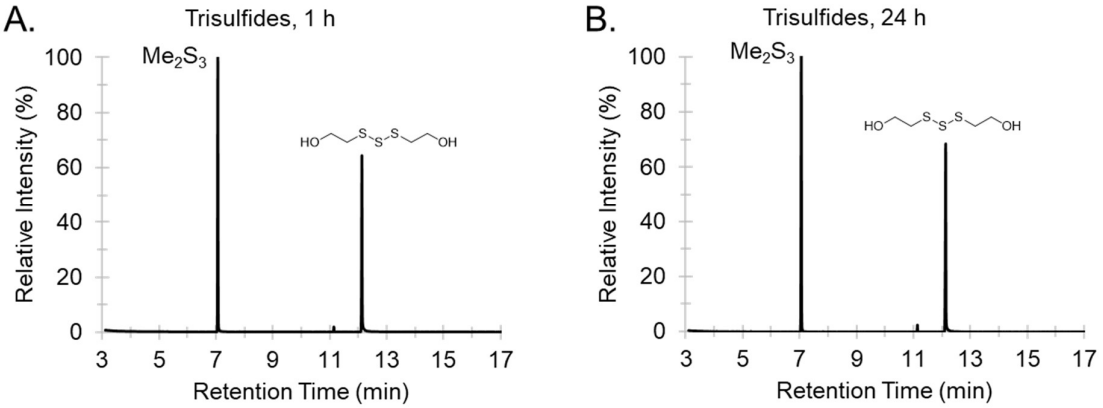

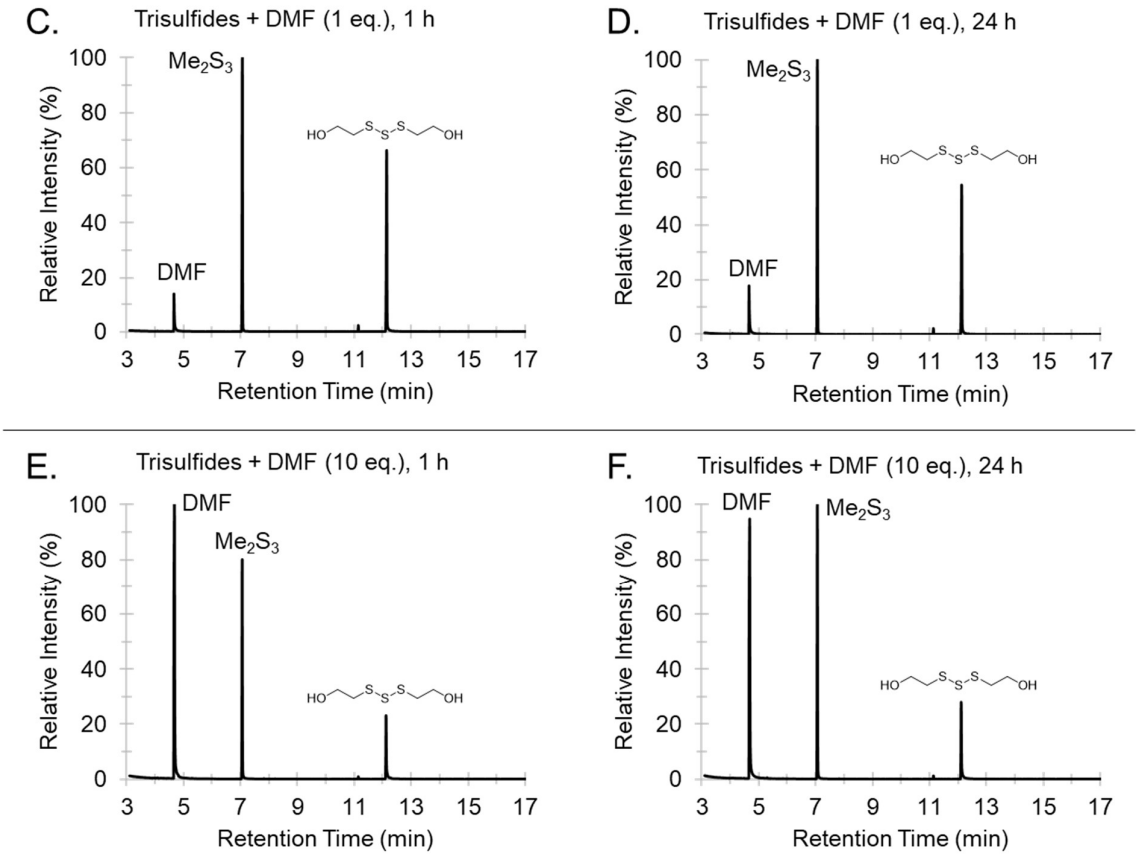

Figure S3.71: GC-MS traces for crossover reaction between bis(2-hydroxyethyl) trisulfide ($HOCH_2CH_2S_3CH_2CH_2OH$) and dimethyl trisulfide (Me_2S_3) with *N*,*N*-dimethylformamide (DMF) over 24 hours at room temperature (8 – 15 °C). (A, B) The trisulfides (1 eq. each) after 1 h and 24 h (no solvent). (C, D) The trisulfides (1 eq. each) and DMF (1 eq.) after 1 h and 24 h. (E, F) The trisulfides (1 eq. each) and DMF (10 eq.) after 1 h and 24 h. GC-MS method A. Retention time: DMF (4.67 min), Me_2S_3 (7.06 min) and $HOCH_2CH_2S_3CH_2CH_2OH$ (12.12 min).

Bis(2-trimethylsiloxyethyl) trisulfide ($Me_3SiOC_2H_4)_2S_3$ and dimethyl trisulfide (Me_2S_3) crossover

(This experiment was performed by Dr. Harshal D. Patel)

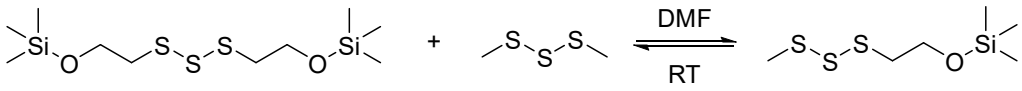

Bis(2-trimethylsiloxyethyl) trisulfide (16 mg, 48 µmol, 1.0 eq.), dimethyl trisulfide (5.09 µL, 48.4 µmol, 1.0 eq.) and *N*,*N*-dimethylformamide (37.3 µL, 484 µmol, 10.0 eq.) were added to a 1.5 mL GC vial equipped with a stir bar and sealed with a lid. A control experiment was carried out between the trisulfides without *N*,*N*-dimethylformamide. After 1 h and 22 h of stirring at room temperature, a 10 µL aliquot was removed and diluted to 1 mL with chloroform for GC-MS analysis for the reaction in DMF. For the control experiment, a 1 µL aliquot was removed and diluted to 1 mL with chloroform for GC-MS analysis. The crossover reaction of bis(2-trimethylsiloxyethyl) trisulfide with Me_2S_3 occurs in *N*,*N*-dimethylformamide, giving methyl 2-trimethylsiloxyethyl trisulfide ($Me_3SiOC_2H_4S_3Me$).

Bis(2-trimethylsiloxyethyl) trisulfide

GC-MS (EI, 70 eV) *m/z* (rel. intensity): *m/z* calcd. for $C_6H_{16}OS_3Si^+$: 228.0[*M*]$^+$, found: 228.0 (M+, 35), 213.0 (5), 182.0 (16), 151.0 (4), 133.0 (38), 117.1 (31), 103.1 (33), 79.0 (14), 73.1 (100), 59.0 (9).

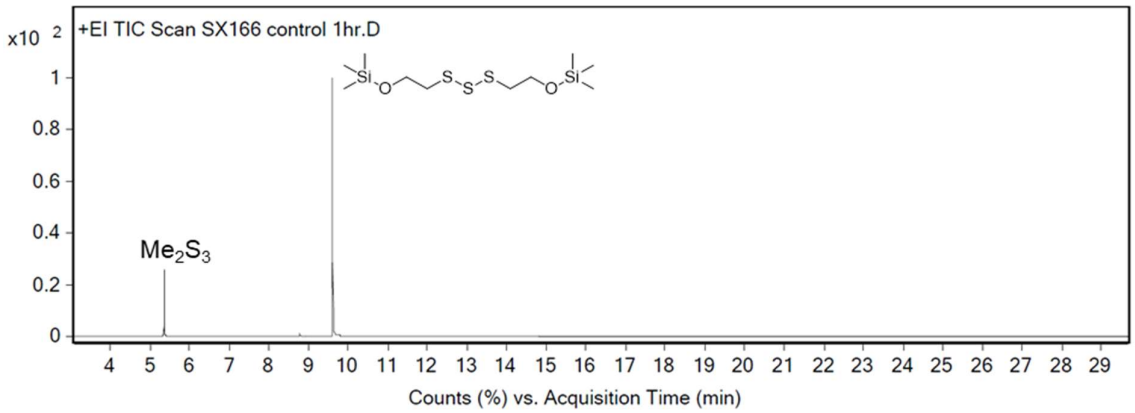

Figure S3.72: Gas chromatogram of the reaction between Me_2S_3 and bis(2-trimethylsiloxyethyl) trisulfide, without DMF after 1 hour. GC-MS method G. Retention time: Me_2S_3 (5.358 min), $(Me_3SiOC_2H_4)_2S_3$ (9.604 min).

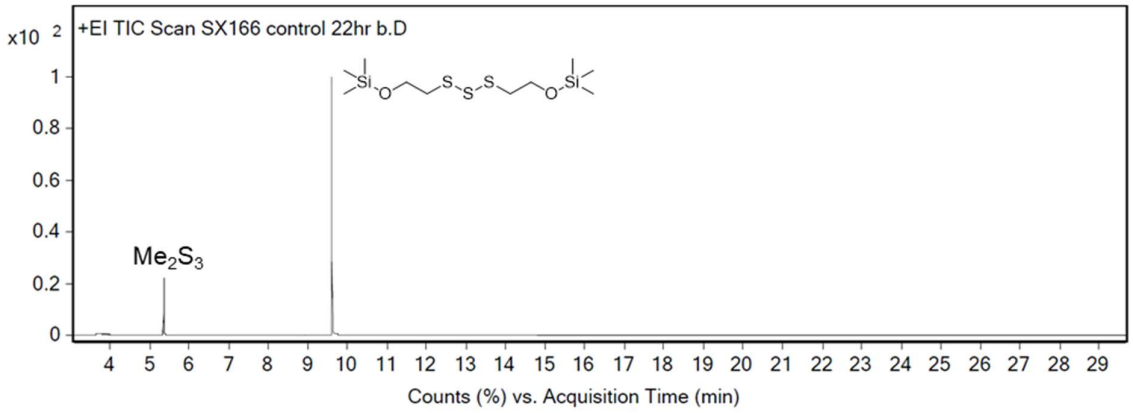

Figure S3.73: Gas chromatogram of the reaction between Me_2S_3 and bis(2-trimethylsiloxyethyl) trisulfide, without DMF after 22 hours. GC-MS method G. Retention time: Me_2S_3 (5.358 min), $(Me_3SiOC_2H_4)_2S_3$ (9.604 min).

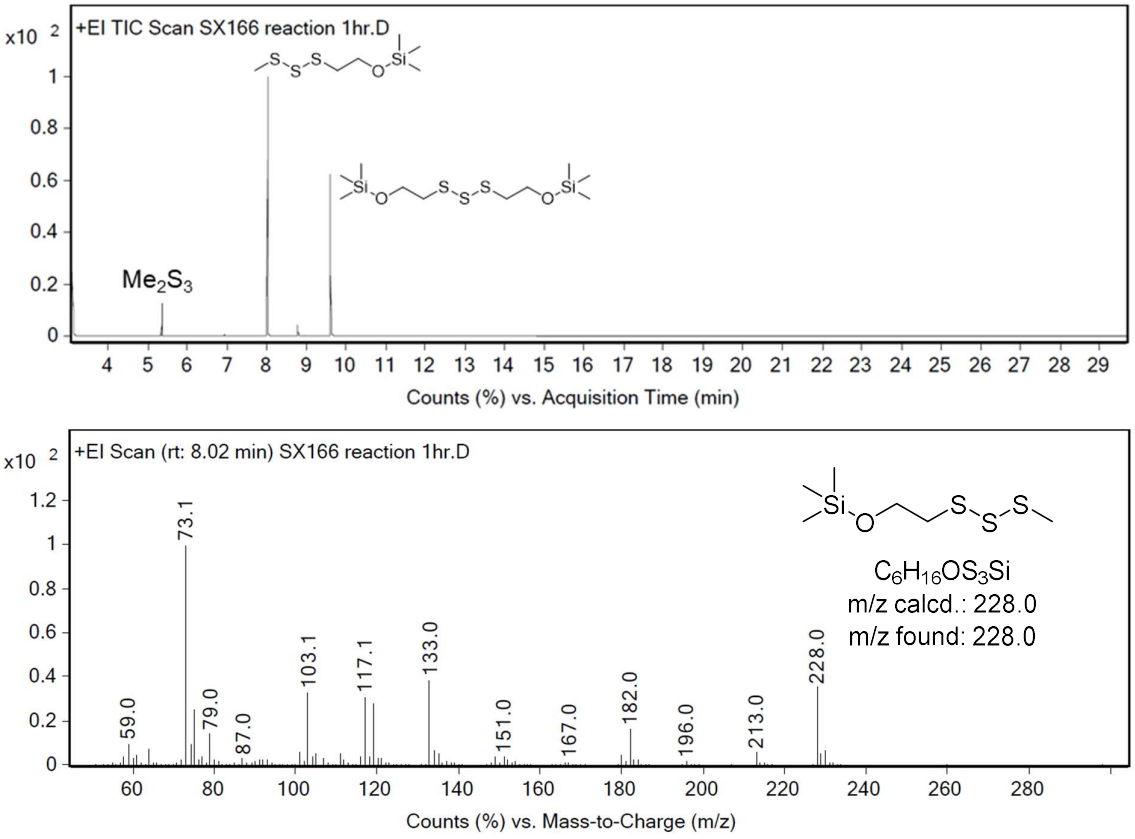

Figure S3.74: Gas chromatogram of the reaction between Me_2S_3 and bis(2-trimethylsiloxyethyl) trisulfide, with DMF after 1 hour, and the mass spectrum of the $Me_3SiOC_2H_4S_3Me$ peak. GC-MS method G. Retention time: Me_2S_3 (5.358 min), $Me_3SiOC_2H_4S_3Me$ (8.019 min), $(Me_3SiOC_2H_4)_2S_3$ (9.604 min).

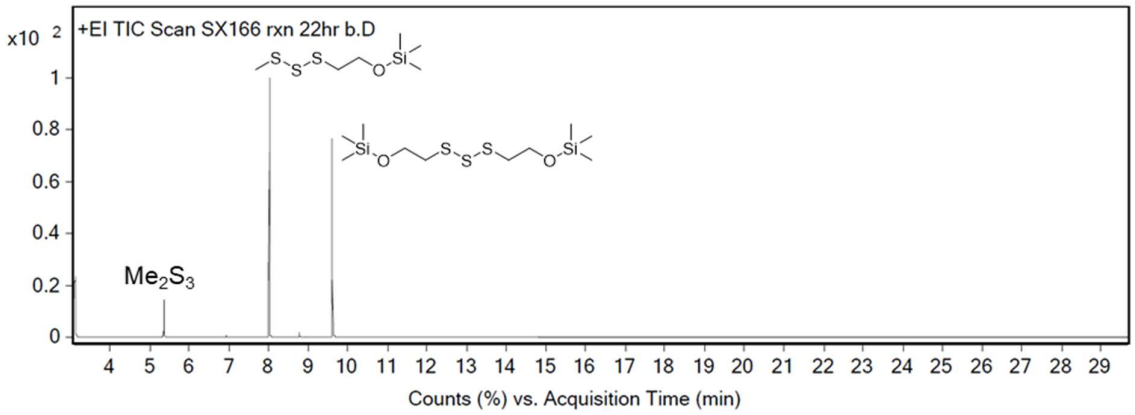

Figure S3.75: Gas chromatogram of the reaction between Me_2S_3 and bis(2-trimethylsiloxyethyl) trisulfide, with DMF after 22 hours. GC-MS method G. Retention time: Me_2S_3 (5.358 min), $Me_3SiOC_2H_4S_3Me$ (8.019 min), $(Me_3SiOC_2H_4)_2S_3$ (9.604 min).

Dimethyl trisulfide (Me_2S_3) and norbornene trisulfide (NBTS) crossover

Norbornene trisulfide purification

The synthesis protocol of norbornene trisulfide was described somewhere else.[6] Crude norbornene trisulfide (260.8 mg, ~6 months in the fridge) was purified by flash column chromatography (silica, 100% hexane as mobile phase) to give the titled compound as a yellow oil (170.2 mg, recovery yield 65%, R_f = 0.58).

^{1}H NMR (600 MHz, $CDCl_3$) δ 3.65 (d, *J* = 1.6 Hz, 2H), 2.49 – 2.46 (m, 2H), 1.96 – 1.92 (m, 1H), 1.76 – 1.71 (m, 2H), 1.29 – 1.24 (m, 2H), 1.09 – 1.05 (m, 1H). **^{13}C NMR** (150 MHz, $CDCl_3$) δ 70.0, 40.9, 32.5, 27.8.

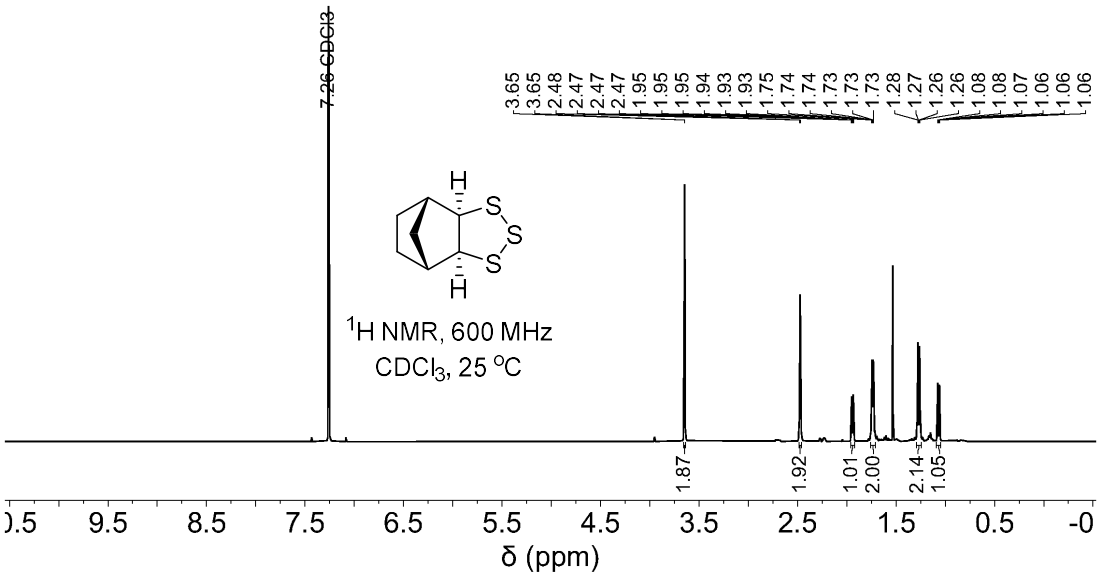

Figure S3.76: ^{1}H NMR spectrum of norbornene trisulfide.

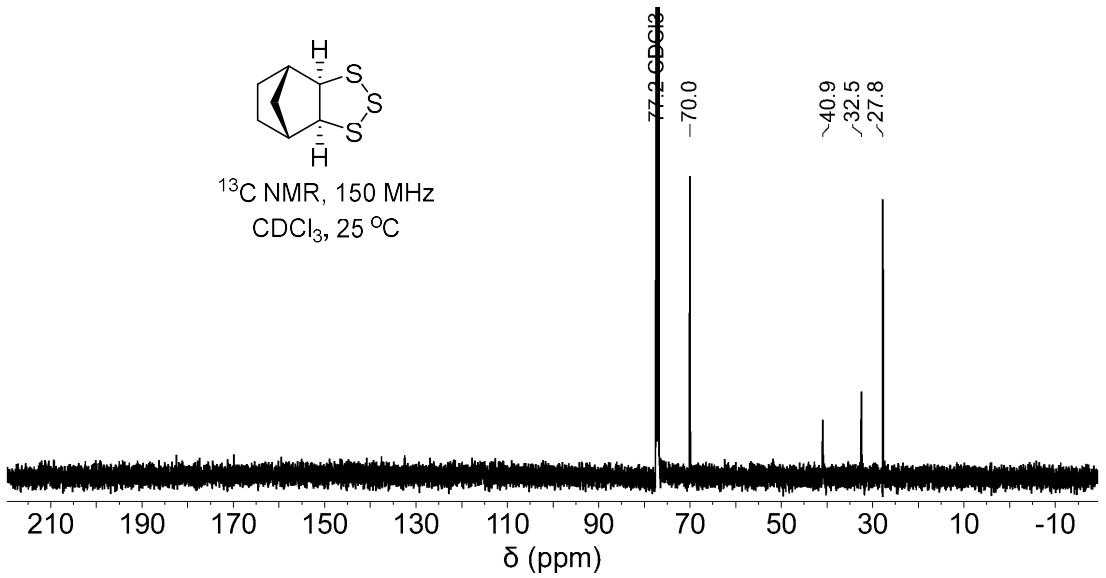

Figure S3.77. ^{13}C NMR spectrum of norbornene trisulfide.

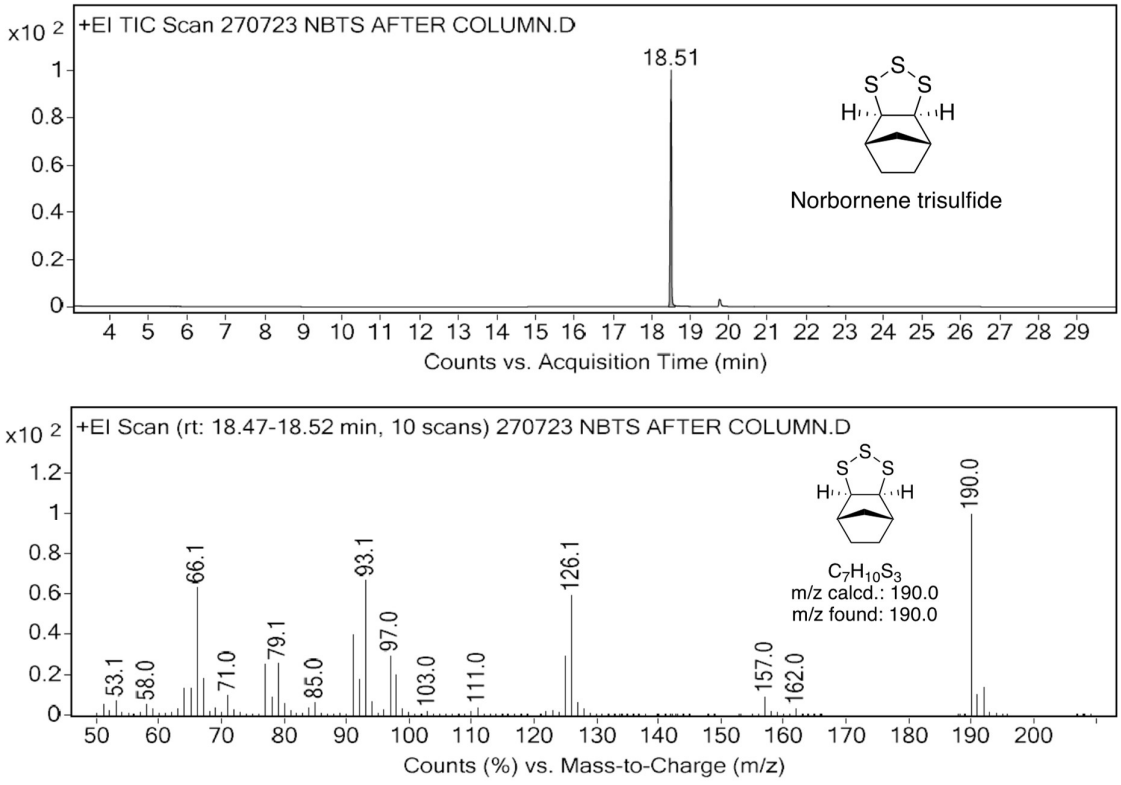

Figure S3.78: Gas chromatogram and mass spectrum of norbornene trisulfide. GCMS method H. Retention time: 18.51 min (Norbornene trisulfide)

Norbornene trisulfide (NBTS) and dimethyl trisulfide (Me_2S_3) crossover

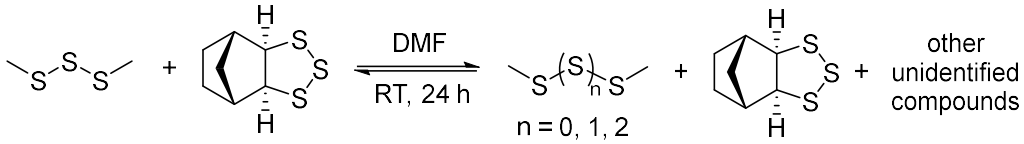

Norbornene trisulfide (38 mg, 0.2 mmol), dimethyl trisulfide (21 µL, 0.2 mmol), and *N*,*N*-dimethylformamide (15.5 µL, 0.2 mmol, for 1 eq., or 154.8 µL, 2 mmol, for 10 eq.) were added to a 2 mL glass vial. The mixture was stirred (300 rpm) at room temperature (19 – 22 ºC) for 24 hours. After 1 h and 24 h, a 5 µL aliquot was removed and diluted to 1 mL with chloroform for GCMS analysis. Control experiments were also carried out between: (1) dimethyl trisulfide and norbornene trisulfide without the presence of DMF, (2) dimethyl trisulfide (42 µL, 0.4 mmol, 1 eq.) and DMF (310 µL, 4.0 mmol, 10 eq.), and (3) norbornene trisulfide (38 mg, 0.2 mmol) and DMF (155 µL, 2.0 mmol, 10 eq.).

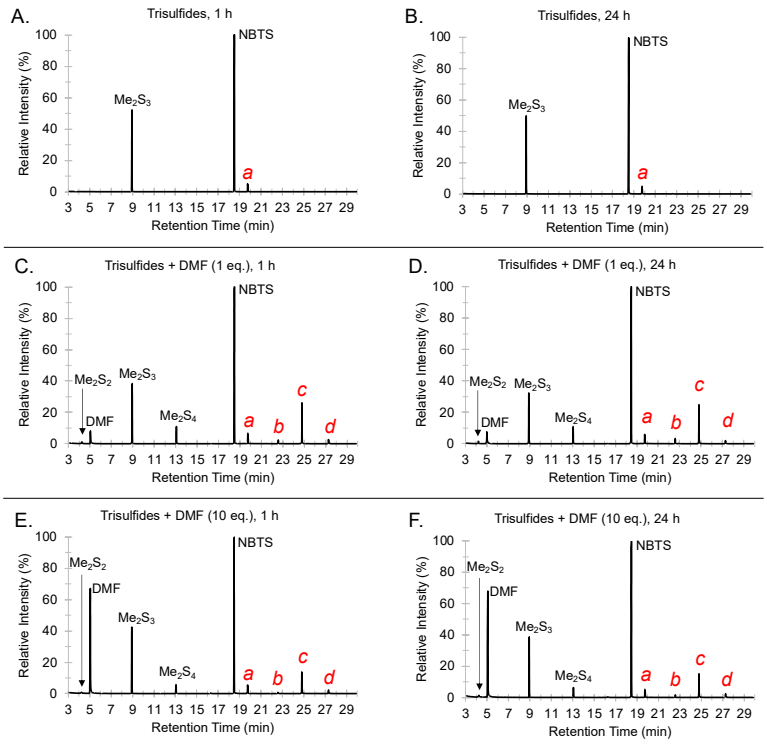

Figure S3.79: GCMS traces for the room temperature crossover reaction between norbornene trisulfide, dimethyl trisulfide, and *N*,*N*'-dimethylformamide. (A, B) Trisulfides neat (1 eq. each) after 1 h and 24 h. (C, D) Trisulfides (1 eq. each) and DMF (1 eq.) after 1 h and 24 h. (E, F) Trisulfides (1 eq. each) and DMF (10 eq.) after 1 h and 24 h. GCMS method H. Retention time: Me_2S_2 (4.32 min), DMF (5.03 min), Me_2S_3 (8.93 min), Me_2S_4 (13.07 min), NBTS (18.48 min), a (19.75 min), b (22.60 min), c (24.81min), and d (27.29 min).

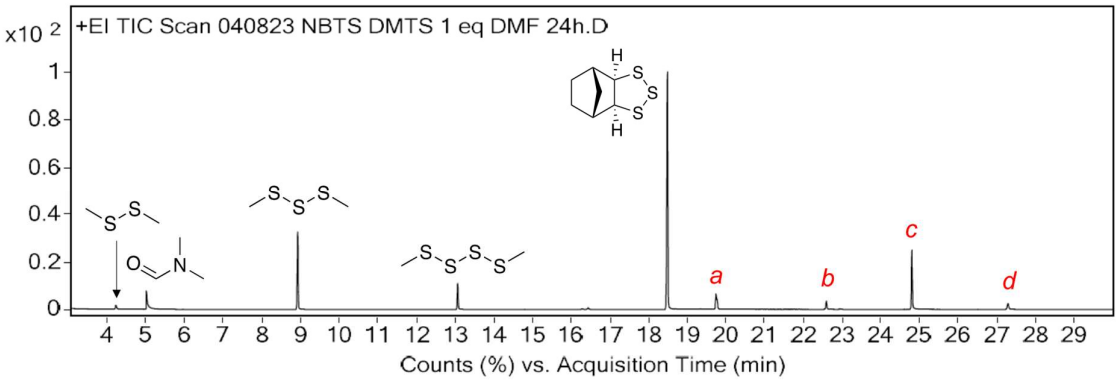

Figure S3.80: A GC trace for the crossover reaction between norbornene trisulfide (NBTS), dimethyl trisulfide (Me_2S_3), and DMF after 1 h. The predicted compound a, b, c, and d are shown below in MS data section. GCMS method H. Retention time: Me_2S_2 (4.32 min), DMF (5.03 min), Me_2S_3 (8.93 min), Me_2S_4 (13.07 min), NBTS (18.48 min), a (19.75 min), b (22.60 min), c (24.81min), and d (27.29 min).

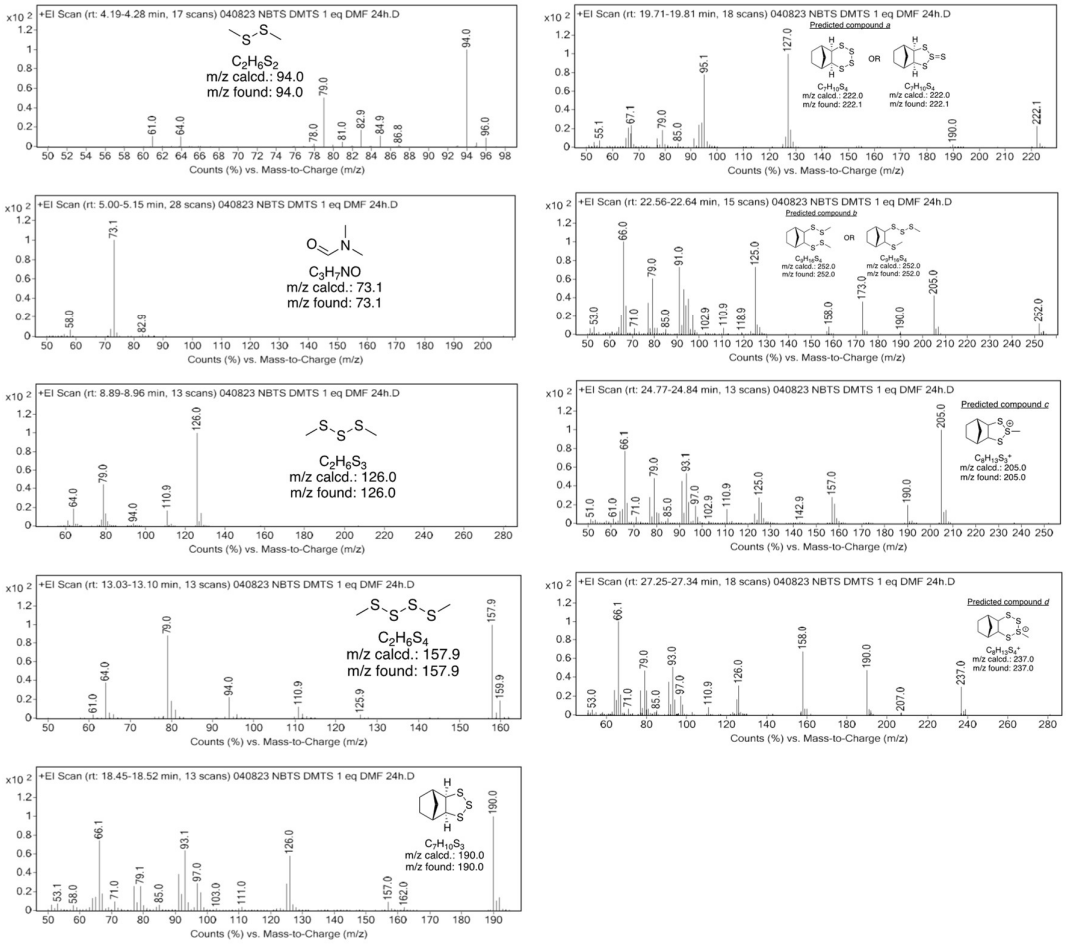

Figure S3.81: MS data for the crossover reaction between norbornene trisulfide (NBTS), dimethyl trisulfide (Me_2S_3), and DMF after 1 h.

Control experiments: Dimethyl trisulfide and DMF only, and norbornene trisulfide and DMF only

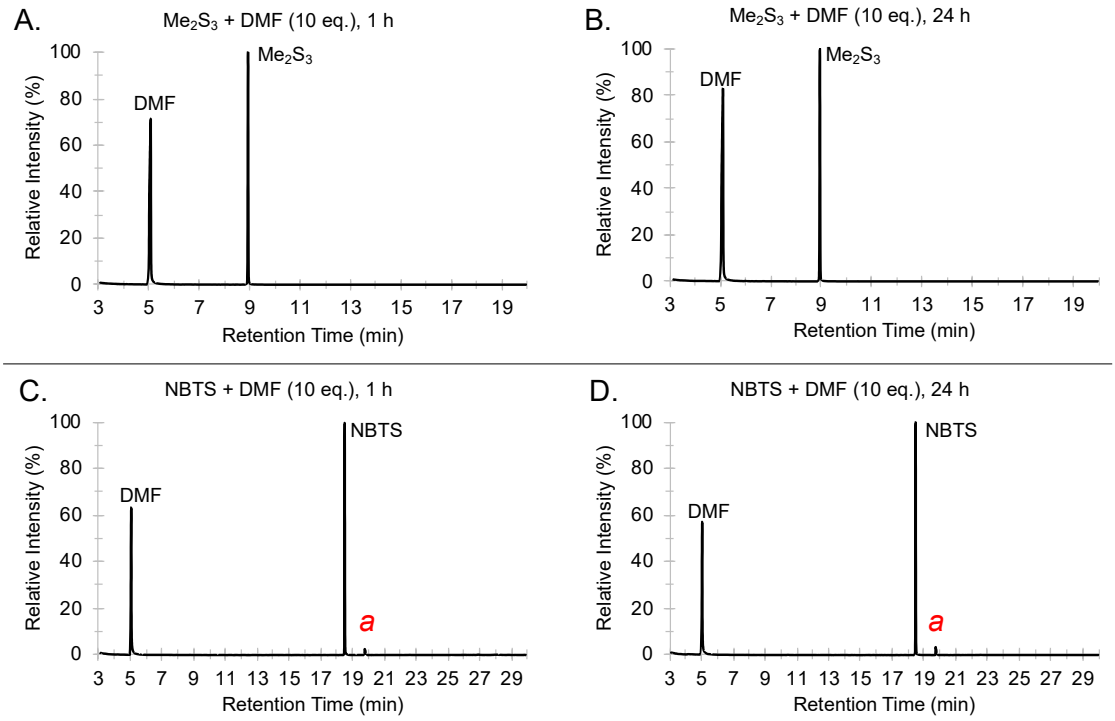

Figure S3.82: GC traces for the control reaction between (A, B) dimethyl trisulfide (0.2 mmol, 1 eq.) and DMF (2.0 mmol, 10 eq.) after 1 h and 24 h, and (C, D) norbornene trisulfide (0.2 mmol, 1 eq.) and DMF (2.0 mmol, 10 eq.) after 1 h and 24 h. GCMS method H. Retention time: DMF (5.03 min), Me_2S_3 (8.93 min), Me_2S_4 (13.07 min), NBTS (18.48 min), and a (19.75 min)

Applications of the trisulfide S-S metathesis induced by DMF

BnS_3Me Synthesis using crossover chemistry

(This experiment was performed by Dr. Harshal D. Patel)

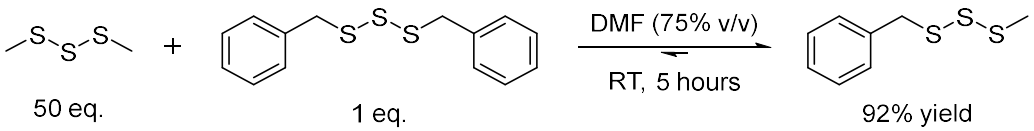

Dimethyl trisulfide (3.78 mL, 35.9 mmol, 50 eq.), dibenzyl trisulfide (200 mg, 0.718 mmol, 1.0 eq.) and 11.3 mL *N,N*-dimethylformamide were added to a 20 mL glass vial equipped with a stir bar and sealed with a lid. The mixture was then stirred at room temperature (19 – 20 ºC) for 5 hours. The reaction mixture was transferred into a separating funnel with *n*-pentane and water. *N,N*-dimethylformamide was removed by washing the organic phase with water seven times. The organic phase was dried with $MgSO_4$, filtered through a sintered glass funnel, and carefully concentrated under reduced pressure (100 mbar, 40 ºC). Short path distillation under reduced pressure (0.44 mbar, 70 ºC oil bath, all glassware wrapped in aluminium foil) provided the excess dimethyl trisulfide distillate as a pale-yellow oil (3.68 g, 81% recovered), and in the distilling flask BnS_3Me was recovered as a pale-yellow oil (269 mg, 92% yield).

BnS_3Me

^{1}H NMR (600 MHz, $CDCl_3$) δ 7.35 (ap. d, J = 4.4 Hz, 4H), 7.31 – 7.27 (m, 1H), 4.10 (s, 2H), 2.50 (s, 3H). **^{13}C NMR** (150 MHz, $CDCl_3$) δ 136.7, 129.6, 128.8, 127.7, 43.2, 22.7. **FTIR** (neat, cm^{-1}): 2914, 1410, 1304, 1135, 1071, 949, 807, 764, 697, 652, 581, 515, 470. **GC-MS** (EI, 70 eV) *m/z* (rel. intensity): *m/z* calcd. for $C_8H_{10}S_3^+$: 202.0 $[M]^+$, found: 202.0 (M^+, 7), 170.0 (1), 137.0 (19), 121.0 (5), 91.1 (100). **Elemental analysis** (CHNS): $C_8H_{10}S_3$ requires C, 47.49%; H, 4.98%; N, 0%; S, 47.53%. Found C, 47.89%; H, 5.90%; N, 0%; S, 44.64%.

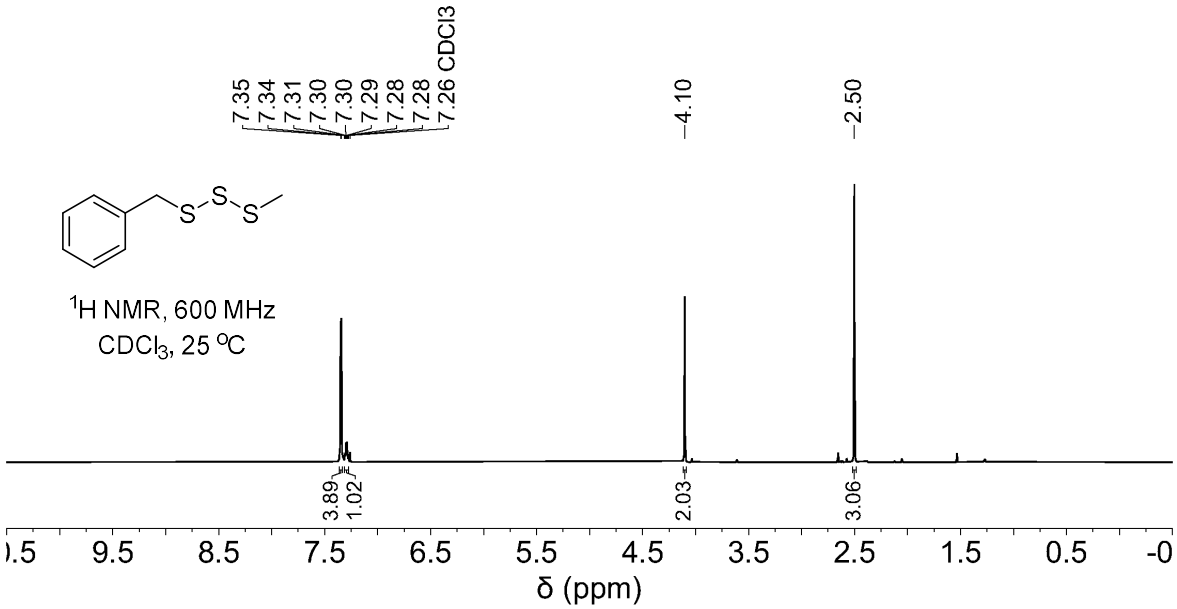

Figure S3.83: ^{1}H NMR spectrum of BnS_3Me (distillate).

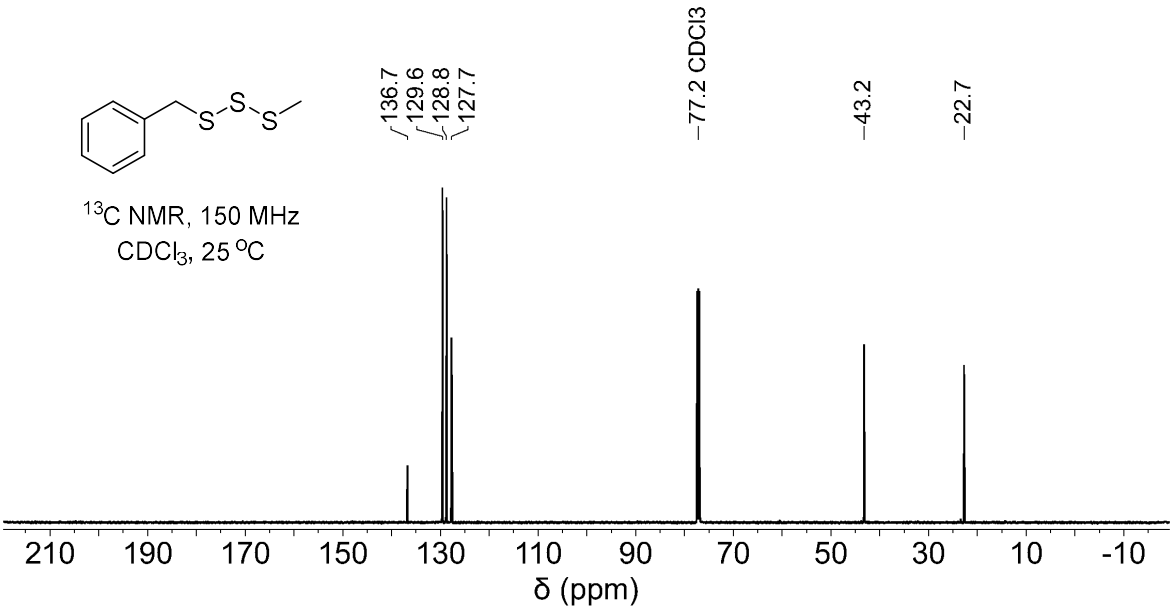

Figure S3.84: ^{13}C NMR spectrum of BnS_3Me (distillate).

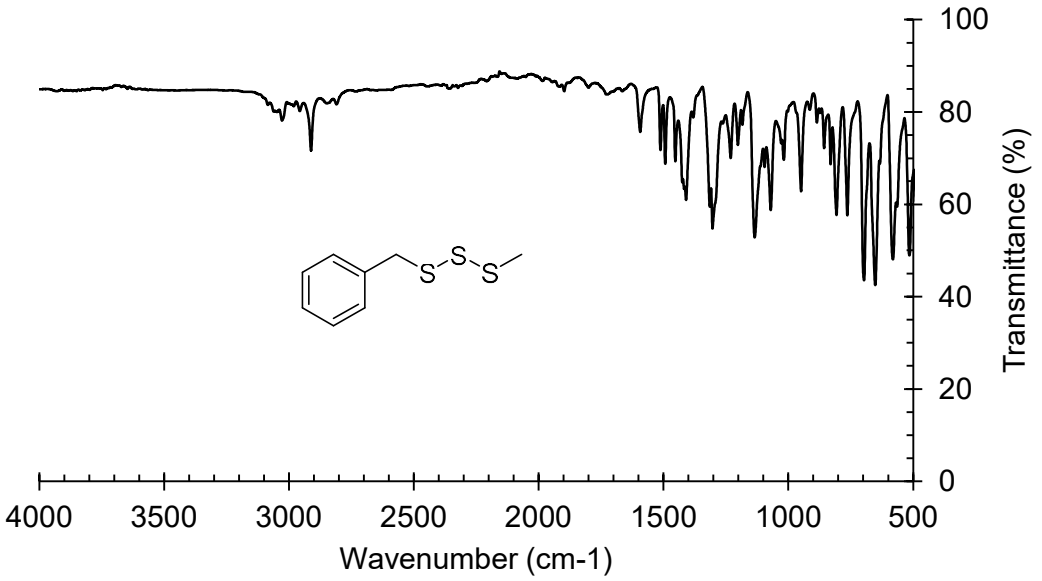

Figure S3.85: FTIR spectrum of BnS_3Me (distillate).

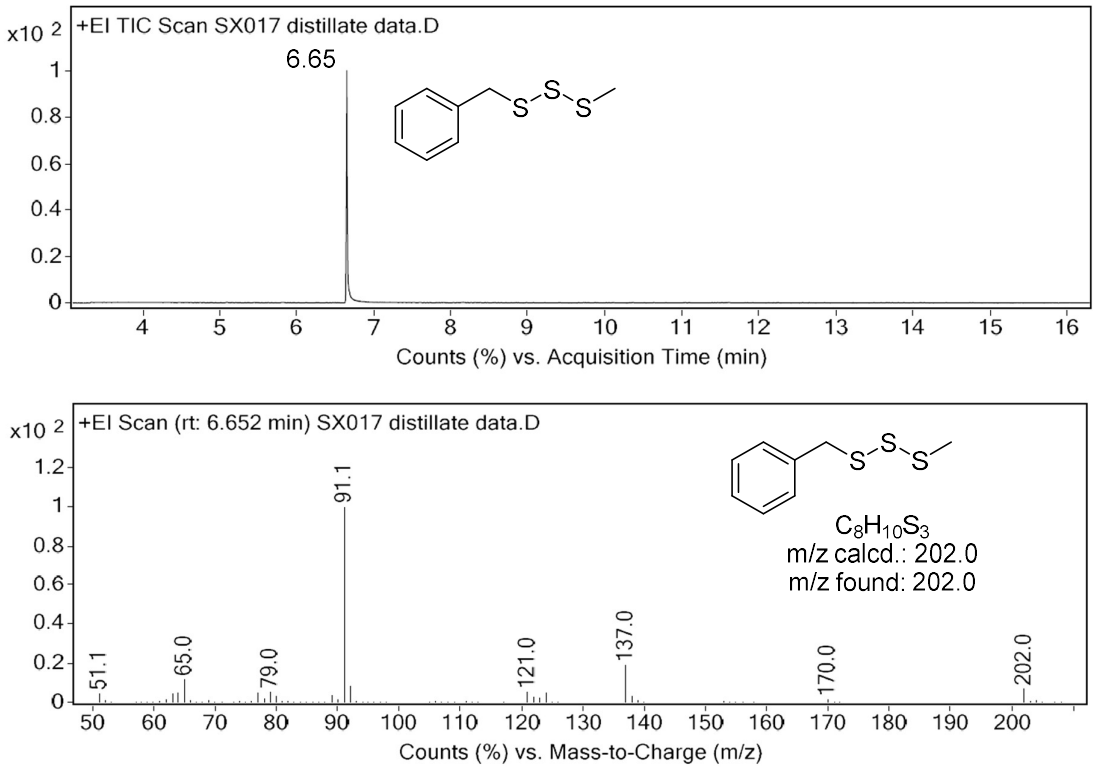

Figure S3.86: Gas chromatogram and mass spectrum of BnS_3Me. GC-MS method F. Retention time: BnS_3Me (6.655 min)

BnS_3Me Disproportionation by S-S metathesis in DMF-d_7

(This experiment was performed by Dr. Harshal D. Patel)

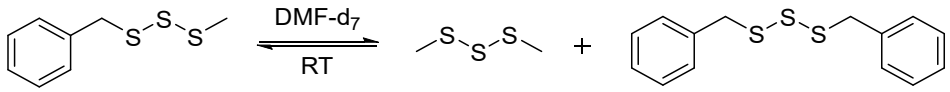

The disproportionation of BnS_3Me (8 mg, 0.04 mmol, 1.0 eq.) in 0.5 mL DMF-d_7 was monitored by ^{1}H NMR. Equilibrium had been reached within 10 minutes, with both dimethyl trisulfide and dibenzyl trisulfide identified in solution through comparison with analytically pure samples in DMF-d_7.

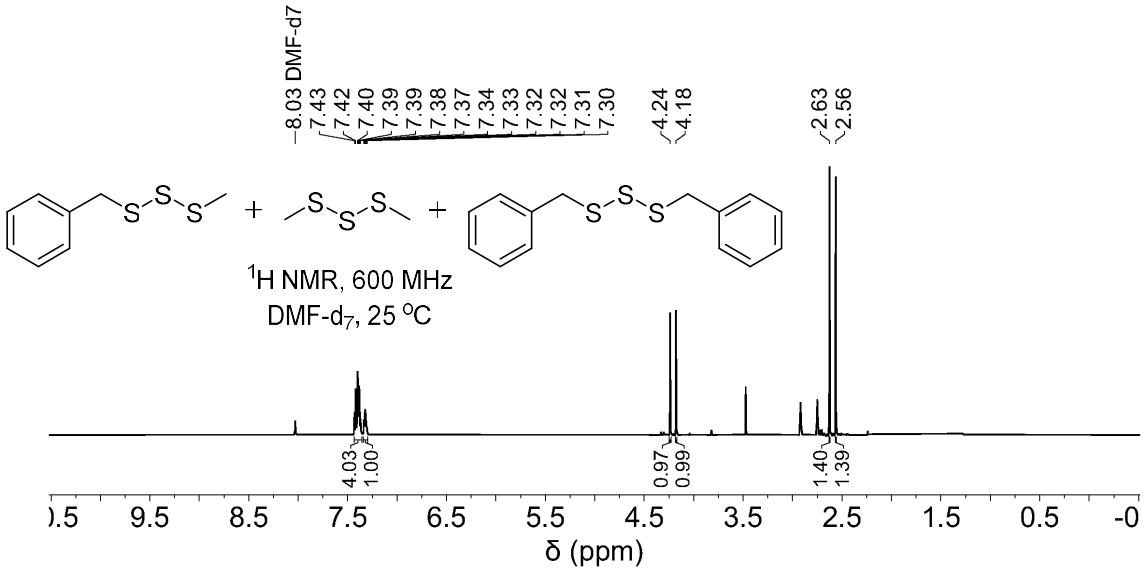

Figure S3.87: ^{1}H NMR spectrum of BnS_3Me (distillate; 4.24 and 2.56 ppm) in DMF-d_7 after 10 minutes. Me_2S_3 (2.63 ppm), Bn_2S_3 (4.18 ppm) were identified in solution through comparison with analytically pure samples in DMF-d_7.

$BnS_3{}^t$Bu thermal disproportionation

(This experiment was performed by Dr. Harshal D. Patel)

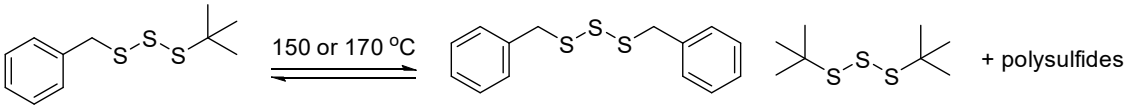

$BnS_3{}^t$Bu (20 mg, 82 µmol, 1.0 eq.) was heated at either 150 ºC or 170 ºC. Aliquots of 5 µL in 1 mL $CHCl_3$ were used for GC-MS analysis after 1 hour and 6 hours of heating. Both Bn_2S_3 and $^tBu_2S_3$ were observed following heating, as well as other related polysulfide compounds – $^tBu_2S_4$, $BnS_2{}^t$Bu, and Bn_2S_2.

$BnS_2{}^tBu$

GC-MS (EI, 70 eV) *m/z* (rel. intensity): *m/z* calcd. for $C_{11}H_{16}S_2^+$: 212.1[*M*]$^+$, found: 212.1 (M+, 18), 156.0 (22), 121.0 (5), 91.1 (100), 57.1 (81).

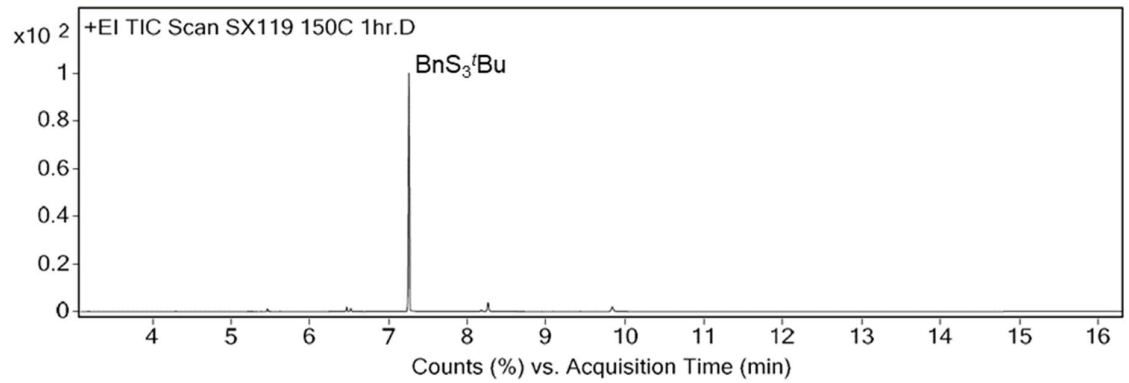

Figure S3.88: Gas chromatogram of BnS_3t-Bu after heating at 150 ºC for 1 hour. GC-MS method F. Retention time: $BnS_3{}^tBu$ (7.258 min).

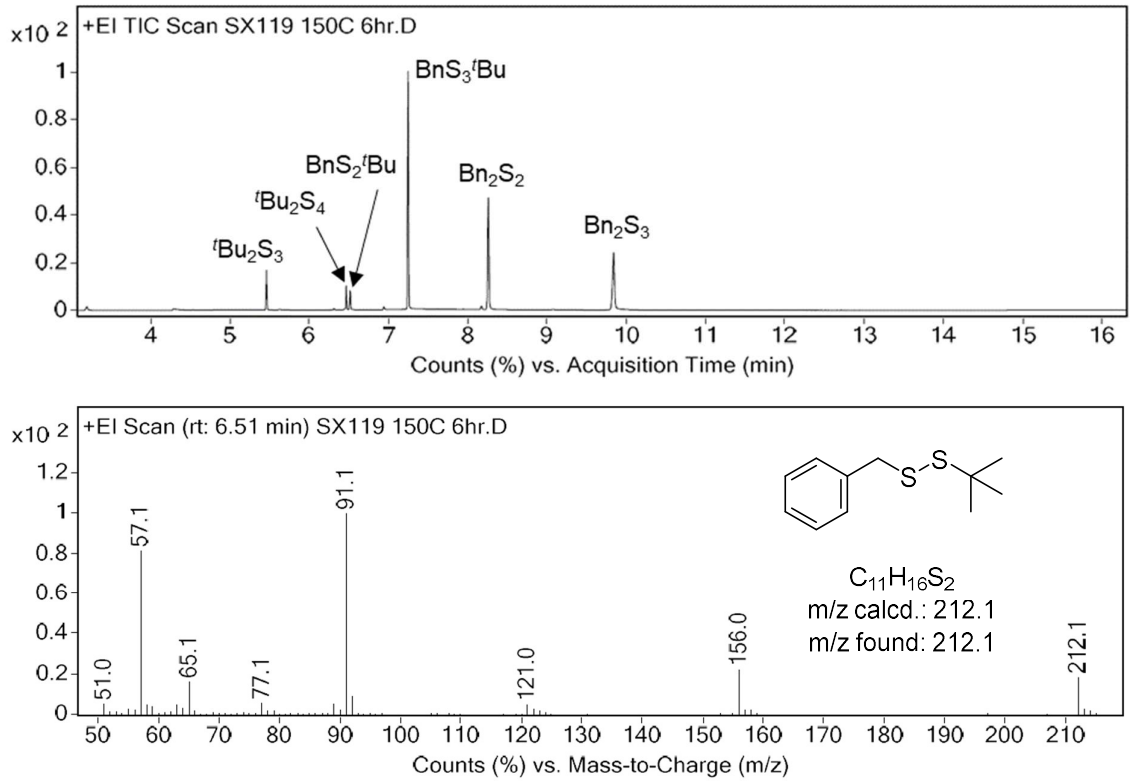

Figure S3.89: Gas chromatogram of $BnS_3{}^tBu$ after heating at 150 ºC for 6 hours, and mass spectrum of $BnS_2{}^tBu$. GC-MS method F. Retention time: $^tBu_2S_3$ (5.462 min), $^tBu_2S_4$ (6.469 min), $BnS_2{}^tBu$ (6.514 min), $BnS_3{}^tBu$ (7.247 min), Bn_2S_2 (8.260 min), Bn_2S_3 (9.839 min).

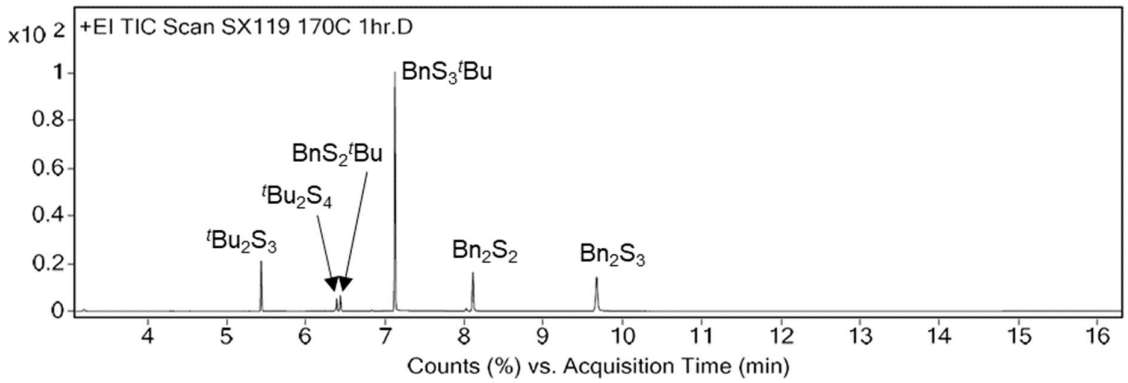

Figure S3.90: Gas chromatogram of $BnS_3{}^tBu$ after heating at 170 ºC for 1 hour. GC-MS method F. Retention time: $^tBu_2S_3$ (5.462 min), $^tBu_2S_4$ (6.469 min), $BnS_2{}^tBu$ (6.514 min), $BnS_3{}^tBu$ (7.247 min), Bn_2S_2 (8.260 min), Bn_2S_3 (9.839 min).

$BnS_3{}^tBu$ disproportionation in DMF

(This experiment was performed by Dr. Harshal D. Patel)

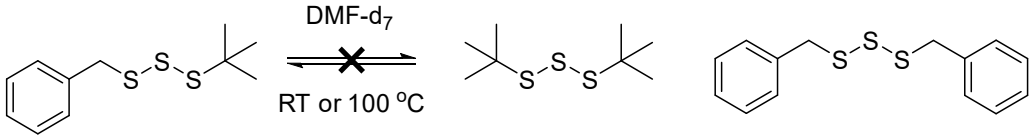

Dissolution of $BnS_3{}^tBu$ in DMF-d_7 resulted in no disproportionation to $^tBu_2S_3$ and Bn_2S_3 at room temperature, or at 100 ºC for 11 hours.

$BnS_3{}^tBu$

^{1}H NMR (600 MHz, DMF-d_7) δ 7.42 – 7.34 (m, 4H), 7.34 – 7.29 (m, 1H), 4.21 (s, 2H), 1.38 (s, 9H).

^{13}C NMR (150 MHz, DMF-d_7) δ 138.1, 130.6, 129.7, 128.6, 49.8, 43.7, 30.5.

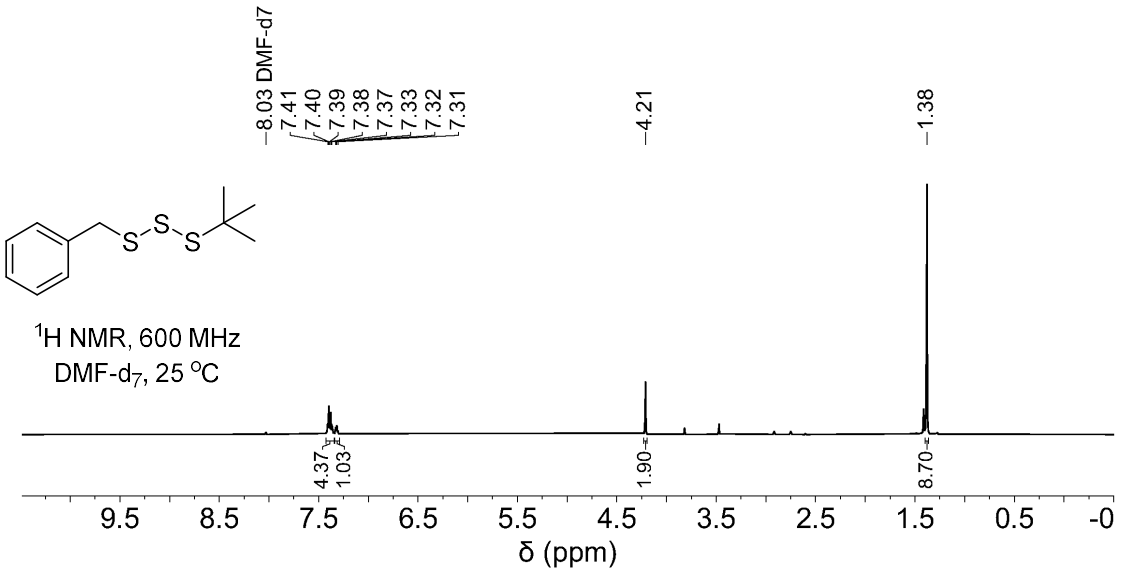

Figure S3.91: ^{1}H NMR spectrum of $BnS_3{}^{t}Bu$ in DMF-d_7 at room temperature; the ^{1}H NMR spectrum remained unchanged after heating at 100 ºC for 11 hours.

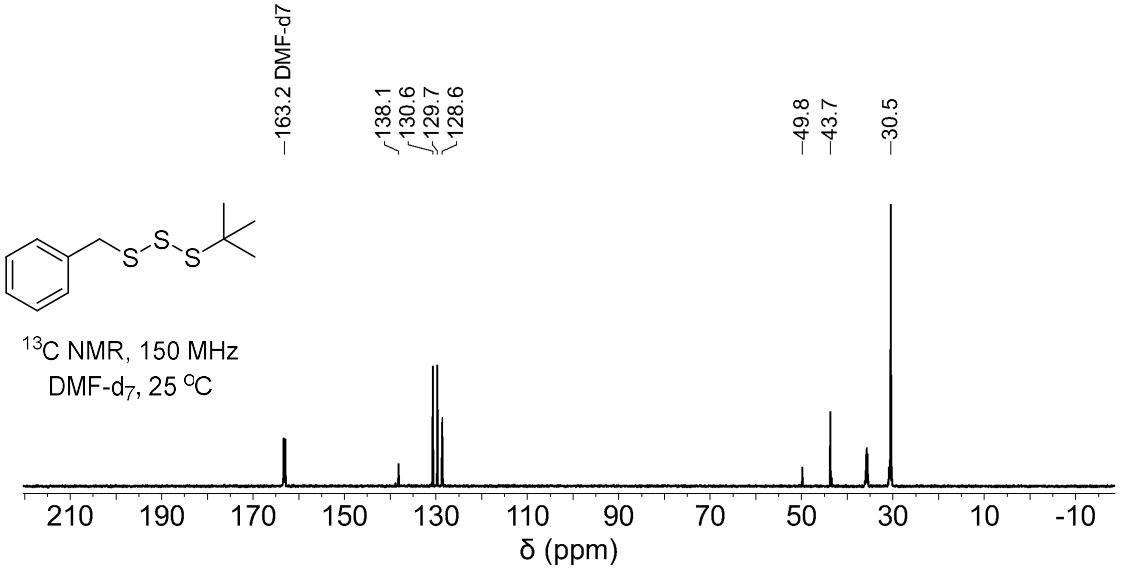

Figure S3.92: ^{13}C NMR spectrum of $BnS_3{}^{t}Bu$ in DMF-d_7 at room temperature.

Me_2S_3 induced disproportionation of $BnS_3{}^tBu$

(This experiment was performed by Dr. Harshal D. Patel)

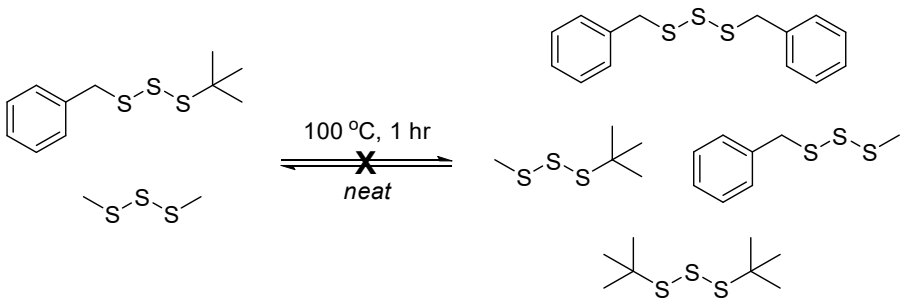

$BnS_3{}^tBu$ (15 mg, 61 µmol, 1.0 eq.) and Me_2S_3 (8 mg, 61 µmol, 1.0 eq.) were heated together neat at 100 ºC. No significant exchange was observed after 1 hour.

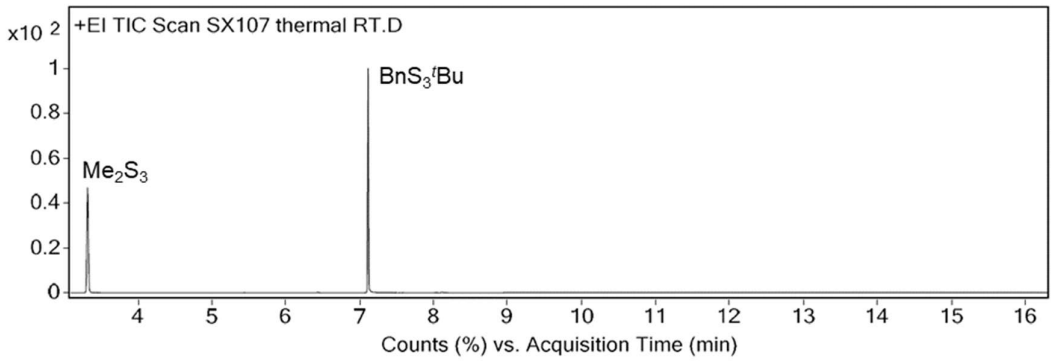

Figure S3.93: Gas chromatogram of $BnS_3{}^tBu$ and Me_2S_3 prior to heating at 100 ºC for 1 hour. GC-MS method F. Retention time: Me_2S_3 (3.322 min), BnS_3t-Bu (7.115 min).

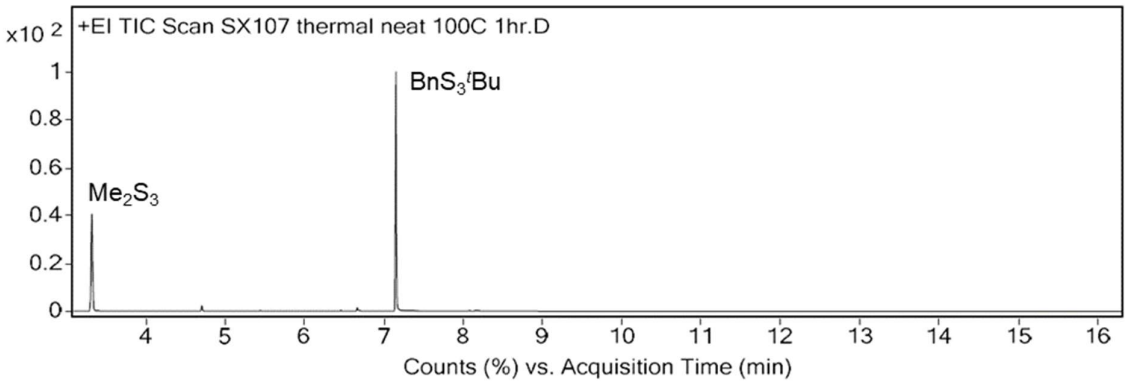

Figure S3.94: Gas chromatogram of $BnS_3{}^tBu$ and Me_2S_3 after heating at 100 ºC for 1 hour. GC-MS method F. Retention time: Me_2S_3 (3.322 min), $BnS_3{}^tBu$ (7.115 min).

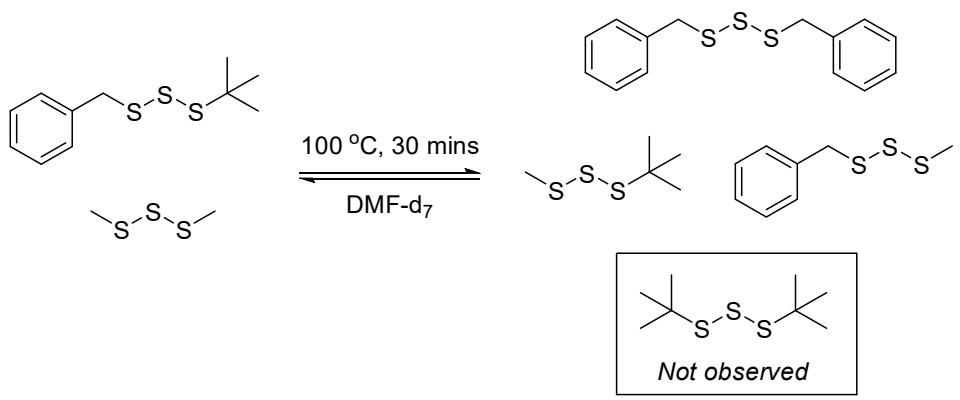

$BnS_3{}^tBu$ (15 mg, 61 µmol, 1.0 eq.) and Me_2S_3 (12 mg, 98 µmol, 1.6 eq.) were placed in 0.5 mL DMF-d_7. No exchange was observed at room temperature. When heated at 100 ºC, equilibrium was established within 30 minutes.

$MeS_3{}^tBu$

GC-MS (EI, 70 eV) *m/z* (rel. intensity): *m/z* calcd. for $C_5H_{12}S_3^+$: 168.0[*M*]$^+$, found: 168.0 (M+, 31), 112.0 (18), 89.0 (7), 79.0 (8), 64.0 (11), 57.1 (100).

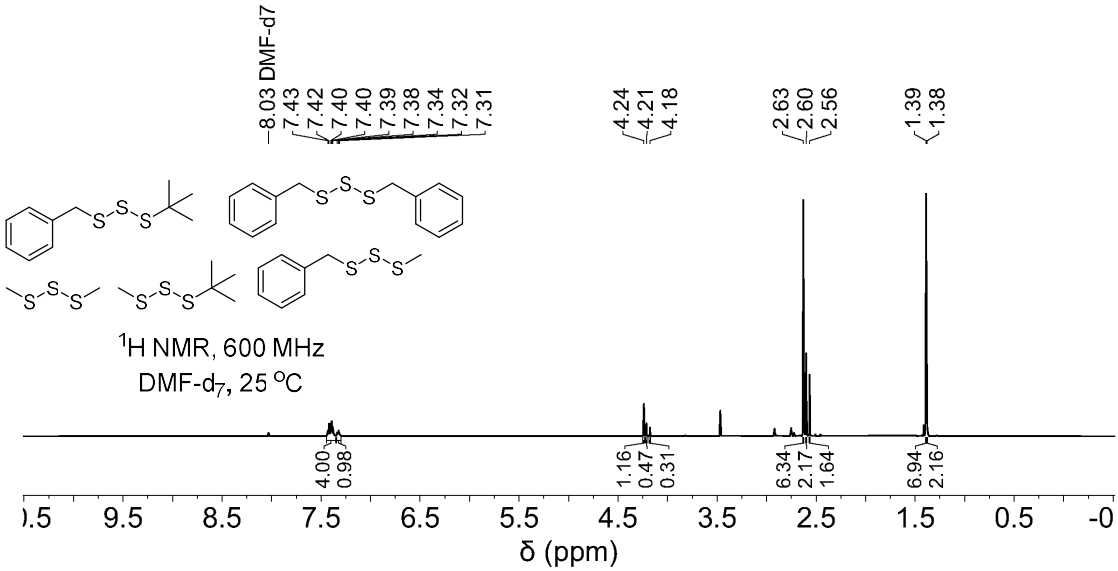

Figure S3.95: ^{1}H NMR spectrum of $BnS_3{}^tBu$ and Me_2S_3 in DMF-d_7 after heating at 100 ºC for 30 minutes. The NMR spectrum remained unchanged upon further heating. $BnS_3{}^tBu$ (4.21 and 1.38 ppm), BnS_3Me (4.24 and 2.56 ppm), Me_2S_3 (2.63 ppm) and Bn_2S_3 (4.18 ppm) were identified in solution through comparison with analytically pure samples in DMF-d_7. $^tBu_2S_3$ was not observed by NMR through comparison with an analytically pure sample in DMF-d_7. $MeS_3{}^tBu$ was identified through GC-MS and assigned to peaks at 2.60 and 1.39 ppm in DMF-d_7.

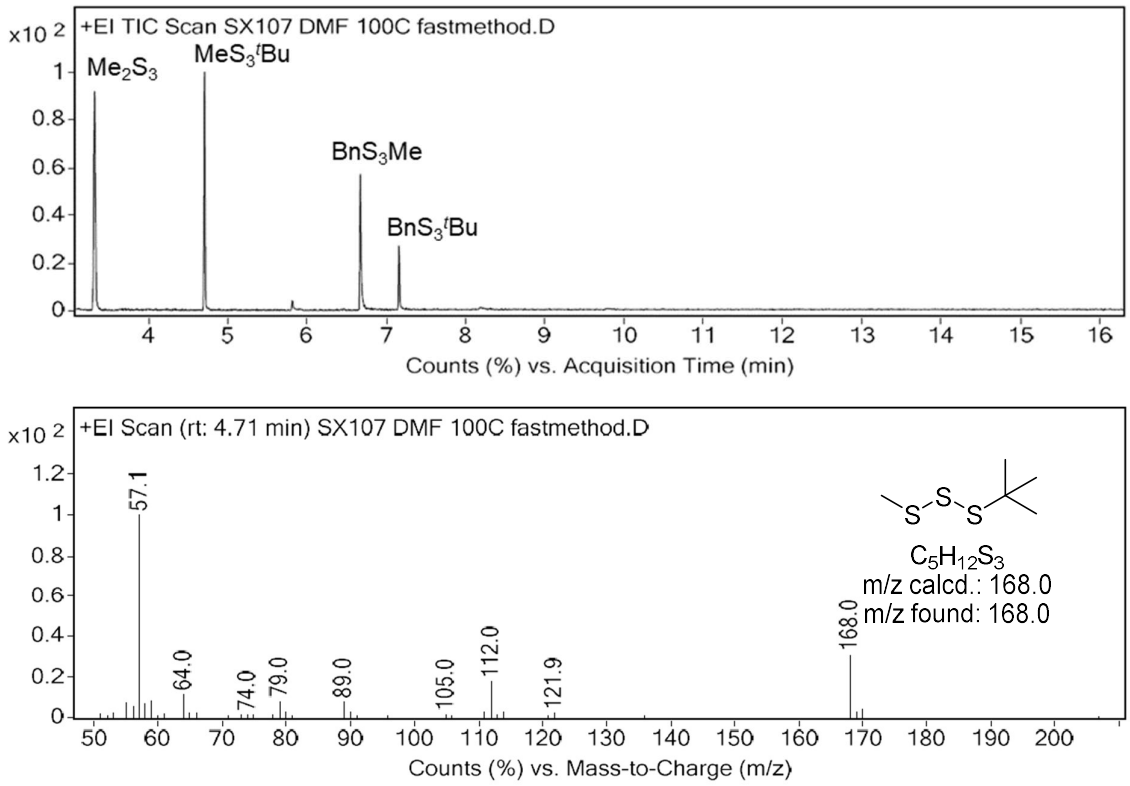

Figure S3.96: Gas chromatogram of the reaction between $BnS_3{}^tBu$ and Me_2S_3 in DMF-d_7 after heating at 100 ºC for 30 minutes, and the mass spectrum of the $MeS_3{}^tBu$ peak. Low abundance of Bn_2S_3 precluded its observation by GC-MS. GC-MS method F. Retention time: Me_2S_3 (3.322 min), $MeS_3{}^tBu$ (4.706 min), BnS_3Me (6.675 min), $BnS_3{}^tBu$ (7.115 min).

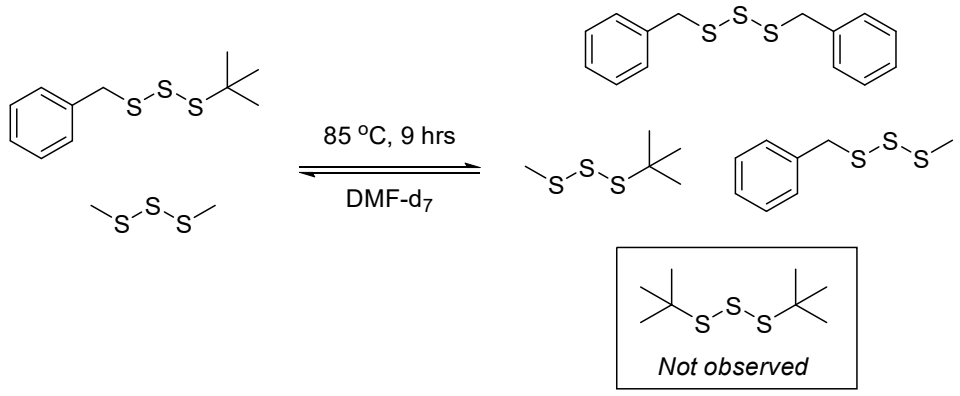

$BnS_3{}^tBu$ (15 mg, 61 µmol, 1.0 eq.) and Me_2S_3 (10 mg, 80 µmol, 1.3 eq.) were placed in 0.5 mL DMF-d_7. No exchange was observed at room temperature. When heated at 85 ºC, equilibrium was established within 9 hours.

$MeS_3{}^tBu$

GC-MS (EI, 70 eV) *m/z* (rel. intensity): *m/z* calcd. for $C_5H_{12}S_3{}^+$: 168.0[*M*]$^+$, found: 168.0 (M+, 34), 111.9 (19), 89.0 (7), 79.0 (8), 63.9 (12), 57.1 (100).

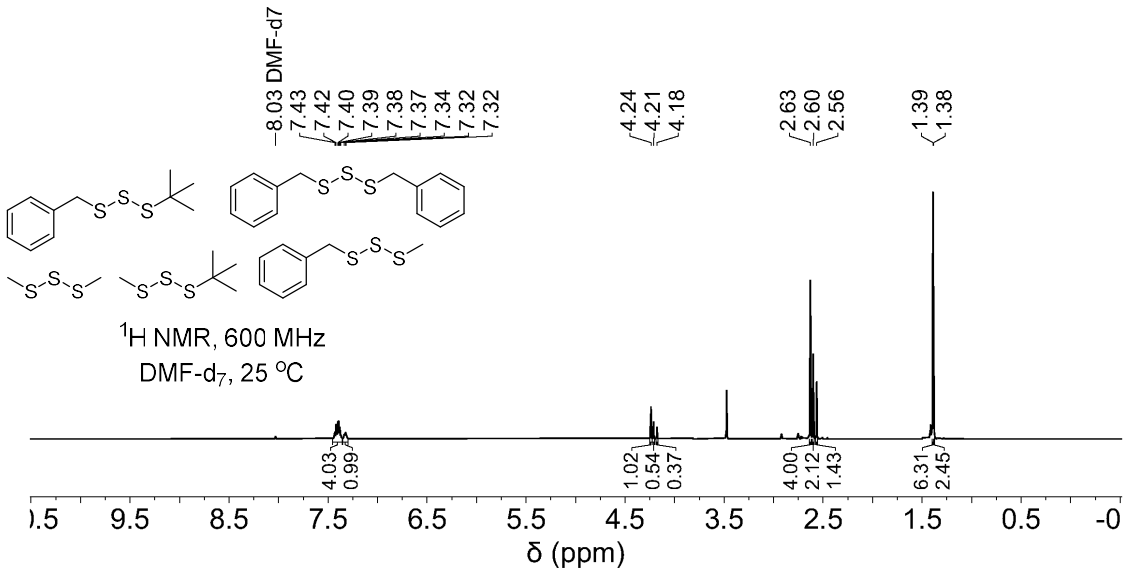

Figure S3.97: ^{1}H NMR spectrum of $BnS_3{}^{t}Bu$ and Me_2S_3 in DMF-d_7 after heating at 85 ºC for 9 hours. The NMR spectrum remained unchanged upon further heating. $BnS_3{}^{t}Bu$ (4.21 and 1.38 ppm), BnS_3Me (4.24 and 2.56 ppm), Me_2S_3 (2.63 ppm) and Bn_2S_3 (4.18 ppm) were identified in solution through comparison with analytically pure samples in DMF-d_7. $^{t}Bu_2S_3$ was not observed by NMR spectroscopy through comparison with an analytically pure sample in DMF-d_7. $MeS_3{}^{t}Bu$ was identified through GC-MS and assigned to peaks at 2.60 and 1.39 ppm in DMF-d_7.

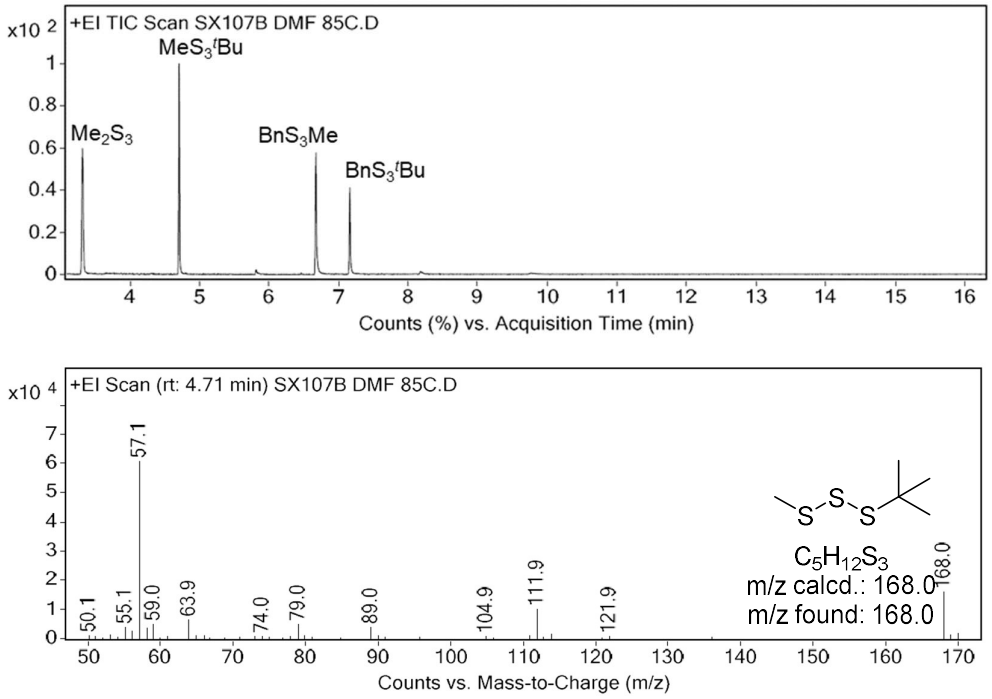

Figure S3.98: Gas chromatogram of the reaction between $BnS_3{}^{t}Bu$ and Me_2S_3 in DMF-d_7 after heating at 100 ºC for 30 minutes, and the mass spectrum of the $MeS_3{}^{t}Bu$ peak. Low abundance of Bn_2S_3 precluded its observation by GC-MS. GC-MS method F. Retention time: Me_2S_3 (3.322 min), MeS_3*t*-Bu (4.706 min), BnS_3Me (6.675 min), BnS_3t-Bu (7.115 min).

Dynamic Trisulfide Libraries

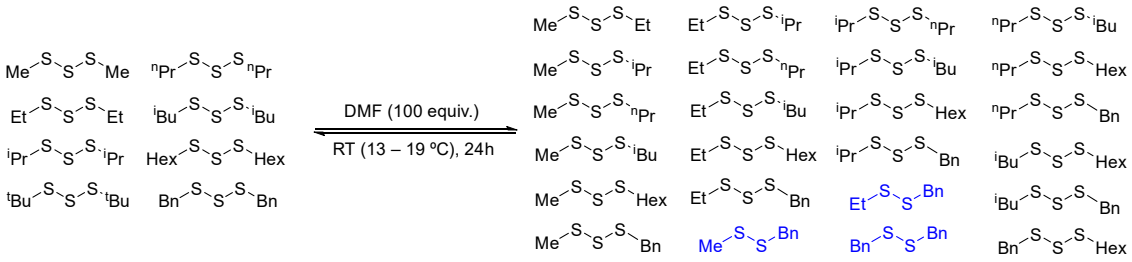

To a 2-mL glass vial equipped with a stir bar was added eight different trisulfides (0.2 mmol each): dimethyl trisulfide (25.3 mg), diethyl trisulfide (30.9 mg), di-isopropyl trisulfide (36.5 mg), di-*tert*-butyl trisulfide (42.1 mg), di-*n*-propyl trisulfide (36.5 mg), di-isobutyl trisulfide (42.1 mg), di-*n*-hexyl trisulfide (53.3 mg), dibenzyl trisulfide (55.7 mg), and *N,N*-dimethylformamide (1.55 mL, 1.46 g, 20 mmol, 100 eq.). The mixture was stirred for 24 hours at room temperature (13 – 19 ºC). After 5 min, 1 hour, and 24 hours, 10 µL of the aliquot was removed and diluted to 1 mL with chloroform for GC-MS analysis. A control experiment was also carried out between the trisulfides only (neat).

Table S3.4: Expected crossover products from the reaction between 8 trisulfides in DMF solvent. Twenty-one (21) crossover products were found within 5 minutes (a total of 29 compounds including the 8 symmetrical trisulfide starting materials). After 24 h, benzyl methyl, benzyl ethyl and dibenzyl disulfide can be observed in the GC trace (these products are not observed at the 5 min time point in the reaction). Seven (7) unsymmetrical trisulfides containing the *tert*-butyl fragment (highlighted yellow) were not observed by GC-MS. The relative abundance of di-*tert*-butyl trisulfide was not changed after 24 hours of the reaction. This indicates that di-*tert*-butyl trisulfide is not reactive enough to proceed the S-S exchange with other trisulfides.

m/z = 126.0								
m/z = 154.0	m/z= 140.0							
m/z = 182.0	m/z= 154.0	m/z= 168.0						
m/z = 210.1	m/z= 168.0	m/z= 182.0	m/z= 196.0					
m/z = 182.0	m/z= 154.0	m/z= 168.0	m/z= 182.0	m/z= 196.0				
m/z= 210.1	m/z= 168.0	m/z= 182.0	m/z= 196.0	m/z= 210.1	m/z= 196.0			
m/z= 266.1	m/z= 196.0	m/z= 210.1	m/z= 224.1	m/z= 238.1	m/z= 224.1	m/z= 238.1		
m/z= 278.0	m/z= 202.0	m/z= 216.0	m/z= 230.0	m/z= 244.0	m/z= 230.0	m/z= 244.0	m/z= 272.1	

Table S3.5: Eight parent trisulfides used in the production of dynamic combinatorial library.

No	Trisulfide compound	Retention time (min)	m/z calcd.	m/z found	Structure
1	Dimethyl trisulfide	7.06	126.0	126.0	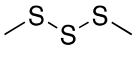
2	Diethyl trisulfide	8.61	154.0	154.0	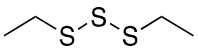
3	Di-isopropyl trisulfide	9.33	182.0	182.0	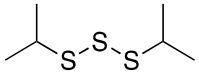
4	Di-*tert*-butyl trisulfide	9.83	210.1	210.1	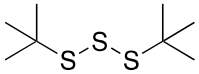
5	Di-*n*-propyl trisulfide	10.03	182.0	182.0	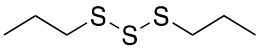
6	Di-isobutyl trisulfide	10.71	210.1	210.1	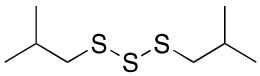
7	Di-*n*-hexyl trisulfide	13.62	266.1	266.2	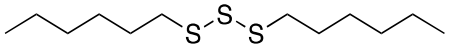
8	Dibenzyl trisulfide	16.09	278.0	278.1	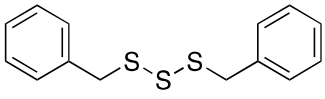

GC traces of neat reaction between the parent trisulfides

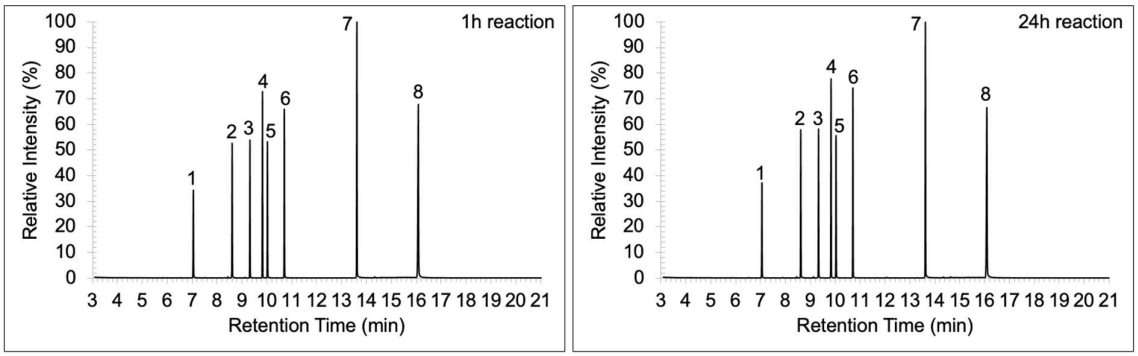

Figure S3.99: Gas chromatograms of eight different trisulfides (neat) after 1 and 24 hour. GC-MS method J. Retention time for each trisulfide compound can be seen in Table S5 above.

GC traces of the trisulfides in the presence of DMF (100 eq.) – 5 min

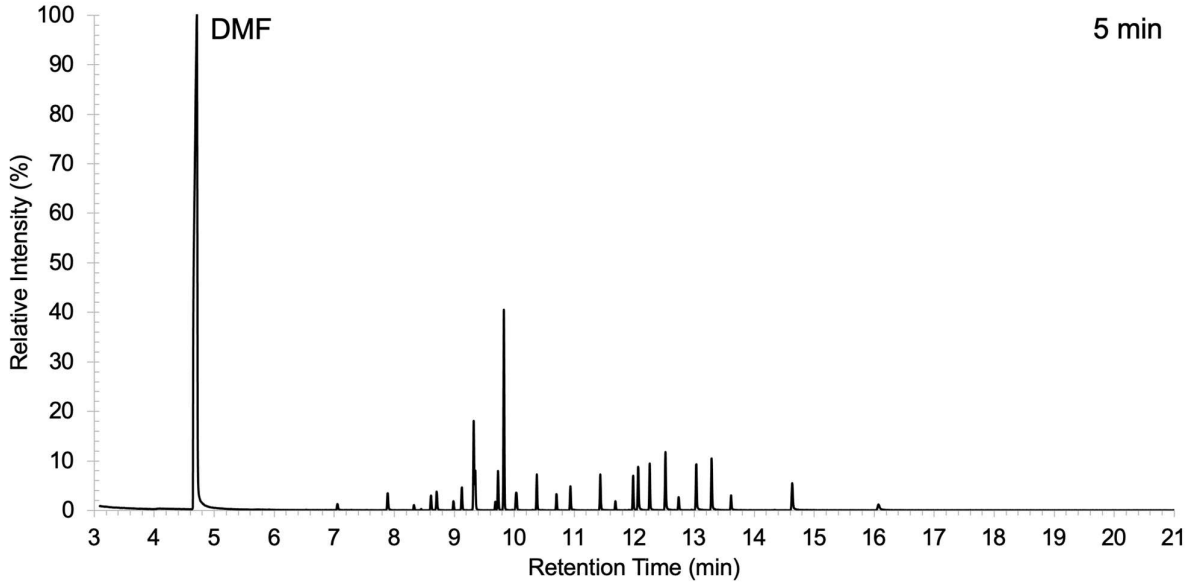

Figure S3.100: Gas chromatogram of the crossover reaction of eight different trisulfides in DMF (100 eq.) after a 5-min reaction. GC-MS method I. Retention time for each trisulfide compound can be seen in Table S6 below.

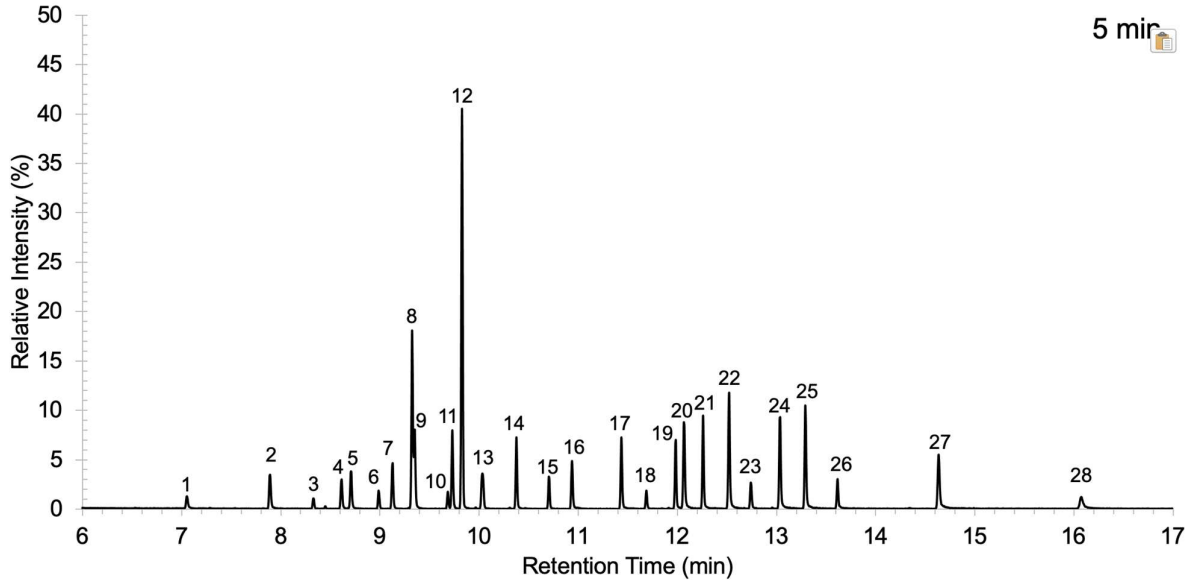

Figure S3.101: Expanded gas chromatogram of the crossover reaction of eight different trisulfides in DMF (100 eq.) after a 5-min reaction (expanded region from 6 to 17 min of retention time, DMF peak excluded). GC-MS method I. Retention time for each trisulfide compound can be seen in Table S6 on the following page.

Table S3.6: m/z for peaks observed in GC-MS of a trisulfides-DMF mixture after 5 min

Peak #	m/z observed	m/z fragments	Retention time (min)	Compound match
1	126.0	126.0, 110.9, 93.9, 79.0, 64.0	7.06	dimethyl trisulfide
2	140.0	140.0, 125.0, 112.0, 93.0, 79.0, 64.0, 61.0	7.89	ethyl methyl trisulfide
3	154.0	154.0, 150.1, 122.0, 111.9, 108.0, 78.9, 64.0	8.33	isopropyl methyl trisulfide
4	154.0	154.0, 124.9, 93.0, 64.0, 61.0	8.61	diethyl trisulfide
5	154.0	154.0, 122.0, 112.0, 108.0, 79.0, 64.0	8.71	methyl *n*-propyl trisulfide
6	168.0	168.0, 135.9, 125.9, 108.0, 94.0, 89.0, 63.9, 61.0	8.99	ethyl isopropyl trisulfide
7	168.0	168.0, 136.0, 122.0, 111.9, 79.0, 64.0, 57.1	9.13	isobutyl methyl trisulfide
8	182.0	182.0, 150.0, 140.0, 117.0, 97.9, 75.0, 64.0	9.32	di-isopropyl trisulfide
9	168.0	168.0, 136.0, 126.0, 108.1, 97.9, 75.0, 63.9, 61.0	9.35	ethyl *n*-propyl trisulfide
10	182.0	182.0, 150.0, 140.0, 117.0, 108.0, 97.9.0, 75.0, 63.9	9.68	isopropyl *n*-propyl trisulfide
11	182.0	182.0, 150.1, 125.9, 119.0, 93.0, 64.0, 61.0, 57.1	9.73	ethyl isobutyl trisulfide
12	210.0	210.1, 154.0, 89.0, 63.9, 57.1	9.83	di-*tert*-butyl trisulfide
13*	182.0	182.0, 150.1, 140.0, 108.0, 75.0, 64.0	10.02	di-*n*-propyl trisulfide
13*	196.1	196.1, 182.0, 164.1, 154.0, 140.0, 122.0, 117.0, 108.0, 97.9.0, 89.0, 75.0, 64.0, 57.1	10.04	isobutyl isopropyl trisulfide
14	196.1	196.1, 164.1, 140.0, 122.0, 108.0, 97.9, 89.0, 75.0, 64.0, 57.1	10.38	isobutyl *n*-propyl trisulfide
15	210.1	210.1, 178.1, 153.9, 122.0, 110.9, 97.9, 89.1, 57.1	10.71	di-isobutyl trisulfide
16	196.1	196.1, 164.1, 150.0, 118.1, 111.9, 92.9, 79.0, 64.0, 57.1, 55.1	10.94	hexyl methyl trisulfide
17	210.1	210.1, 178.1, 150.0, 145.1, 126.0, 117.1, 94.0, 83.1, 69.0, 64.0, 61.0, 57.1, 55.1	11.44	ethyl hexyl trisulfide
18	224.1	224.1, 192.0, 182.0, 159.0, 150.1, 117.1, 108.0, 97.9, 85.0, 83.1, 74.9, 69.0, 63.9, 57.0, 55.0	11.69	isopropyl hexyl trisulfide

19	224.1	224.1, 192.1, 159.1, 150.1, 140.0, 117.1, 108.0, 97.9, 85.1, 83.1, 75.0, 63.9, 57.1, 55.1	11.98	hexyl *n*-propyl trisulfide
20	202.0	202.0, 170.0, 137.0, 121.0, 91.1, 79.0, 77.0, 65.1, 51.1	12.07	benzyl methyl trisulfide
21	238.1	238.1, 206.1, 182.0, 173.1, 150.0, 122.0, 117.1, 111.0, 97.9, 89.0, 85.0, 83.1, 79.0, 73.0, 69.0, 57.1, 55.1	12.26	hexyl isobutyl trisulfide
22	216.0	216.0, 184.0, 151.0, 121.0, 91.1, 77.0, 65.0, 59.0, 51.0	12.52	benzyl ethyl trisulfide
23	230.0	230.0, 198.0, 165.1, 120.9, 108.0, 91.1, 77.0, 65.0, 59.0, 51.0	12.74	benzyl isopropyl trisulfide
24	230.0	230.0, 198.0, 165.1, 121.0, 108.1.0, 91.1, 77.1, 65.1, 51.0	13.03	benzyl *n*-propyl trisulfide
25	244.1	224.1, 212.1, 179.1, 121.0, 91.1, 77.0, 65.0, 57.0, 51.1	13.29	benzyl isobutyl trisulfide
26	266.1	266.1, 234.1, 182.0, 150.1, 117.1, 85.0, 83.1, 79.0, 69.1, 61.0, 57.1, 55.1	13.62	di-*n*-hexyl trisulfide
27	272.1	272.1. 207.1, 150.1, 121.0, 91.1, 77.0, 65.0, 56.1	14.63	benzyl hexyl trisulfide
28	278.0	278.0, 213.1, 124.0, 91.1, 76.9, 65.0, 51.0	16.07	dibenzyl trisulfide

(*) this peak shows two m/z fragments indicating two different compounds i.e., $^{n}PrS_3{}^{n}Pr$ and $^{i}BuS_3{}^{i}Pr$. Rows with highlighted yellow indicate the parent trisulfides.

GC traces of the trisulfides in the presence of DMF (100 eq.) – 1 hour

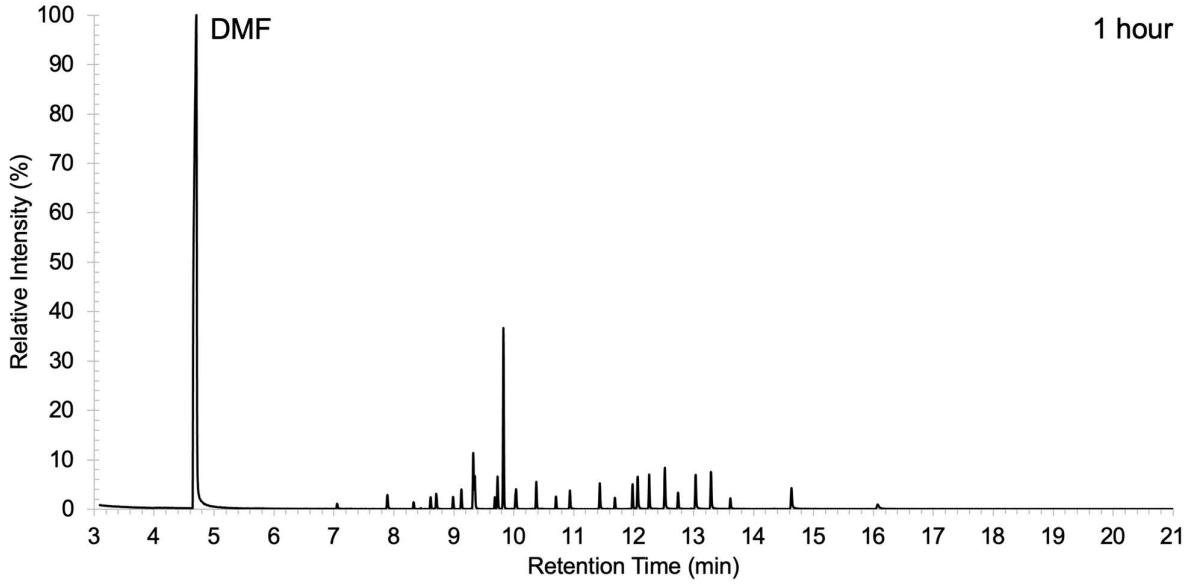

Figure S3.102: Gas chromatogram of the crossover reaction of eight different trisulfides in DMF (100 eq.) after a 1-hour reaction. GC-MS method I.

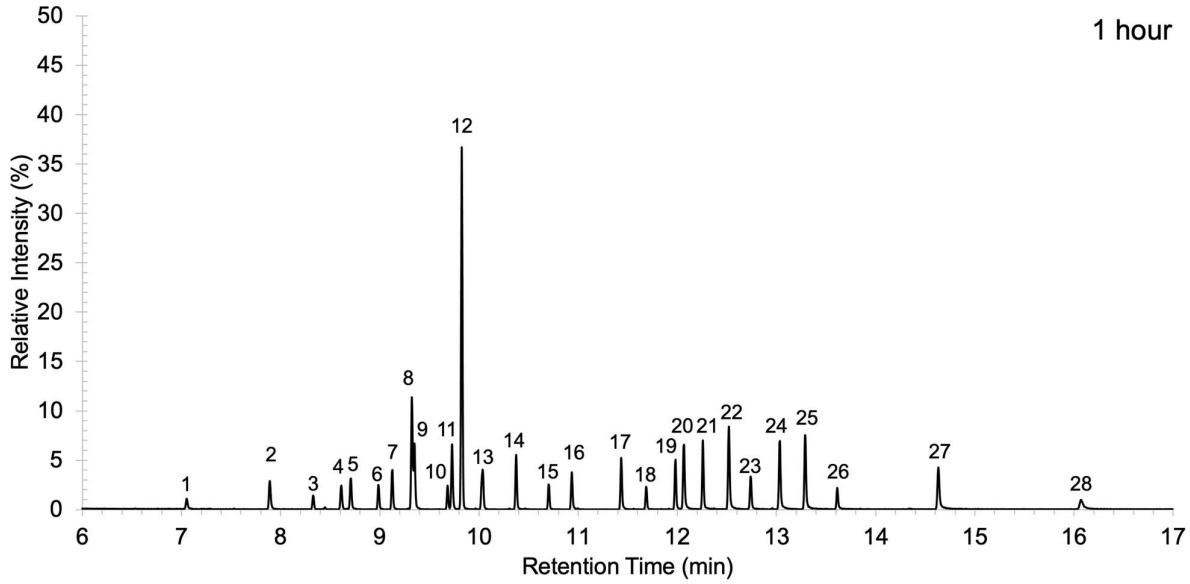

Figure S3.103: Expanded gas chromatogram of the crossover reaction of eight different trisulfides in DMF (100 eq.) after a 1-hour reaction (expanded region from 6 to 17 min of retention time, DMF peak excluded). GC-MS method I. m/z data for peaks observed after 1 hour reaction is the same data as the 5-minute reaction.

GC traces of the trisulfides in the presence of DMF (100 eq.) – 24 hours

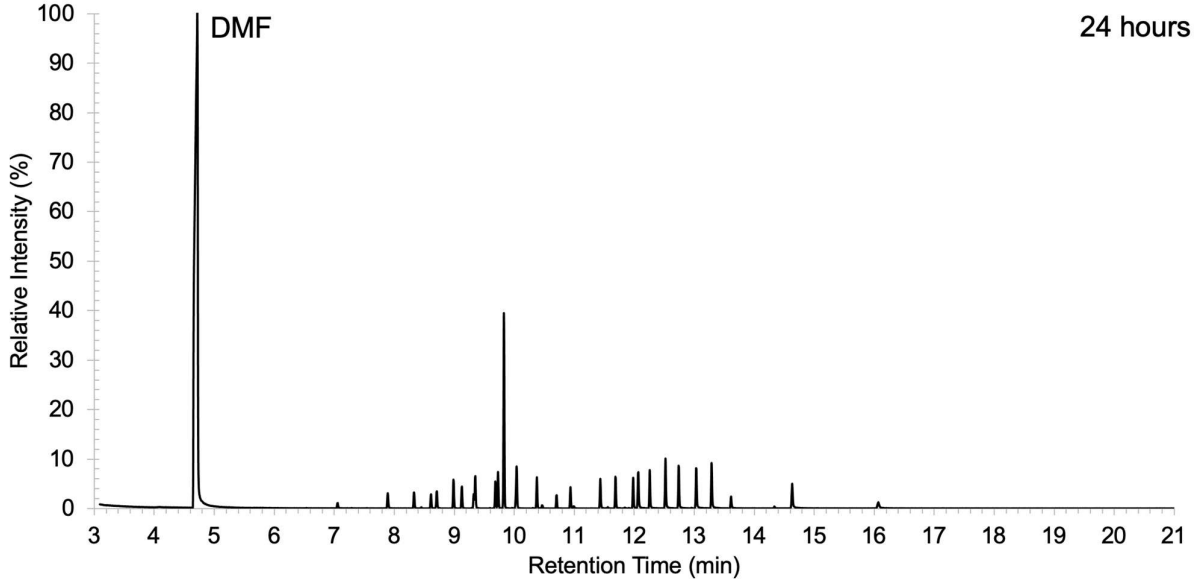

Figure S3.103: Gas chromatogram of the crossover reaction of eight different trisulfides in DMF (100 eq.) after a 24-hour reaction. GC-MS method I.

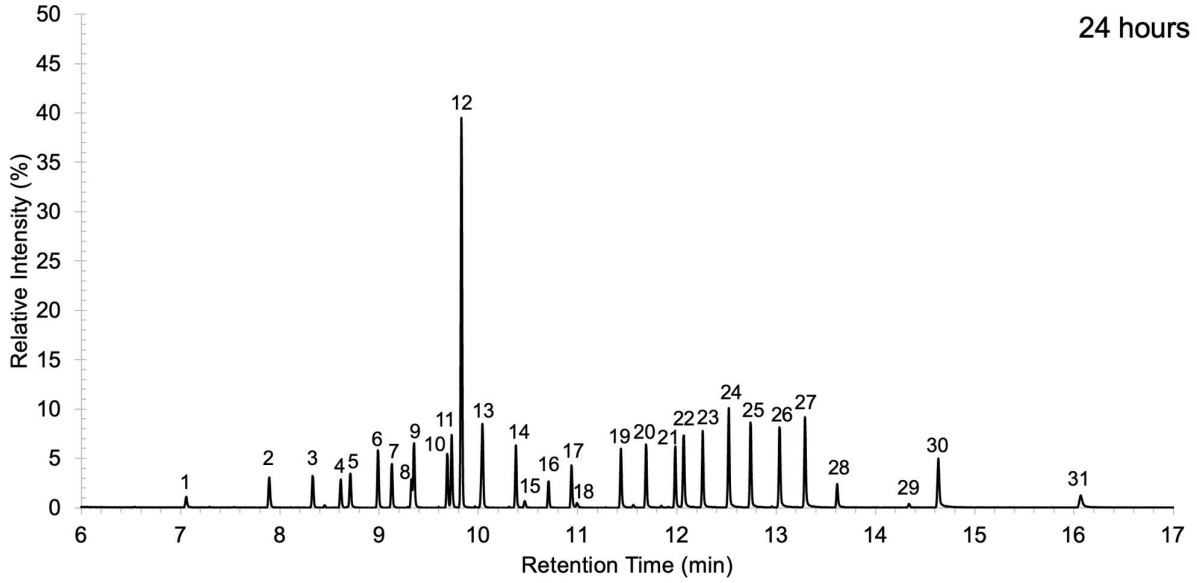

Figure S3.104: Expanded gas chromatogram of the crossover reaction of eight different trisulfides in DMF (100 eq.) after a 24-hour reaction (expanded region from 6 to 17 min of retention time, DMF peak excluded). GC-MS method I.

Table S3.7: m/z for peaks observed in GC-MS of a trisulfides-DMF mixture after 24 h

Peak #	m/z observed	m/z fragments	Retention time (min)	Compound match
1	126.0	126.0, 110.9, 93.9, 79.0, 64.0	7.06	dimethyl trisulfide
2	140.0	140.0, 124.9, 111.9, 93.0, 79.0, 64.0, 61.0	7.89	ethyl methyl trisulfide
3	154.0	154.0, 150.0, 122.0, 111.9, 108.0, 78.9, 64.0	8.33	isopropyl methyl trisulfide
4	154.0	154.0, 125.0, 93.0, 64.0, 61.0	8.61	diethyl trisulfide
5	154.0	154.0, 121.9, 112.0, 108.0, 79.0, 64.0	8.71	methyl *n*-propyl trisulfide
6	168.0	168.0, 136.0, 126.0, 108.0, 94.0, 89.0, 64.0, 61.0	8.99	ethyl isopropyl trisulfide
7	168.0	168.0, 136.1, 122.0, 112.0, 79.0, 64.0, 57.1	9.13	isobutyl methyl trisulfide
8	182.0	182.0, 150.1, 140.0, 117.1, 97.9, 75.0, 64.0	9.32	di-isopropyl trisulfide
9	168.0	168.0, 136.0, 126.0, 108.0, 97.9, 75.0, 63.9, 61.0	9.35	ethyl *n*-propyl trisulfide
10	182.0	182.0, 150.0, 140.0, 117.0, 108.0, 97.9, 75.0, 64.0	9.68	isopropyl *n*-propyl trisulfide
11	182.0	182.0, 150.0, 126.0, 117.0, 93.0, 63.9, 61.0, 57.1	9.73	ethyl isobutyl trisulfide
12	210.0	210.1, 154.0, 89.0, 64.0, 57.1	9.83	di-*tert*-butyl trisulfide
13*	182.0	182.0, 150.1, 140.0, 108.0, 75.0, 64.0	10.02	di-*n*-propyl trisulfide
13*	196.1	196.1, 182.0, 164.1, 154.0, 140.0, 122.0, 117.0, 108.0, 97.9.0, 89.0, 75.0, 64.0, 57.1	10.04	isobutyl isopropyl trisulfide
14	196.1	196.1, 164.1, 140.0, 122.0, 108.0, 97.8, 89.0, 75.0, 64.0, 57.1	10.38	isobutyl *n*-propyl trisulfide
15**	170.0	170.0, 121.0, 91.1, 79.0, 65.1	10.47	benzyl methyl disulfide
16	210.1	210.1, 178.1, 154.0, 122.0, 119.0, 97.0, 89.1, 57.1	10.71	di-isobutyl trisulfide
17	196.1	196.1, 164.1, 149.9. 118.1, 112.0, 92.9, 79.0, 63.9, 57.1, 55.1	10.94	hexyl methyl trisulfide
18**	196.1	196.1, 184.0, 120.8, 91.1, 89.0, 82.8, 73.0, 65.0, 56.0	10.99	benzyl ethyl disulfide
19	210.1	210.1, 178.1, 150.0, 145.1, 126.0, 117.0, 94.0, 83.1, 69.0, 63.9, 61.0, 55.1	11.44	ethyl hexyl trisulfide

20	224.1	224.1, 192.1, 182.0, 159.2, 150.0, 139.9, 117.1, 108.0, 97.9, 85.0, 83.1, 75.0, 69.1, 63.9, 55.1	11.69	isopropyl hexyl trisulfide
21	224.1	224.1, 192.1, 159.0, 150.0, 140.0, 117.1, 108.0, 97.9, 83.1, 75.0, 64.0, 55.1	11.98	hexyl *n*-propyl trisulfide
22	202.0	202.0, 170.0, 137.0, 121.0, 91.1, 79.0, 65.0, 51.0	12.07	benzyl methyl trisulfide
23	238.1	238.1, 206.1, 182.0, 173.1, 150.1, 122.0, 117.1, 110.9, 97.9, 89.1, 85.0, 83.0, 79.0, 73.0, 63.9, 57.1, 55.1	12.26	hexyl isobutyl trisulfide
24	216.0	216.0, 184.0, 151.1, 121.0, 91.1, 77.0, 75.0, 59.0, 51.1	12.52	benzyl ethyl trisulfide
25	230.0	230.0, 198.0, 165.1, 121.0, 107.9, 91.1, 77.0, 65.1, 59.0, 51.0	12.74	benzyl isopropyl trisulfide
26	230.0	230.0, 198.0, 165.1, 121.0, 108.0, 91.1, 77.0, 65.0, 51.0	13.03	benzyl *n*-propyl trisulfide
27	244.1	224.1, 212.1, 179.1, 121.0, 91.1, 77.0, 65.0, 57.0, 51.0	13.29	benzyl isobutyl trisulfide
28	266.1	266.2, 234.2, 182.0, 150.1, 117.1, 85.0	13.62	di-*n*-hexyl trisulfide
29**	246.0	246.0, 207.0, 181.2, 120.9, 91.1, 76.9, 65.0, 55.9	14.34	dibenzyl disulfide
30	272.1	272.1. 207.1, 150.0, 121.0, 91.1, 77.0, 65.0, 56.1	14.63	benzyl hexyl trisulfide
31	278.1	278.1, 246.1, 213.1, 181.1, 123.0, 91.1, 77.1	16.07	dibenzyl trisulfide

(*) this peak shows two m/z fragments indicating two different compounds i.e., $^{n}PrS_3{}^{n}Pr$ and $^{i}BuS_3{}^{i}Pr$.

(**) alkyl benzyl disulfides were only observed after 24 hours. Rows with highlighted yellow indicate the parent trisulfides.

Calicheamicin γ1 Functionalisation

(This experiment was performed by Dr. Harshal D. Patel and James Smith)

Calicheamicin Dimer

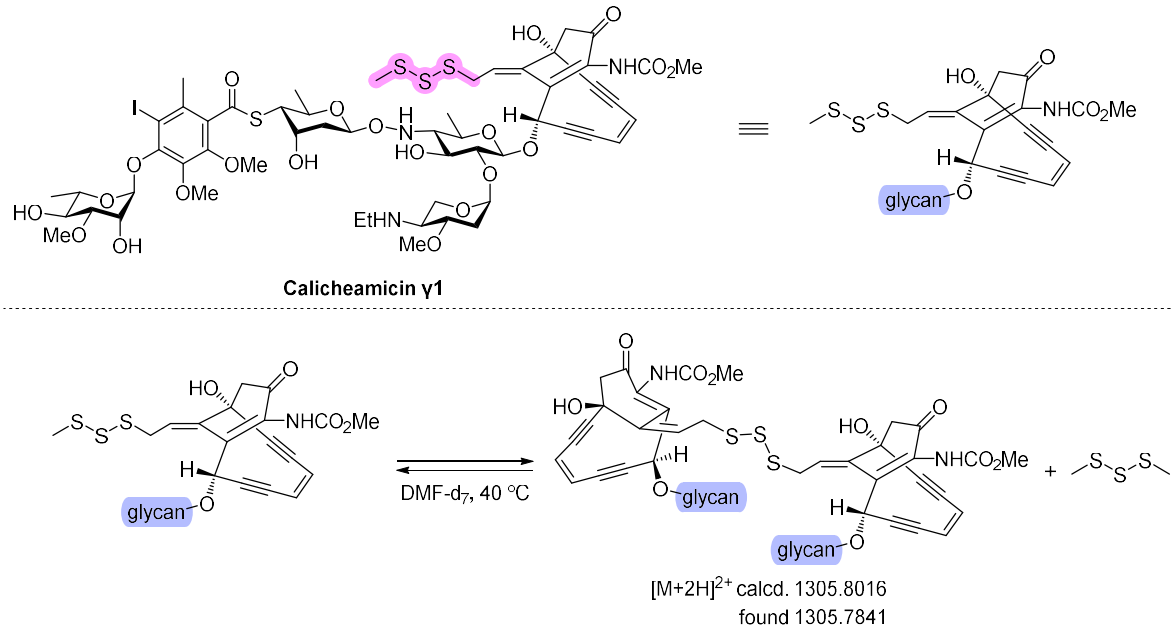

Calicheamicin γ1 (1 mg, 730 nmol, 1.0 eq.) was placed in an NMR tube. Next, 0.45 mL DMF-d_7 was added and a proton NMR was collected immediately. The sample was then heated at 40 °C for 60 minutes. For LC-MS, the DMF-d_7 was removed under high vacuum, and the residue dissolved in 1 mL MeCN for analysis.

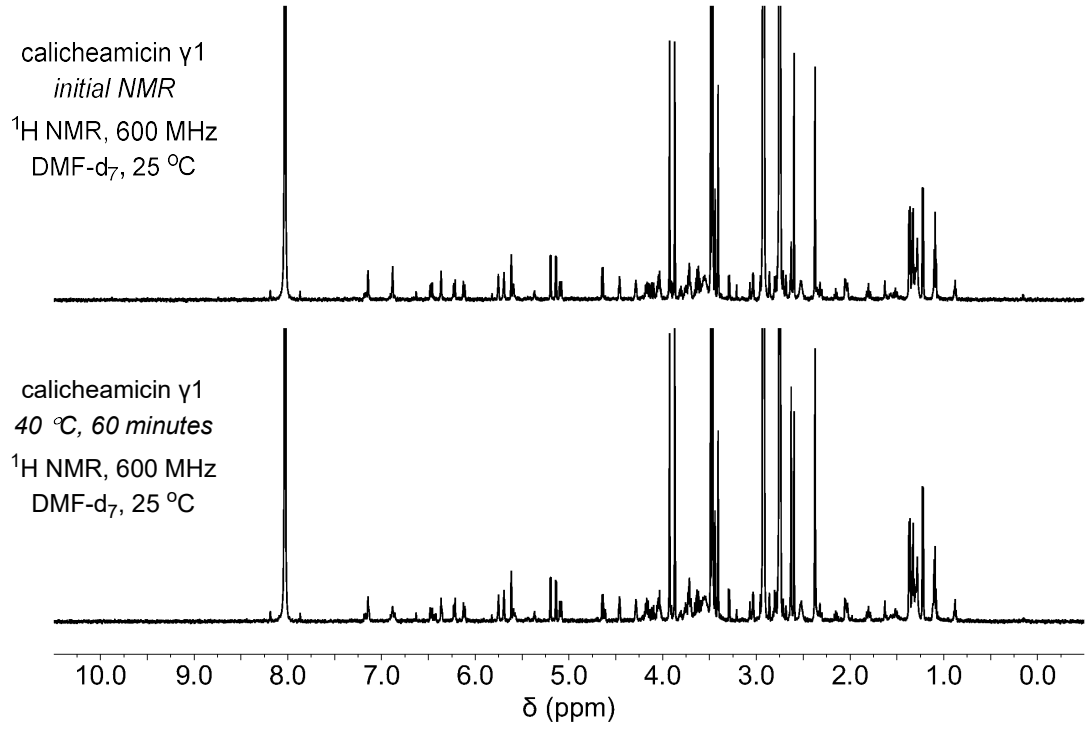

Figure S3.105: ^{1}H NMR spectra in DMF-d_7 of calicheamicin γ1 (top), and the same sample after heating at 40 °C for 60 minutes (bottom).

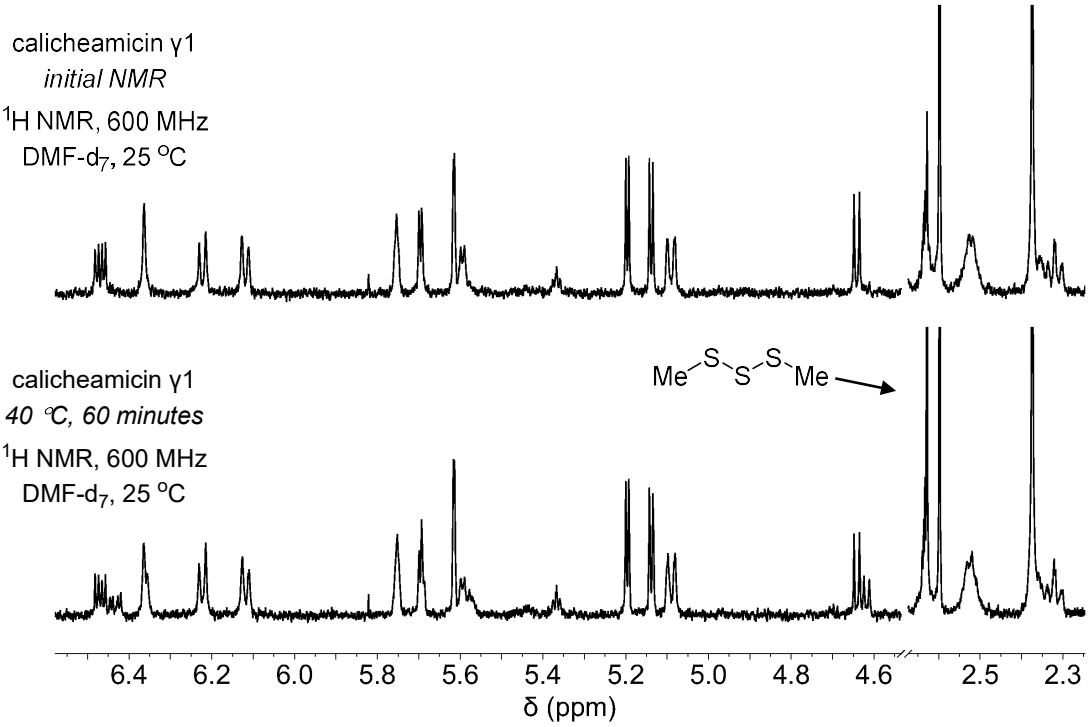

Figure S3.106: Zoomed ^{1}H NMR spectra in DMF-d_7 of calicheamicin γ1 (top), and the same sample after heating at 40 °C for 60 minutes (bottom). A new peak forming at 2.62 ppm corresponds to Me_2S_3.

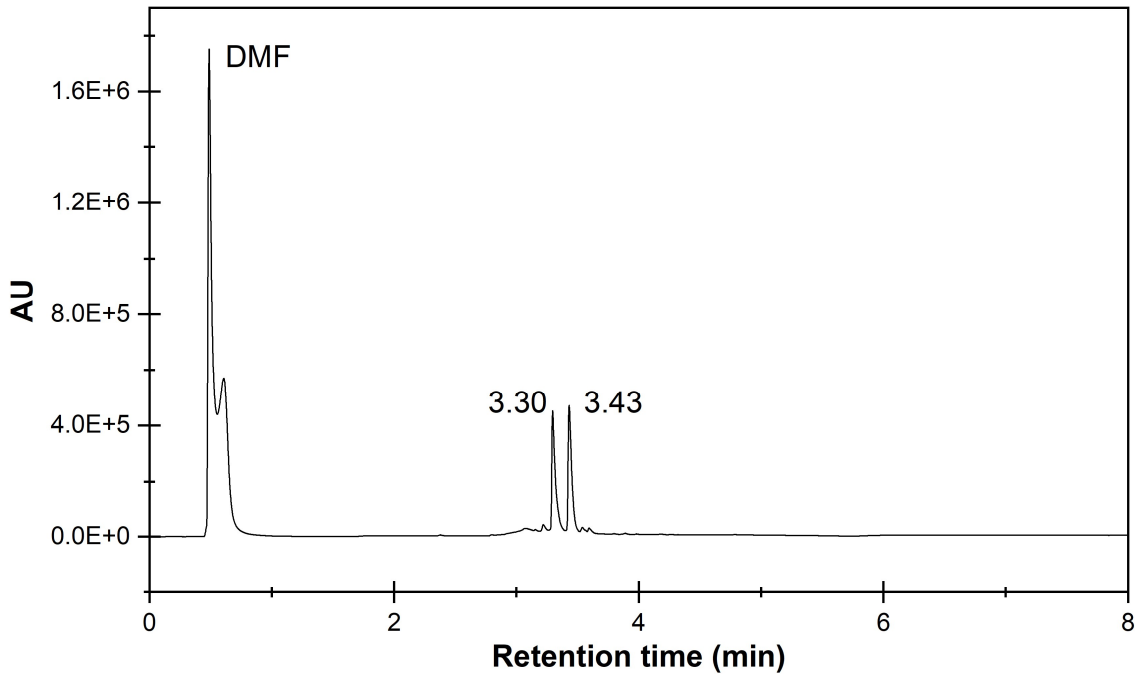

Figure S3.107: LC trace at 214 nm detection: Calicheamicin dimer (3.30 min) and calicheamicin γ1 (3.43 min) in MeCN.

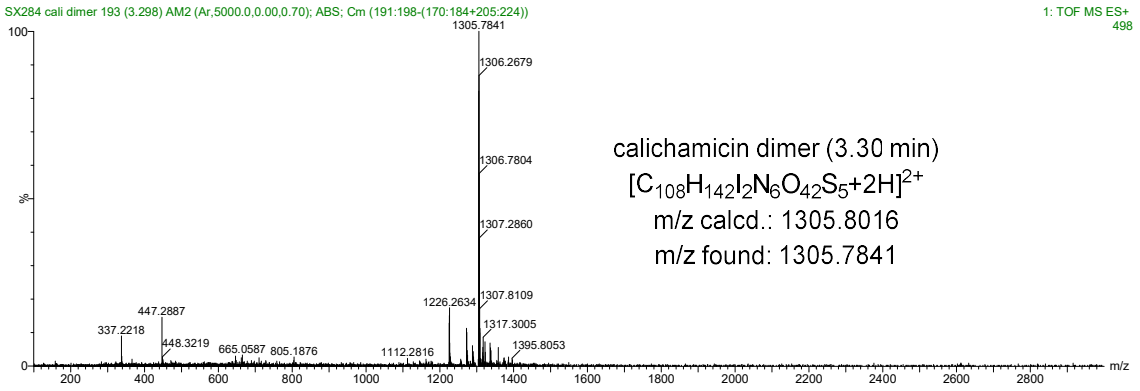

Figure S3.108: Calicheamicin dimer (3.30 min) mass fragment. $[M+2H]^{2+}$ calcd. 1305.8016, found 1305.7841.

Bn_2S_3 Crossover with calicheamicin γ1

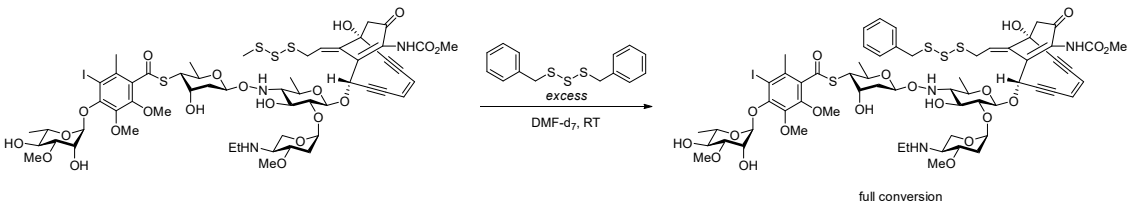

Calicheamicin γ1 (1 mg, 730 nmol, 1.0 eq.) and dibenzyl trisulfide (7 mg, 26 mmol, 35.0 eq.) were placed in an NMR tube. Next, 0.45 mL DMF-d_7 was added and a proton NMR was collected immediately, and at 10, 20, and 30 minutes. The contents of the NMR tube were transferred to a round bottom flask, and the DMF was removed under high vacuum at room temperature. Pentane was added to the round bottom flask which formed a white precipitate. Trituration with pentane and filtering through cotton wool removed excess Bn_2S_3 and BnS_3Me; the pentane was removed under reduced pressure and analysed by NMR spectroscopy and GC-MS. The white precipitate was collected by dissolution in $CDCl_3$, and the solvent was removed under reduced pressure and analysed by NMR in $CDCl_3$. A 0.1 mL sample was removed and diluted to 1 mL with MeCN for analysis by LC-MS.

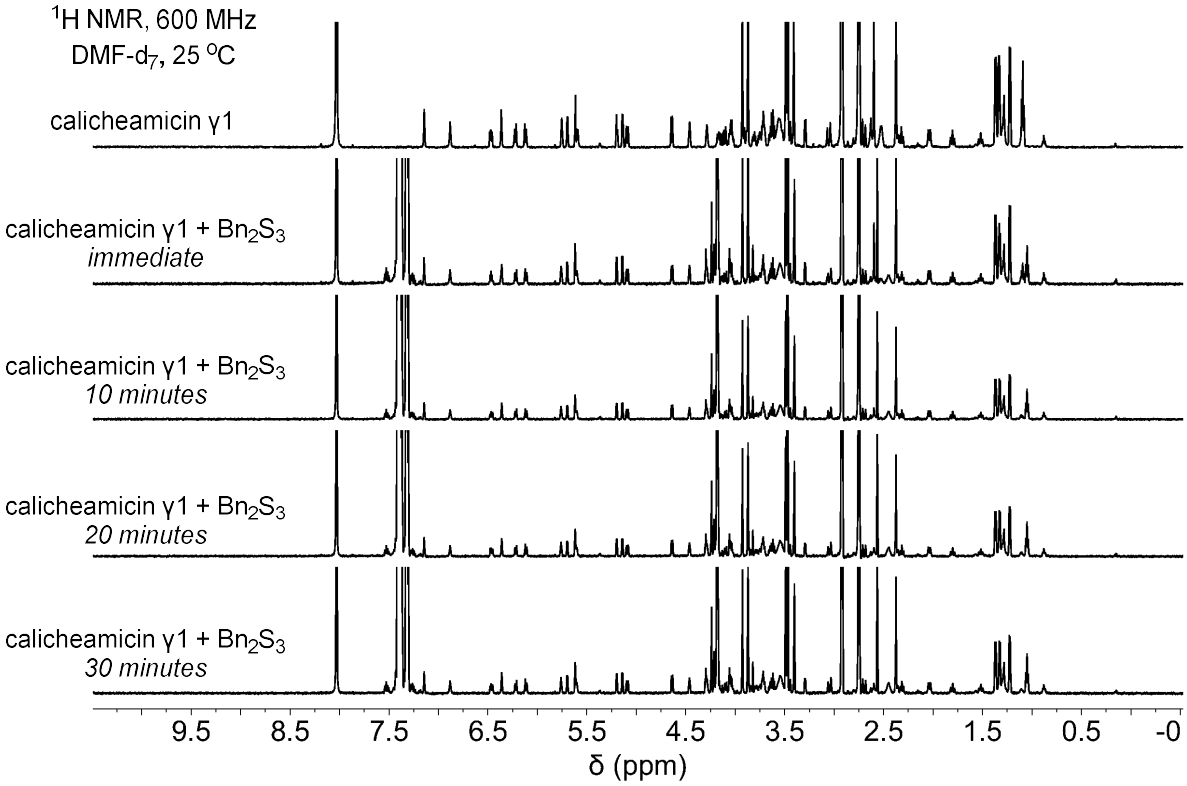

Figure S3.109: ^1H NMR spectra in DMF-d_7, from top to bottom: calicheamicin γ1, calicheamicin γ1 and Bn_2S_3 immediately, calicheamicin γ1 and Bn_2S_3 after 10 minutes, calicheamicin γ1 and Bn_2S_3 after 20 minutes, calicheamicin γ1 and Bn_2S_3 after 30 minutes.

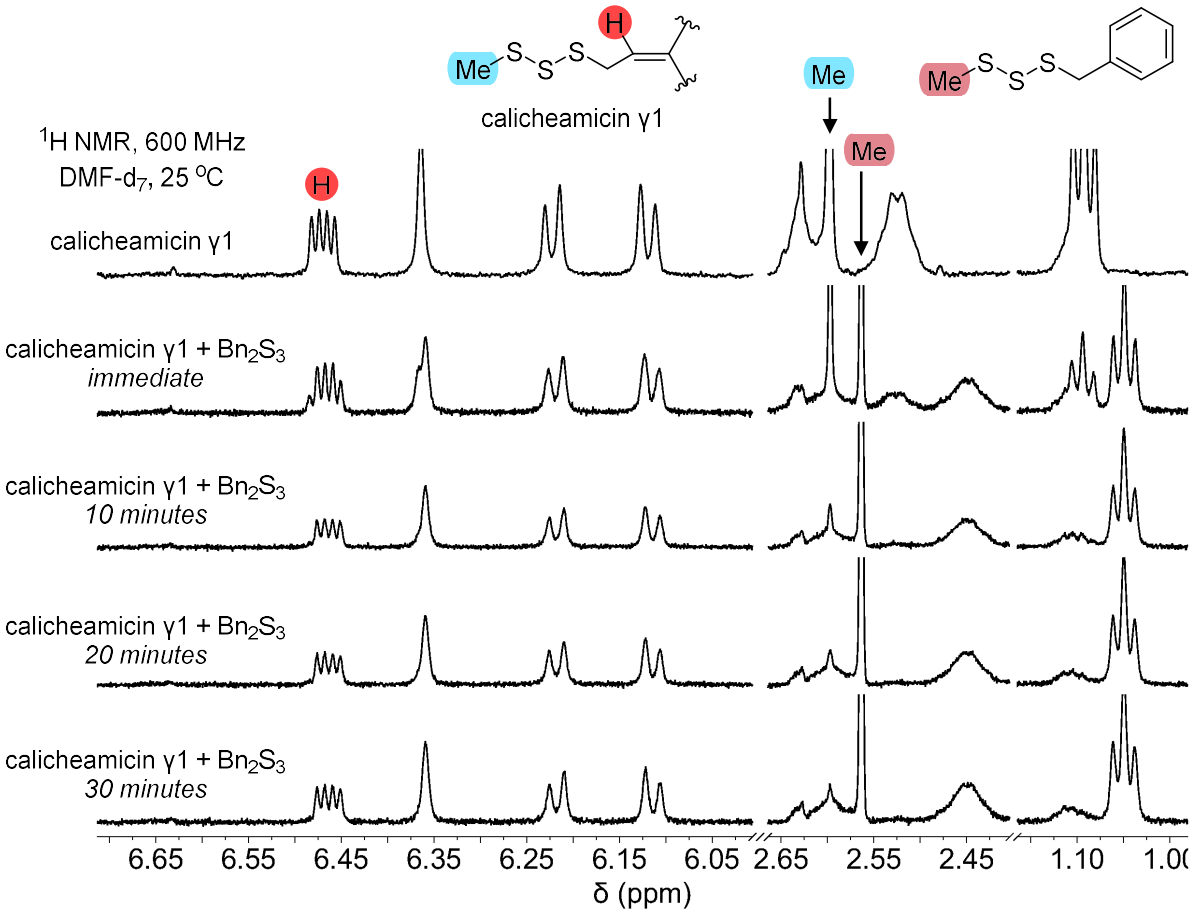

Figure S3.110: ^{1}H NMR spectra in regions of interest in DMF-d$_7$, from top to bottom: calicheamicin γ1, calicheamicin γ1 and Bn$_2$S$_3$ (t = 0), calicheamicin γ1 and Bn$_2$S$_3$ after 10 minutes, calicheamicin γ1 and Bn$_2$S$_3$ after 20 minutes, calicheamicin γ1 and Bn$_2$S$_3$ after 30 minutes. The most noticeable change is the disappearance of the calicheamicin γ1 **Me**-SSS-R, and the formation of the **Me**-SSS-Bn signal.

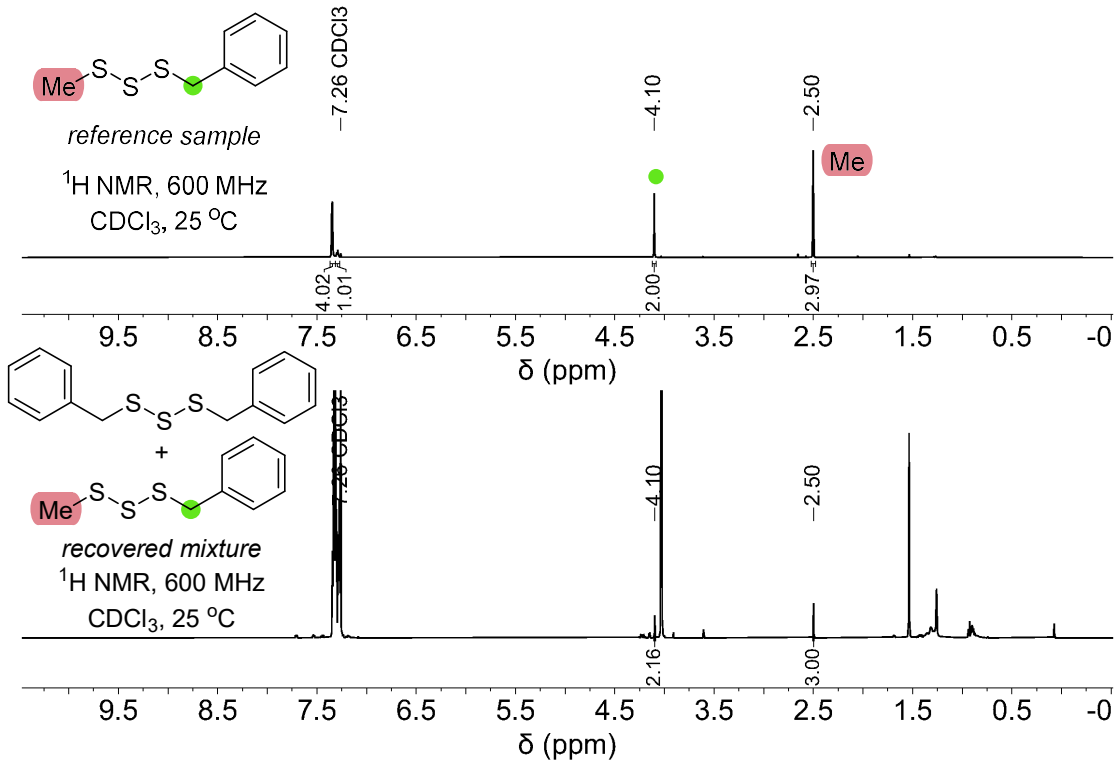

Figure S3.111: ^{1}H NMR spectra in $CDCl_3$ comparing pure BnS_3Me (top) with the recovered mixture of BnS_3Bn and BnS_3Me (bottom).

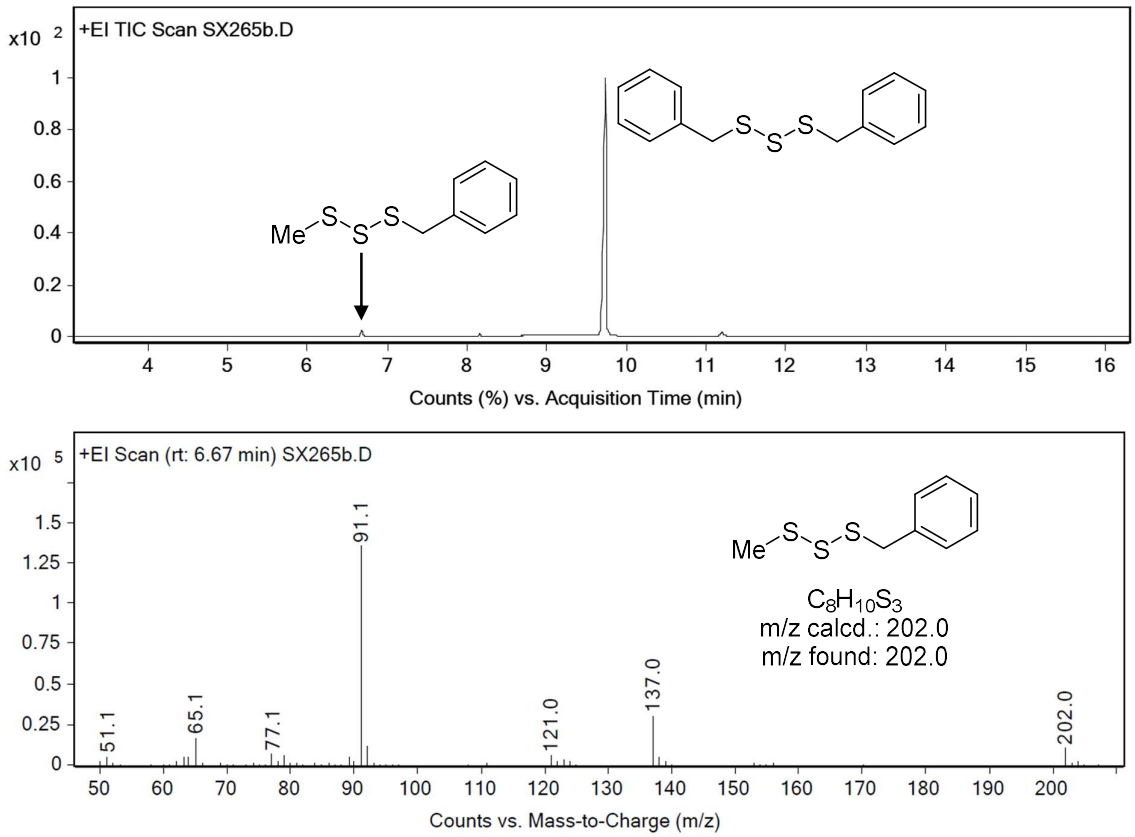

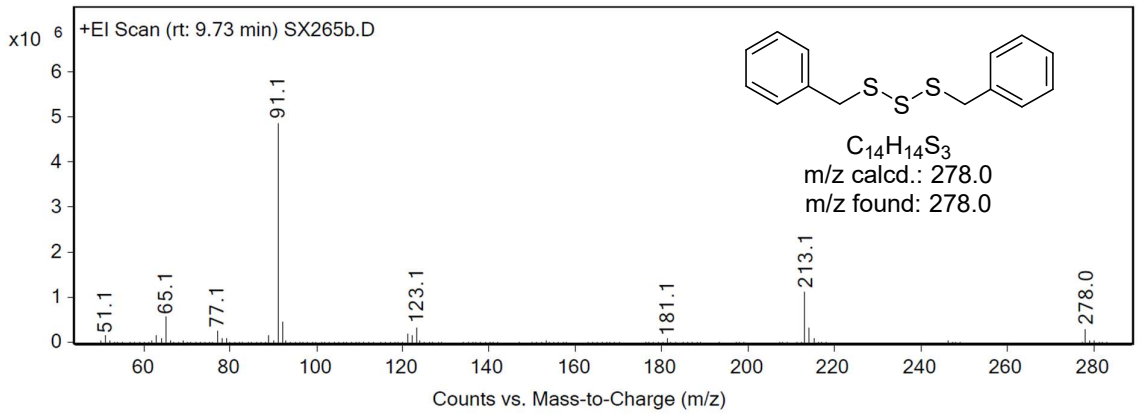

Figure S3.112: Gas chromatogram and mass spectrum of recovered BnS_3Bn and BnS_3Me. GC-MS method E. Retention time: 6.67 min (BnS_3Me) and 9.73 min (Bn_2S_3).

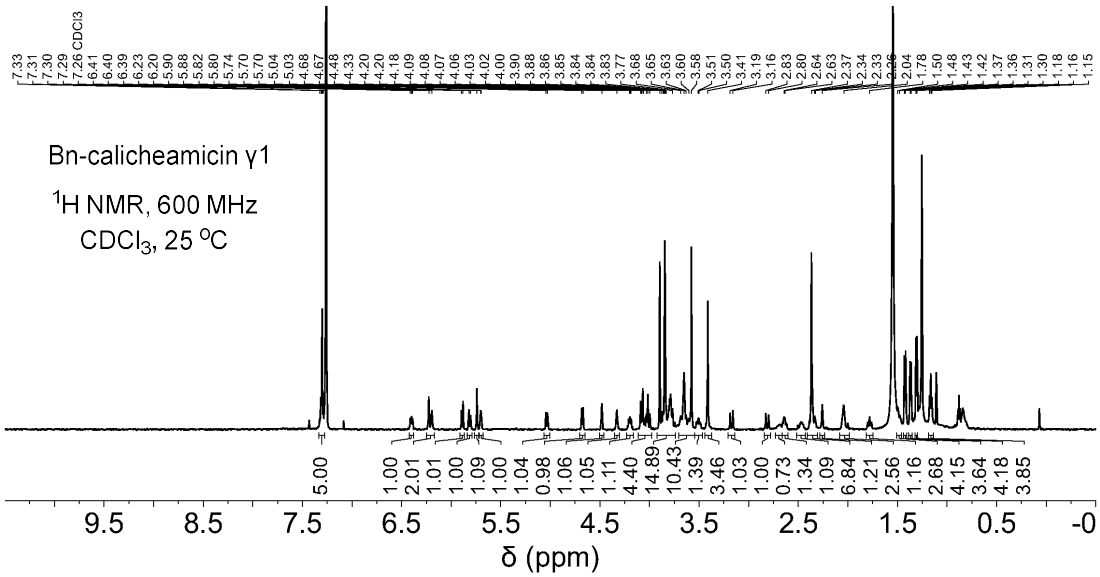

Figure S3.113: ^1H NMR spectrum of purified Bn-calicheamicin γ1 in $CDCl_3$.

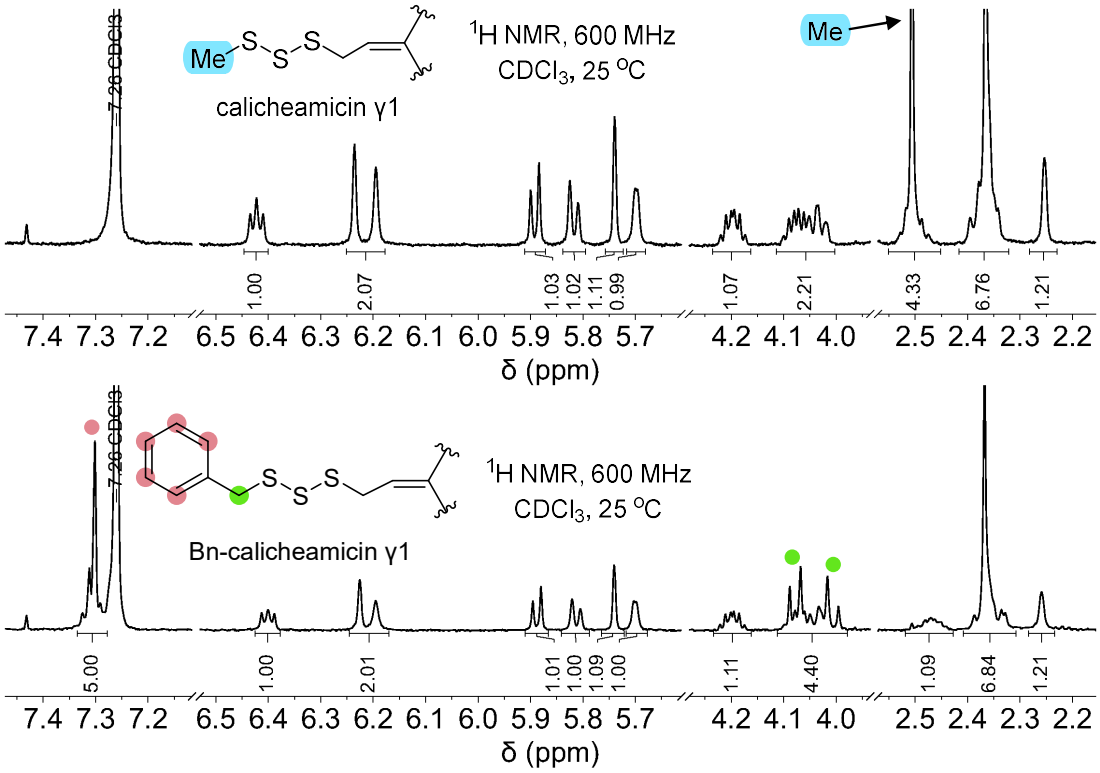

Figure S3.114: ^{1}H NMR spectra of Calicheamicin γ1 (top) with purified Bn-calicheamicin γ1 in $CDCl_3$ (bottom).

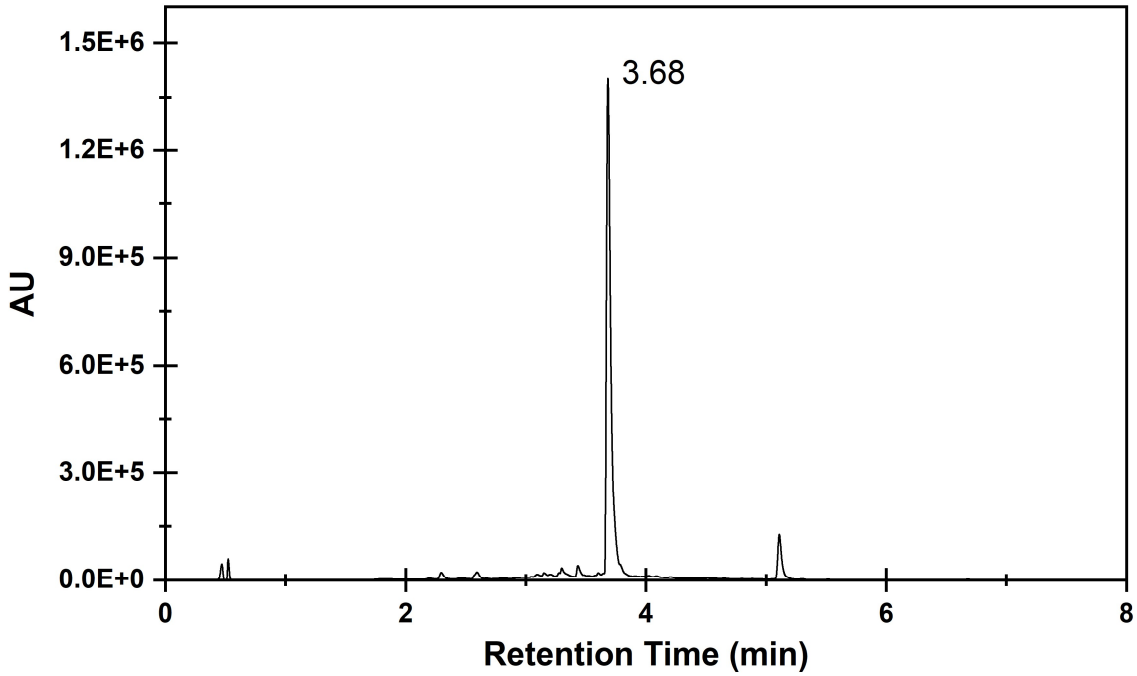

Figure S3.114: LC trace at 214 nm detection: Benzyl calicheamicin (3.68 min) in MeCN.

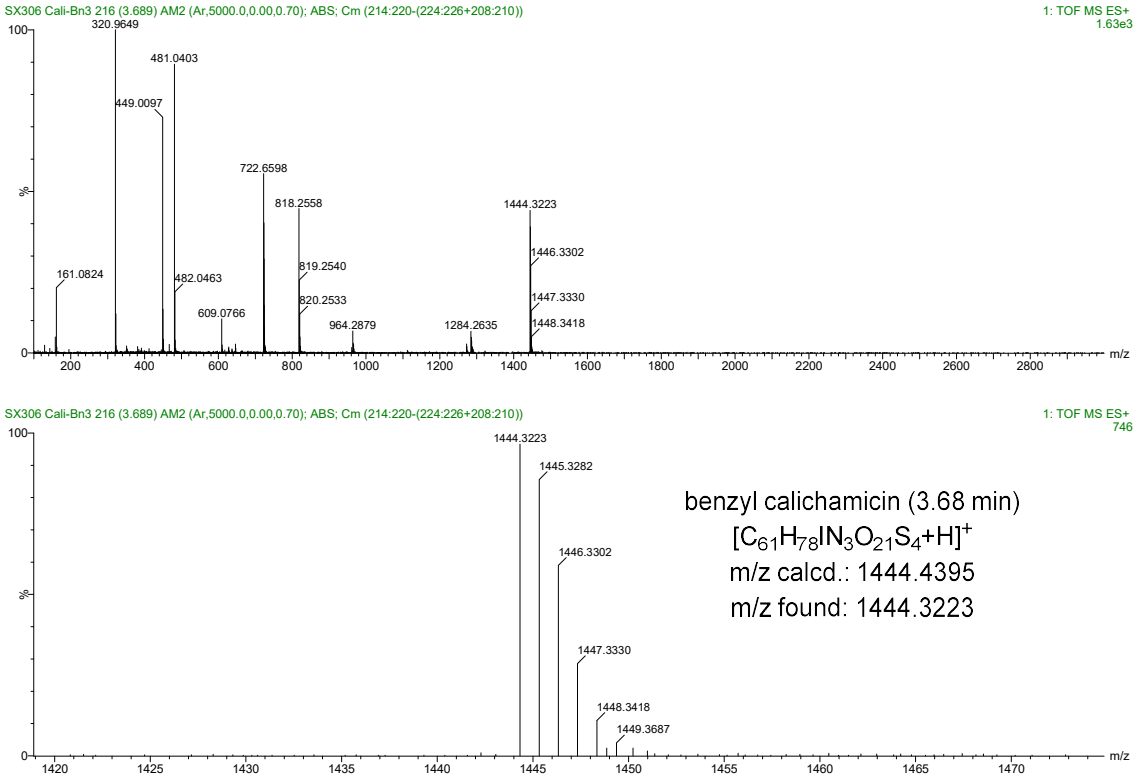

Figure S3.115: Benzyl calicheamicin (3.68 min) mass fragment. $[M+H]^+$ calcd. 1444.4395 found 1444.3223.

nPr_2S_3 Crossover with calicheamicin γ1

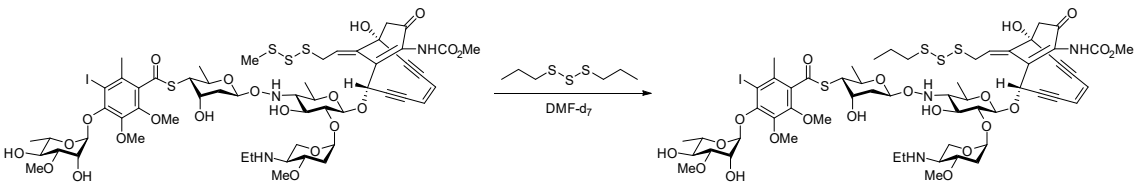

Calicheamicin γ[1] (1 mg, 730 nmol, 1.0 eq.) and *n*Pr_2S_3 (8 µmL, 50 eq.) was added to an NMR tube and dissolved in DMF-d_7 (0.4 mL). The sample was heated at 40 °C for 30 minutes monitoring *via* ^{1}H NMR spectroscopy. The solvent was removed under high vacuum and the residue was triturated with distilled pentane removing excess *n*Pr_2S_3. The residue was dissolved in $CDCl_3$ for further ^{1}H NMR analysis. Solvent was again removed under vacuum and dissolvent in acetonitrile for LC-MS analysis.

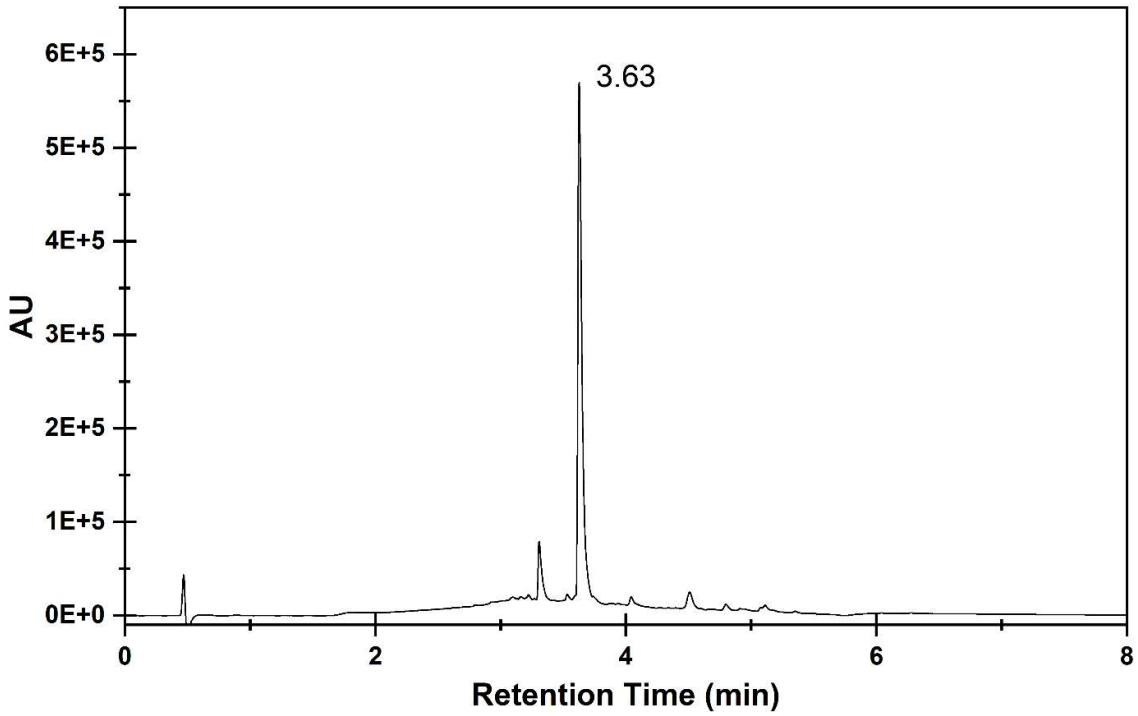

Figure S3.116: LC trace at 214 nm detection: *n*-propyl Calicheamicin (3.63 min) in MeCN.

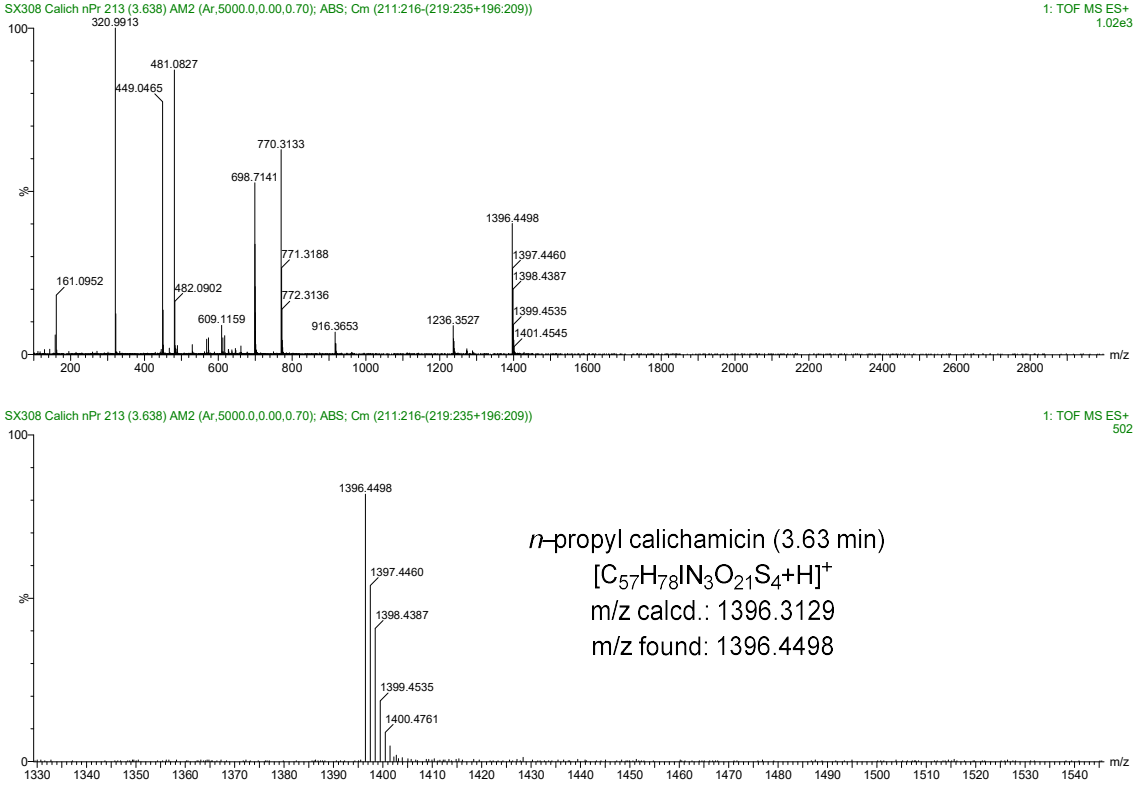

Figure S3.117: *n*-propyl Calicheamicin (3.63 min) mass fragment. $[M+H]^+$ calcd. 1396.3129 found 1396.4498.

Reaction of *n*PrSH with calicheamicin γ1

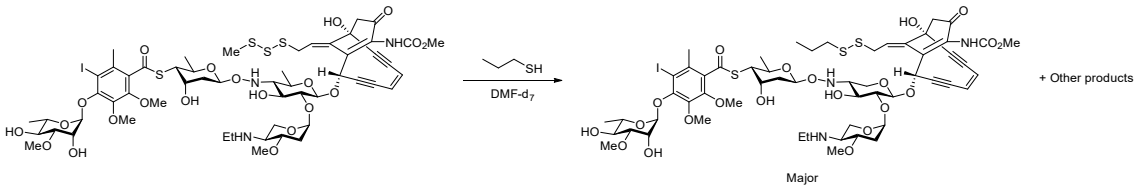

Calicheamicin γ[1] (1 mg, 730 nmol, 1.0 eq.) was dissolved in DMF-d_7 (0.4 mL), to the solution *n*-propyl thiol (3.2 μmL, 36.5 μmol, 50 eq.) was added. ^{1}H NMR spectroscopy was used to monitor the interaction between calicheamicin γ[1] and *n*-propyl thiol and after 1 hour the solvent and excess *n*-propyl thiol was removed under high vacuum leaving a residual oil which was dissolved in $CDCl_3$ to be analysed by ^{1}H NMR spectroscopy. The deuterated solvent was then removed, and residue was dissolved in 1 mL of acetonitrile for LC-MS analysis.

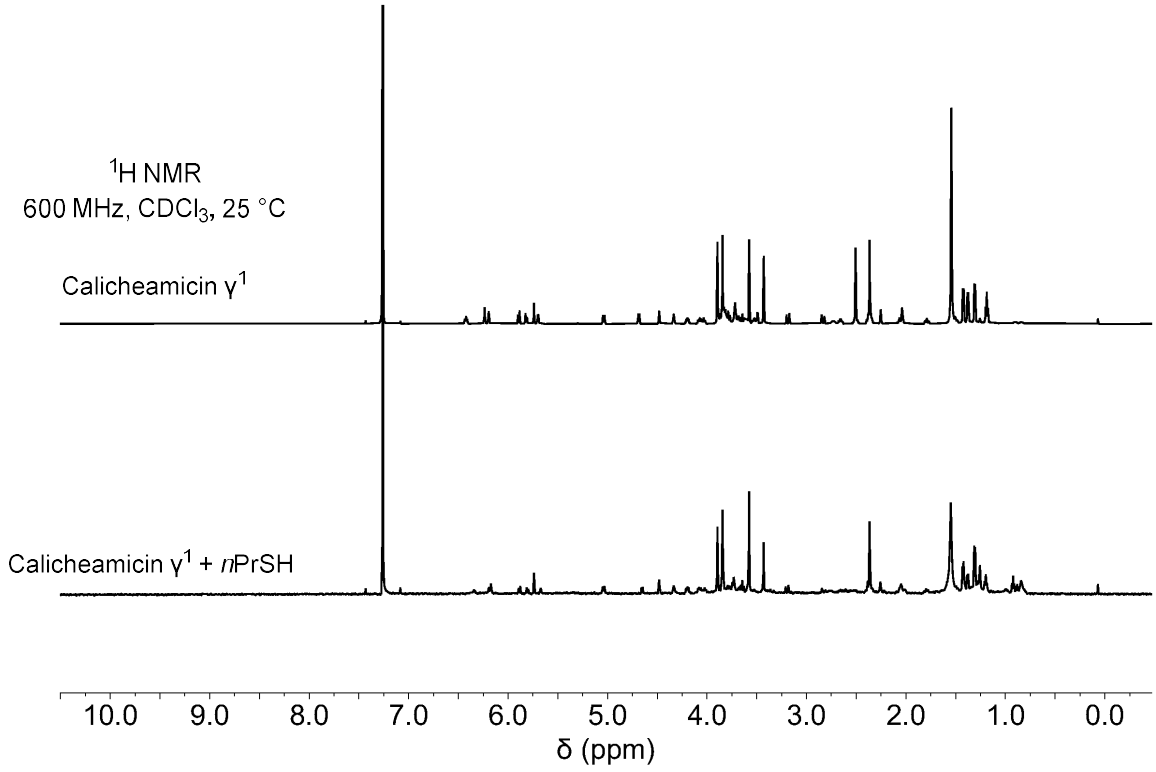

Figure S3.118: ^{1}H NMR spectra of Calicheamicin γ[1] (top), and Calicheamicin γ[1]/*n*-propyl thiol (bottom) in $CDCl_3$.

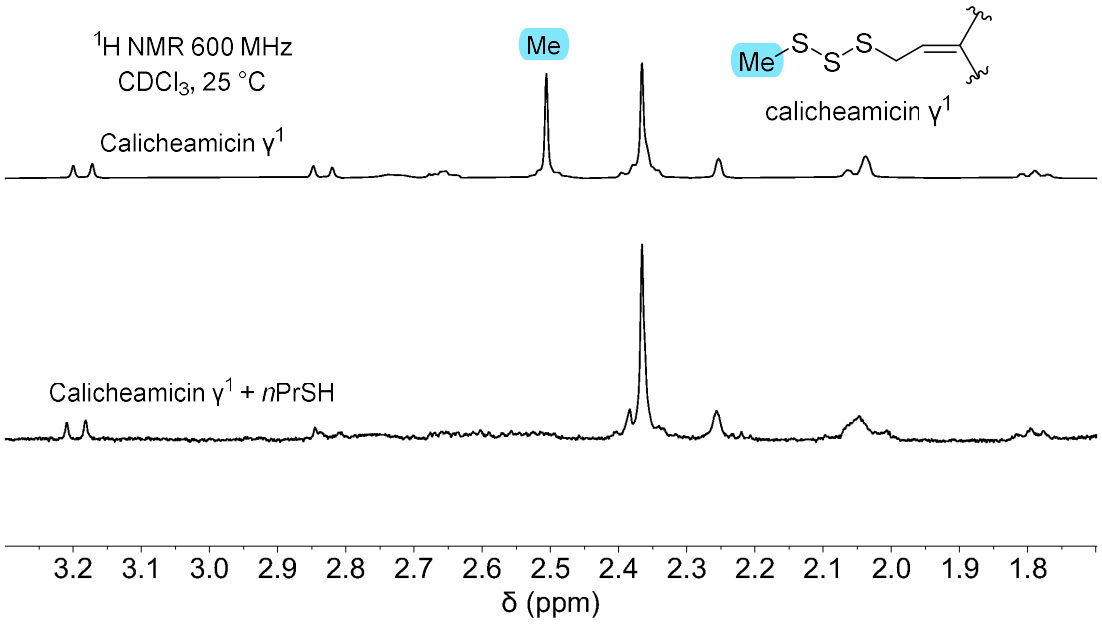

Figure S3.119: Zoomed ^{1}H NMR spectra of Calicheamicin γ^1 (top) and Calicheamicin γ^1/*n*-propyl thiol (bottom) in $CDCl_3$ between 1.7-3.3 ppm.

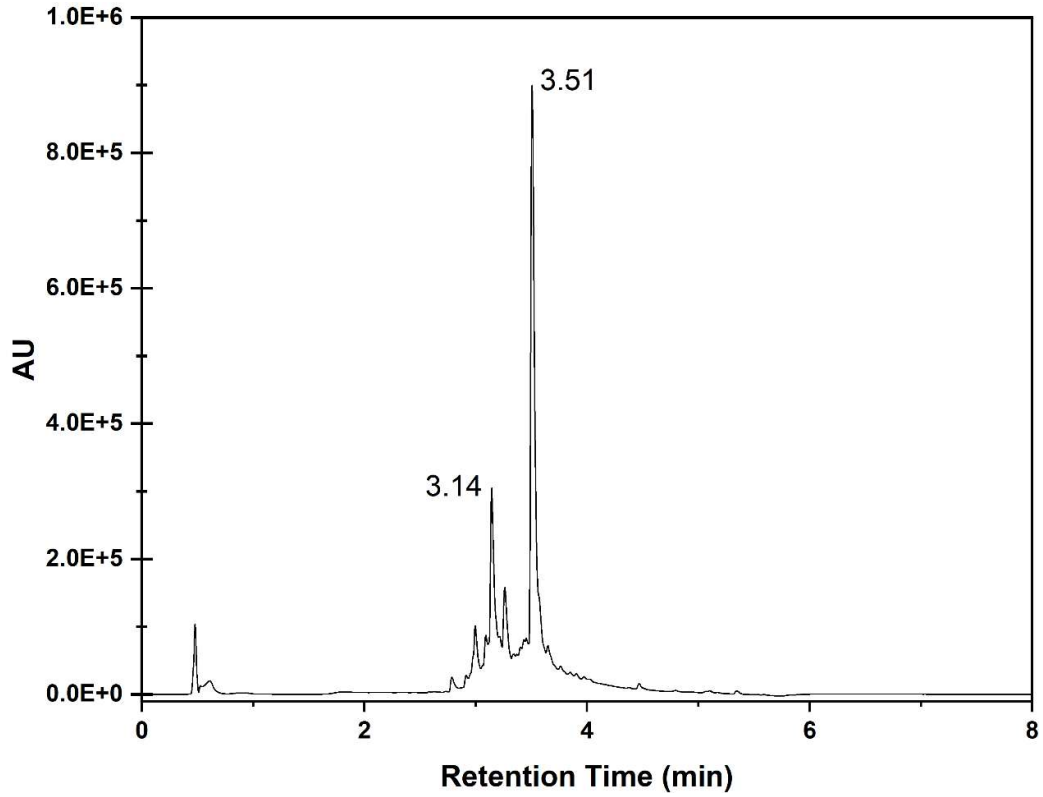

Figure S3.120: LC trace at 214 nm detection: *n*-propyl calicheamicin disulfide (3.51 min) in MeCN.

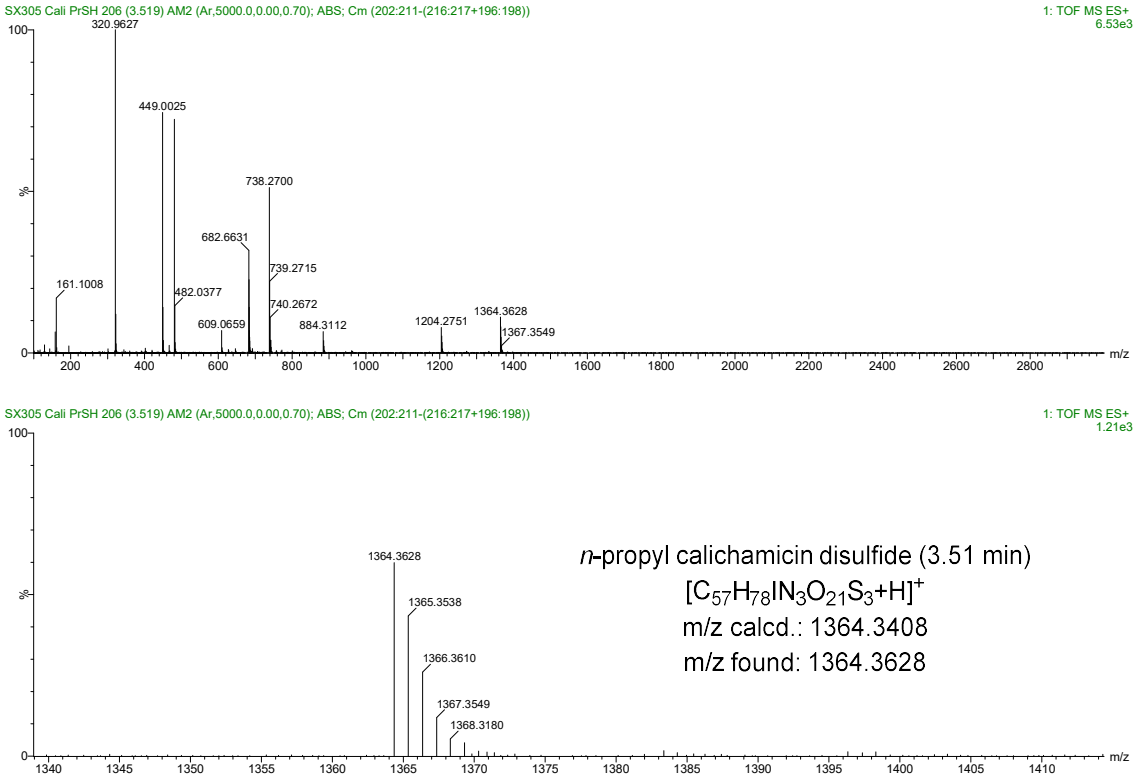

Figure S3.121: *n*-propyl calicheamicin disulfide (3.51 min) mass fragment. $[M+H]^+$ calcd. 1364.3408 found 1364.3628.

Disulfide Crossover

Crossover between dimethyl disulfide (Me_2S_2) and di-*n*-propyl disulfide ($^nPr_2S_2$) – DMF, NMP and DMSO

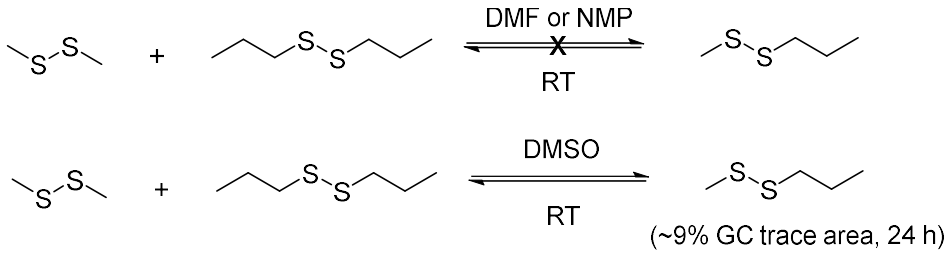

Dimethyl disulfide (36 µL, 0.4 mmol, 1 eq.) and di-*n*-propyl disulfide (62.6 µL, 0.4 mmol, 1 eq.) were added to a 2 mL glass vial, followed by the solvent. The solvents were *N*,*N*-dimethylformamide (DMF) (31 µL, 0.4 mmol, for 1 eq. and 310 µL, 4.0 mmol, for 10 eq.), *N*-methyl-2-pyrrolidone (NMP) (386 µL, 4.0 mmol, 10 eq.) and dimethyl sulfoxide (DMSO) (284 µL, 4.0 mmol, 10 eq.). The mixture was stirred at room temperature for 24 hours. Room temperature was 16 – 21 ºC for crossover with DMF, 15 – 23 ºC for crossover with NMP, and 15 – 28 ºC for crossover with DMSO. After 5 minutes, 1 hour and 24 hours, 10 µL of the aliquot was removed and diluted to 1 mL with chloroform for GC-MS analysis. In general, the crossover reaction between dimethyl disulfide and di-*n*-propyl disulfide does occur in the presence of 10 equivalent of the amide solvents i.e., DMF and NMP. The area percentage of $MeS_2{}^nPr$ crossover product for a 24-hour reaction in DMF and NMP were only 2% and 2.6%, respectively. Results also showed that a mere 9% of $MeS_2{}^nPr$ was observed when the disulfides reacted in DMSO after 24 hours.

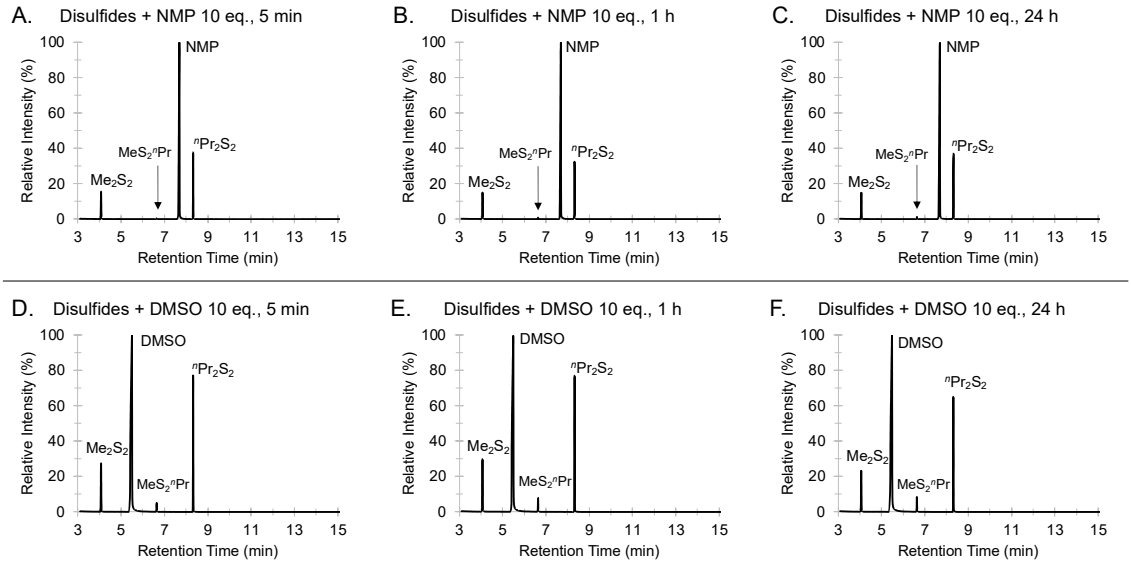

Figure S3.122: GC traces for the crossover reaction between dimethyl disulfide (Me_2S_2) and di-*n*-propyl disulfide ($^nPr_2S_2$) over 24 hours at room temperature. (A, B and C) The disulfides (1 eq. each) and NMP (10 eq.) at 15 – 23 °C after 5 min, 1 h, and 24 h. (D, E and F) The disulfides (1 eq. each) and DMSO (10 eq.) at 15 – 28 ºC after 5 min, 1 h, and 24 h. The GC-MS method A. Retention time: Me_2S_2 (4.07 min), DMSO (5.49 min), $MeS_2{}^nPr$ (6.63 min), NMP (7.69 min) and $^nPr_2S_2$ (8.33 min).

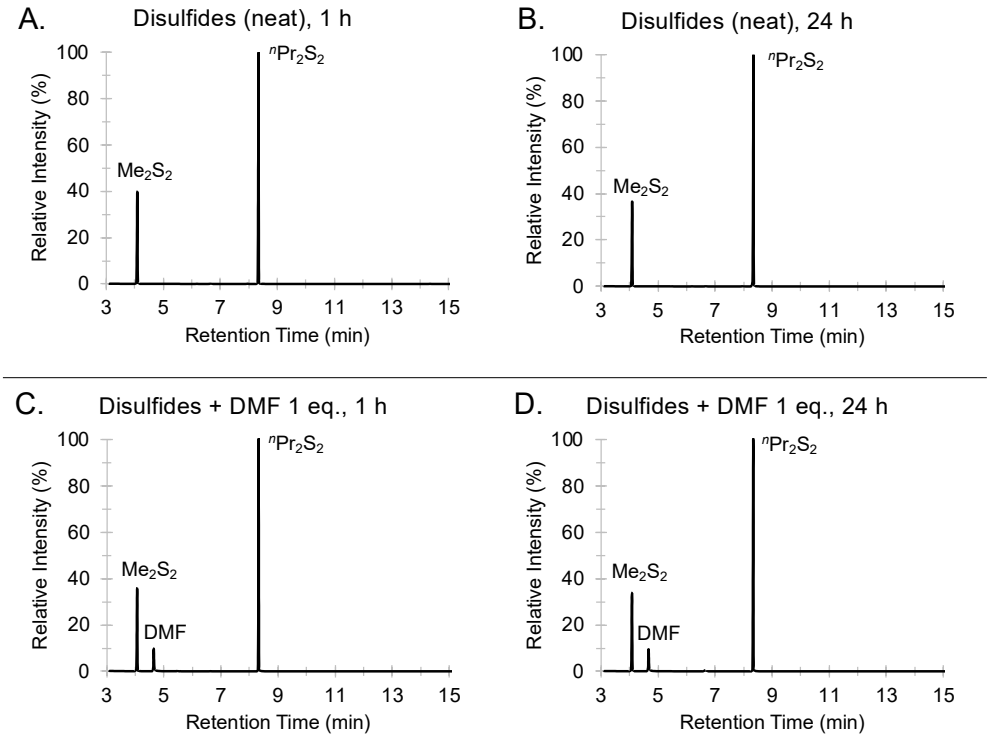

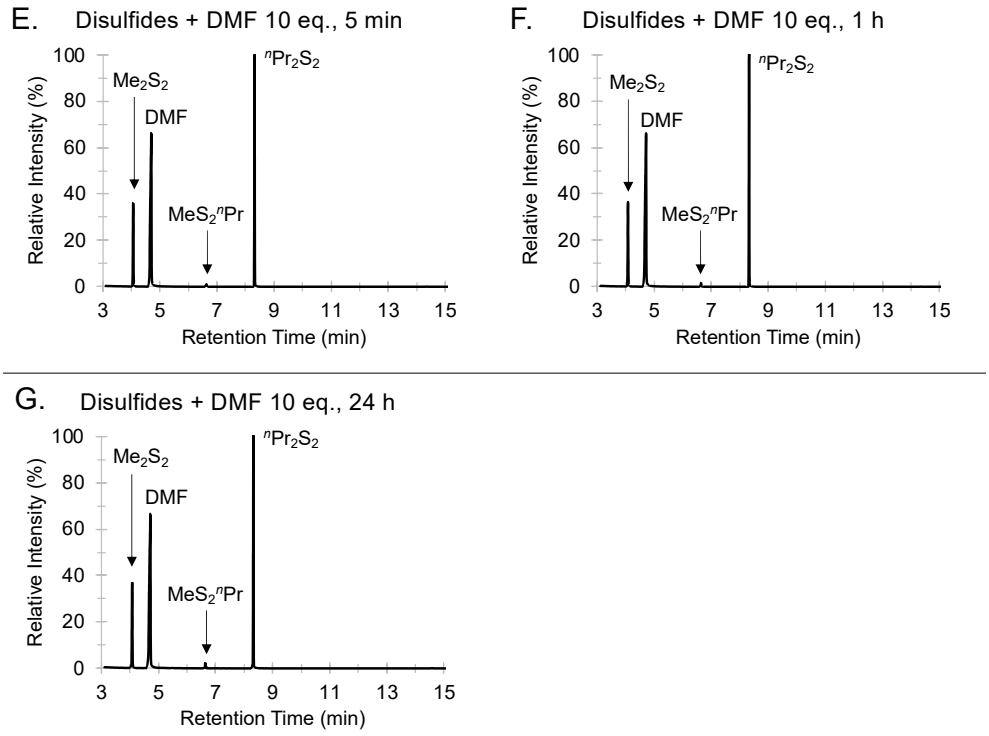

Figure S3.123: GC traces for the crossover reaction between dimethyl disulfide (Me_2S_2) and di-*n*-propyl disulfide ($^nPr_2S_2$) over 24 hours at room temperature (16 – 21 °C). (A, B) The disulfides only (1 eq. each). (C, D) The disulfides and DMF (1 eq. each). (E, F and G) The disulfides (1 eq. each) and DMF (10 eq.). The GC-MS method A. Retention time: Me_2S_2 (4.07 min), DMF (4.70 min), $MeS_2{}^nPr$ (6.63 min), and $^nPr_2S_2$ (8.33 min)

Crossover between dimethyl disulfide (Me_2S_2) and di-*n*-hexyl disulfide ($^nHex_2S_2$) in the presence of DMF

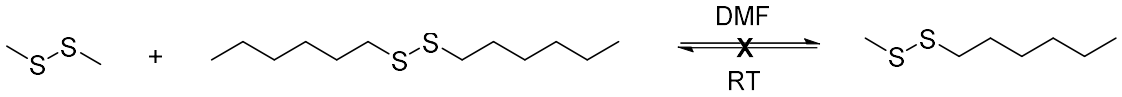

Dimethyl disulfide (36 µL, 0.4 mmol, 1 eq.) and di-*n*-hexyl disulfide (60.1 mg, 0.4 mmol, 1 eq.) were added to a 2 mL glass vial, followed by *N*,*N*-dimethylformamide (DMF) (310 µL, 4.0 mmol, 10 eq.). The mixture was stirred at room temperature (8 – 18 ºC) for 24 hours. After 1 and 24 h, 10 µL of the aliquot was removed and diluted to 1 mL with chloroform for GC-MS analysis. No crossover product ($MeS_2{}^nHex$) was observed.

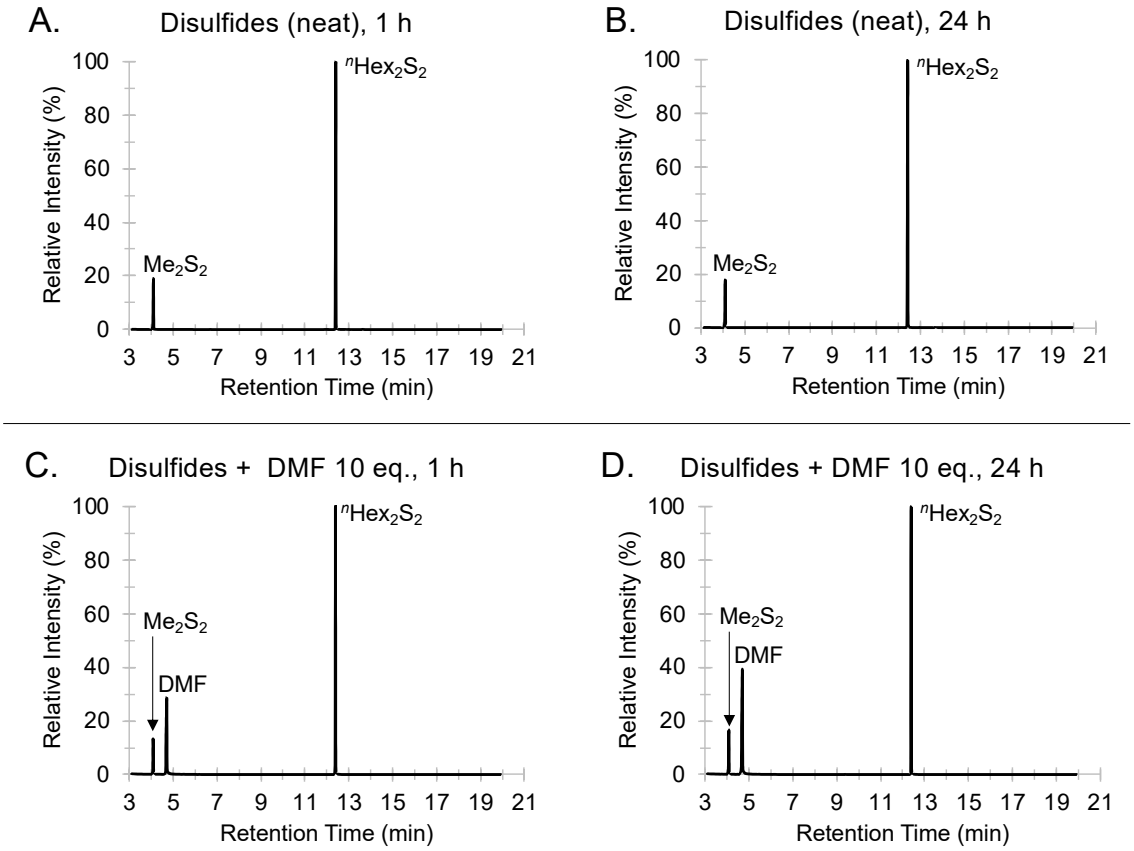

Figure S3.124: GC traces for the crossover reaction between dimethyl disulfide (Me_2S_2) and di-*n*-hexyl disulfide ($^{n}Hex_2S_2$) over 24 hours at room temperature (8 – 18 °C). (A, B) The disulfides only (1 eq. each). (C, D) The disulfides (1 eq. each) and DMF (10 eq.). The GC-MS method A. Retention time: Me_2S_2 (4.07 min), DMF (4.70 min), and $^{n}Hex_2S_2$ (12.39 min)

Crossover between dimethyl disulfide (Me_2S_2) and di-isobutyl disulfide ($^{i}Bu_2S_2$) in the presence of DMF

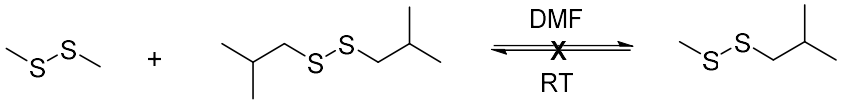

Dimethyl disulfide (36 µL, 0.4 mmol, 1 eq.) and di-isobutyl disulfide (71.3 mg, 0.4 mmol, 1 eq.) were added to a 2 mL glass vial, followed by *N*,*N*-dimethylformamide (DMF) (310 µL, 4.0 mmol, 10 eq.). The mixture was stirred at room temperature (8 – 18 ºC) for 24 hours. After 1 and 24 h, 10 µL of the aliquot was removed and diluted to 1 mL with chloroform for GC-MS analysis. No crossover product ($MeS_2{}^{i}Bu$) was observed.

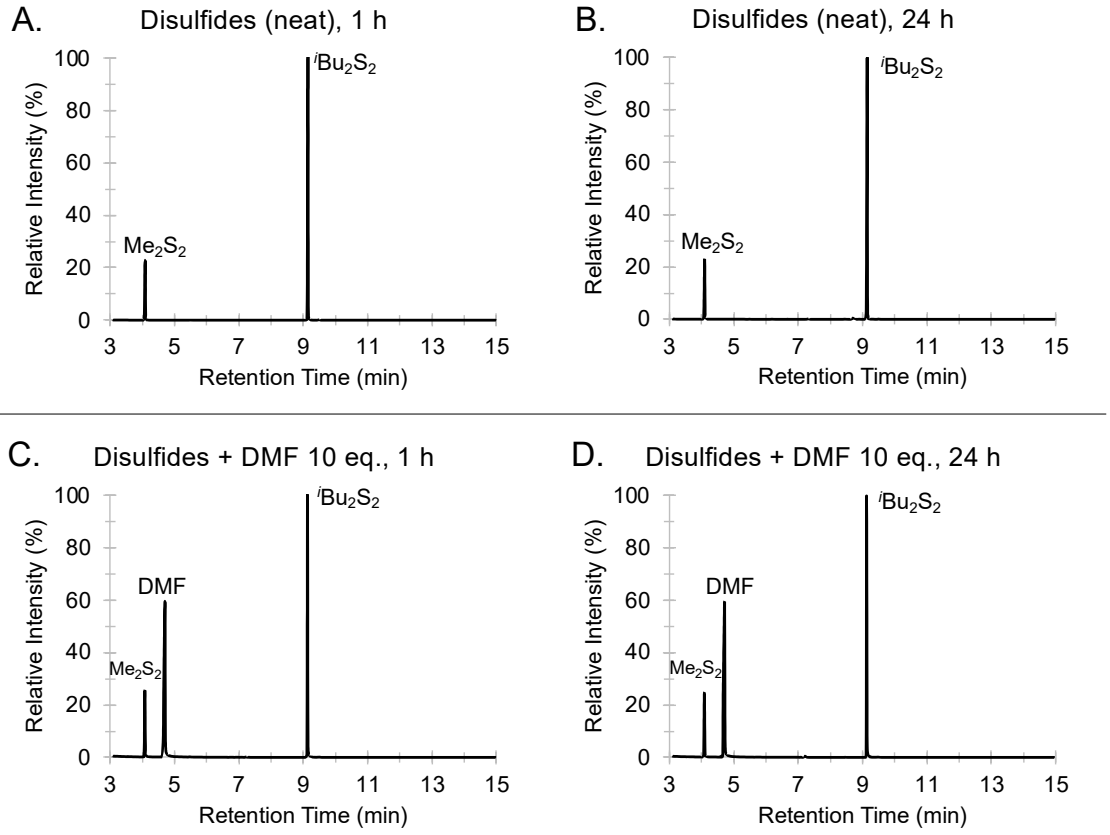

Figure S3.125: GC traces for the crossover reaction between dimethyl disulfide (Me_2S_2) and di-isobutyl disulfide ($^{i}Bu_2S_2$) over 24 hours at room temperature (8 – 18 °C). (A, B) The disulfides only (1 eq. each). (C, D) The disulfides (1 eq. each) and DMF (10 eq.). The GC-MS method A. Retention time: Me_2S_2 (4.07 min), DMF (4.70 min), and $^{i}Bu_2S_2$ (9.13 min)

Crossover between dimethyl disulfide (Me_2S_2) and di-isopropyl disulfide ($^{i}Pr_2S_2$) in the presence of DMF

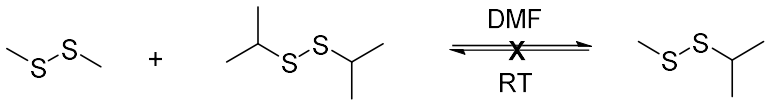

Dimethyl disulfide (36 µL, 0.4 mmol, 1 eq.) and di-isopropyl disulfide (60.1 mg, 0.4 mmol, 1 eq.) were added to a 2 mL glass vial, followed by *N*,*N*-dimethylformamide (DMF) (310 µL, 4.0 mmol, 10 eq.). The mixture was stirred at room temperature (11 – 21 ºC) for 24 hours. After 1 and 24 h, 10 µL of the aliquot was removed and diluted to 1 mL with chloroform for GC-MS analysis. No crossover product ($MeS_2{}^{i}Pr$) was observed.

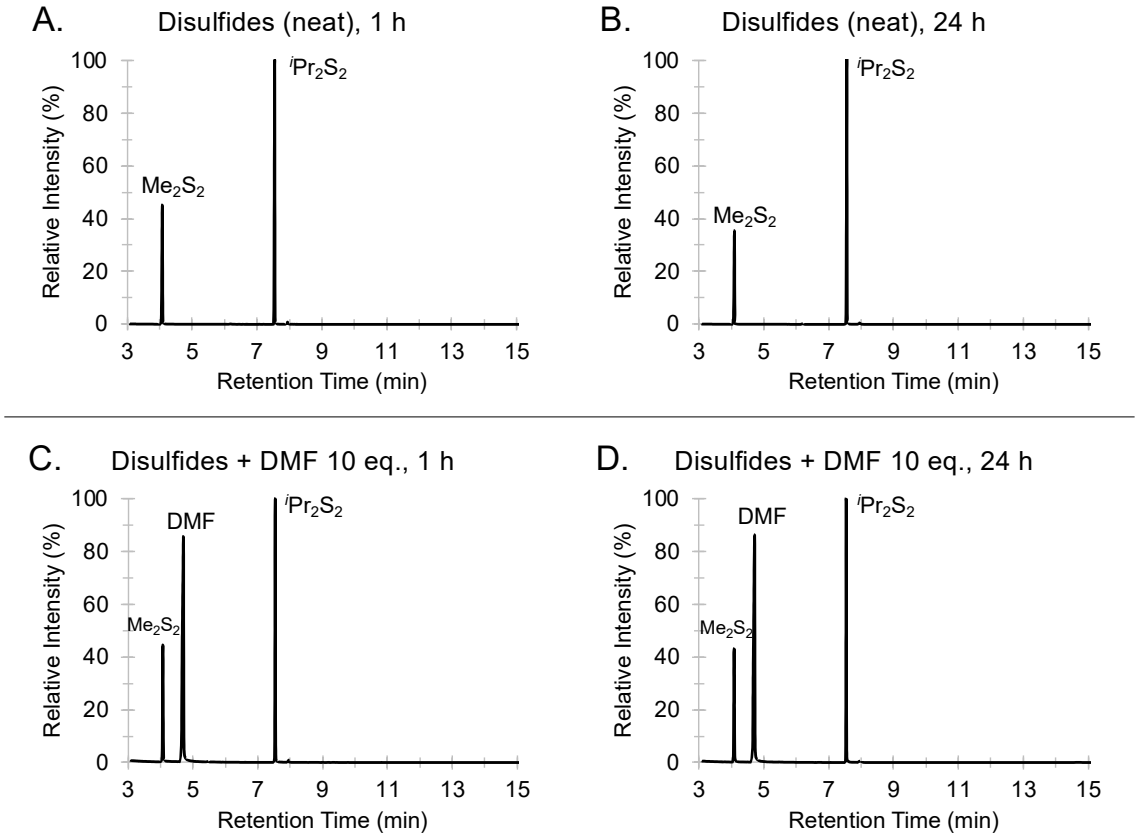

Figure S3.126: GC traces for the crossover reaction between dimethyl disulfide (Me_2S_2) and di-isopropyl disulfide ($^{i}Pr_2S_2$) over 24 hours at room temperature (11 – 21 °C). (A, B) The disulfides (1 eq. each). (C, D) The disulfides (1 eq. each) and DMF (10 eq.). The GC-MS method A. Retention time: Me_2S_2 (4.07 min), DMF (4.70 min), and $^{i}Pr_2S_2$ (7.54 min)

Crossover between dimethyl disulfide (Me_2S_2) and di-*tert*-butyl disulfide ($^{t}Bu_2S_2$) in the presence of DMF

Dimethyl disulfide (36 µL, 0.4 mmol, 1 eq.) and di-*tert*-butyl disulfide (71.3 mg, 0.4 mmol, 1 eq.) were added to a 2 mL glass vial, followed by *N*,*N*-dimethylformamide (DMF) (310 µL, 4.0 mmol, 10 eq.). The mixture was stirred at room temperature (8 – 15 ºC) for 24 hours. After 1 and 24 h, 10 µL of the aliquot was removed and diluted to 1 mL with chloroform for GC-MS analysis. No crossover product ($MeS_2{}^{t}Bu$) was observed.

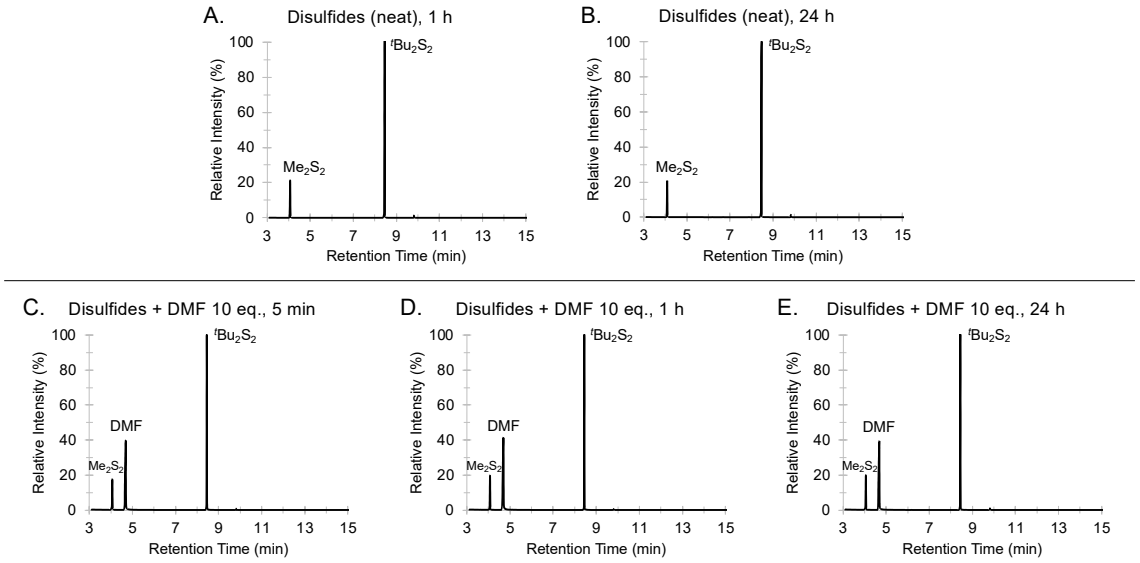

Figure S3.127: GC traces for the crossover reaction between dimethyl disulfide (Me_2S_2) and di-*tert*-butyl disulfide ($^tBu_2S_2$) over 24 hours at room temperature (8 – 15 °C). (A, B) The disulfides only (1 eq. each). (C, D) The disulfides (1 eq. each) and DMF (10 eq.). The GC-MS method A. Retention time: Me_2S_2 (4.07 min), DMF (4.70 min), and $^tBu_2S_2$ (8.45 min)

Crossover between dimethyl disulfide (Me_2S_2) and dibenzyl disulfide (Bn_2S_2) – DMF, NMP and DMSO

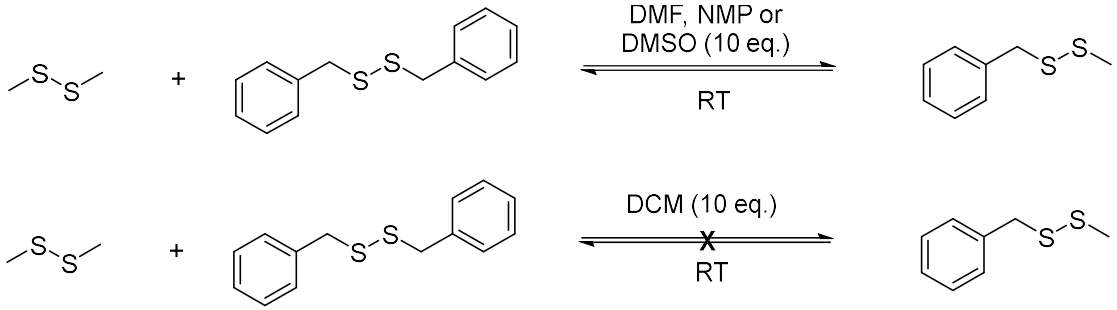

Dimethyl disulfide (36 µL, 0.4 mmol, 1 eq.) and dibenzyl disulfide (98.6 mg, 0.4 mmol, 1 eq.) were added to a 2 mL glass vial, followed by the solvent. The solvents were *N*,*N*-dimethylformamide (DMF) (310 µL, 4.0 mmol, for 10 eq.), *N*-methyl-2-pyrrolidone (NMP) (386 µL, 4.0 mmol, 10 eq.) or dimethyl sulfoxide (DMSO) (284 µL, 4.0 mmol, 10 eq.). The mixture was stirred at room temperature for 24 hours. Room temperature was 16 – 21 ºC for crossover with DMF, 15 – 23 ºC for crossover with NMP, and 11 – 28 ºC for crossover with DMSO. After 5 minutes, 1 hour and 24 hours, 10 µL of the aliquot was removed and diluted to 1 mL with chloroform for GC-MS analysis. In general, the crossover reaction between dimethyl disulfide and dibenzyl disulfide occurs in the presence of DMF, NMP and DMSO. The overall results showed that the crossover reaction might be unique to dibenzyl disulfide. Dibenzyl disulfide (a solid) is not soluble in dimethyl disulfide, so the neat reaction was not carried out. Instead, a control experiment was carried out in dichloromethane (DCM) (255.4 µL, 10 eq.).

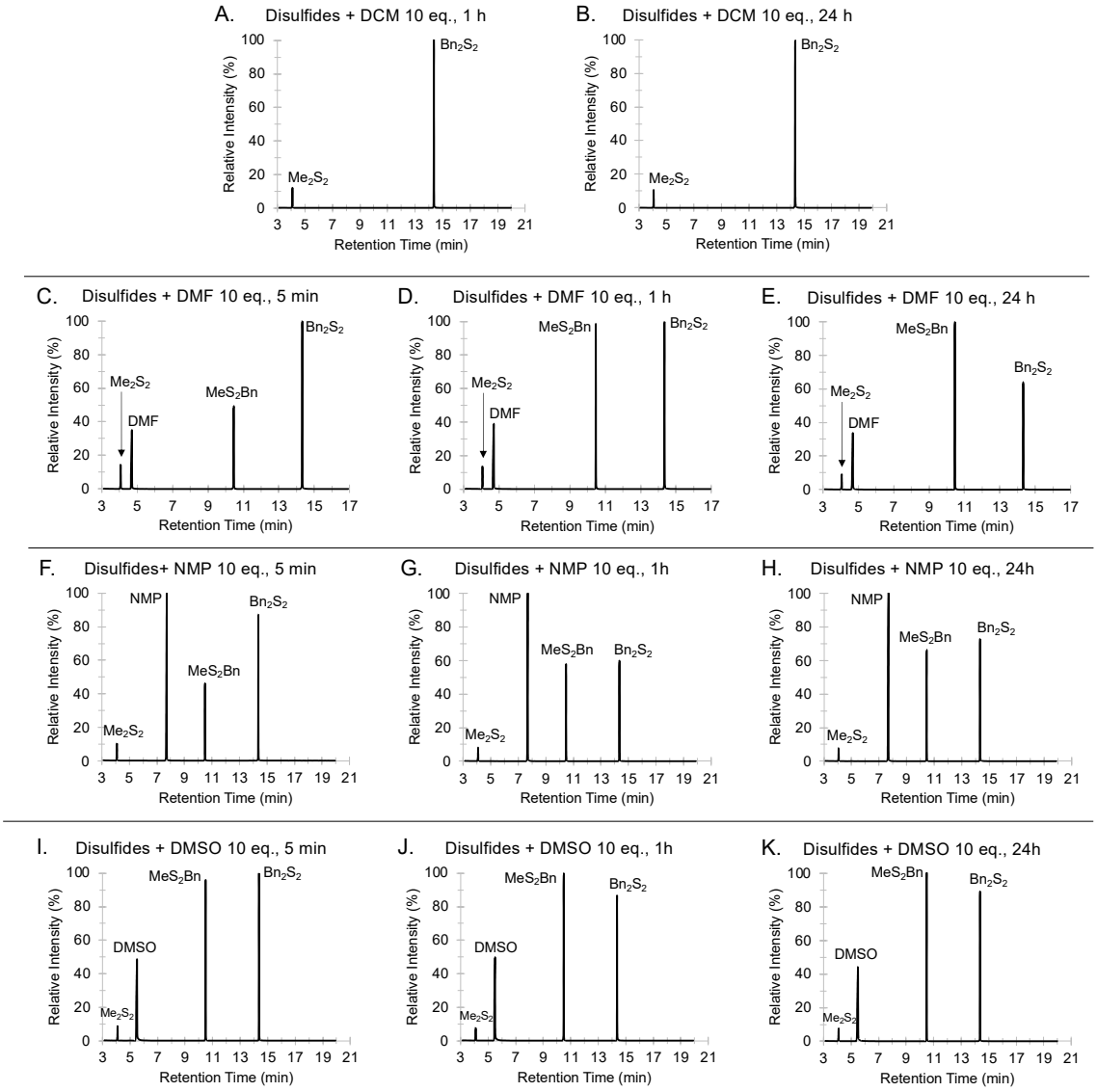

Figure S3.128: GC traces for the crossover reaction between dimethyl disulfide (Me_2S_2) and dibenzyl disulfide (Bn_2S_2) over 24 hours at room temperature. (A, B) The disulfides (1 eq. each) and dichloromethane (DCM) (10 eq.) – control experiment. (C, D, and E) The disulfides (1 eq. each) and *N*,*N*-dimethylformamide (DMF) (10 eq.) after 5 min, 1 h, and 24 h. (F, G, and H) The disulfides (1 eq. each) and *N*-methyl-2-pyrrolidone (NMP) (10 eq.) after 5 min, 1 h, and 24 h. (I, J, and K) The disulfides (1 eq.) and dimethyl sulfoxide (DMSO) (10 eq.) after 5 min, 1 h, and 24 h. The GC-MS method A. Retention time: Me_2S_2 (4.07 min), DMF (4.70 min), DMSO (5.49 min), NMP (7.69 min), MeS_2Bn (10.47 min), and Bn_2S_2 (14.35 min)

Crossover between dimethyl disulfide (Me_2S_2) and dibenzyl disulfide (Bn_2S_2) in Pyridine

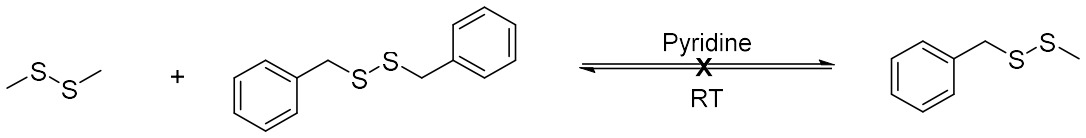

Dimethyl disulfide (36 µL, 0.4 mmol, 1 eq.) and dibenzyl disulfide (98.6 mg, 0.4 mmol, 1 eq.) were added to a 2 mL glass vial, followed by pyridine (322.2 µL, 4.0 mmol, 10 eq.). The mixture was stirred at room temperature (11 – 28 ºC) for 24 hours. After 5 minutes, 1 hour and 24 hours, 10 µL of the aliquot was removed and diluted to 1 mL with chloroform for GC-MS analysis. The crossover reaction between dimethyl disulfide and dibenzyl disulfide does not occur in the presence of pyridine. This result was interesting because the same reaction did occur in DMF, NMP and DMSO.

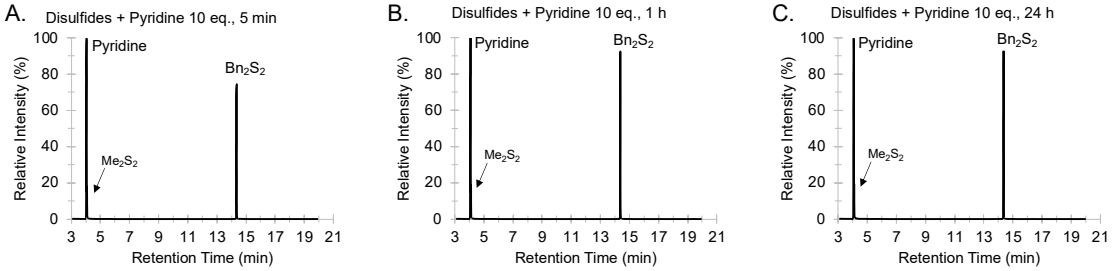

Figure S3.129: GC traces for the crossover reaction between dimethyl disulfide (Me_2S_2) and dibenzyl disulfide (Bn_2S_2) over (A) 5 min, (B) 1 h, and (C) 24 h at room temperature in pyridine (10 eq.). The GC-MS method A. Retention time: pyridine (4.06 min), Me_2S_2 (4.07 min), and Bn_2S_2 (14.35 min).

Crossover between di-*n*-propyl disulfide ($^{n}Pr_2S_2$) and dibenzyl disulfide (Bn_2S_2) in DMF

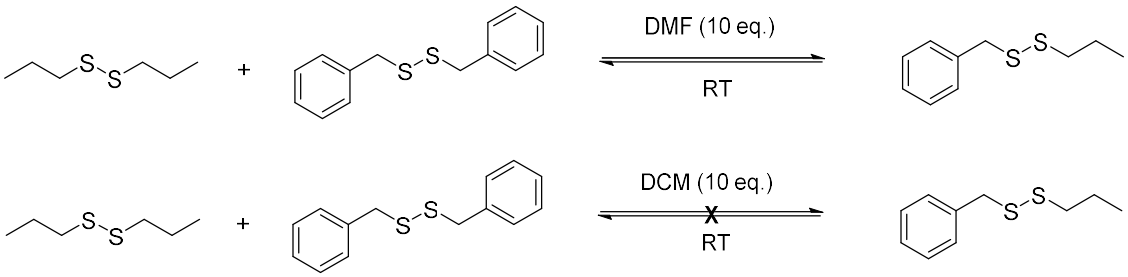

Di-*n*-propyl disulfide (62.6 µL, 0.4 mmol, 1 eq.) and dibenzyl disulfide (98.6 mg, 0.4 mmol, 1 eq.) were added to a 2 mL glass vial, followed by *N*,*N*-dimethylformamide (DMF) (310 µL, 4.0 mmol, for 10 eq.). The mixture was stirred at room temperature (8 – 15 ºC) for 24 hours. After 5 minutes, 1 hour and 24 hours, 10 µL of the aliquot was removed and diluted to 1 mL with chloroform for GC-MS analysis. The crossover reaction between di-*n*-propyl disulfide and dibenzyl disulfide occurs in the presence of DMF. Dibenzyl disulfide (a solid) is not soluble in di-*n*-propyl disulfide, so the neat reaction was not carried out. Instead, a control experiment was carried out in dichloromethane (DCM) (255.4 µL, 10 eq.).

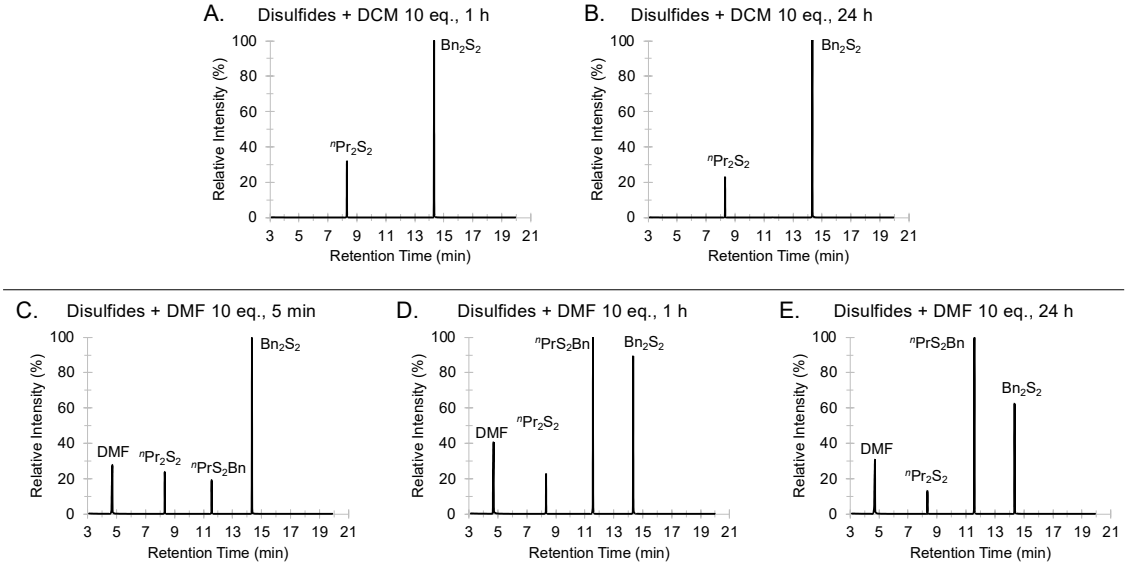

Figure S3.130: GC traces for the crossover reaction between di-*n*-propyl disulfide ($^{n}Pr_2S_2$) and dibenzyl disulfide (Bn_2S_2) over 24 hours at room temperature. (A, B) The disulfides (1 eq. each) and dichloromethane (DCM) (10 eq.) – control experiment. (C, D, and E) in 10 eq. *N*,*N*-dimethylformamide (DMF). The GC-MS method A. Retention time: DMF (4.70 min), $^{n}Pr_2S_2$ (8.32 min), MeS_2Bn (10.47 min), and Bn_2S_2 (14.35 min)

Crossover between di-*tert*-butyl disulfide ($^{t}Bu_2S_2$) and dibenzyl disulfide (Bn_2S_2) in DMF

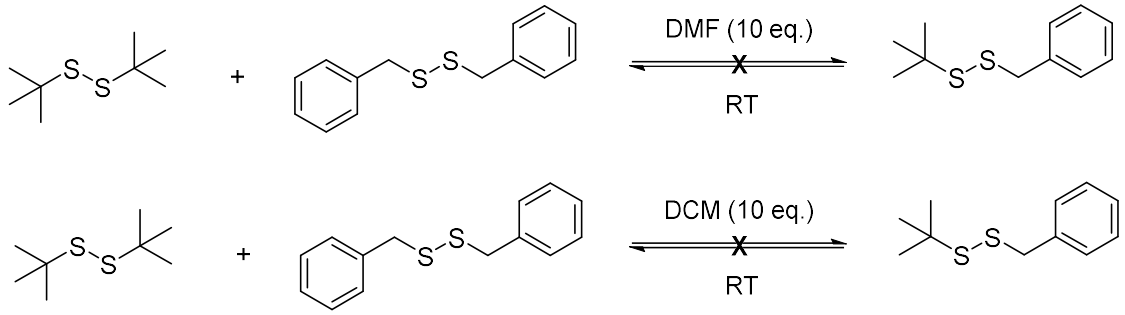

Di-*tert*-butyl disulfide (71.3 mg, 0.4 mmol, 1 eq.) and dibenzyl disulfide (98.6 mg, 0.4 mmol, 1 eq.) were added to a 2 mL glass vial, followed by *N*,*N*-dimethylformamide (DMF) (310 µL, 4.0 mmol, for 10 eq.). The mixture was stirred at room temperature (8 – 15 ºC) for 24 hours. After 5 minutes, 1 hour and 24 hours, 10 µL of the aliquot was removed and diluted to 1 mL with chloroform for GC-MS analysis. The crossover reaction between di- *tert*-butyl disulfide and dibenzyl disulfide does not occurs in the presence of DMF. Dibenzyl disulfide (a solid) is not soluble in di-*tert*-butyl disulfide, so the neat reaction was not carried out. Instead, a control experiment was carried out in dichloromethane (DCM) (255.4 µL, 10 eq.).

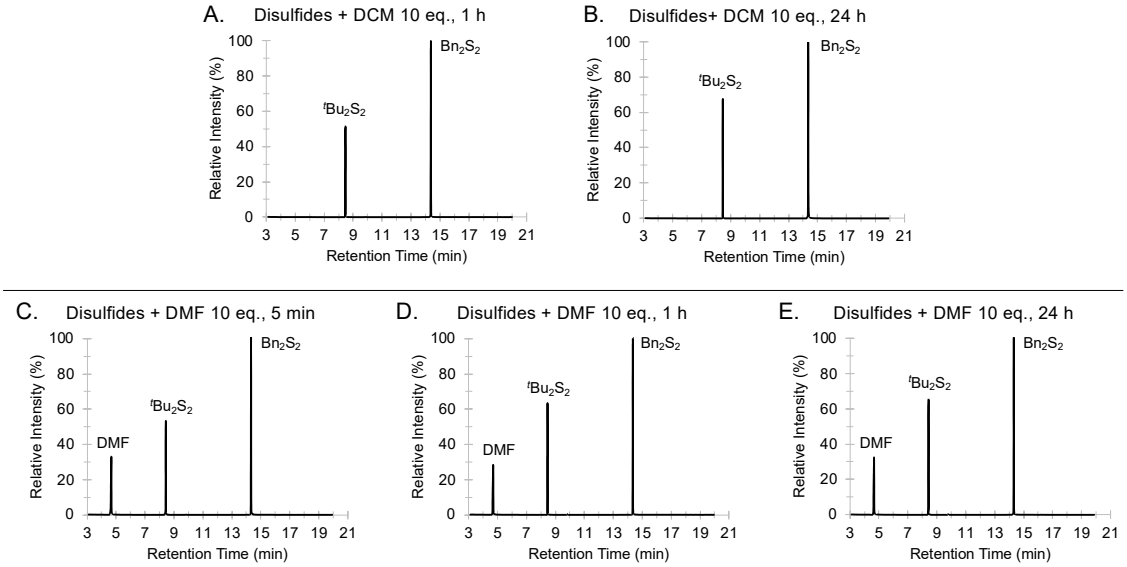

Figure S3.131: GC traces for the crossover reaction between di-*n*-propyl disulfide ($^{t}Bu_2S_2$) and dibenzyl disulfide (Bn_2S_2) over 24 hours at room temperature. (A, B) The disulfides (1 eq. each) and dichloromethane (DCM) (10 eq.) – control experiment. (C, D, and E) The disulfides (1 eq. each) and *N*,*N*-dimethylformamide (DMF) (10 eq.). The GC-MS method A. Retention time: DMF (4.70 min), $^{t}Bu_2S_2$ (8.45 min), and Bn_2S_2 (14.35 min)

Crossover between dimethyl disulfide (Me_2S_2) and dibenzyl disulfide (Bn_2S_2) in the presence of 10 mol% TEMPO in DMF

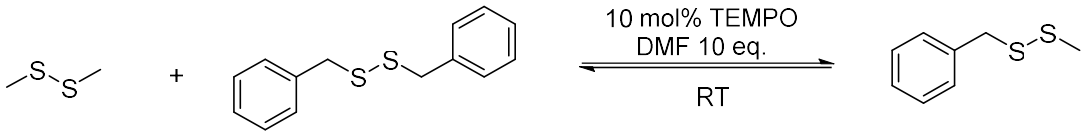

Dimethyl disulfide (36 µL, 0.4 mmol, 1 eq.), dibenzyl disulfide (98.6 mg, 0.4 mmol, 1 eq.), and TEMPO (6.3 mg, 0.04 mmol, 0.1 eq., 10 mol%) were added to a 2 mL glass vial, followed by *N*,*N*-dimethylformamide (DMF) (310 µL, 4.0 mmol, for 10 eq.). The mixture was stirred at room temperature (18 – 21 ºC) for 24 hours. After 1, 5, 15, 30, 60, 180 min, and 24 h, 10 µL of the aliquot was removed and diluted to 1 mL with chloroform for GC-MS analysis. TEMPO slows down the crossover reaction between dimethyl disulfide and dibenzyl disulfide in DMF.

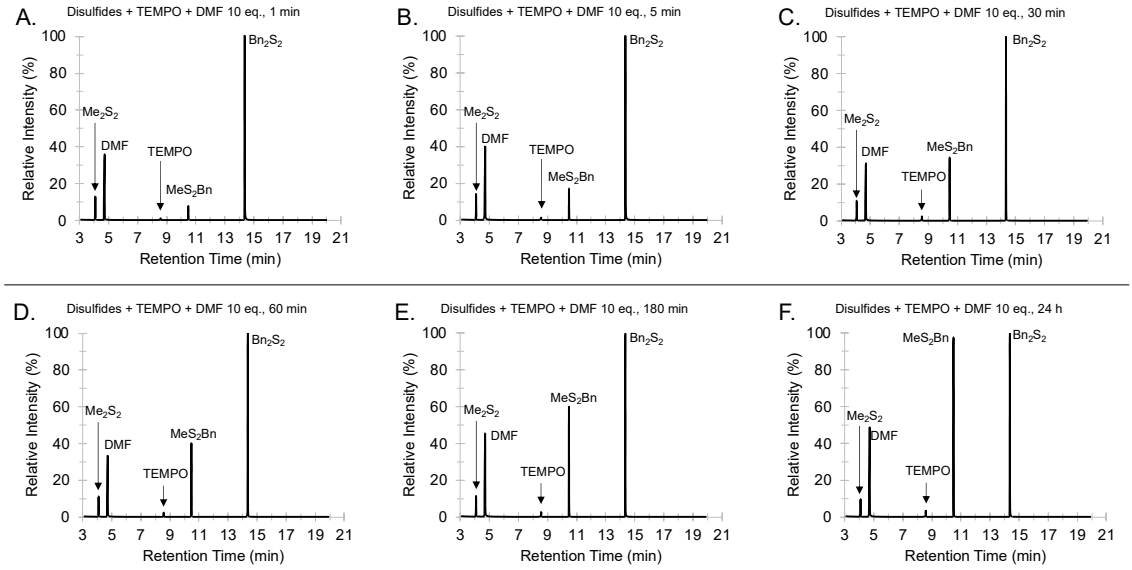

Figure S3.132: GC traces for the crossover reaction between dimethyl disulfide (Me_2S_2) (1 eq.) and dibenzyl disulfide (Bn_2S_2) (1 eq.) with 10 mol% TEMPO at room temperature in *N*,*N*-dimethylformamide (DMF) (10 eq.) after (A) 1 min, (B) 5 min, (C) 30 min, (D) 60 min, (E) 180 min, and (F) 24 h. The GC-MS method A. Retention time: Me_2S_2 (4.07 min), DMF (4.70 min), TEMPO (8.57 min), MeS_2Bn (10.47 min), and Bn_2S_2 (14.35 min).

Tetrasulfide Crossover

Di-*n*-propyl tetrasulfide and dibenzyl tetrasulfide crossover in DMF-d_7

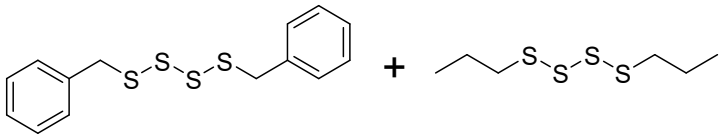

DMF-d_7

Di-*n*-propyl tetrasulfide (7.5 mg, 0.35 mmol, 1 eq.) and dibenzyl tetrasulfide (11 mg, 0.35 mmol. 1 eq.) were added to a GC vial. To the mixture was added DMF-d_7 (600 µL) to dissolve the tetrasulfides. This mixture was then quickly transferred to an NMR tube, and ^{1}H-NMR spectrum was recorded at room temperature (20 ºC) at 5 min, 1 h, and 12 h. No new signals were observed, indicating that the crossover did not take place at room temperature. No reactivity was observed when the sample was heated at 50 ºC for 1 hour, or at 80 ºC for 1 hour. When heated at 100 ºC, new peaks were observed in ^{1}H NMR spectrum, indicating a reaction had occurred.

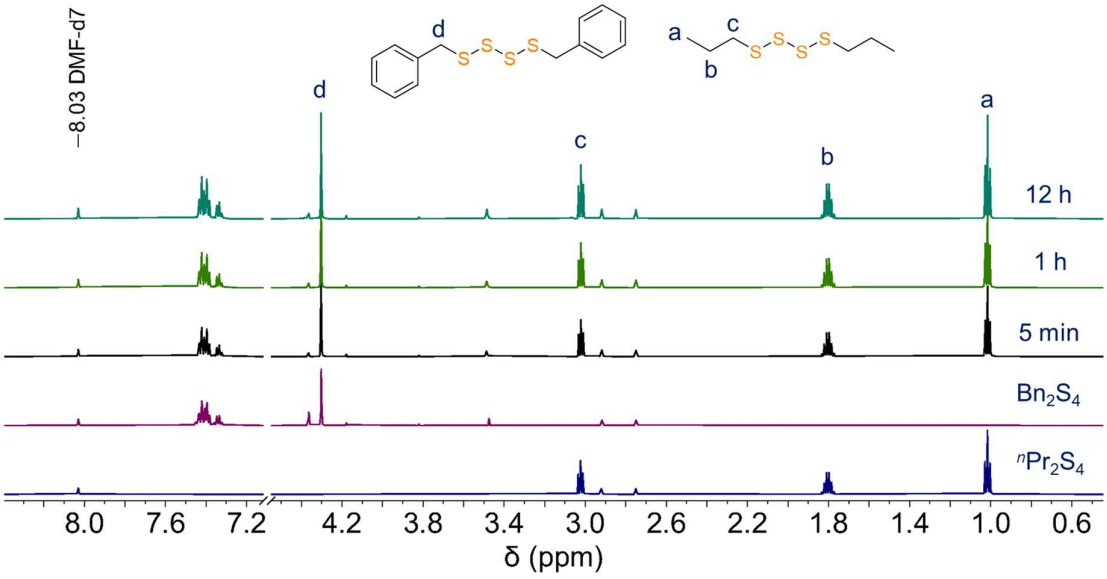

Figure S3.133: Stacked ^{1}H NMR spectra of di-*n*-propyl tetrasulfide and dibenzyl tetrasulfide mixture in DMF-d_7 at room temperature over 12 hours.

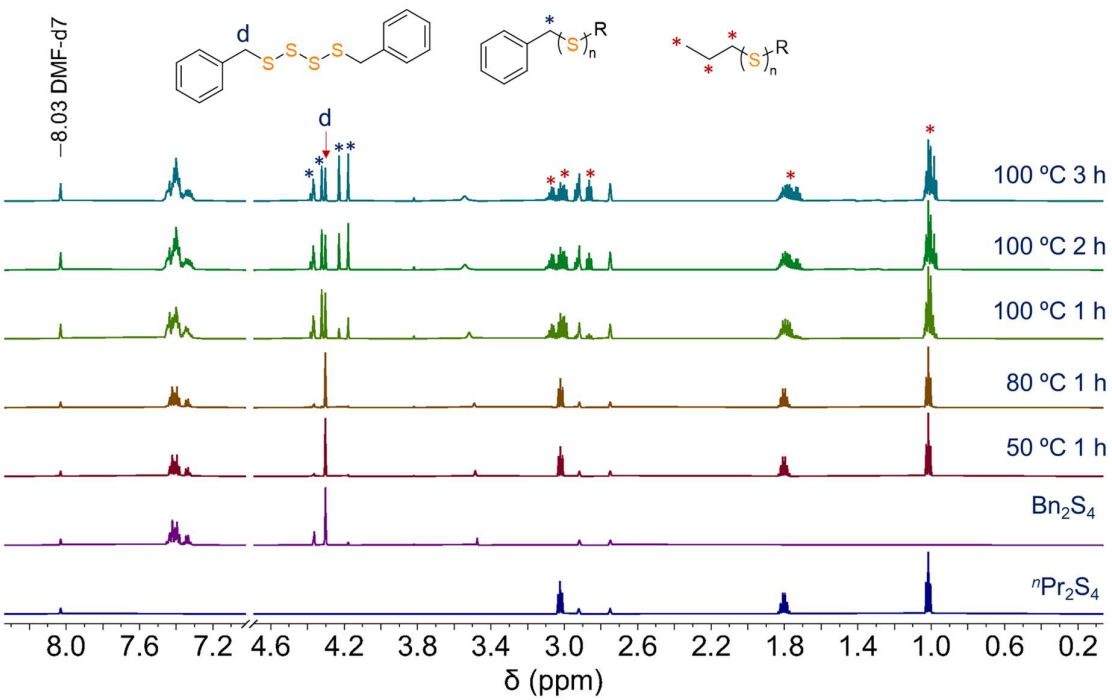

Figure S3.134: Stacked ^{1}H NMR spectra of di-*n*-propyl tetrasulfide and dibenzyl tetrasulfide mixture in DMF-d_7 at elevated temperature. The blue asterisks (*) indicate the benzylic protons of products formed at 100 °C. The red asterisks (*) indicate the methylene and methyl protons of products formed at 100 °C.

Di-*n*-propyl tetrasulfide and dibenzyl tetrasulfide crossover in toluene-d_8

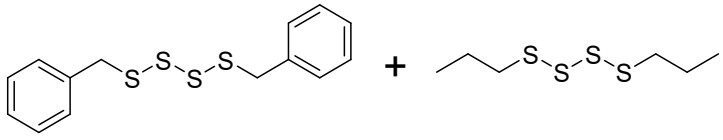

toluene-d_8

Di-*n*-propyl tetrasulfide (11.5 mg, 0.54 mmol, 1 eq.) and dibenzyl tetrasulfide (16.6 mg, 0.54 mmol. 1 eq.) were added to a GC vial. To the mixture was added toluene-d_8 (500 µL) to dissolve the tetrasulfides. This mixture was then quickly transferred to an NMR tube. No reactivity was observed when the sample was heated at 50 °C for 1 hour, or at 80 °C for 1 hour. When heated at 100 °C, new peaks were observed in the ^{1}H NMR spectrum, indicating a reaction had occurred.

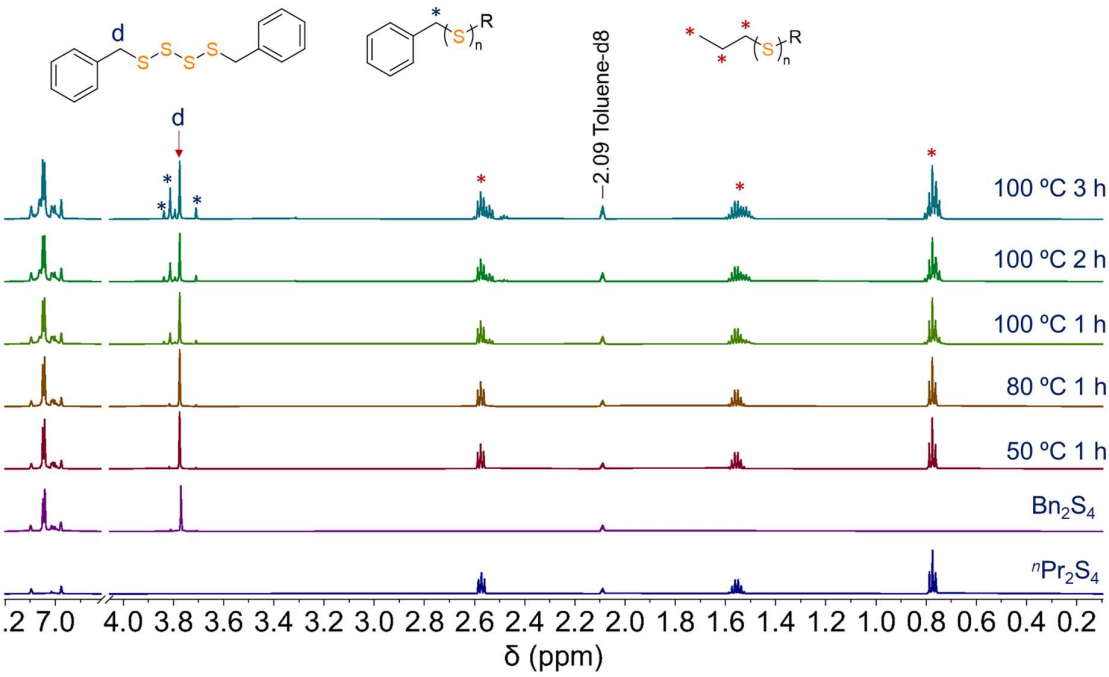

Figure S3.135: Stacked ^{1}H NMR spectra of di-*n*-propyl tetrasulfide and dibenzyl tetrasulfide mixture in Toluene-d_8 at elevated temperature. Blue asterisks (*) indicate the benzylic protons of products formed at 100 ºC. Red asterisks (*) indicate the methylene and methyl protons of products formed at 100 ºC.

Di-*n*-propyl tetrasulfide and bis(4-methoxybenzyl) tetrasulfide crossover in DMF-d_7

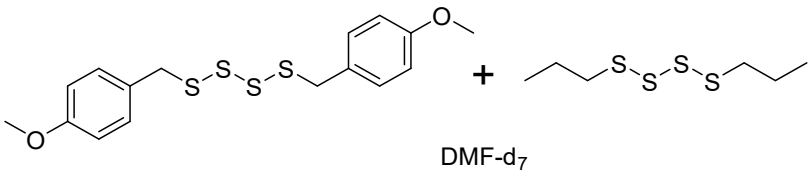

Di-*n*-propyl tetrasulfide (7.5 mg, 0.35 mmol, 1 eq.) and bis(4-methoxybenzyl) tetrasulfide (11 mg, 0.35 mmol. 1 eq.) were added to a GC vial. To the mixture was added DMF-d_7 (600 µL) to dissolve the tetrasulfides. This mixture was then quickly transferred to an NMR tube. No reactivity was observed when the sample was heated at 50 ºC for 1 hour, or at 80 ºC for 1 hour. When heated at 100 ºC, new peaks were observed in the ^{1}H NMR spectrum, indicating a reaction had occurred.

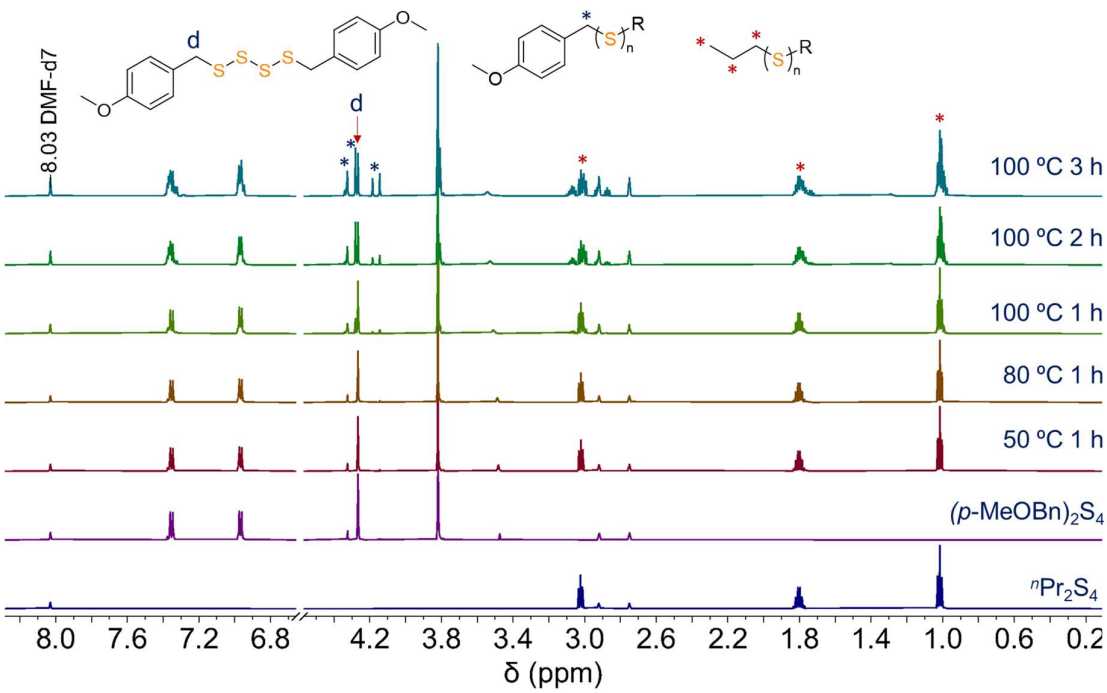

Figure S3.136: Stacked ^{1}H NMR spectra of di-*n*-propyl tetrasulfide and bis(4-methoxybenzyl) tetrasulfide mixture in DMF-d_7 at elevated temperature. Blue asterisks (*) indicate the benzylic protons of products formed at 100 ºC. Red asterisks (*) indicate the methylene and methyl protons of products formed at 100 ºC.

Di-*n*-propyl tetrasulfide and bis(4-methoxybenzyl) tetrasulfide crossover in toluene-d_8

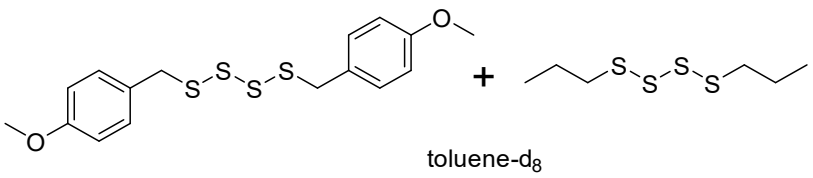

Di-*n*-propyl tetrasulfide (7.5 mg, 0.35 mmol, 1 eq.) and bis(4-methoxybenzyl) tetrasulfide (11 mg, 0.35 mmol. 1 eq.) were added to a GC vial. To the mixture was added toluene-d_8 (600 µL) to dissolve the tetrasulfides. This mixture was then quickly transferred to an NMR tube. No reactivity was observed when the sample was heated at 50 ºC for 1 hour, or at 80 ºC for 1 hour. When heated at 100 ºC, new peaks were observed in the ^{1}H NMR spectrum, indicating a reaction had occurred.

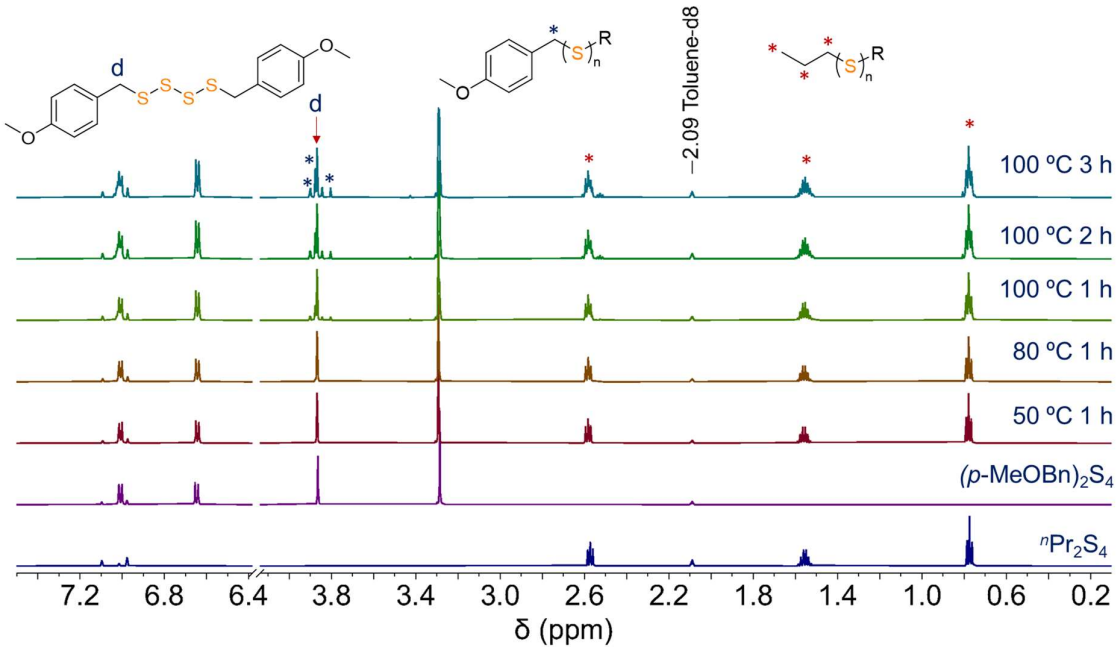

Figure S3.137: Stacked ^{1}H NMR spectra of di-*n*-propyl tetrasulfide and bis(4-methoxybenzyl) tetrasulfide mixture in Toluene-d_8 at elevated temperature. Blue asterisks (*) indicate the benzylic protons in products formed at 100 ºC. Red asterisk (*) indicate the methylene and methyl protons of products formed at 100 ºC.

3.7 References for Experimental Details and Characterizations

1. Gottlieb, H. E.; Kotlyar, V.; Nudelman, A. *J. Org. Chem*. 1997, 62, 7512–7515. DOI: 10.1021/jo971176v
2. S. Budavari, M.J. O'Neil, A. Smith, P.E. Heckelman, The Merck Index, an Encyclopedia of Chemicals, Drugs, and Biologicals - Eleventh Edition, Merck Co., Inc. Rahway, NJ, 1989.
3. Pickering, T. L.; Saunders, K. J.; Tobolsky, A. V. Disproportionation of organic polysulfides. *J. Am. Chem. Soc*. **1967**, 89 (10), 2364-2367. DOI: 10.1021/ja00986a021.
4. Trivette Jr, C.; Coran, A. Polysulfide Exchange Reactions. I. Kinetics and Mechanism of the Thermal Exchange between Diethyl Trisulfide and Di-n-propyl Trisulfide. *J. Org. Chem.* **1966**, *31* (1), 100-104. DOI: 10.1021/jo01339a020.
5. Shapter, R. Investigating reactions of trisulfide system. Undergraduate thesis, Flinders University, Bedford Park, South Australia, 2021.
6. Pople, J.M., Nicholls, T.P., Pham, L.N., Bloch, W.M., Lisboa, L.S., Perkins, M.V., Gibson, C.T., Coote, M.L., Jia, Z. and Chalker, J.M., 2023. Electrochemical synthesis of poly (trisulfides). *J. Am. Chem. Soc.* 2023, 145, 21, 11798–11810

CHAPTER 4: MECHANISTIC INVESTIGATIONS ON THE TRISULFIDE METATHESIS

4.1 Acknowledgement

Dr. Harshal D. Patel for the assistance in EPR studies and inhibition experiments of trisulfides with small molecules. A/Prof. Jeffrey R. Harmer for EPR training and technical assistance in the EPR measurement. Zhipeng Pei for discussions of proposed mechanistic pathways. Prof. Michelle M. Coote for the advice on the reaction mechanisms and computational studies.

4.2 Introduction

Reaction mechanisms of trisulfide S-S metathesis

The S-S exchange of polysulfides catalysed by UV light or thermal treatment is well-documented. This trisulfide S-S metathesis reaction proceeds through a free radical mechanism under these conditions.[1-3] For the S-S exchange between two symmetrical trisulfides, the attack of central sulfur atom in a trisulfide by thiyl radical ($RS^{\bullet}$) or the attack of terminal sulfur atom in a trisulfide by perthiyl radical ($RSS^{\bullet}$) could lead to the formation of unsymmetrical trisulfide as the main product. The central sulfur atom of a trisulfide is electron rich and susceptible to attack by a sulfur radical.[3, 4] Thus, the formation of unsymmetrical trisulfide can only be done via the attack of thiyl radical to the central sulfur atom of a trisulfide. At higher temperature, attack at either sulfur can occur. Furthermore, in the termination process, the radical recombination will lead to the formation of disulfide and tetrasulfide.

In the presence of nucleophiles such as tertiary phosphines and amines, trisulfides can undergo S-S metathesis. This process occurs via S_N2 nucleophilic displacement.[5-8] Depending on the nucleophilicity, phosphine-catalysed trisulfide exchange (R_3P, where R = e.g., Ph, Me_2N, Et_2N, MeO) could lead to a desulfurization – a removal of sulfur atom from trisulfide to disulfide or from disulfide to monosulfide (thioether). Desulfurization can occur at terminal sulfur atom or central sulfur atom of a trisulfide depending on the type of trisulfide, R-SSS-R (R = aryl or alkyl).[6, 9] Figure 4.1 illustrates the reaction between trisulfides with amine or phosphines.

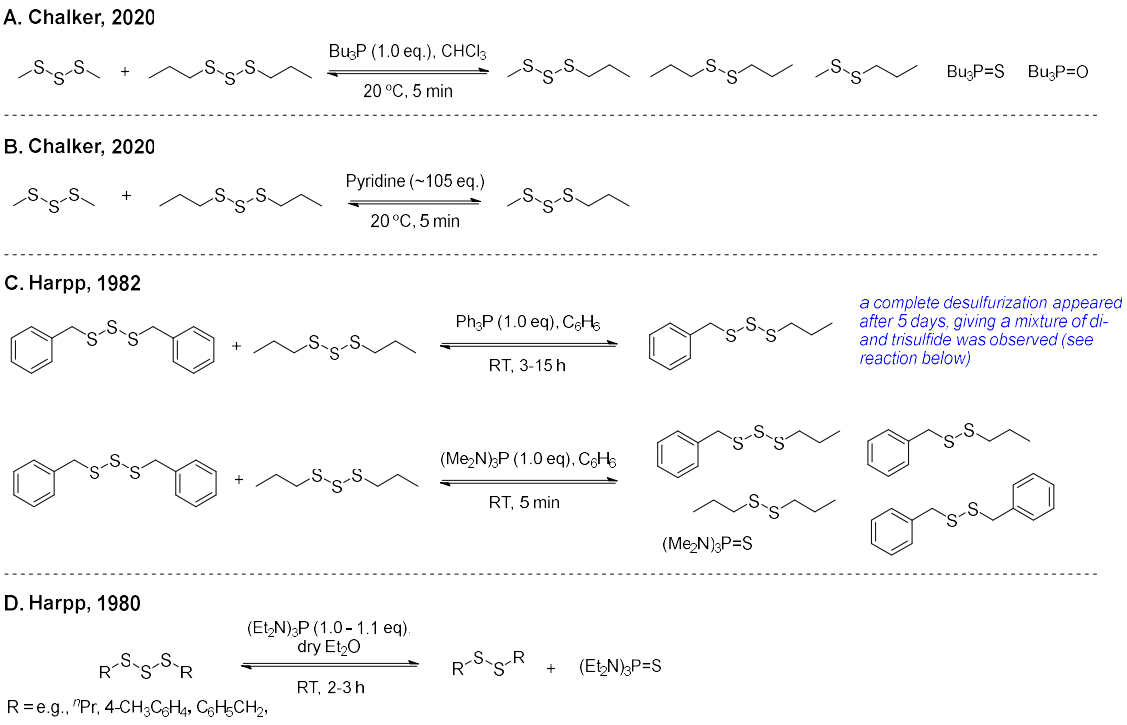

Figure 4.1: Examples of amine or phosphine-promoted trisulfide metathesis and related S-S exchange and desulfurization reactions.[5-7]

It has been proposed by Steudel and co-workers that the S-S metathesis in polysulfides could proceed via thiosulfoxide intermediate **1** (Figure 4.2B). This intermediate **1** has been invoked in the disproportionation of a trisulfide to give a disulfide and a tetrasulfide which could explain the thermal decomposition of dimethyl trisulfide at 80 °C (Figure 3.2, Chapter 3). Clenaan and Stensaas[4] proposed several pathways for the trisulfide exchange via thiosulfoxide intermediate (Figure 4.2B). The trisulfide exchange reaction was suggested to proceed via an addition across the S=S bond to give a sulfurane (pathway a). Nucleophilic attack at terminal (pathway b) and central sulfur atom (pathway c) had also been considered. All these pathways would lead to the formation of disulfide and tetrasulfide as the exchange product. Furthermore, the isomerization of the linear polysulfide to the thiosulfoxide species is endothermic and requires considerably amount of activation energy. For example, the formation of thiosulfoxide from dimethyl disulfide (Me_2S_2) via intermolecular isomerization requires energy of 340 kJ mol^{-1}, which is higher energy than the C-S bond, $D(H_3$**C–S**$SCH_3)$ = 238 kJ mol^{-1}.[10, 11] Therefore, the S-S metathesis is unlikely to occur by this mechanism. Moreover, studies about trisulfide isomerization to thiosulfoxide have not been carried out. The S-S metathesis mechanisms involving thiosulfoxides are therefore only proposals. With that said S=S bonds in thiosulfoxides and related molecules have been observed spectroscopically or by X-ray crystallography in rare cases.[12, 13]

Another mechanism proposed by Steudel is the direct insertion of trisulfide. In this mechanistic proposal, one trisulfide is proposed to attach to another trisulfide to give an intermediate sulfurane **2** (Figure 4.2C). This intermediate could undergo Berry pseudorotation mechanism and then elimination by ligand-coupling gives the unsymmetrical trisulfide as the product.[1, 14, 15] In general, for low-temperature S-S exchange in polysulfides, the mechanism has remained unclear. However, it has been suggested by that the reaction, in some cases, may be due to the trace amounts of nucleophiles present in the solvents or on the surface of the reaction vial.[14]

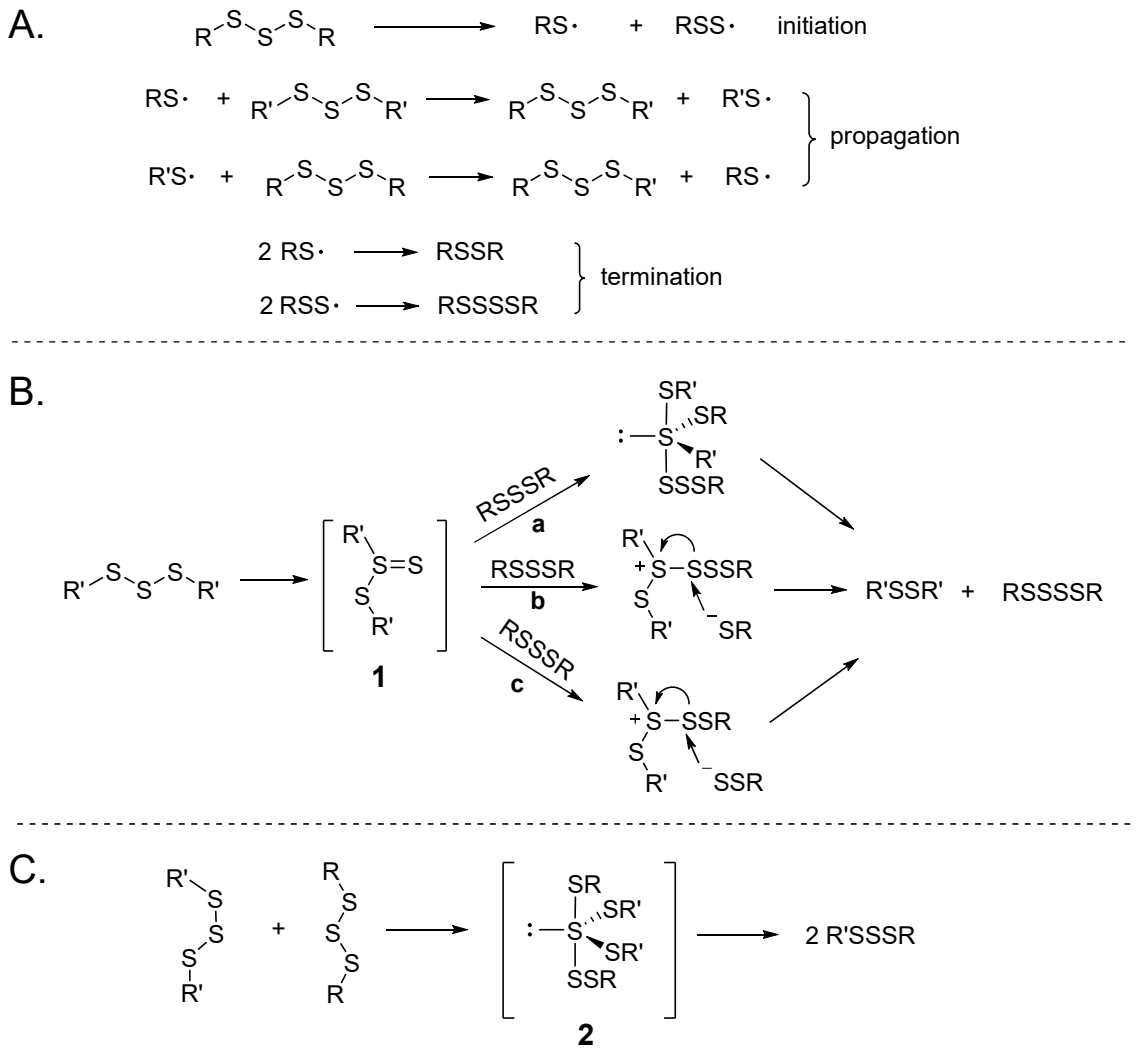

Figure 4.2: Possible proposed mechanisms of trisulfide S-S metathesis summarized by Clennan and Stensaas. Schemes were reprinted under permission from ref. 4. © 2009 Taylor & Francis Group.

Initial mechanistic hypothesis on amides induced trisulfide S-S metathesis

According to recent reports from the Hasell and Chalker laboratories,[16, 17] the S-S metathesis reaction between dimethyl trisulfide and di-*n*-propyl trisulfide occurs rapidly in the presence of amide solvents such as DMF, DMAc, and NMP (Figure 4.3A). It has also been reported that TEMPO was able to inhibit the trisulfide S-S metathesis (Figure 4.3B). Thus, this experimental result suggested that thiyl or perthiyl radicals may be involved in the mechanism. However, the mechanism on how this reaction occurred is poorly understood. If radicals are involved in the reaction, both disulfide and tetrasulfide might be expected to form. However, the trisulfide metathesis in DMF only selectively gives only unsymmetrical trisulfide **3** as the product.

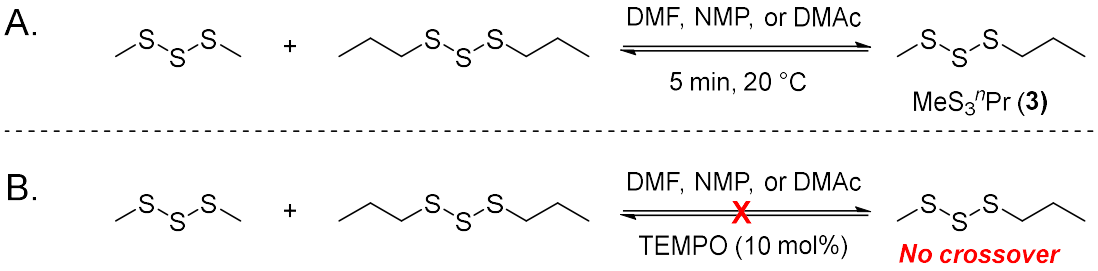

Figure 4.3: A. Rapid trisulfide S-S metathesis in amide solvents. B. TEMPO inhibits the trisulfide S-S metathesis in amide solvents.

The overall aim of this Chapter was to investigate possible mechanisms involved the reaction between trisulfides in DMF. For a direct analysis, we conducted experiments using electron paramagnetic resonance (EPR) spectroscopy to test for the presence of thiyl or perthiyl radicals in the trisulfides-DMF mixture. Radical trapping experiments using perfluoronitroxide stable (PFN-5) radical were also conducted. To test for any ionic intermediates that may form, trapping experiments were completed in an attempt to intercept any thiolates. Other reaction mechanisms will also be discussed and how they align (or not) with the rapid and selected trisulfide metathesis in DMF.

4.3 Results and Discussion

Mechanistic proposal on amides induced trisulfide S-S metathesis

In Chapter 3, we have shown that the S-S metathesis reaction between dimethyl trisulfide and di-*n*-propyl trisulfide occurs at room temperature to give methyl *n*-propyl trisulfide ($MeS_3{}^nPr$) as the metathesis product. This reaction is rapidly induced by the presence of polar solvents such as amides, ureas, phosphoramides, and sulfoxide (e.g., DMSO). Other polar solvents such as alcohols, acetone, acetonitrile, and some nitro compounds were also found to induce the metathesis reaction even though it is much slower compared to those amides. The mechanisms involved in each solvent can be different. Since the focus of this research was to investigate the role of amide solvents in the trisulfide S-S metathesis, the discussion will only be specific to DMF.

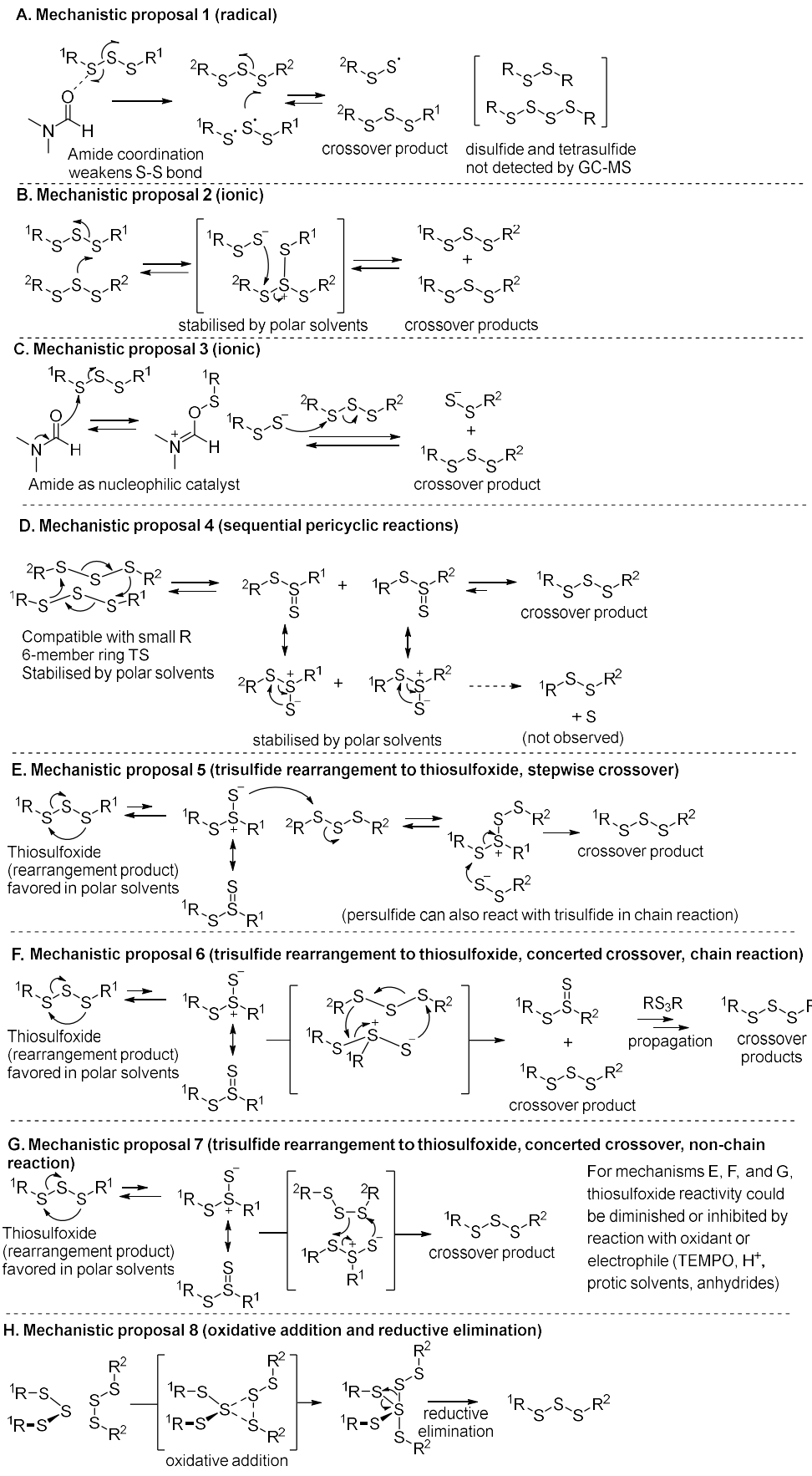

Figure 4.4: Mechanistic proposals for trisulfide S-S metathesis induced by amide solvents.

In our initial studies, TEMPO was found to inhibit the S-S metathesis reaction, which may point to a radical process (Figure 4.3B). However, a critical question remained unanswered: if the trisulfide S-S metathesis reaction follows a radical pathway, why are disulfide and tetrasulfide not formed? The same important question also applies to ionic intermediates that involve thiolates or persulfides. In other words, if a thiyl radical or a thiolate anion is present in the reaction, disulfide or tetrasulfide might be expected to form, but these species are *not* observed.[7, 18, 19] Therefore, experiments were conducted to find answers which mechanisms may be involved in the reaction. Several proposed mechanistic pathways for consideration are shown in Figure 4.4. The rationale for each mechanistic proposal shown in Figure 4.4 is explained below. These hypotheses are designed to be reasonable, testable pathways that cover radical, ionic, and neutral intermediates. The goal of this chapter is to provide evidence to rule out pathways and identify observations that provide support or corroboration of other pathways.

In mechanistic proposal 1 (Figure 4.4A), the hypothesis is based on the coordination of DMF molecules to sulfur atom in a trisulfide which could reduce the S-S bond strength and facilitate the S-S cleavage to generate thiyl and perthiyl radical. In the subsequent step, these radical could participate in the reaction with other trisulfide molecules via a chain radical process to give trisulfide exchange product, along with a disulfide and a tetrasulfide. Since TEMPO has been shown previously to inhibit the trisulfide metathesis, this mechanistic proposal is a radical pathway that may be consistent with TEMPO inhibition while proposing a role for DMF. However, several pieces of evidence against this mechanism are discussed in the next sections of this chapter.

In mechanistic proposal 2 (Figure 4.4B), the reaction is proposed to occur via ionic mechanism. The central sulfur atom in a trisulfide is proposed to attack the terminal sulfur atom of another trisulfide. This would then create a charged pair (perthiolate anion and thiosulfonium ion) which could be stabilised by polar solvents such as DMF. The perthiolate anion is the proposed to attack the positively charged thiosulfonium ion via S_N2 to give the trisulfide crossover product. Another proposed ionic mechanism is that the polar solvents such as DMF could act as a nucleophilic catalyst (Mechanistic proposal 3, Figure 4.4C). DMF is proposed to regioselectively attack the terminal sulfur atom in a trisulfide and break the S-S bond; thus, it produces perthiolate anion which could then attack another trisulfide to give the trisulfide crossover product. During the reaction, the perthiolate anion is reproduced, attacking another trisulfide in a chain reaction.

Mechanistic proposal 4, 5, 6, and 7 (Figure 4.4D–G) depict the involvement of thiosulfoxide species in the trisulfide metathesis. In mechanistic proposal 4, two thiosulfoxides which are generated via a six-membered concerted reaction are proposed. These thiosulfoxides are stabilised by polar solvents (e.g., DMF) and then undergo rearrangement to give the stable linear trisulfide product. Unlike mechanistic proposal 4, the reversible formation of a thiosulfoxide from a linear trisulfide is proposed in the initial reaction for mechanistic proposal 5, 6, and 7. In mechanistic proposal 5, a thiosulfoxide isomer is proposed as a nucleophile in the initial step. This negatively charged sulfur atom is proposed to attack the terminal sulfur atom in a trisulfide, leading to the

formation of a new positively charged sulfur species and a perthiolate. This perthiolate is likely to provoke the formation of trisulfide crossover product. In mechanistic proposal 6, after the formation of the thiosulfoxide isomer a concerted crossover is proposed to occur between the thiosulfoxide isomer and a trisulfide to form a trisulfide crossover product and a new thiosulfoxide. This thiosulfoxide is then proposed to provoke another reaction with the other trisulfide to produce another crossover product and thiosulfoxide in a chain reaction. The chain reaction is proposed as a path for propagation due to the anticipated high energy barrier for a thiosulfoxide formation. For mechanistic proposal 7, the thiosulfoxide isomer is proposed to react with a trisulfide via a 5-membered ring concerted step to directly give a trisulfide crossover product. The concerted step is proposed because the trisulfide metathesis reaction only gives a new trisulfide.

In all mechanistic proposal involving a thiosulfoxide species, there are several aspects that need to be considered. Firstly, as for the disulfide, the energy barrier of a thiosulfoxide formation from a trisulfide may be relatively high. Therefore, in mechanistic proposal 4 the formation of two high energy thiosulfoxide species are unlikely to happen. However, this step is proposed because DMF could play a vital role in lowering the energy barrier and potentially allow the reaction to occur. Secondly, thiosulfoxide species are polar. This could potentially lead to the lower reactivity of thiosulfoxide in protic solvents such as alcohols. The electron rich sulfur in the thiosulfoxide is likely to form an interaction with hydrogen in the hydrogen-bond donor solvents. This interaction could possibly explain why thiosulfoxide reactivity is diminished in wet DMF. In addition to this, that electron rich sulfur could potentially react with TEMPO via redox reactions and anhydrides via nucleophilic attack. Thus, this could explain the S-S metathesis inhibition by these molecules.

In mechanistic proposal 8, the trisulfide metathesis reaction is proposed to occur via oxidative addition, followed by reductive elimination of a species called sulfurane. In the previous study by Steudel[15], it was found that the calculated energy of a sulfurane species obtained from a proposed reaction between Me_2S_2 and Me_2S_3 is too high. However, this mechanism is proposed because the computational calculation with inclusion of DMF as a solvent has never been carried out.

Direct evidence by EPR: No S-centred radical in the S-S metathesis reaction

Following the results by TEMPO inhibition reported by Hasell and co-workers[16], the S-S metathesis reaction between dimethyl trisulfide and di-*n*-propyl trisulfide was examined by means of electron paramagnetic resonance (EPR) spectroscopy. The equimolar mixture of the trisulfide and DMF was first analysed by EPR. No radical signal was observed in the EPR spectrum (Figure 4.5). This result was also similar for different ratios of trisulfides and DMF. If thiyl or perthiyl radicals exist, a strong signal or S-centred radical would show between 340 and 360 mT.[20]

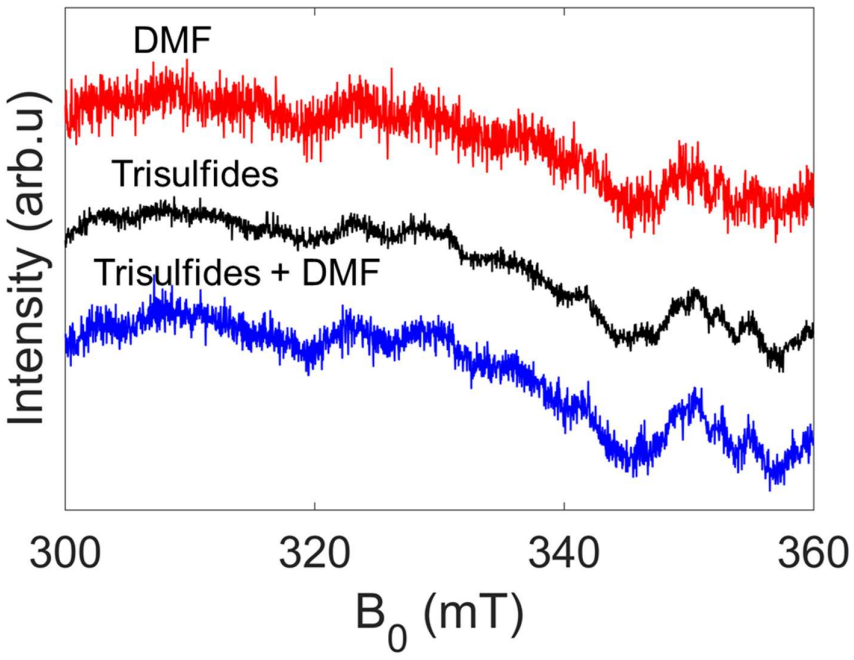

Figure 4.5: EPR spectra of DMF, the equimolar trisulfides (dimethyl trisulfide and di-*n*-propyl trisulfide), and the equimolar trisulfides and DMF mixture. No radical signal observed.

The thiyl or perthiyl radicals which form in the reaction could be short-lived and formed in concentrations lower than the limit of detection by EPR spectroscopy. It has also been shown previously that thiyl radicals can be trapped by 5,5-dimethyl-1-pyrroline-*N*-oxide (DMPO).[21-23] Thus, DMPO and dimethyl trisulfide were employed as a radical trap and trisulfide model, respectively. Prior to the EPR measurement of the DMPO-DMTS mixture, a positive control using Fenton and Haber-Weiss oxidation was tested to see whether or not DMPO radical trap can be used in DMF. A mixture of iron(II) and hydrogen peroxide in DMF should generate hydroxy radical (Figure 4.6A) which is trapped by DMPO to give a strong signal specific to the formation of DMPO-OH species that yield 1:2:2:1 pattern (Figure 4.6B).[24, 25] Figure 4.7 shows the EPR spectrum for the mixture of Fenton reagents and DMPO in DMF which confirms that the expected signal appeared with similar pattern to that of literature report. This result suggested that DMPO can be used in DMF.

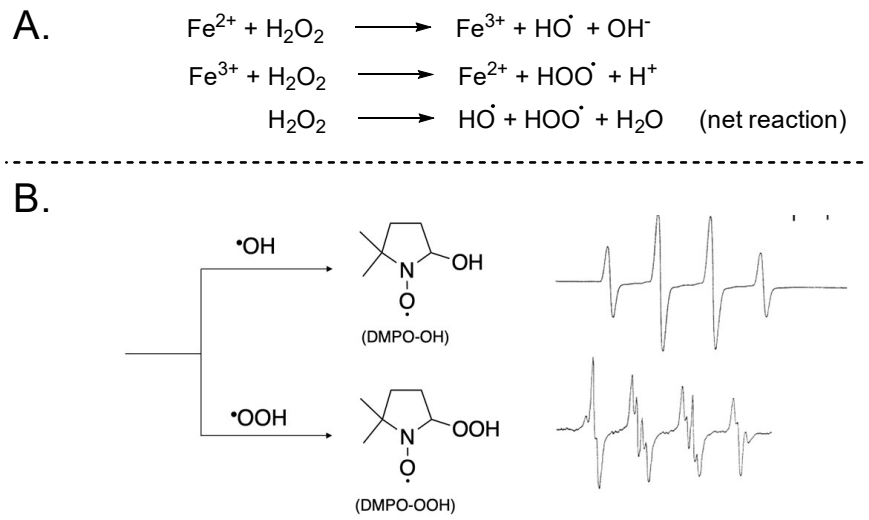

Figure 4.6: A. Hydroxyl and peroxide radical generated from Fenton and Haber-Weiss chemistry. B. Hydroxyl and peroxide radical trapped by DMPO spin trap. The EPR spectra of these DMPO-OH and -OOH adduct were shown next to the structures.[25] EPR spectra of each adduct were reproduced with permission from ref. 25. © 2004 American Chemical Society.

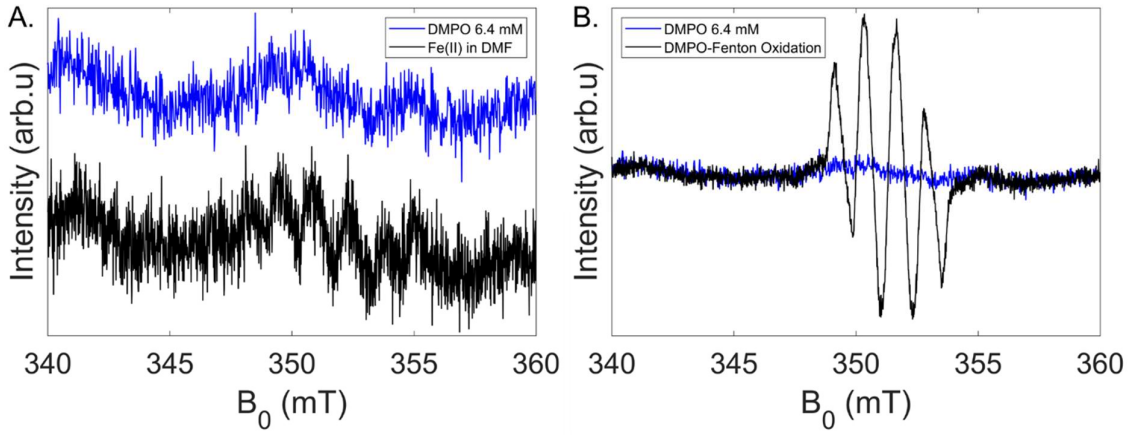

Figure 4.7: A. EPR spectra of DMPO 6400 nM and Fe^{2+} in DMF (control experiment). B. EPR spectra of DMPO 6400 nM and DMPO + Fe^{2+} + H_2O_2 mixture – showing the signal for DMPO adducts.

Next, DMPO was mixed with dimethyl trisulfide in an equimolar ratio. If thiyl or perthiyl radical were present, DMPO would trap them and form the adducts **4** and **5** (Figure 4.8) which would give EPR signals. A mixture of DMPO and dimethyl trisulfide (DMPO:Me_2S_3 =1: 149, 1:1, 1:5, or 5:1) gave no signal or evidence for radicals in the EPR spectra. Hence, the reaction is unlikely to involve a radical pathway.

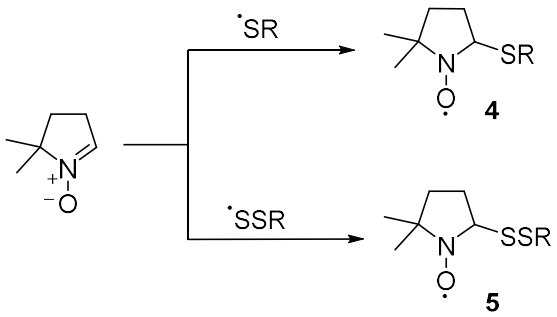

Figure 4.8: Thiyl and perthiyl radical trapping by DMPO.

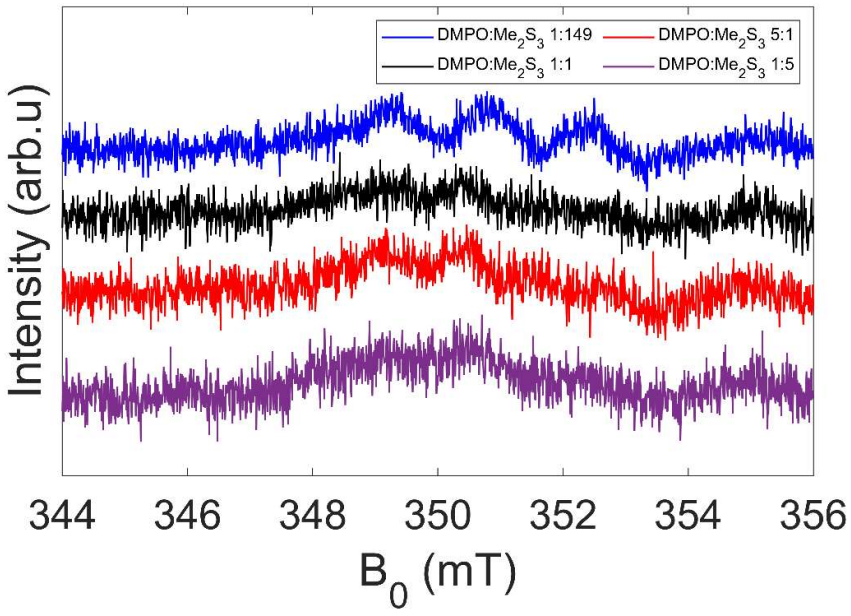

Figure 4.9: EPR spectra of DMPO and dimethyl trisulfide mixtures.

EPR investigation of the reaction between trisulfides and TEMPO in DMF

The question of the mechanism of TEMPO inhibition still remained. Because TEMPO was found to inhibit the crossover reaction, we also study the inhibition by EPR method. TEMPO in DMF gives expected radical signals. In the initial study, it is important to know the minimum concentration of the TEMPO-trisulfides mixture that can still be detected by the instrument. To test this, three TEMPO solutions (64, 640 and 6400 nM in DMF) were freshly prepared from the TEMPO stock solution (6.4 mM). EPR results showed that TEMPO radical can still be detected at a concentration of 640 nM (Figure 4.10).

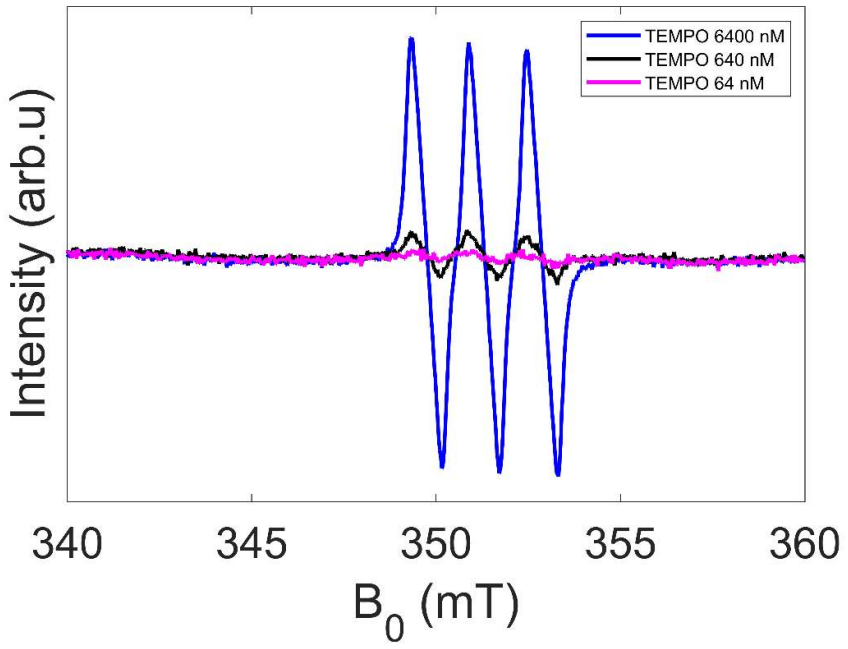

Figure 4.10: EPR spectra of TEMPO in DMF at various concentrations.

With the known minimum concentration of TEMPO in hand, next the EPR experiment of the trisulfides crossover inhibition by TEMPO was carried out. To do this, TEMPO was reacted with the trisulfides at various molar ratios. For example, [TEMPO]:[Me_2S_3]:[$^nPr_2S_3$] = 1:1:1 was prepared by mixing 100 µL TEMPO 6.4 µM (1 eq.), 100 µL Me_2S_3 6.4 µM (1 eq.), and 100 µL $^nPr_2S_3$ 6.4 µM (1 eq.) and diluted to 1 mL with DMF prior to EPR analysis. It should be noted that EPR was run immediately after sample preparation. The resulting intensity of TEMPO radical signal (Figure 4.11A – *blue trace*) did not change at an equimolar concentration but decreased immediately when using the excess of the trisulfides (1,485,000 eq. for each trisulfide relative to the TEMPO concentration, Figure 4.11A – *magenta trace*). For the reaction between TEMPO and excess dimethyl trisulfide, an immediate measurement showed the TEMPO signal was not changed but the disappearance of TEMPO signal intensity was apparent after the reaction left for one hour (Figure 4.11B – *blue trace*).

Overall, the results suggested that TEMPO reacts with the trisulfides, especially when the reaction involves an excess of trisulfide. However, the mechanism of inhibition of the trisulfides crossover reaction by TEMPO remains unclear. TEMPO may undergo a redox process. In other words, TEMPO can be converted to a non-radical species or it undergo a radical-radical recombination to form TEMPO-SR species. In the next section, the efforts had been made to observe this possible TEMPO adduct by NMR spectroscopy.

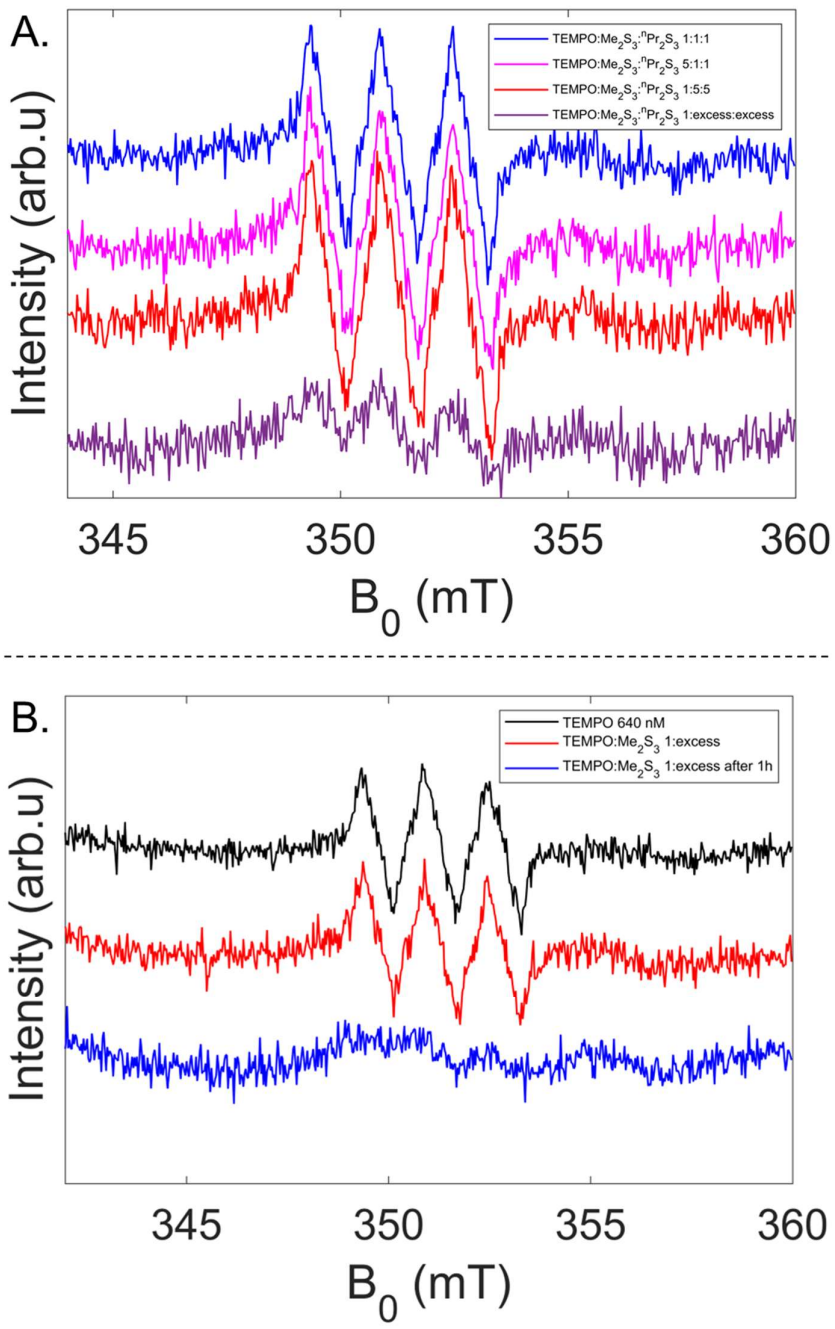

Figure 4.11: A. EPR spectra comparison of TEMPO and both trisulfides reaction at various concentrations (measured immediately). B. EPR spectra comparison between TEMPO and dimethyl trisulfide after immediate measurement and after 1 hour.

NMR studies of trisulfide metathesis inhibition by TEMPO

From the EPR results, if excess trisulfides are used in the reaction TEMPO signal decreases significantly (Figure 4.11), indicating that TEMPO could be transformed into a non-radical species by reaction with a trisulfide or a trisulfide-derived intermediate. TEMPO was dissolved in DMF-d_7 and its ^{1}H-NMR spectrum was recorded. At a chemical shift (δ) of around -15 ppm and +15 ppm, the broad shoulder peaks were observed which indicate the presence of TEMPO radical. Upon addition of both dimethyl trisulfide and di-*n*-propyl trisulfide to TEMPO (10 mol%) in DMF-d_7, these TEMPO peaks were immediately attenuated, especially when more trisulfide was added to TEMPO solution (Figure 4.12). This clearly suggested that TEMPO is being converted to a non-radical species. For the reaction of TEMPO with 1.0 eq. of each trisulfide, the NMR spectra were collected up to 17 h (Figure 4.13). It was found that after the TEMPO signal attenuated, the signal remained the same intensity even after left for 17 h at room temperature. A closer look at the ^{1}H-NMR spectrum of the TEMPO-trisulfide mixture (1 eq. of each trisulfide) indicates no sign of the formation of any TEMPO derivative compounds (Figure 4.14). Similarly, an investigation of TEMPO-trisulfide mixture by means of GC-MS revealed the significant reduction in the S-S metathesis reaction. TEMPO-SR species are unstable and tend to decompose into TEMP-H and sulfinic acid (RS(O)OH) via heterolysis in water.[26] Even if the TEMPO-SR species undergo N-O heterolysis, its decomposition products were difficult to detect and characterised by NMR spectroscopy or GC-MS.

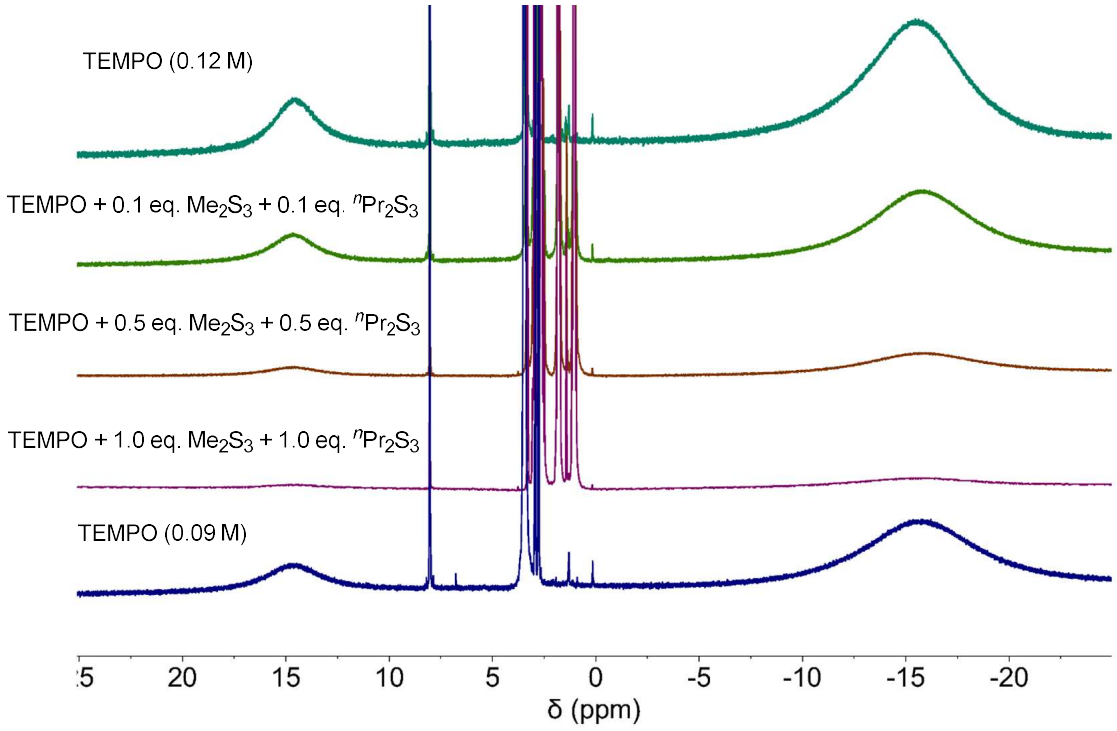

Figure 4.12: Comparison of evenly scaled ^{1}H NMR spectra (DMF-d_7, 600 MHz) of TEMPO and TEMPO-trisulfide mixtures (0.1, 0.5, and 1.0 eq. of each trisulfide).

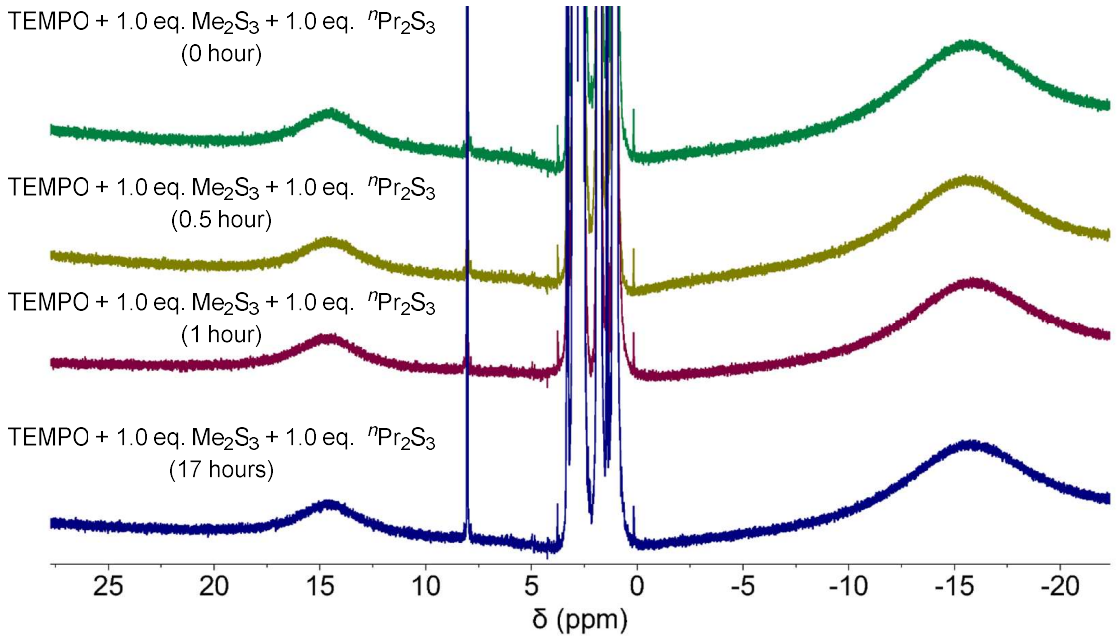

Figure 4.13: Comparison of evenly scaled ^{1}H NMR spectra (DMF-d_7, 600 MHz) of TEMPO-trisulfide mixture at 1.0 eq. at 0, 0.5, 1, and 17 h.

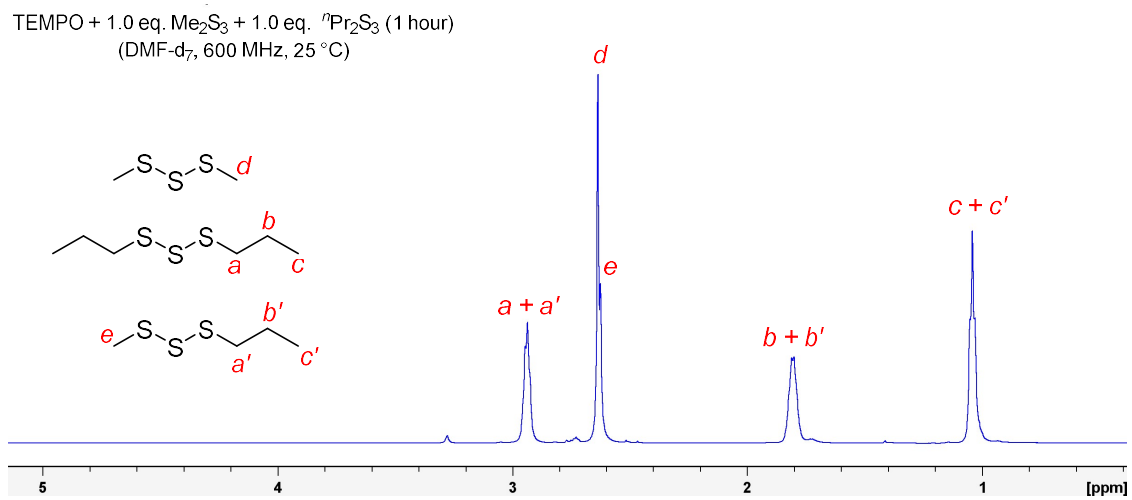

Figure 4.14: Expanded ^{1}H NMR spectrum (DMF-d_7, 600 MHz) of TEMPO-trisulfide mixture at 1.0 eq. at 1 h. Only the trisulfides were observed.

Trisulfide metathesis inhibition by other small molecules

TEMPO is not the only molecule that can inhibit the trisulfide metathesis reaction. Previous investigation by Shapter[17] showed that the addition of acetic acid in DMF had shown a substantial reduction in the rate of S-S metathesis. In fact, we also found that the presence of water in the reaction mixture could significantly reduce the rate of trisulfide metathesis reaction (see section in Chapter 3 – *The effect of water on the trisulfide S-S metathesis*). To obtain more information about

the inhibition process, several small molecules (butylated hydroxytoluene (BHT), dimethyl maleate, succinic anhydride, 1,4-benzoquinone, and maleic anhydride) were employed in the reaction. In all cases, 10 mol% of the small molecule was used in the reaction between dimethyl trisulfide and di-*n*-propyl trisulfide in DMF.

At first, BHT was tested in the reaction. Despite its known radical-trapping behaviour[27, 28], butylated hydroxytoluene (BHT) did not inhibit the trisulfide S-S metathesis reaction. The reaction equilibrium was quickly achieved within the first minute. In contrast, a complete S-S metathesis inhibition was observed when the trisulfides were reacted in the presence of 1,4-benzoquinone and maleic anhydride. 1,4-benzoquinone and maleic anhydride are potent electrophiles which allow to them to undergo a nucleophilic addition by some putative intermediate derived from the trisulfide. This could lead to the formation of substituted benzoquinone and substituted alkylthiosuccinic anhydride, respectively.[29-33] However, nothing of note was observed by GC-MS analysis. For the reaction between the trisulfides and maleic anhydride in DMF-d_7, NMR analysis also showed no changes in the mixture. In other words, the trisulfide S-S metathesis reaction was inhibited under this condition, but no adducts derived from the inhibitor were formed in detectable amounts.

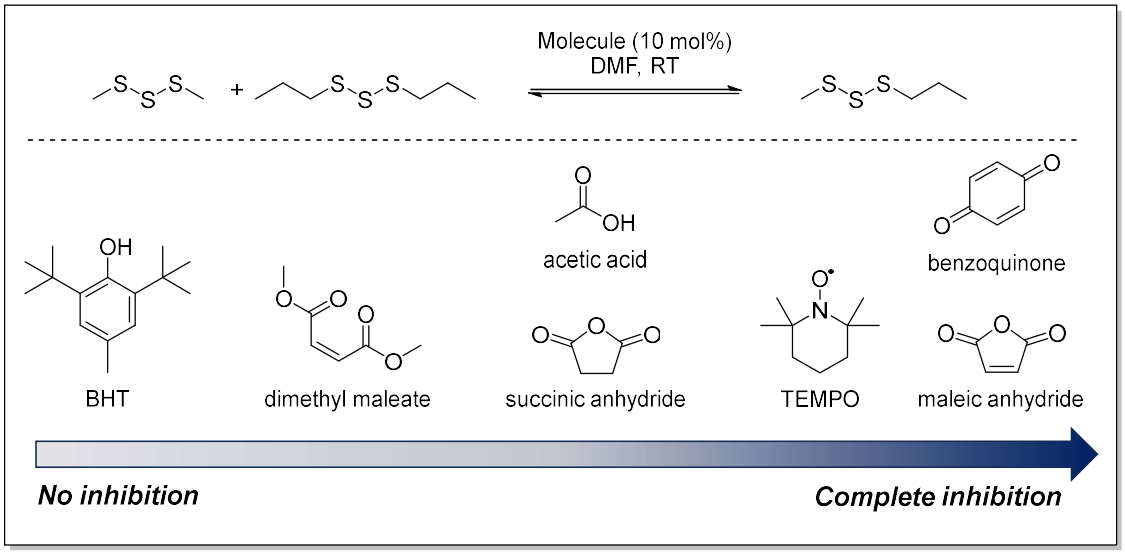

Figure 4.15: Trisulfide metathesis inhibition by small molecules. The scale shown here is only qualitative depiction of the reaction rate based on the formation of the S-S metathesis product.

A significant reduction in the rate of trisulfide metathesis was also observed in the reaction involving succinic anhydride. Although significant portion of S-S metathesis product was observed, the reaction equilibrium had not reached after 1 h. The ability of succinic anhydride to significantly supress the reaction may be due to the presence of a tiny fraction succinic acid which could be generated by hydrolysis of the anhydride. The presence of acid could cause the trisulfide metathesis inhibition in which it is similar to that of acetic acid. Alternatively, a nucleophilic reactive intermediate may have been intercepted by the anhydride. But again, no adduct or hydrolysis product of succinic

acid was detected. Next, another electrophilic molecule tested for the inhibition study was dimethyl maleate. In the presence of this diester, the trisulfide metathesis was able to reach equilibrium within 5 min. Inhibition process did occur but it is slower compared to that reaction in the presence of BHT where the equilibrium being reached within 1 min. Also, no isomerization of dimethyl maleate to dimethyl fumarate was observed. α,β-unsaturated diester compounds are often used for the *cis-trans* isomerization studies. The isomerization process can be catalysed by free radicals, amines, or hydrogen halides.[34-36] Since no isomerization occurred, any ionic or radical intermediates that may form do so in such small quantities that no addition to the alkene is observed by NMR spectroscopy or GC-MS.

The mechanism of trisulfide inhibition by acid or water in the trisulfide metathesis reaction is proposed and shown in Figure 4.16. If the mechanistic proposal 2 or 3 (Figure 4.4) operates, the thiolate could undergo several reactions in the presence of acid or water. In this case, TEMPO was used as a model molecule since it inhibits the trisulfide S-S metathesis reaction. It should be noted that the mechanism for each inhibitor can be different.

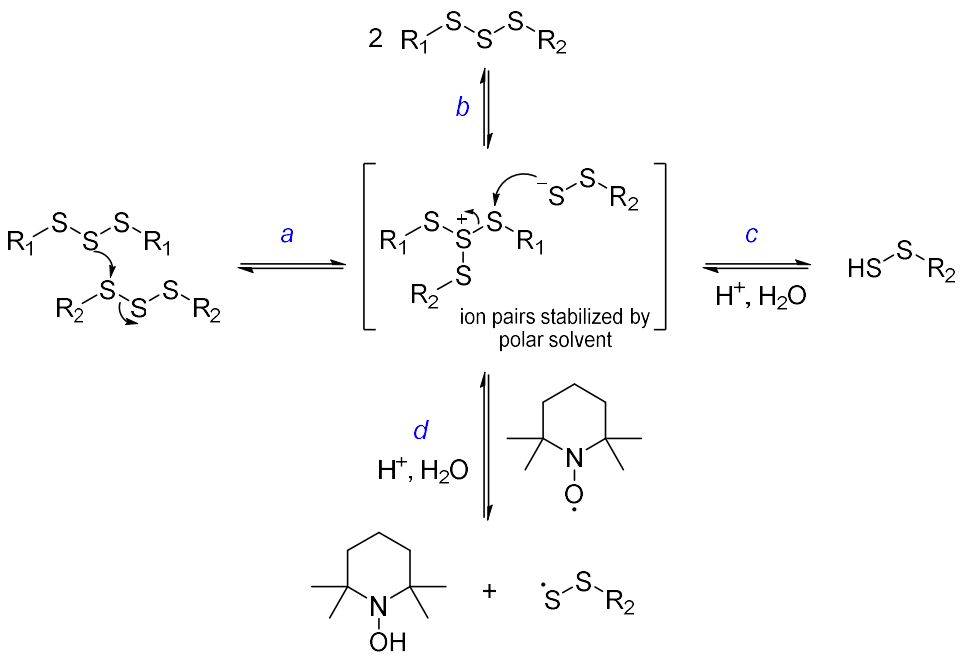

Figure 4.16: Proposed inhibition mechanism of trisulfide S-S metathesis by water or acid in polar solvents. (a) the formation of ion pairs via a nucleophilic attack between trisulfides, (b) a nucleophilic attack by thiolate to form an unsymmetrical trisulfide as the product in a normal pathway – if no water or acid is introduced, (c) thiolate is protonated to form persulfide (RSSH) species, and (d) first the formation of RSSH like in the previous pathway and then TEMPO abstracts hydrogen from RSSH to form TEMPO-H and perthiyl radical (RSS•).

From the figure 4.16 above, the trisulfides will initially react and form a charged pair which could be stabilised by polar solvents such as DMF (pathway ***a***). Next, the thiolate anion would then attack the positively charge species to generate the unsymmetrical trisulfide (pathway ***b***). In the presence of acid or water, the anion would probably be converted to a less reactive persulfide (RSSH) species (pathway ***c***). Therefore, we observed trisulfide metathesis inhibition when the reaction is carried out with wet or acidic solvent. In pathway ***d***, a proton in the persulfide which is formed via pathway ***c*** could be abstracted by TEMPO to give the TEMPO-H and a less reactive perthiyl radical ($RSS^{\bullet}$). However, TEMPO-H was not observed based on the previous NMR experiment, and RSS• could still potentially cause the S-S exchange, so this mechanism is unlikely.

Attempts to trap putative thiyl radical or thiolate anion by *N,N*-dimethyl acrylamide

In a separate study, we attempted to trap the putative thiyl radical or thiolate anion which may be generated from the trisulfides-DMF mixture. If thiyl radical is present, it could be trapped and used to initiate radical polymerisation. And if thiolate is present, it could undergo a thiol-Michael addition reaction to give a conjugate adduct (C-S bond formation) or induce anionic-polymerisation. In the previous work, Shapter[17] attempted to trap putative thiyl radical and use it for polymerization of methyl methacrylate. It was anticipated that polymerization could occur via free-radical chain mechanism and the polymer could be isolated. However, neither polymer nor Michael-addition product were formed. This unsuccessful reaction could be due to several reasons: (1) methyl methacrylate is a less reactive Michael acceptor, (2) the generated thiyl radicals is quenched during the initiation, or (3) no thiyl radicals are actually generated from the reaction.

Hence, we tested the reaction using a more reactive Michael acceptor *N,N*-dimethyl acrylamide (DMAA).[37] In this case, DMAA is an amide and we anticipated that this molecule could induce trisulfide S-S metathesis similar to other amides like DMF. So, DMAA was employed as Michael acceptor as well as polar aprotic medium for the reaction. In equimolar mixture of the trisulfides and DMAA, the S-S metathesis product (methyl *n*-propyl trisulfide) was observed after 1 h of reaction (Figure 4.17A). No effort was made to evaluate this amide for short reaction time, considering that this acrylamide is not commonly used as a solvent but rather a monomer. From this result, another experiment was tested to see whether Michael-addition products could be formed or not. Dimethyl trisulfide and DMAA were used in the reaction with or without the presence of water (Figure 4.17B). No reaction was observed, even after 7 days. Moreover, since the electrophilic unsaturated β-carbon in DMMA is prone to a thiolate (RS^{-}) attack, the enolate is then formed and potentially reacts further with DMAA molecules to give a dimer, oligomer, or polymer (Figure 4.17C). However, none of these products were observed. This finding suggests that neither radical nor thiolate are likely involved in the trisulfide S-S metathesis reaction induced by amide solvents.

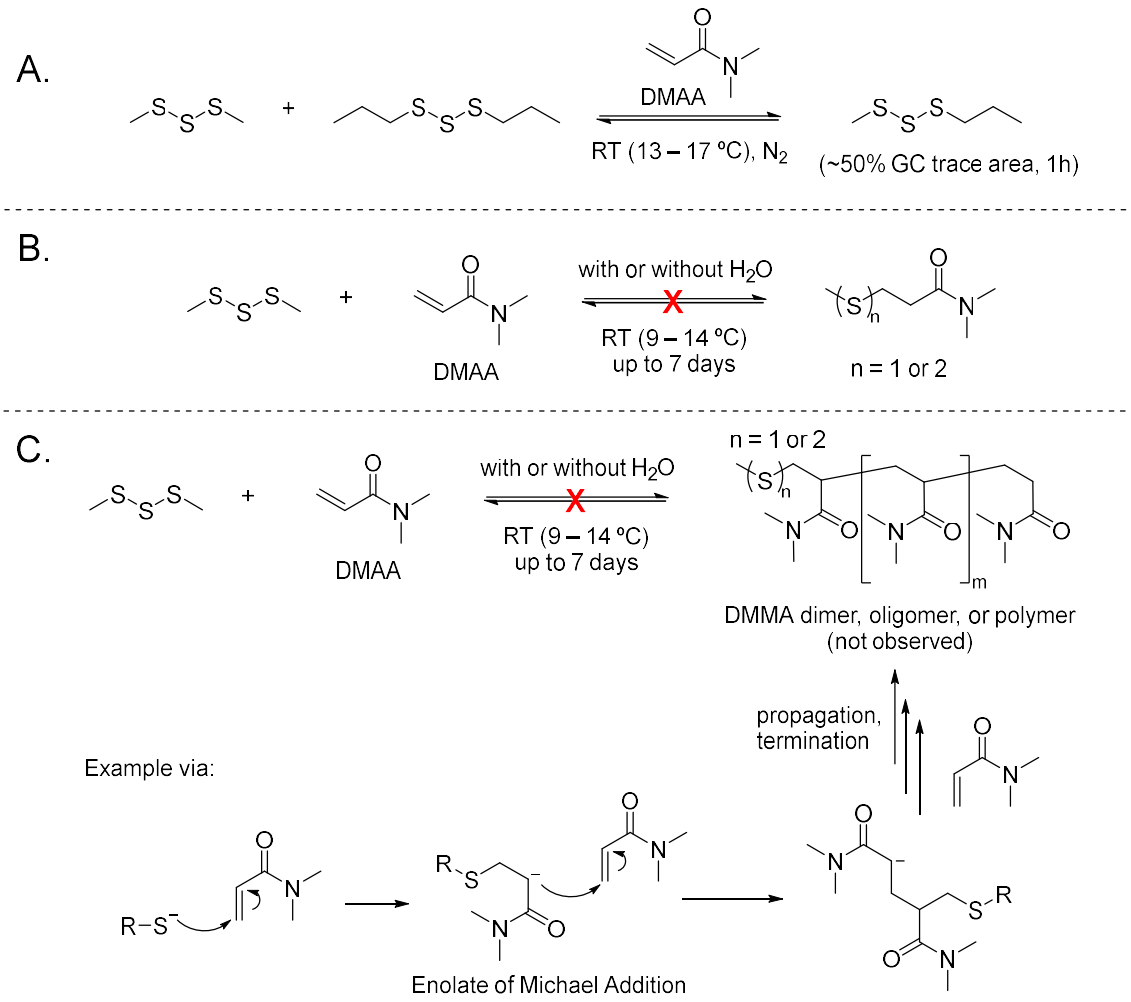

Figure 4.17: A. *N,N*-dimethyl acrylamide (DMAA) induces S-S metathesis between dimethyl trisulfide and di-n-propyl trisulfide. B. No conjugate addition products were observed by GC-MS in the mixture of dimethyl trisulfide and *N,N*-dimethyl acrylamide (DMAA). C. No polymerisation was observed in the reaction of DMAA and dimethyl trisulfide.

UV-light Induced S-S metathesis in trisulfide molecules

If the reaction proceeds through the radical pathway (e.g., UV light-initiated S-S metathesis), it is possible for the trisulfides mixture in DMF to for disulfide and tetrasulfide products. Di-*n*-propyl trisulfide was used as the trisulfide model and exposed to the UV light (λ = 245 nm). Figure 4.18 shows the $^{n}Pr_2S_3$ reaction under UV light and the GC traces of the trisulfide solution after being exposed to UV light for 10 and 30 min. After exposing the trisulfide solution to UV energy of around 4500 mJ cm^{-2} (10 minutes), di-*n*-propyl disulfide was observed by GC-MS. The area percentage of di-*n*-propyl disulfide in the mixture increased after being exposed for an additional energy of 9000 mJ cm^{-2} (20 minutes). Interestingly, with this condition di-*n*-propyl tetrasulfide was not observed in the GC trace. It is possible that the tetrasulfide might have been formed during the reaction but it is not stable to continued irradiation. It is known that S-S bond dissociation energy of a tetrasulfide is

weaker compared to di and trisulfide analogue.[27] Therefore, the result suggests that the trisulfide S-S metathesis in DMF might not occur via a radical pathway.

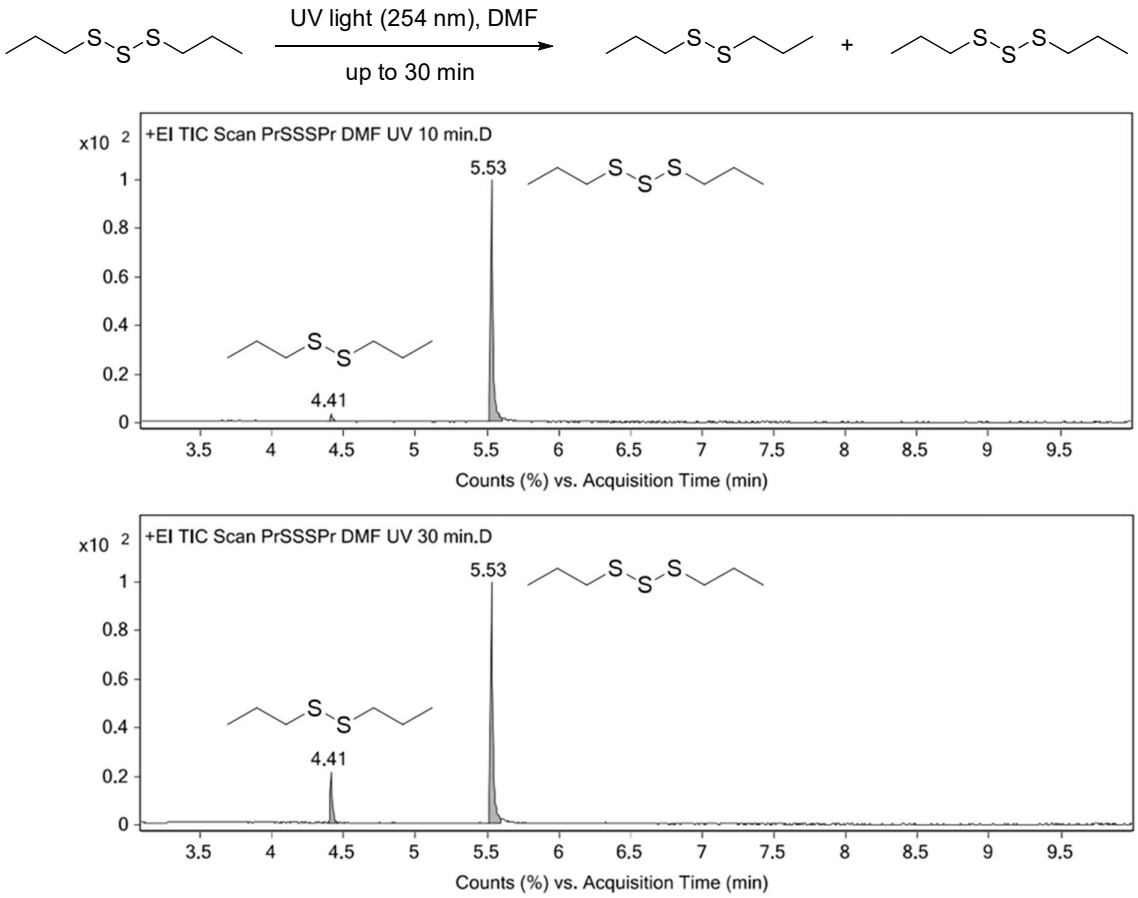

Figure 4.18: UV induced S-S metathesis of di-*n*-propyl trisulfide in DMF and GC traces showing the reaction after 10 and 30 min of 254 nm UV exposure.

Putative thiyl or perthiyl radical trapping experiments using PFN-5 radical scavenger

We also attempted to detect the possible S-centred radical from the trisulfides-DMF mixture indirectly via a radical trapping by perfluoro nitroxide compound, 2,2,6,6-Tetramethyl-4-([7-nitrobenzo[c][1,2,5]oxadiazol-4-yl]-amino) piperidin-1-oxyl radical or PFN-5. This compound was prepared according to the previous report.[38] In the radical form, PFN-5 is weakly fluorescence due to the nature of the nitrobenzofurazan group. The fluorescent signal is restored when the radical traps another radical (e.g., H$^{\bullet}$), and the fluorescence emission intensity will increase. With this knowledge, thiyl or perthiyl radicals which might form during the reaction between the trisulfides in DMF could be trapped by PFN-5 probe, giving a fluorescent PFN-5SR or PFN5-SSR (Figure 4.19).

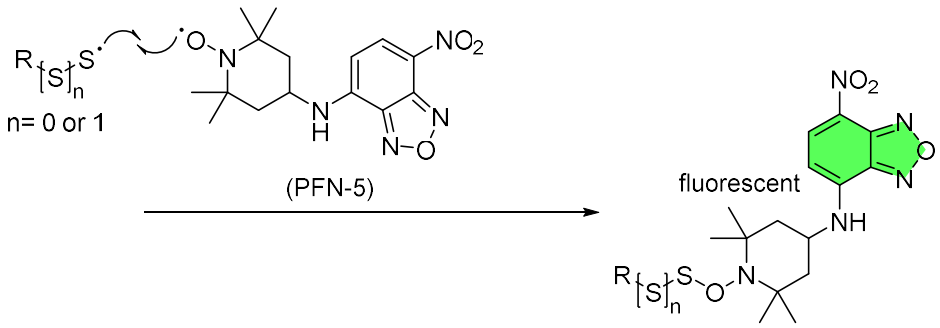

Figure 4.19: Putative thiyl or perthiyl radical trapping by PFN-5.

A solution of PFN-5 (6 x 10^{-5} M) in DCM was used in the test. Whether DMF can induce the crossover reaction via a radical mechanism or not, the mechanistic investigation was carried out by measuring the intensity of the probe after the addition of the trisulfides and DMF. Initial intensity of the PFN-5 probe was measured. Upon addition of the equimolar of trisulfides, the fluorescence intensity of the mixture decreased significantly, accounting for half of the original intensity of the nitroxide probe. In the presence of DMF (~10% v/v), there was a slight increase in the emission intensity. To validate that the cause of this increase is not because of DMF only, we measured the intensity of a mixture of PFN-5 and DMF (~10% v/v). The intensity of the mixture was measured over 60 minutes. Results showed that the emission signal of the radical probe was changing overtime in the presence of DMF only (Figure 4.20). This suggests that the probe might react with DMF. Therefore, attempts on using this method to trap putative radical was discontinued.

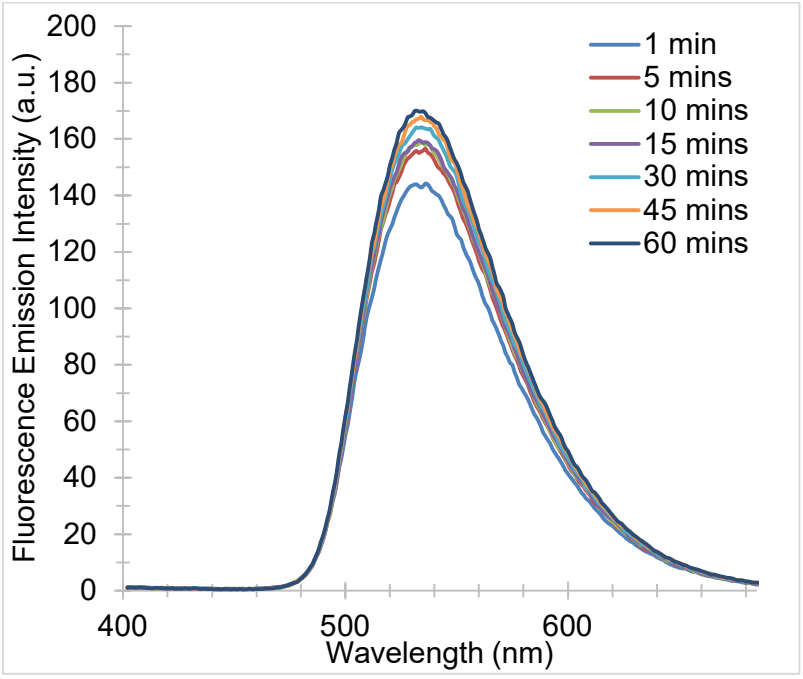

Figure 4.20: Fluorescence emission intensities of the probe after the addition of DMF (312 µL, 4.03 mmol). Spectra parameters setting: Emission slit 5 nm, PMT power set at 600 volts, excitation source set at 350 nm.

Trapping putative thiolate anion (RS^-) by benzyl bromide

DMF induced trisulfide S-S metathesis reaction could occur due to the presence of nucleophilic thiolate anion (RS^-). Suppose the reaction follows the mechanistic proposal 2 or 3, the thiolate formed in the reaction can be trapped using an electrophile such as benzyl chloride or bromide via a S_N2 reaction to give the sulfides (Figure 4.21).[39]

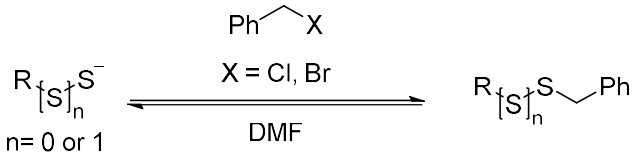

Figure 4.21: A thiolate trapping by an electrophile such as benzyl chloride or bromide

A test was conducted by reacting an equimolar mixture of dimethyl trisulfide, benzyl bromide, and DMF at room temperature. GC-MS analysis showed that only starting materials were observed after 1 hour of reaction. After 24 hours, a very small portion of dimethyl disulfide and tetrasulfide were observed. When the reaction was left for 72 hours, a very small portion of benzyl methyl sulfide **6** was formed (Figure 4.22A). In addition to that, both area percentage of dimethyl disulfide and tetrasulfide were noticeable. In a typical reaction involving a thiolate, e.g., methanethiolate (MeS^-), and alkyl or aryl halide in a polar solvent such as DMF or MeOH, the substitution product can be obtained readily.[39, 40] Since S-S metathesis reaction occurs very quickly, it is unlikely that the thiolate contributes to the reaction. A very interesting observation is that benzyl formate **7** was formed when 5 eq. of DMF was used. However, it is only a negligible portion and it merely started to form after 24 hours of reaction. The formate ester product **7** was apparent after 72 hours of reaction (Figure 4.22B). This result suggests that the behaviour of DMF is somewhat unusual. Besides as a polar aprotic solvent, DMF is a unique chemical and can participate in many types of reactions including formyloxylation.[41, 42] Overall, it can be concluded that the thiolate is unlikely to be involved in this reaction.

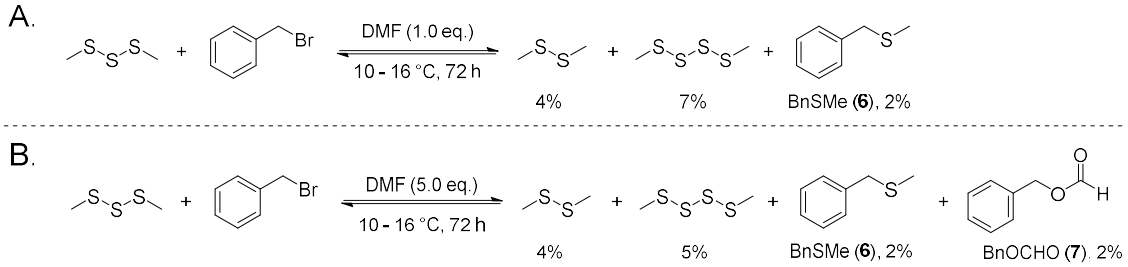

Figure 4.22: Reaction between dimethyl trisulfide and benzyl bromide in (A) 1 eq. of DMF and (B) 5 eq. of DMF after 72 hours at room temperature. Percent area was determined by GC.

Thiolate reaction with trisulfide: a rapid formation of disulfide and tetrasulfide

If the thiolate (RS^-) is present in the mixture of trisulfides (R'SSSR') and DMF, it should readily displace the trisulfide and gives S-S exchange products. We tested the reaction between propanethiolate ($^nPrS^-$) which was prepared from deprotonation of 1-propanethiol by sodium hydride, and di-*n*-propyl trisulfide. In the first test, only half portion of 1-propanethiol was deprotonated (the mixture consists of 1:1 ratio of PrSH:PrS^-) and then reacted it with di-*n*-propyl trisulfide. Within 1 minute, GC-MS analysis revealed the formation of di-*n*-propyl disulfide and tetrasulfide (Figure 4.23A). In addition to this, we have found no significant difference in terms of the products formed when the thiol was fully deprotonated (all thiol converted to propanethiolate). In a control experiment where only thiol (0.1 eq.) is used in the reaction, di-*n*-propyl disulfide and tetrasulfide were also observed but it only made up less than 3% of area percentage for both combined (Figure 4.23B). The results suggest that the thiolate is unlikely to be present in the trisulfide-DMF metathesis reaction system. In the reaction between two unsymmetrical trisulfides, only trisulfides are formed and disulfides and tetrasulfides are not formed. In contrast, the reaction in Figure 4.23A shows that thiolates rapidly generate disulfides and tetrasulfides upon reaction with trisulfides.

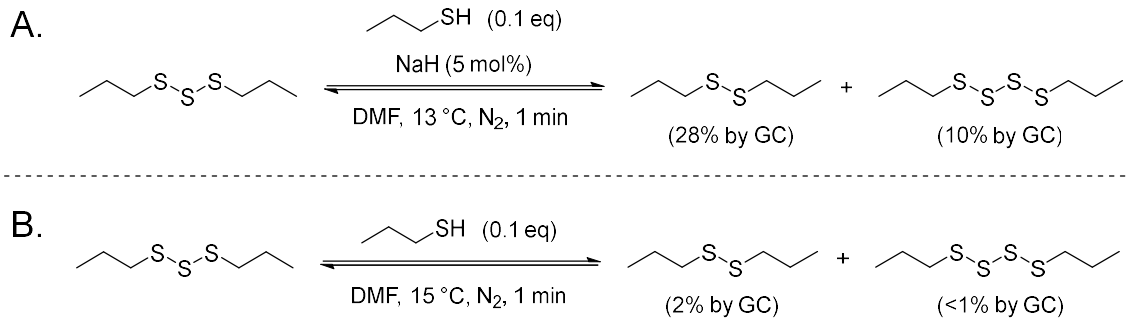

Figure 4.23: A. The reaction between di-*n*-propyl trisulfide and PrSH/PrS^- (1:1) in DMF. B. A control experiment between di-*n*-propyl trisulfide and PrSH in DMF.

Other possible mechanisms: Thiosulfoxide and hypervalent intermediate

In the previous discussion, all experimental results have shown that the trisulfide S-S metathesis may not involve a radical mechanism (Mechanistic proposal 1, Figure 4.4A) or anionic mechanism via a thiolate (Mechanistic proposal 2 and 3, Figure 4.4B and 4.4C). The EPR studies did not provide any evidence for radical formation, so a radical pathway for the trisulfide metathesis is unlikely. Additionally, although TEMPO can inhibit the trisulfide metathesis, it was suspected that this was through a redox reaction with an intermediate, rather than through reaction with a radical. For mechanistic proposal 3 (Figure 4.4C), the amide is weakly nucleophile so the S-S bond breaking in a trisulfide by DMF to form thiolate is unlikely to happen. If DMF would break the S-S bond in the symmetrical trisulfide and formed a thiolate, the reaction should be rapidly generating the unsymmetrical trisulfide along with the disulfide and tetrasulfide. Nevertheless, in a putative thiolate

trapping experiment, no significant portion of thioether product was observed after long reaction time which suggests that mechanistic proposal 2 or 3 might not be operating.

Mechanistic proposal 4, 5, 6 and 7 involve a thiosulfoxide species. Mechanistic proposal 4 (Figure 4.4D) proposes a reaction pathway that could follow a concerted mechanism via thiosulfoxide species. It is possible that the trisulfides will directly react and form a product through a cyclic transition state. In the initial step, the polar solvents such as DMF could stabilise the 6-membered ring TS of two symmetrical trisulfides which then give two thiosulfoxide species. In this process, the thiosulfoxide species undergo a rearrangement to yield an unsymmetrical trisulfide. A caveat for putting forward this proposal is that the simultaneous formation of two thiosulfoxides is unlikely due to the high energy barrier for a thiosulfoxide isomerization from a trisulfide.

In mechanistic proposal 5 (Figure 4.4E), the trisulfide is proposed to undergo a rearrangement to form a thiosulfoxide in the first step and then the thiosulfoxide further reacts with another trisulfide molecule to form a charged pair resulting in a perthiolate ion (RSS^-) in the second step. This perthiolate would then attack the positively charged sulfur species to give the trisulfide crossover product in the last step. It should be noted that the persulfide generated from the second step could react with another trisulfide in chain reaction. When this happens, the perthiolate attack to trisulfide would possibly give not only the unsymmetrical trisulfide as the product but also a tetrasulfide according to the reaction shown in Figure 4.24. Additionally, the thiolate generated from the reaction could attack either terminal sulfur or central sulfur to yield a disulfide and a trisulfide, respectively. Nevertheless, the attack of a terminal sulfur in trisulfide by thiolate or perthiolate was investigated theoretically to be kinetically and thermodynamically favourable.[43]

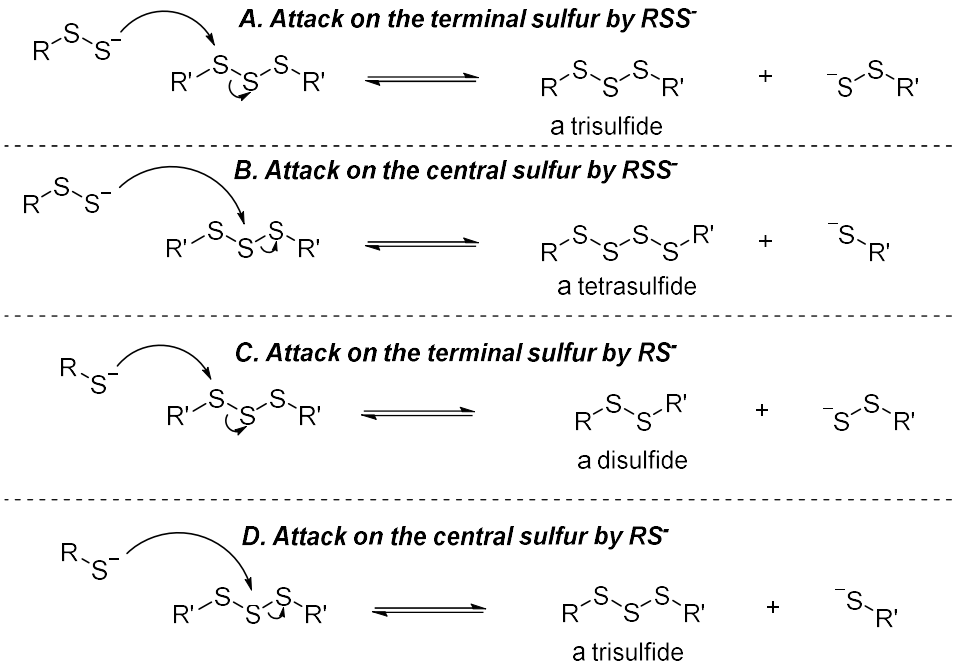

Figure 4.24: Perthiolate (RSS^-) and thiolate (RS^-) could possibly attack on either the terminal or central sulfur atom in a trisulfide to give another disulfide, trisulfide or tetrasulfide crossover product.

In mechanistic proposal 6 (Figure 4.4F), the thiosulfoxide is initially generated from a trisulfide and then proposed to react with another trisulfide in the key step. The reactive thiosulfoxide is stabilised by a polar solvent (i.e., DMF) and proposed to react directly with the trisulfide (Figure 4.25A). This step allows a concerted process via 6-membered TS (transition state) where a new thiosulfoxide and a trisulfide metathesis product are formed. Since the new thiosulfoxide is produced, it could then propagate trisulfide metathesis in a chain reaction. This mechanistic proposal offers a more logical interpretation because of the sequential generation of high energy thiosulfoxide.

In mechanistic proposal 7 (Figure 4.4G), the thiosulfoxide is generated and proposed to react directly with another trisulfide molecule to give the crossover product via concerted mechanism. The reaction, in this case, is depicted proceeding through a 5-membered transition state which can be stabilised by the presence of polar solvents such as DMF (Figure 4.25B).

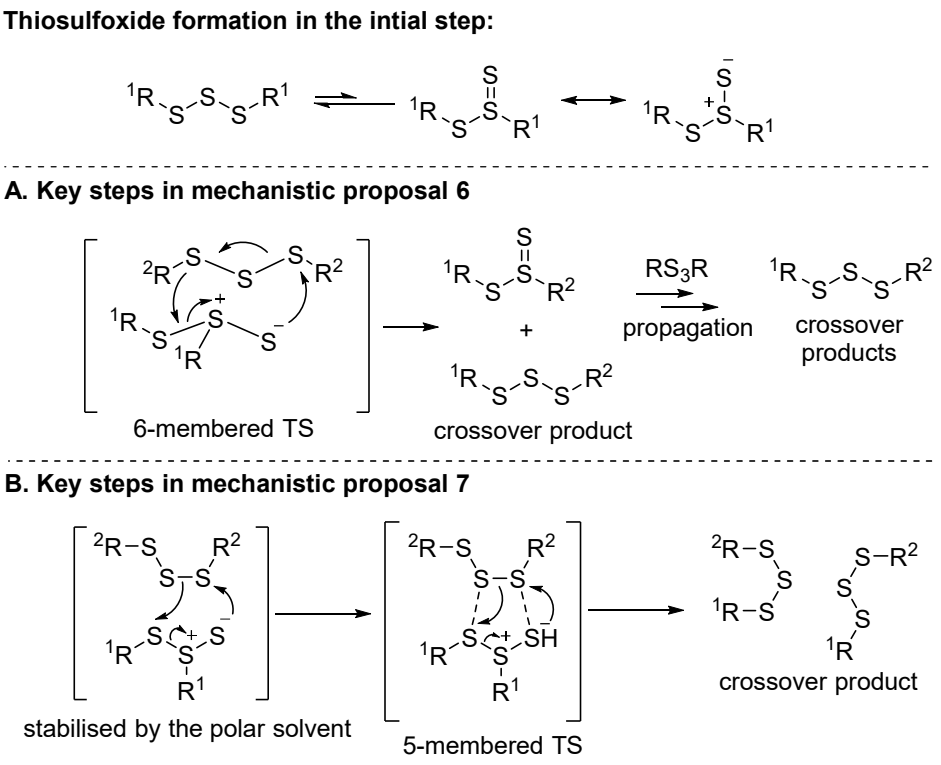

Figure 4.25: Thiosulfoxide reaction with another trisulfide to form: (A) A 6-membered TS to give a thiosulfoxide and a trisulfide metathesis product, and (B) A 5-membered TS to give directly trisulfide metathesis products.

The mechanisms involving thiosulfoxide intermediates were proposed for several reasons. Firstly, the S-S metathesis reaction between two symmetrical trisulfides i.e., Me_2S_3 and $^{n}Pr_2S_3$ in a neat condition can still occur although the rate of reaction was extremely slow. Only in polar solvents such as DMF, the same reaction can reach equilibrium within a minute. The polar solvent is proposed to stabilise the formation of the polar thiosulfoxide intermediate. Secondly, the formation of 6-

membered ring transition state is compatible with small R group. The experimental investigations for the S-S metathesis reaction involving different R groups support this reasoning. In the case of bulkier R groups such as isopropyl, *tert*-butyl, and adamantyl trisulfide, we found that the trisulfide metathesis reaction was slower or simply there is no reaction due to the steric hindrance (Figure 4.26). However, the formation of two thiosulfoxides is again unlikely to occur in a single step due to the high energy required for the thiosulfoxide formation. Thirdly, one might consider the thiosulfoxide as a polar molecule or semipolar structure.[1, 10, 15] The terminal sulfur atom is polarized which could lead to the negatively charged sulfur species. Thus, the thiosulfoxide could be nucleophilic enough to attack S-S bond in another trisulfide via heterolytic cleavage.

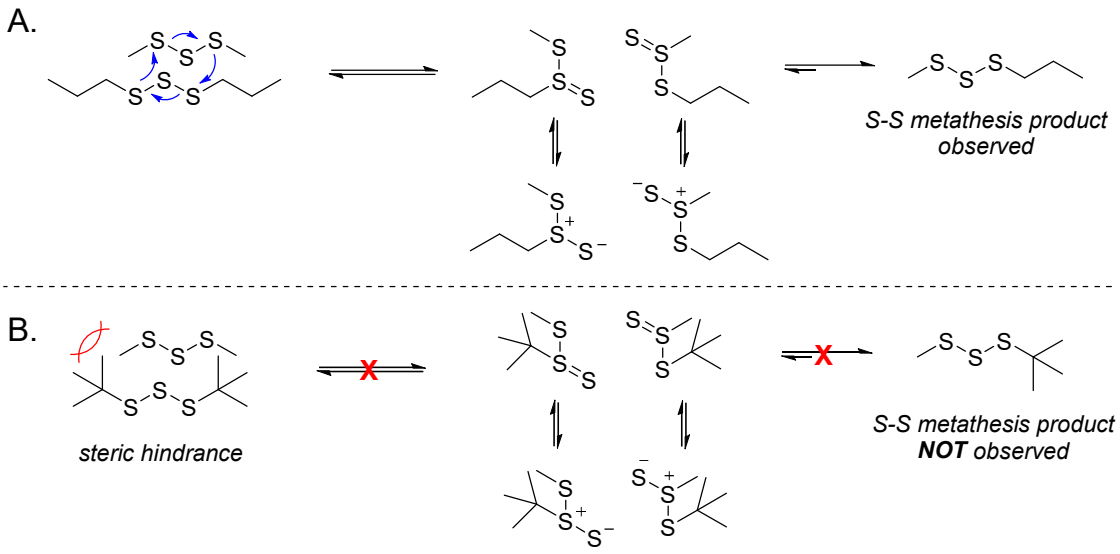

Figure 4.26: A. A possible 6-membered cyclic TS geometry for a reaction between dimethyl trisulfide and di-*n*-propyl trisulfide. B. A possible 6-membered TS geometry for a reaction between dimethyl trisulfide and di-*tert*-butyl trisulfide (steric hindrance).

Another reason why thiosulfoxide could be involved in the trisulfide S-S metathesis mechanism is that the polar thiosulfoxide species could participate in hydrogen bonding and attenuate the reactivity of the thiosulfoxide. (Figure 4.27). This pathway could account for the experimental results where we observed that the trisulfide S-S metathesis inhibition took place when the trisulfide substrate contains -OH group, or the slow reaction in protic or wet solvents.

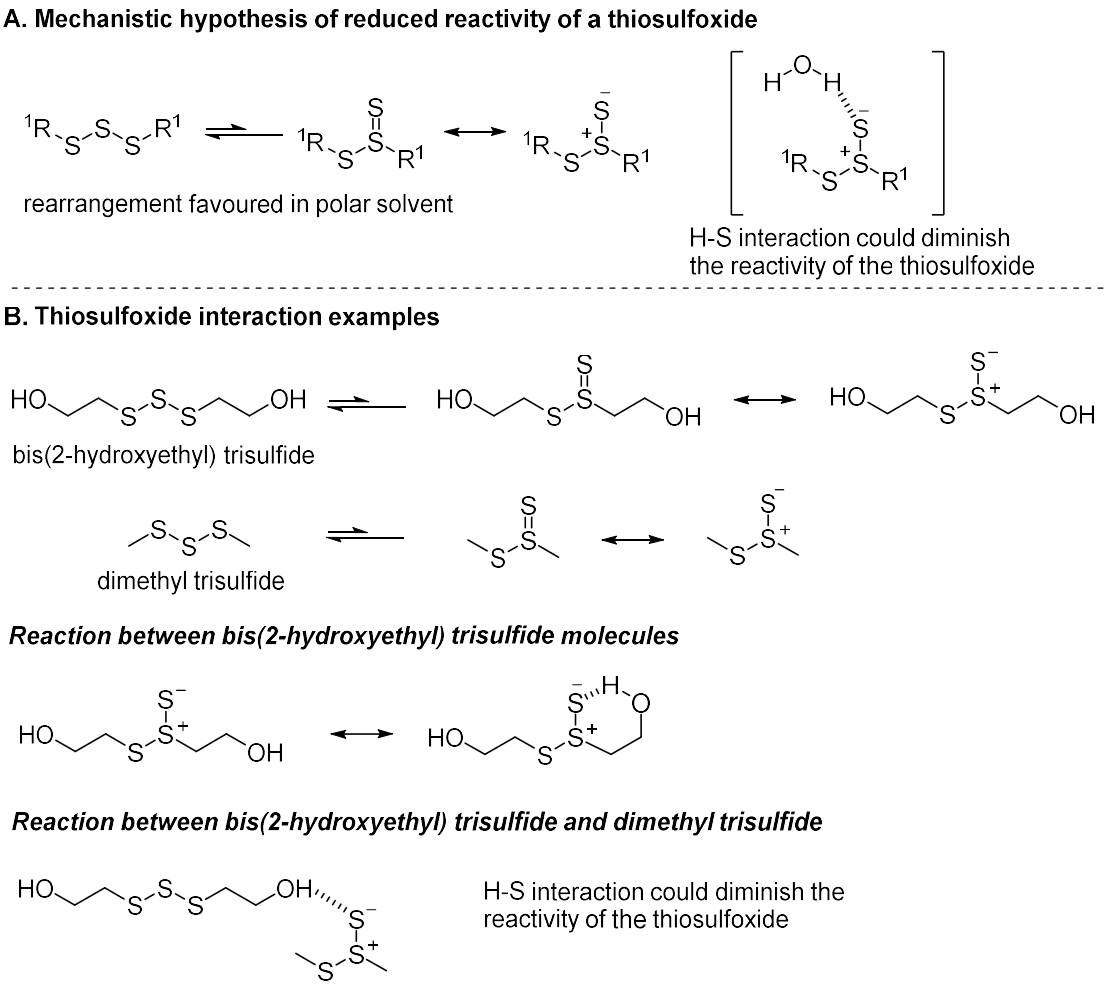

Figure 4.27: A. Mechanistic hypothesis of hydrogen-sulfur interaction in a thiosulfoxide species. B. Examples of H-S interaction of a thiosulfoxide.

The last proposed mechanism is that the trisulfide metathesis could occur via a hypervalent intermediate called sulfurane **8** (Figure 4.28A). The first step is the oxidative addition of a trisulfide to another trisulfide which would form a pseudotrigonal-bipyramidal type of sulfurane molecule with C_{2v} symmetry (Figure 4.28A). This sulfurane is potentially to undergo a Berry pseudorotation at room temperature. Substituents located in axial and equatorial could undergo an exchange. This would then lead the reductive elimination or reverse reaction to give a new trisulfide. This mechanistic proposal was based on the computational study conducted by Steudel and co-workers[15] where they studied the reaction between dimethyl trisulfide (Me_2S_3) and dimethyl disulfide (Me_2S_2). In their calculations, the transition state (**TS 8**, Figure 4.28B) energy was around 90 kJ mol^{-1} higher than that of sulfurane **8**. In addition, they also found that the activation energy for the reaction between dimethyl disulfide and dimethyl trisulfide was around 290 kJ mol^{-1} (Figure 4.28A). Since the S-S bond dissociation energy for Me_2S_3 is 226 kJ mol^{-1}, this indicates that the reaction is not thermodynamically favourable. However, the calculations have not considered DMF as the solvent model which could

possibly interact during each step of the reaction and lower the activation energy. Therefore, the mechanistic proposal 7 has not been ruled out.

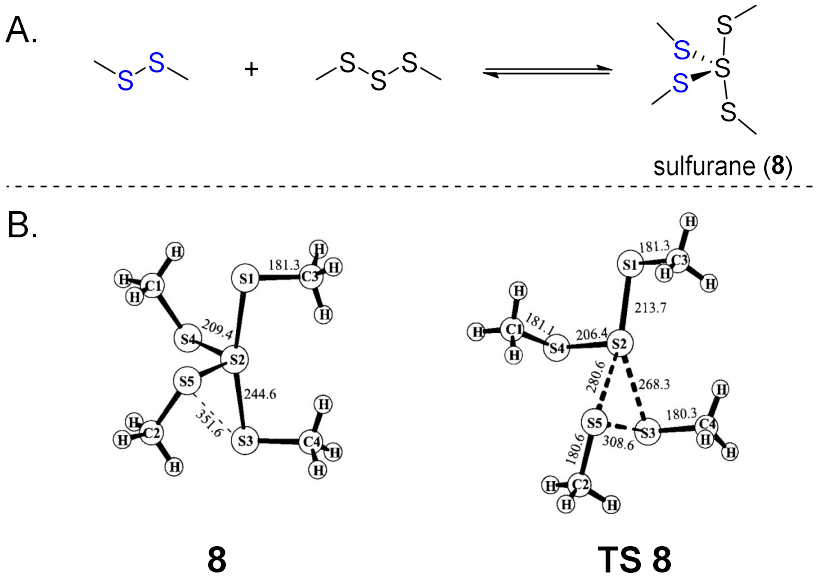

Figure 4.28: A. Formation of sulfurane from dimethyl disulfide and dimethyl trisulfide. B. Structure of sulfurane **8** and its transition state TS **8**.[15] Structures 8 and TS 8 were reproduced with permission from ref. 15. © 2001 WILEY-VCH Verlag GmbH, Weinheim, Fed. Rep. of Germany.

The sulfurane type transition state was found to have a high energy barrier which makes it impossible for the trisulfide S-S metathesis to occur at room temperature. The thiosulfoxide formation from a disulfide is also high, which may suggest the reaction is impossible to occur at room temperature. For the thiosulfoxide from a trisulfide, this may not be the case and the barrier may be lower than that of disulfide. Again, however, the computational calculation involving DMF as a model solvent has not been carried out. Therefore, the mechanistic proposal involving thiosulfoxide intermediate could still be possible for trisulfide.

Future explorations on the mechanistic hypothesis of trisulfide metathesis

The involvement of thiosulfoxide intermediates in the mechanistic hypothesis of trisulfide metathesis reaction is currently the most plausible explanation for the exquisite selectivity for trisulfides and the lack of formation of di- and tetrasulfides in the metathesis process. Radical or ionic pathways cannot account for the trisulfide selectivity. The thiosulfoxide intermediate may also explain the inhibitory effects of water and protic solvents (hydrogen bonding), and TEMPO (redox reaction), and electrophiles (alkylation). Mechanistic proposal 6 (Figure 4.4F) provides a refined proposed pathway for the formation of a trisulfide metathesis product. The thiosulfoxide species is proposed to form in a trace amount and stabilised by the presence of polar aprotic solvents such as DMF during the initial step. The generated thiosulfoxide is sufficient to react with a trisulfide via a concerted reaction

to yield two key products: a new thiosulfoxide and a new trisulfide. The new thiosulfoxide is likely to propagate the chain reaction. This proposal has been considered to account for the selective formation of trisulfide. Also, this proposal aligns well with the current understanding, particularly when considering the production of higher energy thiosulfoxide intermediate during the key reaction step. However, this intermediate has not been detected directly.

It is therefore crucial to design future experiments or to carry out theoretical explorations on the mechanisms to find the most reasonable pathway for the trisulfide metathesis. Hence, multiple approaches may be employed to ascertain the answer. For future investigations, one might explore a combination of spectroscopic analyses such as mass spectrometry, IR, Raman, and NMR spectroscopy, in order to provide a robust method to observe and characterize the proposed thiosulfoxide intermediates. For example, advanced tandem mass spectrometry can be used to observe the presence of thiosulfoxide species, $X_2S{=}S$ (where X = H, CH_3, C_2H_5), in a gas phase.[44] In addition, a non-destructive analysis such as IR and Raman spectroscopy can be employed. The predictive vibrational wavenumber for S=S in Me_2SS (a thiosulfoxide from dimethyl disulfide), which was studied computationally by Steudel and co-workers[10], was found to be 496 cm^{-1} with the maximum relative intensity. This information can help us to observe the S=S bond wavenumber and detect the thiosulfoxide species by using time resolved IR and Raman spectroscopy. So, theoretically, if the vibrational wavenumber of S=S in the thiosulfoxide species generated from a trisulfide is calculated, the result can guide us to observe and compare with the experimental observations.

Furthermore, although it has low sensitivity ^{33}S NMR spectroscopy could be useful to characterise the thiosulfoxide intermediate.[45] To date, ^{33}S NMR studies of organic monosulfides and polysulfides are very rare, and it is usually a theoretical study.[46, 47] Bagno[46] has studied computationally the ^{33}S chemical shifts of MeSMe, MeSSMe, and MeSSSMe using the Hartree-Fock level of theory. For the trisulfide, MeSSSMe, the ^{33}S chemical shifts of the terminal sulfur atom (Me**S**SSMe, δ = –361.40 ppm) and the central sulfur atom (MeS**S**SMe, δ = –343.69 ppm) can be distinguished. Thus, with advances in DFT calculations, the predicted ^{33}S chemical shifts of thiosulfoxide species from a trisulfide can possibly be determined accurately. The ^{33}S chemical shift values obtained from the calculations can be used as references to observe the sulfur signals in thiosulfoxide by ^{33}S NMR spectroscopy. However, a caveat is that the ^{33}S NMR signal of the thiosulfoxide intermediate may not be observed due to the low abundance of isotopic ^{33}S. To overcome this, the synthesis of ^{33}S labelled trisulfides may help. Since elemental ^{33}S (99.8%) is available commercially, one can prepare ^{33}S labelled trisulfides through several methods. For example, Figure 4.29 shows a transformation of elemental sulfur to sulfur dichloride (SCl_2) using chlorine gas, then reaction with a thiol (R-SH) to obtain a trisulfide (R-SSS-R). From SCl_2, sulfur monochloride (S_2Cl_2) can be prepared and the synthesis of trisulfides can also be achieved via *N,N*'-thiobisphthalimide. Again, the proposal offered here is to provide an insight for a future study.

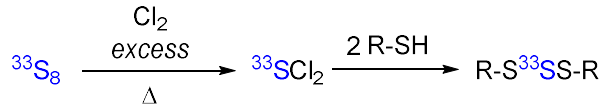

Figure 4.29: Synthetic pathways to prepare a ^{33}S-labelled trisulfide.

Moreover, kinetic rate analysis to determine the rate law is another essential approach to employ. Results obtained from the kinetic rate analysis can help to identify which steps or species are involved in the rate determining step.[48] The trisulfide metathesis reaction involves three starting molecules: trisulfide A (A), trisulfide B (B), and the solvent (S). If thiosulfoxide intermediate (I) is formed during the reaction, it needs to be included in the kinetic rate analysis. Kinetic data from each reactant can be used to determine the rate order and the rate constant. The overall reaction between the trisulfides (e.g., Me_2S_3 and $^nPr_2S_3$) in the presence of polar aprotic solvent (e.g., DMF) is shown in Figure 4.30.

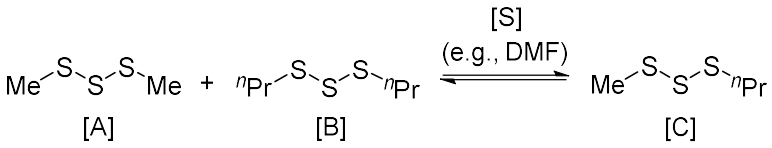

Figure 4.30: The overall trisulfide metathesis reaction.

In this example, we can consider the following steps to evaluate mechanistic proposal 6 (Figure 4.4F):

1. First step is the formation of intermediate (I) from either trisulfide (A) or (B) in the presence of solvent (S) and (I) can revert back to (A) or (B).

   Reaction 1: Intermediate (I) from trisulfide A (where k_1 is the rate constant for the formation of intermediate (I) and k_{-1} is the rate constant for the reverse reaction)

   $$A + S \underset{k_{-1}}{\overset{k_1}{\rightleftharpoons}} I + S$$

   Rate formation of intermediate (I) from reaction 1:

   $$r_1 = k_1[A][S] - k_{-1}[I][S] \qquad \text{Equation 1}$$

   Reaction 2: Intermediate (I) from trisulfide B (where k_2 is the rate constant for the formation of intermediate (I) and k_{-2} is the rate constant for the reverse reaction)

   $$B + S \underset{k_{-2}}{\overset{k_2}{\rightleftharpoons}} I + S$$

   Rate formation of intermediate (I) from reaction 2:

   $$r_2 = k_2[B][S] - k_{-2}[I][S] \qquad \text{Equation 2}$$

The overall rate formation of intermediate (I):

$$r_{1+2} = k_1[\mathrm{A}][\mathrm{S}] - k_{-1}[\mathrm{I}][\mathrm{S}] + k_2[\mathrm{B}][\mathrm{S}] - k_{-2}[\mathrm{I}][\mathrm{S}] \quad \text{Equation 3}$$

$$r_{1+2} = (k_1[\mathrm{A}][\mathrm{S}] + k_2[\mathrm{B}][\mathrm{S}]) - (k_{-1} + k_{-2})[\mathrm{I}][\mathrm{S}] \quad \text{Equation 4}$$

2. Second step is the formation of a trisulfide metathesis product (C) from the reaction between intermediate (I) with either trisulfide (A) or (B).

   Reaction 3: Intermediate (I) and trisulfide (A) react to form trisulfide (C) and regenerates intermediate (I)

$$\mathrm{I} + \mathrm{A} \xrightarrow{k_3} \mathrm{I} + \mathrm{C}$$

   Rate formation of trisulfide (C) from trisulfide (A):

$$r_3 = k_3[\mathrm{I}][\mathrm{A}] \quad \text{Equation 5}$$

   Reaction 4: Intermediate (I) and trisulfide (B) react to form trisulfide (C) and regenerates intermediate (I)

$$\mathrm{I} + \mathrm{B} \xrightarrow{k_4} \mathrm{I} + \mathrm{C}$$

   Rate formation of trisulfide (C) from trisulfide (B):

$$r_4 = k_4[\mathrm{I}][\mathrm{B}] \quad \text{Equation 6}$$

   The overall rate formation of trisulfide (C):

$$r_{3+4} = k_3[\mathrm{I}][\mathrm{A}] + k_4[\mathrm{I}][\mathrm{B}] = [\mathrm{I}](k_3[\mathrm{A}] + k_4[\mathrm{B}]) \quad \text{Equation 7}$$

3. Third step is using a steady state approximation for intermediate (I) to determine the rate formation of trisulfide (C). Because intermediate (I) is regenerated during the reaction, its concentration is assumed to be constant. Therefore, we can consider using a steady-state approximation to determine the rate law. Since intermediate (I) is consumed and regenerated during the metathesis reaction, the rate formation of intermediate (I) is equal to the rate of consumption of intermediate (I).

$$r_{formation\,(I)} = r_{consumption\,(I)}$$

$$r_{1+2} = r_{3+4}$$

$$(k_1[\mathrm{A}][\mathrm{S}] + k_2[\mathrm{B}][\mathrm{S}]) - (k_{-1} + k_{-2})[\mathrm{I}][\mathrm{S}] = k_3[\mathrm{I}][\mathrm{A}] + k_4[\mathrm{I}][\mathrm{B}]$$

$$(k_1[\mathrm{A}][\mathrm{S}] + k_2[\mathrm{B}][\mathrm{S}]) - (k_{-1} + k_{-2})[\mathrm{I}][\mathrm{S}] = (k_3[\mathrm{A}] + k_4[\mathrm{B}])[\mathrm{I}] \quad \text{Equation 8}$$

   [I] can be simplified to:

$$[\mathrm{I}] = \frac{(k_1[\mathrm{A}] + k_2[\mathrm{B}])[\mathrm{S}]}{(k_{-1} + k_{-2})[\mathrm{S}] + k_3[\mathrm{A}] + k_4[\mathrm{B}]} \quad \text{Equation 9}$$

Substituting [I] in Eq. 9 to the rate formation of trisulfide (C) in Eq. 7:

$r_{3+4} = [\mathrm{I}](k_3[\mathrm{A}] + k_4[\mathrm{B}])$

The overall rate becomes:

$$r_{overall} = \frac{(k_1[\mathrm{A}]+k_2[\mathrm{B}])[\mathrm{S}]}{(k_{-1}+k_{-2})[\mathrm{S}] + k_3[\mathrm{A}]+k_4[\mathrm{B}]}(k_3[\mathrm{A}] + k_4[\mathrm{B}]) \qquad \text{Equation 10}$$

If the concentration of trisulfide (A) is equal to trisulfide (B), [A] = [B], the rate becomes:

$$r_{overall,[A]=[B]} = \frac{(k_1[\mathrm{A}] + k_2[\mathrm{A}])[\mathrm{S}]}{(k_{-1} + k_{-2})[\mathrm{S}] + k_3[\mathrm{A}] + k_4[\mathrm{A}]}(k_3[\mathrm{A}] + k_4[\mathrm{A}])$$

$$= \frac{(k_1 + k_2)[\mathrm{A}][\mathrm{S}]}{(k_{-1} + k_{-2})[\mathrm{S}] + (k_3 + k_4)[\mathrm{A}]}(k_3 + k_4)[\mathrm{A}]$$

$$= \frac{(k_1+k_2)(k_3+k_4)[\mathrm{A}]^2[\mathrm{S}]}{(k_{-1}+k_{-2})[\mathrm{S}]+ (k_3+k_4)[\mathrm{A}]} \qquad \text{Equation 11}$$

Now, the overall rate will depend on the square concentration of the trisulfide [A] or [B], the combined rate of intermediate (I), and the solvent concentration [S].

In the case where excess solvent is used ([S] >> [A], [B]), the solvent concentration [S] is constant. The pseudo-first-order approximation can be considered for the rate equation involving solvent (Equation 1 to 4) and the overall rate in Equation 10 is changed. The rate constants for reaction 1 and 2 above become:

$k'_1 = k_1[\mathrm{S}]$; $k'_{-1} = k_{-1}[\mathrm{S}]$ for reaction 1

$k'_2 = k_2[\mathrm{S}]$; $k'_{-2} = k_{-2}[\mathrm{S}]$ for reaction 2

The rate in Equation 1 and 2 become:

$r_1 = k'_1[\mathrm{A}] - k'_{-1}[\mathrm{I}]$ Equation 12

$r_2 = k'_2[\mathrm{B}] - k'_{-2}[\mathrm{I}]$ Equation 13

Using a steady-state approximation, again we assume the intermediate (I) is produced and consumed rapidly so that the concentration of intermediate [I] does not change overtime. Hence, Equation 9 becomes:

$$[\mathrm{I}] = \frac{k'_1[\mathrm{A}] + k'_2[\mathrm{B}]}{k'_{-1} + k'_{-2} + k_3[\mathrm{A}] + k_4[\mathrm{B}]} \qquad \text{Equation 14}$$

Substituting [I] in Eq. 14 to the rate formation of trisulfide (C) in Eq. 7, the overall rate becomes:

$$r_{overall} = \frac{k'_1[\mathrm{A}] + k'_2[\mathrm{B}]}{k'_{-1} + k'_{-2} + k_3[\mathrm{A}] + k_4[\mathrm{B}]}(k_3[\mathrm{A}] + k_4[\mathrm{B}]) \qquad \text{Equation 15}$$

To model and fit the experimental data, first the rate equation needs to be determined. Let us say Eq. 10 will be used so the concentrations of both trisulfides ([A] and [B]) and the solvent [S] are required. Changes in the concentrations of all species participated in the reaction must be determined over time, for example, by using GC-MS or other suitable spectroscopy techniques. In the data analysis, the initial concentrations of all species ($[A]_0$, $[B]_0$, and $[S]_0$) and the changes in concentrations for those species at specific time ($[A]_t$, $[B]_t$, and $[S]_t$) are recorded and checked for their consistency. Since large excess of solvent is used, it is not necessary to record the changes its concentration which means $[S]_t$ can be omitted. After that, we can fit the obtained data using either linear or non-linear regression methods. It is often required a specialised software (e.g., Matlab, Origin) to perform the non-linear square fitting. After the fitting is done, it is important to evaluate the model fit such as the goodness of fit (adjusted R^2), the residual plot analysis, and the error estimation (RMSE). If the fit is not good, it is important to reconsider the rate equation and perhaps the mechanisms (reaction steps). Furthermore, due to the nature of rapid trisulfide metathesis in highly polar aprotic solvents (e.g., DMF), the reaction rate can be altered by changing the solvent polarity. For instance, adding a non-polar solvent such as chlorobenzene can slow down the rate of metathesis reaction. By doing this, the equilibrium can be controlled and the kinetic data can be obtained accurately. This will be done in future studies.

Lastly, the mechanistic proposals for the trisulfide metathesis involving thiosulfoxide species can be supported by the computational calculations. The thiosulfoxide species have been studied computationally using various level of theories.[10] However, the calculations were only done for the thiosulfoxide species in gas phase. Hence, the energy barrier for the thiosulfoxide isomerization in the presence of solvents remains unknown. Since we found that polar aprotic solvents such as DMF, ureas, phosphoramides, and DMSO can induce trisulfide metathesis, the trisulfide metathesis reaction can be studied computationally employing Density Functional Theory (DFT). Each step involved in the proposed mechanism for the trisulfide metathesis can be studied computationally to obtain information about the energy needed to break and reform the S-S bonds as the reaction progresses. Results from the theoretical calculations can assist us to determine which mechanistic steps are the most reasonable so that the reaction pathways can be concluded.

4.4 Conclusion and Outlook

In conclusion, the mechanism of trisulfide S-S metathesis induced by polar solvents still remains unknown. A direct analysis by EPR indicated that radicals are not present in the trisulfides-DMF reaction mixture. TEMPO was found to inhibit the reaction. However, the inhibition only took place for a certain period of time and the S-S metathesis reaction continued to proceed. NMR analysis also supported this where TEMPO NMR signal was attenuated immediately and then levelled off. No addition products such as TEMPO-SR or other related products were detected by GC-MS and NMR spectroscopy.

TEMPO is not the only compound that can inhibit the trisulfide S-S metathesis. Maleic anhydride and 1,4-benzoquionone were potent electrophiles and these molecules severely inhibit the reaction. Succinic anhydride, acetic acid, and dimethyl maleate were found to reduce the reaction rate but not as good as those former molecules. Nucleophilic addition may occur and substituted product may be observed. Nonetheless, no adduct was observed by GC-MS and NMR spectroscopy. Only butylated hydroxytoluene (BHT) did not inhibit the reaction.

N,N-dimethyl acrylamide (DMAA) was found to induce the trisulfide S-S metathesis reaction. This amide was not commonly used as a solvent but instead it is used as a monomer. When used in the reaction, DMAA was able to induce the metathesis reaction between Me_2S_3 and $^nP_2S_3$. Although DMAA is a reactive Michael acceptor, its reaction with Me_2S_3 in the presence of water or without water did not give any adduct or polymer. In other words, no reaction was observed even after long reaction time (~7 days).

In the experiment of exposing $^nP_2S_3$ with UV light, we found that di-*n*-propyl disulfide ($^nP_2S_2$) can be formed. Di-*n*-propyl tetrasulfide ($^nP_2S_4$) should have been formed during the reaction but this compound was not observed. Under the UV condition, the tetrasulfide might have been formed but it could immediately dissociate into ^{n}PrSS$^\bullet$ radical. Yet, the result suggested that the trisulfide S-S metathesis in DMF might not follow a radical pathway. Moreover, in the putative thiolate trapping experiment, we concluded that thiolates are unlikely to present in the reaction. It is because we demonstrated that if thiolates are present in the reaction mixture, both disulfide and tetrasulfide were formed immediately.

Based on the above experimental results, the reaction is unlikely to follow either radical (Mechanistic proposal 1, Figure 4.4A) or ionic pathways (Mechanistic proposal 2 and 3, Figure 4.4B and Figure 4.4C). If those mechanisms are involved, a mixture of disulfide, trisulfide, and tetrasulfide should be observed by GC-MS and NMR spectroscopy. The trisulfide S-S metathesis reaction induced by polar solvents such as DMF selectively yields a trisulfide as the only metathesis product.

Furthermore, other proposed mechanisms such as concerted mechanism, thiosulfoxide stepwise and concerted mechanism, are proposed. A caveat to all mechanistic proposals involving thiosulfoxide is that the thiosulfoxide species is higher energy than the linear trisulfide. Thus, it is unlikely that two thiosulfoxides could be formed in the initial step (Mechanistic proposal 4, Figure 4.4D). For mechanistic proposal 5 (Figure 4.4E), one thiosulfoxide is proposed to form in the initial step. The thiosulfoxide is proposed to undergo a stepwise crossover with a trisulfide, resulting in the formation of ion pair (perthiolate/persulfide and thiosulfonium-like species). The generated perthiolate could react with a trisulfide in chain reaction and give a mixture of disulfide, trisulfide, and tetrasulfide. Again, the trisulfide metathesis in DMF gives exclusively trisulfide as the product. Although the initial step is reasonable, the proposed step on the attack of trisulfide by the thiosulfoxide to generate ion pair could potentially be deviating from the actual reaction pathway. In mechanistic proposal 6 (Figure 4.4F) and 7 (Figure 4.4G), the initial step was the same as the previous proposal. In mechanistic proposal 6, the thiosulfoxide is proposed to react stepwise with a

trisulfide, generating the new thiosulfoxide and the trisulfide metathesis product. Because the high energy thiosulfoxide is regenerated and the process occur in a chain reaction, this step is more reasonable compared to that of direct formation of trisulfide products via a 5-membered concerted crossover in mechanistic proposal 7. Hence, mechanistic proposal 6 could be the most reasonable mechanism considered.

For the hypervalent intermediate (sulfurane), it is unlikely for the trisulfide metathesis by DMF to follow this pathway since the energy barrier for the sulfurane transition state calculated by Steudel and co-workers[15] is too high. However, the interaction between the solvent (e.g., DMF) and the sulfurane species could potentially lower the energy barrier. Therefore, future investigations on the solvent mediated trisulfide metathesis via sulfurane species should be conducted.

Moreover, from the experimental results and literature analysis, the mechanism involved in the trisulfide S-S metathesis could be via thiosulfoxide intermediate with either a concerted or a stepwise mechanism. However, computational analyses with high levels of theory of DFT should be carried out in order to find the answer of which reasonable pathways for the trisulfide metathesis to occur at room temperature in the presence of polar solvents such as DMF. Thus far, mechanistic proposal 6 involving an initial step formation of thiosulfoxide, followed by a 6-membered concerted crossover to give a trisulfide metathesis product and a new thiosulfoxide in a chain reaction, is seen as the most logical pathway for the trisulfide metathesis reaction induced by the polar solvent.

Finally, several approaches can be applied to gain a more comprehensive understanding on the reaction mechanism. While direct structural determination of the putative intermediates is the main limitation of this approach, combinations with general spectroscopic methods such as mass spectrometry, IR, Raman, and NMR can provide direct observation and characterization of the actual species that participate in the reaction. In addition to this, kinetic rate analysis is crucial to obtain useful information about the rate law which impart the rate-determining step, how each reactant involves in the reaction, how the reaction orders suggest the molecular interaction (unimolecular or bimolecular), and whether or not the mechanistic pathway that we proposed need revision based on the match between the predicted rate law and the observed rate law.

4.5 References

(1) Steudel, R. Homocyclic sulfur molecules. *Top. Curr. Chem.* **1982**, 149-176. DOI: 10.1007/3-540-11345-2_10.

(2) Pickering, T. L.; Saunders, K. J.; Tobolsky, A. V. Disproportionation of organic polysulfides. *J. Am. Chem. Soc.* **1967**, *89* (10), 2364-2367. DOI: 10.1021/ja00986a021.

(3) Trivette Jr, C.; Coran, A. Polysulfide Exchange Reactions. I. Kinetics and Mechanism of the Thermal Exchange between Diethyl Trisulfide and Di-n-propyl Trisulfide. *J. Org. Chem.* **1966**, *31* (1), 100-104. DOI: 10.1021/jo01339a020.

(4) Clennan, E. L.; Stensaas, K. L. Recent progress in the synthesis, properties and reactions of trisulfanes and their oxides. *Org. Prep. Proced. Int.* **1998**, *30* (5), 551-600. DOI: 10.1080/00304949809355321.

(5) Tonkin, S. J.; Gibson, C. T.; Campbell, J. A.; Lewis, D. A.; Karton, A.; Hasell, T.; Chalker, J. M. Chemically induced repair, adhesion, and recycling of polymers made by inverse vulcanization. *Chem. Sci.* **2020**, *11* (21), 5537-5546. DOI: 10.1039/D0SC00855A.

(6) Harpp, D. N.; Ash, D. K.; Smith, R. A. Organic sulfur chemistry. 38. Desulfurization of organic trisulfides by tris(dialkylamino)phosphines. Mechanistic aspects. *J. Org. Chem.* **1980**, *45* (25), 5155-5160. DOI: 10.1021/jo01313a026.

(7) Harpp, D. N.; Smith, R. A. Organic sulfur chemistry. 42. Sulfur-sulfur bond cleavage processes. Selective desulfurization of trisulfides. *J. Am. Chem. Soc.* **1982**, *104* (22), 6045-6053. DOI: 10.1021/ja00386a034.

(8) Harpp, D. N.; Smith, R. A. Reaction of trialkyl phosphites with organic trisulfides. Synthetic and mechanistic aspects. *J. Org. Chem.* **1979**, *44* (23), 4140-4144. DOI: 10.1021/jo01337a026.

(9) Fehér, F.; Kurz, D. Über den nucleophilen Abbau von Aryltrisulfanen mit Triphenylphosphin. *Z. Naturforsch. B* **1968**, *23* (8), 1030-1033. DOI: doi:10.1515/znb-1968-0803.

(10) Steudel, R.; Drozdova, Y.; Miaskiewicz, K.; Hertwig, R. H.; Koch, W. How unstable are thiosulfoxides? An ab initio MO study of various disulfanes RSSR (R= H, Me, Pr, all), their branched isomers R2SS, and the related transition states1, 2. *J. Am. Chem. Soc.* **1997**, *119* (8), 1990-1996. DOI: 10.1021/ja9624026.

(11) Benson, S. W. Thermochemistry and kinetics of sulfur-containing molecules and radicals. *Chem. Rev.* **1978**, *78* (1), 23-35. DOI: 10.1021/cr60311a003.

(12) Kuczkowski, R. L. The mass and microwave spectra, structures, and dipole moments of the isomers of sulfur monofluoride. *J. Am. Chem. Soc.* **1964**, *86* (18), 3617-3621. DOI: 10.1021/ja01072a005.

(13) Harpp, D. N.; Steliou, K.; Cheer, C. J. Synthesis and X-ray crystal structure of O,O-bicyclohexyl-1,1′-diyl thiosulphite. *J. Chem. Soc., Chem. Commun.* **1980**, (17), 825-826. DOI: 10.1039/C39800000825.

(14) Steudel, R. The Chemistry of Organic Polysulfanes R− S n− R (n> 2). *Chem. Rev.* **2002**, *102* (11), 3905-3946. DOI: 10.1021/cr010127m

(15) Steudel, R.; Steudel, Y.; Miaskiewicz, K. Does the interconversion of polysulfur compounds proceed via hypervalent intermediates?—An ab initio mo study. *Chem. Eur. J* **2001**, *7* (15), 3281-3290. DOI: 10.1002/1521-3765(20010803)7:15%3C3281::AID-CHEM3281%3E3.0.CO;2-B.

(16) Yan, P.; Zhao, W.; Tonkin, S. J.; Chalker, J. M.; Schiller, T. L.; Hasell, T. Stretchable and Durable Inverse Vulcanized Polymers with Chemical and Thermal Recycling. *Chem. Matter.* **2022**, *34* (3), 1167-1178. DOI: 10.1021/acs.chemmater.1c03662.

(17) Shapter, R. Investigating reactions of trisulfide system. Undergraduate thesis, Flinders University, Bedford Park, South Australia, 2021.

(18) Mönig, J.; Asmus, K.-D.; Forni, L. G.; Willson, R. L. On the reaction of molecular oxygen with thiyl radicals: a re-examination. *Int. J. Radiat. Biol.* **1987**, *52* (4), 589-602. DOI: 10.1080/09553008714552081.

(19) Denes, F.; Pichowicz, M.; Povie, G.; Renaud, P. Thiyl radicals in organic synthesis. *Chem. Rev.* **2014**, *114* (5), 2587-2693. DOI: 10.1021/cr400441m.

(20) Burkey, T.; Hawari, J.; Lossing, F.; Lusztyk, J.; Sutcliffe, R.; Griller, D. The tert-butylperthiyl radical. *J. Org. Chem.* **1985**, *50* (24), 4966-4967. DOI: 10.1021/jo00224a064.

(21) Davies, M. J.; Forni, L. G.; Shuter, S. L. Electron spin resonance and pulse radiolysis studies on the spin trapping of sulphur-centered radicals. *Chem.-Biol. Interact.* **1987**, *61* (2), 177-188. DOI: 10.1016/0009-2797(87)90038-X.

(22) Buettner, G. R. Spin Trapping: ESR parameters of spin adducts 1474 1528V. *Free Radic. Biol. Med.* **1987**, *3* (4), 259-303. DOI: 10.1016/S0891-5849(87)80033-3.

(23) Kalyanaraman, B. Thiyl radicals in biological systems: significant or trivial? In *Biochem. Soc. Symp.*, 1995; Portland Press Limited: Vol. 61, pp 55-63. DOI: 10.1042/bss0610055.

(24) Fontmorin, J. M.; Burgos Castillo, R. C.; Tang, W. Z.; Sillanpää, M. Stability of 5,5-dimethyl-1-pyrroline-N-oxide as a spin-trap for quantification of hydroxyl radicals in processes based on Fenton reaction. *Water Res.* **2016**, *99*, 24-32. DOI: 10.1016/j.watres.2016.04.053.

(25) Rosen, G. M.; Beselman, A.; Tsai, P.; Pou, S.; Mailer, C.; Ichikawa, K.; Robinson, B. H.; Nielsen, R.; Halpern, H. J.; MacKerell, A. D. Influence of conformation on the EPR spectrum of 5, 5-dimethyl-1-hydroperoxy-1-pyrrolidinyloxyl: a spin trapped adduct of superoxide. *J. Org. Chem.* **2004**, *69* (4), 1321-1330. DOI: 10.1021/jo0354894.

(26) Goldstein, S.; Samuni, A.; Merenyi, G. Kinetics of the Reaction between Nitroxide and Thiyl Radicals: Nitroxides as Antioxidants in the Presence of Thiols. *J. Phys. Chem. A* **2008**, *112* (37), 8600-8605. DOI: 10.1021/jp804743g.

(27) Chauvin, J.-P. R.; Griesser, M.; Pratt, D. A. The antioxidant activity of polysulfides: it's radical! *Chem. Sci.* **2019**, *10* (19), 4999-5010. DOI: 10.1039/C9SC00276F.

(28) Boulebd, H. Radical scavenging behavior of butylated hydroxytoluene against oxygenated free radicals in physiological environments: Insights from DFT calculations. *Int. J. Chem. Kinet.* **2022**, *54* (1), 50-57. DOI: 10.1002/kin.21540.

(29) Katritzky, A. R.; Fedoseyenko, D.; Mohapatra, P. P.; Steel, P. J. Reactions of p-benzoquinone with sulfur nucleophiles. *Synthesis* **2008**, *2008* (05), 777-787. DOI: 10.1055/s-2008-1032186.

(30) Snell, J. M.; Weissberger, A. The Reaction of Thiol Compounds with Quinones. *J. Am. Chem. Soc.* **1939**, *61* (2), 450-453. DOI: 10.1021/ja01871a065.

(31) Kutyrev, A. A.; Moskva, V. V. Nucleophilic reactions of quinones. *Russ. Chem. Rev.* **1991**, *60* (1), 72. DOI: 10.1070/RC1991v060n01ABEH001032.

(32) Tallon, M. A. Reactions Involving Maleic Anhydride. In *Handbook of Maleic Anhydride Based Materials: Syntheses, Properties and Applications*, Musa, O. M. Ed.; Springer International Publishing, 2016; pp 59-149.

(33) Sanders, G. C.; Duchateau, R.; Lin, C. Y.; Coote, M. L.; Heuts, J. P. A. End-Functional Styrene–Maleic Anhydride Copolymers via Catalytic Chain Transfer Polymerization. *Macromolecules* **2012**, *45* (15), 5923-5933. DOI: 10.1021/ma301161u.

(34) Chubachi, S.; Chatterjee, P. K.; Tobolsky, A. V. Reaction of dimethyl tetrasulfide with unsaturated compounds. *J. Org. Chem.* **1967**, *32* (5), 1511-1517. DOI: 10.1021/jo01280a046.

(35) Inoue, S.; Ohashi, S. i.; Unno, Y. Asymmetric Addition Catalyzed by Optically Active Polymers. IV. Addition of Lauryl Mercaptan to Dimethyl Maleate and Dimethyl Fumarate. *Polym. J.* **1972**, *3* (5), 611-616. DOI: 10.1295/polymj.3.611.

(36) Simamura, O. The Isomerization of Dimethyl Maleate by Hydrogen Bromide and by Hydrogen Chloride. *Bull. Chem. Soc. Jpn.* **1939**, *14* (1), 22-28. DOI: 10.1246/bcsj.14.22.

(37) Chan, J. W.; Hoyle, C. E.; Lowe, A. B.; Bowman, M. Nucleophile-initiated thiol-Michael reactions: effect of organocatalyst, thiol, and ene. *Macromolecules* **2010**, *43* (15), 6381-6388.

(38) Klinska, M.; Smith, L. M.; Gryn'ova, G.; Banwell, M. G.; Coote, M. L. Experimental demonstration of pH-dependent electrostatic catalysis of radical reactions. *Chem. Sci.* **2015**, *6* (10), 5623-5627. DOI: 10.1039/C5SC01307K.

(39) Ouellette, R. J.; Rawn, J. D. *Organic chemistry: structure, mechanism, synthesis*; Academic Press, 2018.

(40) Zhang, X.-S.; Zhang, Y.-F.; Li, Z.-W.; Luo, F.-X.; Shi, Z.-J. Synthesis of Dibenzo[c,e]oxepin-5(7H)-ones from Benzyl Thioethers and Carboxylic Acids: Rhodium-Catalyzed Double C-H Activation Controlled by Different Directing Groups. *Angew. Chem. Int. Ed.* **2015**, *54* (18), 5478-5482. DOI: 10.1002/anie.201500486.

(41) Abad, A.; Agulló, C.; Cuñat, A. C.; Navarro, I. Conversion of Alkyl Halides into Alcohols via Formyloxylation Reaction with DMF Catalyzed by Silver Salts. *Synthesis* **2005**, *2005* (19), 3355-3361. DOI: 10.1055/s-2005-918453.

(42) Heravi, Majid M.; Ghavidel, M.; Mohammadkhani, L. Beyond a solvent: triple roles of dimethylformamide in organic chemistry. *RSC Adv.* **2018**, *8* (49), 27832-27862. DOI: 10.1039/C8RA04985H.

(43) Mulhearn, D. C.; Bachrach, S. M. Selective Nucleophilic Attack of Trisulfides. An ab Initio Study. *J. Am. Chem. Soc.* **1996**, *118* (39), 9415-9421. DOI: 10.1021/ja9620090.

(44) Gerbaux, P.; Salpin, J.-Y.; Bouchoux, G.; Flammang, R. Thiosulfoxides (X2S=S) and disulfanes (XSSX):: first observation of organic thiosulfoxides. *Int. J. Mass Spectrom.* **2000**, *195-196*, 239-249. DOI: 10.1016/S1387-3806(99)00227-4.

(45) Musio, R. CHAPTER 1 - Applications of 33S NMR Spectroscopy. In *Annual Reports on NMR Spectroscopy*, Webb, G. A. Ed.; Vol. 68; Academic Press, 2009; pp 1-88.

(46) Bagno, A. Ab initio calculation of NMR properties (shielding and electric field gradient) of 33S in sulfur compounds. *J. Mol. Struct. THEOCHEM* **1997**, *418* (2), 243-255. DOI: 10.1016/S0166-1280(96)05013-0.

(47) Gerothanassis, I. P.; Kridvin, L. B. 33S NMR: Recent Advances and Applications. *Molecules* **2024**, *29* (14), 3301. DOI: 10.3390/molecules29143301

(48) House, J. E. *Principles of Chemical Kinetics*; Academic Press, 2007.

4.6 Experimental data and characterizations

General consideration

Materials: All chemicals were purchased from commercial suppliers and used as received. Solvents used for crossover reactions were purchased from the commercial suppliers and used as received, unless otherwise stated. Deionised water was used for chemical reactions.

Analytical thin-layer chromatography and column chromatography

TLC analysis employed commercial aluminium sheets coated with silica gel (Chem-supply, silica gel 60 F254). Compounds were either visualized under UV-light at 254 nm, or by dipping the plates in aqueous potassium permanganate or ceric ammonium molybdate solution followed by heating. Flash column chromatography was performed using a glass chromatography column with silica gel (6 Å, 40 – 63 μm).

NMR (Nuclear magnetic resonance) Spectroscopy

^{1}H and ^{13}C NMR spectra were recorded on a Bruker Ultrashield Plus 600 MHz spectrometer at 600 MHz and 150 MHz respectively, or a Bruker Ascend 400 MHz spectrometer at 400 MHz and 100 MHz respectively. All spectra were obtained at 298 K unless stated otherwise. Deuterated solvents were used as solvent and internal lock unless stated otherwise. Residual solvent peaks were used as an internal reference for ^{1}H NMR spectra [$CDCl_3$ δ 7.26 ppm; DMF-d_7 δ 8.03 ppm; Toluene-d_8 δ 7.09, 2.09 ppm] and for ^{13}C NMR spectra [$CDCl_3$ δ 77.16 ppm, DMF-d_7 δ 163.15 ppm; Toluene-d_8 δ 137.86 ppm].[1,2] Coupling constants (*J*) are quoted to the nearest 0.1 Hz. The following abbreviations, or combinations thereof, were used to describe NMR multiplicities: s = singlet, d = doublet, t = triplet, q = quartet, p = pentet, h = heptet, m = multiplet, ap. = apparent, br. = broad).

GC-MS (Gas chromatography - mass spectrometry)

Many of the trisulfide metathesis reactions were monitored by GC-MS. As a typical example of sample preparation, a 10 μL aliquot was taken from the reaction mixture and diluted with 990 μL of $CHCl_3$, which adequately slows the reaction prior to GC-MS analysis. Where the relative ratio (%) is discussed, values are calculated using the integrated abundance of the species in the chromatogram. GC-MS analysis was performed using an Agilent 5975C series GC-MS system. A 29.4 m x 250 μm x 0.25 μm, (5%-phenyl)-methylpolysiloxane column was used with a helium mobile phase. A 1 μL sample was injected with a split ratio of 60:1 and a gas flow rate of 1.2 mL/min.

The following GC-MS methods were used for experiments as indicated:
GC-MS method **A**: Initial temperature 85 ºC. Hold at 85 ºC for 3 minutes. Ramp rate at 60 ºC/min to 250 ºC. Hold at 250 ºC for 2 minutes. Total run time of 7.75 minutes.

GC-MS method **B**: Initial temperature 30 ºC. Hold at 30 ºC for 3 minutes. Ramp rate at 20 ºC/min to 250 ºC. Hold at 250 ºC for 6 minutes. Total run time was 20 minutes.

GC-MS method **C**: Initial temperature 85 ºC. Hold at 85 ºC for 3 minutes. Ramp rate at 50 ºC/min to 250 ºC. Hold at 250 ºC for 13.7 minutes. Total run time was 20 minutes.

FTIR (Fourier-transform infrared spectroscopy)

FTIR spectra were recorded between 4000 and 450 cm^{-1}, using either a Perkin Elmer Spectrum Two FT-IR Spectrometer equipped with a Universal ATR (Diamond Crystal), or a PerkinElmer Spectrum 100 FT-IR spectrometer equipped with ATR accessory (ZnSe crystal).

EPR (Electron paramagnetic resonance) Spectroscopy

X-band (9.8680 GHz) continuous-wave EPR spectra were acquired at room temperature (298K) using a Bruker Elexsys E500 spectrometer. An aliquot of each sample was transferred to an open ended, quartz capillary tubes capillary tube before being placed in a 10 cm long quartz EPR tube (internal diameter = 2.8 mm, outer diameter = 4.0 mm) for analysis. Spectra were acquired using a microwave power of 5.024 – 20 mW (16 – 10 dB of a 200 mW source), a modulation amplitude of 1 mT and a modulation frequency of 100 kHz. The magnetic field was calibrated with a Gauss Meter. All reagents were degassed with nitrogen for 30 minutes prior to use. EasySpin 5.2.35 in Matlab program (R2023b) was used for EPR spectral data processing and plotting.[3]

Melting point (m.p)

Melting point of crystalline substances was determined using either a Gallenkamp or a DigiMelt 161 SRS (Stanford Research System) melting point apparatus using open ended capillary tubes and are uncorrected.

Trisulfide Crossover – Electron Paramagnetic Resonance (EPR)

EPR spectra were acquired at room temperature (298K). All reagents were degassed with nitrogen for 30 minutes prior to use. An aliquot of each sample was transferred into an open ended, quartz capillary tubes capillary tube before being placed in a 10 cm long quartz EPR tube (internal diameter = 2.8 mm, outer diameter = 4.0 mm) for analysis.

EPR spectra of TEMPO at various concentrations

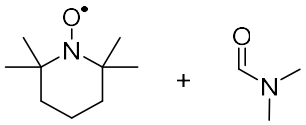

An initial EPR experiment was carried out on TEMPO in DMF, to study the minimum concentration of TEMPO that the instrument can detect. EPR spectra were acquired for three samples of TEMPO: 64, 640, and 6400 nM. The TEMPO radical can still be detected at a concentration of 640 nM.

- TEMPO 6.4 mM (stock A): 10 mg (0.064 mmol) of TEMPO was dissolved in 10 mL of DMF.
- TEMPO 6.4 μM or 6400 nM (stock B): 10 μL of stock A was diluted to 10 mL with DMF.
- TEMPO 640 nM: 100μL of stock B was diluted to 1 mL with DMF.
- TEMPO 64 nM: 10 μL of stock B was diluted to 1 mL with DMF.

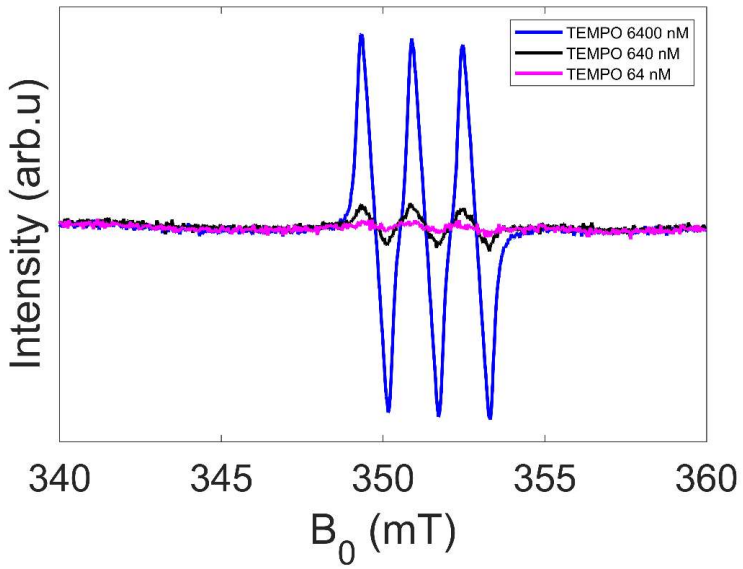

Figure S4.1: EPR spectra of TEMPO in DMF at various concentrations

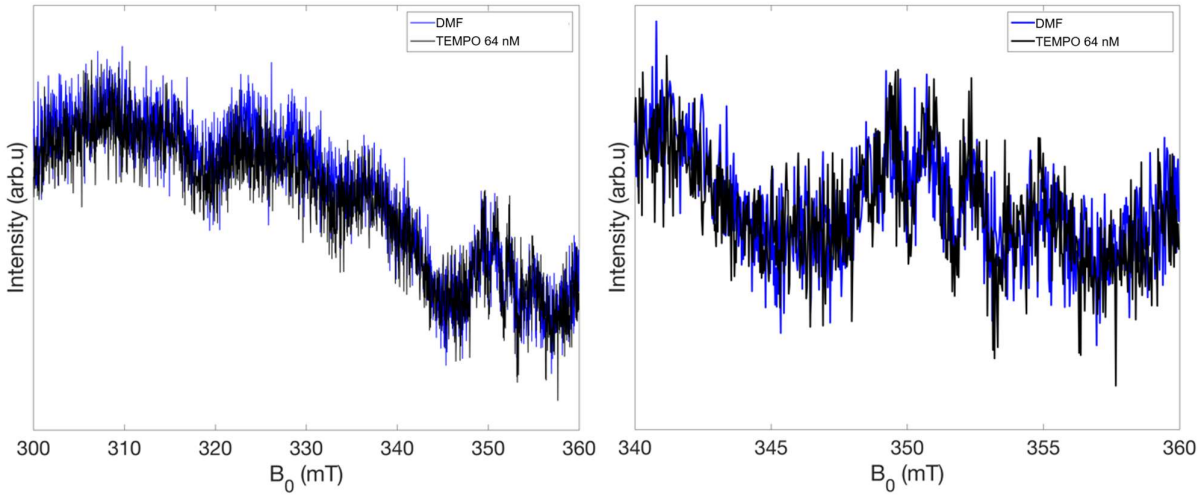

Figure S4.2: EPR spectra comparing DMF only, and 64 nM TEMPO in DMF (right: zoomed at 340 to 360 mT). At a 64 nM TEMPO concentration, EPR signals of TEMPO cannot be observed; the spectrum resembles DMF only

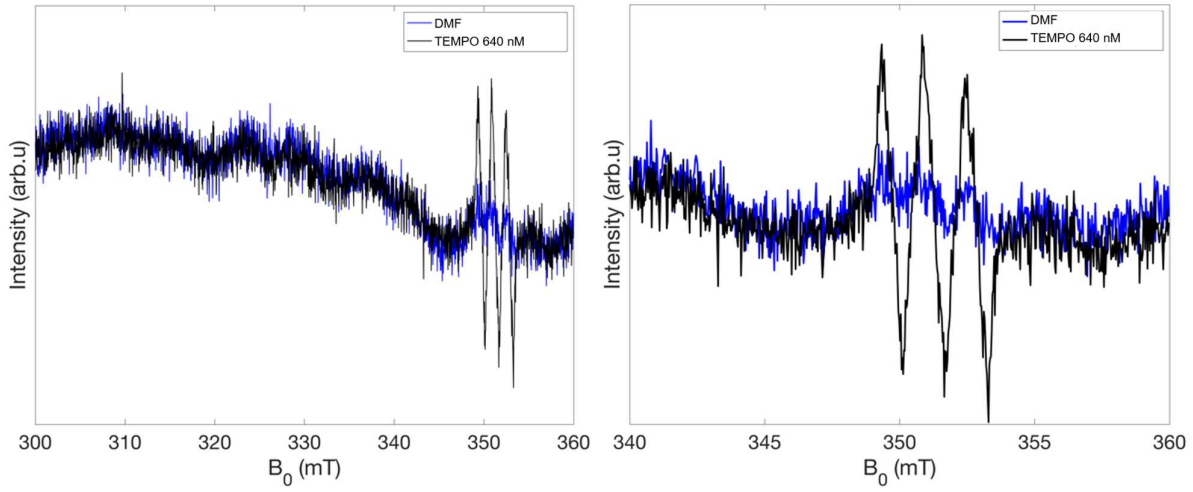

Figure S4.3: EPR spectra comparing DMF only, and 640 nM TEMPO in DMF (right: zoomed at 340 to 360 mT). At a 640 nM TEMPO concentration, EPR signals of TEMPO can be observed.

EPR spectra of Me_2S_3 and $^nPr_2S_3$ – Negative control

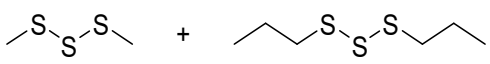

EPR spectra of dimethyl trisulfide, di-*n*-propyl trisulfide and an equimolar mixture of both trisulfides were recorded. Around 100 µL of each trisulfide, and a mixture of both trisulfides, were transferred to a capillary tube and placed into an EPR tube for EPR analysis. No S-centred radical was observed.

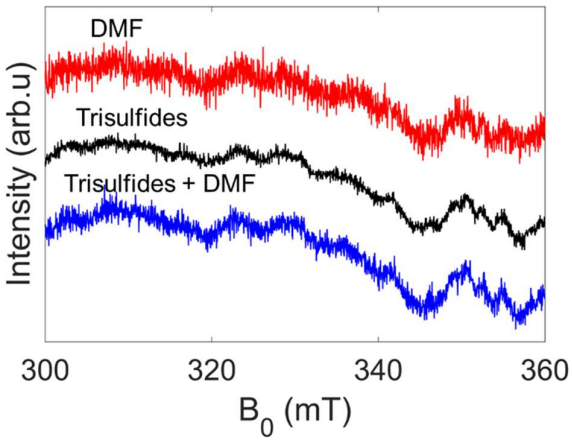

Figure S4.4: EPR spectra of the trisulfides (neat)

EPR spectra of Me_2S_3 in DMF

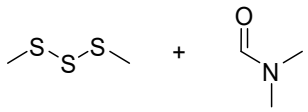

Dimethyl trisulfide was dissolved in DMF at various concentrations. After mixing for 5 minutes, each sample was transferred into a capillary tube and placed into an EPR tube for analysis. No S-centred radical was observed.

- Me_2S_3:DMF 1:4 (40µL, 0.38 mmol Me_2S_3 and 117.3µL, 1.52 mmol DMF – **2.42 M**)
- Me_2S_3:DMF 1:1 (80µL, 0.76 mmol Me_2S_3 and 58.6µL, 0.76 mmol DMF – **5.49 M**)
- Me_2S_3:DMF 4:1 (100µL, 0.95 mmol Me_2S_3 and 18.3µL, 0.24 mmol DMF – **8.04 M**)

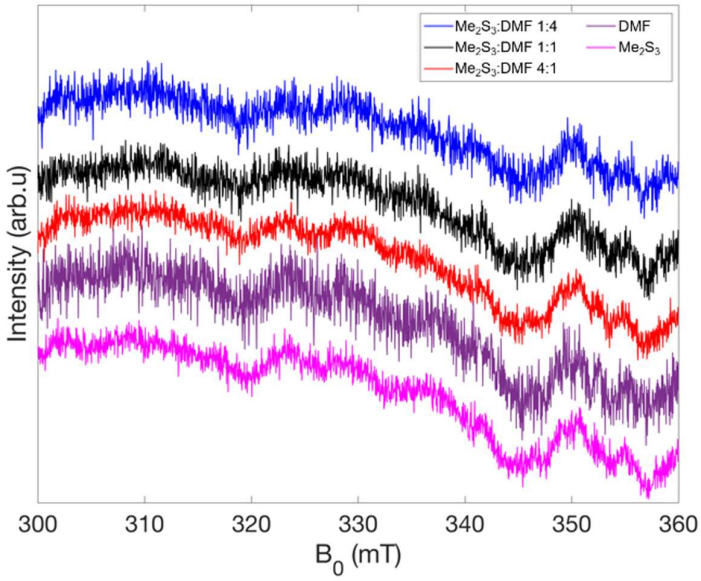

Figure S4.5: EPR spectra of Me_2S_3 in DMF at various concentrations

EPR spectra of Me_2S_3 and $^nPr_2S_3$ in DMF

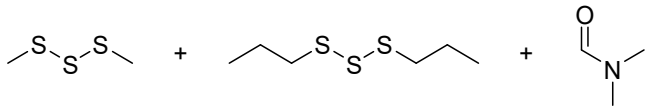

Dimethyl trisulfide and di-*n*-propyl trisulfide were mixed with DMF at various concentrations stated below. After mixing for 5 minutes, each sample was transferred into a capillary tube and placed into an EPR tube for analysis. No S-centred radical was observed.

- Me_2S_3:$^nPr_2S_3$:DMF 1:1:1 (40µL, 0.38 mmol Me_2S_3; 64.2µL, 0.38 mmol $^nPr_2S_3$; and 29.31µL, 0.38 mmol DMF – **2.85 M** for either trisulfide)
- Me_2S_3:$^nPr_2S_3$:DMF 2:2:1 (40µL, 0.38 mmol Me_2S_3; 64.2µL, 0.38 mmol $^nPr_2S_3$; and 14.7µL, 0.19 mmol DMF – **3.20 M** for either trisulfide)
- Me_2S_3:$^nPr_2S_3$:DMF 1:1:8 (20µL, 0.19 mmol Me_2S_3; 32.1µL $^nPr_2S_3$, 0.19 mmol; and 117.3µL, 1.52 mmol DMF – **1.12 M** for either trisulfide).

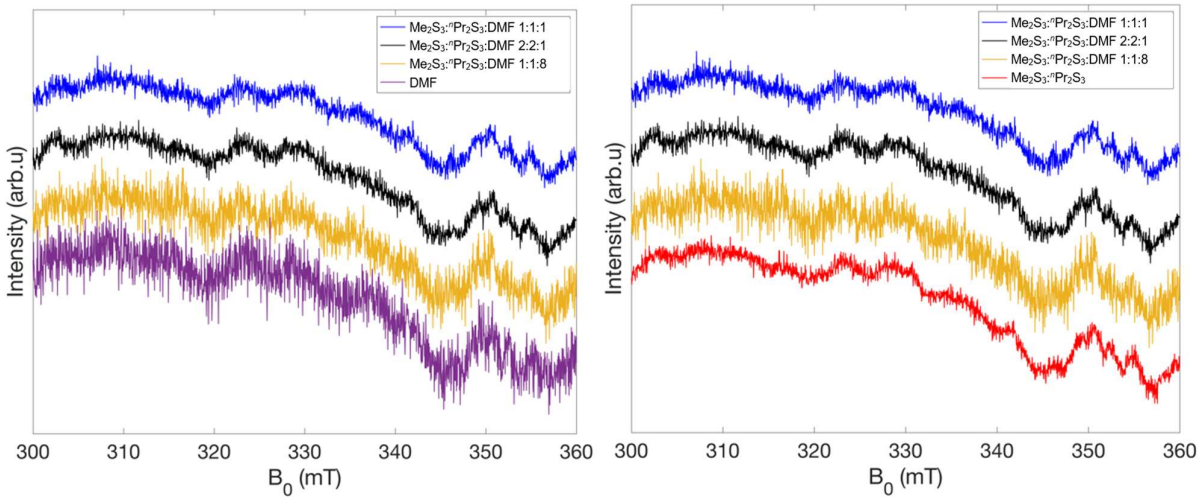

Figure S4.6: EPR spectra of the trisulfides in DMF – comparison with DMF (left) and Me_2S_3/ $^nPr_2S_3$ only (right).

EPR spectra of Me_2S_3 and TEMPO in DMF

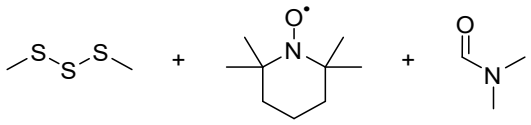

6.72 µL of dimethyl trisulfide (64 µmol) was made up to 10 mL with DMF to give a 6.4 mM dimethyl trisulfide solution (stock C). 10 µL of stock C was diluted to 10 mL with DMF to give a 6.4 µM dimethyl trisulfide solution (stock D). TEMPO stock B (6.4 µM) and trisulfide stock D (6.4 µM) were used for experiments. Samples were prepared as follows:

- TEMPO:$Me_2S_3$1:1 (100 µL TEMPO 6.4µM (1 eq.) and 100 µL Me_2S_3 6.4µM (1 eq.)
- TEMPO:$Me_2S_3$5:1 (100 µL TEMPO 6.4µM (5 eq.) and 20 µL Me_2S_3 6.4µM (1 eq.)
- TEMPO:$Me_2S_3$1:5 (100 µL TEMPO 6.4µM (1 eq.) and 500 µL Me_2S_3 6.4µM (5 eq.)
- TEMPO:$Me_2S_3$1:Excess (100 µL TEMPO 6.4µM (1 eq.) and 100 µL Me_2S_3 (1,485,000 eq. or excess)

Each sample was made up to 1 mL in DMF, resulting in the same TEMPO concentration across all EPR experiments. EPR was ran immediately after sample preparation.

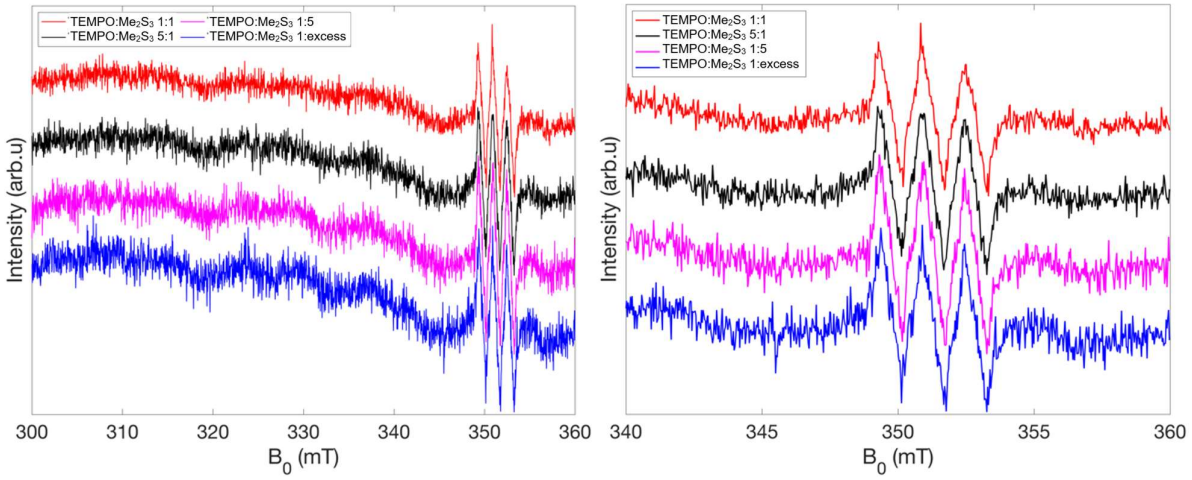

Figure S4.7: EPR spectra of TEMPO and Me_2S_3 mixtures in DMF.

EPR spectra of Me_2S_3, $^nPr_2S_3$, and TEMPO in DMF

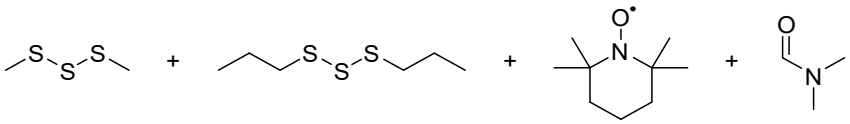

6.72 µL of dimethyl trisulfide (64 µmol) and 10.85 µL of di-*n*-propyl trisulfide (64 µmol) was made up to 10 mL with DMF to give stock E (6.4 mM of each trisulfide). 10 µL of stock E was diluted to 10 mL with DMF to give stock F (6.4 µM of each trisulfide). TEMPO stock B (6.4 µM) and trisulfides stock F (6.4 µM) were used for experiments. Samples were prepared as follows:

- TEMPO:Me_2S_3:$^nPr_2S_3$ 1:1:1 (100 µL TEMPO 6.4µM (1 eq.) and 100 µL Me_2S_3/ $^nPr_2S_3$ 6.4µM (1 eq. each)
- TEMPO:Me_2S_3:$^nPr_2S_3$ 5:1:1 (100 µL TEMPO 6.4µM (5 eq.) and 20 µL Me_2S_3/ $^nPr_2S_3$ 6.4µM (1 eq. each)
- TEMPO:Me_2S_3:$^nPr_2S_3$ 1:5:5 (100 µL TEMPO 6.4µM (1 eq.) and 500 µL Me_2S_3/ $^nPr_2S_3$ 6.4µM (5 eq. each)
- TEMPO:Me_2S_3:$^nPr_2S_3$ 1:Excess:Excess (100 µL TEMPO 6.4µM (1 eq.), 100 µL Me_2S_3 (1,485,000 eq. or excess) and 160.5 µL DPTS (1,485,000 eq. or excess)

Each sample was made up to 1 mL in DMF, resulting in the same TEMPO concentration across all EPR experiments. EPR was ran immediately after sample preparation.

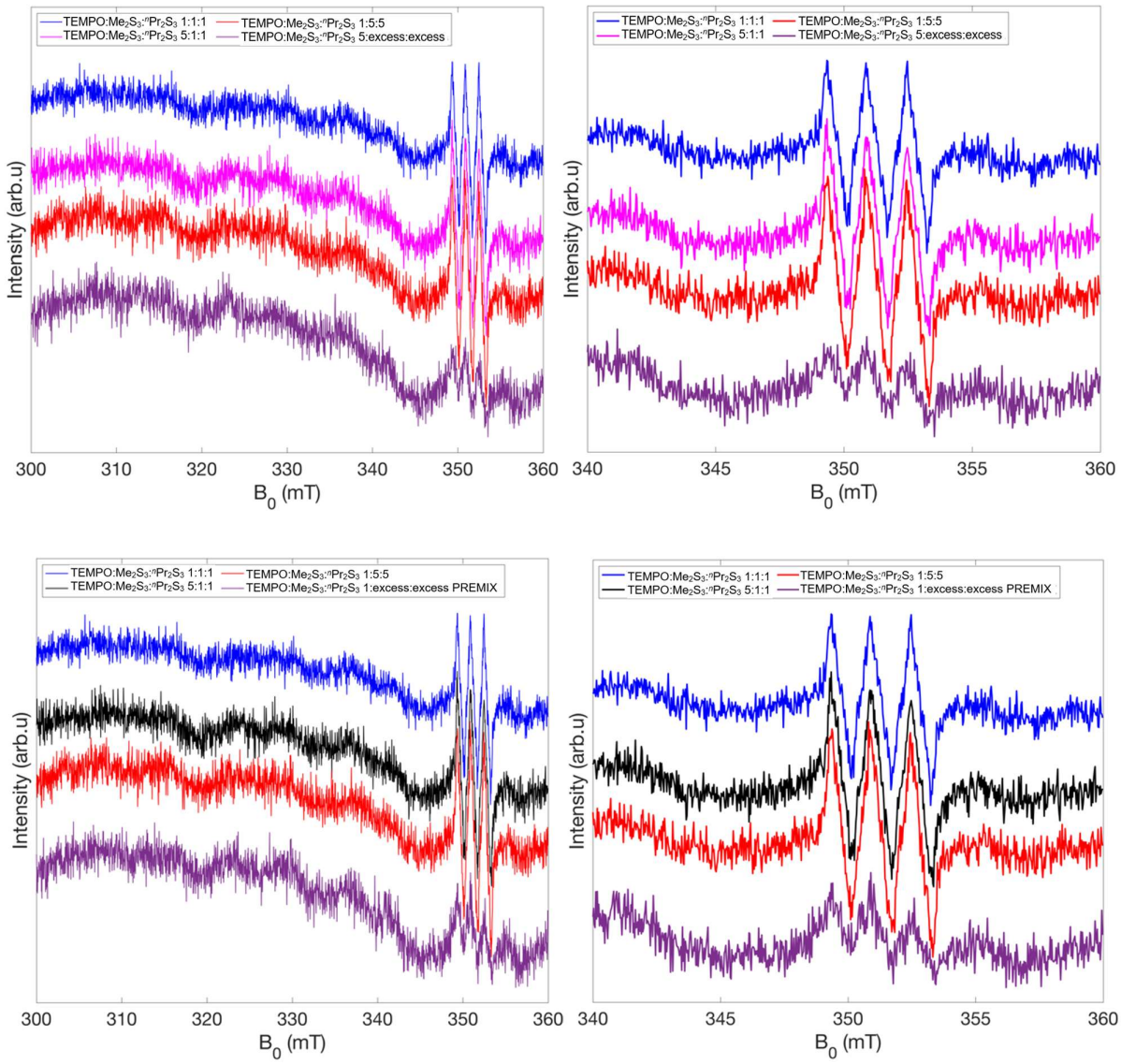

Figure S4.8: EPR spectra of TEMPO/Me_2S_3/ $^nPr_2S_3$ mixtures in DMF. Zoomed spectra from 340 to 360 mT (right).

Radical spin trap experiments with DMPO

5,5-Dimethyl-1-pyrroline *N*-oxide (DMPO) was used as a radical spin trap. If any sulfur centred radical was present in the reaction mixture containing trisulfide(s) and DMF, a DMPO spin adduct would then give EPR signals.[4] Initially, DMPO was tested using Fenton chemistry (to generate •OH). Based on the literature,[5] a DMPO-OH spin adduct gives signals with a 1:2:2:1 pattern. Negative control experiments were also carried out.

EPR spectra of DMPO and iron(II) in DMF – Negative controls

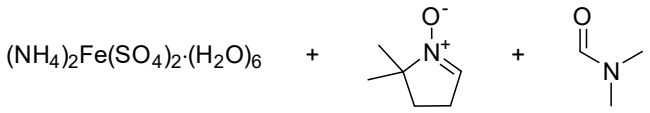

A stock solution of DMPO (6.4 mM) was made by dissolving 9 mg of DMPO in 12.43 mL of DMF. This stock solution was kept cold with dry ice. The EPR spectrum of 6.4 mM DMPO in DMF was recorded.

A solution of 1 mM iron(II) was made by dissolving 7 mg of $(NH_4)_2Fe(SO_4)_2(H_2O)_6$ in 18 mL of water. The EPR spectrum of Fe(II) (12.5 µL, 1 mM Fe(II)) in 100 µL DMF was recorded.

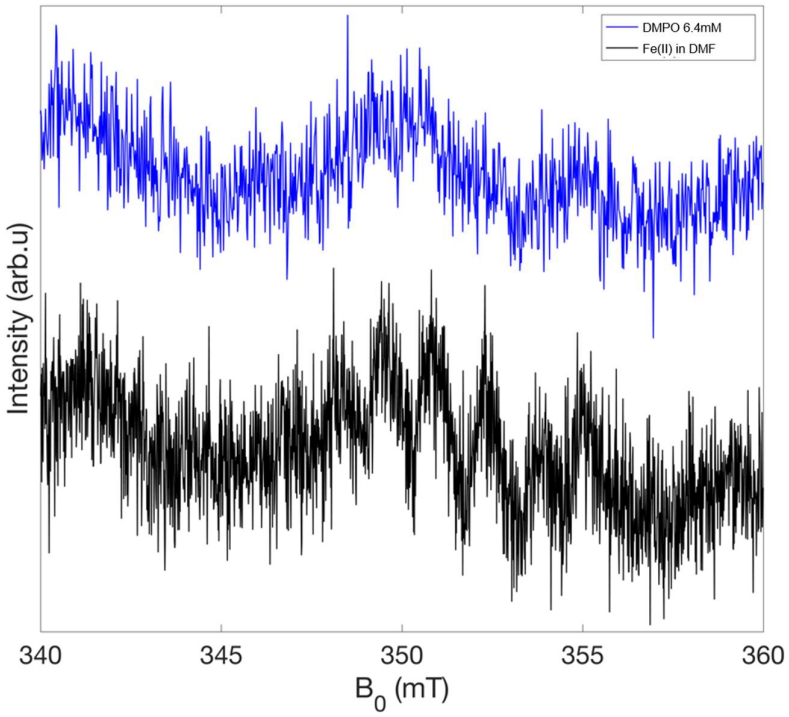

Figure S4.9: EPR spectra of DMPO in DMF (6.4mM) and Fe(II) in DMF (12.5 µL, 1mM Fe(II) and 100 µL of DMF) (negative controls)

EPR spectra of DMPO under Fenton oxidation conditions in DMF – Positive control

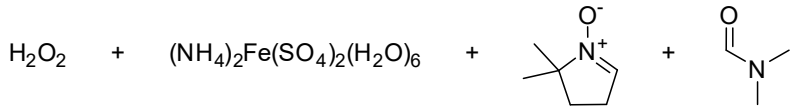

12.5 µL Fe stock (1 mM), 7 µL of ~3% H_2O_2, and 100 µL of stock DMPO (6.4 mM) were mixed. The EPR spectrum of this mixture was recorded immediately.

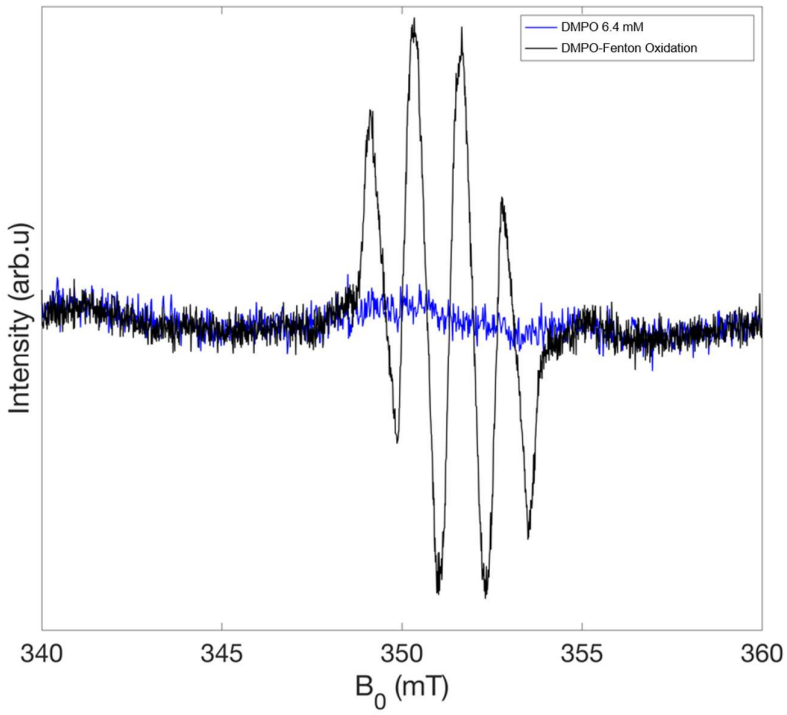

Figure S4.10: EPR spectra of DMPO in DMF (6.4mM), and DMPO under Fenton oxidation conditions.

EPR spectra of DMPO and Me_2S_3 in DMF

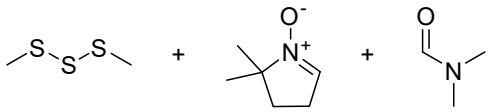

DMPO stock solution 6.4 mM (9 mg DMPO in 12.43 mL DMF). This stock solution was kept cold with dry ice. This sample was run as a negative control. EPR spectrum was recorded from 320 to 360 mT for a full scan and from 340 to 360 mT for a narrow range scan.

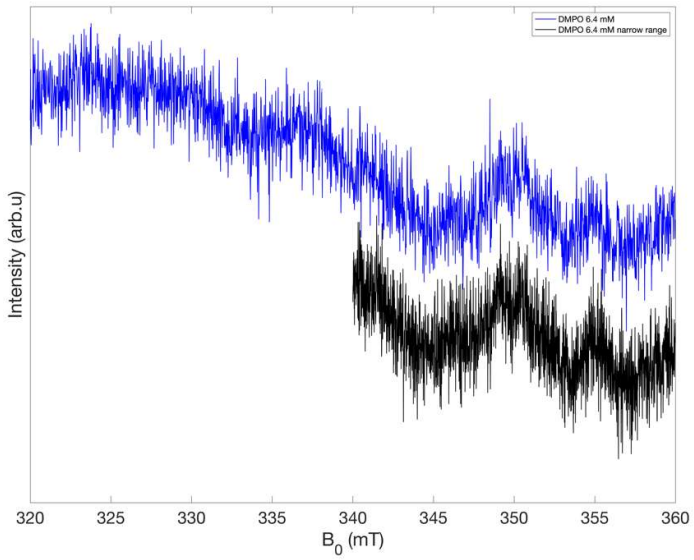

Figure S4.11: EPR spectra of 6.4 mM DMPO solution in DMF.

A stock solution of DMPO (6.4 mM) was made by dissolving 9 mg of DMPO in 12.43 mL of DMF. This stock solution was kept cold with dry ice.

- DMPO + Me_2S_3 149 eq. = 100 µL stock solution of DMPO (6.4 mM, 1 eq.) with 10 µL Me_2S_3 neat (149 eq.)
- DMPO + Me_2S_3 1 eq. each = 100 µL stock solution of DMPO (6.4 mM, 1 eq.) with 100 µL Me_2S_3 stock C (6.4 mM, 1 eq.)
- DMPO 5 eq. + Me_2S_3 1 eq. = 500 µL stock G DMPO (6.4 mM, 1 eq.) with 100 µL Me_2S_3 stock C (6.4 mM, 0.2 eq.)
- DMPO 1 eq. + Me_2S_3 5 eq. = 100 µL stock G DMPO (6.4 mM, 1 eq.) with 500 µL Me_2S_3 stock C (6.4 mM, 1 eq.)

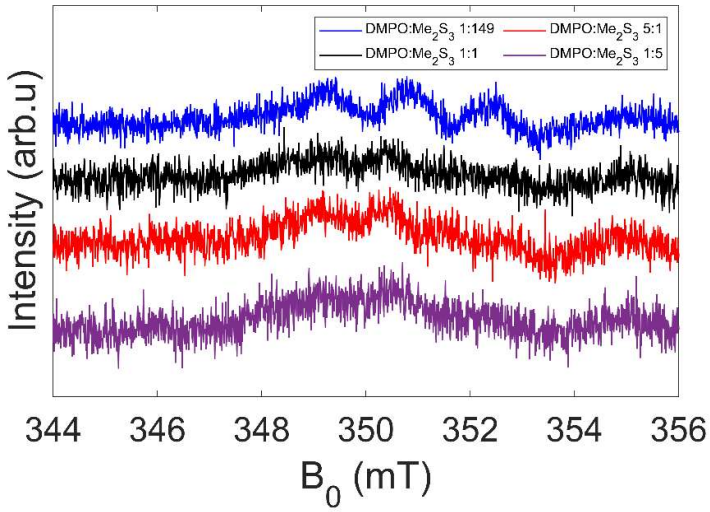

Figure S4.12: EPR spectra of DMPO and Me_2S_3 mixtures.

TEMPO NMR Spectroscopy Experiments

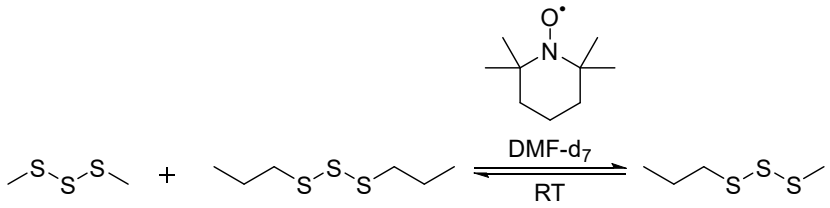

TEMPO (6.9 mg, 44 μmol, 0.10 eq.) in 368 μL of degassed *N*,*N*-dimethylformamide-d_7 (DMF-d_7) was added to an NMR tube under an atmosphere of nitrogen giving a solution 0.12 M in TEMPO (^{1}H NMR –Figure S4.13). Then, dimethyl trisulfide (46.5 μL, 44.2 μmol, 1.0 eq.) and di-*n*-propyl trisulfide (74.6 μL, 44.2 μmol, 1.0 eq.) were added, giving a final TEMPO concentration of 0.09 M. The trisulfide addition was monitored by NMR; 0.1 eq. of each trisulfide in total (^{1}H NMR –Figure S4.14), 0.5 eq. of each trisulfide in total (^{1}H NMR –Figure S4.15), and 1.0 eq. of each trisulfide in total (^{1}H NMR –Figure S4.16). Following the trisulfide additions, the NMR tube was monitored over time at 0.5 hours (^{1}H NMR –Figure S4.17), 1 hour (^{1}H NMR –Figure S4.18), and 17 hours (^{1}H NMR –Figure S4.19).

TEMPO (7.1 mg, 45 μmol, 0.10 eq.) in 496 μL of degassed *N*,*N*-dimethylformamide-d_7 (DMF-d_7) was added to an NMR tube under an atmosphere of nitrogen to give a 0.09 M solution of TEMPO (^{1}H NMR –Figure S4.20). The concentration of this solution mimics the dilution of the 0.12 M TEMPO solution following the addition of 1.0 eq. of both dimethyl trisulfide and di-*n*-propyl trisulfide. For all NMR experiments parameter acquisition was as follows: sw = 100 ppm, aq. = 2.72 sec, d1 = 2.0 sec. and lb = 0.3 Hz. The broad TEMPO signal strength appears to have been attenuated as more of the trisulfides were added (^{1}H NMR –Figure S4.21). Following addition of the trisulfides, the TEMPO signal strength did not appear to change over a 17-hour period (^{1}H NMR –Figure S4.19).

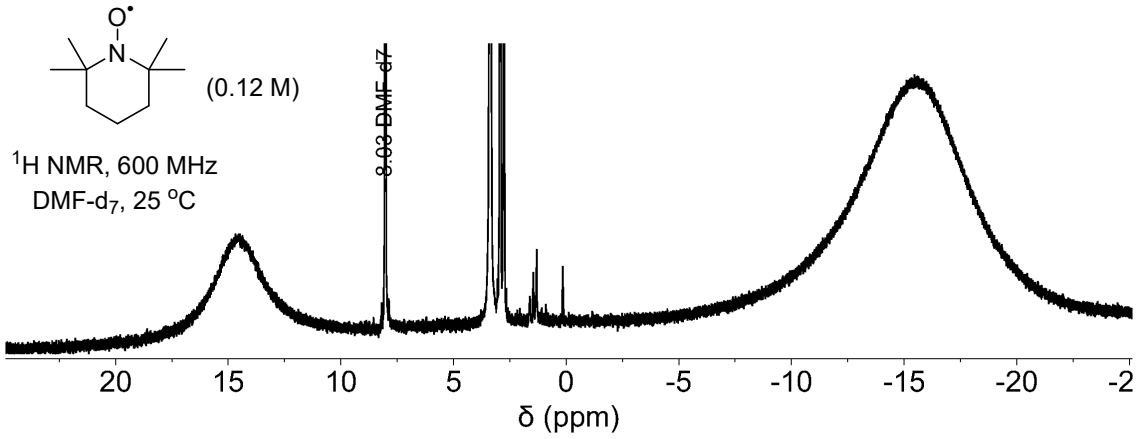

Figure S4.13: ^{1}H NMR spectrum of TEMPO (0.12 M) in DMF-d_7.

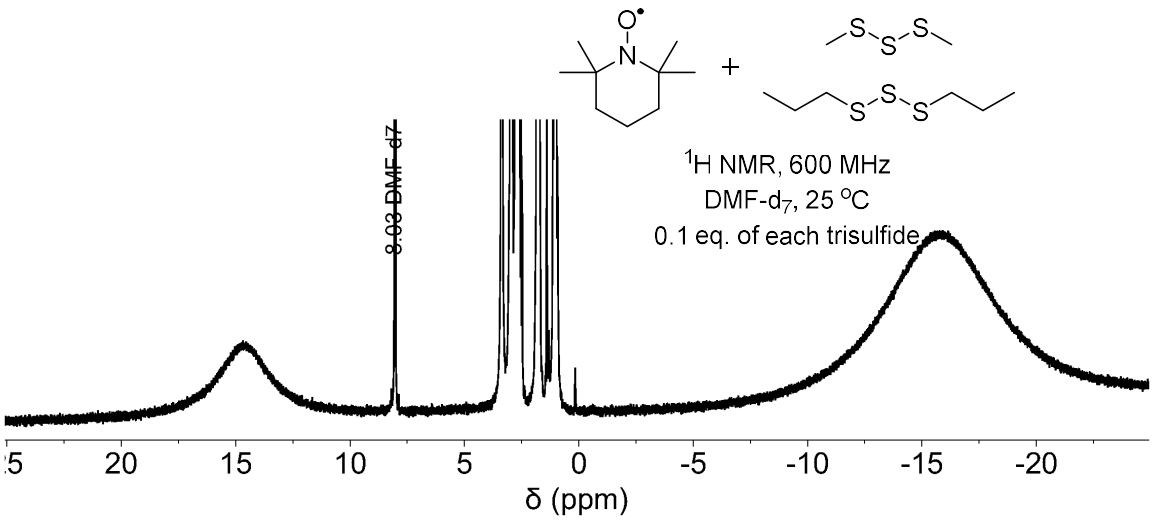

Figure S4.14: ^{1}H NMR spectrum of TEMPO in DMF-d_7 with 0.1 eq. of dimethyl trisulfide (Me_2S_3) and 0.1 eq. of di-*n*-propyl trisulfide ($^{n}Pr_2S_3$).

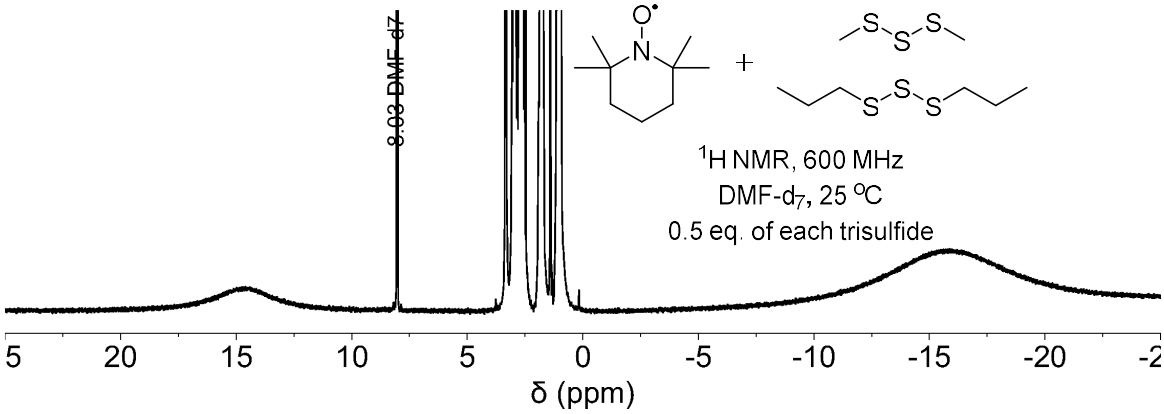

Figure S4.15: ^{1}H NMR spectrum of TEMPO in DMF-d_7 with 0.5 eq. of dimethyl trisulfide (Me_2S_3) and 0.5 eq. of di-*n*-propyl trisulfide ($^{n}Pr_2S_3$).

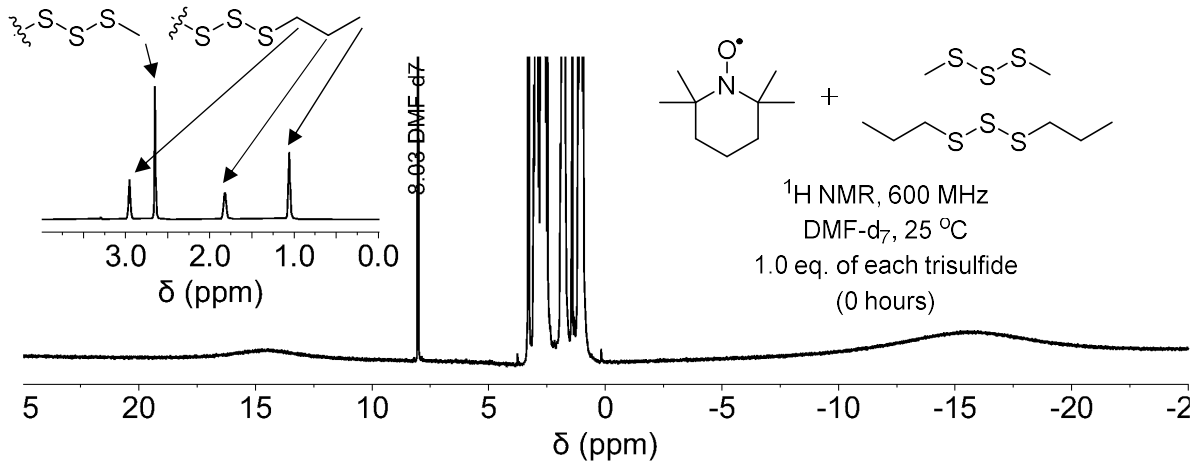

Figure S4.16: ^{1}H NMR spectrum of TEMPO in DMF-d_7 with 1.0 eq. of dimethyl trisulfide (Me_2S_3) and 1.0 eq. of di-*n*-propyl trisulfide ($^{n}Pr_2S_3$) at time 0 hours, and a zoomed in view of the 0 – 4 ppm region where the trisulfide C-H signals are located.

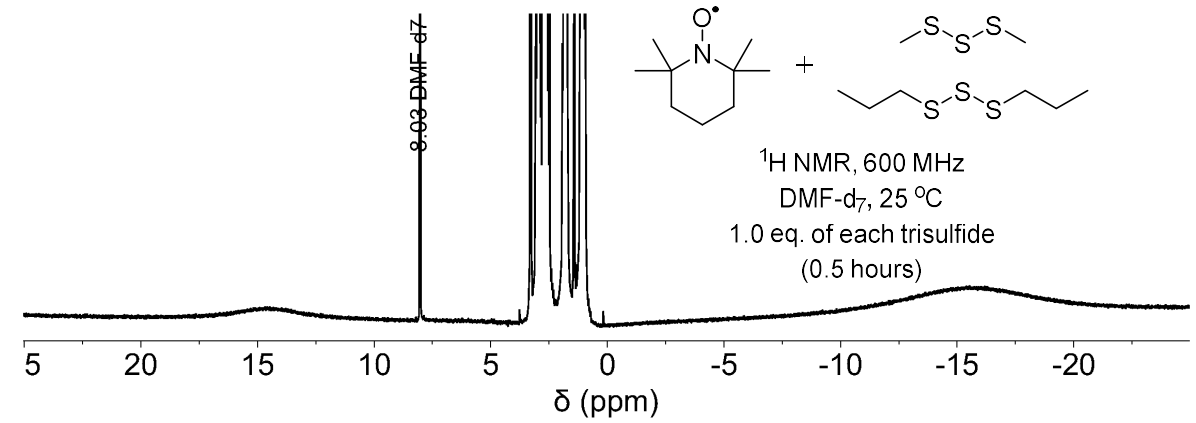

Figure S4.17: ^{1}H NMR spectrum of TEMPO in DMF-d_7 with 1.0 eq. of dimethyl trisulfide (Me_2S_3) and 1.0 eq. of di-*n*-propyl trisulfide ($^{n}Pr_2S_3$), at time 0.5 hours.

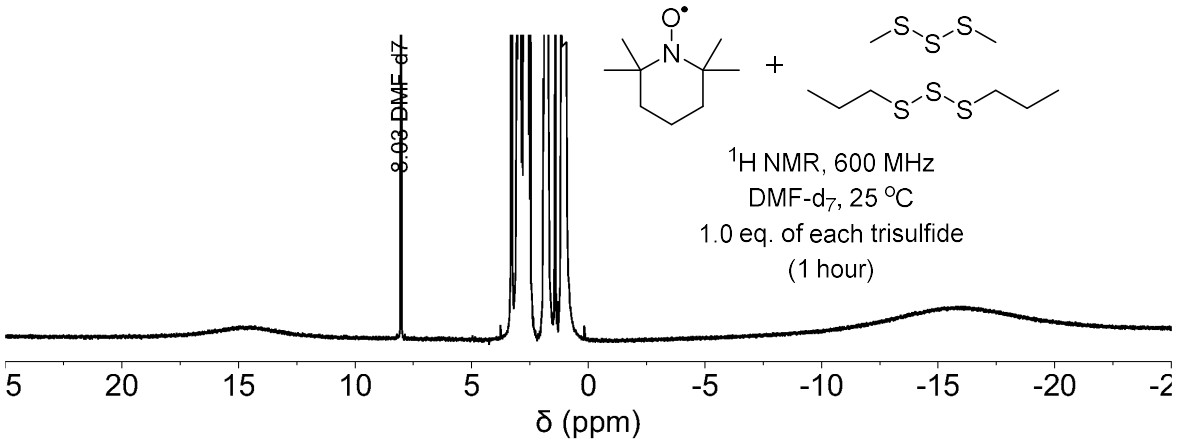

Figure S4.18: ^{1}H NMR spectrum of TEMPO in DMF-d_7 with 1.0 eq. of dimethyl trisulfide (Me_2S_3) and 1.0 eq. of di-*n*-propyl trisulfide ($^{n}Pr_2S_3$), at time 1 hour.

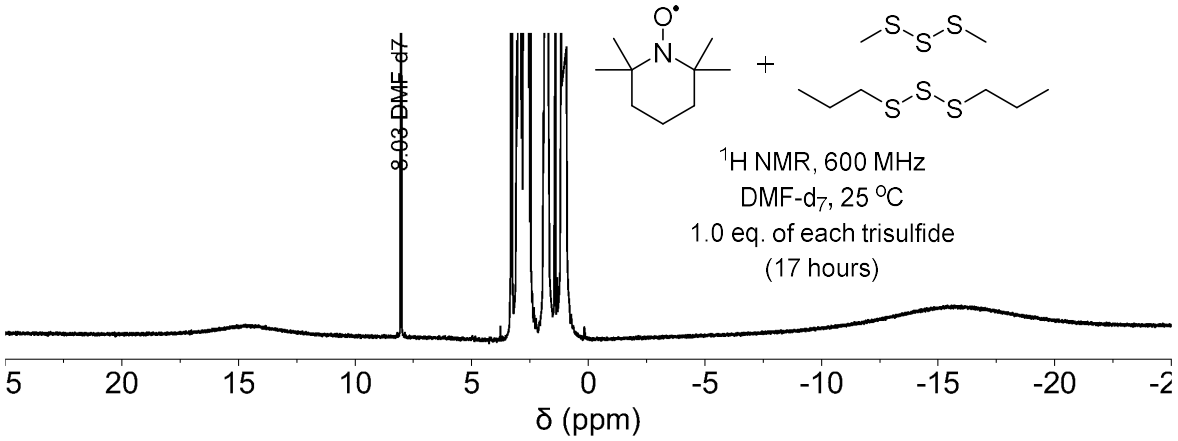

Figure S4.19: ^{1}H NMR spectrum of TEMPO in DMF-d_7 with 1.0 eq. of dimethyl trisulfide (Me_2S_3) and 1.0 eq. of di-*n*-propyl trisulfide ($^{n}Pr_2S_3$), at time 17 hours.

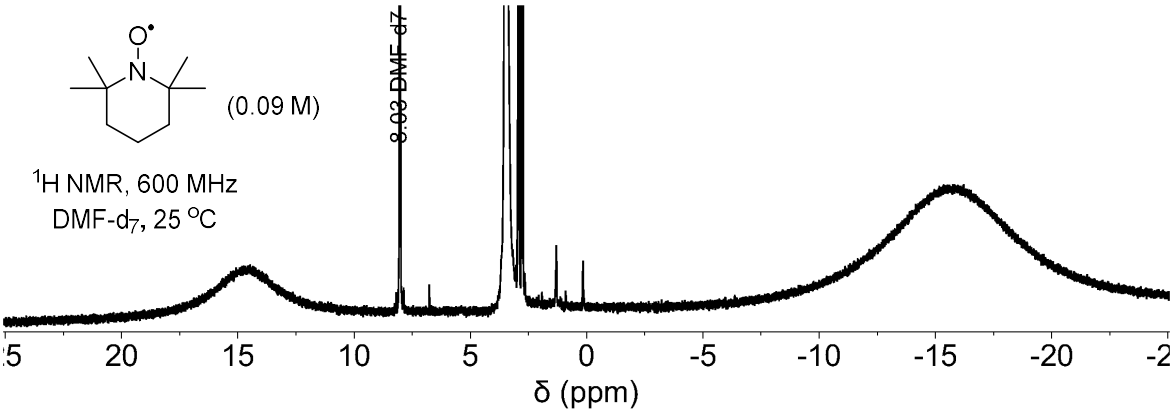

Figure S4.20: ^{1}H NMR spectrum of TEMPO (0.09 M) in DMF-d$_7$.

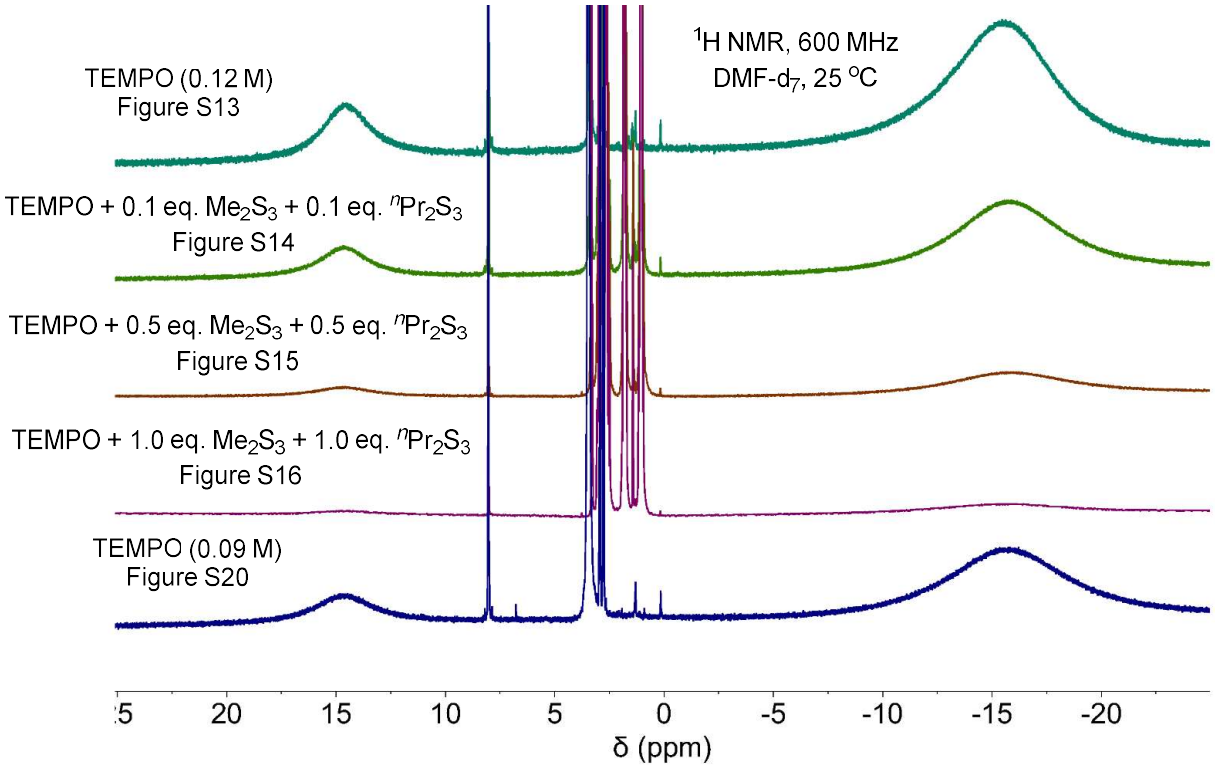

Figure S4.21: Comparison of normalized ^{1}H NMR spectra from (top to bottom). As trisulfides were added to a 0.12 M solution of TEMPO in *N*,*N*-dimethylformamide-d$_7$ (DMF-d$_7$), the broad TEMPO NMR signal strength was attenuated. A 0.09 M solution of TEMPO in *N*,*N*-dimethylformamide-d$_7$ (DMF-d$_7$) mimics the final TEMPO concentration following the addition of 1.0 eq. of both dimethyl trisulfide (Me$_2$S$_3$) and di-*n*-propyl trisulfide (^{n}Pr$_2$S$_3$).

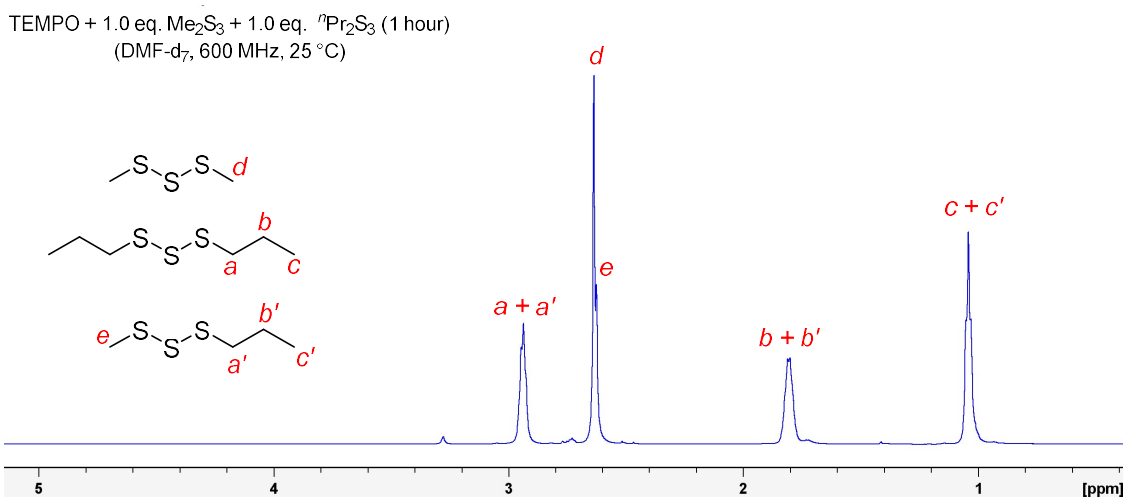

Figure S4.22: Expanded ^{1}H NMR spectrum (DMF-d_7, 600 MHz) of TEMPO-trisulfide mixture at 1.0 eq. at 1 h. Only the trisulfides were observed.

Trisulfide Crossover – Small Molecule Inhibition

Me_2S_3 and $^{n}Pr_2S_3$ crossover in the presence of TEMPO

Me_2S_3 and nPr_2S_3 crossover in DMF (control)

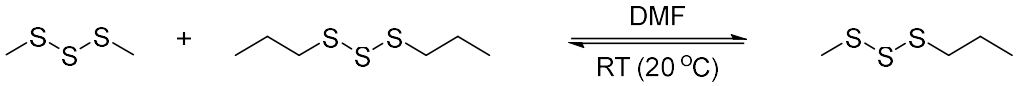

713 µL of degassed *N*,*N*-dimethylformamide (DMF) was added to a vial under an atmosphere of nitrogen. A mixture of dimethyl trisulfide (97.3 µL, 925 µmol, 1.0 eq.) and di-*n*-propyl trisulfide (156 µL, 925 µmol, 1.0 eq.) was added, and the reaction monitored by GC-MS over time: 1 min and 5 min. GC-MS samples were prepared by taking a 10 µL aliquot from the reaction mixture and "quenching" by diluting with 990 µL of $CHCl_3$, which adequately slows the reaction prior to GC-MS analysis. The crossover reaction occurs in DMF.

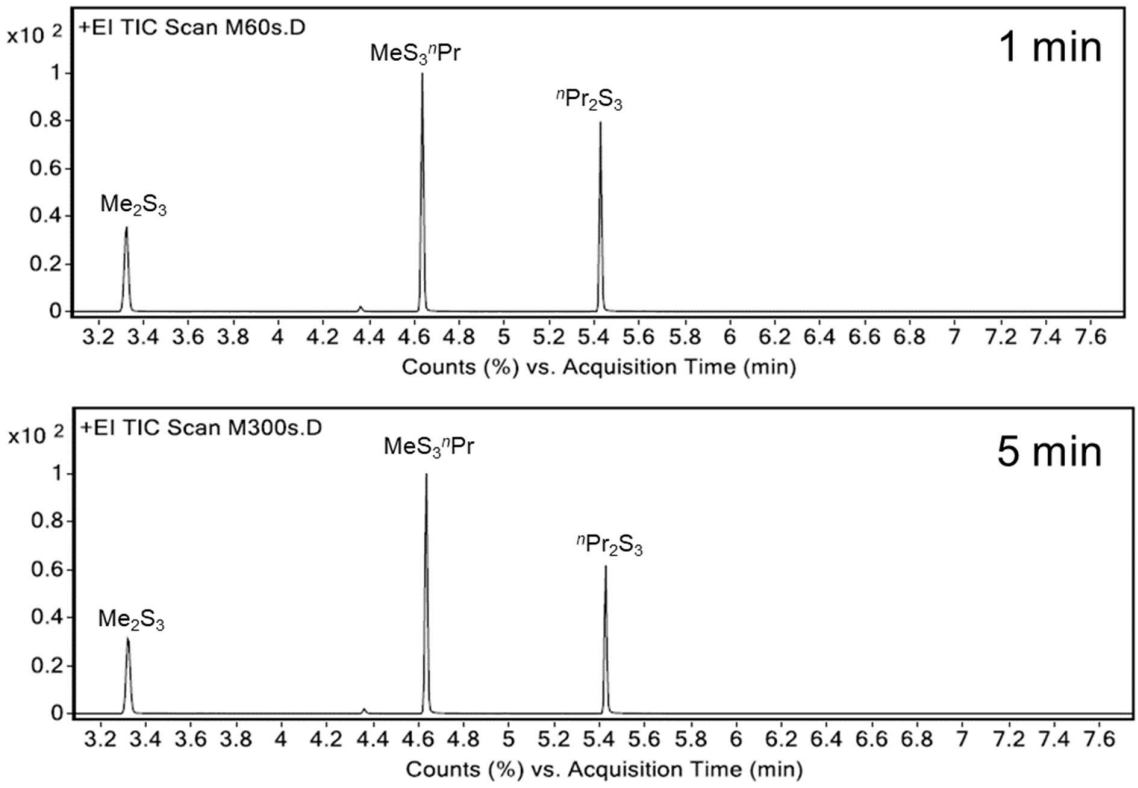

Figure S4.23: Gas chromatogram of the reaction between dimethyl trisulfide (Me_2S_3) and di-*n*-propyl trisulfide ($^nPr_2S_3$) in *N*,*N*-dimethylformamide (DMF) after 1 minute and 5 minutes. GC-MS method A. Retention time: Me_2S_3 (3.33 min), $MeS_3{}^nPr$ (4.64 min), and $^nPr_2S_3$ (5.43 min).

Me_2S_3 and nPr_2S_3 crossover in DMF in the presence of TEMPO (10 mol%)

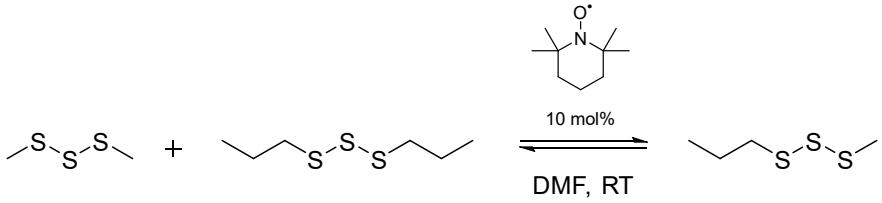

significant reduction in the rate of crossover

TEMPO (14 mg, 93 µmol, 10 mol%) in 713 µL of degassed *N*,*N*-dimethylformamide (DMF) was added to a vial under an atmosphere of nitrogen. Degassed dimethyl trisulfide (97.3 µL, 925 µmol, 1.0 eq.) and di-*n*-propyl trisulfide (156 µL, 925 µmol, 1.0 eq.) were added, and the reaction monitored by GC-MS over time: 1 min, 5 min, 30 min, and 60 min. GC-MS samples were prepared by taking a 10 µL aliquot from the reaction mixture and "quenching" by diluting with 990 µL of $CHCl_3$, which adequately slows the reaction prior to GC-MS analysis. TEMPO inhibited the reaction.

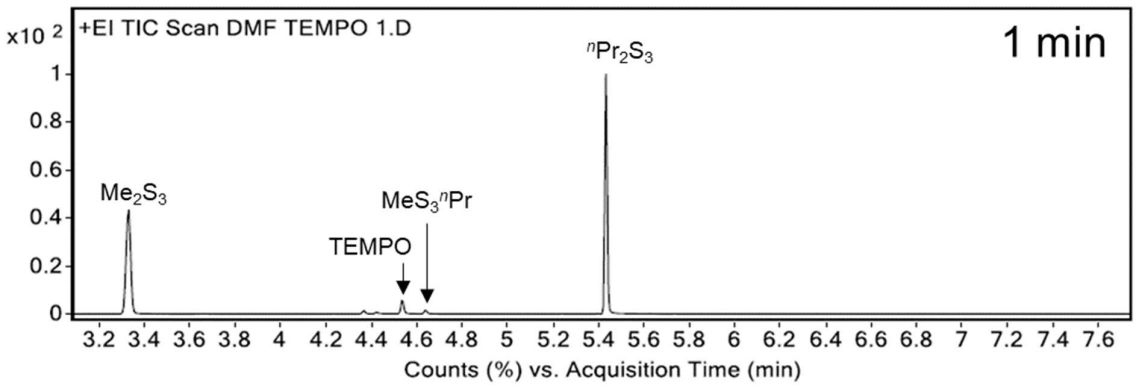
x10 2
+EI TIC Scan DMF TEMPO 1.D
1 min
$^{n}Pr_2S_3$
Me_2S_3
$MeS_3{}^{n}Pr$
TEMPO
0
0.2
0.4
0.6
0.8
1
3.2 3.4 3.6 3.8 4 4.2 4.4 4.6 4.8 5 5.2 5.4 5.6 5.8 6 6.2 6.4 6.6 6.8 7 7.2 7.4 7.6
Counts (%) vs. Acquisition Time (min)

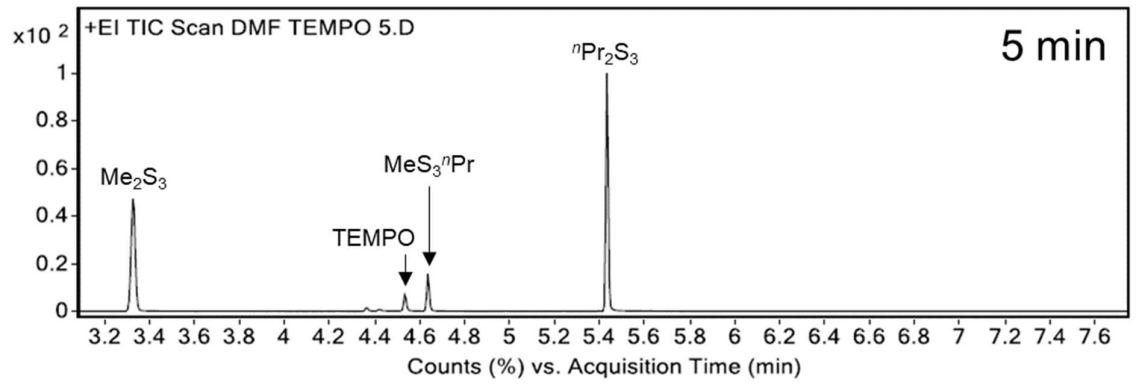
x10 2
+EI TIC Scan DMF TEMPO 5.D
5 min
$^{n}Pr_2S_3$
Me_2S_3
$MeS_3{}^{n}Pr$
TEMPO
0
0.2
0.4
0.6
0.8
1
3.2 3.4 3.6 3.8 4 4.2 4.4 4.6 4.8 5 5.2 5.4 5.6 5.8 6 6.2 6.4 6.6 6.8 7 7.2 7.4 7.6
Counts (%) vs. Acquisition Time (min)

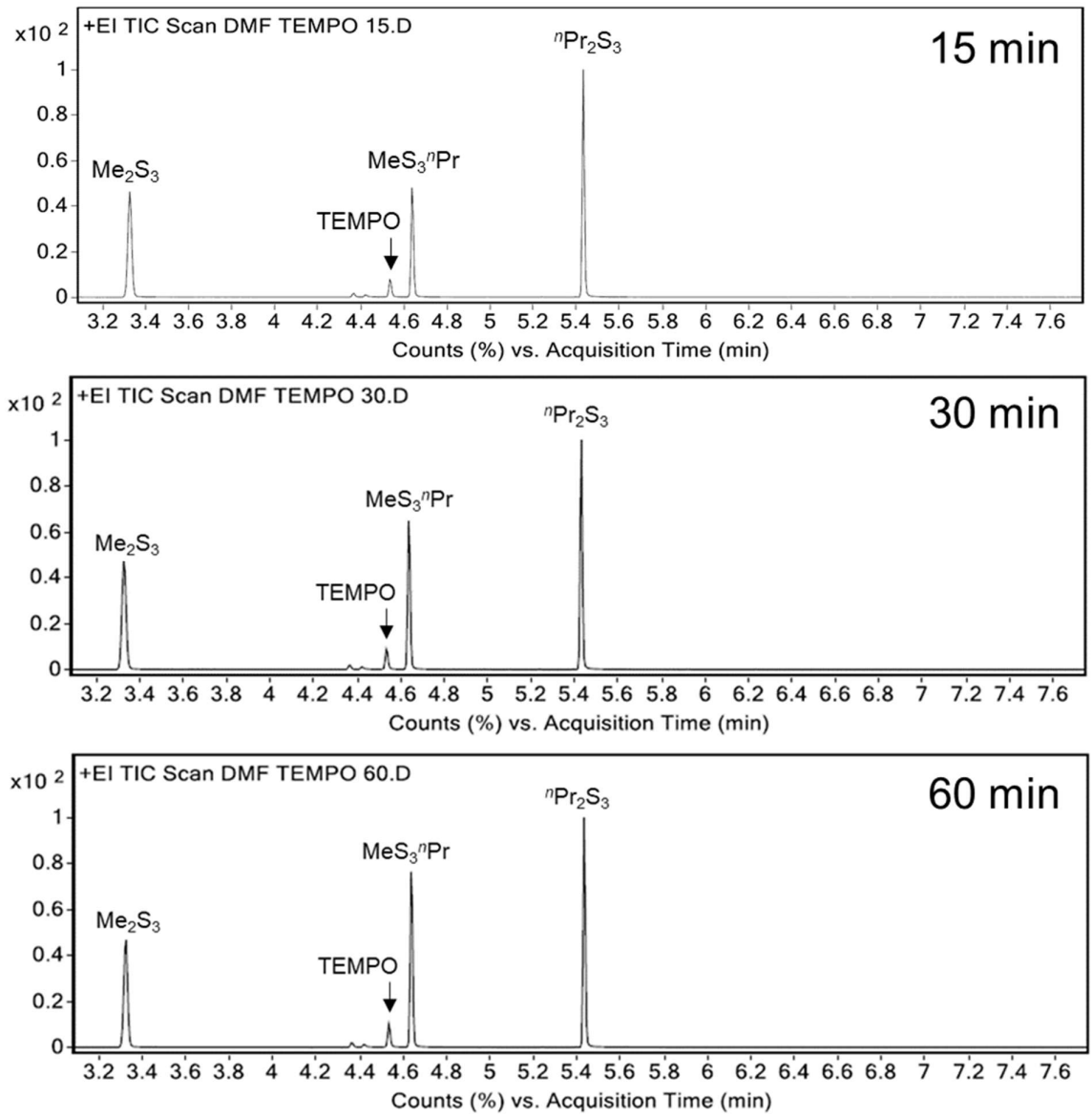

Figure S4.24: Gas chromatograms of the reaction between Me_2S_3 and $^{n}Pr_2S_3$ in DMF, in the presence of TEMPO after 1, 5, 15, 30 and 60 minutes. GC-MS method A. Retention time: Me_2S_3 (3.327 min), TEMPO (4.535 min), $MeS_3{}^{n}Pr$ (4.638 min), and $^{n}Pr_2S_3$ (5.433 min).

Me_2S_3 and nPr_2S_3 crossover in pyridine (control)

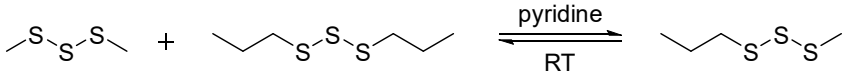

713 µL of degassed pyridine was added to a vial under an atmosphere of nitrogen. A mixture of dimethyl trisulfide (Me_2S_3) (97.3 µL, 925 µmol, 1.0 eq.) and di-*n*-propyl trisulfide ($^nPr_2S_3$) (156 µL, 925 µmol, 1.0 eq.) was added, and the reaction monitored by GC-MS over time: 1 min and 15 min. GC-MS samples were prepared by taking a 10 µL aliquot from the reaction mixture and "quenching" by diluting with 990 µL of $CHCl_3$, which adequately slows the reaction prior to GC-MS analysis. The crossover reaction occurs in pyridine.

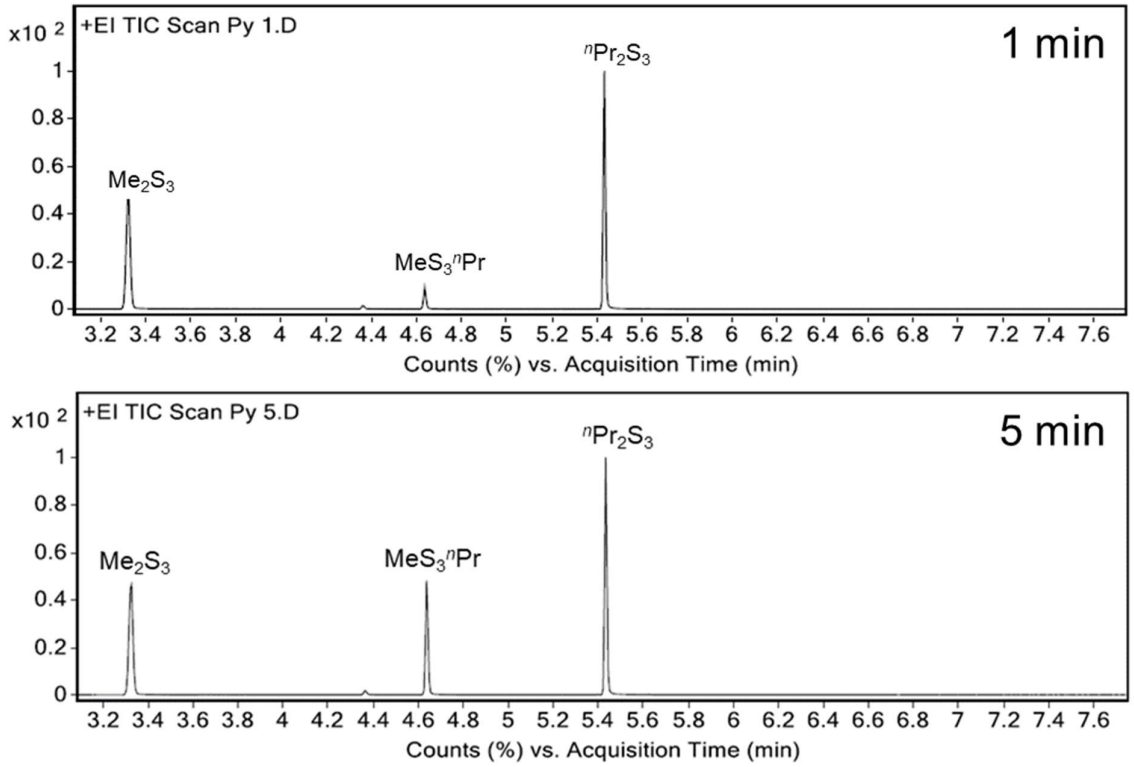

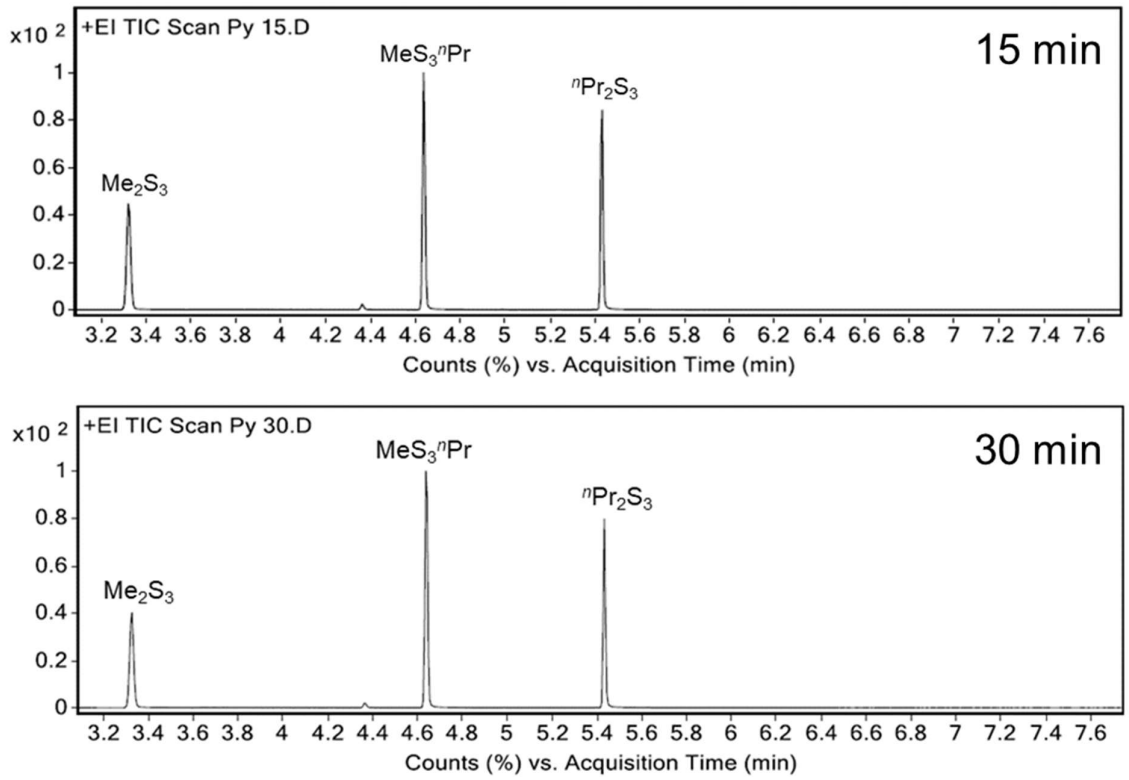

Figure S4.25: Gas chromatograms of the reaction between dimethyl trisulfide (Me_2S_3) and di-*n*-propyl trisulfide ($^nPr_2S_3$) in pyridine after 1, 5, 15, and 30 minutes. GC-MS method A. Retention time: Me_2S_3 (3.327 min), $MeS_3{}^nPr$ (4.638 min), and $^nPr_2S_3$ (5.433 min).

Me_2S_3 and nPr_2S_3 crossover in pyridine in the presence of TEMPO (10 mol%)

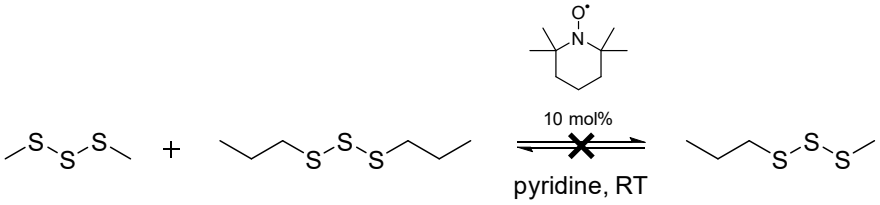

TEMPO (14 mg, 93 µmol, 10 mol%) in 713 µL of degassed pyridine was added to a vial under an atmosphere of nitrogen. A mixture of dimethyl trisulfide (97.3 µL, 925 µmol, 1.0 eq.) and di-*n*-propyl trisulfide (156 µL, 925 µmol, 1.0 eq.) was added, and the reaction monitored by GC-MS over time: 1 min, 5 min, 30 min, and 60 min. GC-MS samples were prepared by taking a 10 µL aliquot from the reaction mixture and "quenching" by diluting with 990 µL of $CHCl_3$, which adequately slows the reaction prior to GC-MS analysis. TEMPO was able to inhibit the reaction in pyridine.

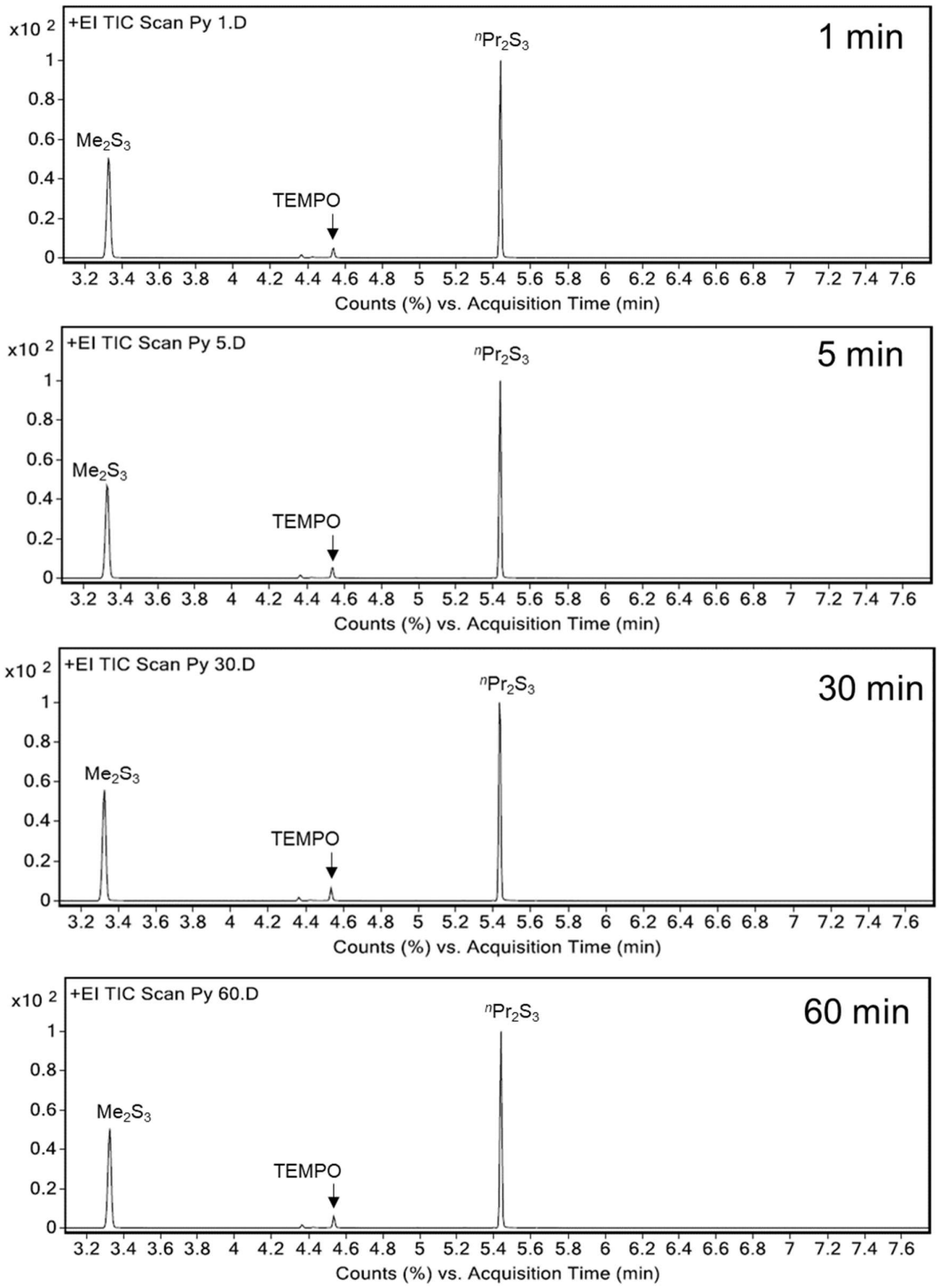

Figure S4.26: Gas chromatogram of the reaction between dimethyl trisulfide (Me_2S_3) and di-*n*-propyl trisulfide ($^{n}Pr_2S_3$) in pyridine, in the presence of TEMPO after 1, 5, 30, and 60 minutes. GC-MS method A. Retention time: Me_2S_3 (3.327 min), TEMPO (4.535 min), and $^{n}Pr_2S_3$ (5.433 min).

Trisulfide crossover inhibition – Other Small Molecules

Crossover in the presence of BHT

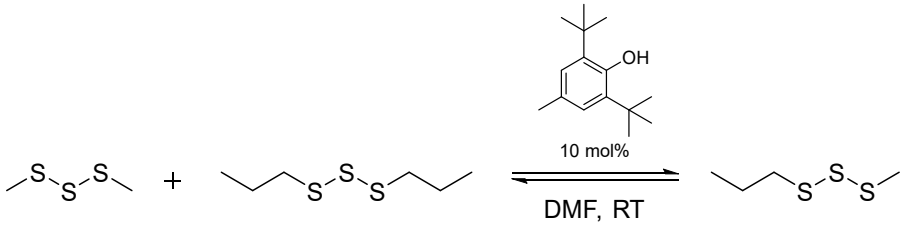

2,6-di-*tert*-butyl-4-methylphenol (BHT) (20 mg, 93 µmol, 10 mol%) in 713 µL of degassed *N*,*N*-dimethylformamide (DMF) was added to a vial under an atmosphere of nitrogen. A mixture of dimethyl trisulfide (97.3 µL, 925 µmol, 1.0 eq.) and di-*n*-propyl trisulfide (156 µL, 925 µmol, 1.0 eq.) was added, and the reaction monitored by GC-MS over time: 1 min, 5 min, 30 min, and 60 min. GC-MS samples were prepared by taking a 10 µL aliquot from the reaction mixture and "quenching" by diluting with 990 µL of $CHCl_3$, which adequately slows the reaction prior to GC-MS analysis. BHT did not inhibit the reaction.

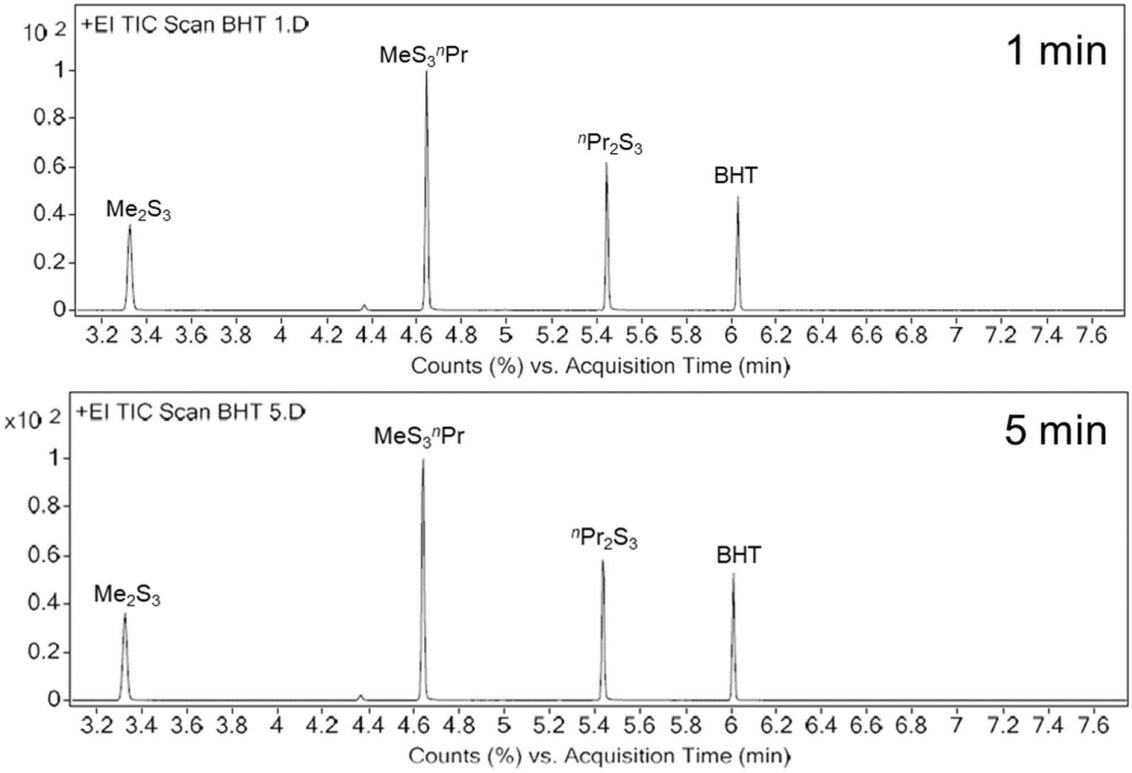

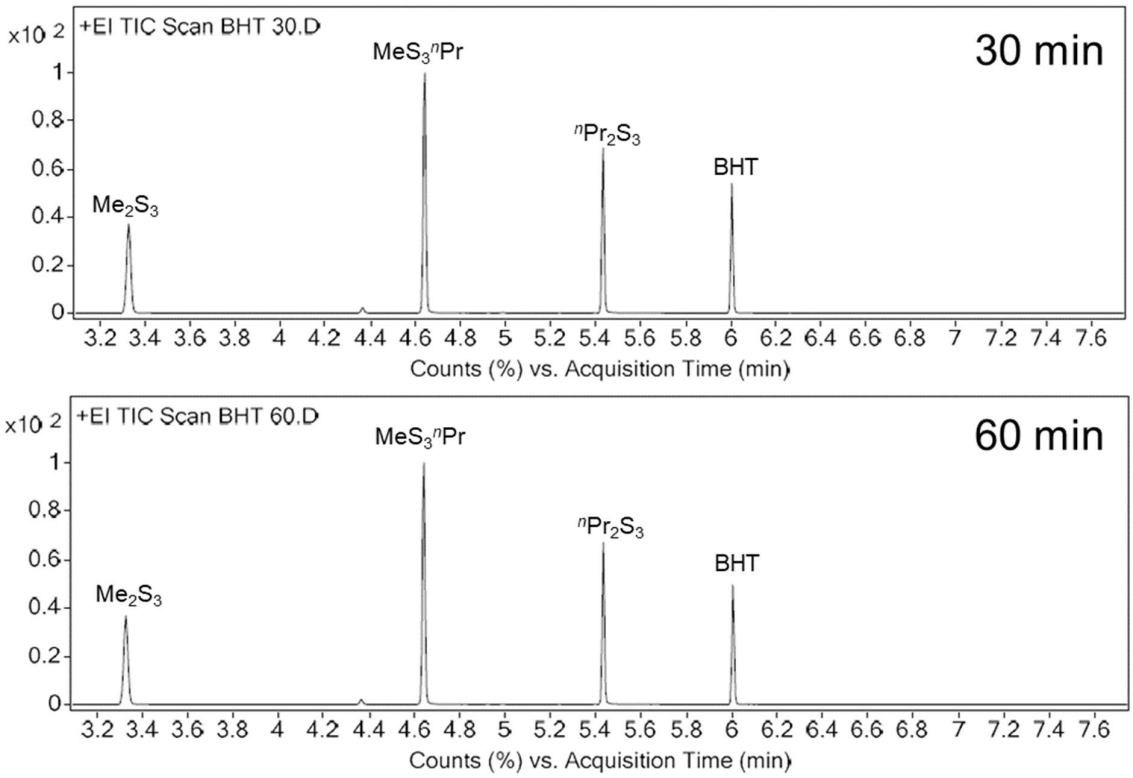

Figure S4.27: Gas chromatogram of the reaction between dimethyl trisulfide (Me_2S_3) and di-*n*-propyl trisulfide ($^nPr_2S_3$) in *N*,*N*-dimethylformamide (DMF), in the presence of 2,6-di-*tert*-butyl-4-methylphenol (BHT) after 1, 15, 30, and 60 minutes. GC-MS method A. Retention time: Me_2S_3 (3.327 min), $MeS_3{}^nPr$ (4.638 min), $^nPr_2S_3$ (5.433 min), BHT (6.028 min).

Crossover in the presence of 1,4-benzoquinone

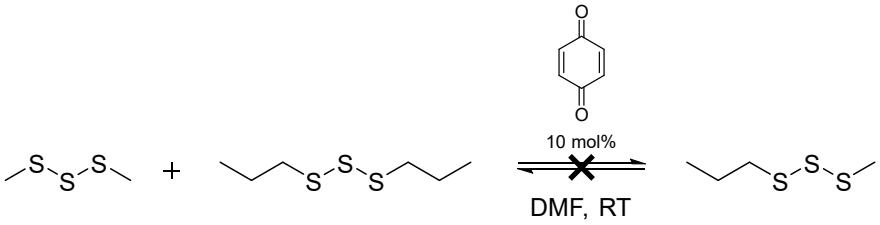

1,4-benzoquinone (10 mg, 93 µmol, 10 mol%) in 713 µL of degassed *N*,*N*-dimethylformamide (DMF) was added to a vial under an atmosphere of nitrogen. A mixture dimethyl trisulfide (97.3 µL, 925 µmol, 1.0 eq.) and di-*n*-propyl trisulfide (156 µL, 925 µmol, 1.0 eq.) was added, and the reaction monitored by GC-MS over time: 1 min, 5 min, 30 min, and 60 min. GC-MS samples were prepared by taking a 10 µL aliquot from the reaction mixture and "quenching" by diluting with 990 µL of $CHCl_3$, which adequately slows the reaction prior to GC-MS analysis. 1,4-Benzoquinone inhibited the reaction.

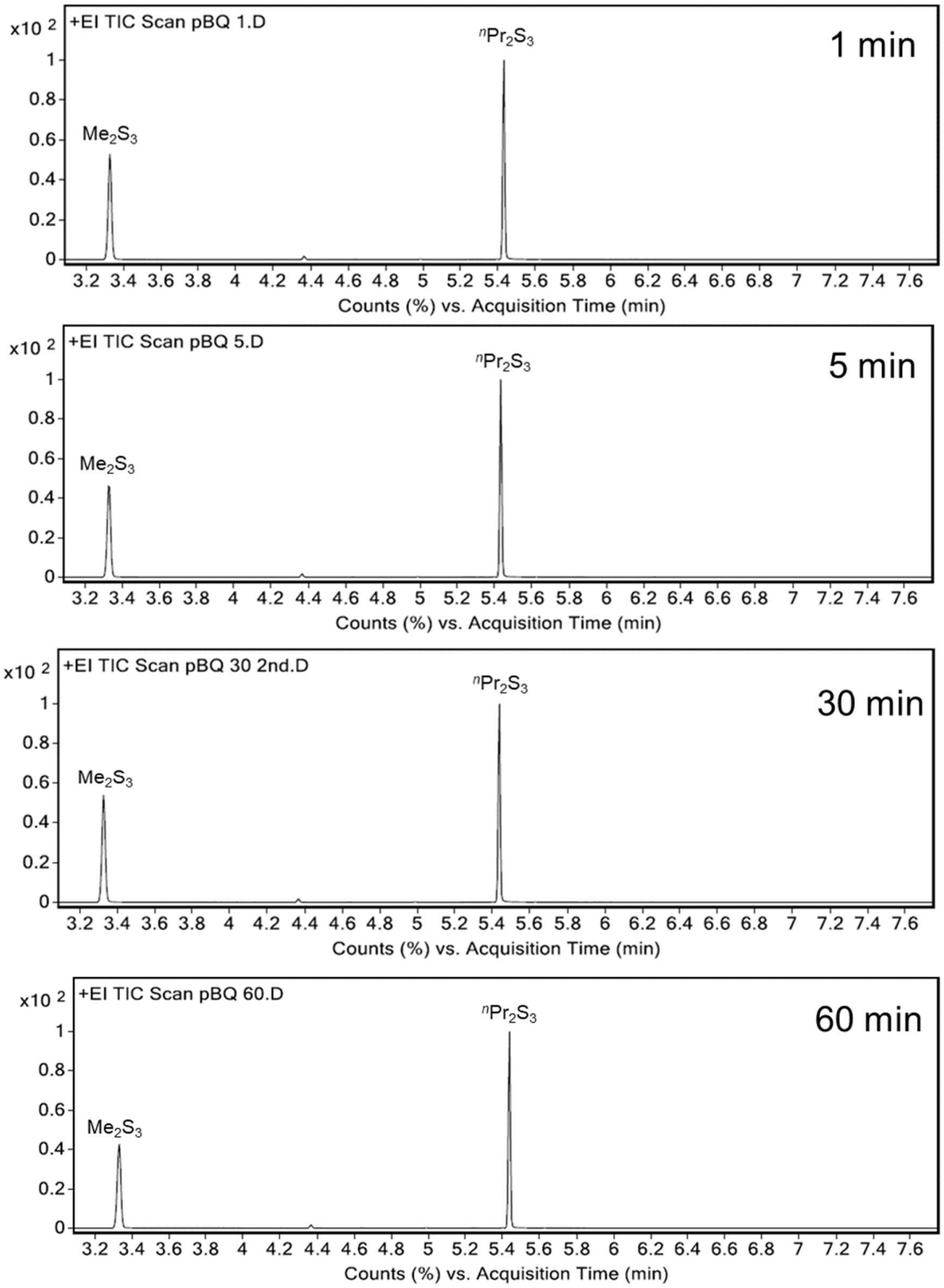

Figure S4.28: Gas chromatogram of the reaction between dimethyl trisulfide (Me_2S_3) and di-*n*-propyl trisulfide ($^{n}Pr_2S_3$) in *N*,*N*-dimethylformamide (DMF), in the presence of 1,4-benzoquinone after 1, 5, 30, and 60 minutes. GC-MS method A. Retention time: Me_2S_3 (3.327 min), $^{n}Pr_2S_3$ (5.433 min).

Crossover in the presence of maleic anhydride

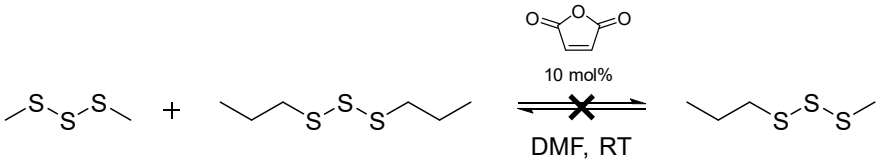

Maleic anhydride (9 mg, 90 µmol, 10 mol%) in 713 µL of degassed *N*,*N*-dimethylformamide (DMF) was added to a vial under an atmosphere of nitrogen. A mixture of dimethyl trisulfide (Me_2S_3) (97.3 µL, 925 µmol, 1.0 eq.) and di-*n*-propyl trisulfide ($^nPr_2S_3$) (156 µL, 925 µmol, 1.0 eq.) was added, and the reaction monitored by GC-MS over time: 1 min, 5 min, 30 min, and 60 min. GC-MS samples were prepared by taking a 10 µL aliquot from the reaction mixture and "quenching" by diluting with 990 µL of $CHCl_3$, which adequately slows the reaction prior to GC-MS analysis. Maleic anhydride inhibited the reaction.

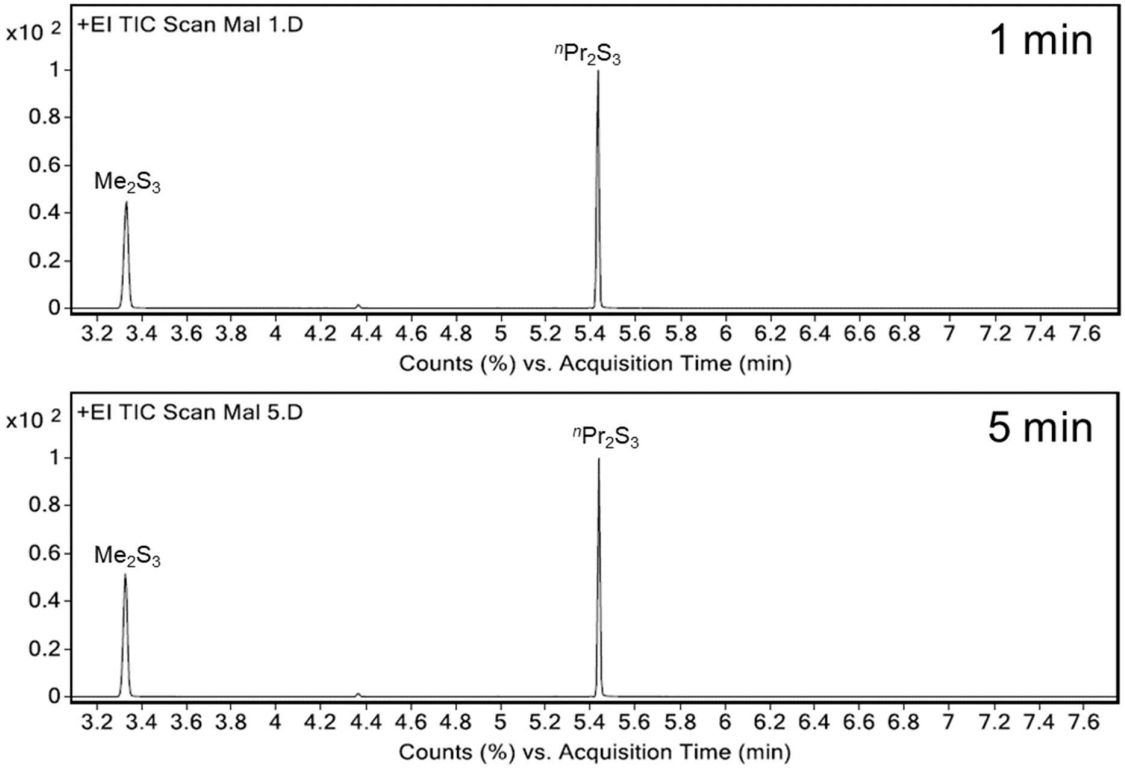

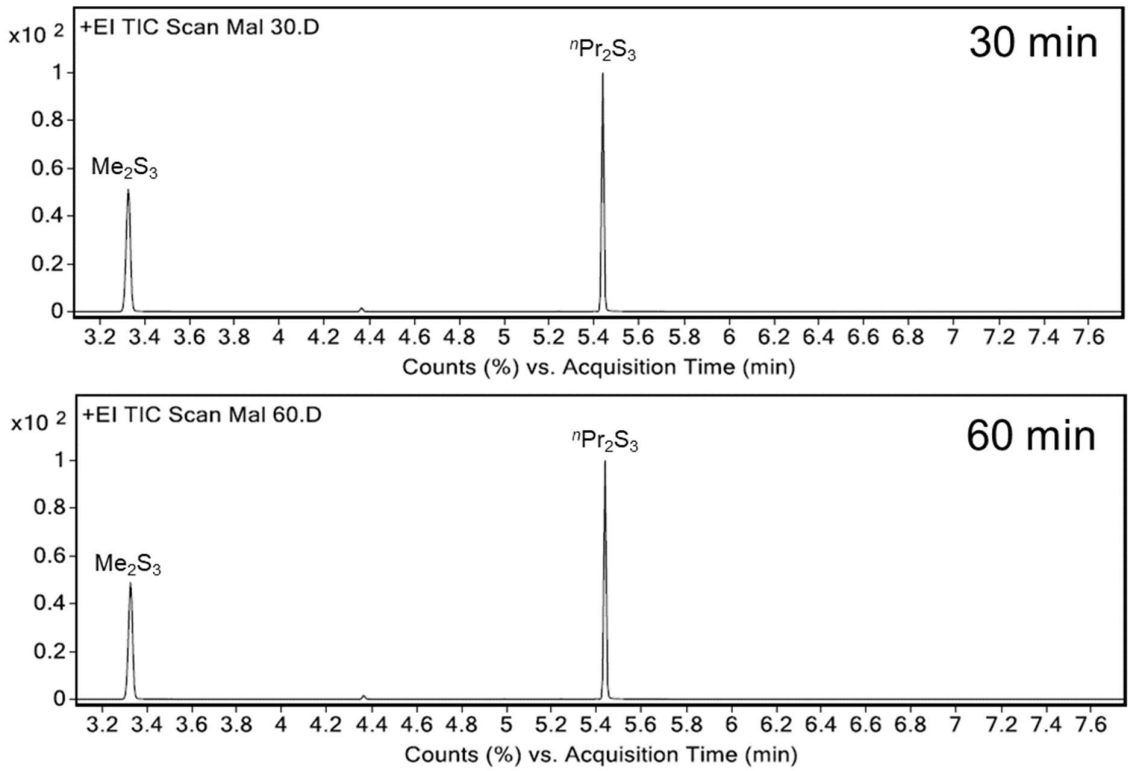

Figure S4.29: Gas chromatogram of the reaction between dimethyl trisulfide (Me_2S_3) and di-*n*-propyl trisulfide ($^{n}Pr_2S_3$) in *N*,*N*-dimethylformamide (DMF), in the presence of maleic anhydride after 60 minutes. GC-MS method A. Retention time: Me_2S_3 (3.327 min), $^{n}Pr_2S_3$ (5.433 min).

^{1}H NMR studies of dimethyl trisulfide and maleic anhydride in DMF-d_7

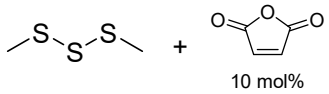

DMF-d_7, RT

Maleic anhydride (14 mg, 140 µmol, 10 mol%) in 427 µL of degassed *N*,*N*-dimethylformamide-d_7 (DMF-d_7) was added to an NMR tube under an atmosphere of nitrogen. Dimethyl trisulfide (Me_2S_3) (150 µL, 1.43 mmol, 1.0 eq.) was added, and the reaction monitored by NMR spectroscopy over 64 hours at room temperature (19 – 20 ºC); nothing of note was observed.

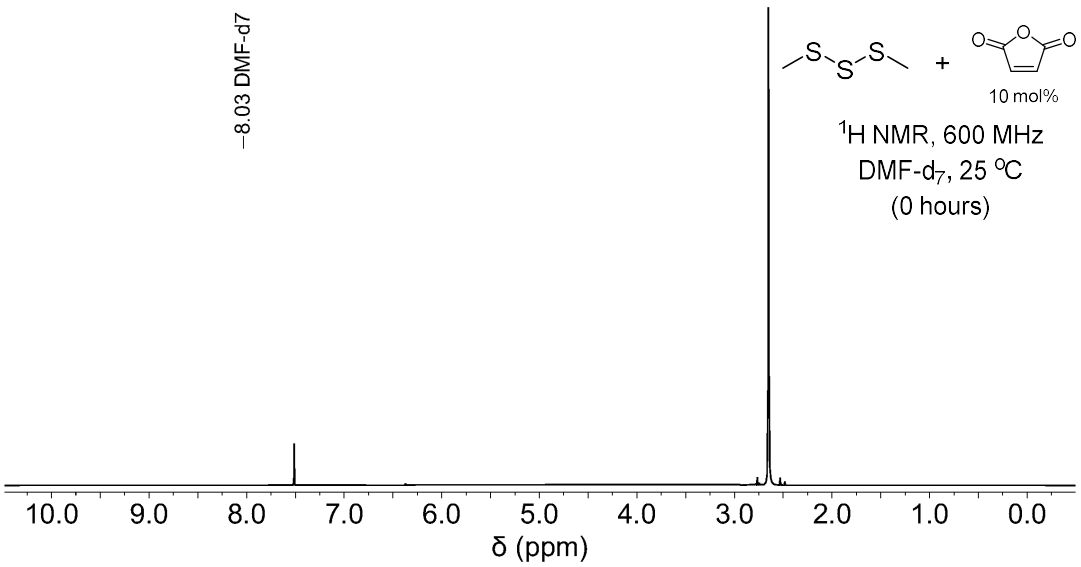

Figure S4.30: ^{1}H NMR spectrum of dimethyl trisulfide (Me_2S_3) and maleic anhydride in *N*,*N*-dimethylformamide-d_7 (DMF-d_7) immediately following NMR tube preparation, at time 0 hours.

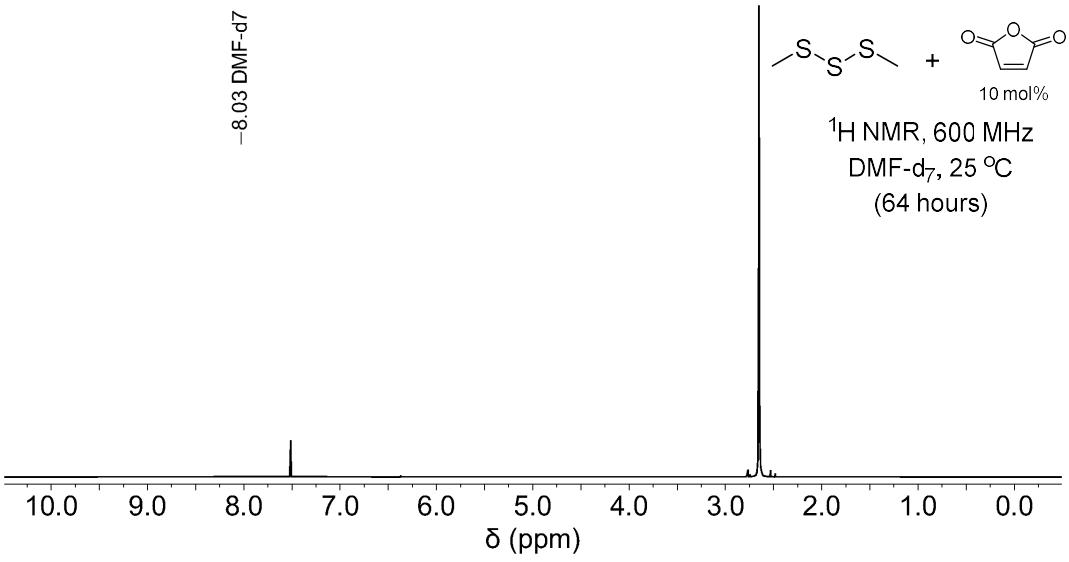

Figure S4.31: ^{1}H NMR spectrum of dimethyl trisulfide (Me_2S_3) and maleic anhydride in *N*,*N*-dimethylformamide-d_7 (DMF-d_7) after 64 hours.

^{1}H NMR studies of Me_2S_3, $^nPr_2S_3$, and maleic anhydride in DMF-d_7

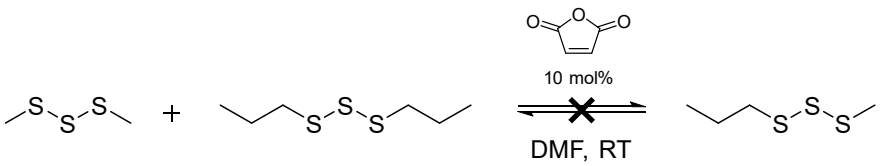

Maleic anhydride (14 mg, 140 μmol, 10 mol%) in 1.11 mL of degassed *N*,*N*-dimethylformamide (DMF) was added to an NMR tube under an atmosphere of nitrogen. Dimethyl trisulfide (Me_2S_3) (150 μL, 1.43 mmol, 1.0 eq.) and di-*n*-propyl trisulfide ($^nPr_2S_3$) (241 μL, 1.43 mmol, 1.0 eq.) were added, and the reaction monitored by NMR in $CDCl_3$ over 1 hour at room temperature (19 – 20 ºC). The crossover reaction was inhibited under these conditions. Nothing of note was observed by NMR spectroscopy.

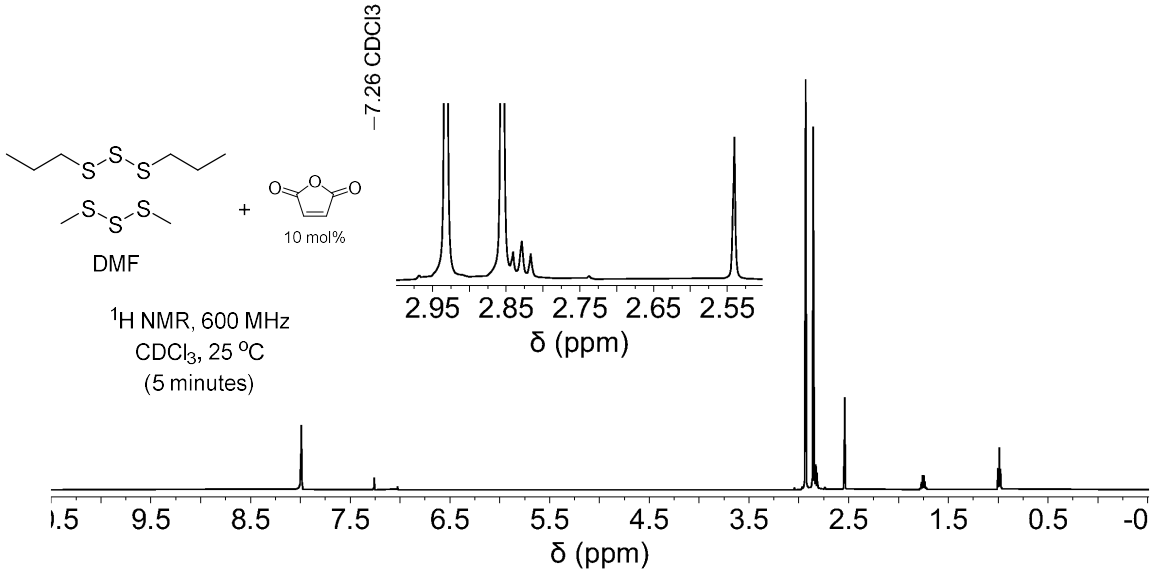

Figure S4.32: ^{1}H NMR spectrum of the reaction aliquot in $CDCl_3$, from dimethyl trisulfide (Me_2S_3), di-*n*-propyl trisulfide ($^nPr_2S_3$), maleic anhydride, and *N*,*N*-dimethylformamide (DMF) after 5 minutes.

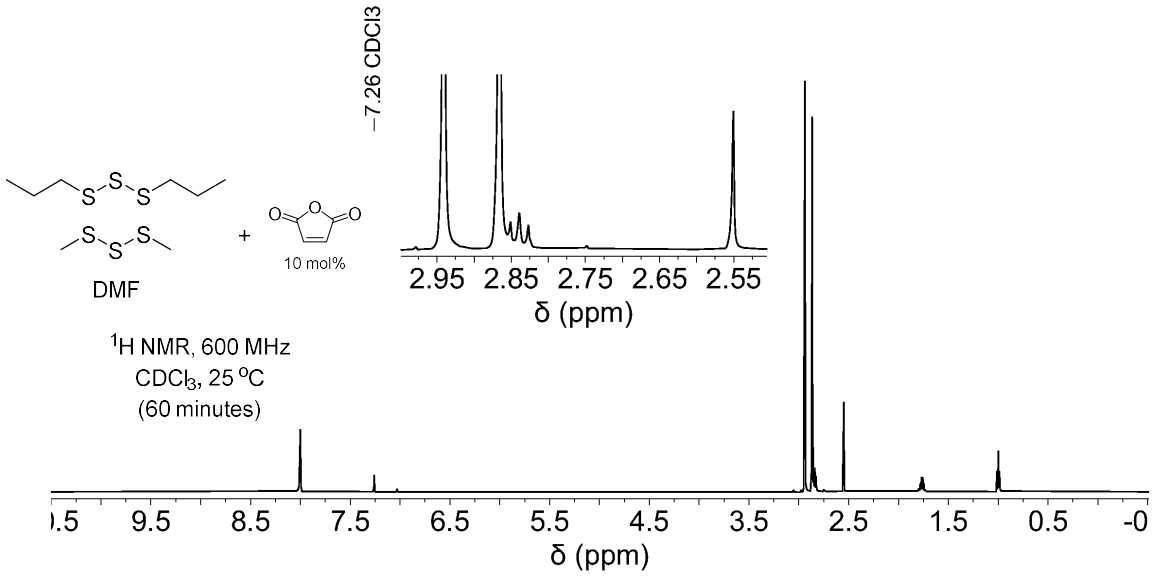

Figure S4.33: ^{1}H NMR spectrum of the reaction aliquot in $CDCl_3$, from dimethyl trisulfide (Me_2S_3), di-*n*-propyl trisulfide ($^{n}Pr_2S_3$), maleic anhydride, and *N*,*N*-dimethylformamide (DMF) after 60 minutes.

Crossover of Me_2S_3 and Pr_2S_3 in the presence of dimethyl maleate

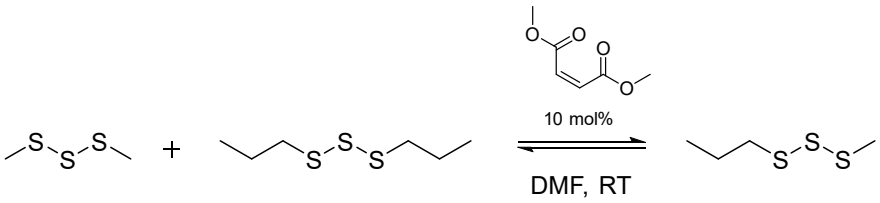

To dimethyl maleate (11.9 µL, 95.1 µmol, 0.10 eq.) in 0.82 mL *N*,*N*-dimethylformamide (DMF) was added a mixture of dimethyl trisulfide (Me_2S_3) (100 µL, 951 µmol, 1.0 eq.) and di-*n*-propyl trisulfide ($^{n}Pr_2S_3$) (160 µL, 951 µmol, 1.0 eq.) at room temperature with stirring. The crossover reaction was slightly inhibited by the presence of dimethyl fumarate as indicated by equilibrium being reached in 5 minutes as opposed to 1 minute. No significant isomerisation of dimethyl maleate to dimethyl fumarate was observed by ^{1}H NMR in $CDCl_3$ after 60 minutes of stirring.

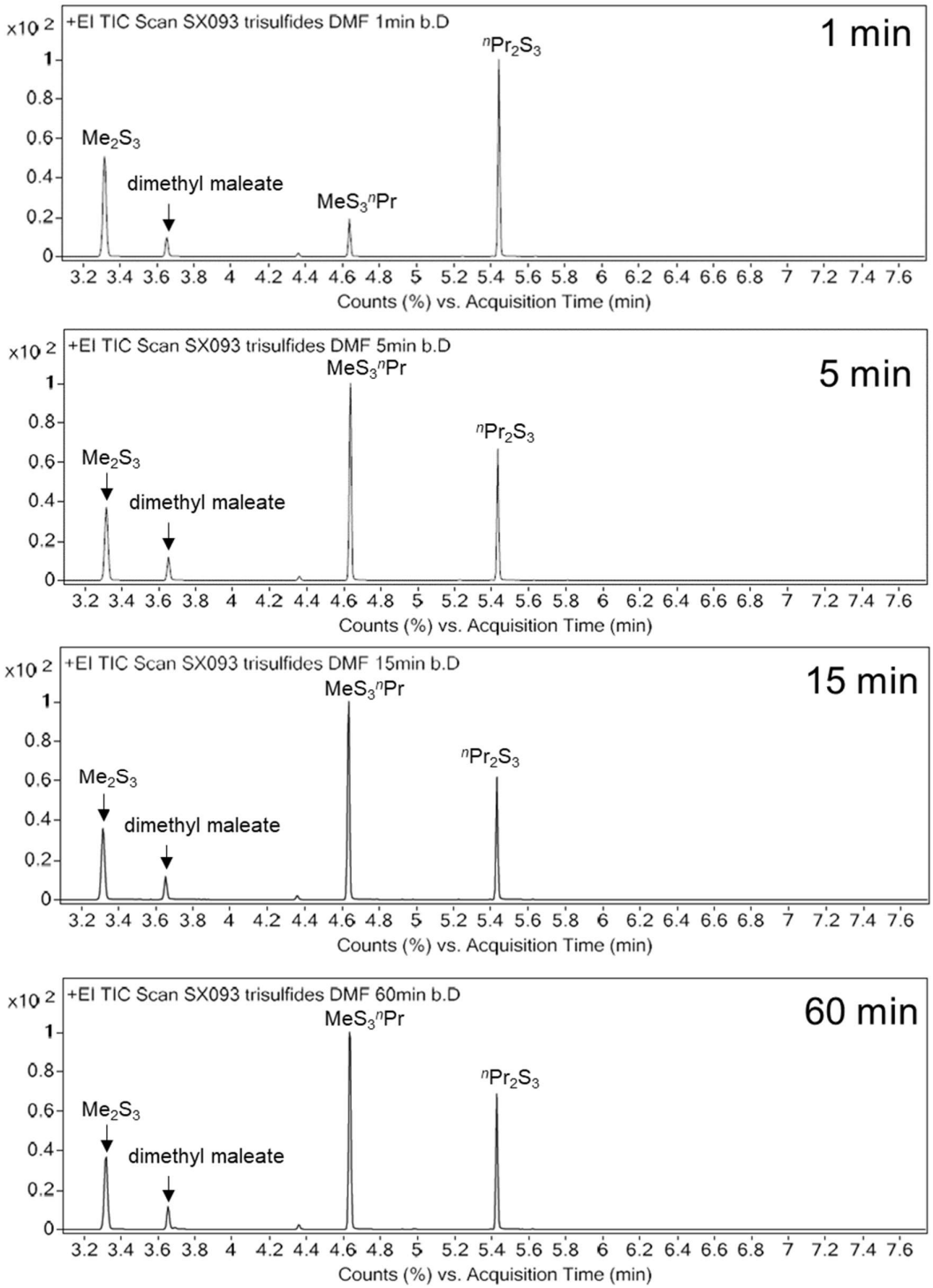

Figure S4.34: Gas chromatogram of the reaction between dimethyl trisulfide (Me_2S_3) and di-*n*-propyl trisulfide ($^{n}Pr_2S_3$) in *N*,*N*-dimethylformamide (DMF), after stirring with dimethyl maleate for 1, 5, 15, and 60 minutes. GC-MS method A. Retention time: Me_2S_3 (3.327 min), dimethyl maleate (3.653 min), $MeS_3{}^{n}Pr$ (4.638 min), $^{n}Pr_2S_3$ (5.433 min).

^{1}H NMR analysis of Me_2S_3, $^nPr_2S_3$, and dimethyl maleate in DMF after 60 min

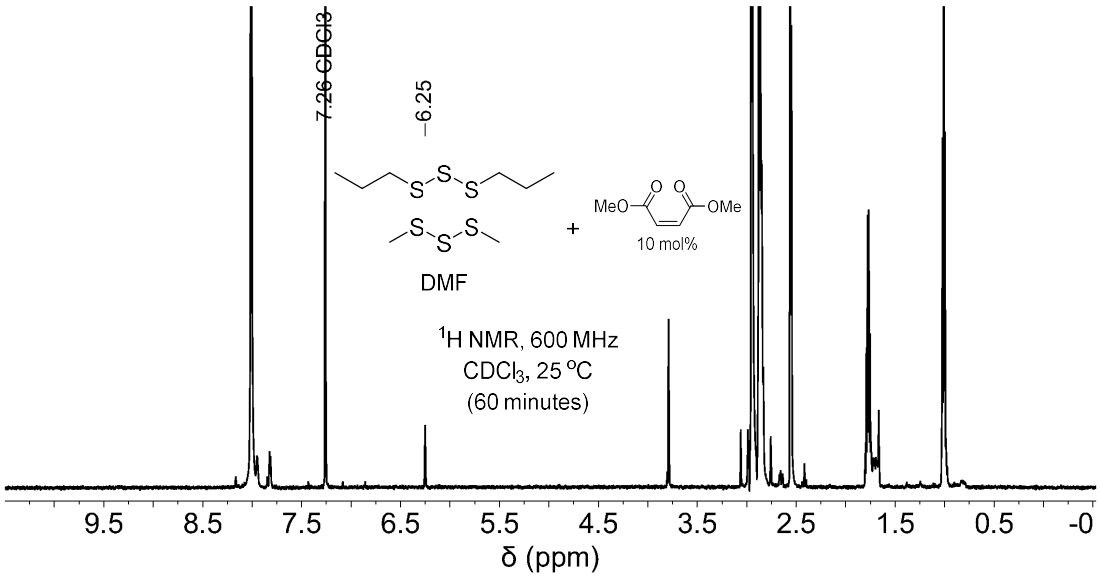

Figure S4.35: ^{1}H NMR spectrum in $CDCl_3$ of an aliquot of the reaction between dimethyl trisulfide (Me_2S_3) and di-*n*-propyl trisulfide ($^nPr_2S_3$) in *N*,*N*-dimethylformamide (DMF), after stirring with dimethyl maleate (6.25 ppm) for 60 minutes. No isomerisation of dimethyl maleate to dimethyl fumarate is apparent.

Crossover of Me_2S_3 and Pr_2S_3 in the presence of succinic anhydride

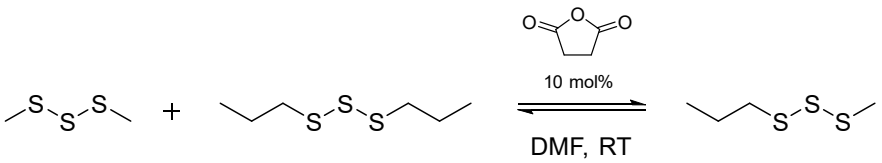

significant reduction in the rate of crossover

To succinic anhydride (10 mg, 95 µmol, 0.10 eq.) in 0.82 mL of *N*,*N*-dimethylformamide (DMF) was added a mixture of dimethyl trisulfide (Me_2S_3) (100 µL, 951 µmol, 1.0 eq.) and di-*n*-propyl trisulfide ($^nPr_2S_3$) (160 µL, 951 µmol, 1.0 eq.) at room temperature with stirring. The crossover reaction was significantly inhibited by the presence of succinic anhydride as indicated by equilibrium not being reached in 60 minutes.

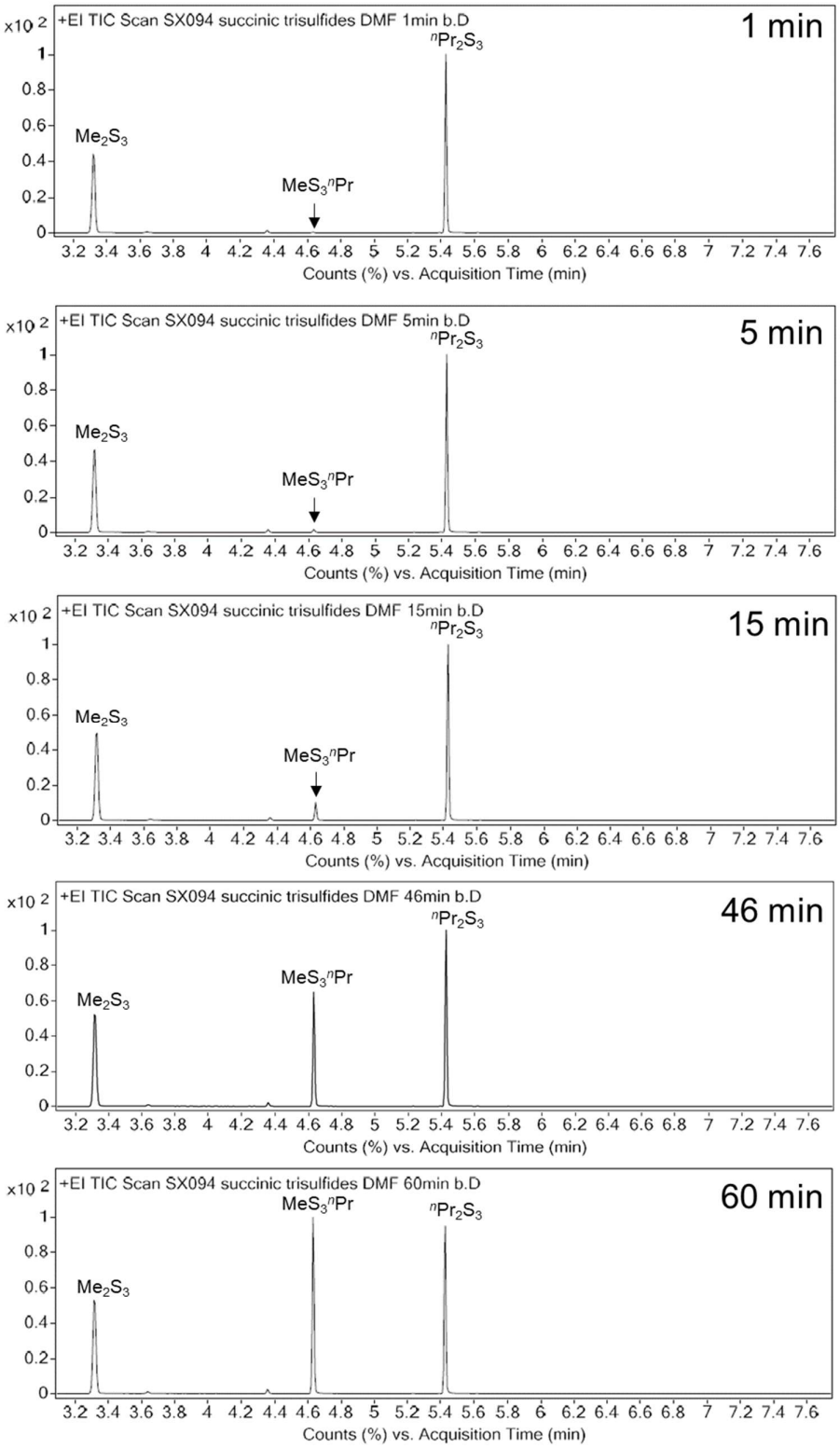

Figure S4.36: Gas chromatogram of the reaction between dimethyl trisulfide (Me_2S_3) and di-*n*-propyl trisulfide ($^nPr_2S_3$) in *N*,*N*-dimethylformamide (DMF), after stirring with succinic anhydride for 60 minutes. GC-MS method A. Retention time: Me_2S_3 (3.327 min), succinic anhydride (3.636 min), $MeS_3{}^nPr$ (4.638 min), $^nPr_2S_3$ (5.433 min).

Me_2S_3 and $^nPr_2S_3$ crossover in N,N-dimethyl acrylamide (DMAA)

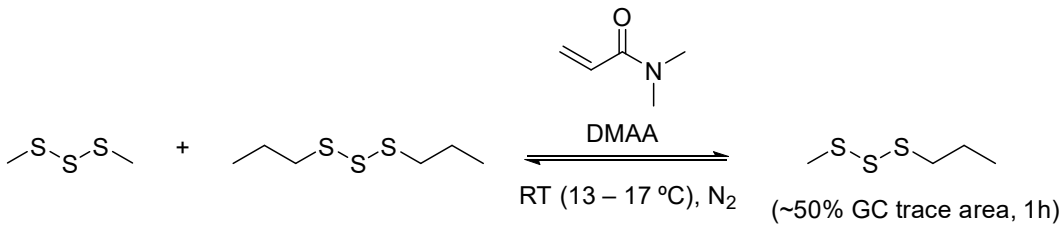

Dimethyl trisulfide (126 µL, 1.2 mmol) and di-*n*-propyl trisulfide (203 µL, 1.2 mmol) were added to a 1.5 mL GC vial equipped with a stir bar, followed by DMAA (123.6 µL, 1.2 mmol), and sealed with a lid. The mixture was then stirred at room temperature (13 – 17 ºC). After 1 and 24 hours, a 10 µL aliquot was removed and diluted to 1 mL with chloroform for GC-MS analysis. The crossover product $MeS_3{}^nPr$ was observed. No adducts resulting from the addition of a trisulfide to the acrylate were observed. DMAA did not polymerize or appear to react in any other way under these conditions.

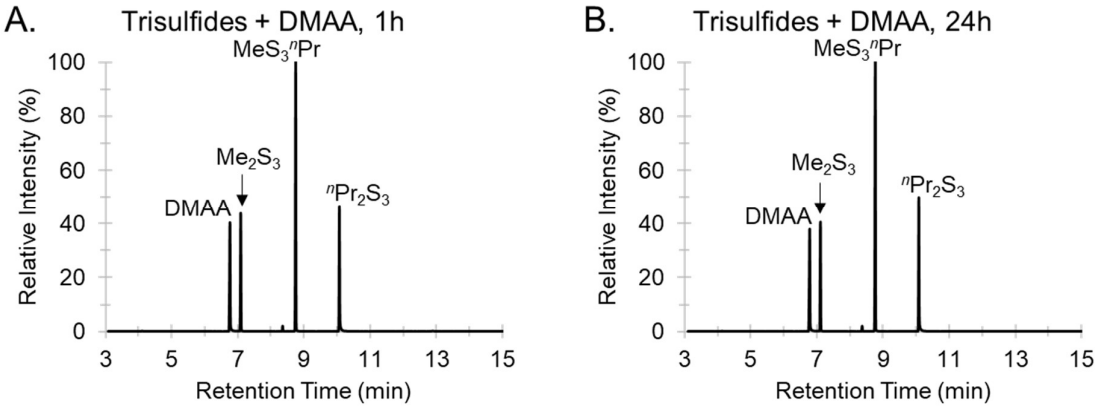

Figure S4.37: GC-MS traces for crossover reaction between dimethyl trisulfide (Me_2S_3) and di-*n*-propyl trisulfide ($^nPr_2S_3$) with DMAA over 24 hours at room temperature (13-17 °C). The reaction reached equilibrium within 1 hour; the GC trace area of $MeS_3{}^nPr$ was around 50%. GC-MS method B. Retention time: DMAA (6.77 min), Me_2S_3 (7.10 min), $^nPr_2S_2$ (8.36 min) – impurity from dipropyl trisulfide, $MeS_3{}^nPr$ (8.75 min), and $^nPr_2S_3$ (10.09 min).

Me_2S_3 and N,N-dimethyl acrylamide (DMAA) in the presence of H_2O

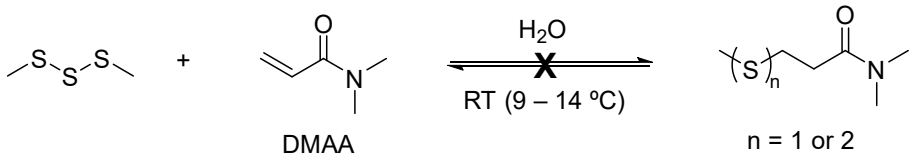

Dimethyl trisulfide (105 µL, 1.0 mmol, 1.0 eq.), DMAA (103 µL, 1.0 mmol, 1.0 eq.) and water (5.0 µL, 0.28 mmol, 0.28 eq.) were added to a 2 mL glass vial equipped with a stir bar and sealed with a lid. The reaction was duplicated using less dimethyl trisulfide (10.5 µL, 0.1 mmol, 0.1 eq.). The mixture was stirred (300 rpm) at room temperature (9 – 14 ºC) for a week. A 5 µL aliquot was removed and diluted to 1 mL with chloroform after 1 h, 24 h, 3 days, and 7 days, for GCMS analysis. Control experiments were carried out between dimethyl trisulfide and DMAA without the addition of water. No adducts resulting from the addition of dimethyl trisulfide to the acrylate were observed.

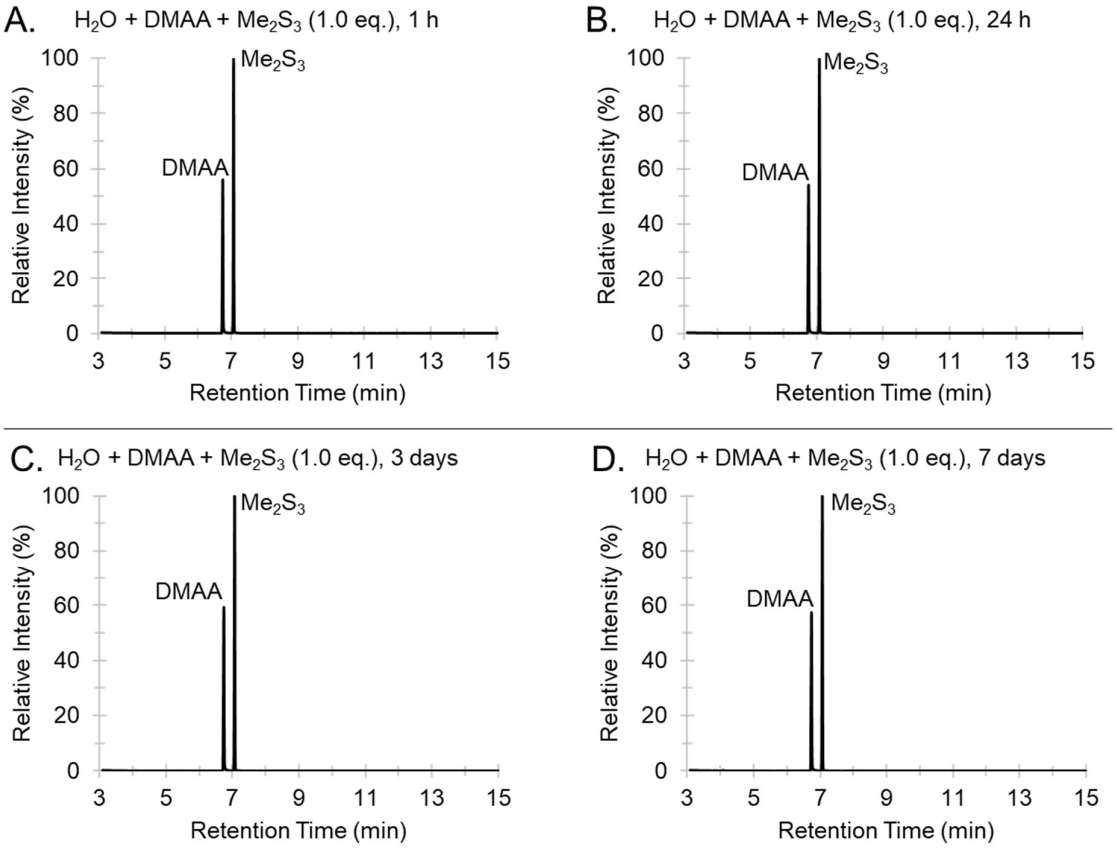

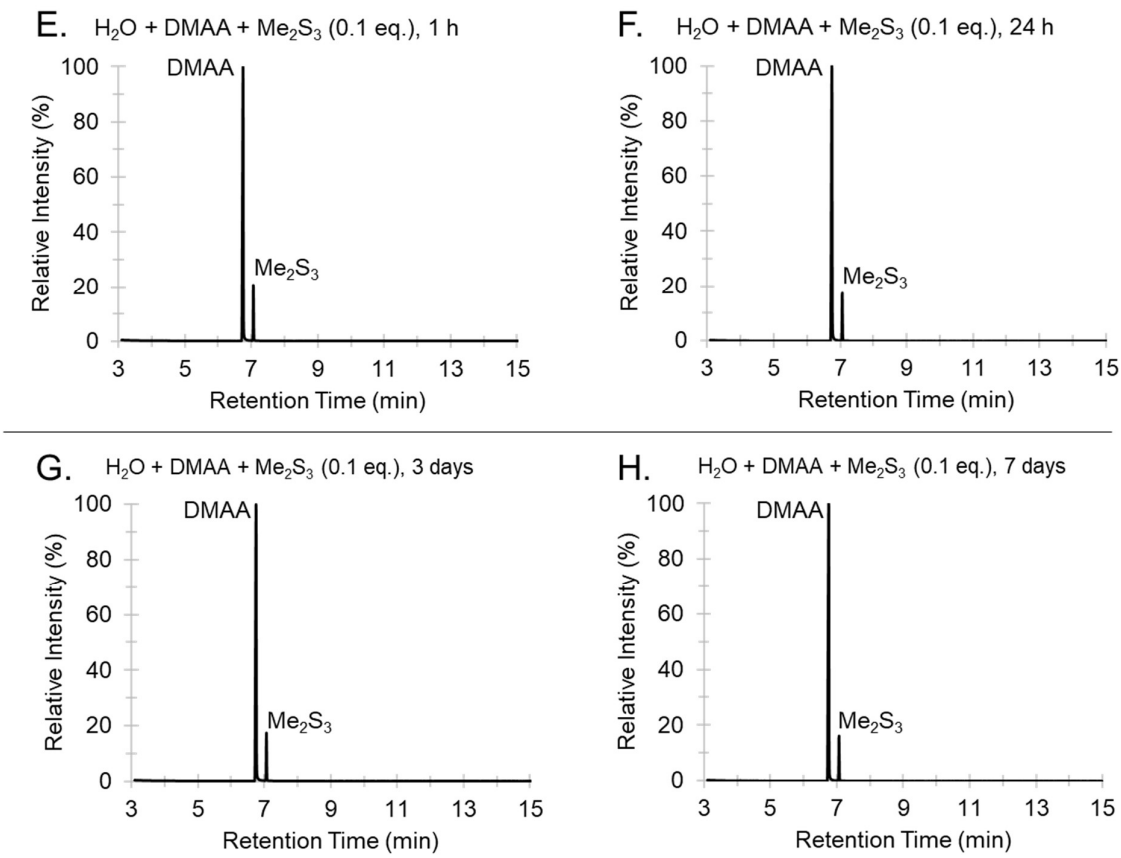

Figure S4.38: GCMS traces for the reaction between dimethyl trisulfide (Me_2S_3) and DMAA over 7 days at room temperature (9-14 °C) in the presence of water, using either (A, B, C, D) 1.0 eq. of dimethyl trisulfide or (E, F, G, H) 0.1 eq. of dimethyl trisulfide. GCMS method B. Retention time: DMAA (6.75 min) and Me_2S_3 (7.10 min).

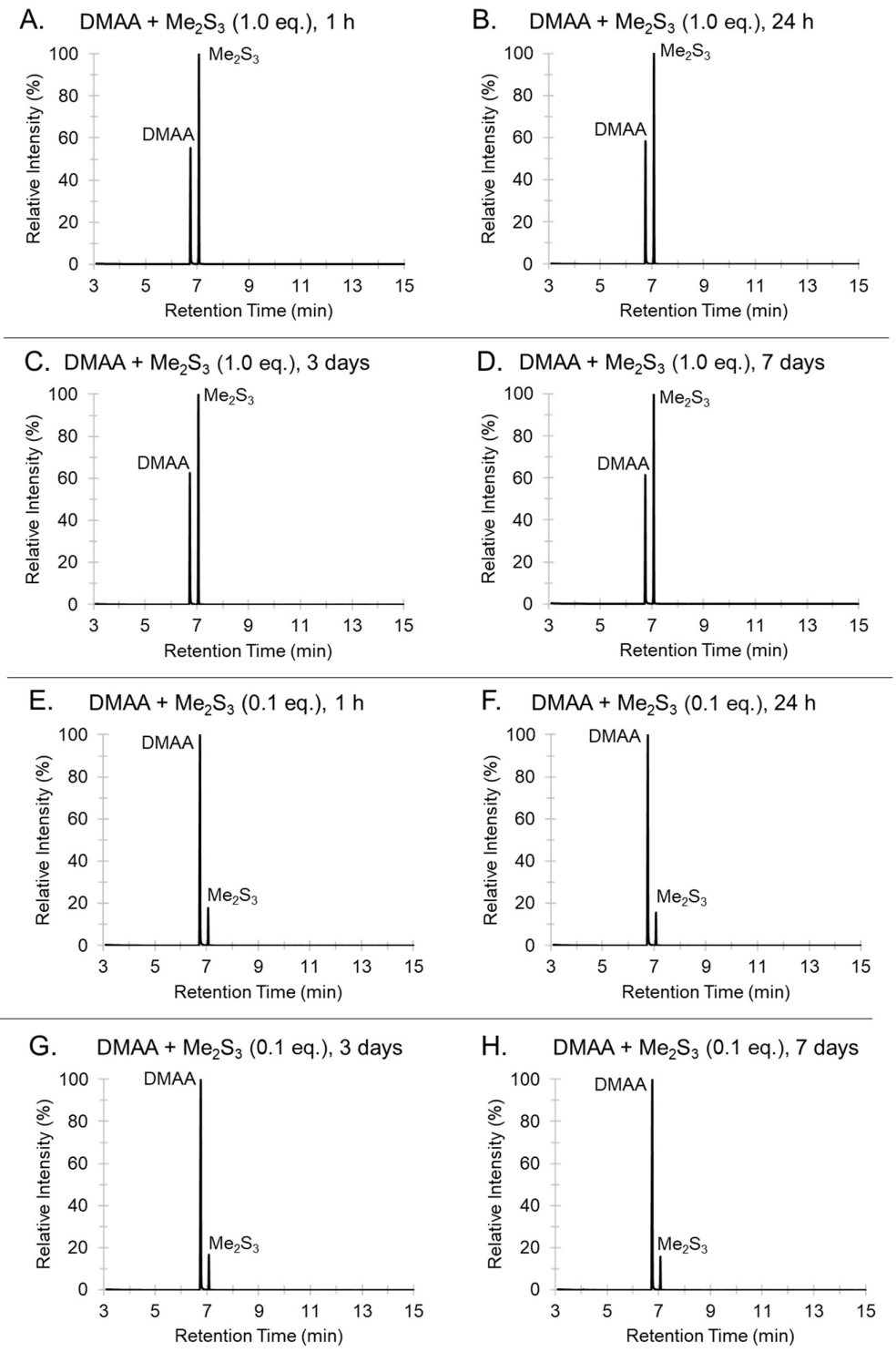

Figure S4.39: GCMS traces for the control reactions between dimethyl trisulfide (Me_2S_3) and DMAA over 7 days at room temperature (9 – 14 °C) in the absence of water, using either (A, B, C, D) 1.0 eq. of dimethyl trisulfide or (E, F, G, H) 0.1 eq. of dimethyl trisulfide. GCMS method B. Retention time: DMAA (6.75 min) and Me_2S_3 (7.10 min).

Reaction of trisulfide in the presence of S-centred radicals (generated by photolysis)

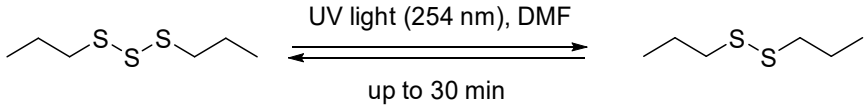

To a dry quartz cuvette (4 windows, 10 x 10 mm path length) was added DMF (1980 μL,128 eq) and di-*n*-propyl trisulfide (34 μL, 0.2 mmol, 1.0 eq.) under a slow stream of nitrogen. The cuvette was closed with the lid and wrapped with parafilm to seal. The mixture was exposed to the UV light (254 nm, UVP crosslinker reactor, Analytik Jena) for 1, 10, and 30 min. After each time, 10 μL of the aliquot was removed and diluted to 1 mL with chloroform for GC-MS analysis. The energy used to induce the reaction was 359 mJ/cm^2 for 1 min, 4208 mJ/cm^2 for an additional of 9 min, and 9290 mJ/cm^2 for an additional 20 min. The total UV exposure time was 30 min.

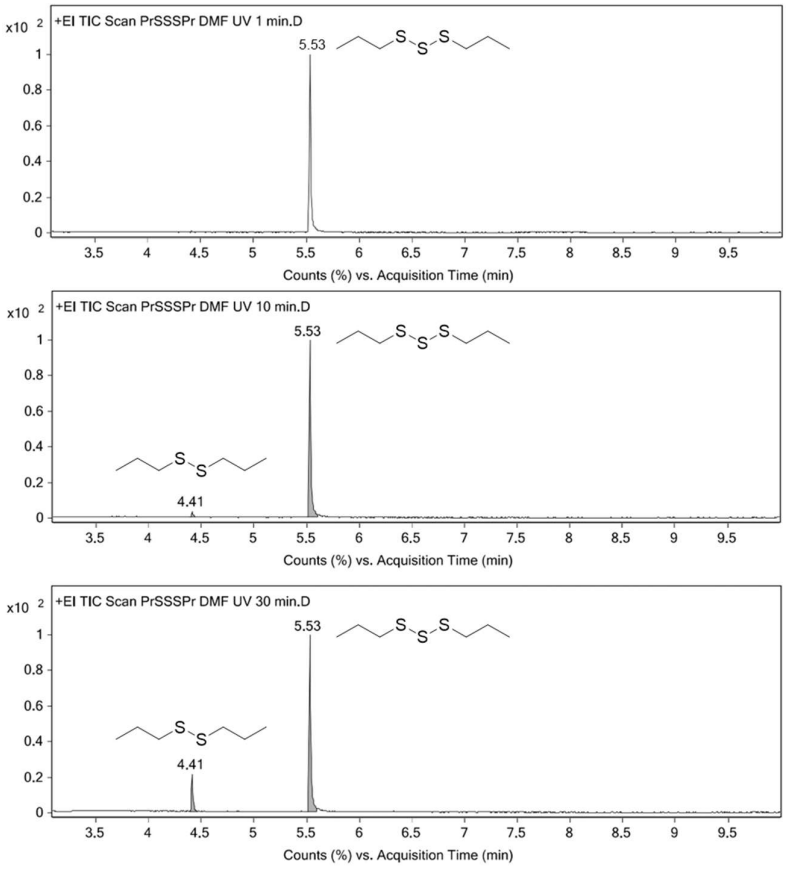

Figure S4.40: GC traces for the UV induced S-S metathesis of di-*n*-propyl trisulfide in DMF. GC-MS method C with a hold time of 3.7 minutes at 250 ºC. No di-*n*-propyl tetrasulfide was observed or it may form during the reaction but it could be easily broken by photolysis.

Control experiments of $^{n}Pr_2S_3$ in DMF under UV light exposure

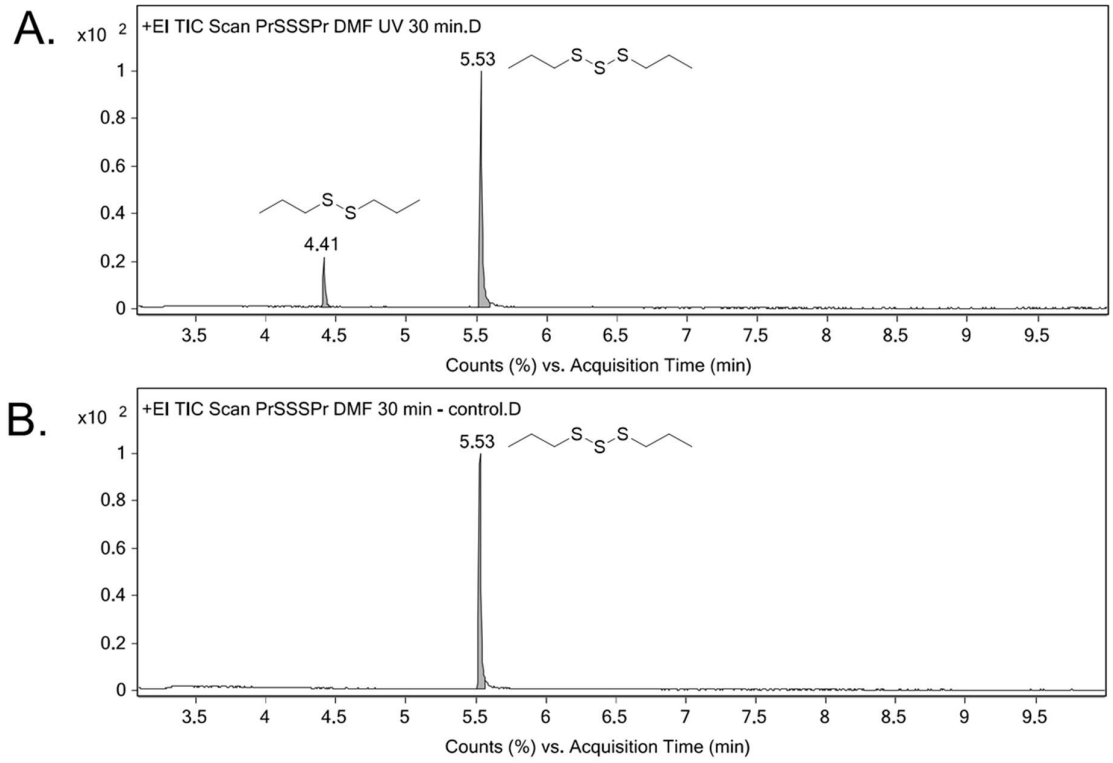

Figure S4.41: GC-MS method C with a hold time of 3.7 minutes at 250 ºC. (A) GC trace for di-*n*-propyl trisulfide in DMF after exposing to UV light for 30 minutes. (B) GC trace for di-*n*-propyl trisulfide in DMF without exposing to UV light for 30 minutes.

Synthesis of 2,2,6,6-Tetramethyl-4-([7-nitrobenzo[c][1,2,5]oxadiazol-4-yl]-amino) piperidin-1-oxyl radical (PFN-5)

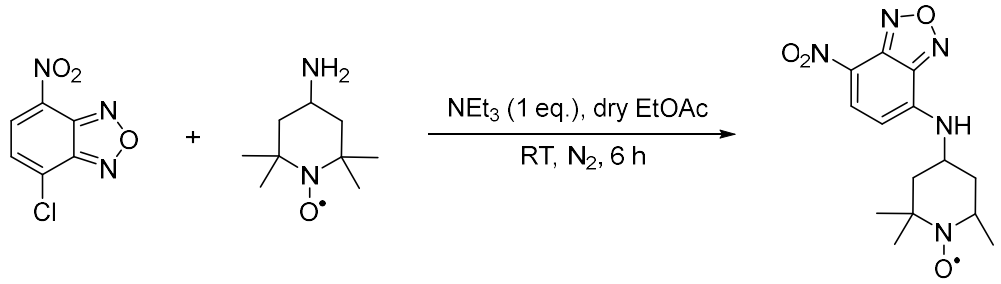

The synthesis protocol of this nitroxide radical was adapted from Klinska et al.[6] A magnetically stirred solution of 4-chloro-7-nitrobenzofurazan (99.8 mg, 0.5 mmol) in dry ethyl acetate (2 mL) is treated, dropwise, with triethylamine (69.6 µL, 0.5 mmol, 1.0 eq.) then 4-amino-TEMPO (85.6 mg, 0.5 mmol, 1.0 eq). The resulting reaction mixture is stirred under a nitrogen atmosphere at room temperature (13-17 ºC) for 6 h then diluted with ethyl acetate (10 mL). The resulting solution is washed with water (1 x 10 mL) and brine (1 x 10 mL) before being dried using sodium sulfate anhydrous, filtered and concentrated under reduced pressure (240 mbar, 40 ºC). The resulting light-yellow oil is subjected to flash column chromatography (silica, 1:9 v/v → 1:1 ethyl acetate/hexane gradient elution) to give the title compound (138.4 mg, 83%) as a bright-orange powder, m.p = 225-228 ºC with decomposition. IR (ATR) ν_{max} 3223, 3065, 2977, 2926, 1578, 1528, 1494, 1313, 1283, 1260, 1237, 1181, 1026 cm^{-1}.

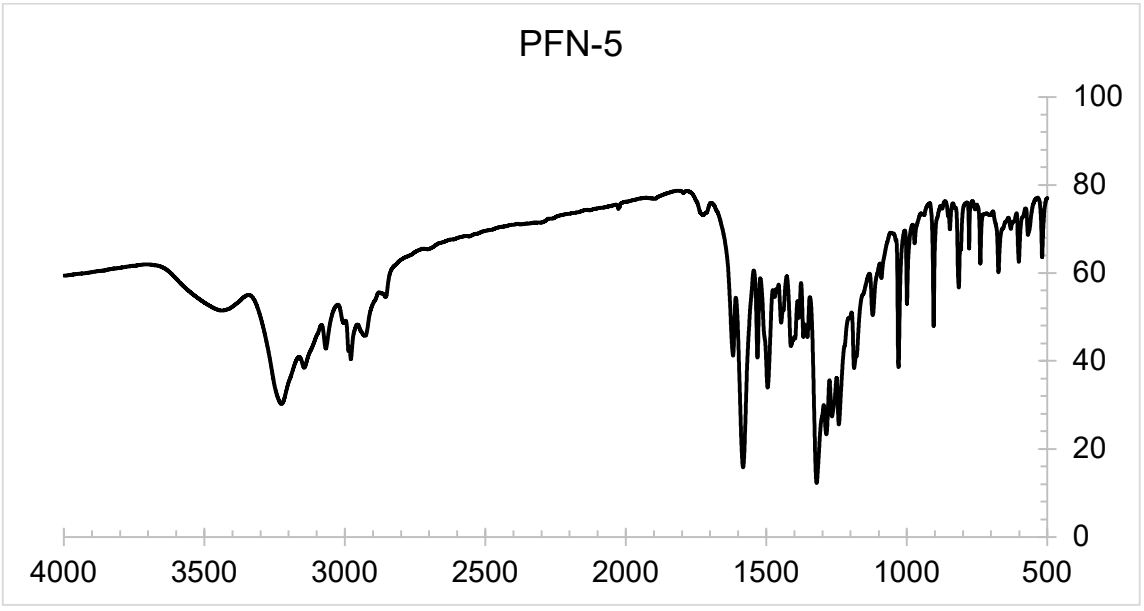

Figure S4.42: FTIR spectrum of PFN-5

Radical trap experiment of the trisulfide crossover reaction using PFN-5

5.0 mg of PFN-5 was dissolved in 250 mL of DCM to give the solution with the concentration of 6 x 10^{-5} M. 2 mL of this probe solution was then placed in a fluorescence cuvette and diluted with the additional 1 mL of DCM (4 x 10^{-5} M). Pre-scanning was carried out to obtain the maximum excitation peak at 476 nm and emission peak at 515 nm (Figure S4.43).

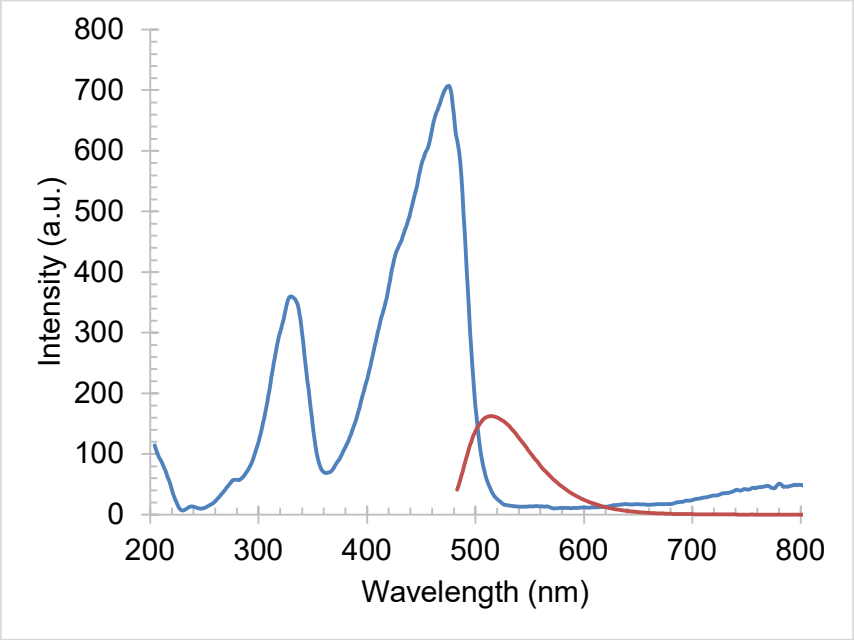

Figure S4.43: Excitation and emission spectra of PFN-5 probe in DCM (4 x 10^{-5} M).

Effect of DMF addition to the probe emission intensity

PFN-5 is a nitroxide radical probe and weakly fluorescence due to the nature of the nitrobenzofurazan/fluorophore group. The signal is restored when the radical traps another radical, and the fluorescence emission intensity will increase. To evaluate the use of this probe for radical analysis in the reaction between dimethyl trisulfide-dipropyl trisulfide and DMF, several experiments were carried out. First, the fluorescence emission intensity was analysed using different amounts of DMF ranging from 0.02 to 6.04 mmol (1, 10, 50, 100, 200, and 300). The samples volume used in the experiment are shown in Table 1. 3 mL of total volume was used due to cuvette capacity.

Table S4.1: PFN-5 probe, DMF and solvent volume used in the experiment.

Volume PFN-5 (mL)	PFN-5 (mmol)	Volume DMF (µL)	DMF (mmol)	DMF mol ratio	Volume DCM to add* (µL)
2.0	1.20×10^{-4}	1.56	0.0201	1	998.44
2.0	1.20×10^{-4}	15.6	0.2015	10	984.4
2.0	1.20×10^{-4}	78	1.0074	50	922
2.0	1.20×10^{-4}	156	2.0148	100	844
2.0	1.20×10^{-4}	312	4.0297	200	688
2.0	1.20×10^{-4}	468	6.0445	300	532

* DCM was added to make the total volume of 3 mL.

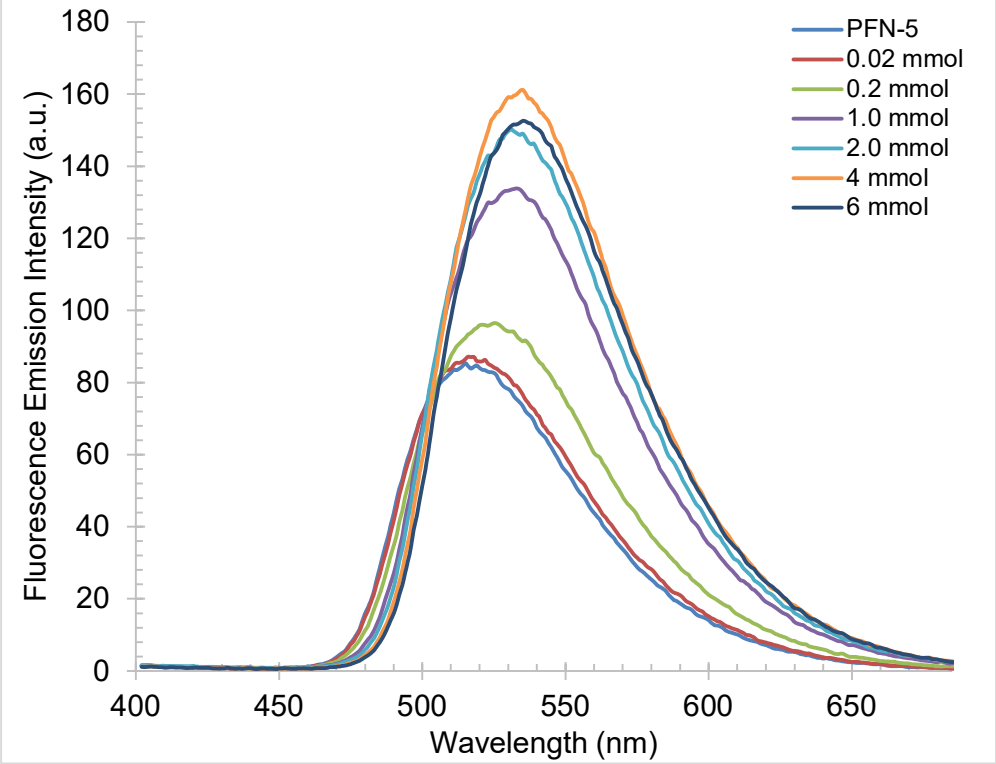

Figure S4.44: Fluorescence emission spectra of PFN-5 probe in DCM (4×10^{-5} M) in the presence of DMF. Spectra were recorded using the following settings: Emission slit 5 nm, PMT power set at 600 volts, excitation source set at 350 nm. The emission spectra were recorded after the addition of DMF.

As shown in Figure S4.44, a noticeable increase in the emission intensity was observed when 0.20 mol DMF was added. This was also followed by the emission wavelength shifting from 517 nm (probe only in DCM) to 521 nm. In general, the emission intensity and the maximum emission wavelength of the probe increases by the addition of DMF. The highest emission intensity was achieved when 200 times amount of DMF (312 µL, 4.03 mmol) was used compared to the initial amount of DMF added. Nevertheless, a turning point of the emission intensity was shown up when more DMF used. In this case, 300 times more DMF (468 µL, 6.04 mmol) was used. The emission intensity of this composition has similar intensity to that of 200 times DMF (fluorescence quenching by the polar solvent does occur).

To validate whether the addition of DMF solely affects the emission fluorescence intensity of the probe, another experiment was carried out. To do this, 312 µL of DMF (4.03 mmol) was added to the fluorescence cuvette containing 2 mL of PFN-5 solution (6 x 10^{-5} M) and then diluted to 3 mL with DCM. This composition was chosen because it provides the highest emission intensity (Figure S4.44). From the results (Figure S4.45), the emission signal of the radical probe was changing overtime in the presence of DMF. The result suggests that DMF could react with the probe. No further exploration was made using this probe.

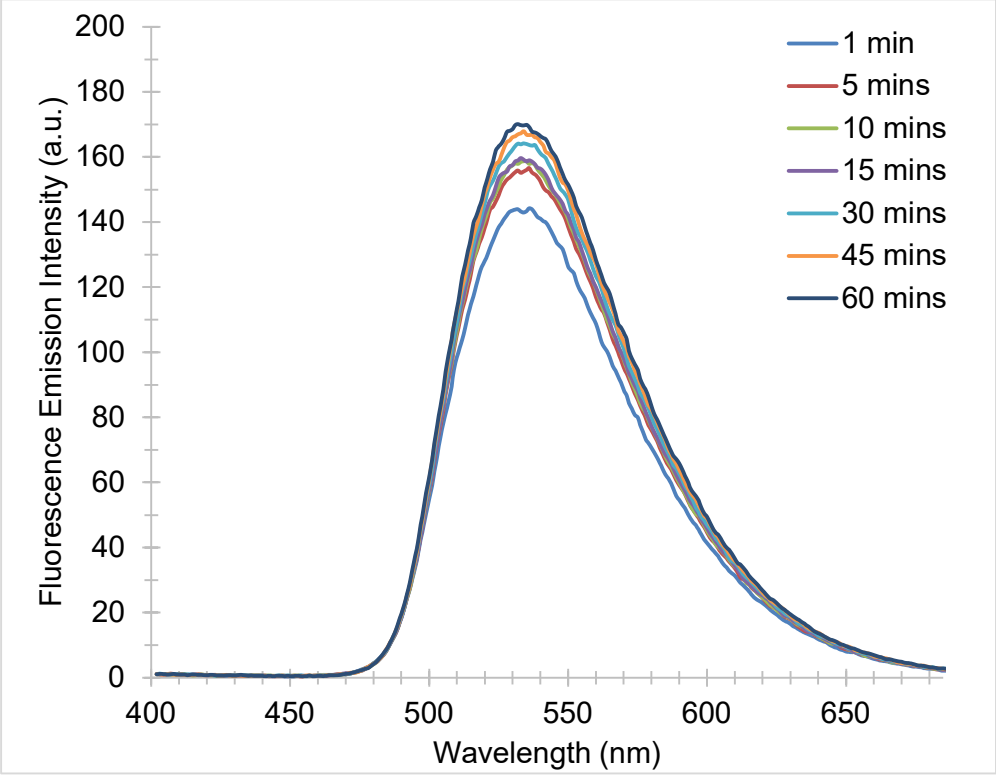

Figure S4.45: Fluorescence emission intensities of the probe after the addition of DMF (312 µL, 4.03 mmol).

Reaction between benzyl bromide and dimethyl trisulfide

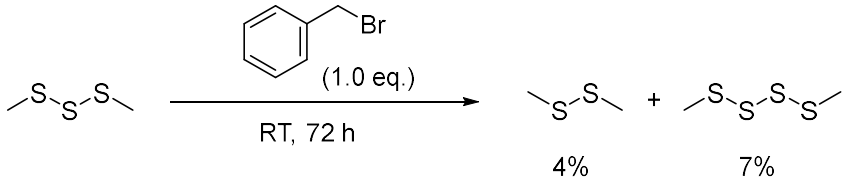

To a GC-MS vial equipped with a magnetic stirrer was added benzyl bromide (118.8 µL, 1 mmol, 1 eq.) and dimethyl trisulfide (105.2 µL, 1 mmol). The mixture was then stirred for 72 hours at room temperature. After 1h, 10 µL of aliquot was removed and diluted to 1 mL using chloroform. The sample was then analysed by GCMS. Analysis was also done for the mixture after 24 and 72 hours.

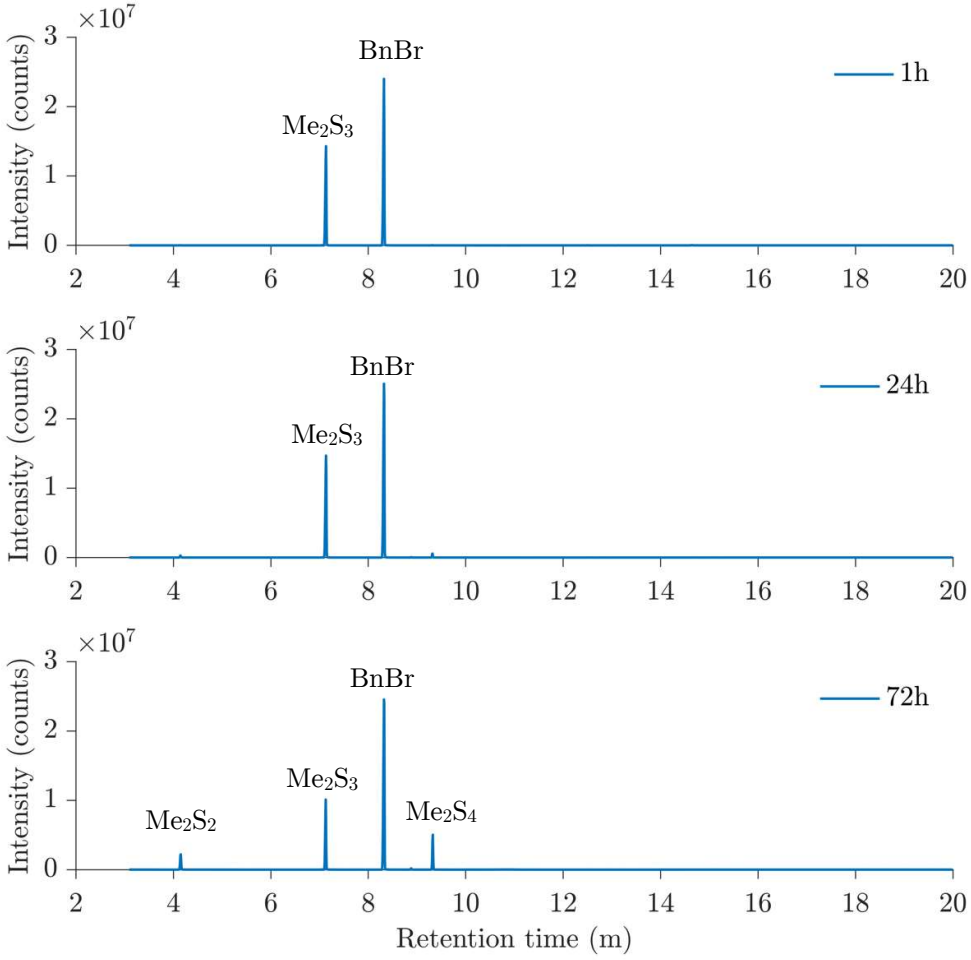

Figure S4.46: GC traces of a reaction between benzyl bromide and dimethyl trisulfide (1 mmol each) after 1, 24, and 72 hours. GCMS method B yields Me_2S_2 (4.14 min), Me_2S_3 (7.12 min), BnBr (8.32 min), Me_2S_4 (9.32 min).

Reaction between benzyl bromide, dimethyl trisulfide and dimethylformamide (1 eq.)

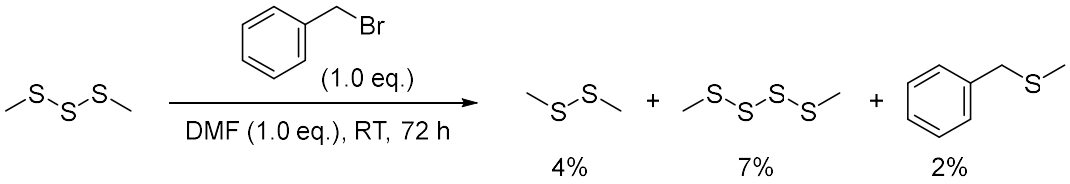

To a GCMS vial equipped with a magnetic stirrer was added benzyl bromide (118.8 µL, 1 mmol, 1 eq.), dimethyl trisulfide (105.2 µL, 1 mmol) and DMF (77.4 µL, 1 mmol). The mixture was then stirred for 72 hours at room temperature. After 1h, 24 and 72 hours, 10 µL of aliquot was removed and diluted to 1 mL using chloroform.

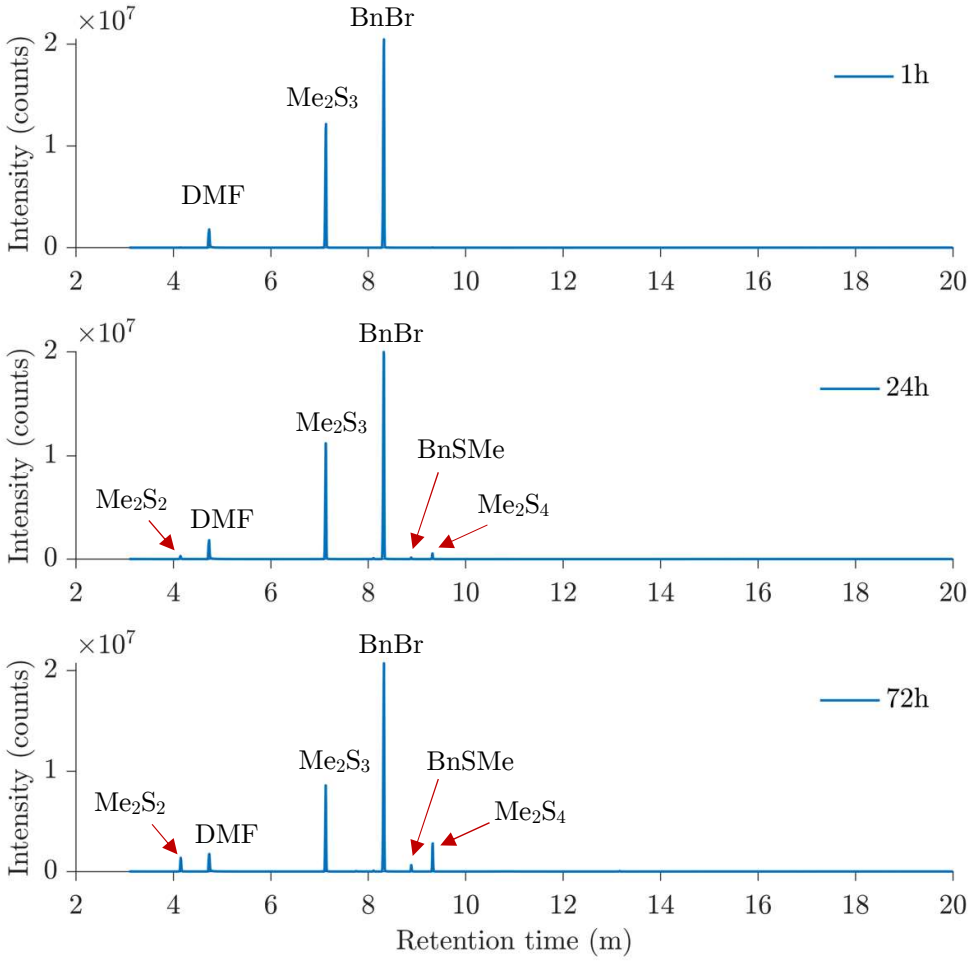

Figure S4.47: GC traces of a reaction between benzyl bromide, dimethyl trisulfide and DMF (1 equiv.). GCMS method B yields Me_2S_2 (4.14 min), DMF (4.74 min) Me_2S_3 (7.12 min), BnBr (8.32 min), BnSMe (8.88 min), Me_2S_4 (9.32 min).

Reaction between benzyl bromide, dimethyl trisulfide and dimethylformamide (5 eq.)

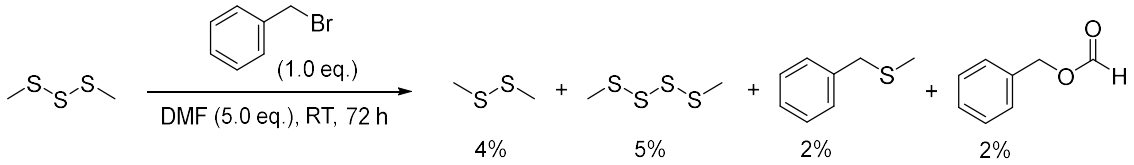

To a GC-MS vial equipped with a magnetic stirrer was added benzyl bromide (118.8 µL, 1 mmol, 1 eq.), dimethyl trisulfide (105.2 µL, 1 mmol) and DMF (387.2 µL, 5 mmol, 5 eq.). The mixture was then stirred for 72 hours at room temperature. After 1h, 24 and 72 hours, 10 µL of aliquot was removed and diluted to 1 mL using chloroform. The sample was then analysed by GC-MS.

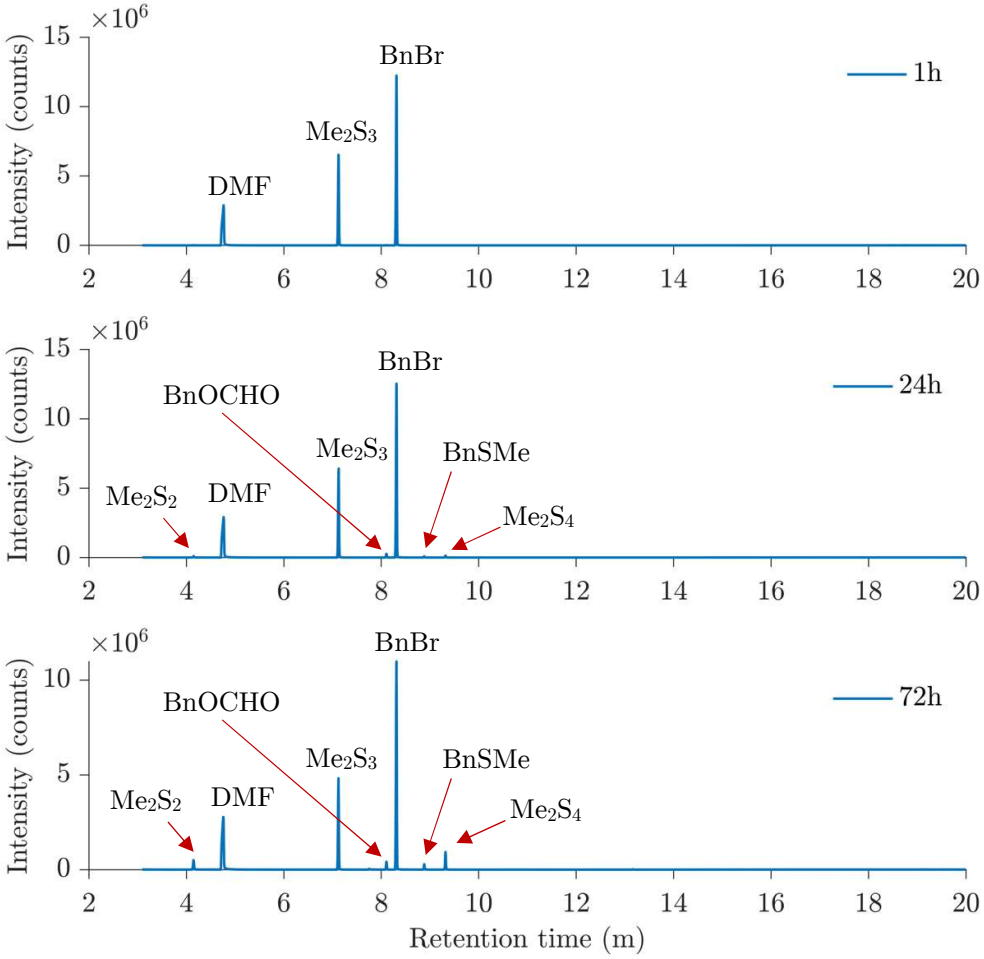

Figure S4.48: GC traces of a reaction between benzyl bromide, dimethyl trisulfide and DMF (5 equiv.). GCMS method B yields Me_2S_2 (4.14 min), DMF (4.74 min) Me_2S_3 (7.12 min), BnOCHO (8.11 min), BnBr (8.32 min), BnSMe (8.88 min), Me_2S_4 (9.32 min).

Reaction of Trisulfides with Thiols, Thiolates, and Thiyl Radicals

Procedure for control experiments:

1-Propane thiol and DMF

To a dry 2 mL glass vial equipped with a stir bar was added 1-propane thiol (27.4 µL, 0.3 mmol, 1 eq.) and DMF (870 µL, 11.2 mmol, 38.1 eq.) via syringe, and the mixture was stirred for 24 h. After 30 min and 24 h, a 10 µL aliquot was removed and diluted to 1 mL using chloroform for GC-MS analysis. Di-*n*-propyl disulfide was formed after 24 h of reaction but only in trace quantities (~0.2% area percentage by GC).

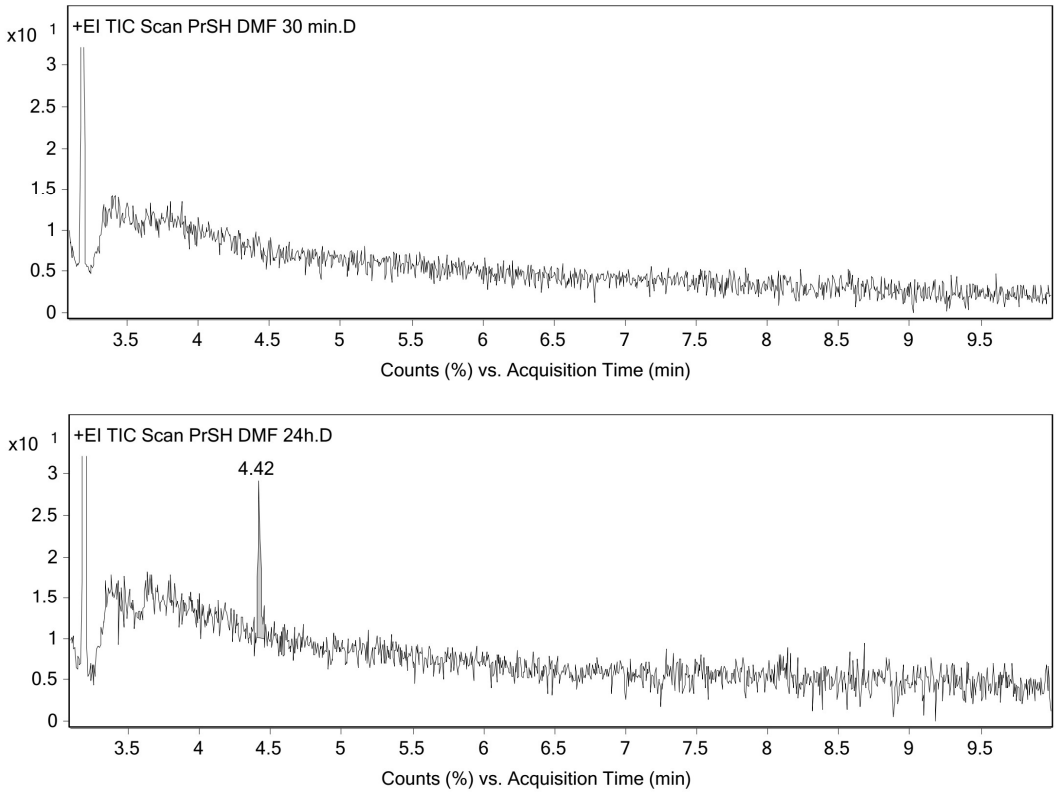

Figure S4.49: GC traces for the mixture of 1-propanethiol and DMF after 30 minutes and 24 h. A negligible portion of di-*n*-propyl disulfide (4.42 min) was formed after 24 h of mixing. GC-MS method C with a hold time of 3.7 minutes at 250 ºC.

Di-*n*-propyl trisulfide and DMF

To a dry 2 mL glass vial equipped with a stir bar was added di-*n*-propyl trisulfide (100 µL, 0.59 mmol, 1 eq.) and DMF (900 µL, 19.6 mmol, 19.7 eq.) via syringe, and the mixture was stirred for 24 h. After 30 min and 24 h, a 10 µL aliquot was removed and diluted to 1 mL using chloroform for GC-MS analysis. No disulfide or tetrasulfide formation was observed.

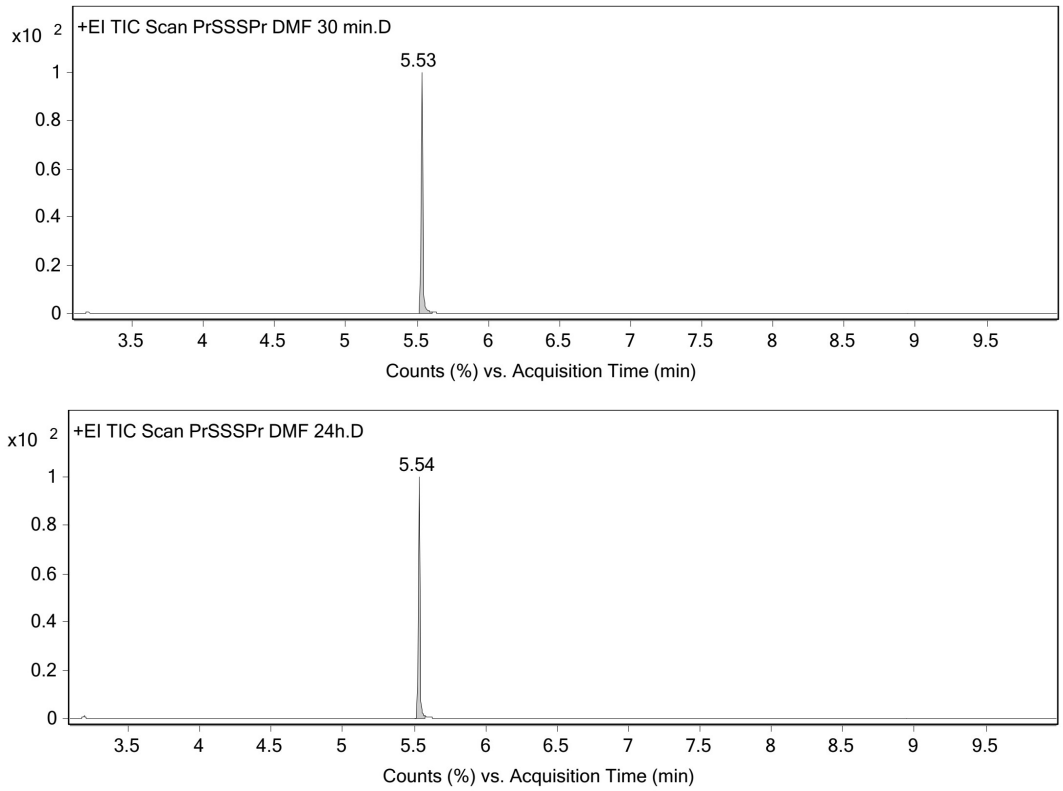

Figure S4.50: GC traces for the mixture of di-*n*-propyl trisulfide and DMF after 30 minutes and 24 h. Neither disulfide nor tetrasulfide were formed after 24 h of mixing. GC-MS method C with a hold time of 3.7 minutes at 250 ºC. Retention time: Pr_2S_3 (5.54 min).

Reaction of trisulfide in the presence of thiols

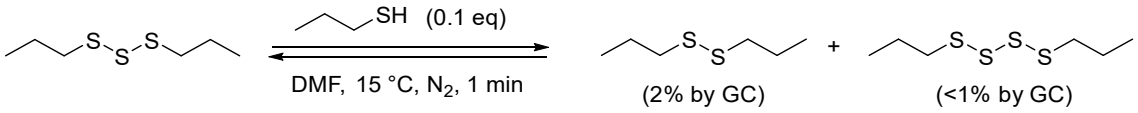

To a dry 2 mL glass vial equipped with a stir bar was added di-*n*-propyl trisulfide (100 μL, 0.59 mmol, 1 eq.) and 1-propane thiol (5.48 μL, 59 μmol, 0.1 eq.) under nitrogen atmosphere. To the thiol-trisulfide mixture was added DMF (890 μL, 11.5 mmol, 19.5 eq.) via syringe, and the mixture was stirred for 24 h. After 1, 5, 30 min, 1 h, and 24 h, a 10 μL aliquot was removed and diluted to 1 mL using chloroform for GC-MS analysis. After 24 hours, the GC area percentage of the disulfide increased to 3.4%. The GC method used (GC-MS method C) allowed detection of di-*n*-propyl disulfide (4.41 min), di-*n*-propyl trisulfide (5.55 min), and di-*n*-propyl tetrasulfide (6.40 min); chloroform solvent and PrSH (b.p. 68 °C) could not be detected by this method.

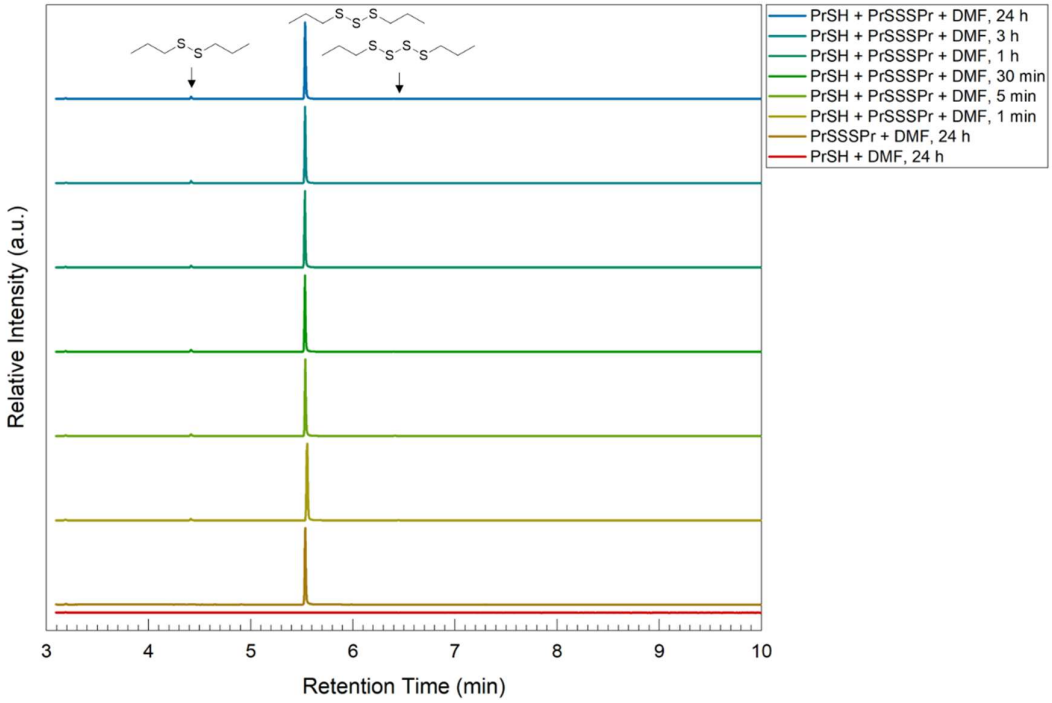

Figure S4.51: Stacked GC traces for the reaction between 1-propane thiol and di-*n*-propyl trisulfide in the presence of DMF. GC-MS method C with a hold time of 3.7 minutes at 250 ºC. Retention time after 1 min, di-*n*-propyl disulfide (4.41 min) and di-*n*-propyl tetrasulfide (6.40 min) were observed in a very small portion (~2%).

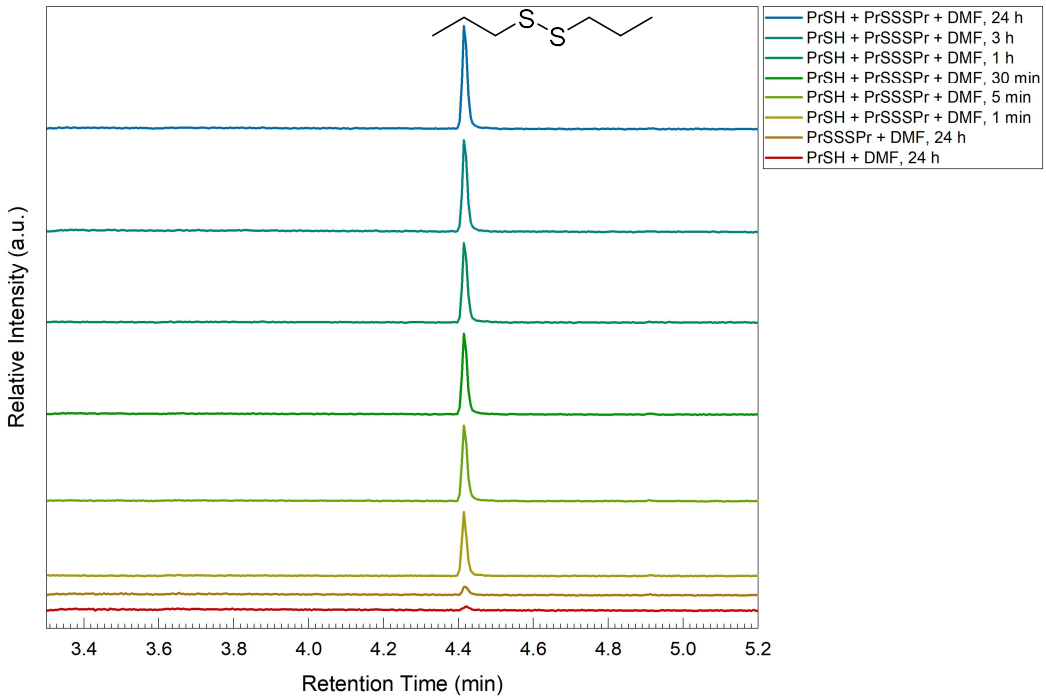

Figure S4.52: Zoomed stacked GC traces for the reaction between 1-propane thiol (0.1 eq.) and di-*n*-propyl trisulfide (1.0 eq.) in the presence of DMF. GC-MS method C with a hold time of 3.7 minutes at 250 ºC. The graph shows the disulfide region (4.41 min).

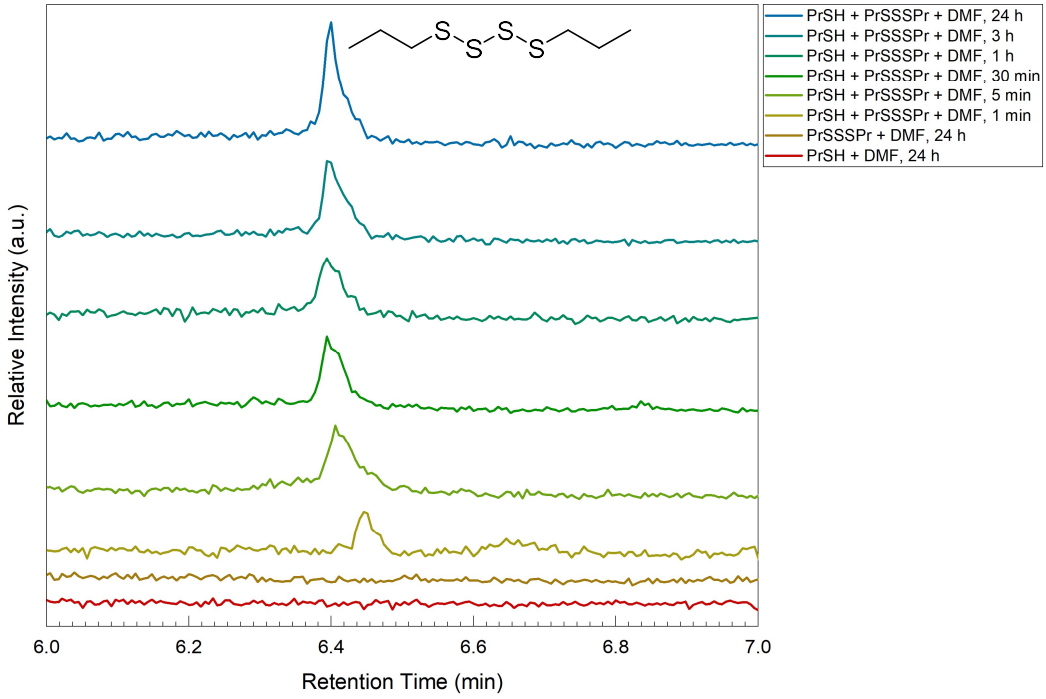

Figure S4.53: Zoomed stacked GC traces for the reaction between 1-propane thiol (0.1 eq.) and di-*n*-propyl trisulfide (1.0 eq.) in the presence of DMF. GC-MS method C with a hold time of 3.7 minutes at 250 ºC. The graph shows the tetrasulfide region (6.40 min).

Reaction of trisulfide in the presence of thiolate

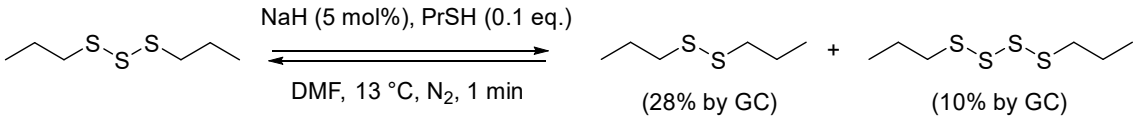

To a dry 2 mL glass vial equipped with a stir bar was added sodium hydride (1.32 mg, 55 μmol, 0.05 eq.) and DMF (810 μL, 10.5 mmol, 9.7 eq.) under nitrogen atmosphere. The mixture was allowed to stir for 1 minute. To this solution was then added 1-propane thiol (10 μL, 108 μmol, 0.1 eq.). The mixture became cloudy, and it was clear after stirring for about 1 minute. This solution was allowed to stir for about 5 minutes to ensure half of the thiol was converted into its thiolate. Next, di-*n*-propyl trisulfide (182.4 μL, 1.08 mmol, 1.0 eq.) was added to the thiol-thiolate solution. When the trisulfide was added, the solution became reddish brown. The mixture was stirred for 24 hours. After 1, 5, 30 minutes, 1 hour and 24 hours, a 20 μL aliquot was diluted to 1.5 mL with chloroform. The chloroform solution was washed with water 1 mL (2 x 0.5 mL) and dried using $MgSO_4$. The dried chloroform layer was filtered using PTFE (0.45 μm pore size) membrane filter directly to the GC-MS vial and ready for analysis. Another reaction was also carried out for a fully deprotonated 1-propane thiol. The amount of the thiol, the trisulfide, and DMF were the same while sodium hydride (2.6 mg,108 μmol, 1 eq. to the thiol) was used.

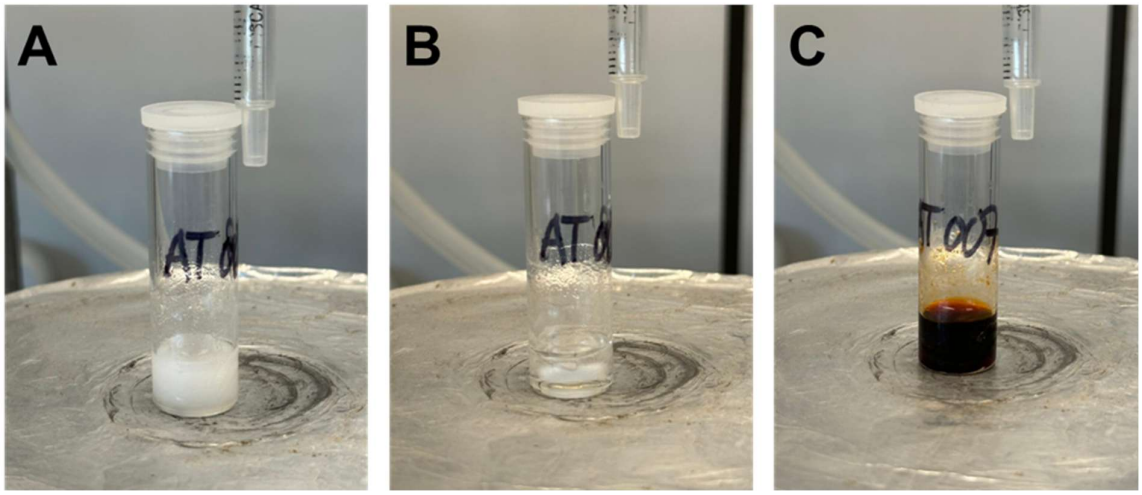

Figure S4.54: (A) NaH and 1-propane thiol dissolution in DMF. (B) NaH and 1-propane thiol in DMF, after around 5 min of stirring the solution turned clear. (C) The colour changed from clear to reddish brown just after the addition of di-*n*-propyl trisulfide to the solution.

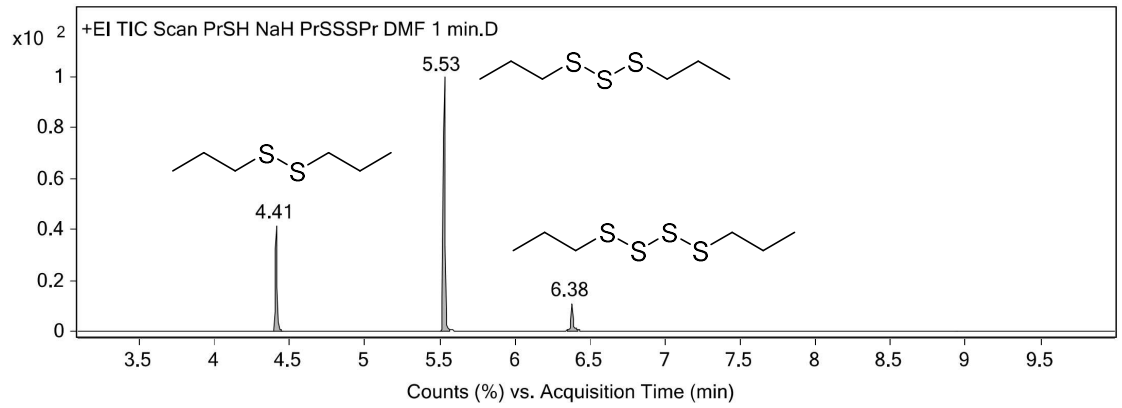

Figure S4.55: A representative GC trace of a reaction between 1-propane thiol/1-propane thiolate and di-*n*-propyl trisulfide in DMF after 1 min. GC-MS method C with a hold time of 3.7 minutes at 250 ºC. The mixture consists of di-*n*-propyl disulfide (28%) and di-*n*-propyl tetrasulfide (10%). After 24 h, the area percentage of di-*n*-propyl disulfide and di-*n*-propyl tetrasulfide were 40% and 13%, respectively.

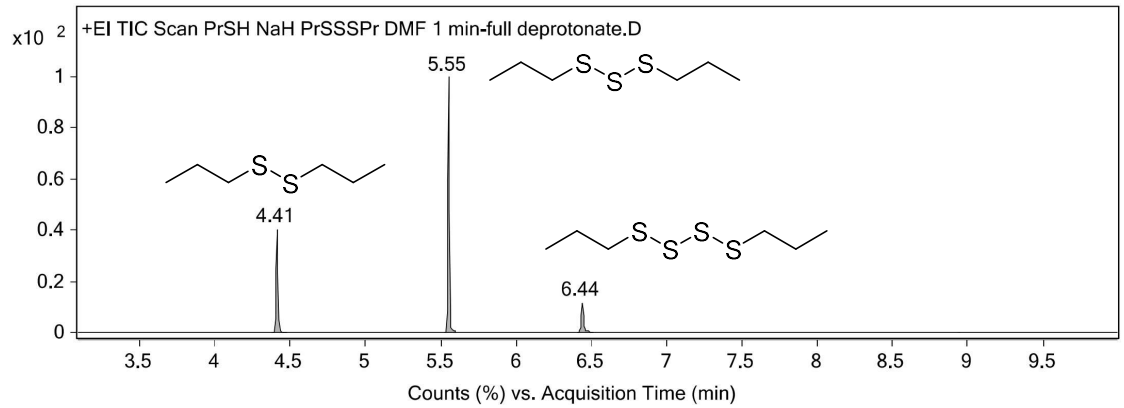

Figure S4.56: A representative GC trace of a reaction between 1-propane thiolate and di-*n*-propyl trisulfide in DMF after 1 min. GC-MS method C with a hold time of 3.7 minutes at 250 ºC. The mixture consists of di-*n*-propyl disulfide (27%) and di-*n*-propyl tetrasulfide (9%). After 24 h, the area percentage of di-*n*-propyl disulfide and di-*n*-propyl tetrasulfide were 44% and 12%, respectively.

4.7 References for Experimental Details and Characterizations

1. Gottlieb, H. E.; Kotlyar, V.; Nudelman, A. NMR Chemical Shifts of Common Laboratory Solvents as Trace Impurities. *J. Org. Chem.* **1997**, *62* (21), 7512-7515. DOI: 10.1021/jo971176v.
2. The MERCK Index: An Encyclopedia of Chemical, Drugs and Biologicals. 11th ed.; S. Budavari Ed.; Merck & Co., Inc., 1989.
3. Stoll, S.; Schweiger, A. EasySpin, a comprehensive software package for spectral simulation and analysis in EPR. *J. Magn. Reson.* **2006**, *178* (1), 42-55. DOI: 10.1016/j.jmr.2005.08.013.
4. Buettner, G. R. Spin Trapping: ESR parameters of spin adducts 1474 1528V. *Free Radic. Biol. Med.* **1987**, *3* (4), 259-303. DOI: 10.1016/S0891-5849(87)80033-3.
5. Rosen, G. M.; Beselman, A.; Tsai, P.; Pou, S.; Mailer, C.; Ichikawa, K.; Robinson, B. H.; Nielsen, R.; Halpern, H. J.; MacKerell, A. D. Influence of conformation on the EPR spectrum of 5, 5-dimethyl-1-hydroperoxy-1-pyrrolidinyloxyl: a spin trapped adduct of superoxide. *J. Org. Chem.* **2004**, *69* (4), 1321-1330. DOI: 10.1021/jo0354894.
6. Klinska, M.; Smith, L. M.; Gryn'ova, G.; Banwell, M. G.; Coote, M. L. Experimental demonstration of pH-dependent electrostatic catalysis of radical reactions. *Chem. Sci.* **2015**, *6* (10), 5623-5627. DOI: 10.1039/C5SC01307K.

CHAPTER 5: CONCLUSIONS AND FUTURE WORK

5.1 Conclusions

Organic trisulfides (R-SSS-R) can be found in various products such as essential oil of alliums (garlic and onion), a potent enediyne antitumor calicheamicin, antioxidant agents in hydrocarbon oils, and sulfur polymers such as sulfur-crosslinked rubber (vulcanized rubber). The reactivity of organic trisulfides is related to their weak S-S bonds which can be broken and reformed through a number of mechanisms. For instance, organic trisulfides can undergo S-S exchange at elevated temperatures (typically above 80 °C) through a radical pathway. This trisulfide metathesis can also occur through an ionic mechanism in the presence of nucleophiles such as phosphines[1] and amines[2]. These trisulfide metathesis reactions typically result in a mixture of polysulfides where a disulfide and a tetrasulfide are observed in the reaction mixture. In 2022, a collaborative study between Chalker group at Flinders University and Hasell group at Liverpool University discovered a unique trisulfide metathesis reaction in the presence of amide solvents (i.e., DMF, NMP, DMAc), and this reaction occurs at room temperature within minutes. An initial investigation on the mechanism in the earlier study was found that TEMPO can inhibit the trisulfide metathesis.[3] This result has led to the initial hypothesis that the S-S exchange in trisulfide might involve a radical pathway. However, a final conclusion on the mechanism has not been drawn due to a lack of supporting experimental data.

To address this problem, in this thesis, trisulfide metathesis has been studied comprehensively. The metathesis studies involve the exploration of various polar and non-polar solvents, the effect of trisulfide substrate scope, and the mechanistic studies to reveal what species contribute to the S-S exchange process. Through a series of experiments, we found that keys for the successful trisulfide metathesis are the use of dry polar aprotic solvents and non-hindered trisulfides. From mechanistic investigations, the driving force for the trisulfide metathesis in polar solvent may not involve radical and ionic mechanisms, but then it was proposed that the metathesis reaction occurs via a thiosulfoxide intermediate which is stabilised by the presence of polar solvents. This chemistry, however, has been very useful in several applications including the synthesis of unsymmetrical trisulfide, a direct modification of natural product containing trisulfide moiety, and the production of trisulfide dynamic combinatorial library.

This thesis presented the effects of various polar and non-polar solvents on the trisulfide metathesis. It was found that polar aprotic solvents such as DMF, NMP, ureas, phosphoramides, and DMSO can promote rapid trisulfide metathesis between two symmetrical trisulfides. While in general, the trisulfide metathesis was found to be very slow or did not occur in non-polar solvents (e.g., THF, DCM, or toluene) or polar protic solvents such as alcohols and acids. More interestingly, the trisulfide metathesis reaction was found to be slower in nucleophilic amines compared to DMF. This nucleophilic experiment, overall, suggests that the rapid S-S metathesis between trisulfides takes place is not simply because of the solvent nucleophilicity. In addition, polar aprotic solvents used in

the trisulfide metathesis reaction must be dry, as wet solvents can slow or severely inhibit the reaction.

In previous study, only dimethyl trisulfide and di-*n*-propyl trisulfide were used as trisulfide models for the metathesis study. We then expanded the study using various trisulfides. The synthesis of various trisulfide compounds was explored using different methods via sodium *S*-alkyl thiosulfate salt (or known as Bunte salt), thiol-sulfur dichloride, and thiol-*N,N'*-thiobisphthalimide as monosulfur transfer reagent. Each method provides pros and cons but all synthesized trisulfides used in thesis were obtained in good to excellent yield and in high purity. In this thesis, we have also made new trisulfides namely diisobutyl trisulfide, di-*n*-hexyl trisulfide, and bis(4-methoxybenzyl) trisulfide. In addition, we have also synthesized several organic tetrasulfides which were used in the tetrasulfide metathesis reaction as a comparison to the trisulfide metathesis.

With the synthesized trisulfides in hand, we examined the trisulfide metathesis employing dimethyl trisulfide and other various trisulfides in the presence of DMF. A rapid S-S metathesis can occur between dimethyl trisulfide and other trisulfides with primary alkyl, allyl, and benzyl groups. Much slower metathesis was observed when the trisulfide with secondary alkyl group (i.e., isopropyl) was employed. The trisulfide metathesis reaction does not work for tertiary butyl, adamantyl, or if the trisulfide contains hydroxyl group. When the hydroxyl group of the trisulfide is protected, the S-S metathesis occurs normally. Thus, it is clear that the steric hindrance and hydroxyl group are also the key factors which influence trisulfide S-S metathesis in DMF. Furthermore, we also tested the metathesis reactions for disulfides and tetrasulfides. As anticipated, in general the disulfide metathesis reaction does not occur. This is due to the strong S-S bond in disulfide compared to that of trisulfides or tetrasulfides. However, we observed an interesting result where disulfide metathesis can occur under the same conditions to that of trisulfide metathesis, and this only works for dibenzyl disulfide and other disulfides with primary alkyl groups (i.e., methyl, *n*-propyl). A more striking result is that DMF does not induce S-S metathesis between tetrasulfides, even though a tetrasulfide has weaker S-S bond compared to those trisulfide and disulfide. Therefore, the S-S metathesis reaction is unique to trisulfides.

In this work, we have hypothesized several mechanistic proposals. The trisulfide metathesis reaction in DMF could occur via a radical, an ionic, or a thiosulfoxide intermediate (concerted) mechanism. The proposed radical pathway can be ruled out based on the experimental results: (1) EPR analysis showed no radical signal. This experiment suggests that no S-centred radical formed in the trisulfide metathesis. (2) A disulfide and a tetrasulfide were not observed in the trisulfides-DMF mixture by analytical methods (i.e., GC-MS and NMR spectroscopy). If a thiyl radical is present, the reaction can lead to the formation of disulfide and tetrasulfide. (3) Benzoquinone and maleic anhydride were potent inhibitors for the trisulfide metathesis. While TEMPO inhibits the metathesis reaction, BHT radical scavenger does not inhibit the reaction. These results suggest other inhibition mechanisms (i.e., redox reaction). (4) The reaction between dimethyl trisulfide and a reactive electrophile dimethyl acrylamide, we observed neither conjugate addition nor polymerisation. If a

radical is present, polymerisation may occur. (5) Thiyl and perthiyl radicals from di-*n*-propyl trisulfide were generated by UV light. In this condition, we observed the formation of di-*n*-propyl disulfide. As mentioned previously, a disulfide and a tetrasulfide could be observed if the trisulfide metathesis generates a radical.

Next, the trisulfide metathesis is unlikely to follow an ionic pathway based on the experimental results: (1) In the reaction between dimethyl trisulfide and dimethyl acrylamide, if a thiolate is present, a Michael addition product can be observed. In fact, only starting materials were observed even after 7 days of reaction. Similarly, a thiolate trapping employing an electrophile benzyl bromide and dimethyl trisulfide in DMF showed an insignificant amount of benzyl methyl sulfide over 3 days which indicates a thiolate is unlikely to present. (2) Following this, a test using a thiolate, which is generated from the reaction between *n*-propyl thiol and sodium hydride, with di-*n*-propyl trisulfide showed a rapid formation of disulfide and tetrasulfide. Therefore, the ionic mechanism can be ruled out.

We also proposed that the trisulfide metathesis could possibly occur via thiosulfoxide intermediate. From several mechanistic proposals, we concluded that the most possible mechanistic pathway is a formation of thiosulfoxide followed by a concerted reaction between thiosulfoxide and a trisulfide to give a trisulfide crossover product and another thiosulfoxide, which can react further with a trisulfide in a chain reaction. The concerted and chain reaction account for the selective formation of trisulfide. In another proposal, we think that the formation of two thiosulfoxide intermediates simultaneously is highly unlikely because the energy barrier could be way much higher compared to the formation of one thiosulfoxide.

We understand that the definitive conclusion on the mechanism for polar solvents induced trisulfide metathesis has not been drawn. However, we have demonstrated several useful applications of this trisulfide metathesis chemistry. First, this chemistry allows one to prepare an unsymmetrical trisulfide directly from two symmetrical trisulfides. Reaction equilibrium can be shifted to obtain the target trisulfide product by using excess one trisulfide starting material, for example, in excess of DMF. We have also explored this synthetic approach to modify an anti-tumour natural product containing trisulfide moiety, calicheamicin-γ_1. For instance, a reaction between calicheamicin-γ_1 and excess dibenzyl trisulfide gave a clean conversion to benzyl–calicheamicin-γ_1. In addition to this, calicheamicin-γ_1 in DMF also underwent a dimerization. Second, this chemistry is useful for the selective and rapid formation of dynamic combinatorial library. Within minutes, 8 parent trisulfides in DMF can be transformed into a 29-trisulfide library. These applications are invaluable for a selective and clean modification of compound containing a trisulfide moiety. This chemical transformation requires no additives (e.g., nucleophiles) and external heating.

Finally, we believe this thesis will contribute valuable knowledge to the exploration of trisulfide metathesis chemistry, from the synthetic approach to their use in various applications such as synthetic modifications of trisulfide-containing molecules and the production of trisulfide dynamic libraries.

5.2 Future Work

For mechanistic studies, we are currently working with our collaborators on the computational calculations of each step in mechanistic proposal 6, which is the most possible mechanism that we proposed, in Chapter 4. Moreover, our work in trisulfide metathesis can be developed further for several applications. Currently, our group is developing polymers containing trisulfide linkages that can be processed by trisulfide metathesis chemistry explored in this thesis. Also, this chemistry can be invaluable for future directions in the synthetic modification of trisulfide containing molecules and the studies of trisulfide-based dynamic combinatorial chemistry.

Theoretical and Experimental Studies for The Proposed Mechanisms via Thiosulfoxide Intermediate

In order to obtain a good mechanistic interpretation of the trisulfide metathesis reaction, we are collaborating with Prof. Michelle L. Coote of Flinders University and Zhipeng Pei (PhD student in Prof. Coote Lab) to carry out computational calculations. The computational analyses include the calculation of energy profile for the overall free energy for the reaction between trisulfide models (i.e., dimethyl trisulfide and di-*n*-propyl trisulfide) in DMF as a solvent model. Next, natural population analysis (NPA) will be carried out to understand the charge distribution in a thiosulfoxide species that we proposed. This result will provide an insight into the bond polarization and the molecular reactivity. For comparison with other proposed mechanisms (i.e., radical and ionic), the bond-dissociation free energy for radical species (thiyl and perthiyl species) and anion species (thiolate and perthiolate) as well as the radical and nucleophilic attack from central sulfur to those species with a trisulfide will be calculated. The calculated energy profile for each reaction will be carried out in DMF as a solvent model.

Furthermore, as discussed in Chapter 4 a detailed kinetic analysis of trisulfide metathesis could offer deeper understanding on the overall mechanism. Information from the rate kinetics can provide key insights such as the reaction order, the rate-determining steps, and possibly the experimental activation energy of the metathesis reaction. For kinetic studies, a set of experiments to obtain the changes in concentration of both trisulfides over time should be carried out. Experiments at different temperatures may be required if the activation energy will be determined. In this case, Arrhenius equation below is used.

$$k = A.e^{-\frac{E_a}{RT}}$$

Where:

k = rate constant at given temperature

A = pre-exponential factor

E_a = activation energy (kJ mol^{-1})

R = universal gas constant (8.314 J mol^{-1} K^{-1})

T = temperature (K)

Solvent Processable Polymers Containing Trisulfide Linkages

Unlike disulfides and tetrasulfides, trisulfide metathesis induced by polar aprotic solvents, particularly for those amide solvents, is unique, rapid, and selective. Due to its selectivity for the formation of a new trisulfide, we thought that if a monomer molecule containing a trisulfide in both sides (R-SSS-X-SSS-R, where R = primary alkyl or aryl; X = polymer backbone), DMF can induce polymerisation. Figure 5.1 shows trisulfide S-S metathesis polymerisation and depolymerisation induced by polar aprotic solvents such as DMF. Other polar aprotic solvents can also be used to induce both processes. There are many routes to obtain a bis(trisulfide) monomer. James Smith (PhD student) and Dr. Harshal D. Patel have prepared a bis(trisulfide) monomer from dihaloalkane using a series of substitution reactions. Currently, our group is still working on producing the polymer via trisulfide metathesis chemistry. Other poly(trisulfides) with different functional groups such as amide, carbonate, and ester, are now under investigation.

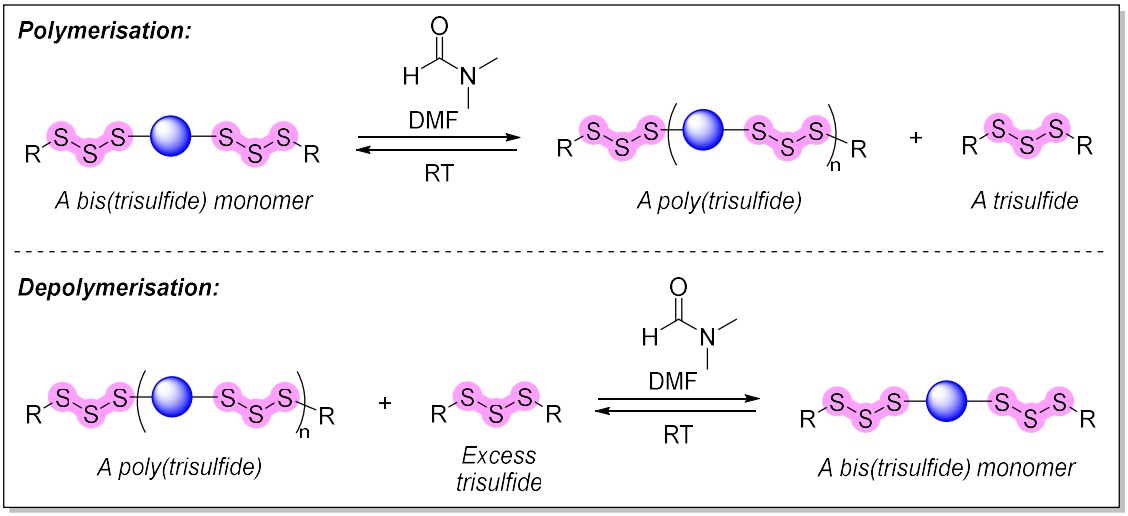

Figure 5.1: Trisulfide metathesis polymerisation and depolymerisation induced by polar aprotic solvents such as DMF.

Direct Modification of Compounds Containing Trisulfide Moiety and Dynamic Combinatorial Library

Following the success of direct modification of an anti-tumour natural product containing trisulfide moiety, calicheamicin-γ_1, the trisulfide metathesis chemistry can be used as a platform for a direct molecular editing specific at trisulfide moiety for all trisulfide molecules. This chemistry can also be useful for a selective modification of peptides and proteins containing trisulfides which is useful for the discovery of therapeutic peptide and proteins. Although disulfides are more prevalent in protein compared to the trisulfides, some antibodies[4] and a protein hormone[5] (i.e., human growth hormone) contain a trisulfide linkage. Hence, there will be opportunities to use trisulfide metathesis chemistry to explore this field.

In addition, our recent study on the production of trisulfide-based dynamic combinatorial library can also be invaluable as a tool to recognize protein ligands which is crucial in protein inhibition and drug discovery studies.[6, 7] Although our study is limited to the use of polar aprotic solvents, it is important that one can explore the trisulfide metathesis reaction under physiological conditions in future research.

5.3 References

(1) Harpp, D. N.; Smith, R. A. Organic sulfur chemistry. 42. Sulfur-sulfur bond cleavage processes. Selective desulfurization of trisulfides. *J. Am. Chem. Soc.* **1982**, *104* (22), 6045-6053. DOI: 10.1021/ja00386a034.

(2) Tonkin, S. J.; Gibson, C. T.; Campbell, J. A.; Lewis, D. A.; Karton, A.; Hasell, T.; Chalker, J. M. Chemically induced repair, adhesion, and recycling of polymers made by inverse vulcanization. *Chem. Sci.* **2020**, *11* (21), 5537-5546. DOI: 10.1039/D0SC00855A.

(3) Yan, P.; Zhao, W.; Tonkin, S. J.; Chalker, J. M.; Schiller, T. L.; Hasell, T. Stretchable and Durable Inverse Vulcanized Polymers with Chemical and Thermal Recycling. *Chem. Matter.* **2022**, *34* (3), 1167-1178. DOI: 10.1021/acs.chemmater.1c03662.

(4) Sun, Z.; Huang, M.; Sokolowska, I.; Cao, R.; Chang, K.; Hu, P.; Mo, J. Impact of Trisulfide on the Structure and Function of Different Antibody Constructs. *J. Pharm. Sci.* **2023**, *112* (10), 2637-2643. DOI: 10.1016/j.xphs.2023.08.010.

(5) Jespersen, A. M.; Christensen, T.; Klausen, N. K.; Nielsen, P. F.; Sørensen, H. H. Characterisation of a trisulphide derivative of biosynthetic human growth hormone produced in Escherichia coli. *Eur. J. Biochem.* **1994**, *219* (1-2), 365-373. DOI: 10.1111/j.1432-1033.1994.tb19948.x.

(6) Mondal, M.; Hirsch, A. K. H. Dynamic combinatorial chemistry: a tool to facilitate the identification of inhibitors for protein targets. *Chem. Soc. Rev.* **2015**, *44* (8), 2455-2488. DOI: 10.1039/C4CS00493K.

(7) Canal-Martín, A.; Pérez-Fernández, R. Protein-Directed Dynamic Combinatorial Chemistry: An Efficient Strategy in Drug Design. *ACS Omega* **2020**, *5* (41), 26307-26315. DOI: 10.1021/acsomega.0c03800.